THE INFLUENCE OF ENVIRONMENTAL FACTORS INCLUDING REACTIVE OXYGEN SPECIES ON THE SPATIAL AND TEMPORAL DISTRIBUTION OF MARINE THAUMARCHAEOTA

by

BRADLEY BURTON TOLAR

(Under the Direction of James T. Hollibaugh)

ABSTRACT

Thaumarchaeota – formerly known as Marine Group I Crenarchaeota – are highly abundant in the world's oceans, making up ~20% of the total prokaryotic population. Members of the Thaumarchaeota are capable of oxidizing ammonia using the ammonia monooxygenase enzyme (*amoA*), which is the first step in nitrification and a key process in the global nitrogen cycle. They are most abundant in deeper, colder waters with appearances in surface waters generally limited to higher latitudes and polar oceans in winter. Reasons for this distribution have been postulated, but no definitive explanation has been found to date. A hypothesis tested with this work is that reactive oxygen species (ROS), particularly hydrogen peroxide (H_2O_2), play a role in exclusion of Thaumarchaeota from surface waters.

This dissertation examines the spatial distribution of Thaumarchaeota in coastal and open-ocean, polar and temperate marine environments, where correlations with increased depth and decreased oxygen were common regardless of sample site. We also investigated the temporal distribution of Thaumarchaeota on Sapelo Island, Georgia, where annual spikes in abundance correlated to summer conditions (increased temperature; decreased pH, oxygen). The potential for Thaumarchaeota to use urea as an alternate substrate for ammonia oxidation was also investigated; our findings suggest that this is not a widespread attribute and is most likely due to removal of amine groups that are subsequently oxidized. Additionally, we found that nitrification is inhibited with increased [H_2O_2] in open ocean samples, with the most sensitive populations coming from the Southern Ocean. Populations from Sapelo Island, Georgia, were not as sensitive, but these microbial communities encounter high daily H_2O_2 concentrations.

In conclusion, we have found that Thaumarchaeota distributions correlate to a variety of environmental factors and it is unlikely that any single one can be used to predict dynamics of the entire group. However, evidence from this work indicates that clades of Thaumarchaeota could be differentially affected by certain conditions, justifying the separation of this group into ecotypes for future studies. We have shown that direct oxidation of urea by Thaumarchaeota is unlikely, and that ROS can inhibit ammonia oxidation. This may explain why Thaumarchaeota are typically absent from surface waters.

INDEX WORDS: Thaumarchaeota, Ammonia oxidation, Ammonia-oxidizing Archaea, Nitrification, 16S rRNA, ammonia monooxygenase (*amoA*), Reactive oxygen species (ROS), Ammonia, Urea, Nitrite, Nitrate, Nitrogen cycle, Quantitative PCR (qPCR)

THE INFLUENCE OF ENVIRONMENTAL FACTORS INCLUDING REACTIVE OXYGEN SPECIES ON THE SPATIAL AND TEMPORAL DISTRIBUTION OF MARINE THAUMARCHAEOTA

by

BRADLEY BURTON TOLAR

B.S., Louisiana State University, 2008

A Dissertation Submitted to the Graduate Faculty of The University of Georgia in Partial Fulfillment of the Requirements for the Degree

DOCTOR OF PHILOSOPHY

ATHENS, GEORGIA

2014

THE INFLUENCE OF ENVIRONMENTAL FACTORS INCLUDING REACTIVE OXYGEN SPECIES ON THE SPATIAL AND TEMPORAL DISTRIBUTION OF MARINE THAUMARCHAEOTA

by

BRADLEY BURTON TOLAR

Major Professor: James T. Hollibaugh

Committee: Mary Ann Moran

William Whitman

Robert Maier

Electronic Version Approved:

Julie Coffield

Interim Dean of the Graduate School

The University of Georgia

December 2014

DEDICATION

This dissertation is dedicated to my high school biology teachers, Mrs. Kay Baggett and Mrs. Renee Hill, who each inspired me to think big, be mindful of the world around me, and pursue science. Without their encouragement and instruction, I would not be where I am today. I also dedicate this work to my grandparents and parents, who always told me that I could be and do anything I wanted, and never allowed me to convince myself otherwise.

ACKNOWLEDGEMENTS

I would like to thank Dr. James “Tim” Hollibaugh for accepting me into his laboratory and teaching me how to explore the world of marine microbiology. He has sent me into the field and onto research vessels to collect water from the Atlantic, Southern, and Pacific Oceans, and I am grateful for all of those experiences. I appreciate Tim’s ability to encourage and push me to do the best science possible, and to constantly question research (including my own) to improve the field. I thank the other members of my advisory committee – Drs. Mary Ann Moran, Barny Whitman, and Rob Maier – for their insightful discussions and helpful comments throughout my studies. I am especially grateful to Mary Ann for allowing me to make use of her laboratory equipment and personnel for many of my research endeavors.

I am thankful for the many contributions of the members of the Hollibaugh Laboratory to my graduate studies throughout the years, especially Dr. Carrie Givens, Christian Edwardson, Qian Liu, Meredith Ross, Drew Duckett, and Chris Abin. Much of this work could not have been possible without their assistance in both the laboratory and field, and with the planning, writing, and presentation stages of research. Dr. Bill Miller and Dr. Leanne Powers have been incredible collaborators, and without them my ROS experiments would not have been possible (or nearly as enjoyable). I also thank Dr. Brian Popp and the members of his laboratory – especially Natalie Wallsgrove and Cassie Ka’apu-Lyons – for teaching me the tricks of the trade for ammonia oxidation rate measurements. Finally, I would like to thank the captains, crew members, and scientists

who took part in each of my research cruises and field expeditions at the UGA Marine Institute – without them I would not have had any samples to analyze.

As is commonly said, “it takes a village”. That is certainly true for a Ph.D., and I am thankful to both of the departments I have been lucky enough to call ‘home’ for the past few years – Microbiology and Marine Sciences. The faculty and staff have been helpful, kind, and welcoming, and have gone above and beyond to help me through any hurdles that have come my way. I am so glad to have entered graduate school with an exceptional class of students; without Dr. Bryn Durham, Dr. Claire Edwards, Dr. Felipe Sarmiento, Dr. Laura Cuff, Dr. Matt Hawkins, Megan Patch, Rupal Prabhu, and Dr. Sarahi Garcia, I would not have made it this far. I also thank the graduate students in both departments for expanding my thoughts outside of the marine Archaea. And to my fellow dissertation-writing partners, the plastics, and other friends at UGA – thanks for all the dinner, study, and birthday parties. You have all made Athens great.

Finally (and most importantly) this work would not have been possible without the constant encouragement, love, and support of my family – Bruce, Susan, Christy, Allie, Connor, Ada, and Laura – and other friends from high school, LSU, and beyond. I am glad you let me teach you about Thaumarchaeota (and how to pronounce the word), understood that I could not tell you when I would actually finish (and eventually stopped asking), and let me escape from the laboratory with vacations, long phone calls, video conferences over cooking and dinner, and random road trips. And especially for always encouraging me to “just keep swimming”, never allowing me stop looking toward the future, and forcing me take time off work to live in and enjoy the present.

TABLE OF CONTENTS

Page

CHAPTER 1

INTRODUCTION AND LITERATURE REVIEW

Marine Thaumarchaeota – An Important Environmental Microorganism

The first evidence of mesophilic marine Archaea was obtained by PCR-based surveys of 16S rRNA genes in the coastal (DeLong, 1992) and open ocean (Fuhrman *et al.*, 1992). It is now estimated that about one-third of all prokaryotic cells in the ocean are planktonic Archaea (Herndl *et al.*, 2005; Karner *et al.*, 2001). DeLong (DeLong, 1992) identified two major groups of Archaea in the oceans: the Marine Group 1 Crenarchaeota (MG1C) and the Marine Group II Euryarchaeota, the former being the most abundant and widespread of all non-extremophilic Archaea (Fuhrman *et al.*, 1992; Karner *et al.*, 2001; Wuchter *et al.*, 2006). MG1C alone is thought to account for around 20% of all the bacterial and archaeal cells in the global ocean (Karner *et al.*, 2001). Recently a new phylum, Thaumarchaeota, has been proposed for the Archaea that would include the MG1C (Brochier-Armanet *et al.*, 2008) and phylogenetic evidence suggests that Thaumarchaeota are the last common ancestor with eukaryotes (Kelly *et al.*, 2011). The first marine isolate from this group ("*Candidatus* Nitrosopumilus maritimus" SCM1) was obtained from gravel in a saltwater aquarium (Könneke *et al.*, 2005). Other Thaumarchaeota have since been isolated or enriched from coastal waters (Qin *et al.*, 2014) and the open ocean (Santoro and Casciotti, 2011); from estuaries (Blainey *et al.*, 2011; Mosier *et al.*, 2012), soils (Jung *et al.*, 2011; Kim *et al.*, 2011; Kim *et al.*, 2012;

Lehtovirta-Morley *et al.*, 2011; Tourna *et al.*, 2011; Zhalnina *et al.*, 2014), and marine sand (Matsutani *et al.*, 2011); from marine (Park *et al.*, 2010; Park *et al.*, 2014) and freshwater (French *et al.*, 2012) sediment; from hot springs (de la Torre *et al.*, 2008; Hatzenpichler *et al.*, 2008; Lebedeva *et al.*, 2013) and a salt flat (Dorador *et al.*, 2008); and some are sponge symbionts (Hallam *et al.*, 2006a).

Ammonia oxidation involves the conversion of ammonia to nitrite, and is a component of the marine nitrogen cycle (Figure 1.1). The reaction is catalyzed by the α-subunit of ammonia monooxygenase, encoded by the *amoA* gene. Initially, researchers thought that only certain Bacteria, such as *Nitrosomonas*, *Nitrosospira*, and *Nitrosococcus* (known as "ammonia-oxidizing Bacteria" or AOB), could oxidize ammonia (reviewed in Capone *et al.*, 2008; Prosser and Nicol, 2008; Ward, 2011b); however, metagenomic surveys of the Sargasso Sea identified a unique *amoA* gene sequence (Venter *et al.*, 2004) located on a contig containing a 16S rRNA gene sequence that was most similar to one retrieved from a soil crenarchaeote (Treusch *et al.*, 2005). This discovery provided the first evidence of putative ammonia oxidation by an archaeon. The subsequent cultivation of "*Ca.* N. maritimus" and studies of its growth dynamics showed that Archaea possessing the *amoA* gene could in fact oxidize ammonia (known as "ammonia-oxidizing Archaea" or AOA; Könneke *et al.*, 2005; Martens-Habbena *et al.*, 2009). Since then, surveys of archaeal *amoA* genes in the water column and sediment have documented its high diversity and wide distribution (e.g., Beman *et al.*, 2008; Church *et al.*, 2010; Coolen *et al.*, 2007; de Corte *et al.*, 2008; Francis *et al.*, 2005; Galand *et al.*, 2009; Hu *et al.*, 2011; Kalanetra *et al.*, 2009; Kirchman *et al.*, 2007; Mosier and Francis, 2008; Santoro *et al.*, 2010; Sintes *et al.*, 2013; Yakimov *et al.*, 2011). Other

studies of ammonia oxidation in the oceans have shown that in most locations, the archaeal *amoA* gene is 10-1000 times more abundant than bacterial *amoA*, suggesting marine AOA play a significant role in the global nitrogen cycle (e.g., Beman *et al.*, 2008; Francis *et al.*, 2007; Mincer *et al.*, 2007; Santoro *et al.*, 2010; Wuchter *et al.*, 2006).

Distribution of Thaumarchaeota in Marine Systems

In marine environments, populations of Thaumarchaeota (and thus AOA) are greatest below 100 m and are generally more abundant in the mesopelagic and bathypelagic zones (Fuhrman *et al.*, 1992; Herndl *et al.*, 2005; Karner *et al.*, 2001; Massana *et al.*, 1998; Mincer *et al.*, 2007; Murray *et al.*, 1999b; Teira *et al.*, 2006a). Additionally, greater concentrations of Thaumarchaeota have been observed at higher latitudes than in subtropical and tropical waters below 200 m depth (Agogué *et al.*, 2008; Church *et al.*, 2010), with elevated abundances in polar regions (Christman *et al.*, 2011; Church *et al.*, 2003; Kalanetra *et al.*, 2009; Kirchman *et al.*, 2007; Murray *et al.*, 1999a; Pedneault *et al.*, 2014).

Seasonal shifts in the abundance of Thaumarchaeota have been observed at high latitudes and in polar regions (Alonso-Sáez *et al.*, 2008; Herfort *et al.*, 2007; Massana *et al.*, 1998; Murray *et al.*, 1998; Pitcher *et al.*, 2011; Wuchter *et al.*, 2006). In the coastal North Sea, Thaumarchaeota become increasingly more abundant in winter of each year and return to background levels in spring (Pitcher *et al.*, 2011; Wuchter *et al.*, 2006). A decrease in abundance from winter to spring has also been observed in surface waters of the Southern Ocean near Palmer Station, Antarctica (Murray *et al.*, 1998), and no Thaumarchaeota were found in the surface layer in summer compared to abundant

populations in deeper water masses (Grzymski *et al.*, 2012; Kalanetra *et al.*, 2009). In contrast to this observed seasonality, populations in a salt marsh-dominated estuary displayed a consistent peak in Thaumarchaeota in August (Gifford *et al.*, 2011; Hollibaugh *et al.*, 2011). The differences in environmental conditions between these two sites suggest that the factors that control seasonal variation in the abundance of Thaumarchaeota are varied or unknown (Biller *et al.*, 2012; Hollibaugh *et al.*, 2014; Pitcher *et al.*, 2011).

Thaumarchaeota Activity and Metabolism

Thaumarchaeota can fix carbon autotrophically through the 3-hydroxypropionate/ 4-hydroxybutyrate pathway (Berg *et al.*, 2007; Hallam *et al.*, 2006b). Major enzymes in this pathway include acetyl-CoA/propionyl-CoA carboxylase (*accA*; Yakimov *et al.*, 2009) and 4-hydroxybutyryl-CoA dehydratase (*hcd*; Offre *et al.*, 2011). Both of these genes have been observed at quantities matching Thaumarchaeota *rrs* abundance in the environment (Hu *et al.*, 2011; Offre *et al.*, 2011; Yakimov *et al.*, 2009; Yakimov *et al.*, 2011), indicating the potential for chemoautotrophic metabolism (with ammonia oxidation) through most of the water column, which is supported by studies of "*Ca.* N. maritimus" (Könneke *et al.*, 2005; Martens-Habbena *et al.*, 2009) and experiments with bicarbonate (Herndl *et al.*, 2005; Wuchter *et al.*, 2003) or CO_2 (Kirchman *et al.*, 2007) uptake in marine systems. However, there is some evidence that Thaumarchaeota can take up organic carbon, including amino acids (Ouverney and Fuhrman, 2000; Teira *et al.*, 2004; Teira *et al.*, 2006b) and α-ketoglutarate (Qin *et al.*, 2014), and may therefore be mixotrophic or heterotrophic.

As mentioned above, ammonia oxidation is thought to be the primary energy-generating metabolism for Thaumarchaeota (combined with autotrophy, heterotrophy, or mixotrophy). Rates of ammonia oxidation have been determined for enrichment cultures (Mosier *et al.*, 2012; Santoro and Casciotti, 2011), isolates (Könneke *et al.*, 2005; Martens-Habbena *et al.*, 2009; Qin *et al.*, 2014), and for a number of locations by measuring overall nitrification rates (reviewed in Ward, 2011a; Yool *et al.*, 2007). It has also been proposed, based on the presence of urease (*ureC*) genes (Alonso-Sáez *et al.*, 2012) and transcripts (Pedneault *et al.*, 2014), that Thaumarchaeota may use urea in place of ammonia when substrate concentrations are low. However, neither oxidation rates nor measurements of urea concentrations were reported in these studies. A comparison of three strains including and similar to "*Ca.* N. maritimus" SCM1 showed that only one was able to convert urea-N to nitrite (almost stochiometrically) at rates similar to ammonia (Qin *et al.*, 2014). Thus the question of whether urea oxidation serves as an alternative source of energy for Thaumarchaeota metabolism has yet to be answered.

Environmental Factors Proposed to Affect Thaumarchaeota

There are a number of theories as to why Thaumarchaeota abundance varies by season, latitude, and depth (as discussed above). The most common of these is that Archaea are simply out-competed by Bacteria (Church *et al.*, 2003; Massana *et al.*, 1997; Massana *et al.*, 1998; Pitcher *et al.*, 2011). Thaumarchaeota abundance was inversely correlated with bacterial biomass and activity in the Southern California Bight (Murray *et al.*, 1999b), for example. It has also been proposed that phytoplankton growth could be inhibitory to Thaumarchaeota in some way (Murray *et al.*, 1999a; Pitcher *et al.*, 2011;

Wells and Deming, 2003), perhaps due to competition for nutrients or production by phytoplankton or associated Bacteria of antimicrobials targeting Thaumarchaeota. It is generally accepted that the Archaea have adapted for slow growth (Valentine, 2007) at greater depths in the ocean where they face less competition (compared to the photic zone), where they have access to an abundance of inorganic nitrogen (e.g. ammonia), and dominate remineralization processes (Church *et al.*, 2003; Massana *et al.*, 1998; Murray *et al.*, 1998; Murray *et al.*, 1999a). These adaptations could explain Thaumarchaeota abundance at depth during the summer in the Southern Ocean, but not their sudden disappearance from the surface layer in spring.

In the Antarctic, a dramatic increase in solar ultraviolet (UV) radiation occurs during the spring as a result of stratospheric ozone depletion (Meador *et al.*, 2002; Smith *et al.*, 1992), which may correspond to the observed decrease in Thaumarchaeota abundance in the Southern Ocean west of the Antarctic Peninsula (Church *et al.*, 2003; Murray *et al.*, 1998; Murray *et al.*, 1999a). Light inhibition of nitrification in marine environments has been postulated previously (Ward, 1987), and has been demonstrated with AOB cultures (Hooper and Terry, 1974; Olson, 1981; Ward, 1985). A comparative study of photosensitivity in isolates of both AOA and AOB showed inhibition of ammonia oxidation by light in both groups, though AOA were more sensitive and did not appear to recover during periods of darkness (Merbt *et al.*, 2012). "*Ca.* N. maritimus" and related isolates displayed differential photoinhibition of ammonia oxidation, but all were inhibited under continuous illumination (Qin *et al.*, 2014).

Since most of what we know about the ecophysiology of Thaumarchaeota has been inferred from studies of natural populations rather than from isolates in pure culture,

our knowledge of the factors affecting their growth is limited. A study of the growth of "*Ca.* N. maritimus" demonstrated its ability to oxidize ammonia under substrate-limited conditions (< 10 nM ammonium) and showed that growth rate and activity were reduced significantly if cultures were slightly aerated or mixed (Martens-Habbena *et al.*, 2009). These results suggest that Thaumarchaeota could be sensitive to unidentified environmental factor(s) other than light.

The tight inverse relationship between light levels and Thaumarchaeota abundance in the environment suggest that if direct damage from sunlight is not influencing Thaumarchaeota abundance, then some other process closely coupled to irradiance might be. One possibility is the production of reactive oxygen species (ROS) – highly reactive compounds that can be generated in the surface water directly from solar irradiation, which can react with oxygen and dissolved organic matter to form ROS, including H_2O_2 (Cabiscol *et al.*, 2000; Kieber *et al.*, 2003). Additionally, a number of cellular processes, such as respiration and photosynthesis, involve reactions that can generate ROS as by-products (Imlay, 2008; Latifi *et al.*, 2009). There are four major types of ROS: singlet oxygen ($^1O_2$), the superoxide anion (O_2^-), the hydroxyl radical ($OH\cdot$), and hydrogen peroxide (H_2O_2). H_2O_2, though less reactive than its counterparts, can be reduced to the more damaging hydroxyl radical via the Fenton reaction:

$$H_2O_2 + Fe^{2+} \rightarrow OH^- + FeO^{2+} + H^+ \rightarrow Fe^{3+} + OH^- + OH\cdot$$

This reaction can occur with a number of divalent transition metal cations (e.g., Fe^{2+}, Cu^{2+}) at a rate constant of 5000-20,000 M^{-1} s^{-1} (Imlay, 2008; Latifi *et al.*, 2009), and as little as 1 μM H_2O_2 can cause massive levels of DNA damage in some bacteria (Imlay, 2008). In seawater, H_2O_2 is detected in concentrations from nM to μM (Miller and

Kester, 1988), with the highest concentrations (~0.1 μM) present at the surface and decreasing with depth to < 25 nM at the base of the photic zone (Miller *et al.*, 2005).

Cellular components – DNA, RNA, proteins, and lipids – can all be damaged by ROS, especially by hydroxyl radicals generated from the breakdown of hydrogen peroxide (Sies and Menck, 1992). These ROS directly attack bases and sugars of nucleic acids, causing single- and double-stranded breaks, cross-links, and replication-blocking lesions (Sies and Menck, 1992). Certain moieties in proteins can also be modified upon exposure to ROS, and polyunsaturated fatty acids in membranes can be directly attacked by free radicals, causing a decrease in membrane fluidity and lipid degradation (Cabiscol *et al.*, 2000).

Prokaryotes possess a number of mechanisms to protect against the harmful effects of ROS, including detoxifying enzymes and DNA repair systems (Imlay, 2008). Some these include enzymes that scavenge ROS and convert them into less harmful forms, like O_2 and water. Superoxide dismutase (SOD) and superoxide reductase both scavenge O_2^- (Imlay, 2008). H_2O_2 can be neutralized by peroxidases (e.g., peroxiredoxins, glutathione peroxidase) and catalases (Cabiscol *et al.*, 2000; Imlay, 2008). Other enzymes are involved in repairing damage to macromolecules, including DNA base excision (*recA*, *xthA*) and recombinational repair (*polA*, *recB*). Disulfide bonds oxidized by ROS can be repaired by thioredoxins and glutaredoxins (Imlay, 2008). Some of these enzymes are grouped together into larger regulatory responses by the cell (OxyR and SoxRS systems) that act against H_2O_2 and O_2^-, respectively. Activation of either response system helps to increase resistance to ROS (Cabiscol *et al.*, 2000).

It is difficult to say whether or not Thaumarchaeota possess these same mechanisms due to limited genomic information, although there seems to be a potential deficiency in ROS-protective genes in the currently annotated Thaumarchaeota genomes available in the Integrated Microbial Genomes (IMG) database (http://img.jgi.doe.gov/) relative to Bacteria and Euryarchaeota (Table 1.1). This suggests that Thaumarchaeota may be more susceptible to ROS than Euryarchaeota or Bacteria, or that they use an unknown alternative mechanism to combat oxidative damage. Most of the information on cellular responses to ROS has been discovered through studies of Bacteria and Eukaryotes. As a result, very little is known about how Archaea respond to ROS, particularly the mesophilic Thaumarchaeota and AOA. However, a hyperthermophilic Crenarchaeota displayed a transcriptional response following UV irradiation that included an increase in the production of UV-protective compounds (Gotz *et al.*, 2007), which may indicate the possibility for similar UV repair mechanisms in marine Thaumarchaeota.

OBJECTIVES

In Chapter Two, we examine natural populations of Thaumarchaeota in the northern Gulf of Mexico to identify factors responsible for their distribution in March 2010, and to support development of experimental methods. We surveyed the region surrounding the Mississippi River plume and collected DNA to determine abundances of Thaumarchaeota genes including 16S rRNA (*rrs*), *amoA* (using two different primer sets), *hcd, and accA.* Genes for Bacteria (*rrs, amoA*) were quantified for comparison to Thaumarchaeota. We measured a suite of environmental variables collected

simultaneously, including depth, temperature, salinity, pH, turbidity, chlorophyll *a* fluorescence, and oxygen concentration to determine if Thaumarchaeota abundance was strongly correlated to any of these factors. Finally, we constructed sequence libraries of Thaumarchaeota *rrs*, *amoA*, and *accA* to assess Thaumarchaeota diversity at one site (Station D5), and we compared *rrs* sequences from Station D5 with others obtained through a pyrosequencing survey of the entire study region.

Chapter Three describes our investigation of Thaumarchaeota distributions in the Southern Ocean west of the Antarctic Peninsula near Palmer Station, Antarctica. We collected samples in austral spring (September 2010) and summer (January 2011) to quantify the abundance of Thaumarchaeota genes (*rrs*, *amoA*, *ureC*) and transcripts (*amoA*), and to measure nitrification rates. We compared samples both by season and water mass sampled, as populations in the surface mixed layer in spring (Antarctic Surface Water, AASW) are isolated deeper in the water column by seasonal stratification during summer (Winter Water, WW). In contrast, the subsurface Circumpolar Deep Water (CDW) layer remains relatively unchanged throughout the year. Similar environmental variables were collected as in Chapter 2, with the addition of measuring dissolved inorganic nitrogen (DIN; ammonia, nitrite, nitrate) concentrations. Finally, we used pyrosequencing to generate libraries of both *rrs* and *amoA* sequences to assess diversity and distribution of phylotypes by season and water mass, and to compare these data from our 2010-2011 survey to one conducted in the same region during the summer of 2006 (Kalanetra *et al.*, 2009).

In Chapter Four, we concentrate on the temporal (seasonal) variability of Thaumarchaeota populations at a single site in a salt marsh-dominated estuary. Through

quarterly sampling (2008-2011) at Marsh Landing in the shallow coastal waters around Sapelo Island, Georgia, an annual "bloom" of Thaumarchaeota (increase in abundance 100- to 1000-times) in August was discovered and described (Gifford *et al.*, 2011; Hollibaugh *et al.*, 2011; Hollibaugh *et al.*, 2014). This seasonal distribution is in stark contrast to distributions seen elsewhere, where Thaumarchaeota are only abundant in deeper waters or are only found in surface waters during winter. We increased the frequency of sampling from quarterly to weekly from March 2011 to the present to quantify fine-scale temporal variability in Thaumarchaeota abundance. We also collected samples to determine DIN concentrations, along with urea, and collected a variety of environmental variables from nearby sensors, including water quality (depth, temperature, salinity, pH, oxygen concentrations), meteorological (air temperature, wind speed and direction, photosynthetically active radiation, precipitation), and nutrient (DIN, phosphate, chlorophyll *a*) data. Finally, we collected samples in shelf waters of the South Atlantic Bight (off the coast of Georgia) to determine the spatial distribution of Thaumarchaeota and nitrification rates around Sapelo Island during bloom (October) and non-bloom (April) seasons for comparison.

Chapter Five investigates the potential for Thaumarchaeota to use urea preferentially as an alternate substrate for ammonia oxidation as proposed by Alonso-Sáez *et al.* (2012). We measured rates of ammonia and urea oxidation at Marsh Landing and in the South Atlantic Bight, Southern Ocean, and Gulf of Alaska to test this in both coastal and open-ocean environments, as well as polar and temperate waters. We also determined the abundance of Thaumarchaeota genes (*rrs*, *amoA*, *ureC*) and transcripts

(*amoA*, *ureC*), and compared them with rates and environmental measurements (including ammonia and urea concentrations) to look for trends.

Finally, Chapter Six describes our investigation of the hypothesis that reactive oxygen species (ROS), specifically hydrogen peroxide (H_2O_2) could explain why Thaumarchaeota are typically absent from surface waters. We collected samples from a variety of open-ocean regions, including the Gulf of Mexico, the Southern Ocean, and the Gulf of Alaska, and set up whole-seawater incubations with varying H_2O_2 additions. We measured transcription and nitrification rates as a response to ROS addition. Additional experiments were performed at Marsh Landing (Sapelo Island) for a coastal comparison; these results are discussed in Appendix E.

REFERENCES

Agogué H, Brink M, Dinasquet J, Herndl GJ (2008). Major gradients in putatively nitrifying and non-nitrifying Archaea in the deep North Atlantic. *Nature* **456:** 788-791.

Alonso-Sáez L, Sanchez O, Gasol JM, Balagué V, Pedrós-Alio C (2008). Winter-to-summer changes in the composition and single-cell activity of near-surface Arctic prokaryotes. *Environ Microbiol* **10:** 2444-2454.

Alonso-Sáez L, Waller AS, Mende DR, Bakker K, Farnelid H, Yager PL, Lovejoy C, Tremblay JE, Potvin M, Heinrich F, Estrada M, Riemann L, Bork P, Pedrós-Alio C, Bertilsson S (2012). Role for urea in nitrification by polar marine Archaea. *Proc Nat Acad Sci USA* **109:** 17989-17994.

Beman JM, Popp BN, Francis CA (2008). Molecular and biogeochemical evidence for ammonia oxidation by marine Crenarchaeota in the Gulf of California. *ISME J* **2:** 429-441.

Berg IA, Kockelkorn D, Buckel W, Fuchs G (2007). A 3-hydroxypropionate/4-hydroxybutyrate autotrophic carbon dioxide assimilation pathway in Archaea. *Science* **318:** 1782-1786.

Biller SJ, Mosier AC, Wells GF, Francis CA (2012). Global Biodiversity of Aquatic Ammonia-Oxidizing Archaea is Partitioned by Habitat. *Front Microbiol* **3:** 252.

Blainey PC, Mosier AC, Potanina A, Francis CA, Quake SR (2011). Genome of a low-salinity ammonia-oxidizing archaeon determined by single-cell and metagenomic analysis. *PLoS ONE* **6:** e16626.

Brochier-Armanet C, Boussau B, Gribaldo S, Forterre P (2008). Mesophilic Crenarchaeota: proposal for a third archaeal phylum, the Thaumarchaeota. *Nat Rev Microbiol* **6:** 245-252.

Cabiscol E, Tamarit J, Ros J (2000). Oxidative stress in bacteria and protein damage by reactive oxygen species. *Int Microbiol* **3:** 3-8.

Capone DG, Bronk DA, Mulholland MR, Carpenter EJ (eds) (2008) Nitrogen in the Marine Environment. Academic Press: Burlington, MA.

Christman GD, Cottrell MT, Popp BN, Gier E, Kirchman DL (2011). Abundance, Diversity, and Activity of Ammonia-Oxidizing Prokaryotes in the Coastal Arctic Ocean in Summer and Winter. *Appl Environ Microbiol* **77:** 2026-2034.

Church MJ, DeLong EF, Ducklow HW, Karner MB, Preston CM, Karl DM (2003). Abundance and distribution of planktonic Archaea and Bacteria in the waters west of the Antarctic Peninsula. *Limnol Oceanogr* **48:** 1893-1902.

Church MJ, Wai B, Karl DM, DeLong EF (2010). Abundances of crenarchaeal *amoA* genes and transcripts in the Pacific Ocean. *Environ Microbiol* **12:** 679-688.

Coolen MJL, Abbas B, van Bleijswijk J, Hopmans EC, Kuypers MMM, Wakeham SG, Damste JSS (2007). Putative ammonia-oxidizing Crenarchaeota in suboxic waters of the Black Sea: a basin-wide ecological study using 16S ribosomal and functional genes and membrane lipids. *Environ Microbiol* **9:** 1001-1016.

de Corte D, Yokokawa T, Varela MM, Agogué H, Herndl GJ (2008). Spatial distribution of Bacteria and Archaea and *amoA* gene copy numbers throughout the water column of the Eastern Mediterranean Sea. *ISME J* **3:** 147-158.

de la Torre JR, Walker CB, Ingalls AE, Konneke M, Stahl DA (2008). Cultivation of a thermophilic ammonia oxidizing archaeon synthesizing crenarchaeol. *Environ Microbiol* **10:** 810-818.

DeLong EF (1992). Archaea in coastal marine environments. *Proc Natl Acad Sci USA* **89:** 5685-5689.

Dorador C, Busekow A, Vila I, Imhoff JF, Witzel K-P (2008). Molecular analysis of enrichment cultures of ammonia oxidizers from the Salar de Huasco, a high altitude saline wetland in northern Chile. *Extremophiles* **12:** 405-414.

Francis CA, Roberts KJ, Beman JM, Santoro AE, Oakley BB (2005). Ubiquity and diversity of ammonia-oxidizing archaea in water columns and sediments of the ocean. *Proc Natl Acad Sci USA* **102:** 14683-14688.

Francis CA, Beman JM, Kuypers MMM (2007). New processes and players in the nitrogen cycle: the microbial ecology of anaerobic and archaeal ammonia oxidation. *ISME J* **1:** 19-27.

French E, Kozlowski JA, Mukherjee M, Bullerjahn G, Bollmann A (2012). Ecophysiological characterization of ammonia-oxidizing archaea and bacteria from freshwater. *Appl Environ Microbiol* **78:** 5773-5780.

Fuhrman JA, McCallum K, Davis AA (1992). Novel Major Archaebacterial Group from Marine Plankton. *Nature* **356:** 148-149.

Galand PE, Lovejoy C, Hamilton AK, Ingram RG, Pedneault E, Carmack EC (2009). Archaeal diversity and a gene for ammonia oxidation are coupled to oceanic circulation. *Environ Microbiol* **11:** 971-980.

Gifford SM, Sharma S, Rinta-Kanto JM, Moran MA (2011). Quantitative analysis of a deeply sequenced marine microbial metatranscriptome. *ISME J* **5:** 461-472.

Gotz D, Pavtubi S, Munro S, Lundgren M, Bernander R, White MF (2007). Responses of hyperthermophilic crenarchaea to UV irradiation. *Genome Biol* **8:** R220.

Grzymski JJ, Riesenfeld CS, Williams TJ, Dussaq AM, Ducklow H, Erickson M, Cavicchioli R, Murray AE (2012). A metagenomic assessment of winter and summer bacterioplankton from Antarctica Peninsula coastal surface waters. *ISME J* **6:** 1901-1915.

Hallam SJ, Konstantinidis KT, Putnam N, Schleper C, Watanabe Y, Sugahara J, Preston C, de la Torre J, Richardson PM, DeLong EF (2006a). Genomic analysis of the uncultivated marine crenarchaeote *Cenarchaeum symbiosum*. *Proc Natl Acad Sci USA* **103:** 18296-18301.

Hallam SJ, Mincer TJ, Schleper C, Preston CM, Roberts KJ, Richardson PM, DeLong EF (2006b). Pathways of Carbon Assimilation and Ammonia Oxidation Suggested by Environmental Genomic Analyses of Marine *Crenarchaeota*. *PLoS Biol* **4:** e95.

Hatzenpichler R, Lebedeva EV, Spieck E, Stoecker K, Richter A, Daims H, Wagner M (2008). A moderately thermophilic ammonia-oxidizing crenarchaeote from a hot spring. *Proc Natl Acad Sci USA* **105:** 2134-2139.

Herfort L, Schouten S, Abbas B, Veldhuis MJW, Coolen MJL, Wuchter C, Boon JP, Herndl GJ, Damste JSS (2007). Variations in spatial and temporal distribution of Archaea in the North Sea in relation to environmental variables. *FEMS Microbiol Ecol* **62:** 242-257.

Herndl GJ, Reinthaler T, Teira E, van Aken H, Veth C, Pernthaler A, Pernthaler J (2005). Contribution of Archaea to Total Prokaryotic Production in the Deep Atlantic Ocean. *Appl Environ Microbiol* **71:** 2303-2309.

Hollibaugh JT, Gifford S, Sharma S, Bano N, Moran MA (2011). Metatranscriptomic analysis of ammonia-oxidizing organisms in an estuarine bacterioplankton assemblage. *ISME J* **5:** 866-878.

Hollibaugh JT, Gifford SM, Moran MA, Ross MJ, Sharma S, Tolar BB (2014). Seasonal variation in the metratranscriptomes of a Thaumarchaeota population from SE USA coastal waters. *ISME J* **8:** 685-698.

Hooper AB, Terry KR (1974). Photoinactivation of Ammonia Oxidation in *Nitrosomonas*. *J Bacteriol* **119:** 899-906.

Hu A, Jiao N, Zhang C (2011). Community structure and function of planktonic Crenarchaeota: Changes with depth in the South China Sea. *Microb Ecol* **62:** 549-563.

Imlay JA (2008). Cellular defenses against superoxide and hydrogen peroxide. *Annu Rev Biochem* **77:** 755-776.

Jung MY, Park SJ, Min D, Kim JS, Rijpstra WI, Sinninghe Damste JS, Kim GJ, Madsen EL, Rhee SK (2011). Enrichment and characterization of an autotrophic ammonia-oxidizing archaeon of mesophilic crenarchaeal group I.1a from an agricultural soil. *Appl Environ Microbiol* **77:** 8635-8647.

Kalanetra KM, Bano N, Hollibaugh JT (2009). Ammonia-oxidizing Archaea in the Arctic Ocean and Antarctic coastal waters. *Environ Microbiol* **11:** 2434-2445.

Karner MB, DeLong EF, Karl DM (2001). Archaeal dominance in the mesopelagic zone of the Pacific Ocean. *Nature* **409:** 507-510.

Kelly S, Wickstead B, Gull K (2011). Archaeal phylogenomics provides evidence in support of a methanogenic origin of the Archaea and a thaumarchaeal origin for the eukaryotes. *Proc Royal Soc B - Bio* **278:** 1009-1018.

Kieber DJ, Peake BM, Scully NM (2003). Reactive oxygen species in aquatic ecosystems. In: Helbling EW, Zagarese H (eds). UV Effects in Aquatic Organisms and Ecosystems. The Royal Society of Chemistry: Cambridge. pp 251-290.

Kim BK, Jung MY, Yu DS, Park SJ, Oh TK, Rhee SK, Kim JF (2011). Genome sequence of an ammonia-oxidizing soil archaeon, "*Candidatus* Nitrosoarchaeum koreensis" MY1. *J Bacteriol* **193:** 5539-5540.

Kim JG, Jung MY, Park SJ, Rijpstra WI, Sinninghe Damste JS, Madsen EL, Min D, Kim JS, Kim GJ, Rhee SK (2012). Cultivation of a highly enriched ammonia-oxidizing archaeon of thaumarchaeotal group I.1b from an agricultural soil. *Environ Microbiol* **14:** 1528-1543.

Kirchman DL, Elifantz H, Dittel AI, Malmstrom RR, Cottrell MT (2007). Standing stocks and activity of Archaea and Bacteria in the western Arctic Ocean. *Limnol Oceanogr* **52:** 495-507.

Könneke M, Bernhard AE, de la Torre JR, Walker CB, Waterbury JB, Stahl DA (2005). Isolation of an autotrophic ammonia-oxidizing marine archaeon. *Nature* **437:** 543-546.

Latifi A, Ruiz M, Zhang CC (2009). Oxidative stress in cyanobacteria. *FEMS Microbiol Rev* **33:** 258-278.

Lebedeva EV, Hatzenpichler R, Pelletier E, Schuster N, Hauzmayer S, Bulaev A, Grigor'eva NV, Galushko A, Schmid M, Palatinszky M, Le Paslier D, Daims H, Wagner M (2013). Enrichment and genome sequence of the group I.1a ammonia-oxidizing Archaeon "Ca. Nitrosotenuis uzonensis" representing a clade globally distributed in thermal habitats. *PLoS ONE* **8:** e80835.

Lehtovirta-Morley LE, Stoecker K, Vilcinskas A, Prosser JI, Nicol GW (2011). Cultivation of an obligate acidophilic ammonia oxidizer from a nitrifying acid soil. *Proc Natl Acad Sci USA* **108:** 15892-15897.

Martens-Habbena W, Berube PM, Urakawa H, de la Torre JR, Stahl DA (2009). Ammonia oxidation kinetics determine niche separation of nitrifying Archaea and Bacteria. *Nature* **461:** 976-979.

Massana R, Murray AE, Preston CM, DeLong EF (1997). Vertical distribution and phylogenetic characterization of marine planktonic Archaea in the Santa Barbara Channel. *Appl Environ Microbiol* **63:** 50-56.

Massana R, Taylor LJ, Murray AE, Wu KY, Jeffrey WH, DeLong EF (1998). Vertical distribution and temporal variation of marine planktonic archaea in the Gerlache Strait, Antarctica, during early spring. *Limnol Oceanogr* **43:** 607-617.

Matsutani N, Nakagawa T, Nakamura K, Takahashi R, Yoshihara K, Tokuyama T (2011). Enrichment of a Novel Marine Ammonia-Oxidizing Archaeon Obtained from Sand of an Eelgrass Zone. *Microbes Environ* **26:** 23-29.

Meador J, Jeffrey WH, Kase JP, Pakulski JD, Chiarello S, Mitchell DL (2002). Seasonal fluctuation of DNA photodamage in marine plankton assemblages at Palmer Station, Antarctica. *Photochem Photobiol* **75:** 266-271.

Merbt SN, Stahl DA, Casamayor EO, Marti E, Nicol GW, Prosser JI (2012). Differential photoinhibition of bacterial and archaeal ammonia oxidation. *FEMS Microbiol Lett* **327:** 41-46.

Miller GW, Morgan CA, Kieber DJ, King DW, Snow JA, Heikes BG, Mopper K, Kiddle JJ (2005). Hydrogen peroxide method intercomparision study in seawater. *Mar Chem* **97:** 4-13.

Miller WL, Kester DR (1988). Hydrogen-Peroxide Measurement in Seawater by (Para-Hydroxyphenyl)Acetic Acid Dimerization. *Anal Chem* **60:** 2711-2715.

Mincer TJ, Church MJ, Taylor LT, Preston C, Karl DM, DeLong EF (2007). Quantitative distribution of presumptive archaeal and bacterial nitrifiers in Monterey Bay and the North Pacific Subtropical Gyre. *Environ Microbiol* **9:** 1162-1175.

Mosier AC, Francis CA (2008). Relative abundance and diversity of ammonia-oxidizing archaea and bacteria in the San Francisco Bay estuary. *Environ Microbiol* **10:** 3002-3016.

Mosier AC, Lund MB, Francis CA (2012). Ecophysiology of an ammonia-oxidizing archaeon adapted to low-salinity habitats. *Microb Ecol* **64:** 955-963.

Murray AE, Preston CM, Massana R, Taylor LT, Blakis A, Wu K, DeLong EF (1998). Seasonal and spatial variability of bacterial and archaeal assemblages in the coastal waters near Anvers Island, Antarctica. *Appl Environ Microbiol* **64:** 2585-2595.

Murray AE, Wu KY, Moyer CL, Karl DM, DeLong EF (1999a). Evidence for circumpolar distribution of planktonic Archaea in the Southern Ocean. *Aquat Microb Ecol* **18:** 263-273.

Murray AE, Blakis A, Massana R, Strawzewski S, Passow U, Alldredge A, DeLong EF (1999b). A time series assessment of planktonic archaeal variability in the Santa Barbara Channel. *Aquat Microb Ecol* **20:** 129-145.

Offre P, Nicol GW, Prosser JI (2011). Community profiling and quantification of putative autotrophic thaumarchaeal communities in environmental samples. *Environ Microbiol Rep* **3:** 245-253.

Olson RJ (1981). Differential Photoinhibition of Marine Nitrifying Bacteria - a Possible Mechanism for the Formation of the Primary Nitrite Maximum. *J Mar Res* **39:** 227-238.

Ouverney CC, Fuhrman JA (2000). Marine planktonic Archaea take up amino acids. *Appl Environ Microbiol* **66:** 4829-4833.

Park BJ, Park S-J, Yoon DN, Schouten S, Sinninghe Damste JS, Rhee S-K (2010). Cultivation of autotrophic ammonia-oxidizing archaea from marine sediments in coculture with sulfur-oxidizing bacteria. *Appl Environ Microbiol* **76:** 7575-7587.

Park S-J, Ghai R, Martin-Cuadrado AB, Rodriguez-Valera F, Chung WH, Kwon K, Lee J-H, Madsen EL, Rhee S-K (2014). Genomes of two new ammonia-oxidizing archaea enriched from deep marine sediments. *PLoS ONE* **9:** e96449.

Pedneault E, Galand PE, Potvin M, Tremblay J-É, Lovejoy C (2014). Archaeal *amoA* and *ureC* genes and their transcriptional activity in the Arctic Ocean. *Sci Rep* **4:** 1-10.

Pitcher A, Wuchter C, Siedenberg K, Schouten S, Damste JSS (2011). Crenarchaeol tracks winter blooms of ammonia-oxidizing Thaumarchaeota in the coastal North Sea. *Limnol Oceanogr* **56:** 2308-2318.

Prosser JI, Nicol GW (2008). Relative contributions of archaea and bacteria to aerobic ammonia oxidation in the environment. *Environ Microbiol* **10:** 2931-2941.

Qin W, Amin SA, Martens-Habbena W, Walker CB, Urakawa H, Devol AH, Ingalls AE, Moffett JW, Armbrust EV, Stahl DA (2014). Marine ammonia-oxidizing archaeal isolates display obligate mixotrophy and wide ecotypic variation. *Proc Nat Acad Sci USA* **111:** 12504-12509.

Santoro AE, Casciotti KL, Francis CA (2010). Activity, abundance and diversity of nitrifying archaea and bacteria in the central California Current. *Environ Microbiol* **12:** 1989-2006.

Santoro AE, Casciotti KL (2011). Enrichment and characterization of ammonia-oxidizing archaea from the open ocean: phylogeny, physiology and stable isotope fractionation. *ISME J* **5:** 1796-1808.

Sies H, Menck CFM (1992). Singlet Oxygen Induced DNA Damage. *Mut Res* **275:** 367-375.

Sintes E, Bergauer K, De Corte D, Yokokawa T, Herndl GJ (2013). Archaeal *amoA* gene diversity points to distinct biogeography of ammonia-oxidizing Crenarchaeota in the ocean. *Environ Microbiol* **15:** 1647-1658.

Smith RC, Prezelin BB, Baker KS, Bidigare RR, Boucher NP, Coley T, Karentz D, Macintyre S, Matlick HA, Menzies D, Ondrusek M, Wan Z, Waters KJ (1992). Ozone Depletion - Ultraviolet-Radiation and Phytoplankton Biology in Antarctic Waters. *Science* **255:** 952-959.

Teira E, Reinthaler T, Pernthaler A, Pernthaler J, Herndl GJ (2004). Combining Catalyzed Reporter Deposition-Fluorescence In Situ Hybridization and Microautoradiography To Detect Substrate Utilization by Bacteria and Archaea in the Deep Ocean. *Appl Environ Microbiol* **70:** 4411-4414.

Teira E, Lebaron P, van Aken H, Herndl GJ (2006a). Distribution and activity of Bacteria and Archaea in the deep water masses of the North Atlantic. *Limnol Oceanogr* **51:** 2131-2144.

Teira E, van Aken H, Veth C, Herndl GJ (2006b). Archaeal uptake of enantiomeric amino acids in the meso- and bathypelagic waters of the North Atlantic. *Limnol Oceanogr* **51:** 60-69.

Tourna M, Stieglmeier M, Spang A, Konneke M, Schintlmeister A, Urich T, Engel M, Schloter M, Wagner M, Richter A, Schleper C (2011). Nitrososphaera viennensis, an ammonia oxidizing archaeon from soil. *Proc Nat Acad Sci USA* **108:** 8420-8425.

Treusch AH, Leininger S, Kletzin A, Schuster SC, Klenk HP, Schleper C (2005). Novel genes for nitrite reductase and Amo-related proteins indicate a role of uncultivated mesophilic crenarchaeota in nitrogen cycling. *Environ Microbiol* **7:** 1985-1995.

Valentine DL (2007). Adaptations to energy stress dictate the ecology and evolution of the Archaea. *Nat Rev Microbiol* **5:** 316-323.

Venter JC, Remington K, Heidelberg JF, Halpern AL, Rusch D, Eisen JA, Wu DY, Paulsen I, Nelson KE, Nelson W, Fouts DE, Levy S, Knap AH, Lomas MW, Nealson K, White O, Peterson J, Hoffman J, Parsons R, Baden-Tillson H, Pfannkoch C, Rogers YH, Smith HO (2004). Environmental genome shotgun sequencing of the Sargasso Sea. *Science* **304:** 66-74.

Ward BB (1985). Light and Substrate Concentration Relationships with Marine Ammonium Assimilation and Oxidation Rates. *Mar Chem* **16:** 301-316.

Ward BB (1987). Nitrogen Transformations in the Southern-California Bight. *Deep-Sea Res* **34:** 785-805.

Ward BB (2011a). Measurement and Distribution of Nitrification Rates in the Oceans. In: Klotz MG (ed). Methods in Enzymology: Research on Nitrification and Related Processes, Part A. Elsevier: Burlington, MA. pp 307-323.

Ward BB (2011b). Nitrification in the Ocean. In: Ward BB, Arp DJ, Klotz MG (eds). Nitrification. ASM Press: Washington, D.C. pp 325-345.

Wells LE, Deming JW (2003). Abundance of Bacteria, the Cytophaga-Flavobacterium cluster and Archaea in cold oligotrophic waters and nepheloid layers of the Northwest Passage, Canadian Archipelago. *Aquat Microb Ecol* **31:** 19-31.

Wuchter C, Schouten S, Boschker HTS, Damste JSS (2003). Bicarbonate uptake by marine Crenarchaeota. *FEMS Microbiol Lett* **219:** 203-207.

Wuchter C, Abbas B, Coolen MJL, Herfort L, van Bleijswijk J, Timmers P, Strous M, Teira E, Herndl GJ, Middelburg JJ, Schouten S, Damste JSS (2006). Archaeal nitrification in the ocean. *Proc Natl Acad Sci USA* **103:** 12317-12322.

Yakimov MM, La Cono V, Denaro R (2009). A first insight into the occurrence and expression of functional amoA and accA genes of autotrophic and ammonia-oxidizing bathypelagic Crenarchaeota of Tyrrhenian Sea. *Deep-Sea Res Pt II* **56:** 748-754.

Yakimov MM, La Cono V, Smedile F, DeLuca TH, Juarez S, Ciordia S, Fernandez M, Albar JP, Ferrer M, Golyshin PN, Giuliano L (2011). Contribution of crenarchaeal autotrophic ammonia oxidizers to the dark primary production in Tyrrhenian deep waters (Central Mediterranean Sea). *ISME J* **5:** 945-961.

Yool A, Martin AP, Fernández C, Clark DR (2007). The significance of nitrification for oceanic new production. *Nature* **447:** 999-1002.

Zhalnina KV, Dias R, Leonard MT, Dorr de Quadros P, Camargo FA, Drew JC, Farmerie WG, Daroub SH, Triplett EW (2014). Genome sequence of *Candidatus* Nitrososphaera evergladensis from group I.1b enriched from Everglades soil reveals novel genomic features of the ammonia-oxidizing archaea. *PLoS ONE* **9:** e101648.

Table 1.1 - Annotated H_2O_2-responsive genes in Bacteria and Archaea (including Thaumarchaeota). Data obtained from the Joint Genome Institute's Integrated Microbial Genome (IMG) database (http://img.jgi.doe.gov/).

	Total Genomes Queried	**1.11.1.1** NADH peroxidase	**1.11.1.5** Cytochrome-c peroxidase	**1.11.1.6** Catalase	**1.11.1.9** Glutathione peroxidase	**1.11.1.10** Chloride peroxidase	**1.11.1.15** Peroxiredoxin	**1.11.1.21** Catalase peroxidase	**1.11.1.** Peroxidases (misc.)	**1.11.1 All Peroxidases**	**1.15.1.1** Superoxide dismutase
Bacteria (excl. Cyanobacteria)*	2578										
Number of Genomes with this Gene		79	754	1362	1402	506	2413	875	79	2457	2210
Percent of Genomes with this Gene		3	29	53	54	20	94	34	3	95	86
Average Gene Dosage per Genome		1.06	1.52	1.69	1.38	1.48	2.50	1.09	1.06	4.75	1.82
Archaea genomes*	167										
Number of Genomes with this Gene		0	5	21	3	1	155	37	0	160	95
Percent of Genomes with this Gene		0	3	13	2	1	93	22	0	96	57
Average Gene Dosage per Genome		0.00	1.00	1.19	1.00	1.00	2.09	1.11	0.00	2.34	1.21
Euryarchaeota genomes*	109										
Number of Genomes with this Gene		0	5	21	3	1	97	37	0	102	54
Percent of Genomes with this Gene		0	5	19	3	1	89	34	0	94	50
Average Gene Dosage per Genome		0.00	1.00	1.19	1.00	1.00	2.10	1.11	0.00	2.49	1.31
Crenarchaeota genomes*	50										
Number of Genomes with this Gene		0	0	0	0	0	50	0	0	50	35
Percent of Genomes with this Gene		0	0	0	0	0	100	0	0	100	70
Average Gene Dosage per Genome		0.00	0.00	0.00	0.00	0.00	2.22	0.00	0.00	2.22	1.00
Thaumarchaeota genomes*	6										
Number of Genomes with this Gene		0	0	0	0	0	6	0	0	6	6
Percent of Genomes with this Gene		0	0	0	0	0	100	0	0	100	100
Average Gene Dosage per Genome		0.00	0.00	0.00	0.00	0.00	1.17	0.00	0.00	1.17	1.50

**only finished genomes queried*

Figure 1.1: The Marine Nitrogen Cycle. Figure from Francis *et al.* (2007) that highlights both aerobic (oxic) and anaerobic (anoxic) microbial processes involved in the nitrogen cycle, including ammonia oxidation which is catalyzed by the enzyme encoded by the ammonia monooxygenase (*amo*) gene.

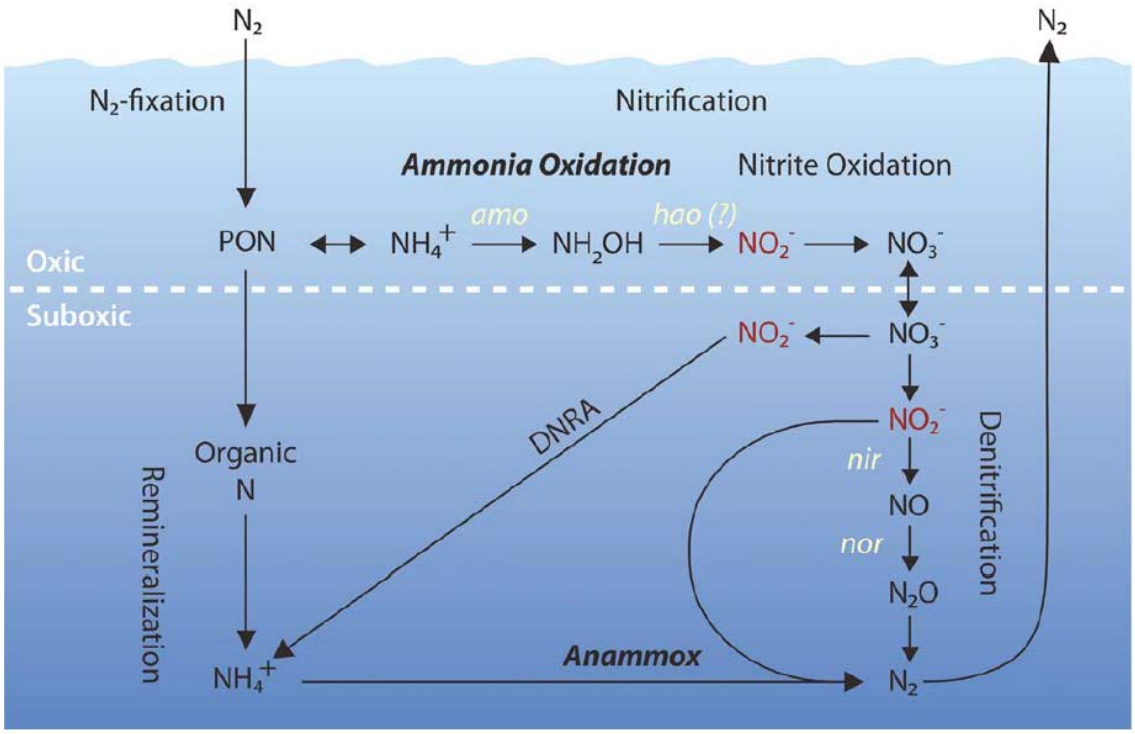
N2
N2
N2-fixation
Nitrification
Ammonia Oxidation
Nitrite Oxidation
amo
hao (?)
PON
NH4+
NH2OH
NO2-
NO3-
Oxic
Suboxic
NO2-
NO3-
DNRA
NO2-
nir
NO
nor
N2O
Organic
N
Remineralization
Denitrification
Anammox
NH4+
N2

CHAPTER 2

AN ANALYSIS OF THAUMARCHAEOTA POPULATIONS FROM THE NORTHERN GULF OF MEXICO[1]

[1] Tolar, B.B., G.M. King, and J.T. Hollibaugh. 2013. *Frontiers in Microbiology*. 4:72. Reprinted here with permission of publisher.

ABSTRACT

We sampled Thaumarchaeota populations in the northern Gulf of Mexico, including shelf waters under the Mississippi River outflow plume that are subject to recurrent hypoxia. Data from this study allowed us to: 1) test the hypothesis that Thaumarchaeota would be abundant in this region; 2) assess phylogenetic composition of these populations for comparison with other regions; 3) compare the efficacy of quantitative PCR (qPCR) based on primers for 16S rRNA genes (*rrs*) with primers for genes in the ammonia oxidation (*amoA*) and carbon fixation (*accA*, *hcd*) pathways; 4) compare distributions obtained by qPCR with the relative abundance of Thaumarchaeota *rrs* in pyrosequenced libraries; 5) compare Thaumarchaeota distributions with environmental variables to help us elucidate the factors responsible for the distributions; 6) compare the distribution of Thaumarchaeota with Nitrite-Oxidizing Bacteria (NOB) to gain insight into the coupling between ammonia and nitrite oxidation.

We found up to 10^8 copies L^{-1} of Thaumarchaeota *rrs* in our samples (up to 40% of prokaryotes) by qPCR, with maximum abundance in slope waters at 200-800 m. Thaumarchaeota *rrs* were also abundant in pyrosequenced libraries and their relative abundance correlated well with values determined by qPCR (r^2=0.82). Thaumarchaeota populations were strongly stratified by depth. Canonical correspondence analysis using a suite of environmental variables explained 92% of the variance in qPCR-estimated gene abundances. Thaumarchaeota *rrs* abundance was correlated with salinity and depth, while *accA* abundance correlated with fluorescence and pH. Correlations of Archaeal *amoA* abundance with environmental variables were primer-dependent, suggesting differential responses of sub-populations to environmental variables. Bacterial *amoA* was at the limit

of qPCR detection in most samples. NOB and Euryarchaeota *rrs* were found in the pyrosequenced libraries; NOB distribution was correlated with that of Thaumarchaeota (r^2=0.49).

INTRODUCTION

The Mississippi River outflow forms a surface plume up to 10 m thick upon entering the northern Gulf of Mexico. Stratification and nutrient (especially nitrogen) enrichment of river water (Turner *et al.*, 2006) lead to elevated primary production in the plume and thus to increased organic matter deposition 10 to 100 km away from river discharge sites (Green *et al.*, 2008; Rabalais *et al.*, 2002). Decomposition of this organic matter is thought to contribute to the formation of a recurrent hypoxic zone in the northern Gulf of Mexico that profoundly affects the ecology, fisheries biology, and geochemistry of the region (Cai *et al.*, 2011; Dagg *et al.*, 2007; Rabalais *et al.*, 2002). Intermittent hypoxia ($[O_2] \leq 2$ ml/L or ~90 μM; Diaz and Rosenberg, 2008) begins to develop in February and typically is most pronounced from mid-May to mid-September (Rabalais *et al.*, 2010).

Processes such as coupled nitrification/denitrification that remove excess fixed nitrogen affect primary production and thus may be important determinants of the extent and duration of hypoxia. Ammonia oxidation is the first step in the biogeochemical pathway leading to denitrification. Members of the β- and γ-subdivisions of the Proteobacteria (Ammonia Oxidizing-Bacteria, AOB) and Marine Group 1 Archaea (Ammonia-Oxidizing Archaea, AOA) can grow chemoautotrophically by oxidizing ammonia to nitrite (Ward, 2011). The nitrite produced can be oxidized further to nitrate

by Nitrite-Oxidizing Bacteria (NOB) and then denitrified (Francis *et al.*, 2007; Jetten, 2001; Ward *et al.*, 2009).

Ammonia monooxygenase genes (*amoA*) from AOA have been observed in marine environments at 10-1,000 times greater abundance than the *amoA* homolog from AOB, suggesting that the AOA play a key role in the marine nitrogen cycle (Francis *et al.*, 2005; Francis *et al.*, 2007; Mincer *et al.*, 2007; Prosser and Nicol, 2008; Santoro *et al.*, 2010; Ward, 2011). Currently, the functional guild of marine AOA includes members of the Marine Group 1 Archaea (DeLong, 1992; Fuhrman *et al.*, 1992) and organisms related to a deeply branching clade (pSL12) of hot spring crenarchaeotes (Barns *et al.*, 1996) that are predicted to possess the *amoA* gene (Mincer *et al.*, 2007). Genomic evidence suggests that Marine Group 1 Archaea and related organisms from benthic, terrestrial, and hot-spring habitats, as well as a sponge symbiont, should be assigned to a new phylum, the Thaumarchaeota, within the kingdom Archaea (Brochier-Armanet *et al.*, 2008; Kelly *et al.*, 2011; Spang *et al.*, 2010). We use this term hereinafter in place of "Marine Group 1 Archaea."

Pelagic marine Thaumarchaeota are typically most abundant below ~100 m depth in the water column (Church *et al.*, 2010; DeLong, 1992; Fuhrman *et al.*, 1992; Karner *et al.*, 2001; Massana *et al.*, 1997; Mincer *et al.*, 2007; Santoro *et al.*, 2010), in surface waters at higher latitudes and polar oceans (Alonso-Sáez *et al.*, 2008; Church *et al.*, 2003; Kalanetra *et al.*, 2009; Massana *et al.*, 1998; Murray *et al.*, 1998; Murray *et al.*, 1999a), and in hypoxic regions and oxygen minimum zones, (OMZs; $[O_2] \leq 0.5$ mL/L or ≤ 22 μM; Levin, 2003) such as the Black Sea, Baltic Sea, Gulf of California, Arabian Sea, and the eastern tropical Pacific Ocean (Beman *et al.*, 2008; Coolen *et al.*, 2007; Labrenz *et*

al., 2010; Lam *et al.*, 2007; Lam *et al.*, 2009; Molina *et al.*, 2010). Previous studies are contradictory but have pointed to environmental factors such as salinity, light, temperature, ammonium, oxygen, and sulfide as major determinants of this distribution (e.g., Bernhard *et al.*, 2010; Caffrey *et al.*, 2007; Gubry-Rangin *et al.*, 2010; Murray *et al.*, 1999a; Santoro *et al.*, 2008; reviewed in Erguder *et al.*, 2009; Nicol *et al.*, 2011; Prosser and Nicol, 2008; Ward, 2011). Bacterial or phytoplankton biomass has also been thought to influence Thaumarchaeota distributions (Church *et al.*, 2003; Murray *et al.*, 1999a; Murray *et al.*, 1999b), perhaps through competition for resources.

One of the goals of the present study was to quantify the distribution of AOA in the northern Gulf of Mexico in the area influenced by the Mississippi River plume and recurrent hypoxia. We hypothesized that ammonia oxidizers would be abundant there because of the high riverine nitrogen loading to the region and the importance of respiration (Cai *et al.*, 2011), and thus presumably nitrogen regeneration, in the region experiencing hypoxia. We also hypothesized that AOA would dominate ammonia oxidizer populations at pelagic stations, although AOB were found to be more abundant than AOA in sediments from Weeks Bay, Alabama (Caffrey *et al.*, 2007). To test these hypotheses, we determined AOA and AOB distributions by quantitative PCR measurements of the abundance of *rrs* and *amoA* genes. We also pyrosequenced *rrs* genes from our samples as an independent check on distributions based on qPCR data. A second goal was to analyze variation in sequences of *rrs* and compare this to genes from two metabolic pathways that are important to AOA, ammonia oxidation and carbon fixation, to provide a more highly resolved description of the composition of Thaumarchaeota populations than can be obtained from analyses of single genes. AOA

can grow autotrophically (Könneke *et al.*, 2005) using the 3-hydroxypropionate/4-hydroxybutyrate pathway (Berg *et al.*, 2007). The potential for AOA autotrophy can be detected in the environment using primers targeting the genes in this pathway, notably acetyl-CoA/propionyl-CoA carboxylase (*accA*; Yakimov *et al.*, 2009) and 4-hydroxybutyryl-CoA dehydratase (*hcd*; Offre *et al.*, 2011). We tested both of these primer sets with our samples. We compared the phylogenetic diversity present in their amplicons with diversity represented in amplicons from more widely-used primer sets for *amoA* and *rrs*. We then used *rrs* sequences from the pyrosequencing effort to extend phylogenetic inferences based on analyses from samples taken at one station more broadly across the study area. A third goal was to investigate the relationship between Thaumarchaeota distributions and environmental variables to provide insight into the factors controlling their distribution. Pyrosequencing data were also used to compare the distribution of NOB with AOA to gain insights into the coupling between these two steps of nitrification.

MATERIALS AND METHODS

Sample collection and DNA extraction

Samples were collected during the *R/V Cape Hatteras* GulfCarbon 5 cruise in the northern Gulf of Mexico (30º 07’ N, 088º 02’ W to 27º 39’ N, 093º 39’W; Figure 2.1) from March 10 to 21, 2010. Samples were collected using Niskin bottles and a General Oceanics rosette sampling system equipped with an SBE25 CTD and sensors for [O_2], beam attenuation (turbidity), and relative fluorescence (calibrated to chlorophyll *a* equivalents). The [O_2] sensor was cross-calibrated against Winkler titrations of [O_2] in

samples collected at fixed depths. pH data were collected using a glass electrode by W-J. Huang of Dr. W.-J. Cai's group. Euphotic depth (defined as 1% PAR, 400-700 nm) was calculated for each station from Aqua MODIS satellite data using an average of the Lee and Morel models (http://oceancolor.gsfc.nasa.gov) by H. Reader and C. Fichot. Nutrient data were collected at some of the station/depths we sampled by Dr. S. Lohrenz's group. Since nutrient sample collections were biased in favor of near-surface samples on the continental shelf, these data were used only in BEST analysis (see Appendix A). Approximately 1 L of water from each Niskin bottle was pressure filtered (at ~60 kPa) through 0.22 µm Durapore filters (Millipore); filters were frozen in 2 mL of lysis buffer (0.75 M sucrose, 40 mM EDTA, 50 mM Tris; pH 8.3). DNA was extracted by enzymatic hydrolysis with lysozyme (50 mg mL^{-1}), proteinase K (20 mg mL^{-1}), and sodium dodecyl sulfate (100 µL of a 10% solution), and then purified by phenol-chloroform extraction as described previously (Bano and Hollibaugh, 2000).

Quantitative PCR

Quantitative PCR (qPCR) was performed using an iCycler iQ™ Real-Time qPCR detection system (Bio-Rad) and the primers listed in Table A.1. qPCR reactions were run in triplicate with standards made from environmental amplicons as described in Appendix A. TaqMan® (Applied Biosystems) chemistry was used to detect amplification of Bacteria and Thaumarchaeota 16S rRNA genes (*rrs*) following Kalanetra *et al.* (2009); all other amplifications were detected using SYBR® Green Supermix (Bio-Rad). We compared two primer sets for detecting Archaeal *amoA*: Arch-amoA-for and Arch-amoA-rev ("Wuchter primers"; Wuchter *et al.*, 2006) and ArchamoAF and ArchamoAR

("Francis primers"; Francis *et al.*, 2005). Reactions using the Wuchter primers were set up as described in Kalanetra *et al.* (2009), while PCR conditions for the Francis primers followed Santoro *et al.* (2010), except that SYBR® Green Supermix (Bio-Rad) was used with no additional $MgCl_2$. Amplification of pSL12 *rrs* followed Mincer *et al.* (2007), with the number of amplification cycles reduced to 40 to prevent quenching of the fluorescence signal. Archaeal *accA* genes were amplified following Yakimov *et al.* (2009) with shorter cycle lengths (Hu *et al.*, 2011). Specificity of SYBR Green® reactions was confirmed by melting curve analysis; *accA* amplicons were also checked by sequencing clones created with qPCR primers Crena_529F and Crena_981R (Yakimov *et al.*, 2009). We also tested published primers for *hcd* genes (Offre *et al.*, 2011), but found that non-specific amplification rendered them unsuitable for quantitative PCR with our samples (see Appendix A). Inhibition of qPCR reactions was tested using dilutions of DNA 10-1000X with the bacterial *rrs* qPCR assay; samples that showed higher copy number than expected from typical dilution were determined to have PCR inhibitors present and run at the dilution which gave the highest copy number for all other gene assays. Calculations of gene abundance and ratios are discussed in the Methods of Appendix A, and qPCR efficiencies for reactions are reported in Table A.1.

Phylogenetic analysis

We sequenced cloned *rrs*, *amoA*, and *accA* amplicons to obtain phylogenetic descriptions of the Thaumarchaeota populations in the study area and to verify specificity of qPCR reactions. Libraries were generated from samples collected at Station D5, located on the southern edge of the area influenced by the Mississippi River plume and

over the continental slope (Figure 2.1) using methods described previously (Kalanetra *et al.*, 2009) and summarized below. This station was chosen for its depth and as representative of slope stations influenced by hypoxia. We compared samples from different depths at this station as others (e.g., Beman *et al.*, 2008; Church *et al.*, 2010; Kalanetra *et al.*, 2009; Lam *et al.*, 2007; Santoro *et al.*, 2010) have shown segregation of Thaumarchaeota populations by depth. *rrs* and *amoA* were amplified from DNA collected at 100 and 200 m, while *accA* amplicons were generated from samples collected at 2, 50, 100, 200, and 450 m to test the *accA* primer set across a wider depth range. PCR amplifications of Archaeal *rrs*, *amoA*, and *accA* used the primers listed in Table A.1. Three separate amplifications were pooled to minimize potential PCR bias and electrophoresed on a 1% agarose gel. The band of the expected DNA product size was excised, extracted and purified using the QIAquick® Gel Extraction Kit (QIAGEN), and incorporated into a TOPO 4 vector (Invitrogen) prior to cloning using chemically competent TOP10 *E. coli* cells with the TOPO TA cloning kit (Invitrogen) following the manufacturer's instructions. Clones from each library were selected randomly and sequenced (Genewiz, Inc.) using the plasmid primer M13F(-21). Euryarchaeota *rrs* sequences were identified by BLAST (Zhang *et al.*, 2000) and not analyzed further.

Sequences were inspected manually and checked for vector contamination using Geneious (v. 5.4; Drummond *et al.*, 2010). Thaumarchaeota *rrs* sequences were checked for chimeras using Bellerophon (Huber *et al.*, 2004); three chimeric sequences were identified and discarded. Nucleotide and inferred amino acid sequences for *amoA* and *accA* were aligned in Geneious, while *rrs* nucleotide sequences were first aligned using the Silva aligner (v.1.2.5; Pruesse *et al.*, 2007) and then imported into ARB (v. 5.2;

Ludwig *et al.*, 2004), manually trimmed, and inspected for alignment errors. Sequences obtained from these libraries have been deposited in GenBank (NCBI) under accession numbers KC330756 to KC330822 (*rrs* – Thaumarchaeota, n = 67), KC330823 to KC330871 (*rrs* – Euryarchaeota, n = 49), KC349137 to KC349317 (*amoA*, n = 181), and KC349318 to KC349551 (*accA*, n = 234).

Operational taxonomic units (OTUs) were determined from sequence alignments using mothur (v. 1.21.1; Schloss *et al.*, 2009) with cutoffs of 0.02 (≥98% similarity) for Thaumarchaeota *rrs* and 0.03 (≥97% similarity) for Archaeal *amoA* and *accA*. Diversity indices and richness estimates (Shannon, Simpson, Chao and ACE) were calculated in mothur. Neighbor-joining trees were constructed using ARB (Ludwig *et al.*, 2004) with the Jukes-Cantor correction and 1,000 bootstrap re-samplings for nucleotide trees; protein trees were constructed without the Kimura correction and re-sampled 100 times. Trees were edited using FigTree (v. 1.3.1; http://tree.bio.ed.ac.uk/).

Pyrosequencing analyses

We also analyzed the distribution of ribotypes in 41 of our 52 samples by massively parallel sequencing (pyrosequencing) using a Roche 454/FLX instrument running Titanium chemistry. *rrs* in DNA extracted from our samples were amplified by PCR using universal *rrs* primers 515F and 806R (Table A.1), modified for bar-coded pyrosequencing. PCR protocols and primer sequences, including barcodes, adaptors, and linkers, followed Bates *et al.* (2011). Purified DNA from 3 reactions for each sample was pooled to produce a mixture in which amplicons from each sample were represented equally. The final mixture was sequenced using standard protocols by Engencore

(University of South Carolina, Columbia, SC). Sequence data have been deposited with MG-RAST (metagenomics.anl.gov) at accession numbers 4509220.3–4509263.3. Metadata are available via the project page: "Analysis of composition and structure of coastal to mesopelagic bacterioplankton communities in the nGoM."

A total of 435,290 sequences were filtered and trimmed (minimum length 200 bp, minimum quality score 20; 221,410 sequences passed) and then sorted into OTUs using the PANGEA pipeline (Giongo *et al.*, 2010). Phylogenetic affiliations of these sequences were determined by a megablast analysis using a reference set of more than 170,000 *rrs* sequences from described isolates obtained from the RDP II database (Giongo *et al.*, 2010). Amplicon sequences were binned into OTUs at domain, phylum, class, order, family, genus and species levels based on megablast results, and then grouped into phylogenetic clusters and sorted by station and depth (average number of sequences per sample: 5,400; range 764 - 9,176). The PANGEA pipeline assigns all Archaea sequences to one group that also includes divergent Bacteria sequences. In order to more accurately assess the proportion of Thaumarchaeota in our samples, we manually enumerated hits to Thaumarchaeota in the megablast output for each sample. We also counted hits to known AOB, NOB, and Euryarchaeota.

Thaumarchaeota *rrs* sequences obtained from pyrosequencing were included for phylogenetic analysis using mothur (v. 1.21.1; Schloss *et al.*, 2009). Unique sequences were grouped together and aligned against the Silva Archaea reference database (http://www.mothur.org/wiki/Silva_reference_files). The resulting alignment, including *rrs* sequences from Station D5 clone libraries and outgroups, was trimmed to a set length and 8 chimeric sequences were removed with Uchime (Edgar *et al.*, 2011); additional

potential chimeras and erroneous sequences were checked manually using BLAST and removed if necessary. The remaining 23,677 Thaumarchaeota sequences were clustered and representatives from each OTU obtained. A maximum likelihood tree was constructing using representative sequences grouped at 98% similarity (2,772 sequences total) with the RAxML program (Stamatakis *et al.*, 2005) within ARB (Ludwig *et al.*, 2004); 100 trees were generated using rapid bootstrap analysis, and the consensus tree was constructed from these iterations. Rarefaction analysis was completed using mothur as described for clone library samples above. The Bacteria populations of these samples are analyzed in King *et al.* (2013).

Statistical analyses

Model II ordinary least squares pairwise regressions were calculated following Legendre and Legendre (1998) using software available at http://adn.biol.umontreal.ca/~numericalecology/indexEn.html. Coefficients of determination and confidence limits of regression equations were calculated from 999 bootstrap permutations. PRIMER (v.6; Clarke and Gorley, 2006) was used to compare environmental and biological data from each station. We normalized environmental data in PRIMER to reduce the influence of variable unit scales before principal components analysis (PCA). The software package CANOCO (v. 4.5; ter Braak and Šmilauer, 2002) was used for canonical correspondence analysis (CCA; ter Braak, 1985) using PCA values and log-transformed qPCR gene abundances. Significance of CCA was determined using 499 Monte-Carlo permutations (reduced model) as recommended in the program documentation. The RAxML tree constructed from 454-generated

Thaumarchaeota *rrs* sequences was used in Fast UniFrac (Hamady *et al.*, 2009) to investigate phylogenetic patterns by sample location and depth. Weighted abundances of sequences within samples were used in both Principal Coordinates Analysis (PCoA) and sample clustering, as well as to calculate pair-wise Unifrac distances. Counts were normalized to reduce the influence of larger sample sizes (greater number of sequences) at certain stations. The significance of sample clusters was tested using 100 jackknife permutations and re-sampling of the minimum (2), first quartile (100), or median (520) number of sequences across all samples; any sample containing less than the number of re-sampled sequences was eliminated from the analysis.

RESULTS

Gene abundance and distribution

The abundance of bacterial *rrs* in these samples ranged from 10^5 to 10^{10} copies L^{-1} (Table 2.1, Table A.2). Thaumarchaeota *rrs* genes were present in the same samples at up to 10^8 copies L^{-1} (Table A.2) with population maxima occurring typically between 100-200m depth and at lower [O_2] and temperature (Figure 2.2). The abundance of *rrs* genes attributable to the pSL12-like clade was much lower, near the limit of detection (see Table A.1) in most samples with a maximum abundance of 10^5 copies L^{-1} (Table A.2). Similar trends with depth for pSL12 *rrs* were observed as Thaumarchaeota *rrs*, though pSL12 *rrs* abundance was generally 100- to 10,000-fold lower (Figure 2.2), except in one sample (Station H1-7 m), where pSL12 *rrs* was 10% of Thaumarchaeota *rrs*. No Thaumarchaeota *rrs* were detected at the freshwater Mississippi River station (MR1-2 m) where pSL12 *rrs* was present at 10^5 copies L^{-1} (Table A.2).

Thaumarchaeota accounted for a high proportion (up to 40% by qPCR, up to 54% of pyrosequenced *rrs*) of the total prokaryotic community in our samples. This percentage varied with depth (Figure 2.3), with deeper (>100 m) samples containing an average of 21% Thaumarchaeota (range 0.5-40%) while samples from near-surface water (≤100 m) contained only 1.8% Thaumarchaeota (range 0-9%). Differences were also observed with distance from shore, with shallower (<100 m) samples from inshore stations having fewer Thaumarchaeota than those from offshore stations (1.1% versus 2.8% of prokaryotes, respectively). Pyrosequencing also showed that Thaumarchaeota *rrs* genes were most abundant in samples from depths of 100-200 m, though they were present at low abundances in all samples with the exception of MR1-2 m (Table A.3), in agreement with qPCR analyses. Thaumarchaeota accounted for 0.1-54% of the prokaryotes in pyrosequencing libraries and their distributions based on qPCR estimates of gene abundance compared favorably with the contribution of Thaumarchaeota ribotypes to pyrosequenced *rrs* libraries from these samples (Figure 2.4; model II regression, n=41, $r^2 = 0.82$, 95% CL of slope = 0.54-0.73).

Archaeal *amoA* was present at up to 10^8 copies L^{-1} (Table 2.1, Figure 2.2, Table A.2). Bacterial *amoA* was at the limit of detection (Table A.1) in most samples, with a maximum of 10^6 copies L^{-1}. The ratio of AOA:AOB *amoA* was found on average to be 2100:1 (Wuchter primers) to 3300:1 (Francis primers). The ratio of bacterial *amoA*:bacterial *rrs* averaged 0.001 across all samples, with a maximum of 0.05 at Station D3-68 m (Figure A.5a). Abundances of *accA* genes ranged from the limit of detection (10^4 copies L^{-1}) to 10^7 copies L^{-1} (Table 2.1, Figure 2.2, Table A.2). Archaeal *amoA* (quantified using Wuchter primers) showed similar distribution by depth as

Thaumarchaeota *rrs* (Figure 2.2). However, *accA* abundances showed opposite trends with depth, leading to higher ratios of *amoA*:*accA* or *rrs*:*accA* in near-surface (≤100 m) water (Figure 2.2).

We used principal components analysis (PCA, Figure A.3) to identify samples from similar environments and group them into a few categories to simplify comparisons. The first two PCA axes explained 63.2% of the variation between samples (Figure A.3; Table A.5), which supported placing stations into three groups: near-surface inshore, near-surface offshore, and deep offshore sets. CCA was included (Figure 2.8) to investigate relationships between gene abundances and environmental conditions (similar to BEST analysis, see Appendix A). The primary CCA axis (CCA1) explained 47.9% of the gene abundance-environment relationship; adding the second axis (CCA2) increased the variance explained by 44% (91.7% total; Figure 2.8, Table A.6). A global permutation test gave a statistical significance of $p < 0.05$ for station groupings based on both canonical axes considered together ($F = 2.26$, $p = 0.014$), while CCA1 considered alone did not explain the gene abundance-environment relationship ($F = 8.43$, $p = 0.086$). Thaumarchaeota *rrs* abundance was negatively correlated with most environmental variables, except for salinity and depth (Figure 2.8). Bacterial *rrs* abundance correlated positively with euphotic zone depth and had a strong negative correlation with pH, with little influence from any variable primarily contributing to CCA2 (beam attenuation, oxygen; Figure 2.8). The distribution of archaeal *amoA* genes as assessed with the Wuchter primers, in contrast, was not strongly influenced by variables contributing to CCA1 (fluorescence, pH, latitude, longitude; Figure 2.8) but showed a weak positive correlation with temperature and beam attenuation (turbidity). Archaeal *amoA* gene

abundance assessed by the Francis primers showed the opposite trend, with strongest positive correlations to latitude (which covaries with distance offshore and depth in this region) and oxygen concentrations (Figure 2.8). Bacterial *amoA* gene abundance correlated with beam attenuation (turbidity) and temperature (positive correlation), as well as depth (negative correlation). *accA* gene abundance had strong positive correlations with relative fluorescence (chlorophyll *a* equivalents) and pH (Figure 2.8).

Thaumarchaeota community composition at Station D5

Phylogenetic analysis of 67 Sanger-sequenced Thaumarchaeota *rrs* sequences obtained from 100 m and 200 m depth at Station D5 revealed 10 different OTUs (Figure 2.5, Table A.4; 98% similarity cutoff). All but one of the sequences retrieved from the 100 m sample clustered into a single OTU, (the "Near-Surface Group", Figure 2.5), that also contained one sequence retrieved from the 200 m sample and the reference sequence from Nitrosopumilus sp. NM25 (Matsutani *et al.*, 2011). We did not retrieve any sequences related to the marine pSL12-like clade. Sequences retrieved from the 200 m sample displayed greater richness and evenness (Table A.4; 9 OTUs) and included some OTUs that appear unique to the northern Gulf of Mexico.

We retrieved 184 *amoA* sequences from Station D5. Phylogenetic analysis of the translated and aligned amino acid sequences revealed two OTUs (similarity cutoff of 97%) of AmoA (Figure 2.6a): one containing primarily near-surface (100 m) sequences ("Group A" following Beman *et al.*, 2008) and the other dominated by sequences from 200 m ("Group B"). *amoA* nucleotide sequences also grouped primarily by depth, but with greater richness and diversity (Table A.4) at a given depth than we observed for

Thaumarchaeota *rrs* genes. Clusters of sequences that appear to be unique to the Gulf of Mexico were observed in both 100 m and 200 m samples (Figure A.1a).

The top BLASTx hits for all but 30 of 257 sequences obtained from *accA* amplicons were to carboxylase or carboxyltransferase genes from Archaea. The remaining 30 amplicons were most similar to non-Thaumarchaeota reference sequences with low (≤65%) sequence identities. Because they did not return hits to Thaumarchaeota reference sequences, we did not consider them further. Phylogenetic analysis of the inferred amino acid sequences for AccA (Figure 2.6b) revealed three major OTUs: OTU 1 contained a majority of near-surface sequences (2, 50, and 100 m), while OTUs 2 and 3 contained mostly sequences from deep water (200 and 450 m). Analysis of *accA* nucleotide sequences revealed similar clusters with depth as inferred amino acid sequences for AccA and Thaumarchaeota *rrs* gene sequences (Figure A.1b) with a total of 51 OTUs observed at a 97% similarity cutoff (Table A.4). Some of these seem unique to the Gulf of Mexico (Figure A.1b), but this may be an artifact of the limited representation of *accA* sequences in reference databases.

Pyrosequencing: Phylogenetic Patterns and Sample Groupings

Microbial community composition varied dramatically with depth as shown by comparisons of libraries from surface (≤ 25 m depth) versus subsurface (≥ 100 m depth) samples (Figure A.2, Table A.3; these data are discussed fully in King *et al.* (2013). Proteobacteria, especially α- and γ-Proteobacteria, dominated the microbial community of near-surface waters at most stations. Consistent with distributions of *rrs* and *amoA* indicated by qPCR analyses, Thaumarchaeota were greatly enriched in deeper waters.

Only 14 (out of a total of 221,410) *rrs* sequences binned to AOB, confirming the much lower abundance of AOB relative to AOA found by qPCR quantification of *amoA*. Half of the AOB sequences were retrieved from one sample: MR1-2m, taken upstream of the mouth of the Mississippi River with a salinity of 0. Only 4 Thaumarchaeota sequences were retrieved from this sample (Table A.3), two of which were most similar to the terrestrial thaumarchaeote, "*Candidatus* Nitrososphaera gargensis" strain EN76, at 15% similarity.

Sequences most closely related to NOB were retrieved from most samples (mean = 0.4%, range 0-1.8% of prokaryotes as calculated in Supplementary Methods (Appendix A, but assuming 2 *rrs* per NOB genome from Mincer *et al.*, 2007). These sequences were primarily identified as *Nitrospina* sp. 3005 (AM110965), though *Nitrospira* ribotypes were also detected. The abundance of NOB *rrs* was greatest at depth (~200 m, Table A.3, Figure 2.7a) and was significantly correlated with the abundance of Thaumarchaeota in the same samples (Figure 2.7a; model II regression, n = 41, r^2 = 0.49, 95% CL of slope = 0.032-0.064). Euryarchaeota only accounted for a few percent of the microbial community (mean 5.8%, range 0.1-17.6 %). Euryarchaeota were most abundant in near surface samples (<100 m; Table A.3) and their abundance was poorly correlated with the abundance of Thaumarchaeota (Figure 2.7b; model II regression, n = 41, r^2 = 0.14, 95% CL of slope = 0.021 to 0.20).

UniFrac distances calculated between samples indicate significant ($p \leq 0.05$) similarities in Thaumarchaeota *rrs* assemblages among offshore, near-surface samples and inshore, near-surface samples from Stations A2, A4, D3, E2, and MR2 (data not shown). The Station D5-100m sample was assigned to the near-surface group ($p \leq 0.05$)

regardless of the method used to obtain *rrs* sequences (pyrosequencing vs. Sanger sequencing from clone libraries). Among deep offshore samples, those from 160-950 m were similar to each other ($p \leq 0.05$); sequences from clone libraries generated from Station D5-200m were also included in this group. The phylogenetic composition of Thaumarchaeota *rrs* in the deepest sample, Station A6-1700m, was only similar to samples from D5-900m and F6-950m ($p \leq 0.05$).

Analysis of phylogenetic patterns across samples using PCoA in Fast UniFrac (Figure 2.9) revealed two major groups of pyrosequenced Thaumarchaeota *rrs* – one of deep (>100 m) samples and another including the near-surface samples (both inshore and offshore), which agrees with PCA groupings (Figure A.3). The primary PCoA axis explained 70% of the variation in phylogenetic composition of the samples, with the secondary axis explaining an additional 11% (total 81 %) of the variation. The sample from Mississippi River Station MR1 was an outlier; however, PCoA analysis with this sample included revealed the same general pattern (Figure A.7). Samples clustered using the minimum re-sampling of 2 sequences (Figure A.4a) only showed significant separation of Station MR1 sample from the rest of the samples (>99.9% jackknife support). For 100 re-sampled sequences (32 of 43 samples; Figure A.4b), a clear separation was observed between surface and deep samples (60% support) and between near-surface inshore samples (excluding Station A4) and near-surface offshore samples (>99.9% support). When the median number of sequences was applied to cluster analysis (520 sequences, 22 of 43 samples; Figure A.4c), the separation of deep and near-surface samples was statistically significant (>99.9% support). Station D3 (inshore, <100 m depth) samples clustered most closely (>99.9% support), followed by inshore Station A4-

43m and offshore Station A6-80m (95% support). Amongst deep samples, a further separation was observed within the deep offshore samples, with the deepest samples (Stations D5-900m and F6-950m) and those from 350-760 m forming distinct clusters 50% and 61% of the time, respectively (Figure A.4c).

DISCUSSION

Community Comparisons

We found a strong correlation between qPCR and pyrosequencing estimates of AOA relative abundance indicating that, despite potential biases associated with individual qPCR primers, qPCR estimates of Thaumarchaeota distributions at this coastal site are robust. Thaumarchaeota were abundant in deeper waters of the northern Gulf of Mexico, increasing in abundance with depth to a broad maximum between ~200 and 800 m (Figures 2.2 and 2.3), coinciding with the oxygen minimum (Figure 2.2). Two shallow water stations (C1, 12 m; MR2, 8 m) contained up to 10^8 copies L^{-1} of Thaumarchaeota *rrs*; both of these stations are near the Mississippi River Plume, which may indicate an influence of riverine nutrients on AOA. It is important to note, however, that these are marine ribotypes and not terrestrial or freshwater ribotypes carried into the Gulf by the Mississippi River, since we did not retrieve similar ribotypes from Mississippi River sample MR1. In contrast, AOB *amoA* genes were below the limit of detection except in a few near-surface samples from inshore stations (Stations C1, D3, D5, G1, and H1) and in river stations MR1 and MR2. Consistent with many other studies of *amoA* in coastal water columns (Beman *et al.*, 2010; Herfort *et al.*, 2007; Wuchter *et al.*, 2006), AOA *amoA* was always >10- to 100-fold more abundant than AOB *amoA*. The relative

abundance of Thaumarchaeota and AOB *rrs* in pyrosequenced libraries (Table A.3) is consistent with the distribution of *amoA* genes determined by qPCR, suggesting that the observed ratio of AOA:AOB *amoA* is not an artifact of primer bias. Although we do not have ammonia oxidation rate measurements for these samples, the greater abundance of AOA than AOB *amoA* suggests that Thaumarchaeota are likely to dominate nitrification in this region (Beman *et al.*, 2008).

We did not quantify the distribution of NOB by qPCR (cf. Santoro *et al.*, 2010), which is limited to *Nitrospina*); however, we were able to determine the distribution of all known NOB relative to Thaumarchaeota from pyrosequenced *rrs* libraries. We found that NOB abundance correlated well with that of Thaumarchaeota ($r^2 = 0.49$), as reported by others (Mincer *et al.*, 2007; Santoro *et al.*, 2010). The correlation between the distributions of these two groups suggests relatively tight coupling between them, presumably leading to efficient conversion of ammonia to nitrate in the northern Gulf of Mexico. However, NOB *rrs* abundance was only ~5% of that of Thaumarchaeota (slope of model II regression; Figure 2.7a), in contrast to estimates of 20-100% reported by Mincer *et al.* (2007) or ~25% reported by Santoro *et al.* (2010). This ratio would change if the *rrs* gene dosages we used in our calculations changed; however, the discrepancy suggests that alternative pathways, e.g. anammox, might be more significant for nitrite removal in the northern Gulf of Mexico than in the temperate Pacific upwelling zone sampled by Mincer *et al.* (2007) and Santoro *et al.* (2010).

Environmental Factors

The connection between pH and AOA abundance has been examined closely in soils, where archaeal *amoA* typically dominates in more acidic samples (reviewed in Erguder *et al.*, 2009; Prosser and Nicol, 2008). The Mississippi River plume is a site of respiration-induced acidification (Cai *et al.*, 2011), and we observed a negative correlation between the abundance of Thaumarchaeota *rrs* and pH in our samples. In contrast, the abundance of archaeal *accA* genes and of AOA *amoA* genes detected by the Francis primers was positively correlated with pH values (Figure 2.8). AOB *amoA* abundance was positively correlated with temperature and negatively correlated with depth, while AOA *amoA* abundance showed the opposite trends (Figure 2.8). These correlations correspond to AOB abundance being greatest in surface samples, versus AOA abundance being greater in samples from deeper, colder water, as observed in other studies (e.g., Santoro *et al.*, 2010). We also observed a strong negative correlation between AOB *amoA* gene abundances and salinity, but we did not find a statistically significant ($p>0.05$) correlation between AOA *amoA* genes and salinity. This contrasts with AOA distributions reported for sediments from an aquifer at Huntington Beach, CA (Santoro *et al.*, 2008) or from the San Francisco Bay Estuary (Mosier and Francis, 2008), where AOB were more abundant in high salinity sediments, while AOA were more prominent in low salinity environments.

Fluorescence (chlorophyll *a*) contributed significantly to PC1 (Figure A.3) and *accA*, pSL12 *rrs*, and archaeal *amoA* gene abundance (Francis primers) were all positively correlated with fluorescence in CCA analysis (Figure 2.8). Most other studies have reported inverse correlations between Thaumarchaeota abundance and chlorophyll *a*

(Kirchman *et al.*, 2007; Murray *et al.*, 1999a; Murray *et al.*, 1999b; Wells and Deming, 2003). A study of AOA and AOB dynamics in estuarine sediments, though, showed that potential nitrification rates and the abundance of archaeal *amoA* genes (Wuchter primers) correlated positively with sediment chlorophyll *a* concentrations (Caffrey *et al.*, 2007). Archaeal abundance in the Arctic Ocean near the Mackenzie River mouth correlated positively with chlorophyll *a* (Wells *et al.*, 2006), although a previous study at similar sites showed the opposite trend (Wells and Deming, 2003). We observed a strong positive correlation between bacterial *amoA* abundance and turbidity in the Gulf of Mexico while archaeal *amoA* genes were inversely correlated with turbidity (Figure 2.8). We detected greatest abundances of AOB *amoA* genes in shallow, near-shore waters (especially at Station C1 and all three Mississippi River stations), which may indicate a salinity effect or an association of AOB with particles originating from estuaries, coastal embayments, or the river. Since we did not sequence the AOB amplicons we obtained, we cannot use the phylogenetic position of the AOB to differentiate between these hypotheses (e.g., O'Mullan and Ward, 2005; Phillips *et al.*, 1999). Caffrey *et al*. (2007) reported that AOB were more abundant than AOA in sediments from Weeks Bay, Alabama, a subembayment of Mobile Bay. Our near-shore waters also had higher ammonia concentrations (up to 3 μM; data not shown) than at other stations, which is consistent with the conceptual model that AOB are more competitive in environments with elevated ammonia concentrations (Martens-Habbena *et al.*, 2009).

Oxygen concentrations are typically higher in surface than deep water, especially in this region of the Gulf of Mexico where bottom waters become seasonally hypoxic (Rabalais *et al.*, 2002; Rabalais *et al.*, 2010). Although samples for this study were

collected before hypoxia had fully developed ([O_2] ranged from 3.5 to 8.4 mg L^{-1}; 150-375 μM), we found clades of AOA similar to those observed in other hypoxic waters (Beman *et al.*, 2008; Labrenz *et al.*, 2010; Molina *et al.*, 2010). Additionally, we determined that the distribution of *amoA* phylotypes detected by the Francis primers correlated positively with [O_2] (as did archaeal *accA* genes), while those detected by the Wuchter primers were not correlated with [O_2] (Figure 2.8). Our data suggests that these primer sets have different PCR biases such that certain AOA ecotypes are amplified more efficiently by one set than the other. As we observed correlations between different environmental variables and *amoA* phylotypes amplified by each primer, we believe these differences may reflect ecotype-specific sequence variation, as proposed for the two primer sets given in Beman *et al*. (2008).

amoA *and* accA *abundance*

The abundance of archaeal *amoA* genes reported in this study (up to 10^8 copies L^{-1}) is comparable to abundances reported for other continental shelf regions (Galand *et al.*, 2006; Kalanetra *et al.*, 2009; Mincer *et al.*, 2007; Santoro *et al.*, 2010), in the mesopelagic Pacific Ocean (Church *et al.*, 2010), and in hypoxic zones (Beman *et al.*, 2008; Mincer *et al.*, 2007). Differences in estimates of *amoA* abundance depended on the primer set used. Previous studies using the Wuchter primers reported low abundance of *amoA* relative to *rrs* in deep waters (Agogué *et al.*, 2008; de Corte *et al.*, 2008) compared to studies that used the Francis primers (Beman *et al.*, 2010; Church *et al.*, 2010; Santoro *et al.*, 2010), suggesting that the Wuchter primers are biased against deep water clades of AOA. Our study supports these conclusions, but we also found that the Francis primers

underestimated *amoA* abundance relative to *rrs* in surface water samples (Figure A.6). Comparisons of primer sequences to alignments of *amoA* sequences from this study show single base-pair differences within Wuchter primer binding sites that could affect primer annealing and thus amplification (Figure A.8). Our findings support the use of two different primer sets for the quantification of archaeal *amoA* in near-surface versus deep water samples, as recommended by Beman *et al.* (2008). Alternatively, Thaumarchaeota abundance in DNA extracted from our samples estimated by qPCR of *rrs* agreed well with an independent assessment based on pyrosequencing. This suggests that the 334F/534R *rrs* primer set originally proposed by Suzuki *et al.* (2000) for quantifying Marine Group 1 Archaea may be more robust than *amoA* primer sets for quantifying Thaumarchaeota.

The *accA* gene, a proposed marker for archaeal autotrophy, was found at abundances almost equal to Thaumarchaeota *rrs* and *amoA* (amplified by the Francis primers) below 100 m depth, in agreement with findings from the original *accA* survey of the Tyrrhenian Sea (Yakimov *et al.*, 2009). *accA* was least abundant in surface water samples (2-70 m depth; e.g., Figure 2.2), especially at inshore stations and in the Mississippi River. A similar trend has been reported for South China Sea samples, where *accA* approached the limit of detection in samples <100 m (Hu *et al.*, 2011). Since the *accA* primers were designed using a very small database, the apparent discrepancy between *accA* and Thaumarchaeota *rrs* abundance in near surface samples may be due to the presence of populations in surface waters with divergent *accA* that are not detected by this primer set.

Community composition

We identified a number of clades that appear to be unique to the northern Gulf of Mexico. These were seen in *rrs* genes from both clone libraries and pyrosequencing reads (e.g., D5-200m-66 [KC330801], -71 [KC330804], -85 [KC330810]; D5-100m-15 [KC330788]; Figure 2.5), in *amoA* gene sequences (e.g., D5-100m-amoA-21 [KC349156], -35 [KC349170], -41 [KC349176], -51 [KC349185]; D5-200m-amoA-30 [KC349251], -44 [KC349264]; Figure A.1a), and in *accA* gene sequences (e.g., D5-2m-accA-05 [KC349402], -44 [KC349436]; D5-50m-accA-53 [KC349545]; D5-100m-accA-21 [KC349333], -29 [KC349340], -47 [KC349355]; D5-200m-accA-11 [KC349365], -27 [KC349380], -36 [KC349389], -41 [KC349393]; D5-450m-accA-20 [KC349475], -26 [KC349480]; Figure A.1b). Since the global distribution of *accA* genes has not been thoroughly surveyed, it is difficult to determine whether these clades are indeed unique to the Gulf of Mexico. Generally, the subpopulations of Thaumarchaeota represented by distinct OTUs of each gene grouped according to sample depth, with the most stringent segregation by depth observed for *rrs* and *accA*, which segregated as deep (200 m and 450 m) and near-surface (2 m, 50 m, and 100 m) OTUs, as has been observed elsewhere for *amoA* (Beman *et al.*, 2008; Beman *et al.*, 2010; Church *et al.*, 2010; Francis *et al.*, 2005; Kalanetra *et al.*, 2009; Santoro *et al.*, 2010). Archaeal *amoA* phylotypes retrieved from Station D5 were also distributed according to sample depth (Figure 2.6a), with a near-surface "Group A" and deep "Group B" (Francis *et al.*, 2005). Since these distributions of each of these genes were determined by independent PCR amplifications, it is not possible to directly associate *rrs*, *amoA* and *accA* genotypes in our samples; however, the coincident groupings of these 3 markers of completely different

physiological functions suggest differentiation of these Thaumarchaeota populations at a genomic level. Unifrac analysis suggests that Thaumarchaeota populations at these stations resolve into 3 subpopulations, segregated by depth and by factors covarying with depth, with strongest separation between surface (depth <100 m) and deep water populations (Figures 2.9, A.4, and A.7).

A few of the *accA* gene sequences retrieved from Station D5 clustered with previously defined ecotypes of the 'Deep Water *accA* Clade' (Yakimov *et al.*, 2009; Yakimov *et al.*, 2011), referred to here as Deep Ecotypes 1a, 1b, and 2 (Figure 2.6b). Inferred amino acid sequences of all but 8 of the 87 *accA* amplicons we retrieved from 200 m and 450 m grouped into Deep Ecotype 2. No representatives of Deep Ecotypes 1a or 1b were identified, although a group of more divergent sequences similar to these ecotypes was evident (Figure 2.6b). Since previous studies concentrated on samples from deeper waters, we have added Near-Surface Ecotypes 1a and 1b to the 'Shallow Water *accA* Clade' (Yakimov *et al.*, 2011). Both of the Sargasso Sea reference sequences from this clade fit into Ecotype 1a, which contained only sequences from near-surface waters (≤100 m) of the northern Gulf of Mexico. The *accA* sequence from "*Candidatus* Nitrosopumilus maritimus" SCM1 (Walker *et al.*, 2010) grouped with marine sediment clones and with "*Candidatus* Nitrosoarchaeum limnia" SFB1 (Blainey *et al.*, 2011); we have thus allocated these sequences to a 'Nitrosopumilus-like group'. We also note a distinct lineage of *accA* (OTU 2, 'Near-Surface Ecotype 1b'; Figure 2.6b) containing sequences from the northern Gulf of Mexico and the South China Sea ('Shallow group II' in Hu *et al.*, 2011). The sequences we retrieved extend coverage of the diversity of *accA*

environmental sequences to near-surface sites and provide additional references for refining ecotype characterizations as more sequences are added to the databases.

CONCLUSIONS

AOA and Thaumarchaeota were abundant in the northern Gulf of Mexico coastal waters we sampled, accounting for up to 40% (qPCR) or 54% (pyrosequencing) of the total bacterioplankton population and outnumbering AOB by 10-100 fold. The ratio of AOA to NOB in our samples was lower than reported in other studies, suggesting that other pathways for nitrite oxidation may be more important in the northern Gulf of Mexico than elsewhere. A diverse community of Thaumarchaeota was observed at Station D5 near the Mississippi River plume in clone libraries constructed from archaeal genes of interest (*rrs*, *amoA*, and *accA*), with clades that seem to be unique to waters of the northern Gulf of Mexico. Consistent with this observation, and in contrast to studies of many other coastal waters, the *amoA* sequence most similar to Nmar_1500, the *amoA* gene from "*Ca.* N. maritimus" strain SCM1, was only 91% similar. Through analysis of *rrs* sequences generated using 454 pyrosequencing, we observed distinct clades of Thaumarchaeota that were distributed primarily by depth, with clear differences between near-surface (≤100 m) and deep (>100 m) populations. The distribution of *rrs* sequences in clone libraries generated from samples collected at Station D5 was consistent with this pattern, suggesting that parallel differences in the composition of Thaumarchaeota populations defined by other genes observed at this station were applicable to the rest of the northern Gulf of Mexico. Finally we found correlations between abundances of Thaumarchaeota genes in this region and environmental variables depth, temperature,

turbidity, pH, and oxygen; however, the manner in which these variables influence Thaumarchaeota metabolism and thus distribution remains unclear.

ACKNOWLEDGEMENTS

This work was supported through National Science Foundation Grants OCE 09-43278 and ANT-08-38996 to J.T.H. Tag pyrosequencing was funded by an award from GoMRI-LSU to G.M.K. We thank L. Powers for helping with sample collection and CTD data processing, and C. Fichot and H. Reader for assistance in collecting satellite data to determine euphotic depth. We would like to express our appreciation to the crew of the R/V *Cape Hatteras,* as well as the scientists from the GulfCarbon 5 cruise that provided environmental data for this study, especially W-J. Huang and W-J. Cai for access to pH data, and S. Lohrenz for access to nutrient data. Funding for the GulfCarbon project was from NSF through awards OCE 07-52110 (W-J. Cai) and OCE 07-52254 (S. Lohrenz). Finally, we would like to thank the reviewers of previous versions of this manuscript for their helpful comments.

REFERENCES

Agogué H, Brink M, Dinasquet J, Herndl GJ (2008). Major gradients in putatively nitrifying and non-nitrifying Archaea in the deep North Atlantic. *Nature* **456:** 788-791.

Alonso-Sáez L, Sanchez O, Gasol JM, Balagué V, Pedrós-Alio C (2008). Winter-to-summer changes in the composition and single-cell activity of near-surface Arctic prokaryotes. *Environ Microbiol* **10:** 2444-2454.

Bano N, Hollibaugh JT (2000). Diversity and distribution of DNA sequences with affinity to ammonia-oxidizing bacteria of the beta subdivision of the class Proteobacteria in the Arctic Ocean. *Appl Environ Microbiol* **66:** 1960-1969.

Barns SM, Delwiche CF, Palmer JD, Pace NR (1996). Perspectives on archaeal diversity, thermophily and monophyly from environmental rRNA sequences. *Proc Nat Acad Sci USA* **93:** 9188-9193.

Bates ST, Berg-Lyons D, Caporaso JG, Walters WA, Knight R, Fierer N (2011). Examining the global distribution of dominant archaeal populations in soil. *ISME J* **5:** 908-917.

Beman JM, Popp BN, Francis CA (2008). Molecular and biogeochemical evidence for ammonia oxidation by marine Crenarchaeota in the Gulf of California. *ISME J* **2:** 429-441.

Beman JM, Sachdeva R, Fuhrman JA (2010). Population ecology of nitrifying archaea and bacteria in the Southern California Bight. *Environ Microbiol* **12:** 1282-1292.

Berg IA, Kockelkorn D, Buckel W, Fuchs G (2007). A 3-hydroxypropionate/4-hydroxybutyrate autotrophic carbon dioxide assimilation pathway in Archaea. *Science* **318:** 1782-1786.

Bernhard AE, Landry ZC, Blevins A, de la Torre JR, Giblin AE, Stahl DA (2010). Abundance of ammonia-oxidizing archaea and bacteria along an estuarine salinity gradient in relation to potential nitrification rates. *Appl Environ Microbiol* **76:** 1285-1289.

Blainey PC, Mosier AC, Potanina A, Francis CA, Quake SR (2011). Genome of a low-salinity ammonia-oxidizing archaeon determined by single-cell and metagenomic analysis. *PLoS ONE* **6:** e16626.

Brochier-Armanet C, Boussau B, Gribaldo S, Forterre P (2008). Mesophilic Crenarchaeota: proposal for a third archaeal phylum, the Thaumarchaeota. *Nat Rev Microbiol* **6:** 245-252.

Caffrey JM, Bano N, Kalanetra K, Hollibaugh JT (2007). Ammonia oxidation and ammonia-oxidizing bacteria and archaea from estuaries with differing histories of hypoxia. *ISME J* **1:** 660-662.

Cai W-J, Hu X, Huang W-J, Murrell MC, Lehrter JC, Lohrenz SE, Chou W-C, Zhai W, Hollibaugh JT, Wang Y, Zhao P, Guo X, Gundersen K, Dai M, Gong G-C (2011). Acidification of subsurface coastal waters enhanced by eutrophication. *Nature Geosci* **4:** 766-770.

Church MJ, DeLong EF, Ducklow HW, Karner MB, Preston CM, Karl DM (2003). Abundance and distribution of planktonic Archaea and Bacteria in the waters west of the Antarctic Peninsula. *Limnol Oceanogr* **48:** 1893-1902.

Church MJ, Wai B, Karl DM, DeLong EF (2010). Abundances of crenarchaeal *amoA* genes and transcripts in the Pacific Ocean. *Environ Microbiol* **12:** 679-688.

Clarke KR, Gorley RN (2006). PRIMER v6. *User Manual / Tutorial*. PRIMER-E: Plymouth.

Coolen MJL, Abbas B, van Bleijswijk J, Hopmans EC, Kuypers MMM, Wakeham SG, Damste JSS (2007). Putative ammonia-oxidizing Crenarchaeota in suboxic waters of the Black Sea: a basin-wide ecological study using 16S ribosomal and functional genes and membrane lipids. *Environ Microbiol* **9:** 1001-1016.

Dagg MJ, Ammerman JW, Amon RMW, Gardner WS, Green RE, Lohrenz SE (2007). A review of water column processes influencing hypoxia in the northern Gulf of Mexico. *Estuar Coasts* **30:** 735-752.

de Corte D, Yokokawa T, Varela MM, Agogué H, Herndl GJ (2008). Spatial distribution of Bacteria and Archaea and *amoA* gene copy numbers throughout the water column of the Eastern Mediterranean Sea. *ISME J* **3:** 147-158.

DeLong EF (1992). Archaea in coastal marine environments. *Proc Natl Acad Sci USA* **89:** 5685-5689.

Diaz R, Rosenberg R (2008). Spreading Dead Zones and Consequences for Marine Ecosystems. *Science* **321:** 926-929.

Drummond AJ, Ashton B, Buxton S, Cheung M, Heled J, Kearse M, Moir R, Stones-Havas S, Sturrock S, Thierer T, Wilson A (2010). Geneious v5.0.

Edgar RC, Haas BJ, Clemente JC, Quince C, Knight R (2011). UCHIME improves sensitivity and speed of chimera detection. *Bioinformatics* **27:** 2194-2200.

Erguder TH, Boon N, Wittebolle L, Marzorati M, Verstraete W (2009). Environmental factors shaping the ecological niches of ammonia-oxidizing archaea. *FEMS Microbiol Rev* **33:** 855-869.

Francis CA, Roberts KJ, Beman JM, Santoro AE, Oakley BB (2005). Ubiquity and diversity of ammonia-oxidizing archaea in water columns and sediments of the ocean. *Proc Natl Acad Sci USA* **102:** 14683-14688.

Francis CA, Beman JM, Kuypers MMM (2007). New processes and players in the nitrogen cycle: the microbial ecology of anaerobic and archaeal ammonia oxidation. *ISME J* **1:** 19-27.

Fuhrman JA, McCallum K, Davis AA (1992). Novel Major Archaebacterial Group from Marine Plankton. *Nature* **356:** 148-149.

Galand PE, Lovejoy C, Vincent WF (2006). Remarkably diverse and contrasting archaeal communities in a large arctic river and the coastal Arctic Ocean. *Aquat Microb Ecol* **44:** 115-126.

Giongo A, Crabb DB, Davis-Richardson AG, Chauliac D, Mobberley JM, Gano KA, Mukherjee N, Casella G, Roesch LFW, Walts B, Riva A, King G, Triplett EW (2010). PANGEA: pipeline for analysis of next generation amplicons. *ISME J* **4:** 852-861.

Green RE, Breed GA, Dagg MJ, Lohrenz SE (2008). Modeling the response of primary production and sedimentation to variable nitrate loading in the Mississippi River plume. *Cont Shelf Res* **28:** 1451-1465.

Gubry-Rangin C, Nicol GW, Prosser JI (2010). Archaea rather than bacteria control nitrification in two agricultural acidic soils. *FEMS Microbiol Ecol* **74:** 566-574.

Hamady M, Lozupone C, Knight R (2009). Fast UniFrac: facilitating high-throughput phylogenetic analyses of microbial communities including analysis of pyrosequencing and PhyloChip data. *ISME J* **4:** 17-27.

Herfort L, Schouten S, Abbas B, Veldhuis MJW, Coolen MJL, Wuchter C, Boon JP, Herndl GJ, Damste JSS (2007). Variations in spatial and temporal distribution of Archaea in the North Sea in relation to environmental variables. *FEMS Microbiol Ecol* **62:** 242-257.

Hu A, Jiao N, Zhang C (2011). Community structure and function of planktonic Crenarchaeota: Changes with depth in the South China Sea. *Microb Ecol* **62:** 549-563.

Huber T, Faulkner G, Hugenholtz P (2004). Bellerophon: a program to detect chimeric sequences in multiple sequence alignments. *Bioinformatics* **20:** 2317-2319.

Jetten MSM (2001). New pathways for ammonia conversion in soil and aquatic systems. *Plant Soil* **230:** 9-19.

Kalanetra KM, Bano N, Hollibaugh JT (2009). Ammonia-oxidizing Archaea in the Arctic Ocean and Antarctic coastal waters. *Environ Microbiol* **11:** 2434-2445.

Karner MB, DeLong EF, Karl DM (2001). Archaeal dominance in the mesopelagic zone of the Pacific Ocean. *Nature* **409:** 507-510.

Kelly S, Wickstead B, Gull K (2011). Archaeal phylogenomics provides evidence in support of a methanogenic origin of the Archaea and a thaumarchaeal origin for the eukaryotes. *Proc Royal Soc B - Bio* **278:** 1009-1018.

King GM, Smith CB, Tolar B, Hollibaugh JT (2013). Analysis of composition and structure of coastal to mesopelagic bacterioplankton communities in the northern Gulf of Mexico. *Front Microbiol*.

Kirchman DL, Elifantz H, Dittel AI, Malmstrom RR, Cottrell MT (2007). Standing stocks and activity of Archaea and Bacteria in the western Arctic Ocean. *Limnol Oceanogr* **52:** 495-507.

Könneke M, Bernhard AE, de la Torre JR, Walker CB, Waterbury JB, Stahl DA (2005). Isolation of an autotrophic ammonia-oxidizing marine archaeon. *Nature* **437:** 543-546.

Labrenz M, Sintes E, Toetzke F, Zumsteg A, Herndl GJ, Seidler M, Jürgens K (2010). Relevance of a crenarchaeotal subcluster related to *Candidatus* Nitrosopumilus maritimus to ammonia oxidation in the suboxic zone of the central Baltic Sea. *ISME J*. **4**: 1496-1508.

Lam P, Jensen MM, Lavik G, McGinnis DF, Müller B, Schubert CJ, Amann R, Thamdrup B, Kuypers MMM (2007). Linking crenarchaeal and bacterial nitrification to anammox in the Black Sea. *Proc Nat Acad Sci USA* **104:** 7104-7109.

Lam P, Lavik G, Jensen MM, van de Vossenberg J, Schmid M, Woebken D, Gutiérrez D, Amann R, Jetten MSM, Kuypers MMM (2009). Revising the nitrogen cycle in the Peruvian oxygen minimum zone. *Proc Nat Acad Sci USA* **106:** 4752-4757.

Legendre P, Legendre L (1998). *Numerical Ecology*, 2nd English edn. edn. Elsevier Science B.V.: Oxford, UK.

Levin LA (2003). Oxygen Minimum Zone Benthos: Adaptation and Community Response to Hypoxia. In: Gibson RN, Atkinson RJA (eds). Oceanography and Marine Biology: An Annual Review. Taylor & Francis: London. pp 1-45.

Ludwig W, Strunk O, Westram R, Richter L, Meier H, Yadhukumar, Buchner A, Lai T, Steppi S, Jobb G, Forster W, Brettske I, Gerber S, Ginhart AW, Gross O, Grumann S, Hermann S, Jost R, Konig A, Liss T, Lussmann R, May M, Nonhoff B, Reichel B, Strehlow R, Stamatakis A, Stuckmann N, Vilbig A, Lenke M, Ludwig T, Bode A, Schleifer KH (2004). ARB: a software environment for sequence data. *Nucl Acids Res* **32:** 1363-1371.

Martens-Habbena W, Berube PM, Urakawa H, de la Torre JR, Stahl DA (2009). Ammonia oxidation kinetics determine niche separation of nitrifying Archaea and Bacteria. *Nature* **461:** 976-979.

Massana R, Murray AE, Preston CM, DeLong EF (1997). Vertical distribution and phylogenetic characterization of marine planktonic Archaea in the Santa Barbara Channel. *Appl Environ Microbiol* **63:** 50-56.

Massana R, Taylor LJ, Murray AE, Wu KY, Jeffrey WH, DeLong EF (1998). Vertical distribution and temporal variation of marine planktonic archaea in the Gerlache Strait, Antarctica, during early spring. *Limnol Oceanogr* **43:** 607-617.

Matsutani N, Nakagawa T, Nakamura K, Takahashi R, Yoshihara K, Tokuyama T (2011). Enrichment of a Novel Marine Ammonia-Oxidizing Archaeon Obtained from Sand of an Eelgrass Zone. *Microbes Environ* **26:** 23-29.

Mincer TJ, Church MJ, Taylor LT, Preston C, Karl DM, DeLong EF (2007). Quantitative distribution of presumptive archaeal and bacterial nitrifiers in Monterey Bay and the North Pacific Subtropical Gyre. *Environ Microbiol* **9:** 1162-1175.

Molina V, Belmar L, Ulloa U (2010). High diversity of ammonia-oxidizing archaea in permanent and seasonal oxygen-deficient waters of the eastern South Pacific. *Environ Microbiol* **12:** 2450-2465.

Mosier AC, Francis CA (2008). Relative abundance and diversity of ammonia-oxidizing archaea and bacteria in the San Francisco Bay estuary. *Environ Microbiol* **10:** 3002-3016.

Murray AE, Preston CM, Massana R, Taylor LT, Blakis A, Wu K, DeLong EF (1998). Seasonal and spatial variability of bacterial and archaeal assemblages in the coastal waters near Anvers Island, Antarctica. *Appl Environ Microbiol* **64:** 2585-2595.

Murray AE, Wu KY, Moyer CL, Karl DM, DeLong EF (1999a). Evidence for circumpolar distribution of planktonic Archaea in the Southern Ocean. *Aquat Microb Ecol* **18:** 263-273.

Murray AE, Blakis A, Massana R, Strawzewski S, Passow U, Alldredge A, DeLong EF (1999b). A time series assessment of planktonic archaeal variability in the Santa Barbara Channel. *Aquat Microb Ecol* **20:** 129-145.

Nicol GW, Leininger S, Schleper C (2011). Distribution and activity of ammonia-oxidizing Archaea in natural environments. In: Ward BB, Arp DJ, Klotz MG (eds). Nitrification. ASM Press: Washington, D.C. pp 157-178.

O'Mullan GD, Ward BB (2005). Relationship of temporal and spatial variabilities of ammonia-oxidizing bacteria to nitrification rates in Monterey Bay, California. *Appl Environ Microbiol* **71:** 697-705.

Offre P, Nicol GW, Prosser JI (2011). Community profiling and quantification of putative autotrophic thaumarchaeal communities in environmental samples. *Environ Microbiol Rep* **3:** 245-253.

Phillips CJ, Smith Z, Embley TM, Prosser JI (1999). Phylogenetic differences between particle-associated and planktonic ammonia-oxidizing bacteria of the beta subdivision of the class Proteobacteria in the Northwestern Mediterranean Sea. *Appl Environ Microbiol* **65:** 779-786.

Prosser JI, Nicol GW (2008). Relative contributions of archaea and bacteria to aerobic ammonia oxidation in the environment. *Environ Microbiol* **10:** 2931-2941.

Pruesse E, Quast C, Knittel K, Fuchs BM, Ludwig WG, Peplies J, Glockner FO (2007). SILVA: a comprehensive online resource for quality checked and aligned ribosomal RNA sequence data compatible with ARB. *Nucl Acids Res* **35:** 7188-7196.

Rabalais NN, Turner RE, Wiseman WJ (2002). Gulf of Mexico hypoxia, aka "The dead zone". *Annu Rev Ecol Syst* **33:** 235-263.

Rabalais NN, Díaz RJ, Levin LA, Turner RE, Gilbert D, Zhang J (2010). Dynamics and distribution of natural and human-caused hypoxia. *Biogeosciences* **7:** 585-619.

Santoro AE, Francis CA, de Sieyes NR, Boehm AB (2008). Shifts in the relative abundance of ammonia-oxidizing bacteria and archaea across physicochemical gradients in a subterranean estuary. *Environ Microbiol* **10:** 1068-1079.

Santoro AE, Casciotti KL, Francis CA (2010). Activity, abundance and diversity of nitrifying archaea and bacteria in the central California Current. *Environ Microbiol* **12:** 1989-2006.

Schloss PD, Westcott SL, Ryabin T, Hall JR, Hartmann M, Hollister EB, Lesniewski RA, Oakley BB, Parks DH, Robinson CJ, Sahl JW, Stres B, Thallinger GG, Van Horn DJ, Weber CF (2009). Introducing mothur: Open-source, platform-independent, community-supported software for describing and comparing microbial communities. *Appl Environ Microbiol* **75:** 7537-7541.

Spang A, Hatzenpichler R, Brochier-Armanet C, Rattei T, Tischler P, Spieck E, Streit W, Stahl DA, Wagner M, Schleper C (2010). Distinct gene set in two different lineages of ammonia-oxidizing archaea supports the phylum Thaumarchaeota. *Trends Microbiol* **18:** 331-340.

Stamatakis A, Ludwig T, Meier H (2005). RAxML-III: a fast program for maximum likelihood-based inference of large phylogenetic trees. *Bioinformatics* **21:** 456-463.

Suzuki MT, Taylor LT, DeLong EF (2000). Quantitative analysis of small-subunit rRNA genes in mixed microbial populations via 5'-nuclease assays. *Appl Environ Microbiol* **66:** 4605-4614.

ter Braak CJF (1985). Canonical correspondence analysis: a new eigenvector technique for multivariate direct gradient analysis. *Ecology* **67:** 1167-1179.

ter Braak CJF, Šmilauer P (2002). CANOCO Reference manual and CanoDraw for Windows User's guide: Software for Canonical Community Ordination (version 4.5). . Microcomputer Power: Ithica, USA.

Turner RE, Rabalais NN, Justić D (2006). Predicting summer hypoxia in the northern Gulf of Mexico: Riverine N, P, and Si loading. *Mar Pollut Bull* **52:** 139-148.

Walker CB, de la Torre JR, Klotz MG, Urakawa H, Pinel N, Arp DJ, Brochier-Armanet C, Chain PSG, Chan PP, Gollabgir A, Hemp J, Hügler M, Karr EA, Könneke M, Shin M, Lawton TJ, Lowe T, Martens-Habbena W, Sayavedra-Soto LA, Lang D, Sievert SM, Rosenzweig AC, Manning G, Stahl DA (2010). *Nitrosopumilus maritimus* genome reveals unique mechanisms for nitrification and autotrophy in globally distributed marine crenarchaea. *Proc Nat Acad Sci USA* **107:** 8818-8823.

Ward BB, Devol AH, Rich JJ, Chang BX, Bulow SE, Naik H, Pratihary A, Jayakumar A (2009). Denitrification as the dominant nitrogen loss process in the Arabian Sea. *Nature* **461:** 78-U77.

Ward BB (2011). Nitrification in the Ocean. In: Ward BB, Arp DJ, Klotz MG (eds). Nitrification. ASM Press: Washington, D.C. pp 325-345.

Wells LE, Deming JW (2003). Abundance of Bacteria, the Cytophaga-Flavobacterium cluster and Archaea in cold oligotrophic waters and nepheloid layers of the Northwest Passage, Canadian Archipelago. *Aquat Microb Ecol* **31:** 19-31.

Wells LE, Cordray M, Bowerman S, Miller LA, Vincent WF, Deming JW (2006). Archaea in particle-rich waters of the Beaufort Shelf and Franklin Bay, Canadian Arctic: Clues to an allochthonous origin? *Limnol Oceanogr* **51:** 47-59.

Wuchter C, Abbas B, Coolen MJL, Herfort L, van Bleijswijk J, Timmers P, Strous M, Teira E, Herndl GJ, Middelburg JJ, Schouten S, Damste JSS (2006). Archaeal nitrification in the ocean. *Proc Natl Acad Sci USA* **103:** 12317-12322.

Yakimov MM, La Cono V, Denaro R (2009). A first insight into the occurrence and expression of functional amoA and accA genes of autotrophic and ammonia-oxidizing bathypelagic Crenarchaeota of Tyrrhenian Sea. *Deep-Sea Res Pt II* **56:** 748-754.

Yakimov MM, La Cono V, Smedile F, DeLuca TH, Juarez S, Ciordia S, Fernandez M, Albar JP, Ferrer M, Golyshin PN, Giuliano L (2011). Contribution of crenarchaeal autotrophic ammonia oxidizers to the dark primary production in Tyrrhenian deep waters (Central Mediterranean Sea). *ISME J* **5:** 945-961.

Zhang Z, Schwartz S, Wagner L, Miller W (2000). A greedy algorithm for aligning DNA sequences. *J Comput Bio* **7:** 203-214.

Table 2.1. Summary of qPCR-estimated gene abundances (copies L^{-1}) determined for samples from the northern Gulf of Mexico. Means for each reaction are listed in bold; ranges follow the mean in parentheses. *amoA* W = amplified with Wuchter *et al.* (2006) *amoA* primer set; *amoA* F = amplified with Francis *et al.* (2005) *amoA* primer set. 'Near-surface' is ≤100 m depth; 'deep' is >100 m depth; 'inshore' = over the continental shelf (seafloor depth <100 m); 'offshore' = shelf break and beyond (depth >100 m).

	Thaum. W *amoA*	Thaum. F *amoA*	Thaum. *accA*	Thaum. *rrs*	pSL12 *rrs*	AOB *amoA*	Bacteria *rrs*
Near-surface inshore	$3.86x10^{7}$ ($9.74x10^{4}$-$1.74x10^{8}$)	$5.82x10^{6}$ ($9.28x10^{2}$-$2.97x10^{7}$)	$1.29x10^{6}$ ($9.09x10^{2}$-$1.00x10^{7}$)	$1.85x10^{7}$ ($1.37x10^{5}$-$1.10x10^{8}$)	$4.77x10^{4}$ ($1.12x10^{2}$-$3.30x10^{5}$)	$3.67x10^{5}$ ($6.09x10^{3}$-$2.10x10^{6}$)	$3.20x10^{9}$ ($3.11x10^{5}$-$1.26x10^{10}$)
Near-surface offshore	$1.16x10^{7}$ ($3.91x10^{4}$ -$3.29x10^{7}$)	$4.19x10^{6}$ ($1.24x10^{5}$-$1.33x10^{7}$)	$5.66x10^{5}$ ($3.16x10^{2}$-$2.79x10^{6}$)	$6.95x10^{6}$ ($4.79x10^{4}$-$2.14x10^{7}$)	$1.30x10^{3}$ ($1.89x10^{1}$-$3.98x10^{3}$)	$2.81x10^{3}$ ($1.67x10^{2}$-$7.07x10^{3}$)	$7.16x10^{8}$ ($3.48x10^{8}$-$1.34x10^{9}$)
Deep offshore	$3.68x10^{6}$ ($4.65x10^{3}$-$2.12x10^{7}$)	$1.11x10^{7}$ ($5.11x10^{5}$-$5.86x10^{7}$)	$8.72x10^{6}$ ($1.48x10^{5}$-$1.80x10^{7}$)	$1.79x10^{7}$ ($3.23x10^{6}$-$5.45x10^{7}$)	$1.00x10^{4}$ ($3.52x10^{3}$-$2.92x10^{4}$)	$2.93x10^{3}$ ($1.34x10^{2}$-$8.80x10^{3}$)	$2.14x10^{8}$ ($2.49x10^{7}$-$1.83x10^{9}$)

Table 2.2. Mean and ranges of the ratios of Thaumarchaeota gene abundances.

Gene ratios were calculated by dividing the abundance of each of the genes tested by the abundance of *rrs* in the same sample. *amoA* W = amplified with Wuchter *et al.* (2006) *amoA* primer set; *amoA* F = amplified with Francis *et al.* (2005) *amoA* primer set.

	amoA W:*rrs*	*amoA* F:*rrs*	*accA*:*rrs*
Near-surface Inshore	2.5 (0.71-6.6)	0.32 (0.002-0.69)	0.06 (0.001-0.22)
Near-surface Offshore	1.2 (0.17-1.8)	0.62 (0.28-1.9)	0.04 (0.0002-0.17)
Deep Offshore	0.19 (0.001-1.0)	0.57 (0.16-1.1)	0.58 (0.07-1.3)

Figure 2.1: Stations occupied during the GulfCarbon 5 cruise, March 10 to 21, 2010. Inshore stations represented with a filled star; offshore stations have an open star.

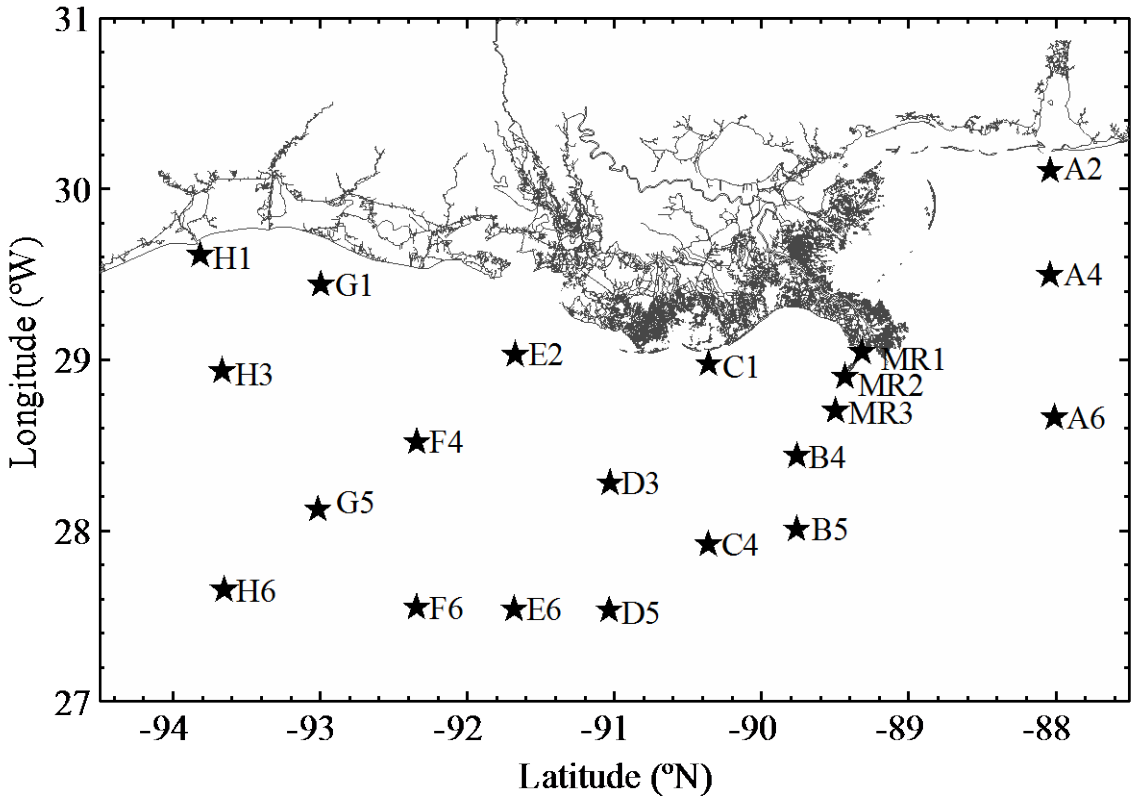
31
30
29
28
27
Longitude (ºW)
-94
-93
-92
-91
-90
-89
-88
Latitude (ºN)
H1
G1
H3
E2
C1
MR1
MR2
MR3
A2
A4
A6
F4
B4
D3
G5
B5
C4
H6
F6
E6
D5

Figure 2.2: Depth profiles of the abundance of selected genes and of environmental variables at Stations **(a)** A6, **(b)** D5, and **(c)** H6. Gene abundances are given as copies L^{-1} of sample filtered as determined from triplicate qPCR amplifications of archaeal and β-Proteobacterial *amoA* and archaeal *accA* (left) and Thaumarchaeota, pSL12, and bacterial *rrs* (center); note that scales for β-Proteobacterial *amoA* and pSL12 *rrs* are reduced by 10-100 to allow for visualization variation with depth. Environmental data were taken from a CTD attached to the frame of the rosette sampler (right). Sampling depths are shown as X's on the depth axis; missing points indicate that the measurement was below the limit of detection (see Table A.1 for detection limits).

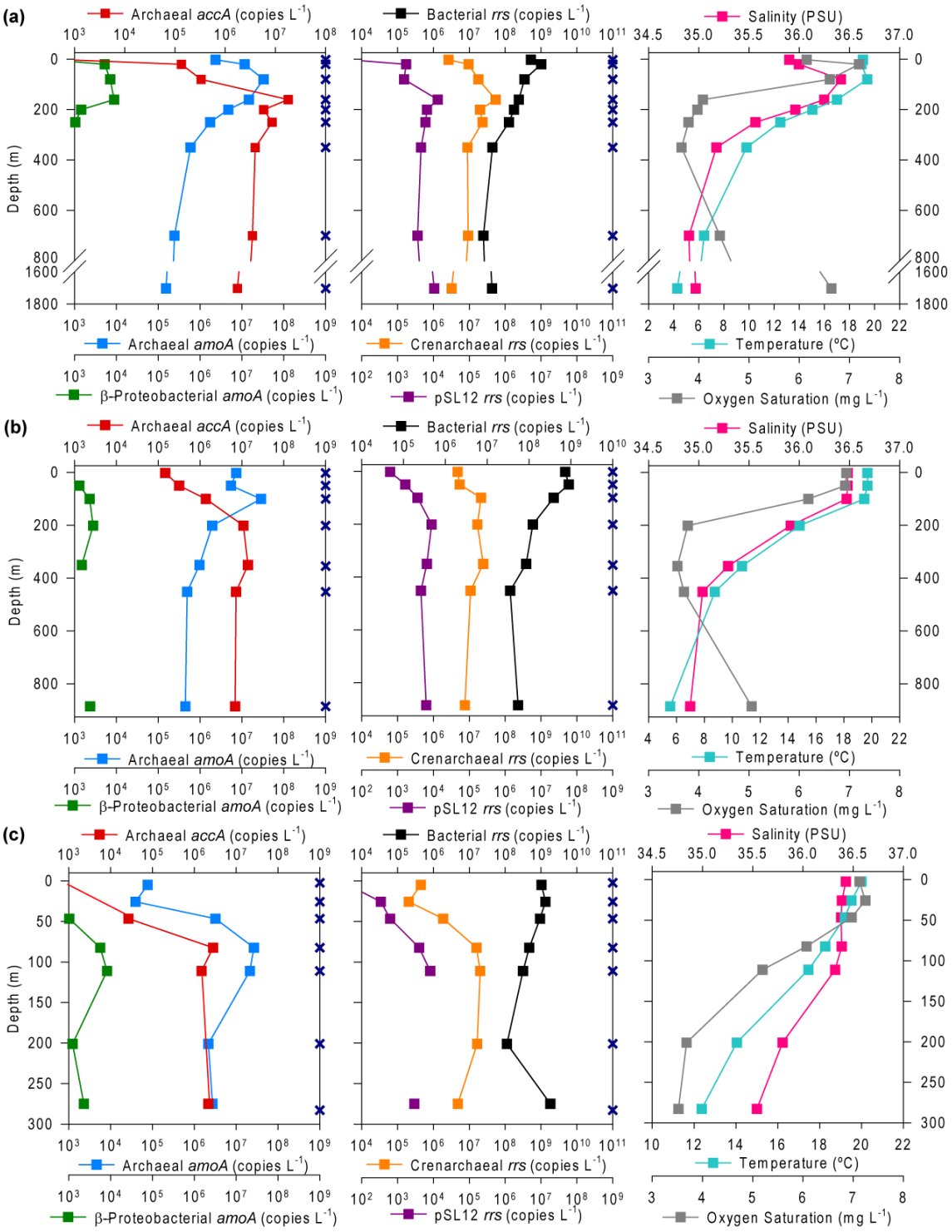
(a)
Archaeal accA (copies L-1)
Bacterial rrs (copies L-1)
Salinity (PSU)
Depth (m)
Archaeal amoA (copies L-1)
Crenarchaeal rrs (copies L-1)
Temperature (ºC)
β-Proteobacterial amoA (copies L-1)
pSL12 rrs (copies L-1)
Oxygen Saturation (mg L-1)
(b)
Archaeal accA (copies L-1)
Bacterial rrs (copies L-1)
Salinity (PSU)
Depth (m)
Archaeal amoA (copies L-1)
Crenarchaeal rrs (copies L-1)
Temperature (ºC)
β-Proteobacterial amoA (copies L-1)
pSL12 rrs (copies L-1)
Oxygen Saturation (mg L-1)
(c)
Archaeal accA (copies L-1)
Bacterial rrs (copies L-1)
Salinity (PSU)
Depth (m)
Archaeal amoA (copies L-1)
Crenarchaeal rrs (copies L-1)
Temperature (ºC)
β-Proteobacterial amoA (copies L-1)
pSL12 rrs (copies L-1)
Oxygen Saturation (mg L-1)

Figure 2.3: Abundance of Thaumarchaeota as a percentage of total bacterioplankton plotted against sample depth.

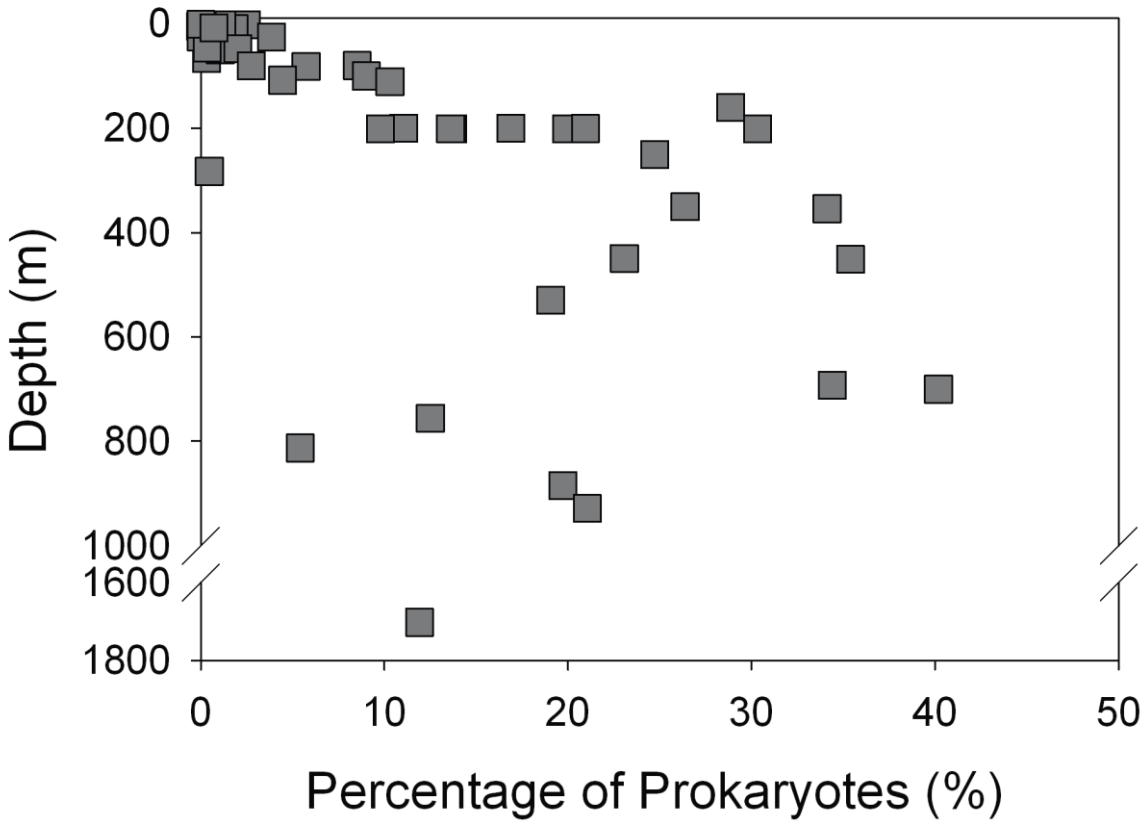
Depth (m)
0
200
400
600
800
1000
1600
1800
0
10
20
30
40
50
Percentage of Prokaryotes (%)

Figure 2.4: Fraction of Thaumarchaeota *rrs* found in 454 pyrosequencing libraries versus the fraction of Thaumarchaeota *rrs* determined from qPCR data. Line represents a model II pairwise regression.

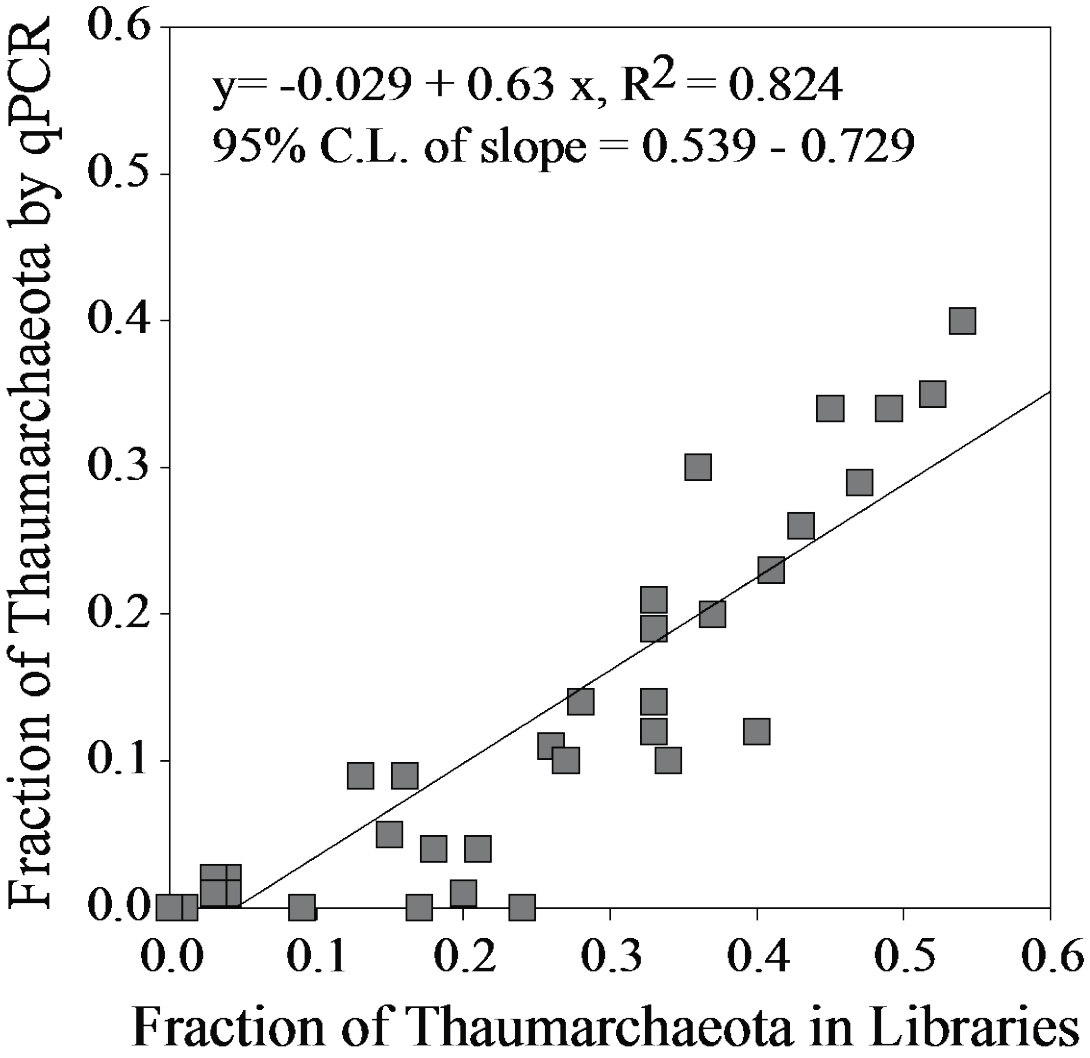
y= -0.029 + 0.63 x, R2 = 0.824
95% C.L. of slope = 0.539 - 0.729
Fraction of Thaumarchaeota by qPCR
Fraction of Thaumarchaeota in Libraries
0.0
0.1
0.2
0.3
0.4
0.5
0.6

Figure 2.5: Phylogenetic analysis of Thaumarchaeota *rrs* genes retrieved from Station D5. Clone libraries were generated from DNA in samples collected at depths of 100 m (green) and 200 m (blue). The Neighbor-Joining tree was constructed using ARB (Ludwig *et al.*, 2004). Reference sequences in bold are from isolates or enrichment cultures of AOA. Bootstrap values obtained from resampling 1000 times; only values above 75% bootstrap support are shown.

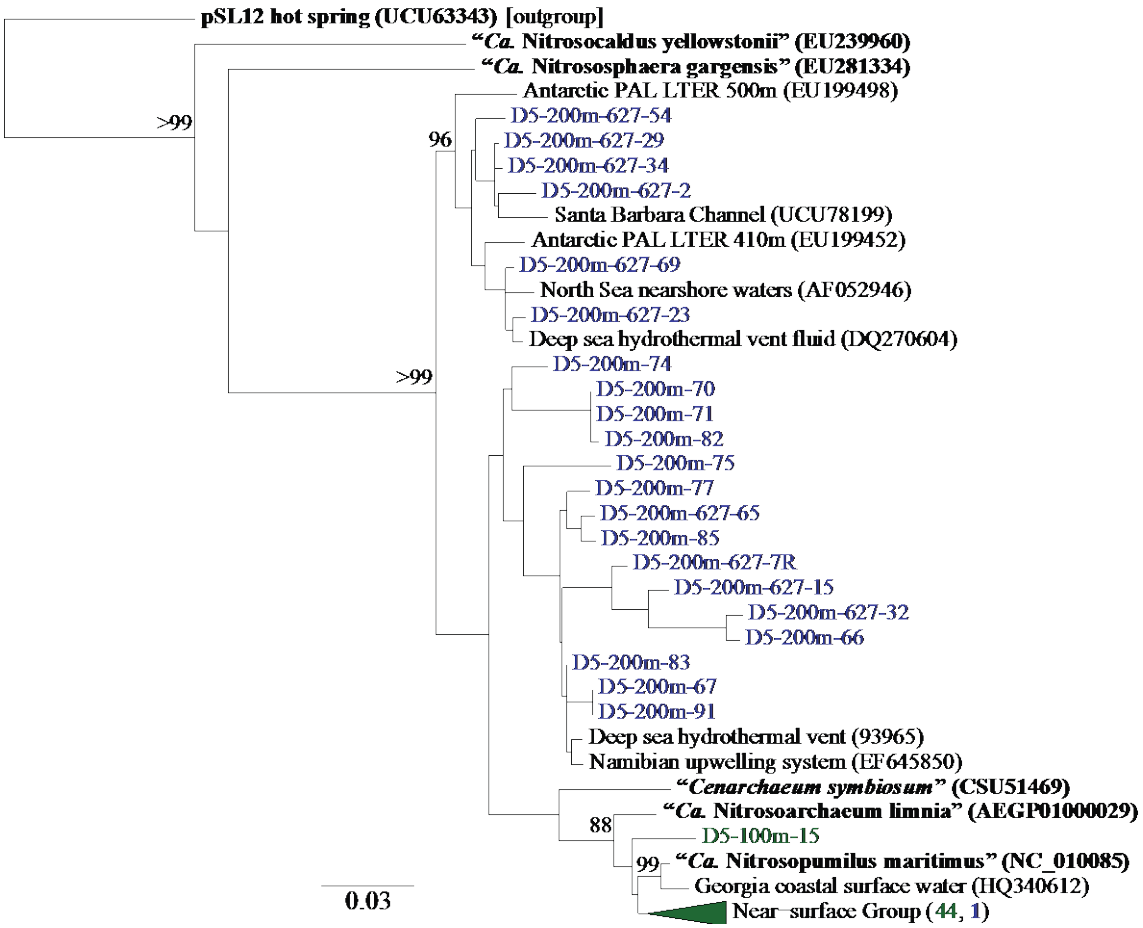
pSL12 hot spring (UCU63343) [outgroup]
"Ca. Nitrosocaldus yellowstonii" (EU239960)
"Ca. Nitrososphaera gargensis" (EU281334)
Antarctic PAL LTER 500m (EU199498)
D5-200m-627-54
D5-200m-627-29
D5-200m-627-34
D5-200m-627-2
Santa Barbara Channel (UCU78199)
Antarctic PAL LTER 410m (EU199452)
D5-200m-627-69
North Sea nearshore waters (AF052946)
D5-200m-627-23
Deep sea hydrothermal vent fluid (DQ270604)
D5-200m-74
D5-200m-70
D5-200m-71
D5-200m-82
D5-200m-75
D5-200m-77
D5-200m-627-65
D5-200m-85
D5-200m-627-7R
D5-200m-627-15
D5-200m-627-32
D5-200m-66
D5-200m-83
D5-200m-67
D5-200m-91
Deep sea hydrothermal vent (93965)
Namibian upwelling system (EF645850)
"Cenarchaeum symbiosum" (CSU51469)
"Ca. Nitrosoarchaeum limnia" (AEGP01000029)
D5-100m-15
"Ca. Nitrosopumilus maritimus" (NC_010085)
Georgia coastal surface water (HQ340612)
Near-surface Group (44, 1)
>99
96
>99
88
99
0.03

Figure 2.6: Phylogenetic analysis of inferred amino acid sequences from (a) *amoA* and (b) *accA* gene sequences retrieved from Station D5. Numbers beside groups (in triangles) indicate the number of sequences from each depth sampled according to color: clades in green are from 2 m, 50 m, or 100 m; clades in blue are from 200 or 450 m. Neighbor-Joining Trees were constructed with ARB (Ludwig *et al.*, 2004) from sequences 199 aa (AmoA) or 137 aa (AccA) in length. Sequences in bold were obtained from isolates or enrichment cultures of AOA. Bootstrap values were obtained from 100 resamplings; only values above 75% bootstrap support are shown.

(a) AmoA Tree

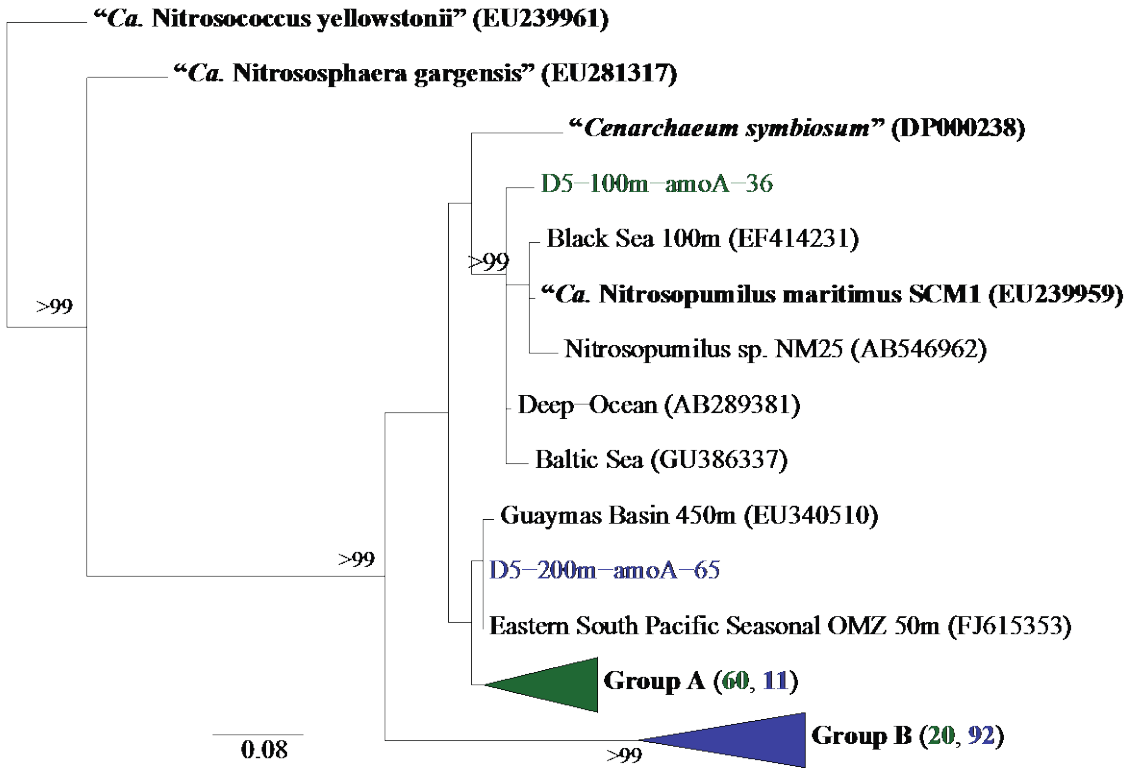
"Ca. Nitrososphaera gargensis" (EU281317)
"Cenarchaeum symbiosum" (DP000238)
D5–100m–amoA–36
Black Sea 100m (EF414231)
"Ca. Nitrosopumilus maritimus SCM1 (EU239959)
Nitrosopumilus sp. NM25 (AB546962)
Deep–Ocean (AB289381)
Baltic Sea (GU386337)
Guaymas Basin 450m (EU340510)
D5–200m–amoA–65
Eastern South Pacific Seasonal OMZ 50m (FJ615353)
Group A (60, 11)
Group B (20, 92)
>99
>99
>99
>99
0.08

(b) AccA Tree

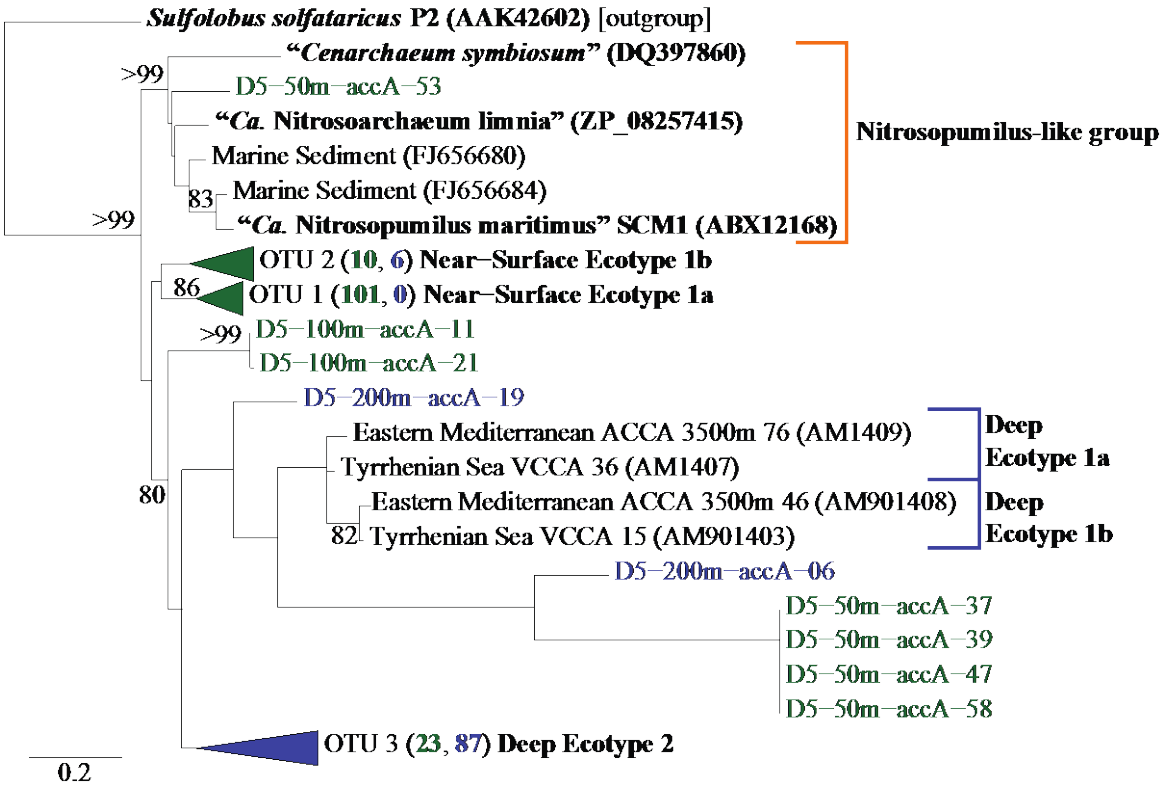
Sulfolobus solfataricus P2 (AAK42602) [outgroup]
"Cenarchaeum symbiosum" (DQ397860)
>99
D5–50m–accA–53
"Ca. Nitrosoarchaeum limnia" (ZP_08257415)
Marine Sediment (FJ656680)
83
Marine Sediment (FJ656684)
"Ca. Nitrosopumilus maritimus" SCM1 (ABX12168)
Nitrosopumilus-like group
>99
OTU 2 (10, 6) Near–Surface Ecotype 1b
86
OTU 1 (101, 0) Near–Surface Ecotype 1a
>99
D5–100m–accA–11
D5–100m–accA–21
D5–200m–accA–19
Eastern Mediterranean ACCA 3500m 76 (AM1409)
Tyrrhenian Sea VCCA 36 (AM1407)
Deep Ecotype 1a
80
Eastern Mediterranean ACCA 3500m 46 (AM901408)
82
Tyrrhenian Sea VCCA 15 (AM901403)
Deep Ecotype 1b
D5–200m–accA–06
D5–50m–accA–37
D5–50m–accA–39
D5–50m–accA–47
D5–50m–accA–58
OTU 3 (23, 87) Deep Ecotype 2
0.2

Figure 2.7: Comparison of the abundance of *rrs* from (a) Nitrite-Oxidizing Bacteria; and (b) Euryarchaeota versus Thaumarchaeota *rrs* in samples from the northern Gulf of Mexico. Triangles = near-surface (≤100 m) samples; squares = Deep (>100 m) samples. Lines are model II regressions (Legendre and Legendre, 1998) of all data.

(a)

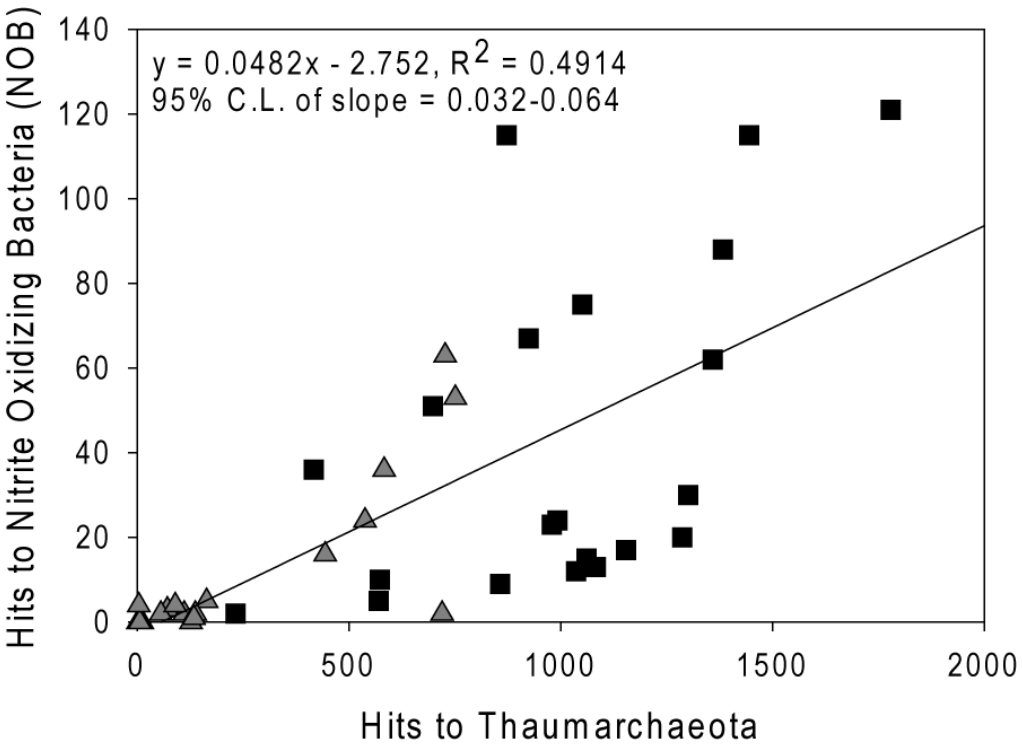
y = 0.0482x - 2.752, R2 = 0.4914
95% C.L. of slope = 0.032-0.064
Hits to Nitrite Oxidizing Bacteria (NOB)
Hits to Thaumarchaeota
0
20
40
60
80
100
120
140
0
500
1000
1500
2000

(b)

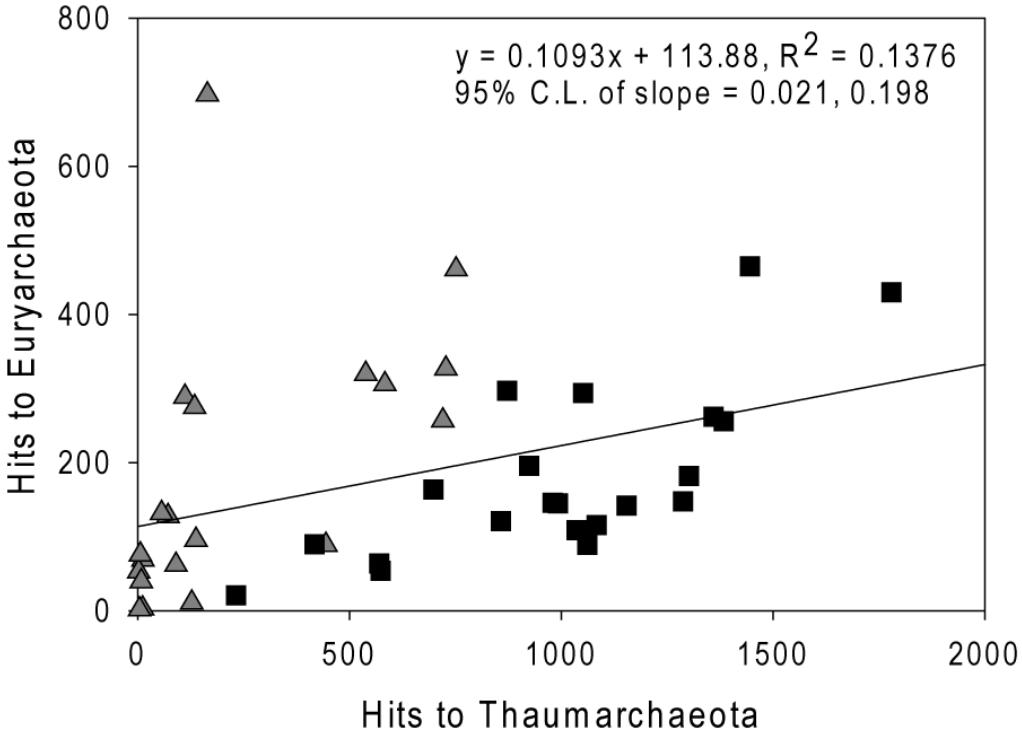
y = 0.1093x + 113.88, R2 = 0.1376
95% C.L. of slope = 0.021, 0.198
Hits to Euryarchaeota
Hits to Thaumarchaeota
0
200
400
600
800
0
500
1000
1500
2000

Figure 2.8: Canonical correspondence analysis (CCA) ordination plot of qPCR-estimated abundances for *rrs*, *amoA*, and *accA* genes and environmental data. The length and angle of arrows shows the contribution of a particular environmental variable to the CCA axes. Fluorescence = relative fluorescence, chlorophyll *a* equivalents; beam attenuation = turbidity. Eigenvalues, correlation values, and percentage variance for CCA are given in Table A.6.

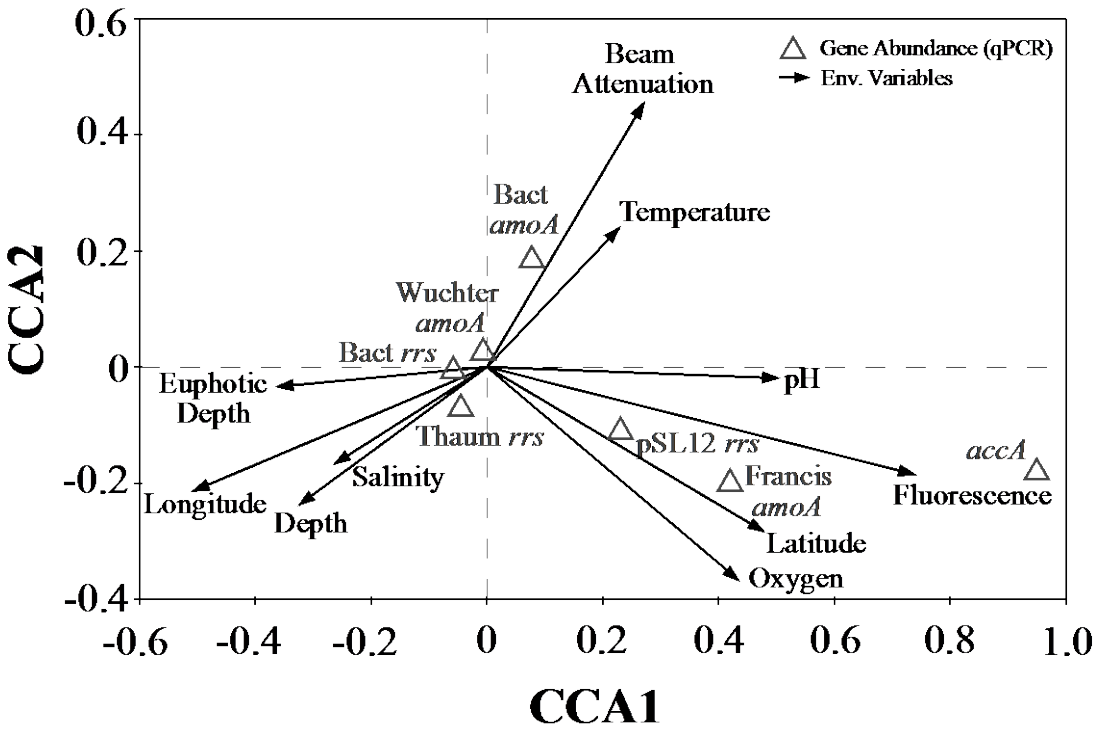
Gene Abundance (qPCR)
Env. Variables
Beam Attenuation
Bact amoA
Temperature
Wuchter amoA
Bact rrs
Euphotic Depth
pH
Thaum rrs
pSL12 rrs
accA
Francis amoA
Fluorescence
Salinity
Longitude
Depth
Latitude
Oxygen
CCA2
CCA1
0.6
0.4
0.2
0
-0.2
-0.4
-0.6
-0.4
-0.2
0
0.2
0.4
0.6
0.8
1.0

Figure 2.9: Principal Coordinates Analysis (PCoA) of Thaumarchaeota *rrs* sequences obtained from 40 samples taken in the northern Gulf of Mexico (excluding Station MR1). Shapes indicate sample groupings: dark grey squares = deep, offshore; open triangles = near-surface, offshore; light grey circles = near-surface, inshore. The percentage of the variance explained by an axis is given in parentheses next to the axis title.

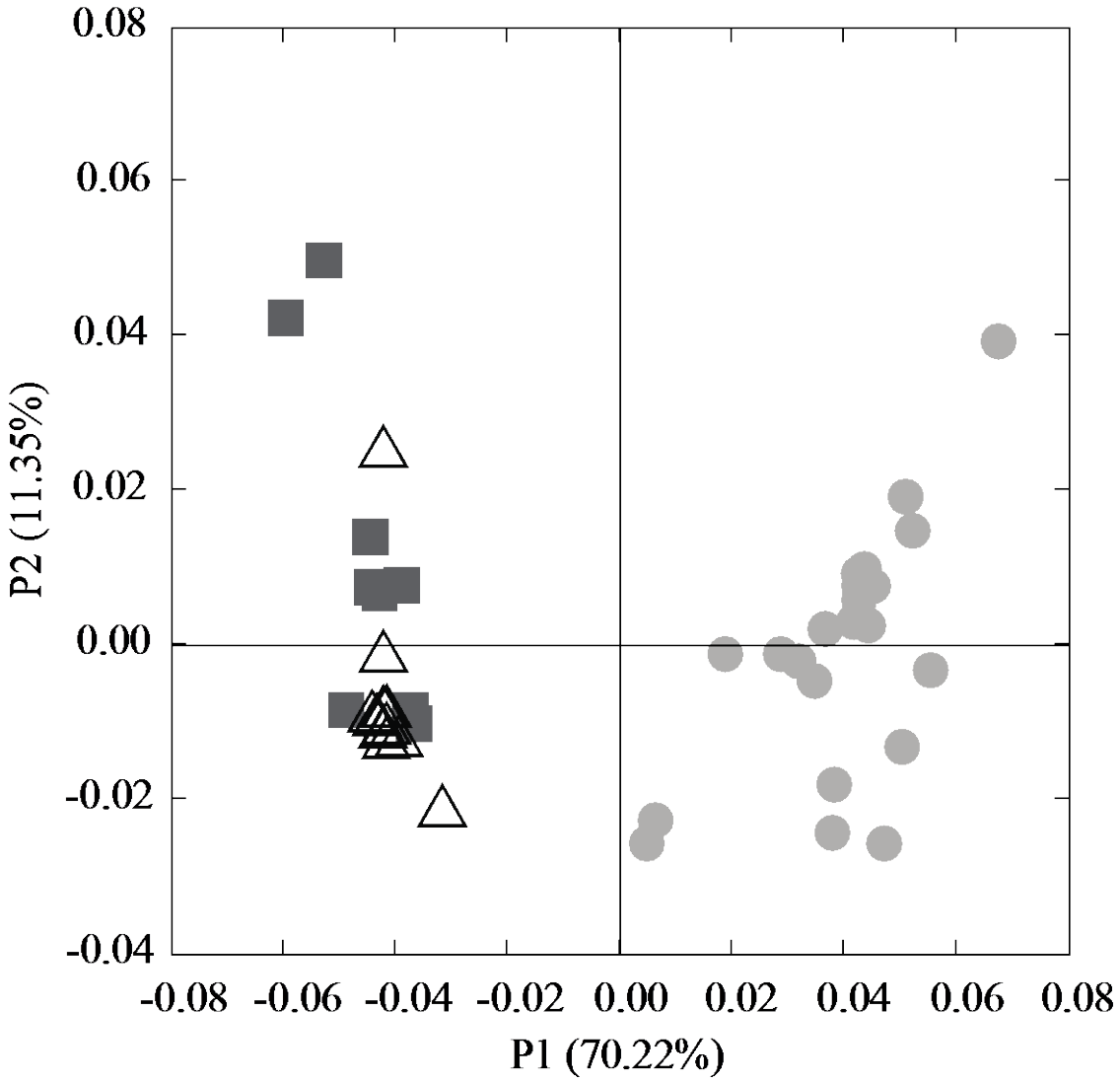
0.08
0.06
0.04
0.02
0.00
-0.02
-0.04
P2 (11.35%)
-0.08 -0.06 -0.04 -0.02 0.00 0.02 0.04 0.06 0.08
P1 (70.22%)

CHAPTER 3

SIGNIFICANT AMMONIA OXIDATION RATES IN ANTARCTIC WATERS ATTRIBUTED TO THAUMARCHAEOTA[1]

[1] Tolar, B.B., M.J. Ross, N.J. Wallsgrove, Q. Liu, L.I. Aluwihare, B.N. Popp, and J.T. Hollibaugh. To be submitted to *The ISME Journal*.

ABSTRACT

We report significant rates of ammonia oxidation (AO; 0.52-140 nM d^{-1}) in spring (Sept 2010) and summer (Jan 2011) samples from the Palmer Long-Term Ecological Research (PAL-LTER) study area in continental shelf waters west of the Antarctic Peninsula, where Thaumarchaeota strongly dominated the population of ammonia-oxidizing organisms. These rates are higher than those previously measured in polar waters and suggest that the contribution of polar regions to oceanic nitrification has been underestimated. Higher AO rates were observed in spring samples from near-surface (0-100 m) waters compared to rates from similar depths (Winter Water; WW) during summer (mean = 56 versus 12 nM d^{-1}, respectively; $p < 0.001$). AO rates in samples from the Circumpolar Deep Water (CDW) did not differ between seasons (mean = 21 versus 25 nM d^{-1}; $p < 0.8$), despite summer samples having 10 to 100-fold greater abundances of Thaumarchaeota genes and transcripts. Overall we observed no consistent relationship between AO rates and archaeal ammonia monooxygenase (*amoA*) gene (10^2-10^8 copies L^{-1}) or transcript (10^3-10^7 copies L^{-1}) abundance; or with the ratio of *amoA* transcripts per gene, which has been used as a proxy for activity. Analysis of partial sequences of Thaumarchaeota 16S rRNA (*rrs*) and *amoA* obtained by pyrosequencing showed greater diversity in CDW populations, and a clear separation of populations by water masses was reflected in statistical analyses of environmental and biotic (both qPCR and pyrosequencing) data. This suggests that distinct communities of Antarctic Thaumarchaeota in both WW and CDW are capable of high rates of ammonia oxidation.

INTRODUCTION

Ammonia oxidation to nitrite is a key reaction of the nitrogen cycle and the first step of nitrification. Two groups of organisms, ammonia-oxidizing Bacteria (AOB) and ammonia-oxidizing Archaea (AOA) are known to catalyze this reaction, while the second step – nitrite oxidation – is carried out by nitrite-oxidizing Bacteria (NOB; reviewed in Prosser and Nicol, 2008; Ward, 2011). AOA are more prominent than AOB in most marine environments, with AOA ammonia monooxygenase genes (*amoA*) 10-1000 times more abundant than bacterial *amoA* in the same sample (e.g., Beman *et al.*, 2008; Francis *et al.*, 2007; Mincer *et al.*, 2007; Santoro *et al.*, 2010; Wuchter *et al.*, 2006). AOA are widely distributed in the marine environment, with population maxima occurring below 100 m depth and at higher latitudes (Karner *et al.*, 2001; reviewed in Erguder *et al.*, 2009; Prosser and Nicol, 2008; Ward, 2011). Rates of nitrification have been measured in most major oceanic regions and range from zero to hundreds of nM d^{-1} (reviewed in Ward, 2008; Ward, 2011; Yool *et al.*, 2007). Nitrification rate measurements have also been made in the Arctic (Christman *et al.*, 2011) and Southern Oceans (Bianchi *et al.*, 1997; Olson, 1981); however, Antarctic data are limited to a handful of sites (only three below 60°S) and to depths ≤100 m.

The waters of the Antarctic continental shelf West of the Antarctic Peninsula (WAP) are characterized by strong seasonal variations in irradiance, sea ice cover, and phytoplankton biomass and production. This region is the site of an ongoing long-term ecological research (LTER) program, the Palmer (PAL) LTER (http://pal.lternet.edu/). The PAL-LTER's multi-decadal studies have revealed dramatic interannual variation in populations of many organisms and processes, with a strong temporal climate signal

(Ducklow *et al.*, 2007; Ducklow *et al.*, 2012). The Southern Ocean in this region is vertically stratified into two distinct water masses in the winter (1: Antarctic Surface Water, AASW; 2: Circumpolar Deep Water, CDW) and three in the summer (1: Summer Surface Water, SSW; 2: Winter Water, WW; 3: CDW; e.g., Church *et al.*, 2003; Hofmann and Klinck, 1998; Kalanetra *et al.*, 2009; Martinson *et al.*, 2008). The CDW is found at depths >150 m year-round, and has temperatures ranging between 0.2-2°C and salinities ranging from 34.4-34.7 PSU. During winter, the surface mixed layer (AASW), which extends from the surface to depths of 100-150 m, is colder (-1.8°C to -0.3°C) and less saline (33.3-34.3 PSU) than the CDW. This AASW layer stratifies during summer as a result of warming and meltwater inputs to form the SSW (temperature 0.5 to 1.5°C, salinity 31.5-33.8 PSU, depth 0-50 m); the remainder of the winter mixed layer deeper in the water column (50-150 m) is known as the WW and retains the characteristics of the AASW. Different microbial communities have been found to inhabit these three layers (Church *et al.*, 2003; Kalanetra *et al.*, 2009; Massana *et al.*, 1998; Murray *et al.*, 1998).

Planktonic Archaea are most abundant in the upper water column of this region during winter and early spring (May-November) and their population is dominated by Thaumarchaeota (Murray *et al.*, 1998). High concentrations of archaeal 16S rRNA (*rrs*) genes have been detected throughout the water column, with maxima occurring around 100 m (Massana *et al.*, 1998; Murray *et al.*, 1998). Archaeal populations decrease as sunlight increases during the transition from winter to summer. These reductions are most significant at the surface, with very few Archaea (1-2% of the population of prokaryotes) remaining in the newly formed SSW, as compared to high abundances in the WW (5-10%) and CDW (13-17%) along the WAP (Church *et al.*, 2003).

Our previous analysis of summer populations of AOA in the WAP found lower abundances of *amoA* and lower ratios of *amoA*:*rrs* in WW than in CDW samples (Kalanetra *et al.*, 2009). We returned to this region to determine whether the distribution of *amoA* genes and transcripts was reflected in the distribution of ammonia oxidation rates. We sampled the region during spring and summer to determine if populations of Thaumarchaeota changed during the transition from AASW to WW in summer. Thaumarchaeota diversity was characterized using 454 pyrosequencing of *rrs* and *amoA* genes, which allowed robust comparisons of assemblage composition by season, as well as by location across nearly the entire WAP region. We also measured biogenic silica (BSi) concentrations and diatom 18S rRNA abundance to test a hypothesis that Thaumarchaeota distributions in the WAP are coupled to ammonia regeneration from sinking diatom blooms, and measured the abundance of *Nitrospina* – a prominent group of NOB – to investigate connections between the two guilds of nitrifying microorganisms. Finally we investigated the distribution of Thaumarchaeota urease (*ureC*) genes after Alonso-Sáez *et al*. (2012) and Pedneault *et al.* (2014), as their presence has been proposed to indicate the use of urea as a substrate for archaeal ammonia oxidation in polar waters.

MATERIALS AND METHODS

Sample Collection

Samples were collected from the ARSV *Laurence M. Gould* in September 2010 (LMG 10-06; LTER 600 line only) and January 2011 (LMG 11-01, entire WAP region) using Niskin bottles attached to a rosette frame equipped with a CTD. Stations were

located on the Antarctic continental shelf West of the Antarctic Peninsula (WAP, Figure B.1, Table B.1) within the PAL-LTER sampling region (http://pal.lternet.edu/). Environmental data – including temperature, salinity, dissolved oxygen (DO), beam attenuation (turbidity), and chlorophyll *a* (chl *a*) fluorescence – were obtained from a CTD during bottle casts. Water masses sampled (Figures B.2, B.3) include the WW and CDW in summer (although the greatest depth sampled was <500 m), and AASW in spring, which was subdivided for analyses into 'Upper AASW' (UAASW; 10 m depth) and 'Lower AASW' (LAASW; 55-75 m depth), as samples collected from the LAASW come from the same depths as WW (Figure B.4; Table B.1). Nutrient samples were collected and analyzed using previously described methods for ammonium (NH_4, Solórzano, 1969); nitrite (NO_2) and nitrite + nitrate (NO_x; Jones, 1984; Strickland and Parsons, 1972); and biogenic silica (BSi; Brzezinski and Nelson, 1989). Additional nutrient data (including the concentrations of NO_x, SiO_4, and PO_4) were collected by the PAL-LTER on LMG 11-01 and are available through their data portal. Seawater samples (0.5-14.5 L) for DNA analysis were filtered onto 0.22 µm pore size Sterivex filters (EMD Millipore, Billerica, MA). Each cartridge received 1.8 mL of lysis buffer (0.75 M sucrose, 40 mM EDTA, 50 mM Tris; pH 8.3), then they were capped and frozen at -80°C until analysis. DNA was recovered from the filters using a phenol-chloroform extraction method (Bano and Hollibaugh, 2000) and eluted in Tris-EDTA buffer (pH 8.0). Seawater samples for RNA analysis were filtered onto 0.22 µm pore size, 47 mm (n = 67; 0.5-3.5 L) or 142 mm (n = 6; 24-33 L) diameter Millipore GVWP filters (EMD Millipore), that were placed in Whirl-Pak (Nalgene, Penfield, NY) bags with 2.0 mL (47 mm filters) or 8.0 mL (142 mm filters) of RNA*later* (Ambion, Austin, TX) and immediately frozen at

-80°C. RNA was extracted as described in Poretsky *et al*. (2009) and Gifford *et al.* (2011) with the substitution of 200 µm zirconium beads (OPS Diagnostics, Lebanon, NJ) in the initial bead-beating step and a final extract volume of 100 µL. DNA was removed from 30 µL of RNA extract with the TURBO DNase-Free Kit (Ambion) following the manufacturer's instructions with a second enzyme treatment at 2X concentration.

Quantitative PCR

Relative abundances of Archaea, Bacteria, and diatom genes were determined on an iCycler iQ™ Real-Time qPCR detection system (BioRad, Hercules, CA) using either SYBR® Green I dye (BioRad) or TaqMan® (Applied Biosystems, Carlsbad, CA) chemistries. Primers and probes used in this study are listed in Table B.2. qPCR reactions were set up in triplicate and analyzed against a range of standards (10^1-10^7 copies μL^{-1} DNA) as described in Tolar *et al.* (2013). qPCR conditions for Archaea and Bacteria *amoA* and *rrs* genes have been described previously (Kalanetra *et al.*, 2009; Tolar *et al.*, 2013). Thaumarchaeota *ureC* genes were quantified under the same conditions as *amoA* with an annealing temperature of 53°C (from Alonso-Sáez *et al.*, 2012). *Nitrospina* (a nitrite-oxidizing Bacteria, NOB) *rrs* genes were quantified as in Mincer *et al.* (2007) and diatom 18S rRNA genes were quantified as described in Nguyen *et al*. (2011) and Baldi *et al*. (2011). *amoA* transcripts from Archaea and Bacteria were quantified as above using the iScript™ One-Step RT-qPCR Kit with SYBR® Green (BioRad) with an additional 10 minute reverse transcription step at 50°C at the beginning of each run. Raw abundance data (copies μL^{-1} of RNA extract) were converted to transcripts L^{-1} using the volume filtered and an elution volume of 100 µL and assuming

100% extraction efficiency. The percent of total prokaryotes that Thaumarchaeota represented was calculated using *rrs* gene abundance (Bacteria and Thaumarchaeota) determined by qPCR and corrected using an average of 1.8 Bacteria *rrs* gene per genome (Biers *et al.*, 2009) and 1.0 Thaumarchaeota *rrs* gene per genome as described previously (Tolar *et al.*, 2013).

Archaeal Diversity

Thaumarchaeal *rrs* and *amoA* amplicons were sequenced from a subset of samples (Table B.1) using a Roche 454 GS-FLX instrument (454 Life Sciences, Branford, CT) with Titanium chemistry (maintained by the Georgia Genomics Facility, University of Georgia, Athens, GA). Thaumarchaeal *rrs* primers were tested for specificity using TestPrime 1.0 (http://www.arb-silva.de/search/testprime/) after Klindworth *et al.* (2012). The first of the five 517F primers used to sequence the Archaea v6-v4 region (5'-GCCTAAAGCATCCGTAGC -3') by the VAMPS project (http://vamps.mbl.edu/) was found to amplify 93.3% of Marine Group I Thaumarchaeota and only 11% of Euryarchaeota (with no mismatches allowed), and so was selected for this study (hereinafter referred to as 517Fa). Primers 517Fa and 1058R (Archaea *rrs*; VAMPS project – http://vamps.mbl.edu/resources/primers.php) and CamoA-19f and CamoA-616r (Archaea *amoA*; Pester *et al.*, 2012) were modified with Titanium (Lib-L) adaptors and sample-specific barcodes.

Samples were amplified in triplicate using 1 µL of DNA extract, Q5® High-Fidelity DNA Polymerase (New England Biolabs, Ipswich, MA), and 1 µL of each primer with the following PCR conditions: initial denaturation at 98°C for 3 minutes; 30

cycles of denaturation at 98°C for 10 seconds, annealing at 63°C (*rrs*) or 59°C (*amoA*) for 30 seconds, and extension at 72°C for 30 seconds; followed by a final extension at 72°C for 2 minutes. PCR reactions were pooled following amplification and purified using the AMPure® XP PCR purification kit (Agencourt Bioscience, Beverly, MA) with a modified 1:1 volume of PCR product to AMPure® bead solution. Purified amplicons were quantified using the Quant-iT™ PicoGreen® dsDNA Kit (Invitrogen, Carlsbad, CA), pooled in equimolar concentrations, and submitted for sequencing at the Georgia Genomics Facility.

Post-sequencing processing of reads to assess the diversity of Thaumarchaeota *rrs* and *amoA* genes followed the Schloss laboratory 454 SOP (http://www.mothur.org/wiki/454_SOP – accessed January 2014; Schloss *et al.*, 2011) using mothur (v. 1.32; Schloss *et al.*, 2009). Chimeric sequences were removed using UCHIME (Edgar *et al.*, 2011) within mothur. Sequences were aligned using the SILVA (Release 115; Quast *et al.*, 2013) database (*rrs*) or the Pester *et al.* (2012) database (*amoA*) before importing into ARB (Ludwig *et al.*, 2004), where neighbor-joining trees were constructed (1000 bootstrap replications) and formatted. Euryarchaeota *rrs* sequences were removed prior to analysis. OTUs were defined using a 98% (*rrs*) or 97% (*amoA*) similarity cutoff, and OTUs containing a single sequence (singletons) were not used in subsequent analyses. Clusters in trees were defined at 95% similarity. Analysis of molecular variance (AMOVA) was calculated using mothur (see 454 SOP for details).

Activity Rates

Nitrification rates (hereinafter referred to as ammonia oxidation rates, or AO rates) were measured in incubations at the *in situ* temperature for 96 h with ^{15}N-labeled ammonium (>99 atom-percent $^{15}NH_4Cl$; Cambridge Isotope Laboratories, Tewksbury, MA) added to a final concentration of 50 nM (Beman *et al.*, 2012; Santoro *et al.*, 2010). Controls were filtered sample water or were frozen immediately after tracer addition. Incubations were terminated by freezing at -80°C. Production of $^{15}NO_x$ was measured using the 'denitrifier method' (Sigman *et al.*, 2001) with *Pseudomonas aureofaciens* cultures maintained in the Stable Isotope Biogeochemistry Laboratory (University of Hawai'i – Mānoa, Honolulu, HI) as described in Popp *et al*. (1995), Dore *et al.* (1998), and Beman *et al.* (2011). Briefly, NO_2 and NO_3 present in each sample were converted to N_2O gas through denitrification by *P. aureofaciens*, transferred from the reaction vial, cryo-focused, and separated from other gases using a CP-PoraBOND Q capillary column (0.32 mm inner diameter x 25 m x 5 μm; Agilent Technologies, Santa Clara, CA) at room temperature. The masses of N_2O were measured using a Finnigan MAT-252 isotope ratio mass spectrometer (Thermo Fisher Scientific, Waltham, MA) to quantify the amount of ^{15}N tracer introduced to the NO_x pool through ammonia oxidation (Beman *et al.*, 2008; Christman *et al.*, 2011). Calculation of the AO rate from δ^{15}N values was performed as described previously (Beman *et al.*, 2012; Christman *et al.*, 2011). Ammonium concentrations were at the limit of detection (<100 nM) in some samples (Table B.1), so the rates measured should be considered as potential rates in some cases.

Statistical Analysis

We used both Principal Components Analysis (PCA) and Non-metric Multi-dimensional Scaling (NMDS) to identify environmental factors that might control Thaumarchaeota distributions and activity. These analyses were performed in R (http://www.r-project.org/) using the prcomp (stats package; PCA), metaMDS (vegan package; NMDS), and lm (stats package; pairwise linear regression) commands as in Hollibaugh *et al.* (2014). PCA analysis was run separately on LMG 11-01 and LMG 10-06 data sets to include variables not collected during LMG 10-06 (turbidity, DO, BSi) and to reduce bias from oversampling along the LTER 600 line. Temperature and salinity were combined into one variable, sigma-t (σ_t, a measure of seawater density; Table B.1, Figure B.3), to describe water mass characteristics, and NO_2 and NO_3 were summed as NO_x for LMG 11-01. Both qPCR-estimated gene abundances and 454-generated OTUs (*rrs* and *amoA*) were used in NMDS analysis (separately). Student's T-test and correlation tests using Pearson's product moment correlation coefficient (r; here we used r^2) were also performed in R using the t.test and cor.test commands (stats package), respectively.

RESULTS

Thaumarchaeota Abundance

Thaumarchaeota genes were detected at all stations and depths sampled in the PAL-LTER study area (Figure B.1) in both spring and summer (Table B.1). In contrast to our previous work in this area (Kalanetra *et al.*, 2009), we found close to a 1:1 ratio of archaeal *amoA*:*rrs* ($r^2 = 0.31$) for all water masses sampled (Figures 3.1, B.5). *amoA* and

rrs genes were more abundant in the CDW (means = 1.2 x 10^7 copies L^{-1}, 1.4 x 10^7 copies L^{-1}, respectively) versus WW (means = 4.0 x 10^6 copies L^{-1}, 2.9 x 10^6 copies L^{-1}, respectively) during summer ($p \leq 0.005$, Student's t-test; Figures 3.2a-b, B.6a-b), though WW exhibited greater variability in abundance (Figure B.7a). The opposite trend was observed in spring, with ~2-fold higher abundances in AASW compared to CDW (during summer, abundance in CDW was 3- to 5-fold greater than in WW) though this difference was not statistically significant ($p < 0.18$ for *rrs*, 0.09 for *amoA*; Student's t-test). Summer populations of Thaumarchaeota accounted for up to 29% of total prokaryotes in the CDW (mean = 14 ± 8.8 %; 1.4 ± 2.4 % in WW samples). Quantification of archaeal *amoA* genes using the Francis *et al.* (2005) primer set led to an underestimation of *amoA* genes in the AASW and WW as compared to analyses made using the Wuchter *et al.* (2006) primer set (Figure B.7b; see also Tolar *et al.*, 2013, Chapter 2), thus the Wuchter primers were used for the remainder of these analyses. The abundance of Thaumarchaeota *ureC* genes was similar to the abundance of *amoA* and *rrs* genes in a sample (Figure B.6c-d, with ratios of *ureC* vs. *rrs* genes (mean = 0.42; Figure B.8) matching values of *amoA* vs. *rrs* (mean = 0.32; $p < 0.4$, Student's t-test).

The abundance of *amoA* transcripts was 10^3-10^7 copies L^{-1} for both AASW and CDW during spring, with 10-fold higher *amoA* transcripts in summer versus spring CDW samples (mean = 2.7 x 10^6 versus 1.3 x 10^5) though not statistically different ($p < 0.10$; Student's t-test). WW and LAASW transcripts averaged 4.4 x 10^6 copies L^{-1} (Table B.1; Figure 3.2c-d), but were only significantly different from CDW transcript abundance in spring ($p < 0.02$). The ratio of archaeal *amoA* transcripts (mRNA) per *amoA* gene (DNA) in summer was 4.4 ± 12 for WW samples and 0.44 ± 0.67 for CDW samples (Figure

3.3a; no significant difference, Student's t-test, $p < 0.1$). Spring data exhibited lower variability and the difference between water masses was statistically significant ($p < 0.02$), with *amoA* transcript to gene ratios of 4.1 ± 3.6 for AASW and 0.22 ± 0.18 for CDW (Figure 3.3a). AOB *amoA* transcripts were either below the limit of detection or on average 29X lower than Archaeal *amoA* transcripts for all samples (Table B.1).

Ammonia Oxidation Rates.

Measured AO rates indicate active ammonia oxidizer populations in all water masses sampled (Table B.1). The highest summer AO rates (n = 47) were found in CDW samples (mean = 25 nM d^{-1}) compared to WW samples (mean = 12 nM d^{-1}; Figure 3.2e-f), though the difference between water masses was not significantly different (Student's t-test, $p < 0.7$). Spring AO rates (n = 18) were significantly higher in samples from the AASW than the CDW (means of 58 nM d^{-1} versus 21 nM d^{-1}, respectively; $p < 0.05$). This is consistent with higher overall *amoA* and *rrs* abundances in the AASW in spring versus WW in summer.

We found significant correlations between AO rates and Thaumarchaeota *amoA* ($r^2 = 0.13$, $p < 0.02$; Figure 3.3b) and *rrs* ($r^2 = 0.20$, $p < 0.002$; Figure B.9a) gene abundances in summer samples, but not with *amoA* transcript abundance ($r^2 = 6.1 \times 10^{-4}$, $p = 0.9$; Figure B.9b) or with the number of *amoA* transcripts per gene ($r^2 = 0.25$, $p = 0.3$; Figure 3.3c). Correlations between AO rates and Thaumarchaeota *rrs* ($r^2 = 0.30$, $p < 0.007$) and *amoA* ($r^2 = 0.32$, $p < 0.003$) gene abundances in the subset of WW samples were significant, but AO rates were not correlated with either measure of Thaumarchaeota abundance in the subset of summer CDW samples. AO rates measured

in spring were not significantly correlated with *rrs* ($r^2 = 0.062$, $p = 0.3$) or *amoA* gene abundances ($r^2 = 7.7 \times 10^{-5}$, $p = 1.0$), *amoA* transcript abundance ($r^2 = 0.16$, $p < 0.1$), or the *amoA* transcript to gene ratio ($r^2 = 0.16$, $p < 0.1$). Correlations between AO rates and AOB *amoA* abundance were not significant. *Nitrospina* (NOB) *rrs* abundance was significantly correlated to AO rates measured in both WW and CDW samples during summer ($r^2 = 0.27$ and 0.18, respectively; $p \leq 0.05$).

Thaumarchaeota Diversity

A total of 399,389 (*rrs*; mean = 353 bp) and 154,037 (*amoA*; mean = 358 bp) useful sequences were retained after processing (Table B.1; unique sequences deposited to GenBank SRA under study PRJNA268106, Accession # SRP050086). Analysis of this data set revealed that Thaumarchaeota populations in the PAL-LTER region were diverse with 76 *rrs* OTUs (defined at 98% similarity) and 175 *amoA* OTUs (defined at 97% similarity). Some of these OTUs were retrieved from all water masses (11 *rrs*, 27 *amoA*; Figure B.10a-b). The diversity of both genes was greater in the CDW population of Thaumarchaeota as compared to AASW and WW populations (46 vs. 3 unique *rrs* OTUs, 71 vs. 14 unique *amoA* OTUs; respectively; Figure B.10a-b). Eighty-five percent of *amoA* sequences retrieved from AASW and WW samples fell into one OTU [OTU #1, within subcluster 13 as defined by Pester *et al*. (2012); Figure 3.4] along with 27% of CDW *amoA* reads. The majority of the remaining CDW sequences grouped into OTU #2 (35%; within subcluster 13) or within subcluster 9.1B (32%; Figure 3.4). The distribution of Thaumarchaeota *rrs* phylotypes was similar to the distribution of *amoA* phylotypes, with a majority of sequences (87%) grouping into a single cluster at 95%

similarity (Cluster #2; Figure B.11). As with *amoA*, WW and AASW *rrs* populations were less diverse (96% and 99% of sequences, respectively, grouped in Cluster #2), while CDW *rrs* populations were more diverse (67% in Cluster #2, 29% in Cluster #1; <5% elsewhere).

AASW samples grouped with WW samples, with no significant difference in the composition of the populations of *amoA* (AMOVA; $p \leq 0.6$) or *rrs* ($p \leq 0.7$) sequences they contain. Thaumarchaeota populations from both the UAASW and LAASW share a majority of *rrs* and *amoA* OTUs with the WW layer (10 and 23 OTUs, respectively; Figure B.10c-d); however, each subset also contained unique OTUs and some that were shared only with WW. This indicates that both AASW populations contribute to the Thaumarchaeota population found in WW samples, despite weak stratification within the AASW observed during spring sampling (Figure B.4). A majority of Thaumarchaeota *rrs* (99.8%) and *amoA* (99.1%) sequences in CDW samples were common to both spring and summer populations; however, because the populations were dominated by a few OTUs, the number of OTUs shared between these populations was much smaller (43 or 37% of OTUs shared, respectively; Figure B.10e-f). Populations of both *rrs* and *amoA* genes differed significantly between WW and CDW samples (AMOVA; $p < 0.001$).

Environmental Correlations

Distributions of AO rates and thaumarchaeal gene abundances within the AASW, WW, or CDW did not show clear spatial trends (Figures 3.2, B.6); therefore, we used PCA and NMDS to relate Thaumarchaeota abundance, activity, and diversity to environmental variables. PCA analysis of the physicochemical characteristics of samples

taken during LMG 11-01 explained 52.3% (axes PC1 and PC2) of the total variation in the dataset and supported division of samples into WW and CDW water masses (Figure 3.5a), which agrees with their characterization based on temperature and salinity alone (Figure B.3). Significant environmental characteristics of the CDW identified in analysis include greater depth, salinity, temperature, AO rate, and [NO_3] along with lower [NO_2], [NH_4], and turbidity (Figure 3.5a). Distributions of DO, PO_4, SiO_4, and chl *a* did not contribute significantly to differences between water masses in the PCA. NMDS based on qPCR-estimated gene abundances also grouped samples by water mass, with samples from the CDW clustering closely based on abundances of Thaumarchaeota genes (*rrs*, *amoA*, and *ureC*) and *Nitrospina rrs*, while grouping of WW samples was driven by increased Bacteria *rrs* and diatom 18S rRNA gene abundances (Figure 3.5b). A pairwise linear regression between sample scores from the primary axes of each analysis (PC1 and MDS1 from PCA and NMDS, respectively) highlighted the correlation ($R^2 = 0.48$; $p < 0.05$) of increased archaeal gene abundances in the CDW. There was no significant correlation between values for MDS1 and PC2, which represented BSi and the LTER line sampled (a surrogate for north-south trends). Similar water mass-associated groupings were observed in PCA and NMDS analyses from LMG 10-06 (Figure B.12), except that increased AO rates corresponded to the AASW. Chl *a* fluorescence was also significant for PC3 during LMG 10-06, though we found no correlation with gene abundance.

NMDS analysis of the distribution of OTUs agreed with analyses based on qPCR estimates of gene abundances (Figure 3.5b), with both different Thaumarchaeota *rrs* and *amoA* OTUs found in WW versus CDW samples (Figure B.13a-b). The primary axis for *rrs* OTUs (MDS1) showed significant correlations with AO rates ($r^2 = 0.14$, $p < 0.05$),

amoA transcript abundance ($r^2 = 0.34$, $p < 0.001$), and the ratio of *amoA* transcripts to genes ($r^2 = 0.15$, $p < 0.04$); however, there were no correlations between MDS1 from *amoA* OTU data and these variables. Increased AO rates and *amoA* transcript abundances therefore correspond to OTUs from CDW samples. Interestingly, MDS1 for Thaumarchaeota *rrs* OTUs also showed a significant correlation to *Nitrospina rrs* abundance ($r^2 = 0.18$, $p < 0.03$). The PCA run on the subset of samples used for 454 pyrosequencing (Figure B.13c) corresponded to that run for all LMG 11-01 samples (Figure 3.5a).

DISCUSSION

Active Thaumarchaeota in Polar Oceans

The pattern of Thaumarchaeota abundances we measured match previous studies of this area of the Southern Ocean, with higher abundances in CDW during summer compared to winter/spring (Church *et al.*, 2003) and in CDW versus WW (Church *et al.*, 2003; Kalanetra *et al.*, 2009). The abundances of both *rrs* and *amoA* genes we measured (10^5-10^8 copies $L^{-1)}$ are of the same order of magnitude as reported for Antarctic waters previously (Alonso-Sáez *et al.*, 2012; Kalanetra *et al.*, 2009) or 10^6-10^7 cells L^{-1} (Church *et al.*, 2003; Murray *et al.*, 1998). The abundance of Thaumarchaeota *ureC* genes (10^4-10^6 copies L^{-1}) in the Amundsen Sea (Alonso-Sáez *et al.*, 2012) and Arctic Ocean (Pedneault *et al.*, 2014) was comparable to that of both *rrs* and *amoA*, which agrees with our findings. The percentage of prokaryotes represented by Thaumarchaeota, estimated by qPCR to be 7.2 ± 8.8% on average (max = 29%; Table B.1), agrees with estimates made using fluorescence *in situ* hybridization (up to 17%; Church *et al.*, 2003; Massana

et al., 1998), and prokaryote abundance determined by qPCR correlates with total cell counts made by the Palmer LTER during LMG 06-01 (Kalanetra *et al.*, 2009) and LMG 11-01 (slope = 0.54, $r^2 = 0.57$, $p < 0.05$; Figure B.14).

Although there are no other comparable data from the Southern Ocean, the abundances of Thaumarchaeota *amoA* transcripts (10^3-10^7 copies L^{-1}) we found are comparable to measurements made in the Arctic Ocean (Pedneault *et al.*, 2014), the Pacific Ocean (Church *et al.*, 2010), and the Baltic Sea (Labrenz *et al.*, 2010). Antarctic Thaumarchaeota have higher ($p < 0.05$) ratios of transcripts per *amoA* gene (WW = 0.03 to 65; CDW = 0.02 to 3.0) relative to populations from below 100 m in the Pacific Ocean (2.8×10^{-4} to 0.52), but WW ratios are of the same magnitude ($p < 0.2$, Student's t-test) as those from ≤ 100 m in the Pacific (0.15 to 56; Church *et al.*, 2010). The ratio of *amoA* mRNA transcripts per *rrs* gene was also higher in our samples (0.13-0.56) than measured in the Baltic Sea (up to 0.4; Labrenz *et al.*, 2010). As we observed higher rates of ammonia oxidation and abundances of *amoA* and *rrs* in spring, Williams *et al.* (2012) also showed increased Thaumarchaeota protein abundance compared to summer.

Rates of ammonia oxidation (AO) have been measured previously in the Southern Ocean, though no measurements have been made with samples from depths >90 m depth (i.e., CDW) or at latitudes >60°S, other than in the Ross Sea (Bianchi *et al.*, 1997; Olson, 1981). Bianchi *et al.* (1997) measured rates of 2.6 nM d^{-1} (averaged over depths 0-100 m) in the southern Indian Ocean (52°S, 62°E) during the fall. AO rates measured in samples from depths <100 m in the Scotia Sea during spring averaged 2.8 nM d^{-1} (55-60°S; Olson, 1980; Olson, 1981). This is an order of magnitude lower than rates we measured in spring (means = 56 and 21 nM d^{-1} for AASW and CDW, respectively) along

the Palmer 600 Line (63.9°S, 66.9°W to 64.7°S, 65.0°W). Two samples retrieved from the Ross Sea during summer (Olson, 1981), had AO rates of 6.0 and 8.9 nM d^{-1} at 30 m and 300 m, respectively; these rates are lower than our summer measurements (mean = 18 nM d^{-1}). We found higher AO rates in our samples (overall mean = 25 nM d^{-1}) compared to Arctic coastal communities, which ranged from 3.6 nM d^{-1} (winter mean) to 0.14 nM d^{-1} (summer mean; Christman *et al.*, 2011). Specific nitrification rates (λ_{nitrif}), calculated by dividing the nitrification rate (nM d^{-1}) by the concentration of ammonia (nM) in a sample, ranged from 10^{-3} to 10^{1} (mean = 0.550 d^{-1}) across the global ocean (Yool *et al.*, 2007), with Antarctic samples from Olson (1981) an order of magnitude lower on average (mean = 0.017 d^{-1}). λ_{nitrif} calculated from our dataset (Table B.1) was on average 2.4 times higher than found in the Olson (1981) study (mean = 0.040 d^{-1}; range = 2.95 x 10^{-4} – 0.307 d^{-1}). This suggests the coastal Southern Ocean may be a "hotspot" for nitrification when compared to the Arctic and in contrast to low rates previously measured at other Southern Ocean sites.

The AO rates we measured were significantly ($p < 0.05$) correlated with Thaumarchaeota gene and transcript abundances for some subsets of samples, in contrast with the lack of correlation between rates and *amoA* abundance reported for the central California Current (Santoro *et al.*, 2010). As postulated by Santoro *et al.* (2010) and others, this may be due to differences in cell-specific ammonia oxidation rates among Thaumarchaeota ecotypes, which has been shown in Monterey Bay by significant correlations between AO rates and *amoA* genes quantified from the "surface water" clade (WCA; Smith *et al.*, 2014a), but not with *amoA* from the "deep water" clade (WCB) or with total *amoA* abundance. While there seems to be a relationship between AO and

gene abundance in some sets of samples (this study, Beman *et al.*, 2008) the inconsistency of this relationship seems to indicate that the only reliable means of estimating AO rates is to measure them directly. Presumable environmental factors like [NH_4], the availability of unknown cofactors, or other as yet unidentified aspects of Thaumarchaeota biology play a more important role in modulating AO rate than gene or transcript abundance.

We found that *Nitrospina* (NOB) abundance in the Southern Ocean co-varied with Thaumarchaeota gene abundance, in agreement with distributions observed by Mincer *et al*. (2007) in the Pacific Ocean. We also observed correlations between *Nitrospina* abundance and AO rates, suggesting a tight coupling of AO and nitrite oxidation in this region.

Diversity and Distribution of Polar Thaumarchaeota

Most of the archaeal *amoA* sequences we retrieved group with 'surface water' clade A (Francis *et al.*, 2005), while only one subcluster (9.1B; 15% of sequences) contained sequences assigned to 'deep water' clade B (Figure 3.4). Since Pester *et al.* (2012) did not include representatives of these established clades in their analysis, we added *amoA* reference sequences belonging to clades A and B to their database before using it in our phylogenetic analysis. Only seven of the 'Nitrosopumilus' subclusters defined by Pester *et al.* (2012) could be confirmed as belonging to clade A (Figure 3.4), while members of both clades A and B were found within subcluster 9.1 (which led to our division of it into subclusters 9.1A and 9.1B; Figure 3.4). Almost all of the WW and AASW *amoA* sequences (94 and 98%, respectively) fit into a cluster with representative

'shallow' clade A *amoA* sequences (subcluster 13; Figure 3.4), indicating that depth distributions of these *amoA* ecotypes (e.g., Beman *et al.*, 2008; Biller *et al.*, 2012; Church *et al.*, 2010; Francis *et al.*, 2005; Hu *et al.*, 2011; Pedneault *et al.*, 2014; Santoro *et al.*, 2010; Sintes *et al.*, 2013) are not driven by water temperature (since shallower WW is colder than deeper CDW in the Southern Ocean; Figure B.2). This strong grouping by depth has also been observed for Thaumarchaeota *rrs*, *accA*, and *ureC* genes (Hu *et al.*, 2011; Tolar *et al.*, 2013; Yakimov *et al.*, 2009; Yakimov *et al.*, 2011) and appears to be a genomic characteristic (Luo *et al.*, 2014).

Previous studies have shown high diversity of Archaea in the CDW (Alonso-Sáez *et al.*, 2011; Kalanetra *et al.*, 2009), which agrees with our data (Figure 3.4, Figure B.11). Archaeal *amoA* and *rrs* sequences collected from the PAL LTER region in 2005-2006 (Kalanetra *et al.*, 2009) clustered with our 2010-2011 sequences, and sequences from both studies had similar distributions by water mass (Table B.3).

Seasonal shifts in the relative abundance of Thaumarchaeota in surface waters of polar regions have been noted previously (Christman *et al.*, 2011; Church *et al.*, 2003; Luria *et al.*, 2014; Murray *et al.*, 1998), with higher abundances in winter compared to summer. We observed a decrease in AO rates in surface waters (AASW and WW) from spring to summer, with no corresponding change in AO rates in the deeper CDW. This suggests that Thaumarchaeota populations in the AASW and WW, which are dominated by a single 'ecotype' (Figures 3.4, B.11; Kalanetra *et al.*, 2009), are more strongly affected changes in water properties accompanying the seasonal transition of spring to summer than the CDW population (Figure B.10), or simply that the physicochemical environment of the CDW is more stable, though we expected CDW populations to

respond to enhanced particle export accompanying melt pack ice and the spring phytoplankton bloom (Ducklow *et al.*, 2008).

We found the strongest correlations between archaeal gene abundance and water mass characteristics (Figure 3.5) that covary strongly with depth: temperature (+), salinity (+), turbidity (-), NH_4 (-), and NO_x (+). Thaumarchaeota abundance also increased with dissolved inorganic nitrogen (NH_4 and NO_x) and PO_4 concentrations in Arctic studies (Kirchman *et al.*, 2007; Pedneault *et al.*, 2014), though we found an inverse correlation with [NH_4] and no correlation with PO_4. Although we found no significant correlations with chl *a* concentration, negative correlations between Archaea abundance and [chl *a*] in the Arctic Ocean have been reported (Wells and Deming, 2003), and Pedneault *et al.* (2014) showed a positive correlation of Thaumarchaeota *rrs* and *amoA* transcripts and [chl *a*]. We did, however, observe a strong positive correlation between diatom 18S rRNA abundance and spring AO rates ($r^2 = 0.59$, $p < 0.003$), potentially displaying a connection in the cycling of DIN between these two groups as discussed previously (Dugdale and Goering, 1967; Ward, 2011; Yool *et al.*, 2007). In contrast, diatom abundance negatively correlated with summer Thaumarchaeota *rrs* ($r^2 = 0.096$, $p < 0.02$) and *ureC* ($r^2 = 0.089$, $p < 0.03$) abundance in our study, which agrees with the proposed phytoplankton competition with Thaumarchaeota for nutrients (e.g., Murray *et al.*, 1998; Murray *et al.*, 1999a; Smith *et al.*, 2014b; Wells and Deming, 2003). Dissolved oxygen (DO) concentrations were reported to be positively correlated to ammonia oxidation rates in the Southern Ocean (Bianchi *et al.*, 1997), but we did not observe such a trend in this study despite differences in [DO] between water masses (Figure B.4).

CONCLUSIONS

Antarctic AO rates ranged from 0.52 to 140 nM day^{-1} and are higher than rates previously reported for other austral waters (Scotia Sea, southern Indian Ocean). AASW AOA populations oxidize ammonia at higher rates than those in WW (Figure 3.3b); however, on average AO rates were highest and most consistent in CDW samples (Figures 2f, 3b). AO rates from CDW populations have not been measured previously, leading to underestimates of the global nitrification rate. Archaeal *amoA* transcripts were more abundant in AASW and WW samples than in CDW samples (Figures 3.3a, B.9b) despite lower average AO rates. Transcript abundance was 0.02 - 40% of *amoA* gene abundance across all water masses – this is greater than or equal to values reported from studies of the Pacific Ocean and the Baltic Sea. Despite this large dynamic range, we only found a significant relationship between AO rates and transcript abundance or transcript/gene ratio in a subset of samples collected in summer, which is suggests that caution is warranted when interpreting transcript abundance or transcript to gene ratios as metabolic activity. Statistical analysis, including PCA and NMDS (Figures 3.5, B.12-13), showed clear separation between WW and CDW samples that match water mass characteristics highlighted in temperature-salinity plots (Figure B.3). The diversity of both Thaumarchaeota *rrs* and *amoA* in our samples also reflects these differences, with sequences clustering primarily by water mass (Figures 3.4, B.11). Phylogenetic composition of these populations was comparable to that reported for this region in previous studies. A distinctive characteristic of Thaumarchaeota populations in WW or AASW samples is strong dominance by one OTU, while the population is more diverse in CDW (Figures 3.2f, B.10).

ACKNOWLEDGEMENTS

We would like to thank the officers and crew of the ARSV *Laurence M. Gould* and the staff of Raytheon Polar Services Company for logistical support during LMG10-06 and LMG11-01, especially E. Pohlman, D. Morehouse, S. Alesandrini, T. Baldwin, and J. Miller. We greatly appreciate the assistance of R. Jellison and members of the Palmer Station 2010-2011 Summer Crew with sample collection, and thank L. Ekern, S. Moret, and C. Guest for their technical and scientific expertise on board the *LMG* and H. Ducklow and the Palmer LTER (funded through grant ANT-0823101) for additional support for LMG11-01. Additionally, we would like to thank J. Wagner, C. Givens, C. Edwardson, C. Ka'apu-Lyons, A. Bratcher, and L. Lim for assistance with sample analysis, and D. Di Iorio for assistance with sigma-t calculations and plotting. This work was supported by the US National Science Foundation through grants ANT-08-38996, OCE-0943278 (both to J.T.H.); and OCE-1129260 (to B.N.P.) and by the University of Georgia Graduate School who funded sample analysis through a 2011 Innovative and Interdisciplinary Research Grant (to B.B.T.).

REFERENCES

Alonso-Sáez L, Andersson A, Heinrich F, Bertilsson S (2011). High archaeal diversity in Antarctic circumpolar deep waters. *Environ Microbiol Rep* **3:** 689-697.

Alonso-Sáez L, Waller AS, Mende DR, Bakker K, Farnelid H, Yager PL, Lovejoy C, Tremblay JE, Potvin M, Heinrich F, Estrada M, Riemann L, Bork P, Pedrós-Alio C, Bertilsson S (2012). Role for urea in nitrification by polar marine Archaea. *Proc Nat Acad Sci USA* **109:** 17989-17994.

Baldi F, Facca C, Marchetto D, Nguyen TNM, Spurio R (2011). Diatom quantification and their distribution with salinity brines in coastal sediments of Terra Nova Bay (Antarctica). *Mar Env Res* **71:** 304-311.

Bano N, Hollibaugh JT (2000). Diversity and distribution of DNA sequences with affinity to ammonia-oxidizing bacteria of the beta subdivision of the class Proteobacteria in the Arctic Ocean. *Appl Environ Microbiol* **66:** 1960-1969.

Beman JM, Popp BN, Francis CA (2008). Molecular and biogeochemical evidence for ammonia oxidation by marine Crenarchaeota in the Gulf of California. *ISME J* **2:** 429-441.

Beman JM, Chow CE, King AL, Feng YY, Fuhrman JA, Andersson A, Bates NR, Popp BN, Hutchins DA (2011). Global declines in oceanic nitrification rates as a consequence of ocean acidification. *Proc Nat Acad Sci USA* **108:** 208-213.

Beman JM, Popp BN, Alford SE (2012). Quantification of ammonia oxidation rates and ammonia-oxidizing archaea and bacteria at high resolution in the Gulf of California and eastern tropical North Pacific Ocean. *Limnol Oceanogr* **57:** 711-726.

Bianchi M, Feliatra F, Tréguer P, Vincendeau M-A, Morvan J (1997). Nitrification rates, ammonium and nitrate distribution in upper layers of the water column and in sediments of the Indian sector of the Southern Ocean. *Deep-Sea Res Pt II* **44:** 1017-1032.

Biers EJ, Sun SL, Howard EC (2009). Prokaryotic Genomes and Diversity in Surface Ocean Waters: Interrogating the Global Ocean Sampling Metagenome. *Appl Environ Microbiol* **75:** 2221-2229.

Biller SJ, Mosier AC, Wells GF, Francis CA (2012). Global Biodiversity of Aquatic Ammonia-Oxidizing Archaea is Partitioned by Habitat. *Front Microbiol* **3:** 252.

Brzezinski MA, Nelson DM (1989). Seasonal changes in the silicon cycle within a GulfStream warm-core ring. *Deep-Sea Res* **36:** 1009-1030.

Christman GD, Cottrell MT, Popp BN, Gier E, Kirchman DL (2011). Abundance, Diversity, and Activity of Ammonia-Oxidizing Prokaryotes in the Coastal Arctic Ocean in Summer and Winter. *Appl Environ Microbiol* **77:** 2026-2034.

Church MJ, DeLong EF, Ducklow HW, Karner MB, Preston CM, Karl DM (2003). Abundance and distribution of planktonic Archaea and Bacteria in the waters west of the Antarctic Peninsula. *Limnol Oceanogr* **48:** 1893-1902.

Church MJ, Wai B, Karl DM, DeLong EF (2010). Abundances of crenarchaeal *amoA* genes and transcripts in the Pacific Ocean. *Environ Microbiol* **12:** 679-688.

Dore JE, Popp BN, Karl DM, Sansone FJ (1998). A large source of atmospheric nitrous oxide from subtropical North Pacific surface waters. *Nature* **396:** 63-66.

Ducklow HW, Baker K, Martinson DG, Quetin LB, Ross RM, Smith RC, Stammerjohn SE, Vernet M, Fraser W (2007). Marine pelagic ecosystems: the West Antarctic Peninsula. *Philos T Roy Soc B* **362:** 67-94.

Ducklow HW, Erickson M, Kelly J, Montes-Hugo M, Ribic CA, Smith RC, Stammerjohn S, Karl DM (2008). Particle export from the upper ocean over the continental shelf of the west Antarctic Peninsula: A long-term record, 1992–2007. *Deep-Sea Res Pt II* **55:** 2118-2131.

Ducklow HW, Schofield O, Vernet M, Stammerjohn S, Erickson M (2012). Multiscale control of bacterial production by phytoplankton dynamics and sea ice along the western Antarctic Peninsula: A regional and decadal investigation. *J Marine Syst* **98-99:** 26-39.

Dugdale RC, Goering JJ (1967). Uptake of new and regenerated forms of nitrogen in marine production. *Limnol Oceanogr* **12:** 196-206.

Edgar RC, Haas BJ, Clemente JC, Quince C, Knight R (2011). UCHIME improves sensitivity and speed of chimera detection. *Bioinformatics* **27:** 2194-2200.

Erguder TH, Boon N, Wittebolle L, Marzorati M, Verstraete W (2009). Environmental factors shaping the ecological niches of ammonia-oxidizing archaea. *FEMS Microbiol Rev* **33:** 855-869.

Francis CA, Roberts KJ, Beman JM, Santoro AE, Oakley BB (2005). Ubiquity and diversity of ammonia-oxidizing archaea in water columns and sediments of the ocean. *Proc Natl Acad Sci USA* **102:** 14683-14688.

Francis CA, Beman JM, Kuypers MMM (2007). New processes and players in the nitrogen cycle: the microbial ecology of anaerobic and archaeal ammonia oxidation. *ISME J* **1:** 19-27.

Gifford SM, Sharma S, Rinta-Kanto JM, Moran MA (2011). Quantitative analysis of a deeply sequenced marine microbial metatranscriptome. *ISME J* **5:** 461-472.

Hofmann EE, Klinck JM (1998). Hydrography and circulation of the Antarctic continental shelf: 150°E to the Greenwich meridian. In: Robinson AR, Brink KH (eds). The Sea. Wiley. pp 997-1042.

Hollibaugh JT, Gifford SM, Moran MA, Ross MJ, Sharma S, Tolar BB (2014). Seasonal variation in the metratranscriptomes of a Thaumarchaeota population from SE USA coastal waters. *ISME J* **8:** 685-698.

Hu A, Jiao N, Zhang C (2011). Community structure and function of planktonic Crenarchaeota: Changes with depth in the South China Sea. *Microb Ecol* **62:** 549-563.

Jones MN (1984). Nitrate Reduction by Shaking with Cadmium - Alternative to Cadmium Columns. *Water Res* **18:** 643-646.

Kalanetra KM, Bano N, Hollibaugh JT (2009). Ammonia-oxidizing Archaea in the Arctic Ocean and Antarctic coastal waters. *Environ Microbiol* **11:** 2434-2445.

Karner MB, DeLong EF, Karl DM (2001). Archaeal dominance in the mesopelagic zone of the Pacific Ocean. *Nature* **409:** 507-510.

Kirchman DL, Elifantz H, Dittel AI, Malmstrom RR, Cottrell MT (2007). Standing stocks and activity of Archaea and Bacteria in the western Arctic Ocean. *Limnol Oceanogr* **52:** 495-507.

Klindworth A, Pruesse E, Schweer T, Peplies J, Quast C, Horn M, Glockner FO (2012). Evaluation of general 16S ribosomal RNA gene PCR primers for classical and next-generation sequencing-based diversity studies. *Nucl Acids Res* **41:** e1.

Labrenz M, Sintes E, Toetzke F, Zumsteg A, Herndl GJ, Seidler M, Jürgens K (2010). Relevance of a crenarchaeotal subcluster related to *Candidatus* Nitrosopumilus maritimus to ammonia oxidation in the suboxic zone of the central Baltic Sea. *ISME J* **4:** 1496-1508.

Ludwig W, Strunk O, Westram R, Richter L, Meier H, Yadhukumar, Buchner A, Lai T, Steppi S, Jobb G, Forster W, Brettske I, Gerber S, Ginhart AW, Gross O, Grumann S, Hermann S, Jost R, Konig A, Liss T, Lussmann R, May M, Nonhoff B, Reichel B, Strehlow R, Stamatakis A, Stuckmann N, Vilbig A, Lenke M, Ludwig T, Bode A, Schleifer KH (2004). ARB: a software environment for sequence data. *Nucl Acids Res* **32:** 1363-1371.

Luo HW, Tolar BB, Swan BK, Zhang CLL, Stepanauskas R, Moran MA, Hollibaugh JT (2014). Single-cell genomics shedding light on marine Thaumarchaeota diversification. *ISME J* **8:** 732-736.

Luria CM, Ducklow HW, Amaral-Zettler LA (2014). Marine bacterial, archaeal and eukaryotic diversity and community structure on the continental shelf of the western Antarctic Peninsula. *Aquat Microb Ecol* **73:** 107-121.

Martinson DG, Stammerjohn SE, Iannuzzi RA, Smith RC, Vernet M (2008). Western Antarctic Peninsula physical oceanography and spatio-temporal variability. *Deep-Sea Res Pt II* **55:** 1964-1987.

Massana R, Taylor LJ, Murray AE, Wu KY, Jeffrey WH, DeLong EF (1998). Vertical distribution and temporal variation of marine planktonic archaea in the Gerlache Strait, Antarctica, during early spring. *Limnol Oceanogr* **43:** 607-617.

Mincer TJ, Church MJ, Taylor LT, Preston C, Karl DM, DeLong EF (2007). Quantitative distribution of presumptive archaeal and bacterial nitrifiers in Monterey Bay and the North Pacific Subtropical Gyre. *Environ Microbiol* **9:** 1162-1175.

Murray AE, Preston CM, Massana R, Taylor LT, Blakis A, Wu K, DeLong EF (1998). Seasonal and spatial variability of bacterial and archaeal assemblages in the coastal waters near Anvers Island, Antarctica. *Appl Environ Microbiol* **64:** 2585-2595.

Murray AE, Wu KY, Moyer CL, Karl DM, DeLong EF (1999a). Evidence for circumpolar distribution of planktonic Archaea in the Southern Ocean. *Aquat Microb Ecol* **18:** 263-273.

Nguyen TNM, Berzano M, Gualerzi CO, Spurio R (2011). Development of molecular tools for the detection of freshwater diatoms. *J Microbiol Methods* **84:** 33-40.

Olson RJ (1980). Nitrate and Ammonium Uptake in Antarctic Waters. *Limnol Oceanogr* **25:** 1064-1074.

Olson RJ (1981). N-15 Tracer Studies of the Primary Nitrite Maximum. *J Mar Res* **39:** 203-226.

Pedneault E, Galand PE, Potvin M, Tremblay J-É, Lovejoy C (2014). Archaeal *amoA* and *ureC* genes and their transcriptional activity in the Arctic Ocean. *Sci Rep* **4:** 1-10.

Pester M, Rattei T, Flechl S, Gröngröft A, Richter A, Overmann J, Reinhold-Hurek B, Loy A, Wagner M (2012). *amoA*-based consensus phylogeny of ammonia-oxidizing archaea and deep sequencing of *amoA* genes from soils of four different geographic regions. *Environ Microbiol* **14:** 525-539.

Popp BN, Sansone FJ, Rust TM, Merritt DA (1995). Determination of Concentration and Carbon Isotopic Composition of Dissolved Methane in Sediments and Nearshore Waters. *Anal Chem* **67:** 405-411.

Poretsky RR, Gifford S, Rinta-Kanto J, Vila-Costa M, Moran MA (2009). Analyzing gene expression from marine microbial communities using environmental transcriptomics. *J Vis Exp* **24**: e1086.

Prosser JI, Nicol GW (2008). Relative contributions of archaea and bacteria to aerobic ammonia oxidation in the environment. *Environ Microbiol* **10:** 2931-2941.

Quast C, Pruesse E, Yilmaz P, Gerken J, Schweer T, Yarza P, Peplies J, Glockner FO (2013). The SILVA ribosomal RNA gene database project: improved data processing and web-based tools. *Nucl Acids Res* **41:** D590-596.

Santoro AE, Casciotti KL, Francis CA (2010). Activity, abundance and diversity of nitrifying archaea and bacteria in the central California Current. *Environ Microbiol* **12:** 1989-2006.

Schlitzer R (2014). Ocean Data View, 4.6.0 edn.

Schloss PD, Westcott SL, Ryabin T, Hall JR, Hartmann M, Hollister EB, Lesniewski RA, Oakley BB, Parks DH, Robinson CJ, Sahl JW, Stres B, Thallinger GG, Van Horn DJ, Weber CF (2009). Introducing mothur: Open-source, platform-independent, community-supported software for describing and comparing microbial communities. *Appl Environ Microbiol* **75:** 7537-7541.

Schloss PD, Gevers D, Westcott SL (2011). Reducing the effects of PCR amplification and sequencing artifacts on 16S rRNA-based studies. *PLoS ONE* **6:** e27310.

Sigman DM, Casciotti KL, Andreani M, Barford C, Galanter M, Böhlke JK (2001). A Bacterial Method for the Nitrogen Isotopic Analysis of Nitrate in Seawater and Freshwater. *Anal Chem* **73:** 4145-4153.

Sintes E, Bergauer K, De Corte D, Yokokawa T, Herndl GJ (2013). Archaeal *amoA* gene diversity points to distinct biogeography of ammonia-oxidizing Crenarchaeota in the ocean. *Environ Microbiol* **15:** 1647-1658.

Smith JM, Casciotti KL, Chavez FP, Francis CA (2014a). Differential contributions of archaeal ammonia oxidizer ecotypes to nitrification in coastal surface waters. *ISME J***:** 1-14.

Smith JM, Chavez FP, Francis CA (2014b). Ammonium uptake by phytoplankton regulates nitrification in the sunlit ocean. *PLoS ONE* **9:** e108173.

Solórzano L (1969). Determination of Ammonia in Natural Waters by the Phenolhypochlorite Method. *Limnol Oceanogr* **14:** 799-801.

Strickland JDH, Parsons TR (1972). Determination of Reactive Silicate. In: Stevenson JC (ed). A Practical Handbook of Seawater Analysis, 2nd edn. Fisheries Research Board of Canada: Ottawa, Canada. pp 65-70.

Tolar BB, King GM, Hollibaugh JT (2013). An analysis of thaumarchaeota populations from the northern Gulf of Mexico. *Front Microbiol* **4:** 72.

Ward BB (2008). Nitrification in Marine Systems. In: Capone DG, Bronk DA, Mulholland MR, Carpenter E (eds). Nitrogen in the Marine Environment, 2nd edn. Elsevier. pp 199-261.

Ward BB (2011). Nitrification in the Ocean. In: Ward BB, Arp DJ, Klotz MG (eds). Nitrification. ASM Press: Washington, D.C. pp 325-345.

Wells LE, Deming JW (2003). Abundance of Bacteria, the Cytophaga-Flavobacterium cluster and Archaea in cold oligotrophic waters and nepheloid layers of the Northwest Passage, Canadian Archipelago. *Aquat Microb Ecol* **31:** 19-31.

Williams TJ, Long E, Evans F, Demaere MZ, Lauro FM, Raftery MJ, Ducklow H, Grzymski JJ, Murray AE, Cavicchioli R (2012). A metaproteomic assessment of winter and summer bacterioplankton from Antarctic Peninsula coastal surface waters. *ISME J* **6:** 1883-1900.

Wuchter C, Abbas B, Coolen MJL, Herfort L, van Bleijswijk J, Timmers P, Strous M, Teira E, Herndl GJ, Middelburg JJ, Schouten S, Damste JSS (2006). Archaeal nitrification in the ocean. *Proc Natl Acad Sci USA* **103:** 12317-12322.

Yakimov MM, La Cono V, Denaro R (2009). A first insight into the occurrence and expression of functional amoA and accA genes of autotrophic and ammonia-oxidizing bathypelagic Crenarchaeota of Tyrrhenian Sea. *Deep-Sea Res Pt II* **56:** 748-754.

Yakimov MM, La Cono V, Smedile F, DeLuca TH, Juarez S, Ciordia S, Fernandez M, Albar JP, Ferrer M, Golyshin PN, Giuliano L (2011). Contribution of crenarchaeal autotrophic ammonia oxidizers to the dark primary production in Tyrrhenian deep waters (Central Mediterranean Sea). *ISME J* **5:** 945-961.

Yool A, Martin AP, Fernández C, Clark DR (2007). The significance of nitrification for oceanic new production. *Nature* **447:** 999-1002.

Figure 3.1: Thaumarchaeota abundance in spring (Sept 2010) compared to summer (Jan 2011). Gene abundance is plotted as a ratio of Thaumarchaeota *rrs* to *amoA*, against depth. Shapes represent water masses sampled, including Upper Antarctic Surface Water (UAASW; circles), Lower AASW (LAASW, filled squares) and Winter Water (WW; open squares), and Circumpolar Deep Water (CDW; triangles). Spring samples are filled dark grey and black; summer samples are filled light grey or white.

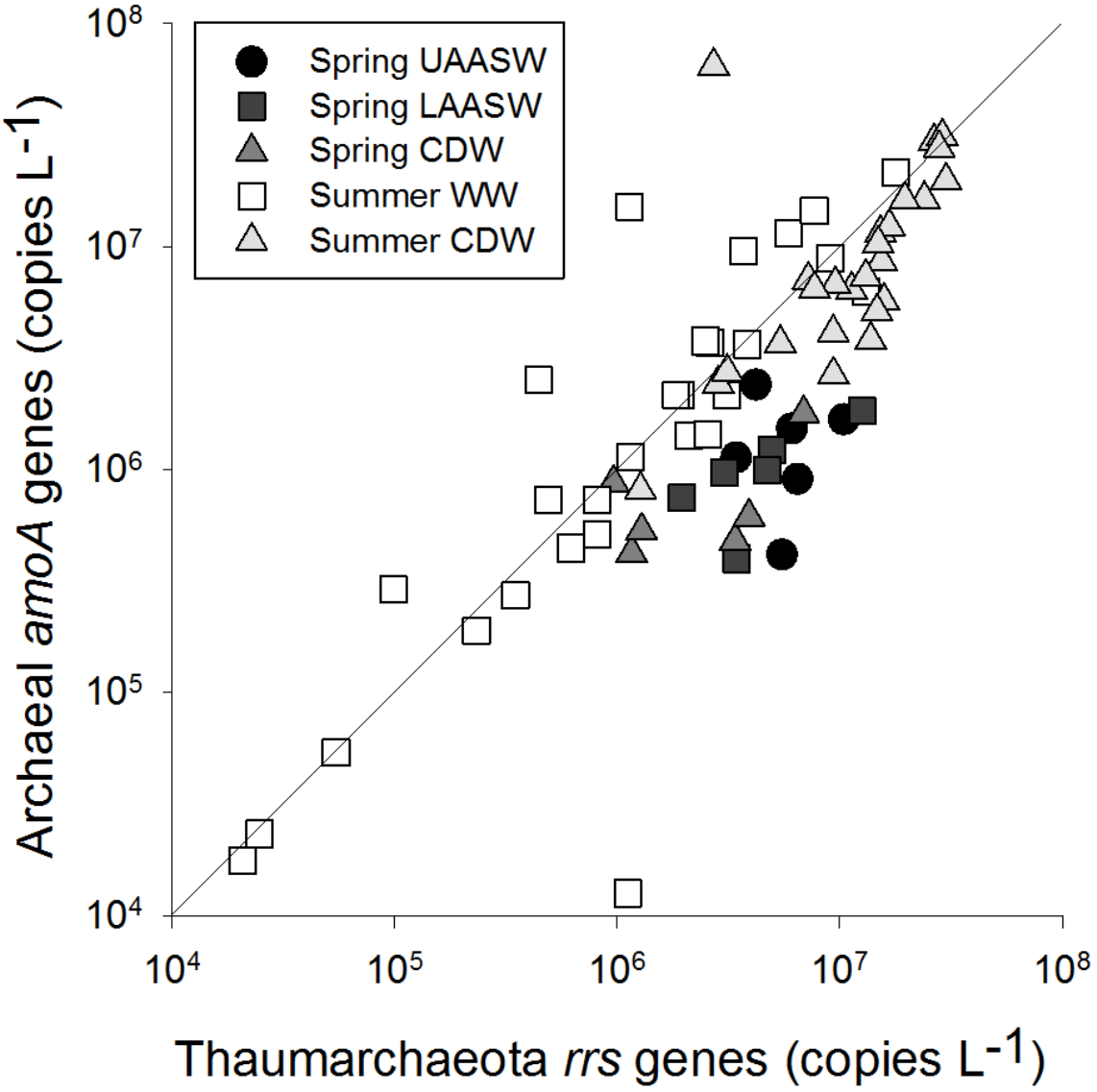
Spring UAASW
Spring LAASW
Spring CDW
Summer WW
Summer CDW
Archaeal amoA genes (copies L-1)
Thaumarchaeota rrs genes (copies L-1)
10^8
10^7
10^6
10^5
10^4

Figure 3.2: Spatial distribution of ammonia oxidation during LMG 11-01.

Distribution of Archaea *amoA* gene **(a-b)** and transcript **(c-d)** abundance, and ammonia oxidation rates **(e-f)** in WW **(a, c, e)** and CDW **(b, d, f)** water masses of the Palmer LTER study region from summer (January 2011). Color scales are identical for each data type. Spatial plots were created with DIVA gridding using Ocean Data View (Schlitzer, 2014).

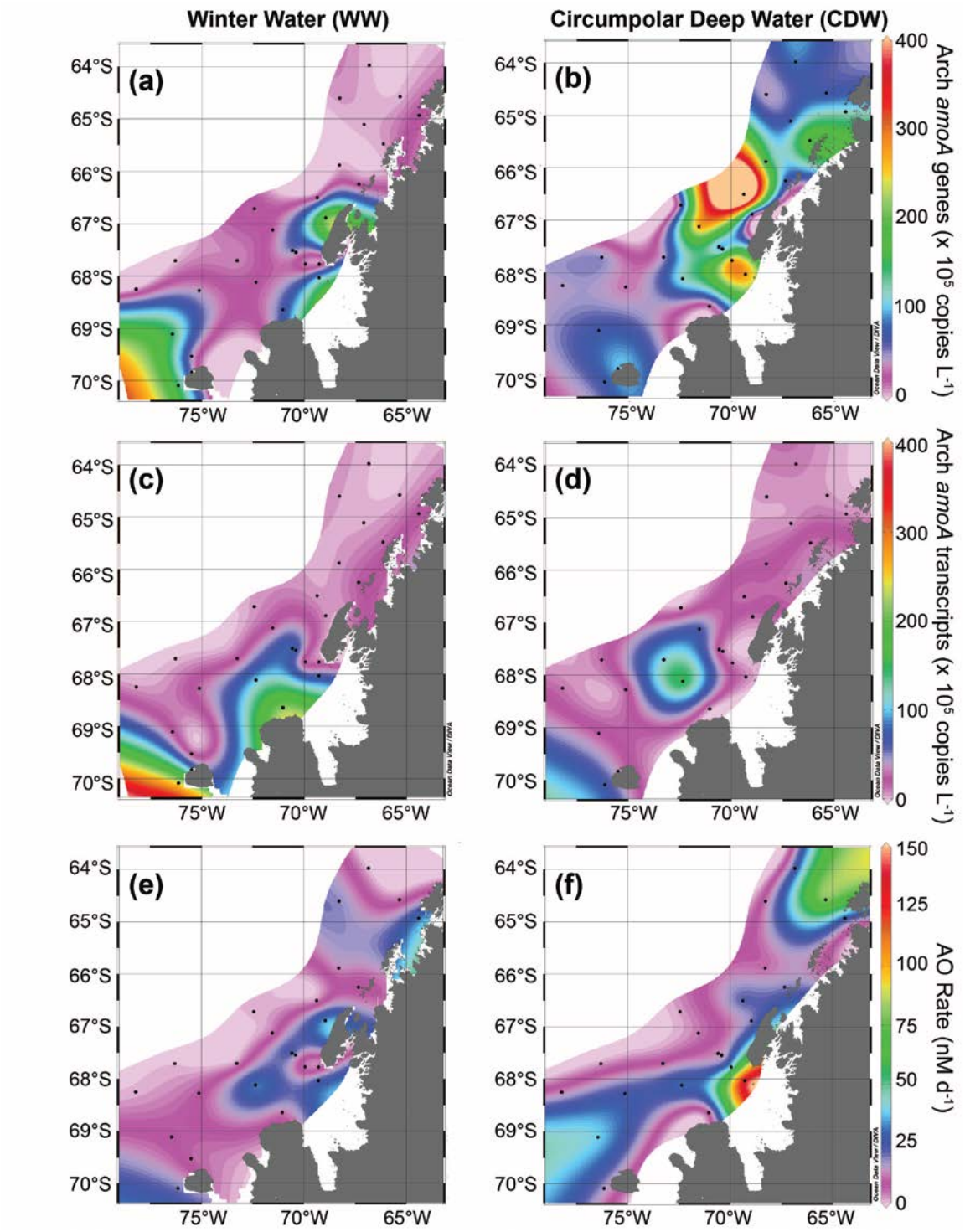
Winter Water (WW)
Circumpolar Deep Water (CDW)
(a)
(b)
(c)
(d)
(e)
(f)
64°S
65°S
66°S
67°S
68°S
69°S
70°S
75°W
70°W
65°W
Arch amoA genes (x 10⁵ copies L⁻¹)
Arch amoA transcripts (x 10⁵ copies L⁻¹)
AO Rate (nM d⁻¹)
0
100
200
300
400
0
25
50
75
100
125
150

Figure 3.3: Thaumarchaeota activity in the Southern Ocean. (a) qPCR-estimated archaeal *amoA* gene versus transcript abundance by season (the 1:1 line indicates which populations were more transcriptionally active; samples that fall above this line have more transcripts per *amoA* gene), and ^{15}N-ammonia oxidation rates plotted against **(b)** archaeal *amoA* gene abundance and **(c)** the ratio of *amoA* transcripts (mRNA) to genes (DNA).

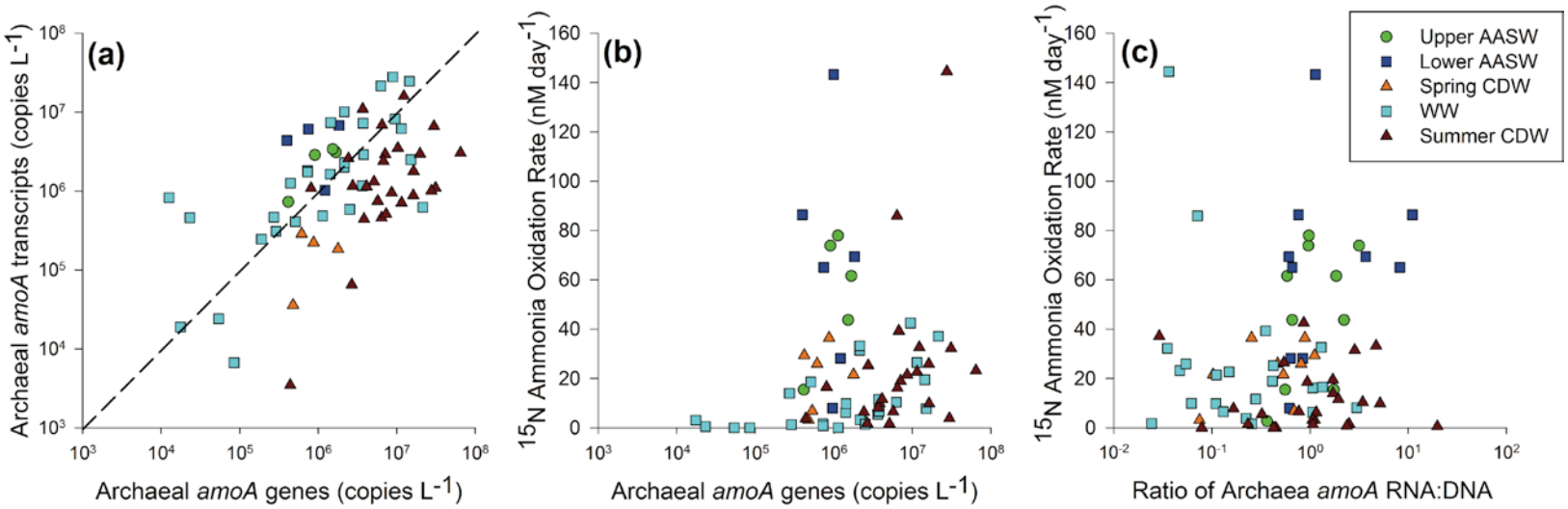
(a)
Archaeal amoA transcripts (copies L-1)
Archaeal amoA genes (copies L-1)
(b)
15N Ammonia Oxidation Rate (nM day-1)
Archaeal amoA genes (copies L-1)
(c)
15N Ammonia Oxidation Rate (nM day-1)
Ratio of Archaea amoA RNA:DNA
Upper AASW
Lower AASW
Spring CDW
WW
Summer CDW

Figure 3.4: Phylogenetic tree of archaeal *amoA* genes. Partial sequences (359 bp) of Thaumarchaeota *amoA* genes were obtained by pyrosequencing and were aligned against the Pester *et al.* (2012) database with OTUs defined at 97% similarity. Numbers following each OTU give the number of sequences and % of total sequences it represents. For the four major clusters, additional notations indicate % of sequences from each water mass (AASW, WW, CDW) sampled. OTU color indicates the water mass that contributed the most sequences in the OTU. Dashed boxes represent archaeal *amoA* groups A (surface water) and B (deep water) as defined in Francis *et al.* (2005). Only bootstrap values ≥ 50% are shown.

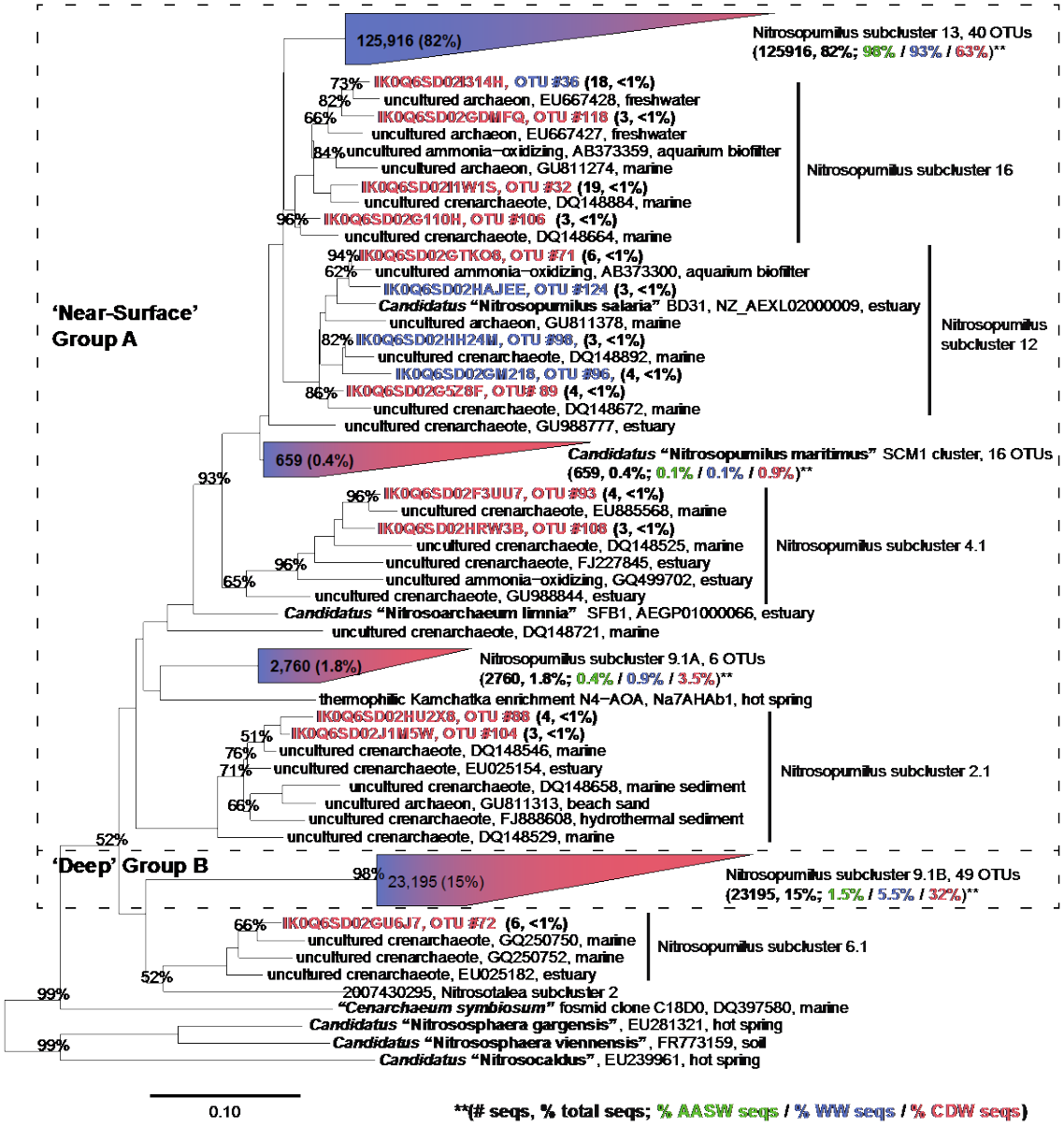
125,916 (82%)
Nitrosopumilus subcluster 13, 40 OTUs
(125916, 82%; 98% / 93% / 63%)**
73% IK0Q6SD02I314H, OTU #36 (18, <1%)
82% uncultured archaeon, EU667428, freshwater
66% IK0Q6SD02GD4IFQ, OTU #118 (3, <1%)
uncultured archaeon, EU667427, freshwater
84% uncultured ammonia−oxidizing, AB373359, aquarium biofilter
uncultured archaeon, GU811274, marine
IK0Q6SD02I1W1S, OTU #32 (19, <1%)
uncultured crenarchaeote, DQ148884, marine
96% IK0Q6SD02G110H, OTU #106 (3, <1%)
uncultured crenarchaeote, DQ148664, marine
Nitrosopumilus subcluster 16
94% IK0Q6SD02GTKO6, OTU #71 (6, <1%)
62% uncultured ammonia−oxidizing, AB373300, aquarium biofilter
IK0Q6SD02HAJEE, OTU #124 (3, <1%)
'Near-Surface'
Group A
Candidatus "Nitrosopumilus salaria" BD31, NZ_AEXL02000009, estuary
uncultured archaeon, GU811378, marine
82% IK0Q6SD02HH24M, OTU #98, (3, <1%)
uncultured crenarchaeote, DQ148892, marine
IK0Q6SD02GM218, OTU #96, (4, <1%)
86% IK0Q6SD02G5Z8F, OTU# 89 (4, <1%)
uncultured crenarchaeote, DQ148672, marine
uncultured crenarchaeote, GU988777, estuary
Nitrosopumilus subcluster 12
659 (0.4%)
Candidatus "Nitrosopumilus maritimus" SCM1 cluster, 16 OTUs
(659, 0.4%; 0.1% / 0.1% / 0.9%)**
93%
96% IK0Q6SD02F3UU7, OTU #93 (4, <1%)
uncultured crenarchaeote, EU885568, marine
IK0Q6SD02HRW3B, OTU #108 (3, <1%)
uncultured crenarchaeote, DQ148525, marine
96% uncultured crenarchaeote, FJ227845, estuary
65% uncultured ammonia−oxidizing, GQ499702, estuary
uncultured crenarchaeote, GU988844, estuary
Nitrosopumilus subcluster 4.1
Candidatus "Nitrosoarchaeum limnia" SFB1, AEGP01000066, estuary
uncultured crenarchaeote, DQ148721, marine
2,760 (1.8%)
Nitrosopumilus subcluster 9.1A, 6 OTUs
(2760, 1.8%; 0.4% / 0.9% / 3.5%)**
thermophilic Kamchatka enrichment N4−AOA, Na7AHAb1, hot spring
IK0Q6SD02HU2X8, OTU #88 (4, <1%)
51% IK0Q6SD02J1WW5W, OTU #104 (3, <1%)
76% uncultured crenarchaeote, DQ148546, marine
71% uncultured crenarchaeote, EU025154, estuary
uncultured crenarchaeote, DQ148658, marine sediment
66% uncultured archaeon, GU811313, beach sand
uncultured crenarchaeote, FJ888608, hydrothermal sediment
uncultured crenarchaeote, DQ148529, marine
Nitrosopumilus subcluster 2.1
52%
'Deep' Group B
98% 23,195 (15%)
Nitrosopumilus subcluster 9.1B, 49 OTUs
(23195, 15%; 1.5% / 5.5% / 32%)**
66% IK0Q6SD02GU6J7, OTU #72 (6, <1%)
uncultured crenarchaeote, GQ250750, marine
uncultured crenarchaeote, GQ250752, marine
uncultured crenarchaeote, EU025182, estuary
Nitrosopumilus subcluster 6.1
52%
99% 2007430295, Nitrosotalea subcluster 2
"Cenarchaeum symbiosum" fosmid clone C18D0, DQ397580, marine
Candidatus "Nitrososphaera gargensis", EU281321, hot spring
Candidatus "Nitrososphaera viennensis", FR773159, soil
99% Candidatus "Nitrosocaldus", EU239961, hot spring
0.10
**(# seqs, % total seqs; % AASW seqs / % WW seqs / % CDW seqs)

Figure 3.5: Multivariate statistical analysis of data from LMG 11-01. (a) Principal Components Analysis (PCA) plot of samples in environmental data space, displayed on the first two axes, representing 52.3% of the variability in the dataset; AO Rate = ammonia oxidation rate, LTER.Line = Palmer LTER Line (proxy for north-south variability), BSi = biogenic silica. **(b)** Nonmetric Multidimensional Scaling (NMDS) plot of samples distributed by qPCR-based estimates of gene abundance; AOB = ammonia-oxidizing bacteria, Thaum = Thaumarchaeota. Both graphs highlight distinct features of Winter Water (WW) and Circumpolar Deep Water (CDW) masses in the Southern Ocean.

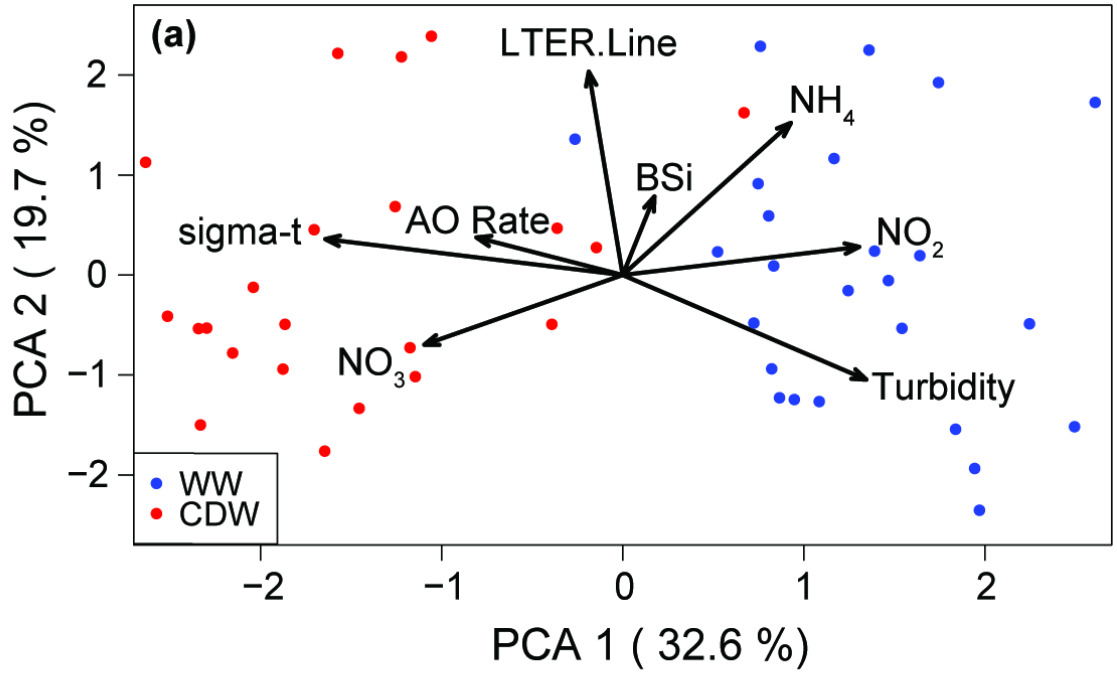
(a)
LTER.Line
NH4
BSi
AO Rate
sigma-t
NO2
NO3
Turbidity
WW
CDW
PCA 2 (19.7 %)
PCA 1 (32.6 %)
2
1
0
−1
−2
−2
−1
0
1
2

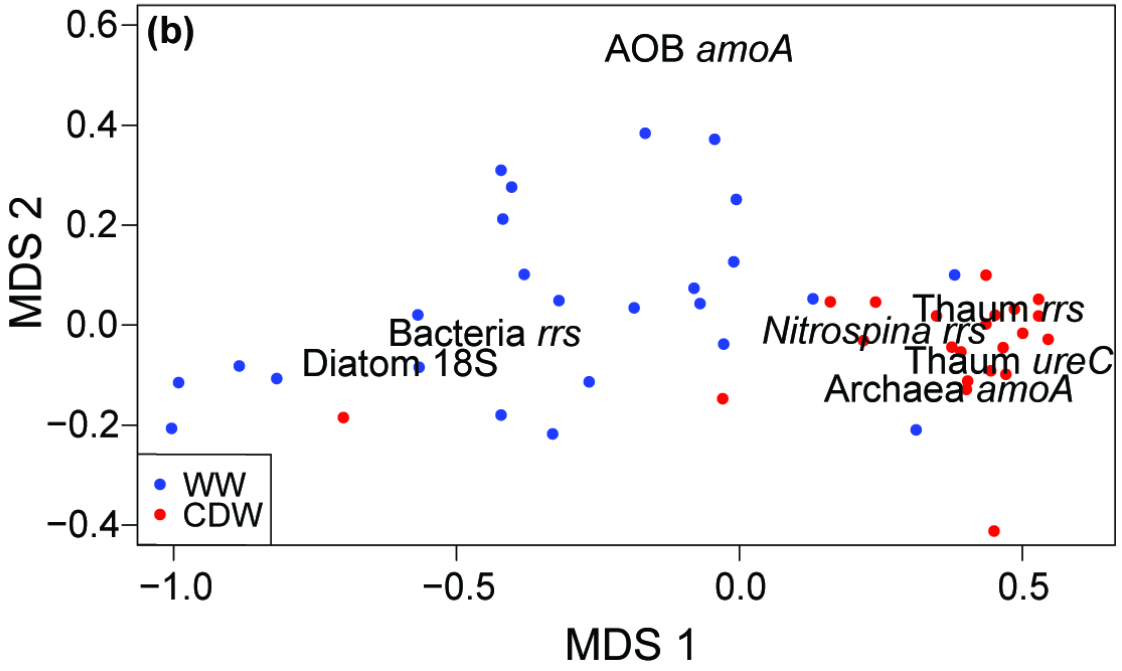
(b)
AOB amoA
Bacteria rrs
Diatom 18S
Nitrospina rrs
Thaum rrs
Thaum ureC
Archaea amoA
WW
CDW
MDS 2
MDS 1
0.6
0.4
0.2
0.0
−0.2
−0.4
−1.0
−0.5
0.0
0.5

CHAPTER 4

SHORT-TERM VARIABILITY OF AMMONIA OXIDIZER POPULATIONS IN A SE USA SALT MARSH ENVIRONMENT[1]

[1] Tolar, B.B., P. Hagan, M.J. Ross, and J.T. Hollibaugh. To be submitted to *The ISME Journal*.

ABSTRACT

We have monitored the population dynamics of ammonia-oxidizing Archaea (AOA, Thaumarchaeota), ammonia-oxidizing Bacteria (AOB), and nitrite-oxidizing Bacteria (NOB) since 2008 at Marsh Landing, Sapelo Island, Georgia; initially quarterly then at weekly intervals. AOA display pronounced, mid-summer blooms (~100-fold increases in abundance to 6.4% of prokaryotes) at this site, while AOB and NOB population levels remain low and do not fluctuate seasonally. The maximum net population growth rate we observed was ~0.4 d^{-1}, comparable to specific growth rates reported in pure cultures (0.78 d^{-1}). The bloom has a profound effect on the composition of dissolved inorganic nitrogen (DIN), with a peak of NO_x concentration (up to 14 μM) in August correlating with AOA abundance. Similar patterns in DIN dynamics are observed at other salt marsh-dominated sites along the SE USA coast, suggesting that this is a general characteristic of these ecosystems. Statistical analysis indicates that the bloom coincides with a variety of factors (temperature, dissolved oxygen, pH) associated with the summer increase in net ecosystem heterotrophy reported for the study site.

INTRODUCTION

Excess nitrogen loading to watersheds and the transport of fixed nitrogen through them has resulted in increasing dissolved inorganic nitrogen (DIN) concentrations in coastal regions (Seitzinger *et al.*, 2005; Turner *et al.*, 2012; Verity, 2002), leading to eutrophication and the formation of "dead zones" (Diaz and Rosenberg, 2008; Doney, 2010). A significant fraction of this nitrogen introduced to the coastal zone is removed by denitrification, a process that can depend on nitrification – the oxidation of ammonia

to nitrite and subsequently nitrate (Seitzinger, 1988; Seitzinger *et al.*, 2005). Nitrification and denitrification can both release nitrous oxide (N_2O), a powerful greenhouse gas (Santoro *et al.*, 2011). Because of these connections to other processes, nitrification is central to the global nitrogen cycle and to ameliorating the effects of excess nitrogen loading in coastal waters (reviewed in Capone *et al.*, 2008; Ward, 2011).

Our understanding of the organisms responsible for nitrification has expanded greatly over the last decade with the adoption of molecular techniques by microbial ecologists and geochemists. Formerly, ammonia-oxidizing Bacteria (AOB) – composed of members of the β-Proteobacteria (e.g. *Nitrosomonas*, *Nitrosospira*) and γ-Proteobacteria (*Nitrosococcus*) – were assumed to be the dominant nitrifiers in marine systems (Kowalchuk and Stephen, 2001; Ward *et al.*, 2000). However, recent evidence from a variety of sources (reviewed in Francis *et al.*, 2007; Jetten, 2001; Schleper, 2010; Ward, 2011) strongly suggests that Archaea of the phylum Thaumarchaeota are chemoautotrophs, depending on ammonia oxidation to supply the energy needed for carbon fixation (also referred to as "ammonia-oxidizing Archaea", or AOA). Although they are abundant and widely distributed (Church *et al.*, 2010; Fuhrman and Hagström, 2008; Karner *et al.*, 2001; Nicol *et al.*, 2011), Thaumarchaeota have proven difficult to culture. Thus what is known about Thaumarchaeota is based primarily on inferences from culture-independent methods (e.g., Francis *et al.*, 2005; Hollibaugh *et al.*, 2011; Kirchman *et al.*, 2007; Ouverney and Fuhrman, 2000; Teira *et al.*, 2004; Treusch *et al.*, 2005; Tully *et al.*, 2012; Venter *et al.*, 2004; Wuchter *et al.*, 2006) and our understanding of their metabolism has remained obscure until recently.

Successful isolation of a thaumarchaeote into pure culture has led to an understanding of the basic features of their ecophysiology (Könneke *et al.*, 2005; Martens-Habbena *et al.*, 2009; Urakawa *et al.*, 2010; Walker *et al.*, 2010a), including their reliance on ammonia oxidation to generate energy; however, the factors controlling their seasonal abundance are not known (Biller *et al.*, 2012; Pitcher *et al.*, 2011). A seasonal cycle of Thaumarchaeota populations – abundant in surface waters in the winter, essentially absent in the summer – is commonly observed at high latitudes (Alonso-Sáez *et al.*, 2008; Herfort *et al.*, 2007; Massana *et al.*, 1998; Pitcher *et al.*, 2011; Wuchter *et al.*, 2006). Most authors have attributed this difference to competition with phytoplankton for nutrients during the onset of the spring bloom, or with Bacteria that are hypothesized to be able to respond more rapidly to this bloom than Thaumarchaeota (Church *et al.*, 2003; Massana *et al.*, 1998; Murray *et al.*, 1998; Pitcher *et al.*, 2011; Wuchter *et al.*, 2006).

Analysis of a set of samples collected quarterly at a site on the Georgia coast (Marsh Landing, Sapelo Island; Gifford *et al.*, 2011; Hollibaugh *et al.*, 2011) revealed a midsummer Thaumarchaeota "bloom", as Thaumarchaeota were ~3 orders of magnitude more abundant in August than in samples collected in February, May or November (Hollibaugh *et al.*, 2011; Hollibaugh *et al.*, 2014). The bloom was detected consistently; however, the relative magnitude of the peak in Thaumarchaeota abundance varied from year to year. This could be due either to true interannual variation in the magnitude of the bloom or, since samples were always collected during the same week in early August, to interannual variation in the timing of the bloom, which may have peaked before or after sampling in some years. In order to distinguish between these two alternatives, we

began sampling Marsh Landing on a weekly basis in March 2011. We report here the results of those analyses and of accompanying changes in DIN concentrations. Comparison of annual cycles of DIN speciation at this site with data from other locations along the eastern United States suggests that these blooms are a common feature of salt marsh-dominated coastal ecosystems.

MATERIALS AND METHODS

Study site

The Duplin River is a salt marsh-dominated tidal creek on the Georgia (USA) coast (Figure 4.1). Despite the name, freshwater inflow to the Duplin "River" is via groundwater from adjacent Sapelo Island or rainfall – it is overall a marine system. Near-surface water samples were collected approximately weekly at or around the daytime high tide from a floating dock at Marsh Landing (31° 25' 4.08 N, 81° 17' 43.26 W) from March 2011 to September 2014 (Table C.1). Samples were collected by immersing a clean, sample-rinsed, 2 L wide-mouth bottle ~10 cm below the surface with the mouth facing upstream. The sample was taken directly to the laboratory where it was filtered through 0.2 um pore size, 47 mm diameter Durapore (polyvinylidene difluoride, PVDF; Millipore) filters. The filter was placed in a 4 oz. WhirlPak bag (Nasco) with 1 mL of lysis buffer (0.75 M sucrose, 40 mM EDTA, 50 mM Tris; pH 8.3) then frozen at -20°C before storage at -80°C until analysis. Fifty milliliters of the filtrate was retained for nutrient analysis, frozen and stored as above.

DNA extraction and qPCR analysis

In the laboratory, an additional 1 mL lysis buffer was added to filters (2 mL total) prior to DNA extraction. Briefly, a phenol:chloroform extraction method was used (Bano and Hollibaugh, 2000) with a two-step enzymatic lysis (1st: lysozyme, 50 mg/mL; 2nd: 20% SDS + proteinase K, 20 mg/mL) performed within the WhirlPak bag following Tolar *et al.* (2013). DNA was eluted in Tris-EDTA buffer (pH 8.0) and diluted 10-1000X to reduce PCR inhibitors found in coastal samples prior to using the eluent as template for quantitative PCR (qPCR). The amount of dilution for each sample was determined from measuring the abundance of Bacteria 16S rRNA (*rrs*) by qPCR across a dilution series and selecting the dilution yielding the highest, and thus presumably non-inhibited, concentration estimate. Primers and protocols used to determine the abundance of Bacteria (*rrs*), Archaea (Marine Group I Archaea, or Thaumarchaeota, *rrs*), AOA (archaeal *amoA*), AOB (β-proteobacterial *amoA*), and NOB (*Nitrospina rrs*) using an iCycler iQ5 (BioRad, Inc.) have been described in detail previously (Hollibaugh *et al.*, 2014; Kalanetra *et al.*, 2009; Tolar *et al.*, 2013; Table C.2). Calculation of gene copies per 1,000 cells used the following equation:

$$\frac{\text{Gene copies}}{\text{1000 cells}} = \frac{\text{Average of triplicate qPCR (copies } \mu L^{-1})}{\left(\frac{Bacteria\ rrs}{1.8} + \frac{Archaea\ rrs}{1.0}\right)} \times 1000$$

Bacteria and Archaea *rrs* are corrected for the total *rrs* copies per genome after Biers *et al*. (2009) and genome queries using the Integrated Microbial Genomes (IMG) database (http://img.jgi.doe.gov/), respectively.

Net population growth rates (μ, d^{-1}) were calculated from the time series of qPCR estimates for Thaumarchaeota *rrs* and *amoA* abundance using an exponential growth model:

$$N = N_0 \times e^{\mu t} \text{ or } \mu = \frac{\ln(\frac{N_t}{N_{t-1}})}{\Delta t} \text{ or } \mu = \frac{\ln(N_t) - \ln(N_{t-1})}{\Delta t}$$

Where N is the standardized qPCR abundance (here, copies L^{-1}, smoothed using a centered, 3-point running average) at time *t*, and Δt represents the difference between sampling dates in days.

Environmental data

Dissolved inorganic nitrogen (DIN) concentrations were determined spectrophotometrically using previously described methods for ammonia (NH_4; Solórzano, 1969), nitrite (NO_2) and nitrite + nitrate (NO_x; Jones, 1984; Strickland and Parsons, 1972). Urea was also measured during the last year and a half of the study (April 2013 to August 2014) with the diacetylmonoxime method (Rahmatullah and Boyde, 1980) as modified for use in seawater by Mulvenna and Savidge (1992). Additional environmental data were obtained from the Sapelo Island National Estuarine Research Reserve web portal (http://cdmo.baruch.sc.edu), including water quality (water temperature, salinity, pH, dissolved oxygen concentration, chlorophyll fluorescence, and turbidity sampled at 15 min intervals using YSI 6600 datasondes), meteorological (air temperature, wind speed, photosynthetically-active radiation or PAR, and precipitation sampled at 15 min intervals), and nutrient (DIN, chlorophyll a, and phosphate concentrations sampled over two days monthly) data. SINERR data were block averaged

over the day of sampling (water quality, meteorological) or by month (nutrients) for use in statistical analyses that follow.

Statistical analysis

Principal components analysis (PCA; environmental data) and non-metric multi-dimensional scaling (MDS; gene abundance data) were performed in R (http://www.r-project.org/) after Hollibaugh *et al*. (2014) using the prcomp (stats package; PCA), metaMDS (vegan package; MDS), and lm (stats package; pairwise linear regression) commands. Data were classified by season based on standard date ranges for spring (March 21 – June 20), summer (June 21 – September 20), fall (September 21 – December 20), and winter (December 21 – March 20).

RESULTS

An annual peak in Thaumarchaeota abundance was observed in August or September of each of the four years sampled (Figure 4.2a), consistent with previous observations at this site (Figure C.1; Hollibaugh *et al.*, 2014). Weekly sampling reveals that the bloom commences in June with rapid growth during July, with abundance peaking in mid-August before declining more slowly throughout the fall. By late November, Thaumarchaeota relative abundance returned to background levels (10^6 *amoA* and *rrs* copies L^{-1}), 1% of their abundance during the peak of the bloom when they were present at 10^8 copies L^{-1} (Figure 4.2a; Table 4.1; Table C.1). In contrast, neither AOB (β-Proteobacteria) nor NOB (*Nitrospina*) show the same seasonal dynamic (Figure 4.2b), with AOB *amoA* and NOB *rrs* gene abundances remaining between 10^5-10^6 copies L^{-1}

throughout the year (Table 4.1; Table C.1). AOB gene abundance increases slightly (on average 4-fold) in summer, but this is much less than the 35- to 95-fold increases of Thaumarchaeota genes. Little or no seasonality was observed with Bacteria *rrs* (2-fold average increase in summer) or Diatom 18S rRNA (1.4-fold increase from spring to summer, 1.8-fold increase from fall to winter; Figure C.2; Table 4.1).

This spike in AOA abundance [and presumably activity – additional samples collected less frequently indicate an increase in both nitrification rates (4.1 to 450 nmole L^{-1} d^{-1}) and *amoA* transcription in August versus April 2012 (Figure D.3)] is accompanied by a biogeochemical signal from nitrite concentrations that increase relative to the background (0.1 to 2 μM) during the AOA bloom (Figures 4.2c, 4.3). We attribute this to enhanced ammonia oxidation over nitrite oxidation, since the NOB population of *Nitrospina* (which is the most abundant NOB at Sapelo Island – GCE-LTER MIRADA Data, http://vamps.mbl.edu/portals/mirada/mirada.php) does not appear to respond to the 'pulse' of nitrite (Figure 4.2b). Further, the net accumulation of NO_x in the system (Figures 4.2c, 4.3) suggests that the AOA bloom also uncouples ammonia oxidation from denitrification.

Seasonality of AOA abundance and DIN composition was reflected in both Multi-Dimensional Scaling (MDS) and Principal Components Analysis (PCA), respectively. A strong separation along the primary MDS axis (MDS1) clearly shows that AOA abundance relative to other microbial groups is distinct during the summer and fall (Figure 4.4a). Variation in the abundance of both Thaumarchaeota *rrs* and AOA *amoA* genes contributed significantly to the distribution of samples on MDS1 (0.57 and 0.51,

respectively), while all other microbial genes measured did not contribute significantly to either MDS axis (Table C.3).

Environmental data (Figure 4.2d; Figure C.3) also distinguished samples by the season in which they were collected (Figure 4.4b), with the primary PCA axis (PC1) explaining 28% of the overall variance (Table C.4). Nitrite – the product of ammonia oxidation – was a strong contributor to PC1 (+0.68, correlation coefficient), in addition to nitrate (+0.53) and total DIN (+0.56). Dissolved oxygen (DO; -0.92), temperature (both air and water; +0.81 and +0.88, respectively), and pH (-0.85) – all variables with strong seasonal signals – were also components of PC1. Other variables were significantly correlated with other PC axes (PC axes 1-5 were statistically significant; Table C.4), including ammonia (PC2; +0.44). Comparison of PCA and NMDS scores showed that seasonal variation in AOA *amoA* and Thaumarchaeota *rrs* was most strongly correlated with variation in PC1 ($R^2 = 0.37$, $p < 0.0001$; Figure C.4a; Table C.5), while the correlations with other PC axes were very weak ($r^2 < 0.1$), even if statistically significant. When we subdivided our environmental data (water quality, nutrient, or meteorological data), we observed primarily the same patterns as above (Figures C.4b-d, C.5a-c). The only exception was that ammonia became more significant when using nutrient data alone (+0.79, PC2 – 29% of variance explained; Table C.4), and was negatively correlated with AOA gene abundance ($R^2 = 0.30$, $p < 0.0001$; Figure C.4d, Table C.5).

We also used the SINERR nutrient dataset (monthly) for PCA (Figure C.5d), which added phosphate (PO_4) and chlorophyll *a* (chl *a*) to measurements of nitrite, NO_x, and ammonia, which we collected separately. The results using SINERR nutrients agreed with analysis using only our nutrient data (Table C.4), with nitrite (+0.77) and NO_x

(+0.91) as significant contributors to PC1 (45% of variance explained), as well as PO_4 (+0.83). PC2, which explained 26% of the variance in the dataset, was comprised of ammonia (+0.75), nitrite (-0.52), and chl *a* (-0.67). However, only PC1 showed a significant correlation ($R^2 = 0.55$, $p < 0.0001$) with a reduced MDS1 from SINERR data only (Figures C.4e, C.5f; Table C.5), indicating that increased [PO_4], in addition to nitrite and NO_x, is indicative of AOA bloom conditions. Finally, PCA of a reduced data set (April 2013 to August 2014) to include urea concentrations measured at Marsh Landing (Figure C.5e) showed that the abundance of Thaumarchaeota *rrs* (but not *amoA*; Figures C.4f, C.5g; Table C.4) was negatively correlated with urea ($R^2 = 0.39$, $p < 0.0001$; Table C.5). Urea was also a significant contributor (+0.58) to PC2 in this analysis (23% of variance explained; Table C.4) along with nitrite (-0.75), which again positively correlated with Thaumarchaeota genes.

We estimated the net population growth rate (which would include mortality, as well as dilution and mixing in the water column) of Thaumarchaeota using both *rrs* and *amoA* genes (Figure 4.5a-c). During the bloom (summer), net growth rates averaged 0.04 d^{-1} for *amoA* (range = -0.13 to 0.42 d^{-1}) and 0.06 d^{-1} for *rrs* (range = -0.13 to 0.43 d^{-1}), and showed a strong linear relationship ($R^2 = 0.58$, Figure 4.5d). This net population growth rate was highest in 2013, but all years showed similar growth rates during the immediate bloom period (Figure 4.5c, Table 4.1). Calculated net population growth rates of *amoA* and *rrs* during non-bloom periods averaged 0.01 and 0.02 d^{-1} for spring, -0.03 and -0.05 d^{-1} for fall, and -0.01 and -0.01 d^{-1} for winter, respectively.

DISCUSSION

The magnitude of the mid-summer peak in Thaumarchaeota relative abundance at Marsh Landing varies from year to year (Figure 4.2a). This appears to be a true interannual variation in the magnitude of the bloom rather than an artifact of the quarterly sampling interval used previously (Hollibaugh *et al.*, 2011; Hollibaugh *et al.*, 2014). The data also provide evidence for a shift in the start date and duration of the bloom, depending on the year sampled. A similar seasonal "bloom" of Thaumarchaeota has been described in the coastal North Sea, where shifts in the timing of population maxima were also observed, though in winter (Herfort *et al.*, 2007; Pitcher *et al.*, 2011; Wuchter *et al.*, 2006). Mid-winter blooms have also been reported elsewhere, including the Southern Ocean (Church *et al.*, 2003; Murray *et al.*, 1998), Arctic Ocean (Alonso-Sáez *et al.*, 2008), California coastal waters (Massana *et al.*, 1997), and Mediterranean coastal waters near Spain (Galand *et al.*, 2010). In contrast, the Thaumarchaeota bloom in Georgia coastal waters occurs in mid-summer, making it a relatively unique event.

The North Sea Thaumarchaeota bloom is quite abrupt, ramping up over a period of weeks (Wuchter *et al.*, 2006) to approximately the same standing stock each year (Pitcher *et al.*, 2011). Elevated abundances persisted for a period of 2-3 months before rapidly returning to background levels. The start of each of these two blooms is comparable, with rapid growth at the beginning; however, the Sapelo Island bloom shows a more gradual rate of decline throughout the fall as the bloom is dispersed (Figure 4.2a). Calculated net population growth rates from Sapelo Island (Figure 4.5) approached the maximum growth rate of the "*Candidatus* Nitrosopumilus maritimus" SCM1 culture (0.78 d^{-1}; Könneke *et al.*, 2005). In both the North Sea and around Sapelo Island,

Thaumarchaeota transition from being members of the "rare biosphere" (Sogin *et al.*, 2006) to being one of the more abundant taxa in the sample, which appears to differ significantly from the apparently stable population abundance observed in the mesopelagic ocean and oxygen minimum zones (e.g., Church *et al.*, 2010; Fuhrman and Hagström, 2008; Karner *et al.*, 2001; Mincer *et al.*, 2007; Santoro *et al.*, 2010; Ward, 2011). The population dynamics we observed at Marsh Landing (and at the other sites mentioned above) contrast with the model of Archaea adaptive strategy proposed by Valentine *et al*. (2007), which posits that Archaea are adapted to cope with "environmental stress" by maintaining low but constant activity (k- versus r-selected) and thus are not a group whose population dynamics should include significant blooms.

The Thaumarchaeota bloom in Georgia coastal waters seems to cause an uncoupling of the two steps of the nitrification process, resulting in the transient accumulation of nitrite produced by AOA before it can be oxidized to nitrate by NOB (Figures 4.2c, 4.3). This was also observed with winter blooms in the North Sea (Pitcher *et al.*, 2011; Wuchter *et al.*, 2006), and the Mediterranean Sea (Galand *et al.*, 2010); however, these studies did not include NOB data to test the hypothesis that NOB populations don't increase in response to enhanced nitrite fluxes resulting from elevated ammonia oxidation during AOA blooms. The geochemical response was most obvious in Georgia coastal waters in 2011 (Figure 4.3) when AOA abundances were the highest observed in the time series, and NO_x and NO_2 concentrations measured in September reached a maximum of 14.0 and 6.8 μM respectively (most of the NO_x measured in these samples is NO_2). This proposed uncoupling appears to be a common feature of the nitrogen dynamics of many east-coast, salt-marsh dominated estuaries, as GCE-LTER

data from Sapelo and Doboy Sounds (Figure 4.6a) show a similar, August spike in NO_x concentration (nitrite was not determined). The same pattern is seen in nitrite data from the Skidaway River (near Savannah GA; Figure 4.6b) and from the Virginia Coast Reserve (VCR) LTER (Figure 4.6c). All of these data sets also show interannual variation in the magnitude of the spike. Interestingly, samples from river-dominated systems (Altamaha Sound, GCE-LTER data; Neuse River, Mod-Mon program/H. Paerl laboratory; or the CM stations in the VCR-LTER data set, data not shown) do not display this seasonal pattern, or it is obscured by the high DIN concentrations (10's to 100's of μM) found in these systems.

The variation in nitrogen dynamics that seems to accompany these population-level responses might also affect the fluxes of other compounds (e.g. the greenhouse gas N_2O) and other geochemical processes (e.g. anammox, an anaerobic process that uses nitrite to oxidize ammonia directly). Santoro *et al*. (2010) demonstrated a link between AOA abundance and N_2O concentration in waters off the central California coast. Further work presented in Santoro *et al*. (2011) demonstrated that the N_2O was derived from AOA metabolism and that AOA (versus denitrifiers, which also produce N_2O as a by-product of their metabolism) are the major source of the oceanic N_2O flux. Walker *et al*. (2010b) have shown significant N_2O production in hypoxic waters of the northern Gulf of Mexico, and further that N_2O production was enhanced by water column oxygenation associated with the passage of a storm. Tolar *et al*. (2013) showed that this area contains high populations of AOA (Chapter 2). If changes in DO affect N_2O production, the Thaumarchaeota bloom at Sapelo Island may be a significant source of N_2O, since decreased [DO] was characteristic of environmental conditions during the

bloom. Nitrite concentration has been shown to be a key regulator of the abundance of anammox organisms in sediment (Dang *et al.*, 2010), suggesting the possibility that the anammox assemblage in sediment around Sapelo Island might respond to the nitrite pulse resulting from the AOA bloom. However, the net accumulation of NOx during the fall suggests that neither anammox nor denitrification is occurring at the same rate as ammonia oxidation in this system. As neither NO_2, NO_3, nor carbon should be limiting during this period, some other factor must be involved in limiting anammox and denitrification in this system.

What causes a Thaumarchaeota "bloom"? The increase in coastal North Sea populations coincides with a mid-winter increase in ammonia (Pitcher *et al.*, 2011); however, ammonia concentrations were higher (1-3 μM) than those thought to limit AOA growth (≤ 10 nM; Martens-Habbena *et al.*, 2009), and both temperature and salinity co-varied with Thaumarchaeota abundance. In the Puget Sound estuary, Thaumarchaeota abundance and nitrification was correlated with low ammonia concentrations (Urakawa *et al.*, 2014); however, we did not observe a connection of our bloom with ammonia in Sapelo Island waters (Figure 4.4b; Tables C.4, C.5). At our study site, there is strong seasonal variation in temperature, DO, phosphate and to some degree, pH (Figure 4.2d; Figure C.3). All of these variables were significantly correlated to Thaumarchaeota gene abundance during the bloom (Figure 4.4b; Tables C.4, C.5), indicating a strong connection based solely on conditions present during summer. Temperature was significant in our analysis, as in Pitcher *et al.* (2011, but with the opposite sign), and additional laboratory experiments with AOA enrichments from Sapelo Island (Appendix C; Figure C.6) show a link between temperature and ammonia oxidation (and also nitrite

oxidation), in contrast to findings in Hood Canal, Washington (Horak *et al.*, 2013). Phosphate concentrations have also been indicated as potentially important to Thaumarchaeota distributions based on the absence of a high-affinity phosphate uptake operon in metagenomic samples from the Gulf of Maine (Tully *et al.*, 2012).

Other environmental variables that seemed to characterize the summer bloom period included elevated NOx, which are cycled through nitrification. Increases in nitrite and nitrate should correspond to increased Thaumarchaeota abundances if AOA are actively oxidizing ammonia, which is indicated by data presented here and by rates measured during the bloom period (Appendix E). We found only a negative correlation between levels of ammonia and abundances of AOA or AOB on the Georgia coast (Figure C.4d, Table C.5), indicating that ammonia concentrations cannot be used reliably to predict the prevalence of one type of ammonia oxidizer, as proposed by Urukawa *et al.* (2010). Thaumarchaeota abundance on Sapelo Island also showed a negative correlation with urea concentrations, perhaps indicating oxidation of urea as suggested by Alonso-Sáez *et al.* (2012) although rates measured during the bloom are much slower than ammonia oxidation rates (Chapter 5; Tables 5.1, 5.2; Figures 5.2a-b, 5.3).

The water at Marsh Landing is turbid (Figure 4.1; Figure C.3d), but Thaumarchaeota abundance was not significantly correlated with turbidity in the analysis presented here and preliminary experiments (Hollibaugh lab, unpublished data) have shown that the Thaumarchaeota population is not associated with particles, indicating that the summer peak is not simply a resuspension event. Surveys around Sapelo Island in August (2011, 2012) indicate that the AOA bloom is a general feature of the salt marsh-

dominated portions of the GCE-LTER study site (Figure D.4). Offshore transects also indicate that the bloom is restricted to shallow coastal waters (Figure D.5).

As no single variable emerged in our statistical analyses, Thaumarchaeota blooms may ultimately be controlled by combinations of environmental factors indicating general ecosystem characteristics such as net heterotrophy. Alternatively, the bloom may be triggered by an unidentified single variable that co-varies with those that we measured, for example trace metal availability (Amin *et al.*, 2013; Jacquot *et al.*, 2014; Morel and Price, 2003; Mosier and Francis, 2008). This highlights the necessity for more substantial exploration of factors controlling Thaumarchaeota growth, both inside and outside the laboratory. The consistent, annual bloom of Thaumarchaeota on Sapelo Island makes it an ideal site to study how environmental conditions can impact this abundant and important phylum of marine nitrifying organisms. Additionally, this site appears to be representative of coastal estuaries throughout the southeastern United States, and therefore whatever factor(s) control(s) the Sapelo Island bloom could have a profound effect on a much greater scale.

CONCLUSIONS

We have shown here that Thaumarchaeota populations in an estuary on the Georgia coast have a dynamic range in abundance of at least 2 orders of magnitude, featuring an annual summer bloom. In contrast, the dynamic range of AOB or NOB abundance during the same period of observation was much smaller, < 1 order of magnitude. This bloom of AOA leads to a rapid oxidation of ammonia, depletion of the NH_4 pool and accumulation of NO_x. Ammonia oxidation apparently outstrips the ability

of NOB to oxidize the NO_2 produced further to NO_3 and of denitrifiers to remove the accumulated NOx by conversion to N_2. Although we found significant relationships between Thaumarchaeota abundance and various environmental factors (e.g., temperature, DO, pH, PO_4, DIN), most of these factors co-vary and no single factor clearly explained the seasonal distribution of Thaumarchaeota. Ammonium concentration did not stand out as a significant variable at Sapelo Island, in contrast to its relationship with Thaumarchaeota blooms in the North Sea. Finally, as evidenced by the August nitrite spikes at other locations, the bloom seems to happen at more or less the same time up and down the US east coast, which suggests that whatever is driving it is a pervasive annual phenomenon, at least in salt marsh environments.

ACKNOWLEDGEMENTS

We would like to thank D. Duckett, A. Bratcher, E. Malagón, L. Lim, J. Cheek, and M. Wolfe for assistance with sample analysis in the laboratory. Additionally, we would like to thank the GCE-LTER personnel, especially M. Alber, and the staff at the UGA Marine Institute on Sapelo Island, especially M. Booth, G. Townsend, and M. Price. Funding for this research was provided by U.S. National Science Foundation grants OCE 09-43278 (EAGER), OCE 13-35838, and OPP 08-38996 to J.T.H.

REFERENCES

Alonso-Sáez L, Sanchez O, Gasol JM, Balagué V, Pedrós-Alio C (2008). Winter-to-summer changes in the composition and single-cell activity of near-surface Arctic prokaryotes. *Environ Microbiol* **10:** 2444-2454.

Alonso-Sáez L, Waller AS, Mende DR, Bakker K, Farnelid H, Yager PL, Lovejoy C, Tremblay JE, Potvin M, Heinrich F, Estrada M, Riemann L, Bork P, Pedrós-Alio C, Bertilsson S (2012). Role for urea in nitrification by polar marine Archaea. *Proc Nat Acad Sci USA* **109:** 17989-17994.

Amin SA, Moffett JW, Martens-Habbena W, Jacquot JE, Han Y, Devol A, Ingalls AE, Stahl DA, Armbrust EV (2013). Copper requirements of the ammonia-oxidizing archaeon *Nitrosopumilus maritimus* SCM1 and implications for nitrification in the marine environment. *Limnol Oceanogr* **58:** 2037-2045.

Bano N, Hollibaugh JT (2000). Diversity and distribution of DNA sequences with affinity to ammonia-oxidizing bacteria of the beta subdivision of the class Proteobacteria in the Arctic Ocean. *Appl Environ Microbiol* **66:** 1960-1969.

Biers EJ, Sun SL, Howard EC (2009). Prokaryotic Genomes and Diversity in Surface Ocean Waters: Interrogating the Global Ocean Sampling Metagenome. *Appl Environ Microbiol* **75:** 2221-2229.

Biller SJ, Mosier AC, Wells GF, Francis CA (2012). Global Biodiversity of Aquatic Ammonia-Oxidizing Archaea is Partitioned by Habitat. *Front Microbiol* **3:** 252.

Capone DG, Bronk DA, Mulholland MR, Carpenter EJ (eds) (2008) Nitrogen in the Marine Environment. Academic Press: Burlington, MA.

Church MJ, DeLong EF, Ducklow HW, Karner MB, Preston CM, Karl DM (2003). Abundance and distribution of planktonic Archaea and Bacteria in the waters west of the Antarctic Peninsula. *Limnol Oceanogr* **48:** 1893-1902.

Church MJ, Wai B, Karl DM, DeLong EF (2010). Abundances of crenarchaeal *amoA* genes and transcripts in the Pacific Ocean. *Environ Microbiol* **12:** 679-688.

Dang H, Chen R, Wang L, Guo L, Chen P, Tang Z, Tian F, Li S, Klotz MG (2010). Environmental factors shape sediment anammox bacterial communities in hypernutrified Jiaozhou Bay, China. *Appl Environ Microbiol* **76:** 7036-7047.

Diaz R, Rosenberg R (2008). Spreading Dead Zones and Consequences for Marine Ecosystems. *Science* **321:** 926-929.

Doney SC (2010). The growing human footprint on coastal and open-ocean biogeochemistry. *Science* **328:** 1512-1516.

Francis CA, Roberts KJ, Beman JM, Santoro AE, Oakley BB (2005). Ubiquity and diversity of ammonia-oxidizing archaea in water columns and sediments of the ocean. *Proc Natl Acad Sci USA* **102:** 14683-14688.

Francis CA, Beman JM, Kuypers MMM (2007). New processes and players in the nitrogen cycle: the microbial ecology of anaerobic and archaeal ammonia oxidation. *ISME J* **1:** 19-27.

Fuhrman JA, Hagström Å (2008). Bacterial and archaeal community structure and its patterns. Microbial Ecology of the Oceans, 2nd edn. Wiley. pp 45-90.

Galand PE, Gutiérrez-Provecho C, Massana R, Gasol JM, Casamayor EO (2010). Inter-annual recurrence of archaeal assemblages in the coastal NW Mediterranean Sea. *Limnol Oceanogr* **55:** 2117-2125.

Gifford SM, Sharma S, Rinta-Kanto JM, Moran MA (2011). Quantitative analysis of a deeply sequenced marine microbial metatranscriptome. *ISME J* **5:** 461-472.

Herfort L, Schouten S, Abbas B, Veldhuis MJW, Coolen MJL, Wuchter C, Boon JP, Herndl GJ, Damste JSS (2007). Variations in spatial and temporal distribution of Archaea in the North Sea in relation to environmental variables. *FEMS Microbiol Ecol* **62:** 242-257.

Hollibaugh JT, Gifford S, Sharma S, Bano N, Moran MA (2011). Metatranscriptomic analysis of ammonia-oxidizing organisms in an estuarine bacterioplankton assemblage. *ISME J* **5:** 866-878.

Hollibaugh JT, Gifford SM, Moran MA, Ross MJ, Sharma S, Tolar BB (2014). Seasonal variation in the metratranscriptomes of a Thaumarchaeota population from SE USA coastal waters. *ISME J* **8:** 685-698.

Horak RE, Qin W, Schauer AJ, Armbrust EV, Ingalls AE, Moffett JW, Stahl DA, Devol AH (2013). Ammonia oxidation kinetics and temperature sensitivity of a natural marine community dominated by Archaea. *ISME J* **7:** 2023-2033.

Jacquot JE, Horak REA, Amin SA, Devol A, Ingalls AE, Armbrust EV, Stahl DA, Moffett JW (2014). Assessment of the potential for copper limitation of ammonia oxidation by Archaea in a dynamic estuary. *Mar Chem* **162:** 37-49.

Jetten MSM (2001). New pathways for ammonia conversion in soil and aquatic systems. *Plant Soil* **230:** 9-19.

Jones MN (1984). Nitrate Reduction by Shaking with Cadmium - Alternative to Cadmium Columns. *Water Res* **18:** 643-646.

Kalanetra KM, Bano N, Hollibaugh JT (2009). Ammonia-oxidizing Archaea in the Arctic Ocean and Antarctic coastal waters. *Environ Microbiol* **11:** 2434-2445.

Karner MB, DeLong EF, Karl DM (2001). Archaeal dominance in the mesopelagic zone of the Pacific Ocean. *Nature* **409:** 507-510.

Kirchman DL, Elifantz H, Dittel AI, Malmstrom RR, Cottrell MT (2007). Standing stocks and activity of Archaea and Bacteria in the western Arctic Ocean. *Limnol Oceanogr* **52:** 495-507.

Könneke M, Bernhard AE, de la Torre JR, Walker CB, Waterbury JB, Stahl DA (2005). Isolation of an autotrophic ammonia-oxidizing marine archaeon. *Nature* **437:** 543-546.

Kowalchuk GA, Stephen JR (2001). Ammonia-oxidizing bacteria: a model for molecular microbial ecology. *Annu Rev Microbiol* **55:** 485-529.

Martens-Habbena W, Berube PM, Urakawa H, de la Torre JR, Stahl DA (2009). Ammonia oxidation kinetics determine niche separation of nitrifying Archaea and Bacteria. *Nature* **461:** 976-979.

Massana R, Murray AE, Preston CM, DeLong EF (1997). Vertical distribution and phylogenetic characterization of marine planktonic Archaea in the Santa Barbara Channel. *Appl Environ Microbiol* **63:** 50-56.

Massana R, Taylor LJ, Murray AE, Wu KY, Jeffrey WH, DeLong EF (1998). Vertical distribution and temporal variation of marine planktonic archaea in the Gerlache Strait, Antarctica, during early spring. *Limnol Oceanogr* **43:** 607-617.

Mincer TJ, Church MJ, Taylor LT, Preston C, Karl DM, DeLong EF (2007). Quantitative distribution of presumptive archaeal and bacterial nitrifiers in Monterey Bay and the North Pacific Subtropical Gyre. *Environ Microbiol* **9:** 1162-1175.

Morel FMM, Price NM (2003). The biogeochemical cycles of trace metals in the oceans. *Science* **300:** 944-947.

Mosier AC, Francis CA (2008). Relative abundance and diversity of ammonia-oxidizing archaea and bacteria in the San Francisco Bay estuary. *Environ Microbiol* **10:** 3002-3016.

Mulvenna PF, Savidge G (1992). A modified manual method for the determination of urea in seawater using diacetylmonoxime reagent. *Estuar Coast Shelf S* **34:** 429-438.

Murray AE, Preston CM, Massana R, Taylor LT, Blakis A, Wu K, DeLong EF (1998). Seasonal and spatial variability of bacterial and archaeal assemblages in the coastal waters near Anvers Island, Antarctica. *Appl Environ Microbiol* **64:** 2585-2595.

Nicol GW, Leininger S, Schleper C (2011). Distribution and activity of ammonia-oxidizing Archaea in natural environments. In: Ward BB, Arp DJ, Klotz MG (eds). Nitrification. ASM Press: Washington, D.C. pp 157-178.

Ouverney CC, Fuhrman JA (2000). Marine planktonic Archaea take up amino acids. *Appl Environ Microbiol* **66:** 4829-4833.

Pitcher A, Wuchter C, Siedenberg K, Schouten S, Damste JSS (2011). Crenarchaeol tracks winter blooms of ammonia-oxidizing Thaumarchaeota in the coastal North Sea. *Limnol Oceanogr* **56:** 2308-2318.

Rahmatullah M, Boyde TR (1980). Improvements in the determination of urea using diacetyl monoxime; methods with and without deproteinisation. *Clin Chim Acta* **107:** 3-9.

Santoro AE, Casciotti KL, Francis CA (2010). Activity, abundance and diversity of nitrifying archaea and bacteria in the central California Current. *Environ Microbiol* **12:** 1989-2006.

Santoro AE, Buchwald C, McIlvin MR, Casciotti KL (2011). Isotopic Signature of N2O Produced by Marine Ammonia-Oxidizing Archaea. *Science* **333:** 1282-1285.

Schleper C (2010). Ammonia oxidation: different niches for bacteria and archaea? *ISME J* **4:** 1092-1094.

Seitzinger SP (1988). Denitrification in freshwater and coastal marine ecosystems: Ecological and geochemical significance. *Limnol Oceanogr* **33:** 702-724.

Seitzinger SP, Harrison JA, Dumont E, Beusen AHW, Bouwman AF (2005). Sources and delivery of carbon, nitrogen, and phosphorus to the coastal zone: An overview of Global Nutrient Export from Watersheds (NEWS) models and their application. *Global Biogeochem Cy* **19:** GB4S01.

Sogin ML, Morrison HG, Huber JA, Welch DM, Huse SM, Neal PR, Arrieta JM, Herndl GJ (2006). Microbial diversity in the deep sea and the underexplored "rare biosphere". *Proc Nat Acad Sci USA* **103:** 12115-12120.

Solórzano L (1969). Determination of Ammonia in Natural Waters by the Phenolhypochlorite Method. *Limnol Oceanogr* **14:** 799-801.

Strickland JDH, Parsons TR (1972). Determination of Reactive Silicate. In: Stevenson JC (ed). A Practical Handbook of Seawater Analysis, 2nd edn. Fisheries Research Board of Canada: Ottawa, Canada. pp 65-70.

Teira E, Reinthaler T, Pernthaler A, Pernthaler J, Herndl GJ (2004). Combining Catalyzed Reporter Deposition-Fluorescence In Situ Hybridization and Microautoradiography To Detect Substrate Utilization by Bacteria and Archaea in the Deep Ocean. *Appl Environ Microbiol* **70:** 4411-4414.

Tolar BB, King GM, Hollibaugh JT (2013). An analysis of thaumarchaeota populations from the northern Gulf of Mexico. *Front Microbiol* **4:** 72.

Treusch AH, Leininger S, Kletzin A, Schuster SC, Klenk HP, Schleper C (2005). Novel genes for nitrite reductase and Amo-related proteins indicate a role of uncultivated mesophilic crenarchaeota in nitrogen cycling. *Environ Microbiol* **7:** 1985-1995.

Tully BJ, Nelson WC, Heidelberg JF (2012). Metagenomic analysis of a complex marine planktonic thaumarchaeal community from the Gulf of Maine. *Environ Microbiol* **14:** 254-267.

Turner RE, Rabalais NN, Justić D (2012). Predicting summer hypoxia in the northern Gulf of Mexico: redux. *Mar Pollut Bull* **64:** 319-324.

Urakawa H, Martens-Habbena W, Stahl DA (2010). High Abundance of Ammonia-Oxidizing Archaea in Coastal Waters, Determined Using a Modified DNA Extraction Method. *Appl Environ Microbiol* **76:** 2129-2135.

Urakawa H, Martens-Habbena W, Huguet C, de la Torre JR, Ingalls AE, Devol AH, Stahl DA (2014). Ammonia availability shapes the seasonal distribution and activity of archaeal and bacterial ammonia oxidizers in the Puget Sound Estuary. *Limnol Oceanogr* **59:** 1321-1335.

Valentine DL (2007). Adaptations to energy stress dictate the ecology and evolution of the Archaea. *Nat Rev Microbiol* **5:** 316-323.

Venter JC, Remington K, Heidelberg JF, Halpern AL, Rusch D, Eisen JA, Wu DY, Paulsen I, Nelson KE, Nelson W, Fouts DE, Levy S, Knap AH, Lomas MW, Nealson K, White O, Peterson J, Hoffman J, Parsons R, Baden-Tillson H, Pfannkoch C, Rogers YH, Smith HO (2004). Environmental genome shotgun sequencing of the Sargasso Sea. *Science* **304:** 66-74.

Verity PG (2002). A decade of change in the Skidaway River estuary. I. Hydrography and nutrients. *Estuaries* **25:** 944-960.

Walker CB, de la Torre JR, Klotz MG, Urakawa H, Pinel N, Arp DJ, Brochier-Armanet C, Chain PSG, Chan PP, Gollabgir A, Hemp J, Hügler M, Karr EA, Könneke M, Shin M, Lawton TJ, Lowe T, Martens-Habbena W, Sayavedra-Soto LA, Lang D, Sievert SM, Rosenzweig AC, Manning G, Stahl DA (2010a). *Nitrosopumilus maritimus* genome reveals unique mechanisms for nitrification and autotrophy in globally distributed marine crenarchaea. *Proc Nat Acad Sci USA* **107:** 8818-8823.

Walker JT, Stow CA, Geron C (2010b). Nitrous oxide emissions from the gulf of Mexico hypoxic zone. *Environ Sci Technol* **44:** 1617-1623.

Ward BB, Martino DP, Diaz MC, Joye SB (2000). Analysis of ammonia-oxidizing bacteria from hypersaline Mono Lake, California, on the basis of 16S rRNA sequences. *Appl Environ Microbiol* **66:** 2873-2881.

Ward BB (2011). Nitrification in the Ocean. In: Ward BB, Arp DJ, Klotz MG (eds). Nitrification. ASM Press: Washington, D.C. pp 325-345.

Wuchter C, Abbas B, Coolen MJL, Herfort L, van Bleijswijk J, Timmers P, Strous M, Teira E, Herndl GJ, Middelburg JJ, Schouten S, Damste JSS (2006). Archaeal nitrification in the ocean. *Proc Natl Acad Sci USA* **103:** 12317-12322.

Table 4.1: Summary of gene abundances, net population growth rates, and DIN concentrations, averaged by season, for the three years sampled.

Year	Season	qPCR Data*						Growth Rate		Nutrient Data^				
		Thaum. *rrs*	Archaea *amoA*	Bacteria *rrs*	Bacteria *amoA*	*Nspina rrs*	Diatom 18S rRNA	Thaum. *rrs*	Archaea *amoA*	NO_2	NO_x	NH_4	DIN	Urea
2011	Spring	6.08E+05	2.91E+05	6.24E+09	7.98E+05	5.13E+05	4.33E+09	0.048	0.045	0.16	0.85	4.05	5.05	ND
	Summer	1.29E+08	7.37E+07	1.45E+10	7.83E+06	7.42E+05	7.25E+09	0.045	0.043	3.66	5.83	1.20	10.69	ND
	Fall	8.23E+06	8.85E+06	2.20E+09	1.73E+05	4.01E+05	1.96E+09	-0.043	-0.027	0.88	3.73	2.68	7.28	ND
2012	Winter	1.34E+06	9.40E+05	1.04E+10	3.62E+05	2.02E+05	2.84E+09	0.005	-0.018	0.03	0.47	1.25	1.77	ND
	Spring	7.11E+05	5.27E+05	4.30E+10	6.37E+05	4.15E+05	2.95E+09	0.002	0.004	0.07	0.38	1.33	1.71	ND
	Summer	9.11E+07	4.32E+07	3.08E+11	1.46E+06	1.02E+06	7.43E+09	0.047	0.030	1.13	2.20	1.14	3.34	ND
	Fall	1.06E+07	7.54E+06	1.72E+11	7.31E+05	6.98E+05	7.79E+09	-0.056	-0.050	0.58	1.85	1.99	3.83	ND
2013	Winter	2.79E+05	2.81E+05	9.03E+10	4.59E+05	4.02E+05	8.82E+09	-0.026	-0.017	0.13	0.93	2.27	3.21	ND
	Spring	1.26E+06	5.32E+05	7.05E+10	9.90E+05	6.41E+05	1.13E+10	0.030	0.017	0.20	0.93	2.03	3.48	0.54
	Summer	9.48E+07	3.19E+07	6.10E+10	8.72E+05	6.33E+05	1.12E+10	0.069	0.063	1.34	2.69	2.13	5.75	0.65
	Fall	2.30E+07	1.14E+07	3.64E+10	1.87E+05	9.64E+05	4.37E+09	-0.049	-0.024	0.85	2.27	1.68	2.39	0.35
2014	Winter	2.32E+06	4.26E+06	4.16E+10	6.89E+05	5.96E+05	1.20E+10	-0.019	0.000	0.07	0.01	0.73	0.44	0.25
	Spring	1.54E+06	4.21E+06	1.05E+11	4.41E+05	5.43E+05	8.91E+09	-0.010	-0.008	0.11	1.06	1.40	2.46	0.27
	Summer	7.61E+07	4.74E+07	1.31E+11	1.80E+06	6.56E+05	1.20E+10	0.073	0.030	0.43	1.02	1.30	2.60	0.43

*= qPCR data is copies L^{-1} filtered sample; *Nspina* = *Nitrospina* (genera of NOB).

^= Nutrient data is μM

Figure 4.1: Map of Sapelo Island, GA (USA), indicating where samples were collected weekly from a floating dock at Marsh Landing (31° 25.075' N, 81° 17.75' W). Note the turbidity of this strongly tidally mixed water.


Sapelo Sound
Blackbeard Island
National Wildlife Refuge
99
Sapelo Island,
Georgia, USA
Marsh Landing
Altamaha State
Waterfowl...
Wolf Island National
Wildlife Refuge
Map data ©2014 Google Imagery ©2014 TerraMetrics

Figure 4.2: Time series of weekly sampling at Marsh Landing, Sapelo Island, GA, showing: qPCR measurements of gene abundance for **(a)** Archaeal *amoA* and *rrs*, and **(b)** AOB *amoA* and *Nitrospina* (NOB) *rrs* (note the difference in scales for abundance); **(c)** DIN and urea concentrations; and **(d)** temperature and salinity measured from March 2011 to September 2014.

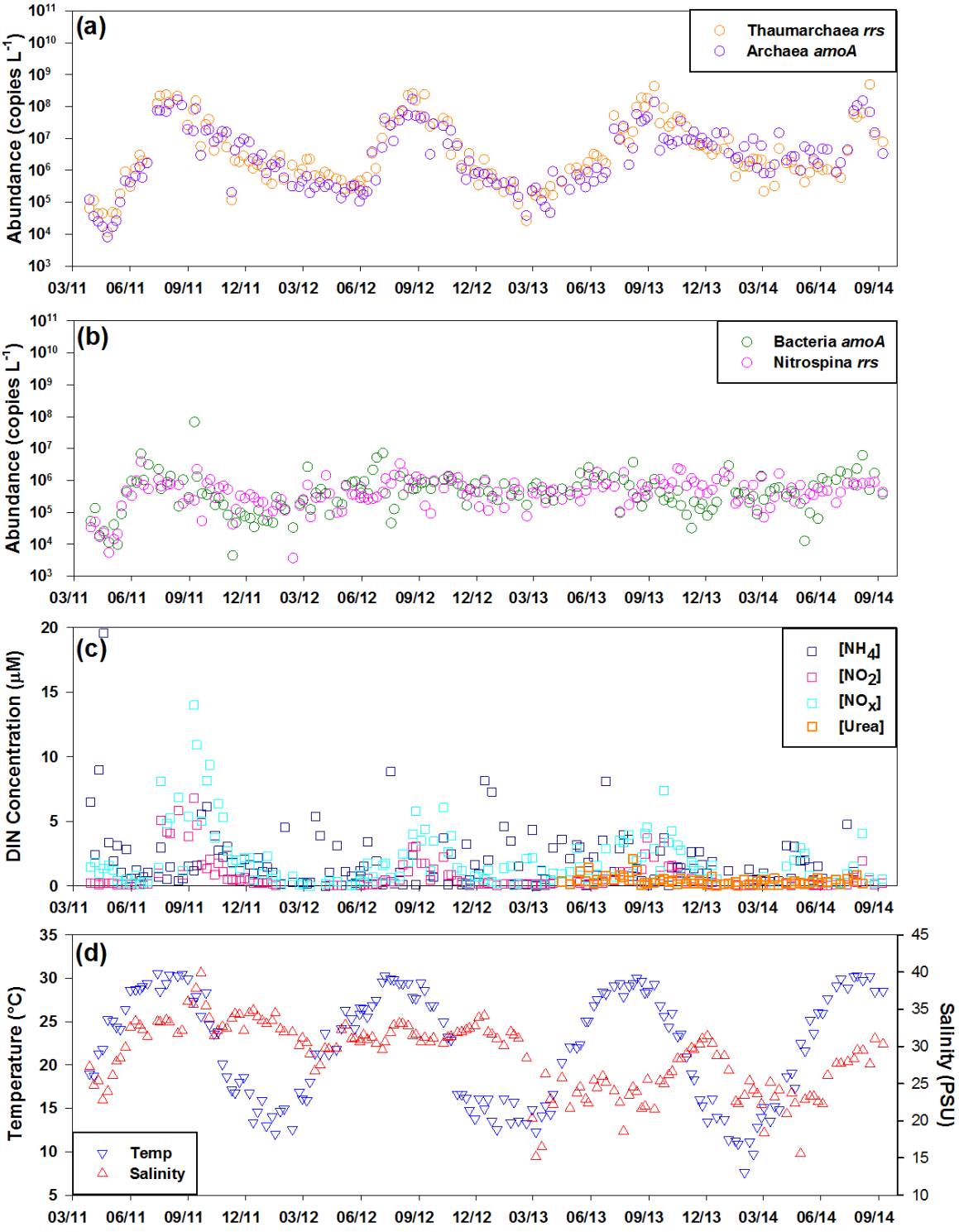
(a)
Thaumarchaea rrs
Archaea amoA
Abundance (copies L-1)
(b)
Bacteria amoA
Nitrospina rrs
Abundance (copies L-1)
(c)
[NH4]
[NO2]
[NOx]
[Urea]
DIN Concentration (µM)
(d)
Temp
Salinity
Temperature (°C)
Salinity (PSU)
03/11
06/11
09/11
12/11
03/12
06/12
09/12
12/12
03/13
06/13
09/13
12/13
03/14
06/14
09/14

Figure 4.3: DIN concentrations from weekly sampling, binned by month, averaged across the four years sampled.

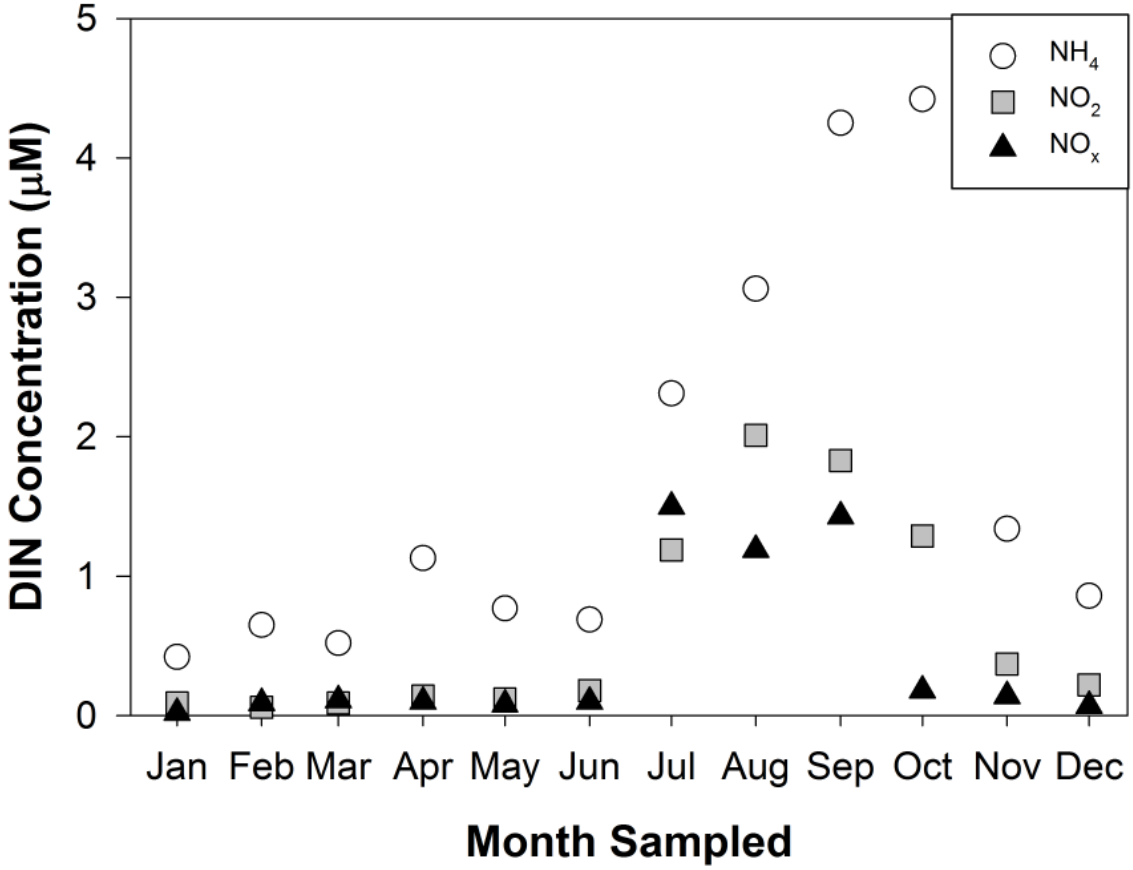
DIN Concentration (µM)
0
1
2
3
4
5
Jan
Feb
Mar
Apr
May
Jun
Jul
Aug
Sep
Oct
Nov
Dec
Month Sampled
NH4
NO2
NOx

Figure 4.4: Statistical analysis of seasonal variability in **(a)** gene abundance (Multidimensional Scaling, MDS) and **(b)** environmental variables measured, including DIN (Principal Components Analysis, PCA). Samples are represented in both plots as circles colored by the season in which each was collected. Gene names plotted in MDS space are plotted with the center of each name representing a gene's score. DO = dissolved oxygen, BP = barometric pressure, RH = relative humidity, Sal = salinity, DIN = dissolved inorganic nitrogen, Precip. = cumulative (48h) precipitation, PAR = total photosynthetically-active radiation, Wind Dir. = wind direction.

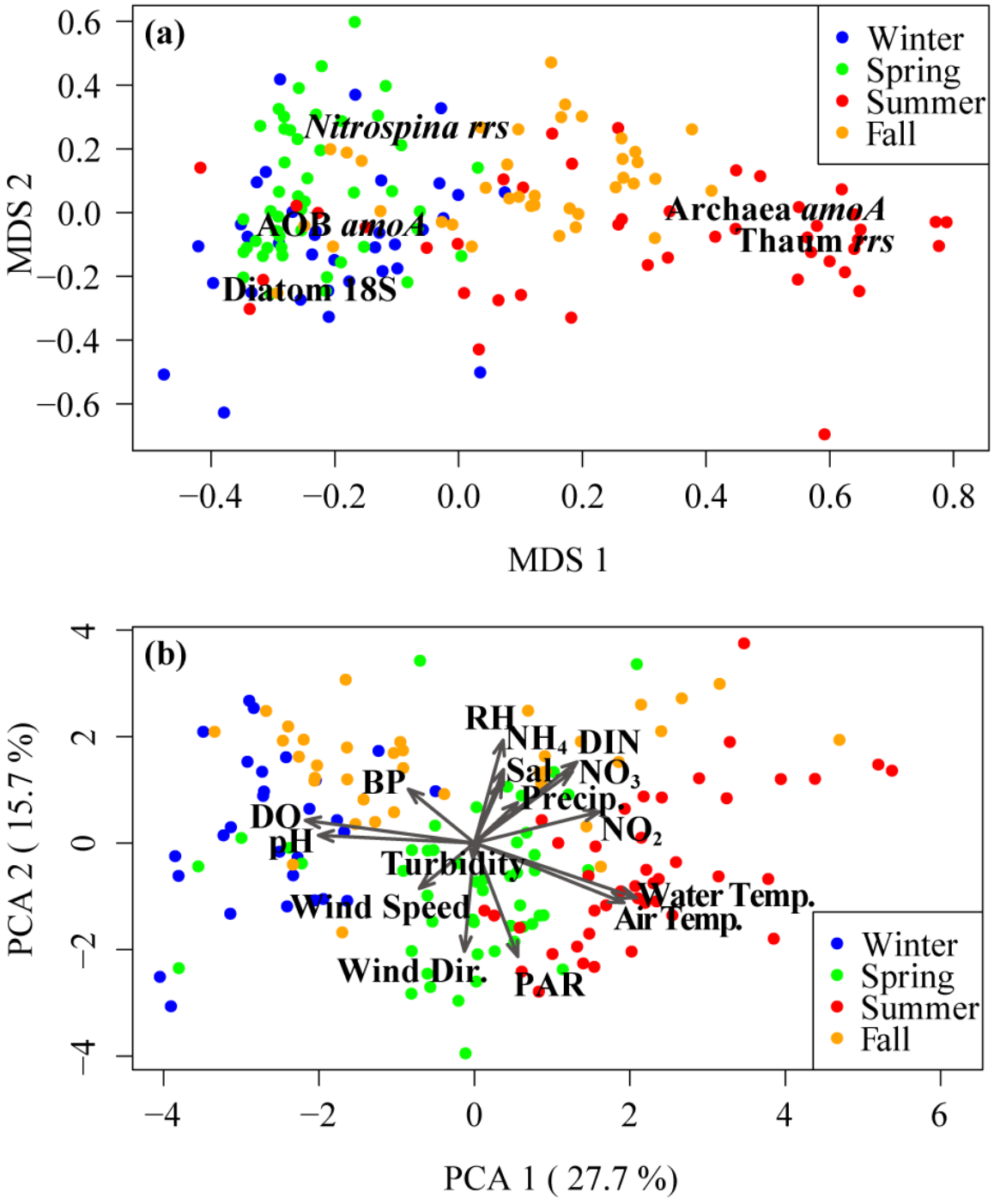
(a)
Winter
Spring
Summer
Fall
Nitrospina rrs
AOB amoA
Archaea amoA
Thaum rrs
Diatom 18S
MDS 2
MDS 1
0.6
0.4
0.2
0.0
−0.2
−0.4
−0.6
−0.4
−0.2
0.0
0.2
0.4
0.6
0.8
(b)
RH
NH4
DIN
Sal
NO3
BP
Precip
DO
NO2
pH
Turbidity
Water Temp.
Wind Speed
Air Temp.
Wind Dir.
PAR
Winter
Spring
Summer
Fall
PCA 2 (15.7 %)
PCA 1 (27.7 %)
4
2
0
−2
−4
−4
−2
0
2
4
6

Figure 4.5: Growth rate of Thaumarchaeota populations during the Sapelo Island bloom. Raw gene abundance data (closed circles) versus smoothed (3-point running average) data (open circles) for **(a)** Thaumarchaeota *rrs* and **(b)** Archaea *amoA*. **(c)** Calculated net population growth rate of *rrs* (closed circles) and *amoA* (open circles). Shaded area represents negative growth (below 0 d^{-1}). **(d)** Relationship between calculated growth rates of Thaumarchaeota *rrs* and *amoA* genes. The linear regression equation is included in the figure.

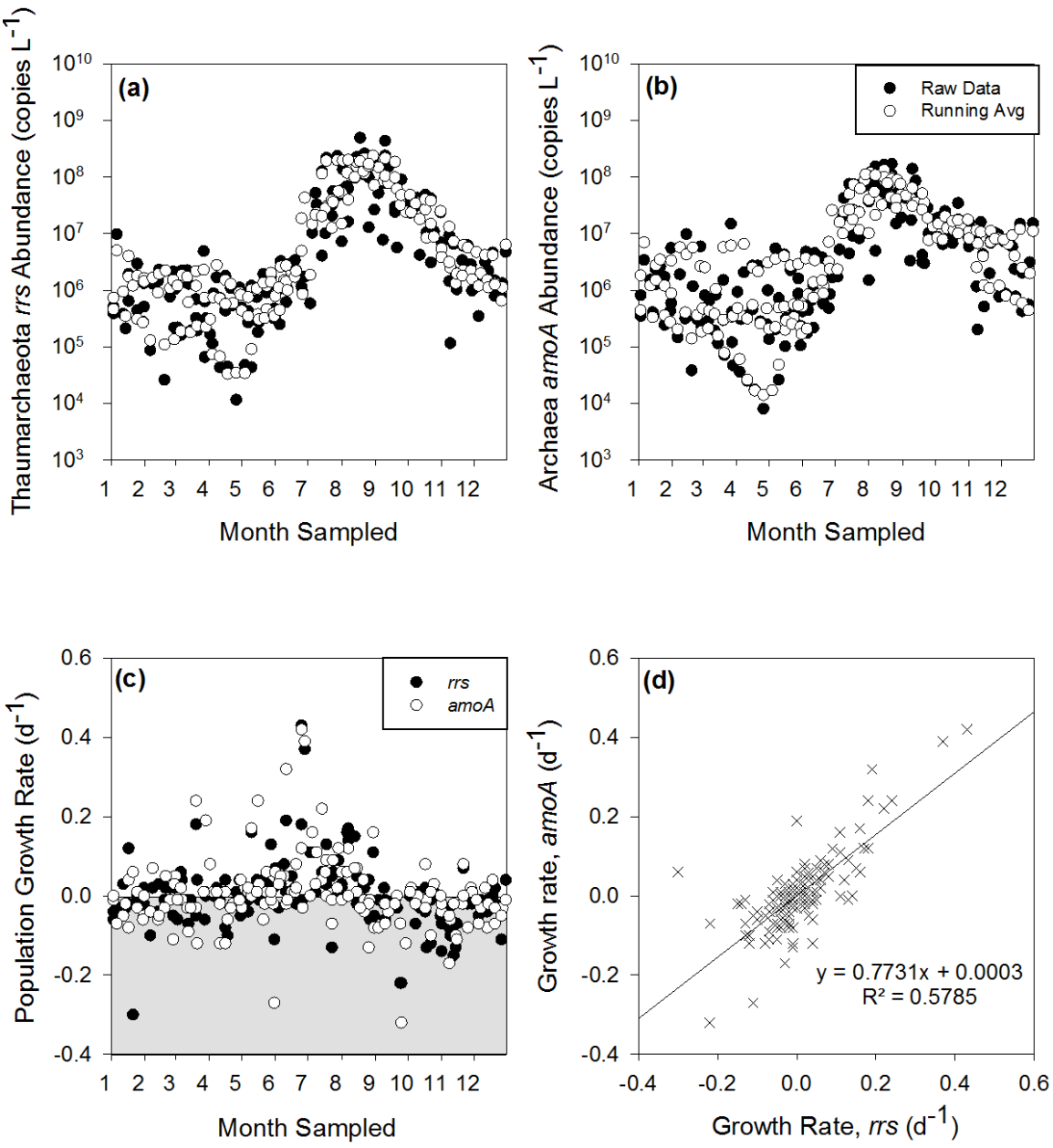
(a)
Thaumarchaeota rrs Abundance (copies L-1)
Month Sampled
(b)
Archaea amoA Abundance (copies L-1)
Raw Data
Running Avg
Month Sampled
(c)
Population Growth Rate (d-1)
rrs
amoA
Month Sampled
(d)
Growth rate, amoA (d-1)
y = 0.7731x + 0.0003
R² = 0.5785
Growth Rate, rrs (d-1)

Figure 4.6: **DIN concentrations, binned by month from estuarine sites along the SE USA**, **(a)** at stations near Sapelo Island (GCE-LTER data); **(b)** in the Skidaway River, GA (data courtesy P. Verity/SkIO); and at stations in the **(c)** Machipongo and Oyster Bay (excluding CM stations) transects (coastal Virginia, USA; VCR-LTER data).

(a) GCE-LTER Data (2001-2009)

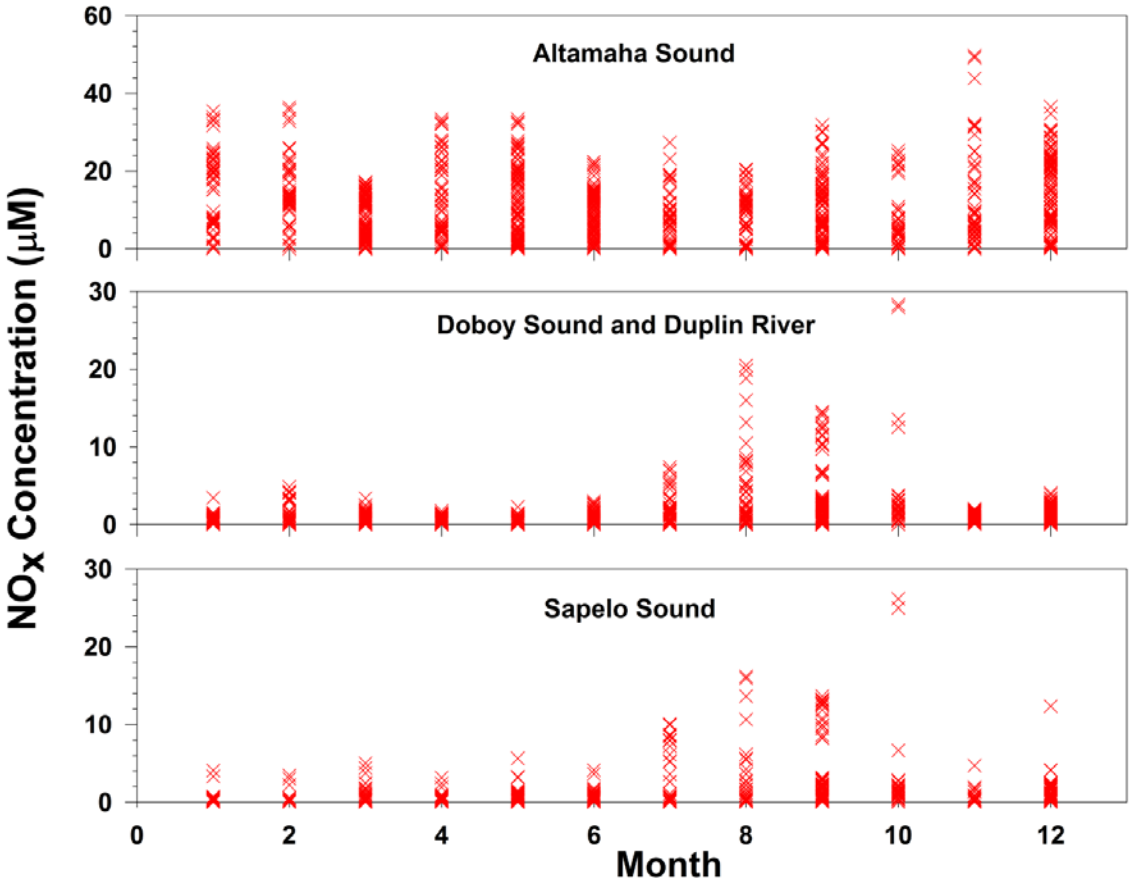

(b) Skidaway River Data (1986-2009)

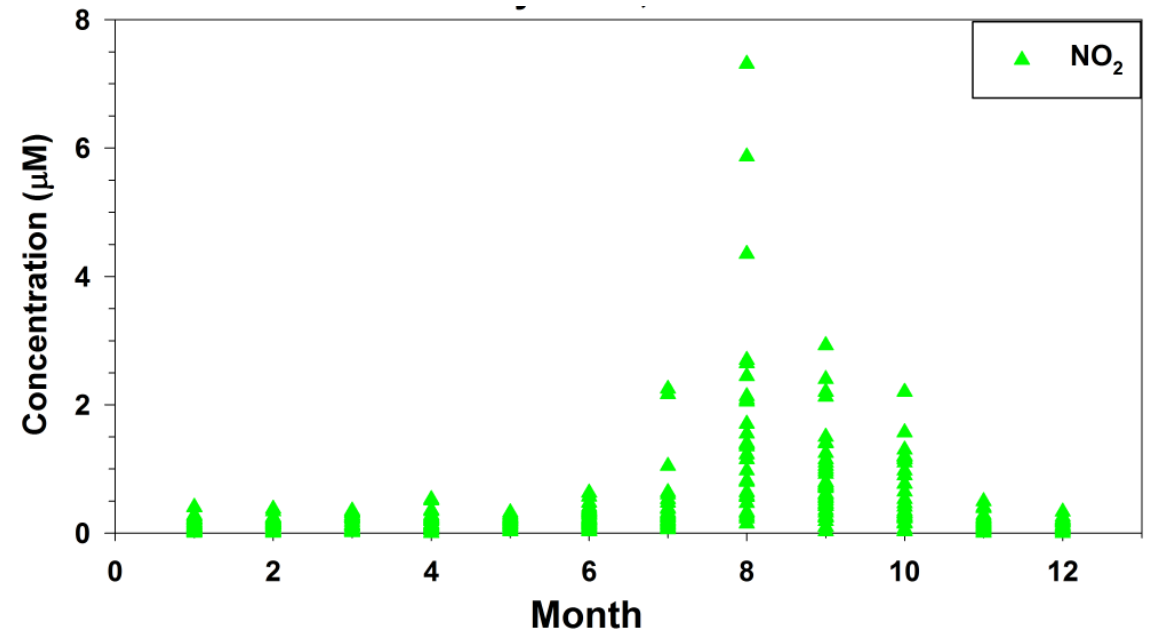

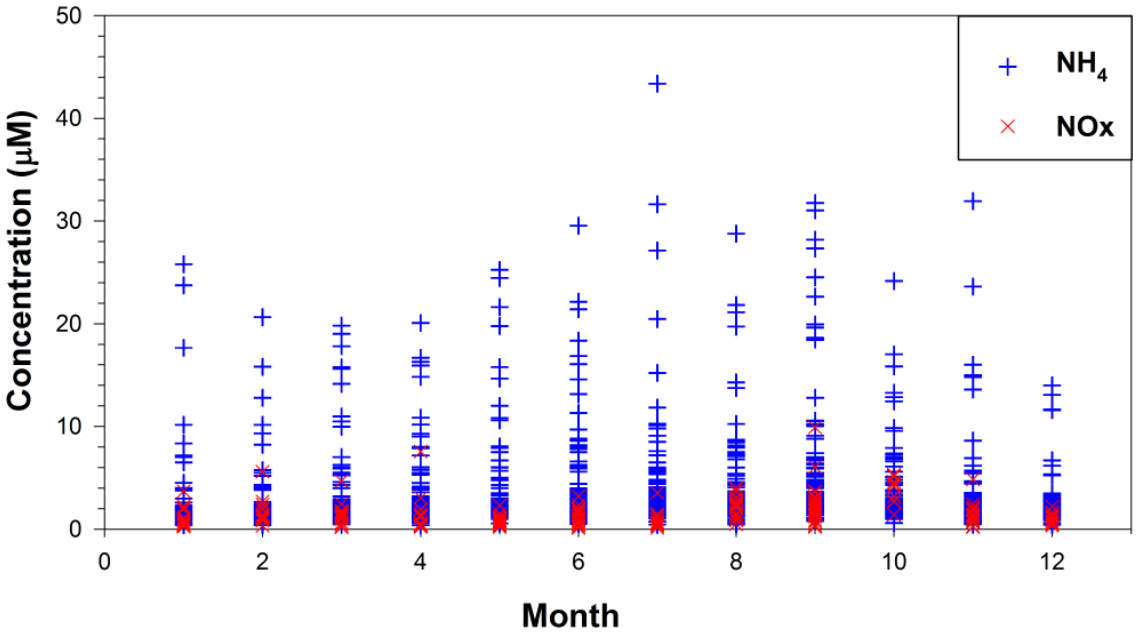

(c) VCR-LTER Data (2005-2008)

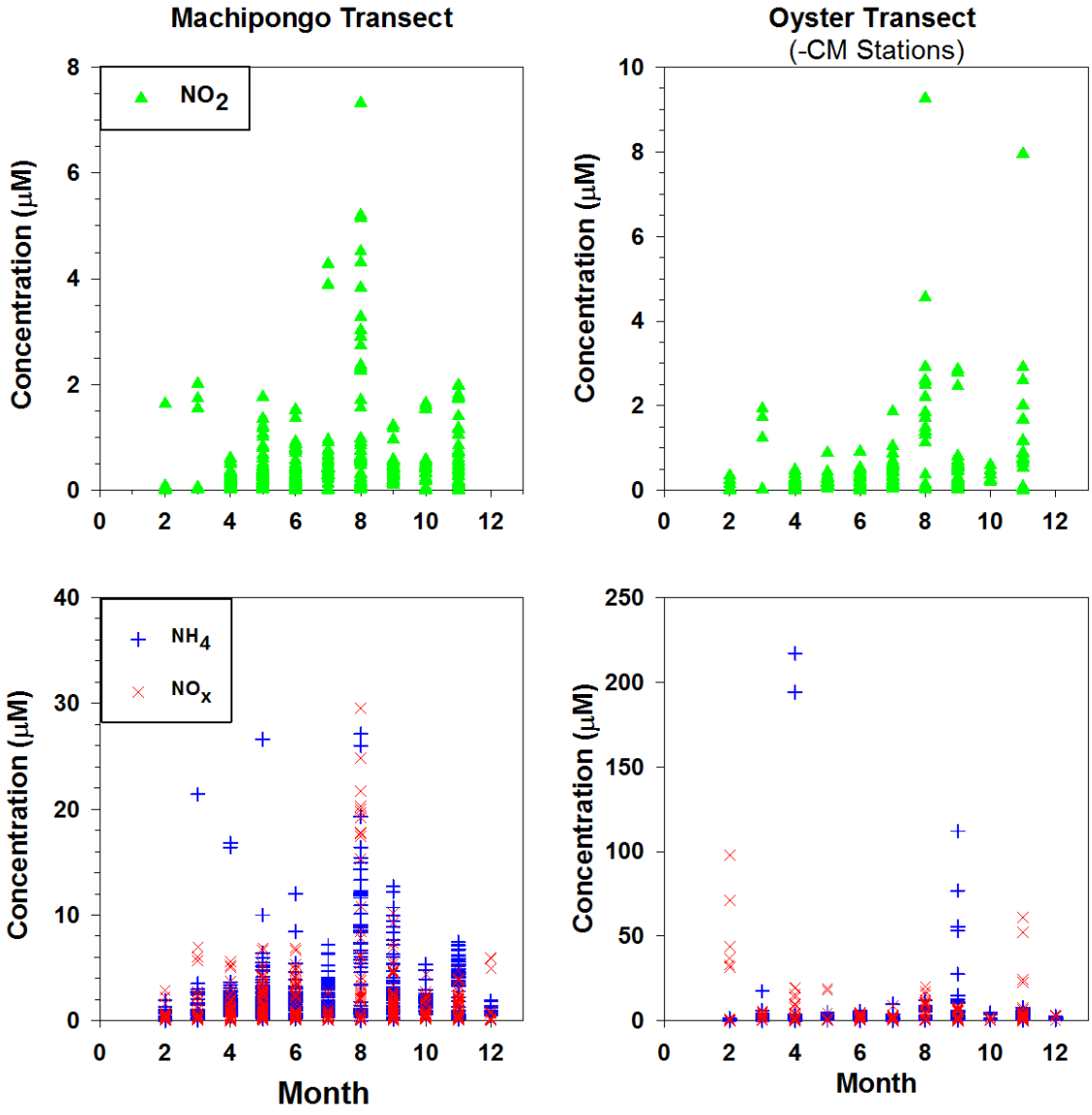

CHAPTER 5

COMPARISON OF OXIDATION OF AMMONIA VERSUS UREA BY MARINE NITRIFYING ORGANISMS[1]

[1] Bradley B. Tolar, Natalie J. Wallsgrove, Brian N. Popp, and James T. Hollibaugh. To be submitted to *Nature Geoscience*.

SUMMARY

Thaumarchaeota are found in almost every environment and all may be capable of oxidizing ammonia to nitrite for energy – the first part of nitrification. Some thaumarchaeote genomes contain a gene that is homologous to urease and it has been proposed that thaumarchaeotes oxidize urea-N when ammonia concentrations are low; and that they preferentially incorporate urea C versus DIC. We compared rates of ammonia and urea-N oxidation in marine nitrifier communities dominated by Thaumarchaeota in both polar and temperate ocean regions. Ammonia oxidation rates were always higher (1.3 - to 120-fold difference) than urea-N oxidation rates (means = 210 vs. 34 nmole L^{-1} d^{-1}, respectively) in temperate waters (coastal Georgia, USA; South Atlantic Bight). Rates of ammonia oxidation were only exceeded by urea-N oxidation rates in samples from 70-200 m from the Southern Ocean and the Gulf of Alaska (mean = 3.3 versus 9.5 nmole L^{-1} d^{-1}); while ammonia oxidation rates were higher in all other high-latitude samples (7.3 versus 22 nmole L^{-1} d^{-1}), most of which were 350-800 m depth. Isotope dilution experiments indicated that urea is hydrolyzed to ammonia extracellularly prior to oxidation. Our data suggest that the contribution of urea-N to nitrification is likely minor at most locations but may represent a significant portion of the nitrification flux in polar waters. We have also shown that urea could be a significant source of ammonia and can thus provide the substrate for nitrification despite a lack of preferential oxidation of urea-N.

MAIN TEXT

Thaumarchaeota, members of a deeply-branching phylum of the kingdom Archaea, are one of the most abundant groups of prokaryotic organisms in the ocean (Karner *et al.*, 2001). They play an important role in the marine nitrogen cycle through the autotrophic oxidation of ammonia (NH_3) to nitrite (reviewed in Capone *et al.*, 2008; Prosser and Nicol, 2008; Ward, 2011). These ammonia-oxidizing Archaea (AOA) are the primary ammonia-oxidizing organisms (AOO) in most marine systems, with abundances of the gene encoding their catalytic subunit of ammonia monooxygenase (*amoA*) up to 10^8 copies L^{-1} (e.g., Beman *et al.*, 2010; Church *et al.*, 2010; Kalanetra *et al.*, 2009; Santoro *et al.*, 2010; Tolar *et al.*, 2013; Wuchter *et al.*, 2006). Bacteria from the β- and γ-Proteobacteria can also take part in ammonia oxidation (known as ammonia-oxidizing Bacteria, or AOB), but they are thought to be relatively minor contributors in most marine environments (reviewed in Ward, 2011).

Observations of reduced incorporation of bicarbonate and high abundance of urease genes in plankton communities from the Arctic and Southern Oceans have suggested that Thaumarchaeota can use urea as an alternative source of energy when NH_3 availability is low (Alonso-Sáez *et al.*, 2012; Pedneault *et al.*, 2014). These studies propose that the Thaumarchaeota urease enzyme can be used to break down urea into NH_3 for ammonia oxidation and CO_2 for carbon fixation (shown by increased ^{14}C-urea uptake; Alonso-Sáez *et al.*, 2012). However, these studies only provided indirect evidence for this conclusion based upon the abundance of urease (*ureC*) genes and transcripts, and lacked direct rate measurements. A recent study examined the capacity for urea oxidation among "*Candidatus* Nitrosopumilus maritimus" SCM1 and two new

isolates (both within the Nitrosopumilus cluster). One strain (PS0) showed an almost stoichiometric conversion of urea to nitrite, though ammonia concentrations were not reported (Qin *et al.*, 2014).

Here we compared the oxidation of ammonia and urea by nitrifying communities from a variety of marine environments to determine whether AOA populations were capable of directly oxidizing urea-N (i.e., without prior hydrolysis of urea to yield ammonia and CO_2). We measured the production of nitrite and nitrate (NO_x) from ^{15}N-labeled ammonia and urea in samples from near-shore, coastal, and offshore environments, and temperate and polar oceans (Figure 5.1; Table 5.1). Incubations proceeded at *in situ* temperatures with tracer-level additions (50 nM) of each substrate (see Methods). We also compared rates of ^{15}N-ammonia oxidation in the presence of unlabeled urea and ammonia, and measured the production of ^{15}N-ammonia in experiments amended with ^{15}N-urea to quantify urea hydrolysis. Finally, we extracted DNA and RNA from samples to investigate relationships between *amoA* and *ureC* transcripts and ammonia and urea oxidation rates, respectively.

Continental shelf waters of the South Atlantic Bight (SAB) are characterized by two water masses: a near-shore plume that is strongly influenced by river runoff and tidal exchange with salt marsh-dominated estuaries, and an offshore water mass that exchanges with slope waters (Atkinson and Menzel, 2013; Cai *et al.*, 2003; Gardner and Stephens, 1978; Liu *et al.*, in press). The turbid near-shore water mass has lower salinity, higher dissolved organic matter, and higher suspended particulate loads than the continental shelf water further offshore. Rates of NO_x production from NH_3 (Table 5.1) were higher in samples from the near-shore water mass (n = 18, mean = 380, range 160-

780 nM d^{-1}; Figures 5.2a-b, 5.3a) compared to samples taken further offshore in the SAB (n=15, mean = 21, range 0-120 nM d^{-1}; Figures 5.2c-d). Rates of urea-N oxidation by Antarctic samples (n = 6, mean = 19, range 6.3-40.0 nM d^{-1}; Figure 5.2e) were comparable to rates measured in the SAB, while the lowest urea-N oxidation rates were found in Gulf of Alaska (GoA) samples (n = 5, mean = 11, range 0-20 nM d^{-1}; Figure 5.2f). However, when normalized to the abundance of Thaumarchaeota in these samples, rates were more narrowly constrained (n = 40, mean 14, range 0-50 fmole $cell^{-1}$ d^{-1}), with little difference between populations from the Antarctic or from coastal Georgia (Sapelo Island): mean rates of 5.5 versus 8.2 fmole $cell^{-1}$ d^{-1}, respectively (Table 5.1). This was surprising given the large difference in environmental factors between these sites.

We found that nitrogen supplied as urea was oxidized in most samples; however, urea-N always contributed less than ammonia to total nitrification by the same population of AOO. This contribution was lowest with samples from Sapelo Island (mean = 21%, range = 3.5-75% of the ammonia oxidation rate; Figures 5.2a-b, 5.3a) and the SAB (mean = 9.4%, range 0.83-29%; Figures 5.2c-d). Ammonia was oxidized 1.7 or 32-fold faster than urea-N by nitrifiers in most samples from the Antarctic and GoA, respectively (Antarctic mean = 130%, range = 27-320% of the ammonia oxidation rate; GoA mean = 69%, range = 1.1-180%; Figures 5.2e-f). In contrast to this general trend, urea-N was oxidized more rapidly than ammonia in 5 samples from below the euphotic zone (70-200 depth) in the GoA and Southern Ocean (Table 5.1). Urea oxidation was higher in Antarctic samples from the Winter Water (50-100 m; Church *et al.*, 2003) versus the Circumpolar Deep Water (150-400 m; mean = 8.7 versus 2.3 fmole $cell^{-1}$ d^{-1}, respectively; $p < 0.003$, Student's t-test), while there was no significant difference in

ammonia oxidation rates between these water masses (mean 6.0 vs. 5.1 fmole $cell^{-1}$ d^{-1}, respectively; $p < 0.8$, Student's t-test). This is especially interesting given the marked differences in phylogenetic composition of Thaumarchaeota in Winter Water compared to Circumpolar Deep Water (Kalanetra *et al.*, 2009; Chapter 2), where Winter Water communities were dominated (~98% of sequences; Chapter 2) by a single phylotype of thaumarchaeote.

Rates of oxidation of urea-N were most comparable to NH_3 in Antarctic samples (15 versus 19 nM d^{-1}, respectively; 130% of ammonia oxidation rate on average); however, in all other samples, including all samples from Georgia coastal waters, the rate of urea-N oxidation was lower than that of ammonia in the same sample (Sapelo Island = 20% of ammonia oxidation rate, SAB = 9.4%, GoA = 69%). We should not be underestimating the rate of urea-N oxidation as urea concentrations are on the same order of magnitude as ammonia concentrations (0.47 versus 0.87 μM on average across all sample sites, respectively), and pool turnover rates were comparable for both urea and ammonia (mean = 0.14 versus 0.19 d^{-1}, respectively). Additionally, urease genes are not highly transcribed in Georgia coastal Thaumarchaeota populations (Hollibaugh *et al.*, 2011; Hollibaugh *et al.*, 2014; Table 5.1) compared to polar populations sampled by Pedneault *et al.* (2014) and those in this study. This suggests that the contribution of urea to thaumarchaeote chemoautotrophy is more important at high latitudes and in polar oceans, which contribute significantly to global nitrification (Christman *et al.*, 2011; Olson, 1980; Chapter 3).

There was no clear trend of urea oxidation in Georgia coastal waters with tide or time of day during either year sampled (Figures 5.2a-b), and rates were on the same order

of magnitude each year. We also examined the competition between these substrates in a sample from Sapelo Island (2013). Production of $^{15}N\text{-}NO_x$ from $^{15}N\text{-}NH_4$ decreased significantly following the addition of unlabeled ammonia to the sample (20.0 ± 6.3 nM d^{-1} vs. 484.9 ± 29.6 nM d^{-1} in the unamended control; $p < 0.003$; Figure 5.3b). Adding unlabeled urea had no effect on the rate of $^{15}N\text{-}NO_x$ production from $^{15}N\text{-}NH_4$ (478.6 ± 52.5 nM d^{-1}; $p > 0.5$ vs. control). Incorporation of $NaH^{14}CO_3$ by a thaumarchaeote-dominated enrichment culture growing on NH_4 decreased when unlabeled urea was added (0.13 versus 1.5 pM h^{-1}, in the urea-amended versus unamended control, respectively). This seems to indicate that urea-N is not being used to promote chemoautotrophy for thaumarchaeotes present in coastal waters around Georgia. Nonetheless, urea-C could be preferentially incorporated (as both a C source and for ammonia oxidation) as suggested by Alonso-Sáez *et al*. (2012) for polar waters.

Additionally, we examined the extent of urea hydrolysis to ammonia in some experiments by measuring production of $^{15}N\text{-}NH_4$ in urea-amended treatments following Holmes *et al.* (1998). We found that ^{15}N-labeled ammonia was recovered from ^{15}N-urea amended treatments in samples taken from both Sapelo Island (Figure 5.4a) and the Gulf of Alaska (Figure 5.4b). This suggests that urea hydrolysis precedes oxidation of urea-N, with subsequent oxidation of the ammonia produced.

Finally, we examined the relationship between *amoA* and *ureC* transcripts with oxidation of ammonia or urea, respectively (Table 5.2). No significant relationships were observed when comparing rates (nM d^{-1}) with transcript abundance (data not shown); however, there were weak correlations between cell-specific oxidation rates (fmole $cell^{-1}$ d^{-1}) and the transcript:gene ratio (Figure 5.5). The strongest relationship we found was

between AO rates and *amoA* gene abundance in the South Atlantic Bight in April 2011 ($r^2 = 0.85$; Figure 5.5c) and the Gulf of Alaska ($r^2 = 0.50$; Figure 5.5f).

Overall, we have shown that oxidation of urea-N can occur with populations of marine nitrifiers dominated by Thaumarchaeota (Table 5.2); however, the contribution of urea to nitrification is almost always significantly less than that of ammonia. Therefore, it appears that the ability and preference of Thaumarchaeota for urea as an alternate substrate is variable and highly dependent on sample location and likely determined by the ecotypes present. Additionally, isotope dilution experiments suggest that it is likely that urea is hydrolyzed to release ammonium, which is then oxidized, rather than being oxidized directly.

METHODS

Sample Collection

A variety of marine environments were sampled to compare rates of ammonia and urea oxidation (Table 5.1). Samples were collected from surface waters at Marsh Landing on Sapelo Island, Georgia – a coastal estuary dominated by salt marshes – in August 2011 and 2012, and September 2013, during the annual Thaumarchaeota bloom (Figure 5.1a). The South Atlantic Bight (SAB) was sampled during near- to offshore transects on the *R/V Savannah* in April and October of 2011 (Figure 5.1a). Antarctic experiments were performed with samples from the Winter Water (WW) and Circumpolar Deep Water (CDW) water masses of the Southern Ocean collected on the *ARSV Laurence M. Gould* in January 2011 (Figure 5.1b). Water was collected for

experiments in the Gulf of Alaska (GoA) from 200 m and 800 m on board the *R/V Melville* in August 2013 (Figure 5.1c).

Experimental Setup and Rate Measurements

Stable isotope-labeled ammonium chloride ($^{15}NH_4Cl$; >99 at-% ^{15}N, Cambridge Isotope Laboratories) and urea [$(^{15}NH_2)_2{}^{13}CO$; >99 at-% ^{15}N, CIL] were added to a final concentration of 50 nM. Substrates were tested in either duplicate or triplicate samples of seawater contained in 50 mL polypropylene screw-cap, conical tubes (Sapelo Island, SAB, GoA) or 250 mL polycarbonate bottles (Antarctic). Sample incubations proceeded at *in situ* temperature in the dark for 24 hours (Sapelo Island, SAB), 48 hours (GoA), or 124-139 hours (Antarctic; Table 5.2) before termination by freezing at -80°C; samples were kept frozen until analysis. Concentrations of dissolved inorganic nitrogen and urea were measured using previously described methods [ammonia (Solórzano, 1969); nitrite (NO_2) and nitrite + nitrate (NO_x; (Jones, 1984; Strickland and Parsons, 1972); and urea (Mulvenna and Savidge, 1992; Rahmatullah and Boyde, 1980)], or estimated from the literature, depending on the sample location (Table 5.1). The competition experiment was conducted in September 2013with a sample from Marsh Landing, Sapelo Island, by adding labeled ^{15}N-ammonium (50 nM final conc.) to bottles containing either unlabeled urea or ammonium (5 μM final conc.). Controls with only ^{15}N-ammonium additions were also included.

The amount of ^{15}N oxidized to nitrite or nitrate (NO_x) was measured with the denitrifier method (Sigman *et al.*, 2001) as described previously (Beman *et al.*, 2011; Dore *et al.*, 1998; Popp *et al.*, 1995) using a MAT-252 isotope ratio mass spectrometer

(Finnigan). Ammonia or urea oxidation rates were calculated from $\delta^{15}N$ values as described previously (Beman *et al.*, 2012; Christman *et al.*, 2011), with urea concentrations substituted for ammonia in urea oxidation rate calculations and using 2 moles of ^{15}N added per mole of urea. Formation of $^{15}NO_x$ was negligible in filtered controls or in samples taken immediately after substrate addition, and no $^{15}N_2O$ was formed by direct addition of ^{15}N-labeled substrates to denitrifier cultures of *Pseudomonas aureofaciens* (data not shown), indicating that microbial assemblages are the source of any $^{15}NO_x$ formed in samples.

We also used an enrichment culture [raised from an inoculum collected at Marsh Landing, Sapelo Island in August 2012, and grown on ammonium-amended (50 μM) filtered seawater] to measure incorporation of ^{14}C-labeled bicarbonate ($NaH^{14}CO_3$, Perkin Elmer; 40 μCi per 200 mL sample) with either ammonia or urea as a substrate for chemoautotrophic metabolism (10 or 5 μM final conc., respectively). The experiment was sampled over a 52-hour period. At each time point, samples were filtered onto 0.22 GSWP filters (Millipore), dissolved with 1 mL of ethyl acetate, suspended in 7 mL EcoLume scintillation cocktail (MP Biomedicals), and counted using a Packard 2910 liquid scintillation counter.

Urea hydrolysis was determined using a modified ammonia diffusion method (Holmes *et al.*, 1998) to measure ^{15}N-NH_4 in treatments with 50 nM amendments of either ^{15}N-urea or ^{15}N-ammonia. Water samples were from Sapelo Island, Georgia (September 2013) and the Gulf of Alaska (August 2013). An ammonia trap [filter pack; containing combusted 1 cm GF/D filters (Whatman) acidified with H_2SO_4 and sealed between two 2.5 cm, 10 μm Teflon membranes (Millipore LCWP)] was added to each

sample, followed by addition of 1.5 g MgO = to convert all NH_4^+ to NH_3. Samples were incubated for 4 weeks with shaking at 40°C to allow NH_3 to diffuse onto the filter pack. Each filter was then dried and the $\delta^{15}N$ of ammonia from each sample was obtained using an isotope ratio mass spectrometer (maintained by T. Maddox, UGA School of Ecology Analytical Chemistry Laboratory).

DNA and RNA Extraction and Quantification

Quantification of bacterial 16S rRNA, AOB *amoA*, Marine Group I Archaea (Thaumarchaeota) 16S rRNA, and archaeal *amoA* genes was performed after a phenol:chloroform DNA extraction (Bano and Hollibaugh, 2000) using primers and protocols as described previously (Kalanetra *et al.*, 2009; Tolar *et al.*, 2013; Table B.2) with an iCycler iQ™ Real-Time qPCR detection system (BioRad). Archaeal *ureC* genes were quantified under the same conditions as *amoA* with an annealing temperature of 53°C (Alonso-Sáez *et al.*, 2012; Chapter 3). RNA was extracted following previous protocols (Gifford *et al.*, 2011; Poretsky *et al.*, 2009) with 200 µm zirconium beads (OPS Diagnostics) used for the initial bead-beating step. The TURBO DNase-Free Kit (Ambion) was used to remove DNA after extraction, and manufacturer's instructions were followed with a second enzyme treatment at 2X concentration. Both *amoA* (AOA and AOB) and *ureC* (Thaumarchaeota) transcripts were quantified with the iScript™ One-Step RT-qPCR Kit with SYBR® Green (BioRad). Each transcript RT-qPCR assay used the same cycling conditions as the gene qPCR assay, with the addition of a 10 minute reverse transcription step at 50°C before the initial denaturation step.

ACKNOWLEDGMENTS

We would like to thank the captain and crew of the *R/V Savannah* (SAV-11-10 and SAV-11-30), *R/V Melville* (MV1310), and *ARSV Laurence M. Gould* (LMG11-01), and the staff at the UGA Marine Institute on Sapelo Island for their role in the sampling programs that led to these experiments. We would also like to thank PAL-LTER personnel and the project PI H. Ducklow (funded by NSF ANT 08-23101), as well as support staff from Raytheon Polar services for their assistance on cruise LMG 11-01. We thank D. Hansell and W. Miller for the ability to participate in MV1310 (funded by NSF OCE 11-53930 and OCE 12-34388). Finally, we would like to thank L. Aluwihare, L. Powers, F. Cao, and Q. Liu for assistance in the field, and N. Wallsgrove, C. Ka'apu-Lyons, A. Bratcher, and E. Malagón for assistance with sample analysis. This work was funded by grants from the National Science Foundation OPP 08-38996, OCE 10-29742, and OCE 06-20959 (J.T.H.), and OCE 11-29260 (B.N.P.).

REFERENCES

Alonso-Sáez L, Waller AS, Mende DR, Bakker K, Farnelid H, Yager PL, Lovejoy C, Tremblay JE, Potvin M, Heinrich F, Estrada M, Riemann L, Bork P, Pedrós-Alio C, Bertilsson S (2012). Role for urea in nitrification by polar marine Archaea. *Proc Nat Acad Sci USA* **109:** 17989-17994.

Atkinson LP, Menzel DW (2013). Introduction: Oceanography of the Southeast United States Continental Shelf. In: Atkinson LP, Menzel DW, Bush KA (eds). Oceanography of the Southeastern US Continental Shelf. American Geophysical Union: Washington, D. C. pp 1-9.

Bano N, Hollibaugh JT (2000). Diversity and distribution of DNA sequences with affinity to ammonia-oxidizing bacteria of the beta subdivision of the class Proteobacteria in the Arctic Ocean. *Appl Environ Microbiol* **66:** 1960-1969.

Beman JM, Sachdeva R, Fuhrman JA (2010). Population ecology of nitrifying archaea and bacteria in the Southern California Bight. *Environ Microbiol* **12:** 1282-1292.

Beman JM, Chow CE, King AL, Feng YY, Fuhrman JA, Andersson A, Bates NR, Popp BN, Hutchins DA (2011). Global declines in oceanic nitrification rates as a consequence of ocean acidification. *Proc Nat Acad Sci USA* **108:** 208-213.

Beman JM, Popp BN, Alford SE (2012). Quantification of ammonia oxidation rates and ammonia-oxidizing archaea and bacteria at high resolution in the Gulf of California and eastern tropical North Pacific Ocean. *Limnol Oceanogr* **57:** 711-726.

Cai W-J, Wang ZA, Wang Y (2003). The role of marsh-dominated heterotrophic continental margins in transport of CO_2 between the atmosphere, the land-sea interface and the ocean. *Geophys Res Lett* **30:** 1849.

Capone DG, Bronk DA, Mulholland MR, Carpenter EJ (eds) (2008) Nitrogen in the Marine Environment. Academic Press: Burlington, MA.

Christman GD, Cottrell MT, Popp BN, Gier E, Kirchman DL (2011). Abundance, Diversity, and Activity of Ammonia-Oxidizing Prokaryotes in the Coastal Arctic Ocean in Summer and Winter. *Appl Environ Microbiol* **77:** 2026-2034.

Church MJ, DeLong EF, Ducklow HW, Karner MB, Preston CM, Karl DM (2003). Abundance and distribution of planktonic Archaea and Bacteria in the waters west of the Antarctic Peninsula. *Limnol Oceanogr* **48:** 1893-1902.

Church MJ, Wai B, Karl DM, DeLong EF (2010). Abundances of crenarchaeal *amoA* genes and transcripts in the Pacific Ocean. *Environ Microbiol* **12:** 679-688.

Dore JE, Popp BN, Karl DM, Sansone FJ (1998). A large source of atmospheric nitrous oxide from subtropical North Pacific surface waters. *Nature* **396:** 63-66.

Francis CA, Roberts KJ, Beman JM, Santoro AE, Oakley BB (2005). Ubiquity and diversity of ammonia-oxidizing archaea in water columns and sediments of the ocean. *Proc Natl Acad Sci USA* **102:** 14683-14688.

Gardner WS, Stephens JA (1978). Stability and composition of terrestrially derived dissolved organic nitrogen in continental shelf surface waters. *Mar Chem* **6:** 335-342.

Gifford SM, Sharma S, Rinta-Kanto JM, Moran MA (2011). Quantitative analysis of a deeply sequenced marine microbial metatranscriptome. *ISME J* **5:** 461-472.

Hollibaugh JT, Gifford S, Sharma S, Bano N, Moran MA (2011). Metatranscriptomic analysis of ammonia-oxidizing organisms in an estuarine bacterioplankton assemblage. *ISME J* **5:** 866-878.

Hollibaugh JT, Gifford SM, Moran MA, Ross MJ, Sharma S, Tolar BB (2014). Seasonal variation in the metratranscriptomes of a Thaumarchaeota population from SE USA coastal waters. *ISME J* **8:** 685-698.

Holmes RM, McClelland JW, Sigman DM, Fry B, Peterson BJ (1998). Measuring ^{15}N–NH_4^+ in marine, estuarine and fresh waters: An adaptation of the ammonia diffusion method for samples with low ammonium concentrations. *Mar Chem* **60:** 235-243.

Jones MN (1984). Nitrate Reduction by Shaking with Cadmium - Alternative to Cadmium Columns. *Water Res* **18:** 643-646.

Kalanetra KM, Bano N, Hollibaugh JT (2009). Ammonia-oxidizing Archaea in the Arctic Ocean and Antarctic coastal waters. *Environ Microbiol* **11:** 2434-2445.

Karner MB, DeLong EF, Karl DM (2001). Archaeal dominance in the mesopelagic zone of the Pacific Ocean. *Nature* **409:** 507-510.

Liu Q, Lu X, Tolar BB, Mou X, Hollibaugh JT (in press). Concentrations, Turnover Rates, and Fluxes of Polyamines in Coastal Waters of the South Atlantic Bight. *Biogeochemistry*.

Mulvenna PF, Savidge G (1992). A modified manual method for the determination of urea in seawater using diacetylmonoxime reagent. *Estuar Coast Shelf S* **34:** 429-438.

Olson RJ (1980). Nitrate and Ammonium Uptake in Antarctic Waters. *Limnol Oceanogr* **25:** 1064-1074.

Pedneault E, Galand PE, Potvin M, Tremblay J-É, Lovejoy C (2014). Archaeal *amoA* and *ureC* genes and their transcriptional activity in the Arctic Ocean. *Sci Rep* **4:** 1-10.

Popp BN, Sansone FJ, Rust TM, Merritt DA (1995). Determination of Concentration and Carbon Isotopic Composition of Dissolved Methane in Sediments and Nearshore Waters. *Anal Chem* **67:** 405-411.

Poretsky RR, Gifford S, Rinta-Kanto J, Vila-Costa M, Moran MA (2009). Analyzing gene expression from marine microbial communities using environmental transcriptomics. *J Vis Exp* **24:** e1086.

Prosser JI, Nicol GW (2008). Relative contributions of archaea and bacteria to aerobic ammonia oxidation in the environment. *Environ Microbiol* **10:** 2931-2941.

Qin W, Amin SA, Martens-Habbena W, Walker CB, Urakawa H, Devol AH, Ingalls AE, Moffett JW, Armbrust EV, Stahl DA (2014). Marine ammonia-oxidizing archaeal isolates display obligate mixotrophy and wide ecotypic variation. *Proc Nat Acad Sci USA* **111:** 12504-12509.

Rahmatullah M, Boyde TR (1980). Improvements in the determination of urea using diacetyl monoxime; methods with and without deproteinisation. *Clin Chim Acta* **107:** 3-9.

Santoro AE, Casciotti KL, Francis CA (2010). Activity, abundance and diversity of nitrifying archaea and bacteria in the central California Current. *Environ Microbiol* **12:** 1989-2006.

Sigman DM, Casciotti KL, Andreani M, Barford C, Galanter M, Böhlke JK (2001). A Bacterial Method for the Nitrogen Isotopic Analysis of Nitrate in Seawater and Freshwater. *Anal Chem* **73:** 4145-4153.

Solórzano L (1969). Determination of Ammonia in Natural Waters by the Phenolhypochlorite Method. *Limnol Oceanogr* **14:** 799-801.

Strickland JDH, Parsons TR (1972). Determination of Reactive Silicate. In: Stevenson JC (ed). A Practical Handbook of Seawater Analysis, 2nd edn. Fisheries Research Board of Canada: Ottawa, Canada. pp 65-70.

Tolar BB, King GM, Hollibaugh JT (2013). An analysis of thaumarchaeota populations from the northern Gulf of Mexico. *Front Microbiol* **4:** 72.

Ward BB (2011). Nitrification in the Ocean. In: Ward BB, Arp DJ, Klotz MG (eds). Nitrification. ASM Press: Washington, D.C. pp 325-345.

Wuchter C, Abbas B, Coolen MJL, Herfort L, van Bleijswijk J, Timmers P, Strous M, Teira E, Herndl GJ, Middelburg JJ, Schouten S, Damste JSS (2006). Archaeal nitrification in the ocean. *Proc Natl Acad Sci USA* **103:** 12317-12322.

Table 5.1: Summary of nutrient and ^{15}N-oxidation rate data collected for experiments.

Sample Location	Station ID	Time or Depth*	[NO_2]	[NO_x]	[NH_4]	[Urea]#	Incubation Time (h)	$^{15}NH_4$ Rate (nM d^{-1})	^{15}N Urea Rate (nM d^{-1})	$^{15}NH_4$ Rate Per Cell$	$^{15}Urea$ Rate Per Cell$
Sapelo Island August 2011	MLD1-11	04:55 PM	5.14	8.57	0.95	1.31	24.53	394	296	7.68	5.77
	MLD2-11	10:33 PM	2.34	3.85	1.15	1.20	24.13	405	95.2	33.6	7.90
	MLD3-11	09:12 AM	5.42	7.53	0.48	0.64	24.18	314	10.9	3.44	0.12
	MLD4-11	11:10 AM	4.42	5.81	0.69	0.48	24.18	326	50.2	11.5	1.77
	MLD5-11	05:11 PM	3.64	5.28	0.98	0.73	24.13	245	74.0	4.53	1.37
	MLD6-11	11:10 PM	3.33	4.26	0.52	*0.89*	24.24	382	167	17.7	7.73
	ML7-11	10:13 AM	7.10	10.57	0.13	0.40	24.15	160	27.4	4.74	0.81
Sapelo Island August 2012	MLD1-12	04:29 AM	2.57	3.81	1.58	*0.37*	23.71	393	ND	5.89	ND
	MLD2-12	08:48 AM	2.52	4.04	2.08	*0.37*	27.76	330	17.9	2.90	0.16
	MLD3-12	11:18 AM	3.29	4.69	2.05	*0.37*	25.06	647	ND	6.35	ND
	MLD4-12	03:20 PM	1.36	2.56	3.12	*0.37*	24.33	271	12.9	2.13	0.10
	MLD5-12	06:32 PM	2.68	4.13	1.38	*0.37*	24.95	369	ND	21.4	ND
	MLD5R-12	06:45 PM	2.84	4.01	1.42	*0.37*	26.01	327	ND	3.21	ND
	MLD6-12	09:40 PM	2.61	5.93	1.79	*0.37*	24.66	457	26.0	5.58	0.32
	MLD7-12	12:03 AM	2.58	7.11	3.15	*0.37*	47.42	775	ND	9.32	ND
	MLD8-12	03:25 AM	2.17	5.23	1.04	*0.37*	26.33	428	37.6	5.27	0.46
Sapelo Island September 2013	ML13-2F	11:30 AM	2.98	17.16	5.43	0.02	26.05	273	42.6	1.49	0.23
	ML13-3F	11:30 AM	3.13	11.13	0.46	0.03	25.35	268	55.3	1.46	0.30
South Atlantic Bight April 2011	SAB-P #4	1.5	0.02	1.49	0.49	0.12	24.99	1.12	**-0.01**	50.5	ND
	SAB-P #4	13	0.02	0.81	0.44	0.22	24.99	0.27	0.03	0.49	0.06
	SAB-P #8	2	0.04	0.96	0.24	0.15	25.70	**-1.14**	0.01	ND	1.08
	SAB-P #8	30.5	0.00	0.62	-0.03	0.13	25.70	1.31	**-0.01**	23.11	ND
	SAB-P #12	10	-0.01	0.59	-0.09	*0.10*	24.62	**-0.05**	**-0.001**	ND	ND
	SAB-P #12	70	2.03	3.07	2.41	0.26	24.62	82.9	4.20	3.19	0.16
	SAB-P #12	500	0.00	32.26	-0.13	0.08	24.65	0.62	**-0.98**	0.02	ND

Sample Location	Station ID	Time or Depth*	[NO_2]	[NO_x]	[NH_4]	[Urea]#	Incubation Time (h)	$^{15}NH_4$ Rate (nM d^{-1})	^{15}N Urea Rate (nM d^{-1})	$^{15}NH_4$ Rate Per Cell$	^{15}Urea Rate Per Cell$
South Atlantic Bight October 2011	SAB-P2 #12	20	0.01	1.48	-0.77	0.83	24.11	0.17	**-0.63**	10.8	ND
	SAB-P2 #12	80	0.14	3.13	-1.26	0.04	24.11	6.04	0.67	0.21	0.02
	SAB-P2 #12	200	0.05	17.46	1.25	0.20	24.11	3.84	0.38	0.08	0.01
	SAB-P2 #12	445	0.00	22.89	-0.79	1.00	24.11	1.60	0.01	0.20	0.00
	SAB-P2 #8	4	0.05	0.09	0.46	1.34	24.76	7.90	1.15	26.9	39.1
	SAB-P2 #8	32	0.09	0.09	-0.39	0.08	24.76	0.01	**-0.08**	0.10	ND
	SAB-P2 #4	4	0.07	1.02	1.71	0.28	24.91	120	1.31	4.83	0.05
	SAB-P2 #4	9	0.13	0.68	0.85	1.18	24.91	86.5	24.8	18.4	5.27
Southern Ocean January 2011	600.040	80	0.19	30.22	0.91	*0.52*	138.75	22.1	17.6	1.89	9.19
	600.040	400	0.08	25.65	2.39	*0.55*	138.77	39.9	10.6	0.07	0.69
	200.040	70	0.19	31.16	0.59	*0.52*	124.88	9.81	21.9	0.31	8.60
	200.040	400	0.07	36.35	0.05	*0.55*	124.05	17.8	11.2	1.02	3.93
	000.100	100	0.09	25.26	1.91	*0.52*	126.89	6.34	20.5	0.01	8.21
	000.100	350	0.02	29.49	0.91	*0.55*	127.65	20.2	7.43	0.71	2.37
Gulf of Alaska August 2013	Stn 002	200	0.22	36.73	0.05	0.13	48.56	LD	1.79	ND	0.15
	Stn 002	800	0.31	47.13	0.03	0.13	48.90	20.4	**-0.35**	0.71	ND
	Stn 015	180	0.11	38.24	-0.63	0.11	48.11	16.8	3.71	0.10	0.08
	Stn 017	200	0.11	47.47	0.27	0.09	49.05	0.24	0.44	0.01	0.01
	Stn 017	800	0.12	38.85	0.08	0.11	49.05	15.4	0.17	8.10	0.07
	Stn 033	200	-0.29	41.67	-0.42	0.20	49.34	**-0.21**	3.02	0.00	0.23

Units for nutrient samples (NO_2, NO_x, NH_4, Urea) are μM. Negative rates in **bold** should be viewed as below the limit of detection.

*Time for surface samples collected from Sapelo Island; depth (m) from all other locations

#Actual concentrations measured or estimated from literature or other nearby sample sites (italic)

$Per cell rates (fmol $cell^{-1}$ d^{-1}) calculated using Thaumarchaeota *rrs* copies L^{-1} as copies $cell^{-1}$, using 1.0 *rrs* per genome (see text).

Table 5.2: Summary of data collected for ammonia versus urea oxidation experiments, including gene and transcript abundance.

Station ID	Depth (m)	Date	Latitude	Longitude	DNA Vol. Filt. (L)	RNA Vol. Filt. (L)	Thaum. *rrs*	Archaea *amoA* W	Archaea *amoA* W mRNA
MLD1-11	0.2	8/14/2011	31° 25' 4.08 N	81° 17' 43.26 W	0.5	0.9	5.13E+07	6.62E+07	4.63E+05
MLD2-11	0.2				0.7	ND	1.21E+07	4.67E+07	ND
MLD3-11	0.2	8/15/2011			0.575	ND	9.15E+07	7.79E+07	ND
MLD4-11	0.2				0.65	ND	2.84E+07	5.15E+07	ND
MLD5-11	0.2				0.75	ND	5.41E+07	9.39E+07	ND
MLD6-11	0.2				0.65	ND	2.16E+07	2.73E+07	ND
ML7-11	0.2				0.6	0.65	3.36E+07	5.84E+07	3.44E+05
MLD1-12	0.2	8/7/2012	31° 25' 4.08 N	81° 17' 43.26 W	0.6	0.6	6.67E+07	9.43E+07	5.35E+04
MLD2-12	0.2				0.6	0.6	1.14E+08	1.74E+08	1.94E+06
MLD3-12	0.2				0.6	0.6	1.02E+08	1.27E+08	6.06E+05
MLD4-12	0.2				0.6	0.6	1.27E+08	1.22E+08	6.27E+04
MLD5-12	0.2				0.6	0.6	1.73E+07	6.53E+07	3.98E+04
MLD5R-12	0.2				0.6	0.6	1.02E+08	1.12E+08	1.29E+06
MLD6-12	0.2				0.65	0.65	8.19E+07	9.52E+07	7.91E+04
MLD7-12	0.2				0.6	0.6	8.32E+07	8.61E+07	6.04E+04
MLD8-12	0.2	8/8/2012			0.6	0.6	8.13E+07	1.24E+08	6.47E+04
ML13-2F	0.2	9/1/2013	31° 25' 4.08 N	81° 17' 43.26 W	0.35	ND	1.83E+08	4.75E+07	ND
ML13-3F	0.2				0.35	ND	1.83E+08	4.75E+07	ND
SAB-P #4	1.5	4/20/2011	30° 42.92' N	81° 21.36' W	0.9	0.9	2.23E+04	1.18E+05	5.47E+04
	13				0.9	0.9	5.45E+05	1.81E+05	2.27E+04
SAB-P #8	2	4/20/2011	30° 31.38' N	80° 42.86' W	1.0	1.0	1.07E+04	4.36E+04	3.29E+03
	30.5				1.1	1.1	5.68E+04	1.37E+05	1.52E+04
SAB-P #12	10	4/20/2011	30° 19.05' N	79° 56.12' W	1.2	1.2	8.04E+02	3.20E+02	3.23E+02
	70				1.0	1.1	2.60E+07	6.82E+07	5.68E+06
	500				1.0	1.0	2.56E+07	1.13E+06	5.93E+04

Station ID	Depth (m)	Date	Latitude	Longitude	DNA Vol. Filt. (L)	RNA Vol. Filt. (L)	Thaum. *rrs*	Archaea *amoA* W	Archaea *amoA* W mRNA
SAB-P2 #12	20	10/4/2011	30° 19.05' N	79° 56.12' W	1	1	1.61E+04	1.56E+04	5.10E+03
	80				1	1	2.82E+07	2.12E+07	1.49E+07
	200				1	1	4.89E+07	2.24E+06	1.57E+05
	445				1	1	7.98E+06	7.30E+05	4.99E+05
SAB-P2 #8	4	10/4/2011	30° 31.38' N	80° 42.86' W	1.01	1	2.94E+05	1.26E+05	8.59E+03
	32				0.8	0.8	1.44E+05	5.01E+05	7.87E+03
SAB-P2 #4	4	10/4/2011	30° 42.92' N	81° 21.36' W	0.95	1	2.49E+07	1.96E+07	7.93E+05
	9				0.95	1	4.70E+06	5.09E+06	8.36E+05
ANT 11 600.040	80	1/11/2011	64° 55.900' S	64° 24.160' W	4.5	1.1	1.92E+06	6.42E+06	2.01E+06
	400				3.95	1.1	1.53E+07	3.07E+07	7.11E+05
ANT 11 200.040 #2	70	1/23/2011	67° 30.731' S	70° 35.350' W	4	0.9	2.55E+06	5.97E+06	7.43E+06
	400				3.2	0.95	2.84E+06	2.10E+06	2.58E+06
ANT 11 000.100	100	1/30/2011	68° 16.625' S	75° 7.576' W	4	1	2.49E+06	4.50E+06	2.91E+06
	350				4	1	3.13E+06	4.16E+06	1.16E+06
GoA Stn 002	200	8/5/2013	48° 58.191' N	130° 40.128' W	1.25	1.1	1.18E+07	1.05E+07	7.57E+06
	800				1.45	1.1	8.42E+06	3.71E+05	9.22E+04
GoA Stn 015	180	8/12/2013	58° 59.968' N	140° 59.956' W	1.50	1.00	4.75E+07	5.43E+07	6.63E+06
GoA Stn 017	200	8/13/2013	57° 09.242' N	148° 42.755' W	1.80	1.1	3.40E+07	1.86E+07	8.29E+06
	800				1.60	1.1	2.39E+06	1.30E+05	7.75E+04
GoA Stn 033	200	8/21/2013	49° 57.343' N	132° 40.094' W	2.60	1.1	1.31E+07	8.86E+06	3.91E+04

Station ID	Depth (m)	Archaea *amoA* F mRNA	Archaea *amoA* F mRNA	Thaum. *ureC*	Thaum. *ureC* mRNA	Bacteria *rrs*	AOB *amoA*	AOB *amoA* mRNA
MLD1-11	0.2	ND	ND	2.97E+06	LD	2.72E+09	1.16E+05	LD
MLD2-11	0.2	ND	ND	1.20E+06	ND	1.44E+09	9.38E+04	ND
MLD3-11	0.2	ND	ND	1.66E+06	ND	3.09E+09	2.98E+05	ND
MLD4-11	0.2	ND	ND	2.20E+06	ND	2.25E+09	1.72E+05	ND
MLD5-11	0.2	ND	ND	3.02E+06	ND	2.60E+09	1.85E+05	ND
MLD6-11	0.2	ND	ND	1.92E+06	ND	9.40E+08	9.84E+04	ND
ML7-11	0.2	ND	ND	2.79E+06	LD	4.19E+09	2.40E+05	LD
MLD1-12	0.2	ND	ND	2.09E+07	9.50E+03	1.01E+11	1.87E+05	LD
MLD2-12	0.2	ND	ND	3.44E+07	3.39E+02	1.93E+11	6.60E+05	LD
MLD3-12	0.2	ND	ND	2.24E+07	LD	7.82E+10	1.11E+06	LD
MLD4-12	0.2	ND	ND	4.75E+07	LD	1.79E+11	6.58E+05	LD
MLD5-12	0.2	ND	ND	1.05E+07	LD	1.33E+10	7.91E+05	LD
MLD5R-12	0.2	ND	ND	1.86E+07	LD	1.37E+11	5.45E+05	LD
MLD6-12	0.2	ND	ND	2.98E+07	LD	1.21E+11	9.22E+05	LD
MLD7-12	0.2	ND	ND	2.79E+07	LD	8.54E+10	6.27E+05	LD
MLD8-12	0.2	ND	ND	3.59E+07	LD	1.18E+11	7.34E+05	LD
ML13-2F	0.2	ND	ND	ND	ND	9.48E+10	6.29E+05	ND
ML13-3F	0.2	ND	ND	ND	ND	9.48E+10	6.29E+05	ND
SAB-P #4	1.5	ND	ND	3.04E+05	2.85E+04	4.78E+09	5.56E+04	1.60E+05
	13	ND	ND	4.13E+04	2.97E+04	6.35E+09	1.52E+06	LD
SAB-P #8	2	ND	ND	1.16E+05	LD	5.25E+09	5.65E+05	9.55E+03
	30.5	ND	ND	2.10E+05	3.45E+03	2.42E+09	3.13E+04	6.57E+03
SAB-P #12	10	7.29E+01	ND	1.85E+04	LD	1.60E+08	9.44E+02	3.02E+03
	70	4.31E+07	ND	2.65E+07	5.47E+03	6.45E+08	7.13E+03	7.49E+03
	500	1.68E+07	1.27E+04	1.33E+06	8.15E+03	1.85E+08	3.94E+03	LD

Station ID	Depth (m)	Archaea *amoA* F	Archaea *amoA* F mRNA	Thaum. *ureC*	Thaum. *ureC* mRNA	Bacteria *rrs*	AOB *amoA*	AOB *amoA* mRNA
SAB-P2 #12	20	2.17E+04	ND	2.10E+05	LD	5.92E+08	4.53E+03	2.90E+03
	80	2.28E+07	ND	3.31E+07	LD	1.12E+09	1.27E+04	5.30E+03
	200	2.36E+07	3.08E+04	4.53E+06	LD	1.81E+08	8.19E+03	1.42E+04
	445	2.17E+07	7.75E+04	2.96E+06	6.70E+03	3.38E+07	9.05E+02	3.55E+03
SAB-P2 #8	4	ND	ND	1.36E+06	6.00E+03	4.37E+09	4.66E+04	1.17E+04
	32	ND	ND	4.46E+06	5.19E+03	6.66E+09	8.28E+04	1.44E+04
SAB-P2 #4	4	ND	ND	2.35E+06	LD	4.18E+09	1.78E+05	4.05E+04
	9	ND	ND	3.73E+06	LD	2.75E+09	5.76E+05	LD
ANT 11 600.040	80	1.65E+04	8.45E+03	2.07E+06	1.04E+03	5.22E+08	3.78E+04	1.11E+05
	400	2.18E+06	3.09E+04	2.97E+07	4.44E+03	1.51E+08	4.65E+04	3.17E+03
ANT 11 200.040 #2	70	3.38E+05	3.90E+02	4.98E+06	3.94E+02	7.13E+07	1.13E+04	6.83E+04
	400	4.57E+02	2.20E+04	7.41E+05	8.95E+03	6.13E+08	1.64E+04	5.99E+03
ANT 11 000.100	100	3.41E+03	ND	1.19E+06	1.19E+03	2.61E+08	1.30E+05	4.44E+05
	350	7.91E+05	ND	8.52E+06	4.96E+03	1.19E+08	8.44E+03	3.02E+03
GoA Stn 002	200	1.01E+07	ND	5.89E+07	4.10E+03	1.24E+09	4.08E+04	3.17E+03
	800	1.05E+07	1.52E+04	4.75E+06	LD	6.38E+08	1.24E+04	LD
GoA Stn 015	180	2.07E+07	4.12E+05	2.32E+08	2.54E+04	6.19E+09	1.32E+06	7.84E+03
GoA Stn 017	200	5.68E+07	ND	2.01E+08	1.78E+04	3.14E+09	1.21E+04	1.94E+04
	800	4.88E+06	1.47E+04	1.84E+06	LD	4.34E+08	9.92E+03	LD
GoA Stn 033	200	1.89E+07	8.00E+03	4.77E+07	LD	8.27E+08	8.38E+03	LD

*ND = not determined; LD = below the limit of detection.

Gene and transcript abundance data are given in copies L^{-1} sample filtered. For Archaea *amoA* genes, "W" refers to Wuchter *et al.* (2006) primers and "F" refers to Francis *et al.* (2005) primers (see Table A.1 and Chapter 2 Discussion)

Figure 5.1: Sample locations for experiments, including **(a)** Sapelo Island, Georgia, and the South Atlantic Bight, **(b)** the Gulf of Alaska, and **(c)** the Southern Ocean near Palmer Station (P), Antarctica.

(a) Sapelo Island, Georgia, and the South Atlantic Bight

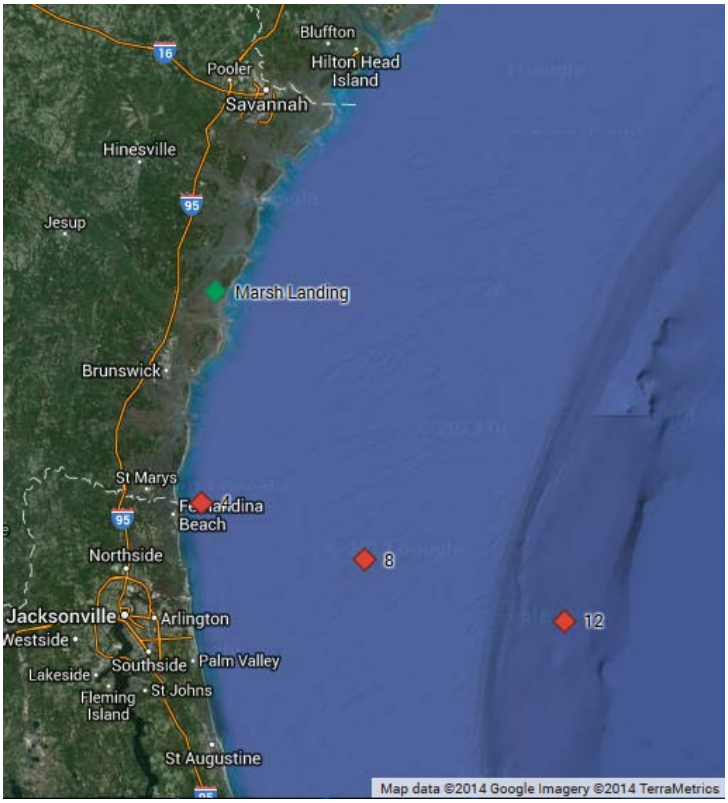

(b) Gulf of Alaska

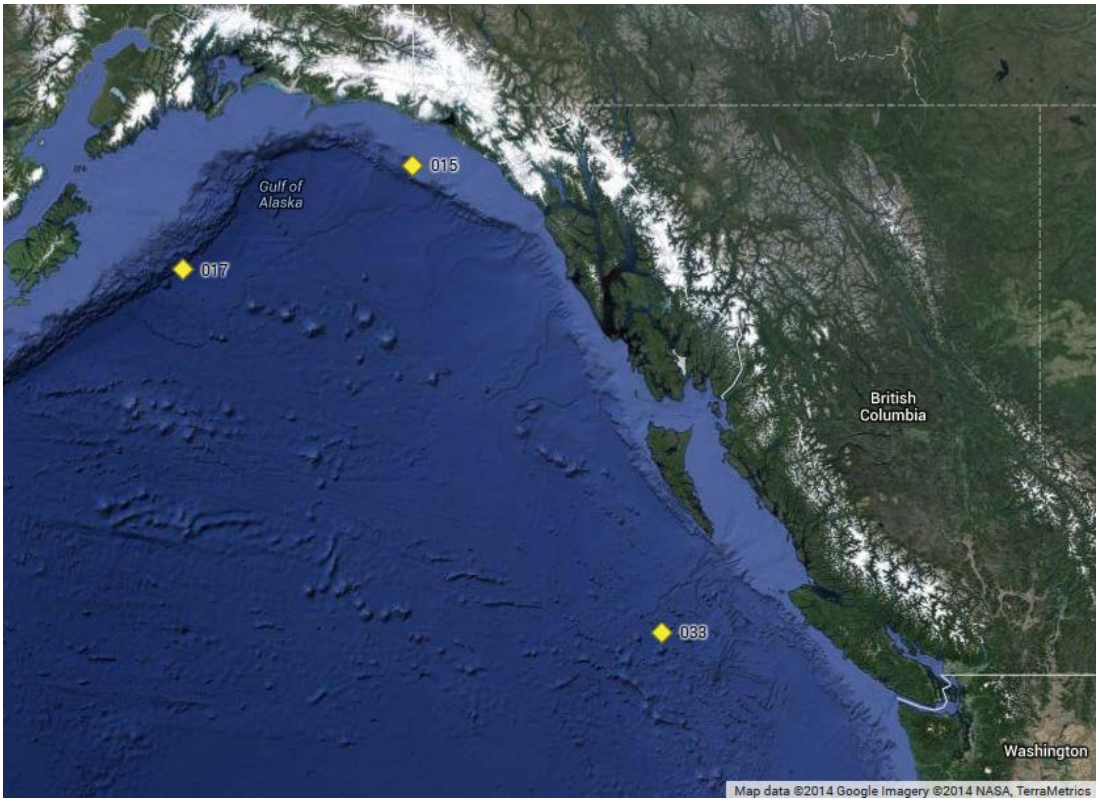

(c) Southern Ocean near Palmer Station (P), Antarctica

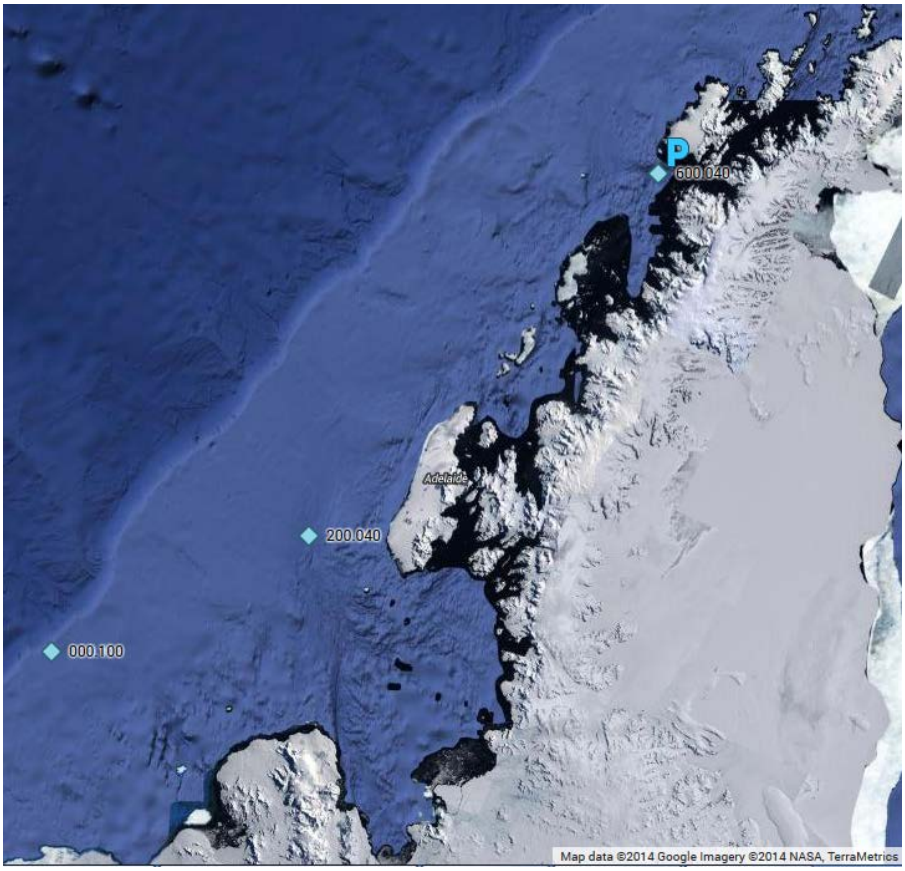

Figure 5.2: Comparison of $^{15}N\text{-}NO_x$ production rates from ^{15}N-ammonia and ^{15}N-urea in samples taken from Sapelo Island, Georgia **(a-b)**; transects into the Atlantic Ocean from the coast of Georgia – South Atlantic Bight **(c-d)**; the Southern Ocean **(e)**; and the Gulf of Alaska **(f)**. Black (blue) bars indicate ammonia oxidation rate, gray (orange) bars indicate urea-N oxidation rate. Urea oxidation was not measured at some time points (indicated by a *; ND in Table 5.1).

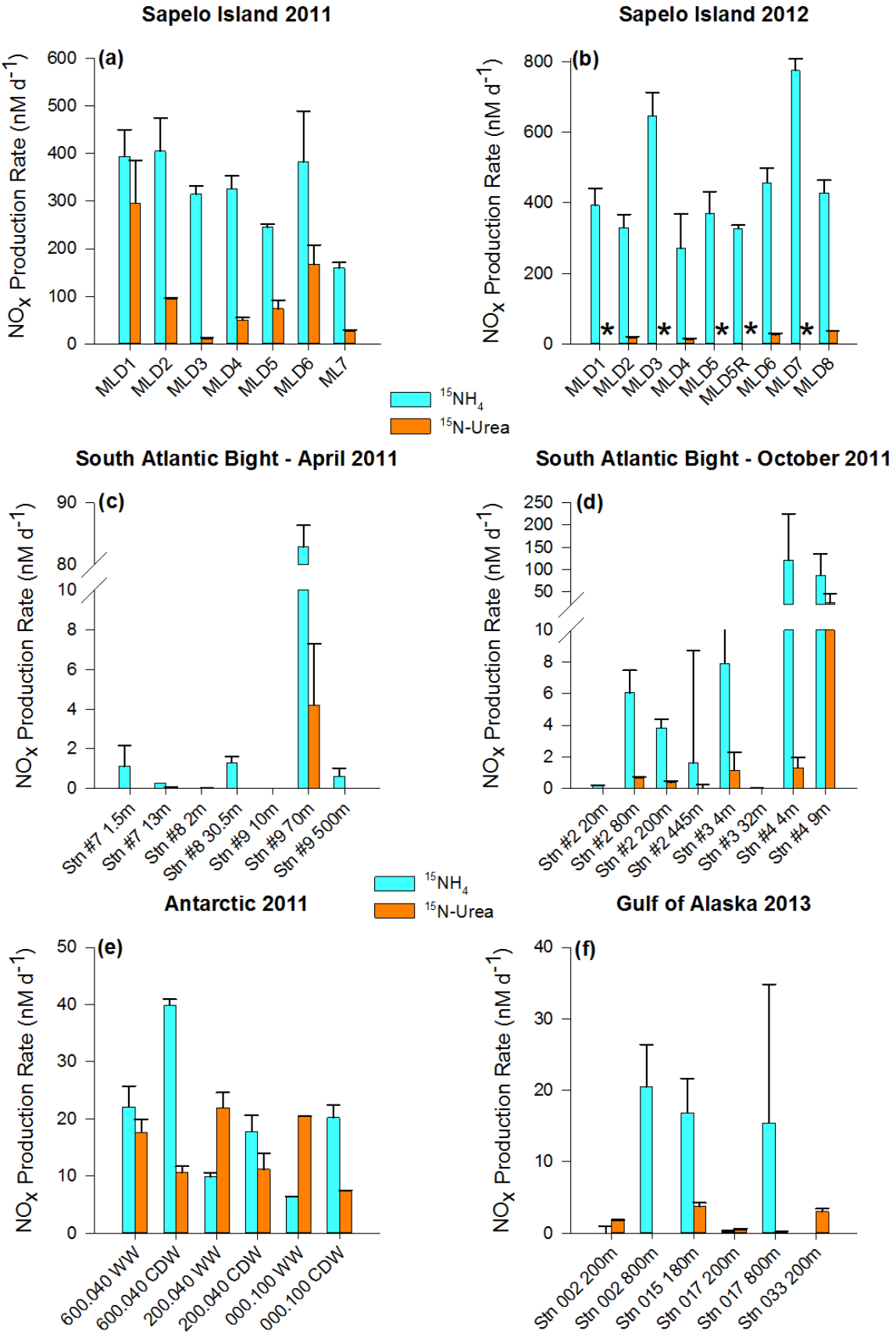
Sapelo Island 2011
(a)
NOX Production Rate (nM d-1)
600
500
400
300
200
100
0
MLD1
MLD2
MLD3
MLD4
MLD5
MLD6
ML7
Sapelo Island 2012
(b)
800
600
400
200
0
*
MLD1
MLD2
MLD3
MLD4
MLD5
MLD5R
MLD6
MLD7
MLD8
15NH4
15N-Urea
South Atlantic Bight - April 2011
(c)
90
80
10
8
6
4
2
0
Stn #7 1.5m
Stn #7 13m
Stn #8 2m
Stn #8 30.5m
Stn #9 10m
Stn #9 70m
Stn #9 500m
South Atlantic Bight - October 2011
(d)
250
200
150
100
50
10
8
6
4
2
0
Stn #2 20m
Stn #2 80m
Stn #2 200m
Stn #2 445m
Stn #3 4m
Stn #3 32m
Stn #4 4m
Stn #4 9m
15NH4
15N-Urea
Antarctic 2011
(e)
50
40
30
20
10
0
600.040 WW
600.040 CDW
200.040 WW
200.040 CDW
000.100 WW
000.100 CDW
Gulf of Alaska 2013
(f)
40
30
20
10
0
Stn 002 200m
Stn 002 800m
Stn 015 180m
Stn 017 200m
Stn 017 800m
Stn 033 200m

Figure 5.3: Replicate experiments performed with the same water sample from Sapelo Island (2013) showing $^{15}N\text{-}NO_x$ production rates. **(a)** A comparison of ^{15}N-ammonia and ^{15}N-urea oxidation rates in two separate experiments set up similar to those in Figure 5.2. **(b)** Competition experiment investigating whether ammonia oxidation rates from samples amended with ^{15}N-labeled ammonia (50 nM) would change with the addition of unlabeled ammonia or urea (5 μM). Two separate non-addition controls (Controls #1, #2) were also run, showing that only ammonia decreased oxidation of ^{15}N-ammonia.

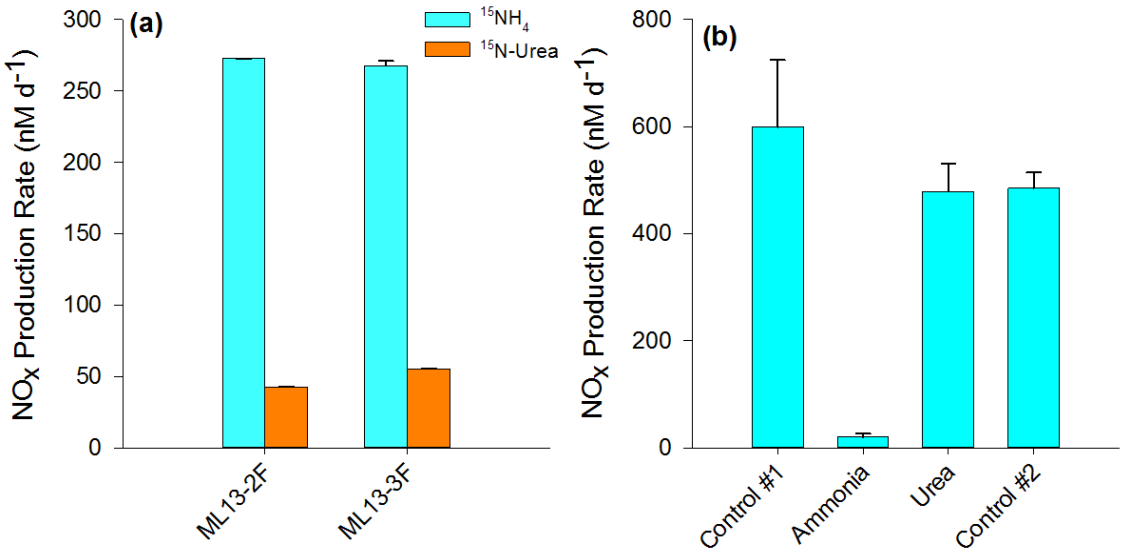
(a)
$^{15}NH_4$
^{15}N-Urea
NO_X Production Rate (nM d^{-1})
300
250
200
150
100
50
0
ML13-2F
ML13-3F
(b)
NO_X Production Rate (nM d^{-1})
800
600
400
200
0
Control #1
Ammonia
Urea
Control #2

Figure 5.4: Hydrolysis of urea in samples collected **(a)** near Sapelo Island, Georgia, and **(b)** in the Gulf of Alaska.

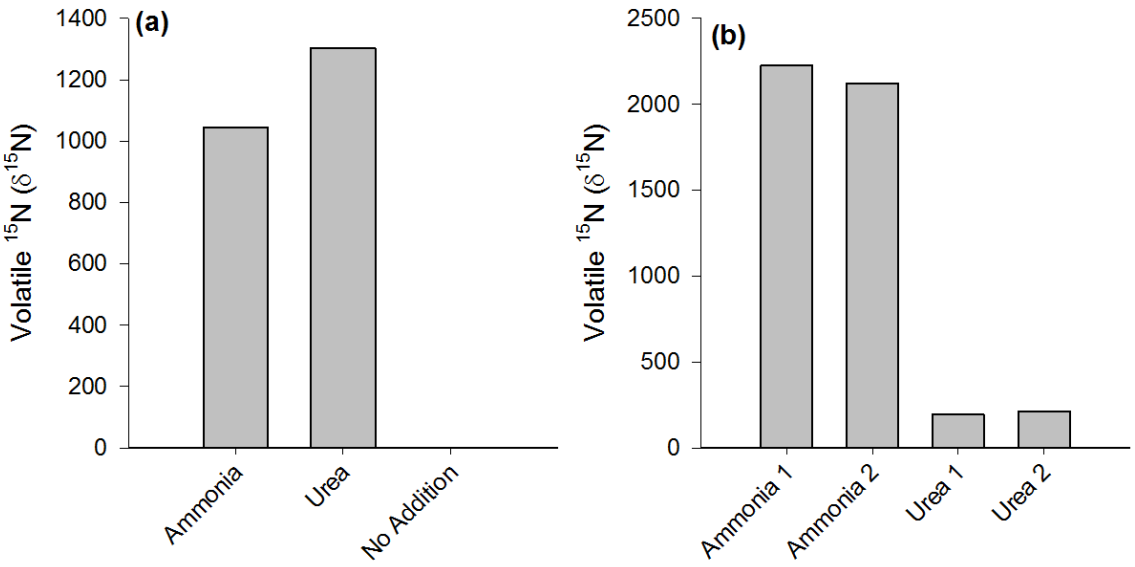
(a)
Volatile ^{15}N ($\delta^{15}N$)
1400
1200
1000
800
600
400
200
0
Ammonia
Urea
No Addition
(b)
Volatile ^{15}N ($\delta^{15}N$)
2500
2000
1500
1000
500
0
Ammonia 1
Ammonia 2
Urea 1
Urea 2

Figure 5.5: Cell-specific rates of ammonia (blue circles) **or urea-N** (orange circles) **oxidation plotted against the transcript:gene ratio of *amoA* or *ureC***, respectively, for each of the sample sites: Sapelo Island, Georgia in 2011 **(a)** and 2012 **(b)**; transects into the Atlantic Ocean from the coast of Georgia – South Atlantic Bight in April **(c)** and October **(d)**; the Southern Ocean **(e)**; and the Gulf of Alaska **(f)**. Regression lines and r^2 values are shown for sites with more than two data points.

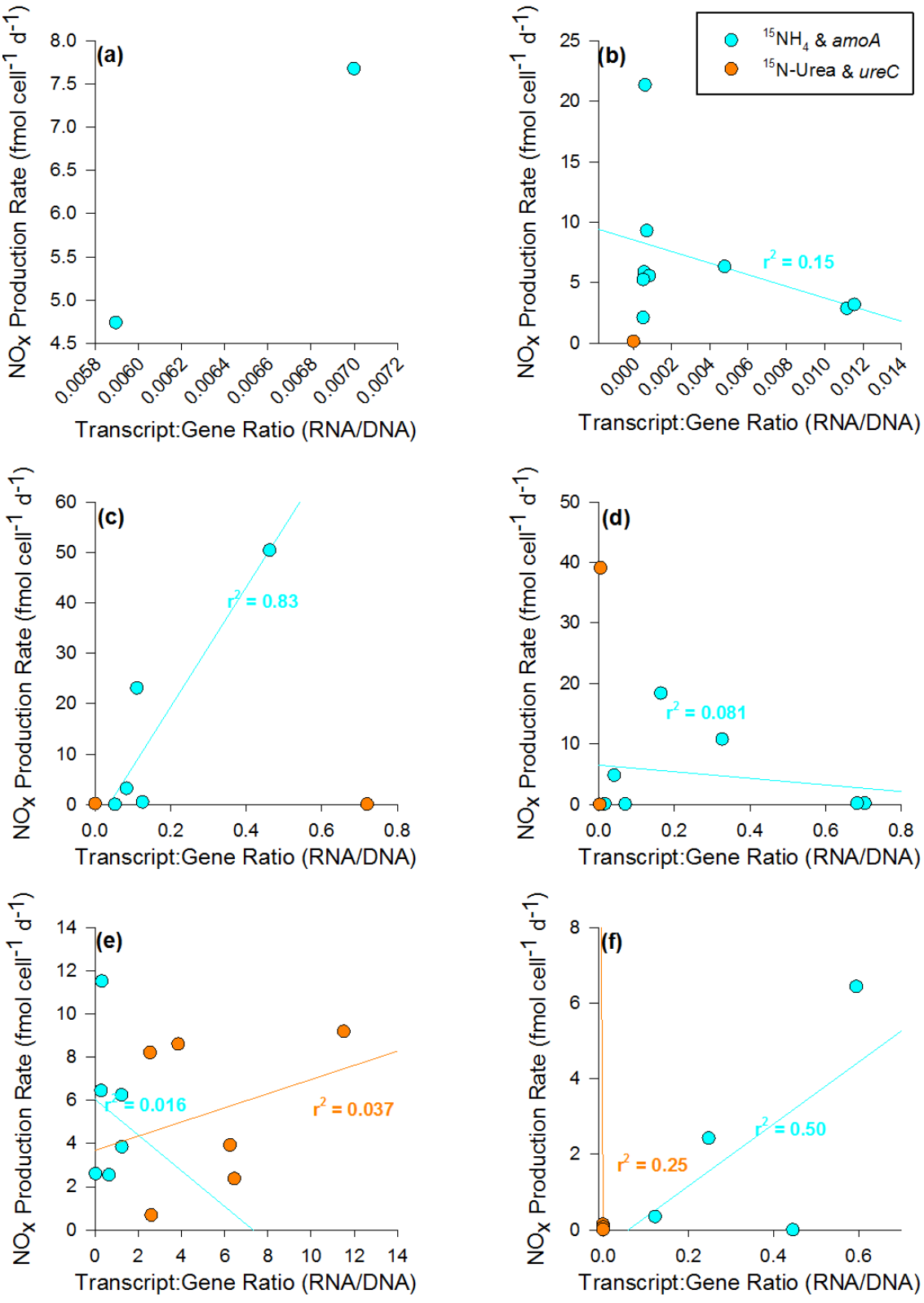
(a)
(b)
(c)
(d)
(e)
(f)
$^{15}NH_4$ & *amoA*
^{15}N-Urea & *ureC*
r^2 = 0.15
r^2 = 0.83
r^2 = 0.081
r^2 = 0.016
r^2 = 0.037
r^2 = 0.50
r^2 = 0.25
NO_X Production Rate (fmol cell^{-1} d^{-1})
Transcript:Gene Ratio (RNA/DNA)

CHAPTER 6

AMMONIA OXIDATION IN THE OPEN OCEAN IS INHIBITED BY HYDROGEN PEROXIDE[1]

[1] Tolar, B.B., L.C. Powers, W.L. Miller, N.J. Wallsgrove, B.N. Popp, and J.T. Hollibaugh. To be submitted to *Nature Geoscience*.

SUMMARY

Thaumarchaeota are one of the most abundant groups of microorganisms, estimated to be about 20% of total picoplankton in the ocean. They are chemoautotrophs that oxidize ammonia to nitrite, mediating a key step in the global nitrogen cycle and are thought to generate the greenhouse gas N_2O in the process. Despite their almost ubiquitous distribution, marine Thaumarchaeota are rarely observed in open-ocean surface (<100 m) waters. We tested the hypothesis that this vertical distribution is driven by reactive oxygen species (ROS), specifically by H_2O_2, which is generated by photochemical and biological processes. Here we show that H_2O_2 can be surprisingly toxic to open-ocean Thaumarchaeota, with ammonia oxidation in Southern Ocean samples inhibited by additions of as little as 10 nM H_2O_2. This sensitivity could explain the seasonal disappearance of Thaumarchaeota from polar surface waters and suggests a potential impact on the global nitrogen cycle.

MAIN TEXT

Photoinhibition has been postulated to reduce ammonia oxidation (AO), the first step of nitrification, in both ammonia-oxidizing Bacteria (AOB; Hooper and Terry, 1973; Olson, 1981; Ward, 1985) and Archaea (AOA; Church *et al.*, 2003; Murray *et al.*, 1998; Murray *et al.*, 1999a; Qin *et al.*, 2014). Nitrification links key processes within the nitrogen cycle (e.g., nutrient regeneration, assimilation, respiration) by converting the most reduced form of inorganic N (ammonium) into the most oxidized (nitrate), which can then be used by phytoplankton for primary production or denitrified and removed from the pool of fixed N (reviewed in Ward, 2011). Early measurements of nitrification

showed reduced or undetectable rates in surface waters (reviewed in Alleman *et al.*, 1987), which were attributed to light sensitivity of AOB. AOA are now generally regarded as the dominant ammonia-oxidizing organisms (AOO) in marine environments (reviewed in Ward, 2011) and are members of the marine Thaumarchaeota (Spang *et al.*, 2010) – a group estimated to account for ~20% of the total prokaryotic cells in the ocean (Karner *et al.*, 2001). However, Thaumarchaeota do not often achieve high abundances in the surface ocean (Agogué *et al.*, 2008; Fuhrman *et al.*, 1992; Herndl *et al.*, 2005; Karner *et al.*, 2001; Massana *et al.*, 1998; Mincer *et al.*, 2007), with notable exceptions during winter at higher latitudes and in polar regions (Massana *et al.*, 1998; Murray *et al.*, 1998; Murray *et al.*, 1999a; Pitcher *et al.*, 2011; Wuchter *et al.*, 2006). Attempts to explain these patterns have focused primarily on competition with bacteria or phytoplankton and on light inhibition (Church *et al.*, 2003; Merbt *et al.*, 2012; Murray *et al.*, 1999a; Smith *et al.*, 2014b; Wells and Deming, 2003). However, most of these theories are derived from negative correlations between environmental variables and abundance. In the Southern Ocean, Thaumarchaeota populations decrease – especially in surface waters (Church *et al.*, 2003) – as irradiance increases during the transition from winter to summer (Murray *et al.*, 1998). This could indicate that photoinhibition or a product of increased irradiance (such as reactive oxygen species, or ROS) has an impact on Thaumarchaeota and, perhaps, on nitrification in general.

The photochemical production of ROS (i.e., H_2O_2, superoxide, singlet oxygen, and hydroxyl radical; Imlay, 2008) proceeds at significant rates in sunlit waters (Figure 6.1a-d), creating a daily increase in ROS concentration that is ubiquitous in surface seawater (Kieber *et al.*, 2003). Since ROS can also be formed internally as by-products

of biochemical reactions like photosynthesis and respiration, they must be removed to prevent cell damage (Diaz *et al.*, 2013; Dixon *et al.*, 2013; Marshall *et al.*, 2005). Prokaryotes possess a number of mechanisms to protect themselves against the harmful effects of ROS, including detoxifying enzymes and DNA repair systems (Imlay, 2008; Figure 6.1e). A survey of the Integrated Microbial Genomes (IMG) database (http://img.jgi.doe.gov/), however, indicated a potential deficiency of ROS-related genes in Thaumarchaeota relative to Bacteria or Euryarchaeota (Table 1.1). All Thaumarchaeota genomes sequenced to date possess at least one copy of superoxide dismutase, which converts superoxide into H_2O_2; however, only *Nitrososphaera gargensis* (isolated from a hot spring; Hatzenpichler *et al.*, 2008) has an annotated catalase (Table 1.1) – the most efficient enzyme known for detoxifying H_2O_2 (Imlay, 2008). Thaumarchaeota have genes annotated as peroxiredoxin; however, peroxiredoxin is less efficient than catalase and has been shown to remove H_2O_2 effectively only at low intracellular concentrations (Imlay, 2008). The other peroxidases encoded in Thaumarchaeota genomes may or may not directly detoxify H_2O_2 (Mishra and Imlay, 2012). It is therefore possible that the distribution of Thaumarchaeota could be explained by the absence of ROS detoxifying enzymes rather than by "competition" with Bacteria or phytoplankton for ammonia.

Here we test the hypothesis that apparent photoinhibition of AO is actually the result of toxic effects of H_2O_2 generated external to the cell. We examined the sensitivity of AO to the ROS species H_2O_2 in AOO assemblages dominated by Thaumarchaeota (Table 6.1) from a wide range of marine environments, including the Southern Ocean near Palmer Station (Antarctica), the Gulf of Mexico, and the Gulf of Alaska (Figure

6.2). Whole-seawater incubations were performed at *in situ* temperatures with additions of ^{15}N-labeled ammonium to determine rates of AO in the presence of H_2O_2 added at environmentally relevant (nM) concentrations (see Methods). We also quantified the abundance of transcripts from *amoA*, which encodes one subunit of the ammonia monooxygenase enzyme that catalyzes ammonia oxidation. Finally, we measured overall microbial activity using leucine incorporation to determine the effects of H_2O_2 on a general cellular function (protein synthesis) for comparison.

AO rates were below detection in the Southern Ocean following addition of 30 nM H_2O_2 to samples (Figure 6.3a-b), indicating that AOO in this region are extremely sensitive to H_2O_2. This sensitivity could be due to typically low [H_2O_2] during winter, allowing microorganisms to survive without ROS detoxification systems. Measurements of H_2O_2 made in spring are low (2.9-14 nM) and match previous ranges (Resing *et al.*, 1993). The abundance of AOA *amoA* transcripts did not reflect the drastic decrease in AO rates observed in treatments with H_2O_2 additions (this was observed at all sites sampled; Figure 6.4). Southern Ocean leucine incorporation rates were also reduced with increasing H_2O_2 concentration (Figure 6.5a); this reduction was less than that in AO rates and was significantly different (average 17% vs. 67% reduction; t-test, $p < 0.01$).

The AO response to H_2O_2 additions was variable in both the Gulf of Mexico (Figure 6.3c) and the Gulf of Alaska (Figure 6.3d), with the greatest inhibition observed at Stations B4 (GoM) and 033 (GoA) with any H_2O_2 addition. At Station C4 (GoM) there was no difference in AO between samples with 0 or 100 nM added H_2O_2, and no change was observed with amendments of up to 300 nM H_2O_2 at Station 015 (coastal GoA, 50 m). This may be due to the efficiency with which the surrounding microbial

community detoxified H_2O_2 (Table 6.2; Figure 6.6); however, differences in net decay rate do not fully explain this variability, which may indicate a difference in the composition of thaumarchaeote populations where some 'ecotypes' could be more or less resistant to ROS stress. Rates of leucine incorporation (protein synthesis) also varied with sample location; for example, we found no significant difference with increased additions of H_2O_2 at Stations C4 or A6 (GoM; Figure 6.5b).

Our data show that nanomolar concentrations of H_2O_2 are harmful to open-ocean AOO, with the most sensitive communities found in polar waters. We observed a significant reduction of AO rates measured after the introduction of H_2O_2 when evaluating the entire dataset together (ANOVA, $F = 14.85$, $p < 0.001$). Rates from both low (target: 10-100 nM) and high (target: 30-300 nM; Table 6.2) H_2O_2 additions were significantly lower than control incubations ($p < 0.001$; Tukey's HSD). There was no significant difference between treatments when examining leucine incorporation rates ($F = 0.17$, $p < 0.9$), indicating that AO is more sensitive to H_2O_2 toxicity than general microbial metabolism.

Controlled light inhibition experiments have indicated that AO is reduced in the presence of increased light for both AOB (Guerrero and Jones, 1996; Hooper and Terry, 1973; Hyman and Arp, 1992) and AOA (Merbt *et al.*, 2012). None of these studies measured concentrations of ROS produced in experiments. We have shown that environmentally relevant [H_2O_2] can inhibit AO in bacterioplankton where Thaumarchaeota are the dominant AOO. The sensitivity of AOA ammonia oxidation to H_2O_2 could explain their absence from surface waters, consistent with early theories for photoinhibition of AO (Alleman *et al.*, 1987); additionally, Hooper and Terry (1973)

indicated that AO by *Nitrosomonas europaea* was inhibited by the addition of catalase inhibitors. H_2O_2 is produced in all sunlit marine waters, through both abiotic and biotic processes where it can enter and damage cells that do not have detoxifying enzymes (Figure 6.1).

The question remains as to why some Thaumarchaeota are sensitive to H_2O_2 (especially compared to Bacteria), given that they likely evolved in an oxygenic world (Kelly *et al.*, 2011; Spang *et al.*, 2010). Most Thaumarchaeota reside in deeper waters (Agogué *et al.*, 2008; Fuhrman *et al.*, 1992; Herndl *et al.*, 2005; Karner *et al.*, 2001; Massana *et al.*, 1998; Mincer *et al.*, 2007) with lower H_2O_2 concentrations, but some clades have been found in the surface and coastal oceans, primarily at higher latitudes (Massana *et al.*, 1998; Murray *et al.*, 1998; Murray *et al.*, 1999a; Pitcher *et al.*, 2011; Wuchter *et al.*, 2006). However, we have also described an abundant and active community of Thaumarchaeota in coastal Georgia (Hollibaugh *et al.*, 2011; Hollibaugh *et al.*, 2014; Chapter 4, Appendices C and D), where [H_2O_2] are high especially during summer (Appendix E). These Thaumarchaeota are less sensitive to H_2O_2 (Figure E.1), and the overall community at Sapelo Island appears to be distinct from other open-ocean 'ecotypes' and more similar to "*Candidatus* Nitrosopumilus maritimus" SCM1 (Hollibaugh *et al.*, 2011; Hollibaugh *et al.*, 2014). Thus, it appears that sensitivity to H_2O_2 may be a characteristic that could assist in subdivision of Thaumarchaeota into meaningful ecotypes and could also support the previously described differences between 'Group A' (near-surface) and 'Group B' (deep) phylogeny (Beman *et al.*, 2008; Beman *et al.*, 2010; Francis *et al.*, 2005; Luo *et al.*, 2014) and activity (Smith *et al.*, 2014a).

Mechanisms of H_2O_2-induced stress for Thaumarchaeota include iron, which can increase oxidative damage through the Fenton reaction, leading to the formation of the toxic hydroxyl radical (Imlay, 2008) and inactivation of iron-containing enzymes (Anjem and Imlay, 2012; Sobota and Imlay, 2011). This process could occur inside the cell; in addition, membrane-bound enzymes or transporters could also be damaged by exogenous ROS. Enzyme damage can be reversed (or prevented) by replacement of Fe(III) with a divalent metal, such as manganese (Anjem and Imlay, 2012), and analysis of Thaumarchaeota genomes indicate replacement of Fe by Cu in the active site of many enzymes, including ammonia monooxygenase and proteins in the electron transport system (Amin *et al.*, 2013; Walker *et al.*, 2010). It is therefore possible that Thaumarchaeota evolved to use Cu in place of Fe to reduce the burden of ROS stress, rather than as a response to low Fe bioavailability. However, this comes at a cost in that these organisms can now be copper-limited (Amin *et al.*, 2013), particularly in coastal ecosystems where bioavailable [Cu] may be low (Amin *et al.*, 2013; Jacquot *et al.*, 2014).

H_2O_2 inhibition should lead to reduced nitrification, which could have profound effects in systems where coupled nitrification-denitrification is important; for example, in eutrophied coastal waters where this process removes excess fixed N. An increase in concentrations of fixed N in coastal waters can support blooms of harmful algae and excess primary production, which can lead to the formation of hypoxic ("dead") zones that can harm coastal fisheries (Rabalais *et al.*, 2010). However, H_2O_2 addition experiments from Sapelo Island, Georgia, suggest that communities in coastal waters are more resilient to ROS stress (Appendix E). Increased [Fe] in polar waters as a result of glacial meltwater accompanying global warming (Bhatia *et al.*, 2013; Raiswell *et al.*,

2008) should also increase ROS production and phytoplankton growth (Paerl and Otten, 2013), which could lead to an altered N-cycle in these waters. As trends of decreased sea ice cover in polar regions (and thus increased light penetration and photochemical activity) are predicted to continue, the resulting ice melt (and therefore increased exposure of surface communities to light) may negatively impact nitrification in polar waters. Finally, open-ocean waters are where most nitrification occurs (Yool *et al.*, 2007), even in the euphotic zone (Smith *et al.*, 2014a). As we have shown here that open-ocean Thaumarchaeota are sensitive to H_2O_2, the potential impact of ROS on ammonia oxidation worldwide should be a priority for future studies.

METHODS

Experimental Setup

Seawater samples were collected (Figure 6.2) in the Gulf of Mexico (GoM – *R/V Pelican*, May 2012; Station C4 – 27° 55.169' N, 90° 22.072' W; Station B4 – 28° 26.551' N, 89° 45.577' W; Station A6 – 28° 39.744' N, 88° 00.443' W), along the Palmer LTER 600 line in the Southern Ocean (Pal – *ARSV Laurence M. Gould*, September 2010; Station 600.160 – 64º 12.657' S, 66º 15.600' W; and Station 600.080 – 64º 41.682' S, 65º 01.849' W), and in the Gulf of Alaska (GoA – *R/V Melville*, August 2013; Station 004 – 49° 34.194' N, 138° 40.188' W; Station 015 – 58° 59.968' N, 140° 59.956' W; Station 033 – 49° 57.343' N, 132° 40.094' W). Seawater was added to 4 L (Pal) or 10 L (GoM, GoA) carboys and kept at *in situ* temperature (shipboard incubators – Pal; seawater flow-through tank – GoM, GoA) in the dark. ^{15}N-labeled ammonium ($^{15}NH_4Cl$; Cambridge Isotope Laboratories) was added at a concentration of 50 nM (Beman *et al.*, 2012;

Santoro *et al.*, 2010) to determine ammonia oxidation (AO) rates, and hydrogen peroxide (H_2O_2; Fisher – Pal; J.T. Baker – GoM, GoA) was added to experimental treatments at target concentrations designated as either 'low' (10-100 nM) or 'high' (30-300 nM); approximate H_2O_2 additions varied by sample site (Table 6.2). H_2O_2 concentrations in stock solutions were determined by absorbance at 240 nm and a molar absorptivity of 38.1 M^{-1} cm^{-1} (Miller and Kester, 1988). Due to variability in measuring stock solutions, adding H_2O_2 to carboys, and subsequent mixing, measured concentrations of H_2O_2 additions at T=0 did not always correspond to the target concentration. Therefore, initial [H_2O_2] was estimated by modeling H_2O_2 decay (Table 6.2) when possible.

RNA Extraction and Quantification

After incubation for 6 hours with H_2O_2, samples were filtered directly onto 47 mm (Pal) or 142 mm (GoM, GoA) 0.22 µm pore size GVWP filters (Millipore), which were frozen in RNA*later* (Ambion) until extraction. RNA was extracted following previously described methods (Gifford *et al.*, 2011; Poretsky *et al.*, 2008) with the replacement of 200 µm zirconium beads (OPS Diagnostics) for the initial bead-beating step. DNA was removed after extraction with the TURBO DNase-Free Kit (Ambion) following manufacturer's instructions with an additional enzyme treatment at 2X concentration. RT-qPCR reactions targeting *amoA* transcripts were performed using the One-Step RT-qPCR SYBR Mix (BioRad), archaeal *amoA* primers (Wuchter *et al.*, 2006), and 1-2 µL of RNA template. AOB *amoA* transcripts were either not detected or below the limit of detection in any of our samples (data not shown). qPCR reaction conditions follow previous methods Kalanetra *et al.* (2009) with the addition of a 15 minute

incubation step at 50°C for reverse transcription of RNA to cDNA prior to the initial denaturation at 95°C. Raw transcript abundance (copies μL^{-1} of RNA extract) was converted to transcripts L^{-1} using the volume filtered and an elution volume of 100 µL, assuming 100% extraction efficiency. DNA extraction, quantification of Archaeal and Bacterial genes using qPCR, and calculation of gene copies L^{-1} were performed as previously described (Tolar *et al.*, 2013; Chapter 2).

Ammonia Oxidation Rate Measurements

Ammonia oxidation **(**AO) rates were measured during dark incubations at *in situ* temperature for 24 h (GoM), 48 h (GoA), or 96 h (Pal) with $^{15}NH_4Cl$. Controls were filtered sample water or frozen immediately after addition of tracer. Incubations were terminated by freezing samples at -20 or -80°C and kept frozen until analysis. Samples were analyzed using the 'denitrifier' method (Sigman *et al.*, 2001) with *Pseudomonas aureofaciens* cultures maintained in the Stable Isotope Biogeochemistry Laboratory at the University of Hawai'i – Mānoa and the $\delta^{15}N$ value of the resultant N_2O measured as described previously (Dore *et al.*, 1998; Popp *et al.*, 1995). Briefly, NO_2 and NO_3 present in each sample were converted to N_2O gas through denitrification by *P. aureofaciens*, transferred from the reaction vial, cryofocused, and separated from other gases using a CP-PoraBOND Q capillary column (0.32 mm inner diameter x 25 m x 5 µm) at 20-25°C. The mass of N_2O was measured using a MAT-252 isotope ratio mass spectrometer (Finnigan) to determine how much of the $^{15}NH_3$ tracer was introduced to the NO_x pool through AO (Beman *et al.*, 2008; Christman *et al.*, 2011). Catalase (0.6 µg L^{-1} final concentration) was added to thawed samples that were then incubated at room

temperature for 30-60 minutes to prevent inhibition of *P. aureofaciens* growth or denitrification ability by residual H_2O_2. Calculation of the AO rate from $\delta^{15}N$ values was performed as previously described (Beman *et al.*, 2012; Christman *et al.*, 2011).

Leucine Incorporation Rate Measurements

The response of all prokaryotes to H_2O_2 was measured using ^{13}C-leucine (GoM, GoA) or ^{3}H-leucine (Pal), added to a final concentration of 100 nM. For ^{13}C-leucine incorporation, samples were incubated for 6 hours at *in situ* temperature, filtered through GF/F filters, and killed using ice-cold 5% trichloroacetic acid. Filters were frozen until analysis on an Isotope Ratio Mass Spectrometer (IRMS) after flash combustion of sample carbon to $^{13}CO_2$ by R. Culp (UGA Center for Applied Isotope Studies; GoA) and T. Maddox (UGA School of Ecology Analytical Chemistry Laboratory; GoM). Samples from the Antarctic amended with ^{3}H-leucine (100 nM) were incubated for 6 hours in 10 mL test tubes at *in situ* temperature in the dark, filtered onto 0.22 µm GSWP filters (Millipore), dissolved in ethyl acetate, and counted directly using a Perkin Elmer Tri-carb 2900 liquid scintillation counter.

Hydrogen Peroxide Concentrations

H_2O_2 was measured first in the Southern Ocean using the POHPAA method (Miller and Kester, 1988) on samples that were first reacted, then frozen and measured on an Aqualog fluorometer (Horiba Scientific). As this was a preliminary experiment, only a subset of samples had detectable H_2O_2 concentrations (Table 6.2). For the remaining experiments, we switched to a more sensitive method using a FeLume

chemiluminescence (CL) system (Waterville Analytical; Figure 6.7) with modifications to previous protocols (King *et al.*, 2007). Briefly, H_2O_2 reacts with 10-methyl-0-(p-formylphenyl)-acridinium carboxylate trifluoromethanesulfonate (acridinium ester, AE; provided by James Kiddle, University of Western Michigan) at alkaline pH, forming a chemiluminescent product that can be quantified using flow injection analysis. In the FeLume system, we used a peristaltic pump (Rainin, operated at 15 RPM) to run the reagent and the carrier/sample plug to a flow cell located in front of a photomultiplier tube (PMT) detector (Hamamatsu HC135 photon counter, operated at 900 V with an integration time of 400 ms). The sample loop (195 μL volume) was filled with sample seawater using a plastic syringe to flush at least 1 mL of sample through the loop. This system takes about 60 seconds for each measurement, and H_2O_2 can be measured in solution in real time. In addition, it is very sensitive, with a limit of detection of 350 pM for open ocean seawater (King *et al.*, 2007).

Operating conditions and instrument set-up (Figure 6.7) were as follows: (1) sample syringe, (2) peristaltic pump: carrier – 0.2 M HCl, CL reagent – 1 μM AE, carbonate buffer – 0.1 M pH 10.4, (3) acid wash loop (unused), (4) 10-port valve dual injection (VICI), (5) sample loop, and (6) flow cell. The optimal pH for the reaction of H_2O_2 and AE is 11.3 (King *et al.*, 2007), but mixing seawater and alkaline carbonate buffer causes the precipitation of magnesium hydroxide in the flow cell. To prevent this precipitate from blocking the flow cell and decreasing the PMT signal, King *et al.* (2007) added an acid wash loop to the injection valve. Instead, we decided to lower the buffer pH to 10.4 and to use dilute acid as the carrier, which also helped to deceased background CL. A 2 mM H_2O_2 stock solution was prepared from 30% H_2O_2 (J.T. Baker) in ultrapure

water and checked spectrophotometrically as above. Standards were prepared in aged seawater and checked for low H_2O_2 with H_2O_2 blanks of aged seawater with added catalase (20 μL of 100 units L^{-1} catalase to 20 mL seawater). Under these conditions, the H_2O_2 detection limit, defined as three times the standard deviation of the blank, was 2-5 nM.

While the overall decay of hydrogen peroxide should be second order (Zepp *et al.*, 1987), decay in addition experiments generally followed first-order kinetics with respect to hydrogen peroxide concentration,

$$\frac{d[H_2O_2]}{dt} = -k_{obs}[H_2O_2] \tag{6.1}$$

where k_{obs} is the observed rate constant (h^{-1}). By integrating Equation (6.1), H_2O_2 decay can be modeled with the following equation

$$[H_2O_2] = [H_2O_2]_0 e^{-k_{obs}t} \tag{6.2}$$

where $[H_2O_2]_0$ is the initial peroxide concentration. For each experiment, H_2O_2 data were fit to Equation (6.2) with a non-linear regression of H_2O_2 vs. time using the curve fitting toolbox in MATLAB® and both $[H_2O_2]_0$ and k_{obs} were used as fitting parameters. Half-lives varied for each environment, ranging from 5 to over 120 h (Table 6.2).

Statistical analysis was performed with R (http://www.r-project.org/) using the commands 'aov' for one-way analysis of variance (ANOVA), 'TukeyHSD' for the Tukey's honestly significant difference (HSD) test, and 't.test' for Student's t-test (all from the stats package included with R). Rate data were scaled to remove negative values and log-transformed to prevent bias from higher rates obtained in some samples.

Percent reduction of rates (AO and leucine incorporation) was calculated by dividing a given rate by the average rate from a non-H_2O_2 addition control.

ACKNOWLEDGEMENTS

Funding for this research was provided by a University of Georgia Innovative and Interdisciplinary Research Grant (IIRG) to B.B.T. and U.S. National Science Foundation grants OCE 09-43278 (EAGER) and OPP 08-38996 to J.T.H., OCE-1234388 to W.L.M., and OCE-1129260 to B.N.P. We thank R. Jellison for assistance in field sampling, as well as the scientific parties and crew of the *ARSV Laurence M. Gould*, *R/V Pelican*, and *R/V Melville*, and the Palmer Station 2010-2011 support staff. We also thank A. Bratcher, D. Duckett, E. Malagón, L. Lim, J.L. Shih, J. Fackrell, and C. Ka'apu-Lyons for assistance in the laboratory, and M. Moran for comments on the manuscript.

REFERENCES

Agogué H, Brink M, Dinasquet J, Herndl GJ (2008). Major gradients in putatively nitrifying and non-nitrifying Archaea in the deep North Atlantic. *Nature* **456:** 788-791.

Alleman JE, Keramida V, Panteakiser L (1987). Light-Induced *Nitrosomonas* Inhibition. *Water Res* **21:** 499-501.

Amin SA, Moffett JW, Martens-Habbena W, Jacquot JE, Han Y, Devol A, Ingalls AE, Stahl DA, Armbrust EV (2013). Copper requirements of the ammonia-oxidizing archaeon *Nitrosopumilus maritimus* SCM1 and implications for nitrification in the marine environment. *Limnol Oceanogr* **58:** 2037-2045.

Anjem A, Imlay JA (2012). Mononuclear Iron Enzymes Are Primary Targets of Hydrogen Peroxide Stress. *J Biol Chem* **287:** 15544-15556.

Beman JM, Popp BN, Francis CA (2008). Molecular and biogeochemical evidence for ammonia oxidation by marine Crenarchaeota in the Gulf of California. *ISME J* **2:** 429-441.

Beman JM, Sachdeva R, Fuhrman JA (2010). Population ecology of nitrifying archaea and bacteria in the Southern California Bight. *Environ Microbiol* **12:** 1282-1292.

Beman JM, Popp BN, Alford SE (2012). Quantification of ammonia oxidation rates and ammonia-oxidizing archaea and bacteria at high resolution in the Gulf of California and eastern tropical North Pacific Ocean. *Limnol Oceanogr* **57:** 711-726.

Bhatia MP, Kujawinski EB, Das SB, Breier CF, Henderson PB, Charette MA (2013). Greenland meltwater as a significant and potentially bioavailable source of iron to the ocean. *Nature Geosci* **6:** 274-278.

Christman GD, Cottrell MT, Popp BN, Gier E, Kirchman DL (2011). Abundance, Diversity, and Activity of Ammonia-Oxidizing Prokaryotes in the Coastal Arctic Ocean in Summer and Winter. *Appl Environ Microbiol* **77:** 2026-2034.

Church MJ, DeLong EF, Ducklow HW, Karner MB, Preston CM, Karl DM (2003). Abundance and distribution of planktonic Archaea and Bacteria in the waters west of the Antarctic Peninsula. *Limnol Oceanogr* **48:** 1893-1902.

Diaz JM, Hansel CM, Voelker BM, Mendes CM, Andeer PF, Zhang T (2013). Widespread Production of Extracellular Superoxide by Heterotrophic Bacteria. *Science* **340:** 1223-1226.

Dixon TC, Vermilyea AW, Scott DT, Voelker BM (2013). Hydrogen peroxide dynamics in an agricultural headwater stream: Evidence for significant nonphotochemical production. *Limnol Oceanogr* **58:** 2133-2144.

Dore JE, Popp BN, Karl DM, Sansone FJ (1998). A large source of atmospheric nitrous oxide from subtropical North Pacific surface waters. *Nature* **396:** 63-66.

Francis CA, Roberts KJ, Beman JM, Santoro AE, Oakley BB (2005). Ubiquity and diversity of ammonia-oxidizing archaea in water columns and sediments of the ocean. *Proc Natl Acad Sci USA* **102:** 14683-14688.

Fuhrman JA, McCallum K, Davis AA (1992). Novel Major Archaebacterial Group from Marine Plankton. *Nature* **356:** 148-149.

Gifford SM, Sharma S, Rinta-Kanto JM, Moran MA (2011). Quantitative analysis of a deeply sequenced marine microbial metatranscriptome. *ISME J* **5:** 461-472.

Guerrero MA, Jones RD (1996). Photoinhibition of marine nitrifying bacteria. I. Wavelength-dependent response. *Mar Ecol-Prog Ser* **141:** 183-192.

Hatzenpichler R, Lebedeva EV, Spieck E, Stoecker K, Richter A, Daims H, Wagner M (2008). A moderately thermophilic ammonia-oxidizing crenarchaeote from a hot spring. *Proc Natl Acad Sci USA* **105:** 2134-2139.

Herndl GJ, Reinthaler T, Teira E, van Aken H, Veth C, Pernthaler A, Pernthaler J (2005). Contribution of Archaea to Total Prokaryotic Production in the Deep Atlantic Ocean. *Appl Environ Microbiol* **71:** 2303-2309.

Hollibaugh JT, Gifford S, Sharma S, Bano N, Moran MA (2011). Metatranscriptomic analysis of ammonia-oxidizing organisms in an estuarine bacterioplankton assemblage. *ISME J* **5:** 866-878.

Hollibaugh JT, Gifford SM, Moran MA, Ross MJ, Sharma S, Tolar BB (2014). Seasonal variation in the metratranscriptomes of a Thaumarchaeota population from SE USA coastal waters. *ISME J* **8:** 685-698.

Hooper AB, Terry KR (1973). Specific Inhibitors of Ammonia Oxidation in *Nitrosomonas*. *J Bacteriol* **115:** 480-485.

Hyman MR, Arp DJ (1992). $^{14}C_2H_2$-Labeling and $^{14}CO_2$-Labeling Studies of the Denovo Synthesis of Polypeptides by *Nitrosomonas europaea* during Recovery from Acetylene and Light Inactivation of Ammonia Monooxygenase. *J Biol Chem* **267:** 1534-1545.

Imlay JA (2008). Cellular defenses against superoxide and hydrogen peroxide. *Annu Rev Biochem* **77:** 755-776.

Jacquot JE, Horak REA, Amin SA, Devol A, Ingalls AE, Armbrust EV, Stahl DA, Moffett JW (2014). Assessment of the potential for copper limitation of ammonia oxidation by Archaea in a dynamic estuary. *Mar Chem* **162:** 37-49.

Kalanetra KM, Bano N, Hollibaugh JT (2009). Ammonia-oxidizing Archaea in the Arctic Ocean and Antarctic coastal waters. *Environ Microbiol* **11:** 2434-2445.

Karner MB, DeLong EF, Karl DM (2001). Archaeal dominance in the mesopelagic zone of the Pacific Ocean. *Nature* **409:** 507-510.

Kelly S, Wickstead B, Gull K (2011). Archaeal phylogenomics provides evidence in support of a methanogenic origin of the Archaea and a thaumarchaeal origin for the eukaryotes. *Proc Royal Soc B - Bio* **278:** 1009-1018.

Kieber DJ, Peake BM, Scully NM (2003). Reactive oxygen species in aquatic ecosystems. In: Helbling EW, Zagarese H (eds). UV Effects in Aquatic Organisms and Ecosystems. The Royal Society of Chemistry: Cambridge. pp 251-290.

King DW, Cooper WJ, Rusak SA, Peake BM, Kiddle JJ, O'Sullivan DW, Melamed ML, Morgan CR, Theberge SM (2007). Flow injection analysis of H_2O_2 in natural waters using acridinium ester chemiluminescence: Method development and optimization using a kinetic model. *Anal Chem* **79:** 4169-4176.

Luo HW, Tolar BB, Swan BK, Zhang CLL, Stepanauskas R, Moran MA, Hollibaugh JT (2014). Single-cell genomics shedding light on marine Thaumarchaeota diversification. *ISME J* **8:** 732-736.

Marshall JA, de Salas M, Oda T, Hallegraeff G (2005). Superoxide production by marine microalgae. *Mar Biol* **147:** 533-540.

Massana R, Taylor LJ, Murray AE, Wu KY, Jeffrey WH, DeLong EF (1998). Vertical distribution and temporal variation of marine planktonic archaea in the Gerlache Strait, Antarctica, during early spring. *Limnol Oceanogr* **43:** 607-617.

Merbt SN, Stahl DA, Casamayor EO, Marti E, Nicol GW, Prosser JI (2012). Differential photoinhibition of bacterial and archaeal ammonia oxidation. *FEMS Microbiol Lett* **327:** 41-46.

Miller WL, Kester DR (1988). Hydrogen-Peroxide Measurement in Seawater by (Para-Hydroxyphenyl)Acetic Acid Dimerization. *Anal Chem* **60:** 2711-2715.

Mincer TJ, Church MJ, Taylor LT, Preston C, Karl DM, DeLong EF (2007). Quantitative distribution of presumptive archaeal and bacterial nitrifiers in Monterey Bay and the North Pacific Subtropical Gyre. *Environ Microbiol* **9:** 1162-1175.

Mishra S, Imlay J (2012). Why do bacteria use so many enzymes to scavenge hydrogen peroxide? *Arch Biochem Biophys* **525:** 145-160.

Murray AE, Preston CM, Massana R, Taylor LT, Blakis A, Wu K, DeLong EF (1998). Seasonal and spatial variability of bacterial and archaeal assemblages in the coastal waters near Anvers Island, Antarctica. *Appl Environ Microbiol* **64:** 2585-2595.

Murray AE, Wu KY, Moyer CL, Karl DM, DeLong EF (1999a). Evidence for circumpolar distribution of planktonic Archaea in the Southern Ocean. *Aquat Microb Ecol* **18:** 263-273.

Olson RJ (1981). Differential Photoinhibition of Marine Nitrifying Bacteria - a Possible Mechanism for the Formation of the Primary Nitrite Maximum. *J Mar Res* **39:** 227-238.

Paerl HW, Otten TG (2013). Environmental science. Blooms bite the hand that feeds them. *Science* **342:** 433-434.

Pitcher A, Wuchter C, Siedenberg K, Schouten S, Damste JSS (2011). Crenarchaeol tracks winter blooms of ammonia-oxidizing Thaumarchaeota in the coastal North Sea. *Limnol Oceanogr* **56:** 2308-2318.

Popp BN, Sansone FJ, Rust TM, Merritt DA (1995). Determination of Concentration and Carbon Isotopic Composition of Dissolved Methane in Sediments and Nearshore Waters. *Anal Chem* **67:** 405-411.

Poretsky RR, Bano N, Buchan A, Moran MA, Hollibaugh JT (2008). Environmental transcriptomics: a method to access expressed genes in complex microbial communities. In: Kowalchuk GA, de Bruijn FJ, Head IM, Akkermans ADL, van Elsas JD (eds). Molecular Microbial Ecology Manual. Springer: Dordrecht, Netherlands.

Qin W, Amin SA, Martens-Habbena W, Walker CB, Urakawa H, Devol AH, Ingalls AE, Moffett JW, Armbrust EV, Stahl DA (2014). Marine ammonia-oxidizing archaeal isolates display obligate mixotrophy and wide ecotypic variation. *Proc Nat Acad Sci USA* **111:** 12504-12509.

Rabalais NN, Díaz RJ, Levin LA, Turner RE, Gilbert D, Zhang J (2010). Dynamics and distribution of natural and human-caused hypoxia. *Biogeosciences* **7:** 585-619.

Raiswell R, Benning LG, Tranter M, Tulaczyk S (2008). Bioavailable iron in the Southern Ocean: the significance of the iceberg conveyor belt. *Geochem Transact* **9:** 7.

Resing J, Tien G, Letelier R, Karl DM, Jones D (1993). Palmer LTER: Hydrogen peroxide in the Palmer LTER region: II. Water column distribution. *Antarct J US* **28:** 227-229.

Santoro AE, Casciotti KL, Francis CA (2010). Activity, abundance and diversity of nitrifying archaea and bacteria in the central California Current. *Environ Microbiol* **12:** 1989-2006.

Sigman DM, Casciotti KL, Andreani M, Barford C, Galanter M, Böhlke JK (2001). A Bacterial Method for the Nitrogen Isotopic Analysis of Nitrate in Seawater and Freshwater. *Anal Chem* **73:** 4145-4153.

Smith JM, Casciotti KL, Chavez FP, Francis CA (2014a). Differential contributions of archaeal ammonia oxidizer ecotypes to nitrification in coastal surface waters. *ISME J***:** 1-14.

Smith JM, Chavez FP, Francis CA (2014b). Ammonium uptake by phytoplankton regulates nitrification in the sunlit ocean. *PLoS ONE* **9:** e108173.

Sobota JM, Imlay JA (2011). Iron enzyme ribulose-5-phosphate 3-epimerase in *Escherichia coli* is rapidly damaged by hydrogen peroxide but can be protected by manganese. *Proc Nat Acad Sci USA* **108:** 5402-5407.

Spang A, Hatzenpichler R, Brochier-Armanet C, Rattei T, Tischler P, Spieck E, Streit W, Stahl DA, Wagner M, Schleper C (2010). Distinct gene set in two different lineages of ammonia-oxidizing archaea supports the phylum Thaumarchaeota. *Trends Microbiol* **18:** 331-340.

Tolar BB, King GM, Hollibaugh JT (2013). An analysis of thaumarchaeota populations from the northern Gulf of Mexico. *Front Microbiol* **4:** 72.

Walker CB, de la Torre JR, Klotz MG, Urakawa H, Pinel N, Arp DJ, Brochier-Armanet C, Chain PSG, Chan PP, Gollabgir A, Hemp J, Hügler M, Karr EA, Könneke M, Shin M, Lawton TJ, Lowe T, Martens-Habbena W, Sayavedra-Soto LA, Lang D, Sievert SM, Rosenzweig AC, Manning G, Stahl DA (2010). *Nitrosopumilus maritimus* genome reveals unique mechanisms for nitrification and autotrophy in globally distributed marine crenarchaea. *Proc Nat Acad Sci USA* **107:** 8818-8823.

Ward BB (1985). Light and Substrate Concentration Relationships with Marine Ammonium Assimilation and Oxidation Rates. *Mar Chem* **16:** 301-316.

Ward BB (2011). Nitrification in the Ocean. In: Ward BB, Arp DJ, Klotz MG (eds). Nitrification. ASM Press: Washington, D.C. pp 325-345.

Wells LE, Deming JW (2003). Abundance of Bacteria, the Cytophaga-Flavobacterium cluster and Archaea in cold oligotrophic waters and nepheloid layers of the Northwest Passage, Canadian Archipelago. *Aquat Microb Ecol* **31:** 19-31.

Wuchter C, Abbas B, Coolen MJL, Herfort L, van Bleijswijk J, Timmers P, Strous M, Teira E, Herndl GJ, Middelburg JJ, Schouten S, Damste JSS (2006). Archaeal nitrification in the ocean. *Proc Natl Acad Sci USA* **103:** 12317-12322.

Yool A, Martin AP, Fernández C, Clark DR (2007). The significance of nitrification for oceanic new production. *Nature* **447:** 999-1002.

Zepp RG, Skurlato YI, Pierce JT (1987). Algal-Induced Decay and Formation of Hydrogen Peroxide in Water: Its Possible Role in Oxidation of Anilines by Algae. In: Zika RG, Cooper WJ (eds). Photochemistry of Environmental Systems. American Chemical Society: Washington, D.C.

Table 6.1: Summary of data from ROS Experiments with H_2O_2 additions.

Site	Station	Depth / Time	H_2O_2 Addn (nM)	Avg ^{15}N Oxid. Rate		Avg Leu. Incorp. Rate		Initial [H_2O_2]	
				(nM d^{-1})	SD	(pM h^{-1})	SD	(nM)	SD
Southern Ocean 2010	600.080	10m	0	2.46	0.96	ND	ND	14.27	27.16
	600.080	10m	30	**-0.21**	1.03	ND	ND		
	600.080	10m	100	**-0.04**	0.34	ND	ND		
	600.080	75 m	0	7.96	0.34	ND	ND	2.86	8.85
	600.080	75 m	30	2.56	2.18	ND	ND		
	600.080	75 m	100	**-0.97**	0.79	ND	ND		
	600.080	300m	0	7.06	3.25	ND	ND	6.95	11.88
	600.080	300m	30	0.60	0.55	ND	ND		
	600.080	300m	100	**-3.53**	0.01	ND	ND		
	600.160	10m	0	72.35	6.36	8.80	1.89	ND	ND
	600.160	10m	30	0.69	0.24	6.92	2.92		
	600.160	10m	100	**-0.10**	0.21	2.29	1.82		
	600.160	55m	0	219.53	44.05	13.02	0.23	ND	ND
	600.160	55m	30	**-2.16**	0.71	3.12	1.59		
	600.160	55m	100	**-0.72**	1.14	1.47	0.77		
	600.160	300m	0	34.94	6.16	2.68	1.10	ND	ND
	600.160	300m	30	2.01	1.75	5.59	2.49		
	600.160	300m	100	0.15	0.27	2.71	0.08		
Gulf of Mexico 2012	C4	200 m	0	36.21	0.09	194.04	194.19	16.33	4.57
	C4	200 m	100	27.69	7.72	**-34.62**	23.09		
	C4	200 m	300	24.21	3.11	37.23	59.38		
	B4	200 m	0	42.49	0.45	2.64	4.57	28.06	6.14
	B4	200 m	100	31.81	7.08	22.37	19.09		
	B4	200 m	300	15.82	7.45	114.03	18.38		

Site	Station	Depth / Time	H_2O_2 Addn (nM)	Avg ^{15}N Oxid. Rate		Avg Leu. Incorp. Rate		Initial [H_2O_2]	
				(nM d^{-1})	SD	(pM h^{-1})	SD	(nM)	SD
Gulf of Mexico 2012	A6	200 m	0	8.03	2.65	276.45	291.79	14.62	3.36
	A6	200 m	100	5.95	0.27	55.06	26.25		
	A6	200 m	300	2.73	1.18	280.02	107.54		
Gulf of Alaska 2013	004	200 m	0	24.88	14.36	563.63	184.81	6.87	3.94
	004	200 m	100	23.84	0.09	619.79	58.62		
	004	200 m	300	10.88	9.76	686.16	130.21		
	010	200 m	0	2.88	0.48	ND	ND	12.11	1.67
	010	200 m	30	4.90	0.78	ND	ND		
	010	200 m	100	2.95	0.32	ND	ND		
	010	200 m	300	1.14	0.01	ND	ND		
Gulf of Alaska 2013	015	50 m	0	81.97	1.44	4811.39	9620.10	15.59	3.57
	015	50 m	30	76.04	5.18	6137.09	3802.80		
	015	50 m	100	77.07	5.91	1149.03	4355.20		
	015	50 m	300	77.37	6.17	864.17	7385.51		
	033	200 m	0	32.99	2.61	165.98	12.25	14.27	1.54
	033	200 m	30	20.78	1.98	359.37	163.28		
Gulf of Alaska 2013	015	50 m	0	81.97	1.44	4811.39	9620.10	15.59	3.57
	015	50 m	30	76.04	5.18	6137.09	3802.80		
	015	50 m	100	77.07	5.91	1149.03	4355.20		
	015	50 m	300	77.37	6.17	864.17	7385.51		
	033	200 m	0	32.99	2.61	165.98	12.25	14.27	1.54
	033	200 m	30	20.78	1.98	359.37	163.28		

ND = not determined; LD = below limit of detection; SD = standard deviation

Values in **bold** indicate negative rate values due to a high control - these values are assumed to be zero.

Site	Station	Depth / Time	H_2O_2 Addn (nM)	Archaeal *amoA* mRNA	Archaeal *amoA* gene	Thaum. 16S rRNA	AOB *amoA* gene	Bacteria 16S rRNA
Southern Ocean 2010	600.080	10m	0	3.60E+06	4.80E+06	4.20E+06	1.29E+05	9.53E+07
	600.080	10m	30	1.29E+06				
	600.080	10m	100	1.51E+06				
	600.080	75 m	0	6.86E+06	3.27E+06	3.04E+06	5.06E+04	1.17E+08
	600.080	75 m	30	1.78E+06				
	600.080	75 m	100	1.67E+06				
	600.080	300m	0	1.47E+06	2.15E+06	1.29E+06	7.30E+03	1.06E+07
	600.080	300m	30	1.52E+06				
	600.080	300m	100	5.24E+05				
	600.160	10m	0	6.97E+06	2.84E+06	3.43E+06	8.40E+03	1.11E+08
	600.160	10m	30	1.13E+07				
	600.160	10m	100	3.52E+06				
	600.160	55m	0	8.36E+06	2.69E+06	4.73E+06	7.41E+03	1.44E+08
	600.160	55m	30	3.58E+06				
	600.160	55m	100	5.47E+06				
	600.160	300m	0	1.51E+06	1.88E+06	1.16E+06	4.21E+03	1.23E+07
	600.160	300m	30	1.96E+05				
	600.160	300m	100	1.79E+05				
Gulf of Mexico 2012	C4	200 m	0	7.24E+04	2.22E+06	1.25E+06	9.95E+02	3.13E+09
	C4	200 m	100	3.88E+04				
	C4	200 m	300	7.99E+04				
	B4	200 m	0	2.40E+04	6.99E+06	4.68E+06	3.22E+03	3.83E+09
	B4	200 m	100	7.99E+03				
	B4	200 m	300	4.63E+03				

Site	Station	Depth / Time	H_2O_2 Addn (nM)	Archaeal *amoA* mRNA	Archaeal *amoA* gene	Thaum. 16S rRNA	AOB *amoA* gene	Bacteria 16S rRNA
Gulf of Mexico 2012	A6	200 m	0	1.07E+04	1.07E+05	2.70E+06	3.13E+03	1.97E+09
	A6	200 m	100	6.33E+04				
	A6	200 m	300	1.87E+04				
Gulf of Alaska 2013	004	200 m	0	2.36E+04	1.27E+07	1.33E+07	1.93E+04	2.39E+09
	004	200 m	100	6.57E+04				
	004	200 m	300	1.21E+04				
	010	200 m	0	2.11E+04	1.40E+07	2.20E+07	1.85E+04	3.78E+09
	010	200 m	30	3.66E+04				
	010	200 m	100	4.39E+04				
	010	200 m	300	1.66E+04				
Gulf of Alaska 2013	015	50 m	0	4.76E+05	1.44E+07	1.08E+07	2.47E+06	3.01E+09
	015	50 m	30	1.87E+05				
	015	50 m	100	6.58E+05				
	015	50 m	300	3.32E+05				
	033	200 m	0	ND	5.89E+06	7.05E+06	5.45E+03	8.88E+08
	033	200 m	30	ND				
Gulf of Alaska 2013	015	50 m	0	4.76E+05	1.44E+07	1.08E+07	2.47E+06	3.01E+09
	015	50 m	30	1.87E+05				
	015	50 m	100	6.58E+05				
	015	50 m	300	3.32E+05				
	033	200 m	0	ND	5.89E+06	7.05E+06	5.45E+03	8.88E+08
	033	200 m	30	ND				

ND = Not determined.

Gene (*amoA*, 16S rRNA) and transcript (AOA *amoA* only) abundance data is in copies L^{-1} filtered sample.

Table 6.2: Decay rates and initial H_2O_2 concentrations in ROS incubations.

Sample ID*	Initial $[H_2O_2]$	Nominal $[H_2O_2]$ Addition	Decay Rate (nM/h)[#] m	SD	R^2	Initial $[H_2O_2]$[$] b	SD	Prokarya Cells / L	$[H_2O_2]_0$ (modeled)[^]	k_{obs} (1/h)	R^2	$t_{1/2}$ (h)
GOM12 C4	16.33	100 nM	-0.74	0.05	0.99	163.1	0.84	3.13E+09	200.1	0.025	0.77	27.41
GOM12 C4		300 nM	-4.59	1.75	0.78	464.3	30.60	3.13E+09	560.6	0.031	0.83	22.40
GOM12 B4	28.06	100 nM	-2.83	0.16	0.99	234.2	2.73	3.83E+09	281.2	0.033	0.86	20.82
GOM12 B4		300 nM	-10.93	4.53	0.75	731.0	79.00	3.83E+09	839.3	0.032	0.93	21.61
GOM12 A6	14.62	100 nM	-3.98	0.45	0.98	197.3	8.69	1.97E+09	161.1	0.019	0.73	36.85
GOM12 A6		300 nM	-12.23	2.15	0.94	555.8	41.60	1.97E+09	463.7	0.022	0.74	31.90
GoA Stn 004	6.87	100 nM	-0.51	0.38	0.32	112.2	19.90	2.40E+09	143.1	0.011	0.87	61.45
GoA Stn 004		300 nM	-0.98	0.24	0.81	312.2	12.30	2.40E+09	418.3	0.011	0.91	63.77
GoA Stn 010	8.77	30 nM	-0.46	0.06	0.90	64.19	5.49	2.12E+09	73.37	0.016	0.88	44.49
GoA Stn 010		100 nM	-1.07	0.11	0.94	157.57	9.26	2.12E+09	168.3	0.012	0.84	56.77
GoA Stn 010		300 nM	-2.64	0.39	0.89	402.9	33.48	2.12E+09	418.6	0.011	0.76	63.42
GoA Stn 015	15.59	30 nM	-0.05	0.07	0.05	52.9	3.09	3.02E+09	59.71	0.005	0.55	127.6
GoA Stn 015		100 nM	-0.89	0.22	0.67	160.2	7.58	3.02E+09	168.8	0.010	0.88	70.39
GoA Stn 015		300 nM	-2.71	0.27	0.93	432.9	11.70	3.02E+09	453.5	0.010	0.97	68.97
GoA Stn 033	14.27	30 nM	-2.54	0.81	0.71	69.2	11.60	8.95E+08	83.34	0.129	0.93	5.39

*GOM12 = Gulf of Mexico (May 2012); GoA = Gulf of Alaska (August 2013); Stn = Station.

[#]Decay rate determined from slope, a negative slope indicates decay; [$]Initial $[H_2O_2]$ determined from y-intercept;

[^]Calculations for $[H_2O_2]_0$ modeled are described further in the Methods; Model: $[H_2O_2] = [H_2O_2]_0 * e^{(-k*t)}$

Decomposition of H_2O_2 is overall 2nd order (1st order with respect to $[H_2O_2]$, 1st order with respect to *algal* biomass (Zepp *et al.*, 1987)

*$d[H_2O_2]/dt = -k_{obs}[H_2O_2]$ (modeled using nonlinear curve fit)

*$d[H_2O_2]/dt = -k_d[H_2O_2][biomass]$ (k_d = specific decay rate) $k_d = - k_{obs}/[biomass]$

Figure 6.1: Sources and effects of ROS in marine environments. ROS (here, superoxide and hydrogen peroxide) can be introduced in surface waters via (a) phytoplankton as by-products of photosynthesis, (b) photochemical reactions of colored dissolved organic matter (CDOM) and metals, (c) rain, and (d) production by heterotrophic bacteria. When prokaryotic cells come into contact with ROS (e), molecules such as DNA, protein, and lipids can become damaged unless enzymes like superoxide dismutase (SOD) or catalase (Cat) are produced to detoxify ROS (Imlay, 2008). As shown above, ammonia oxidation by marine Thaumarchaeota (AOA) is particularly sensitive to ROS.

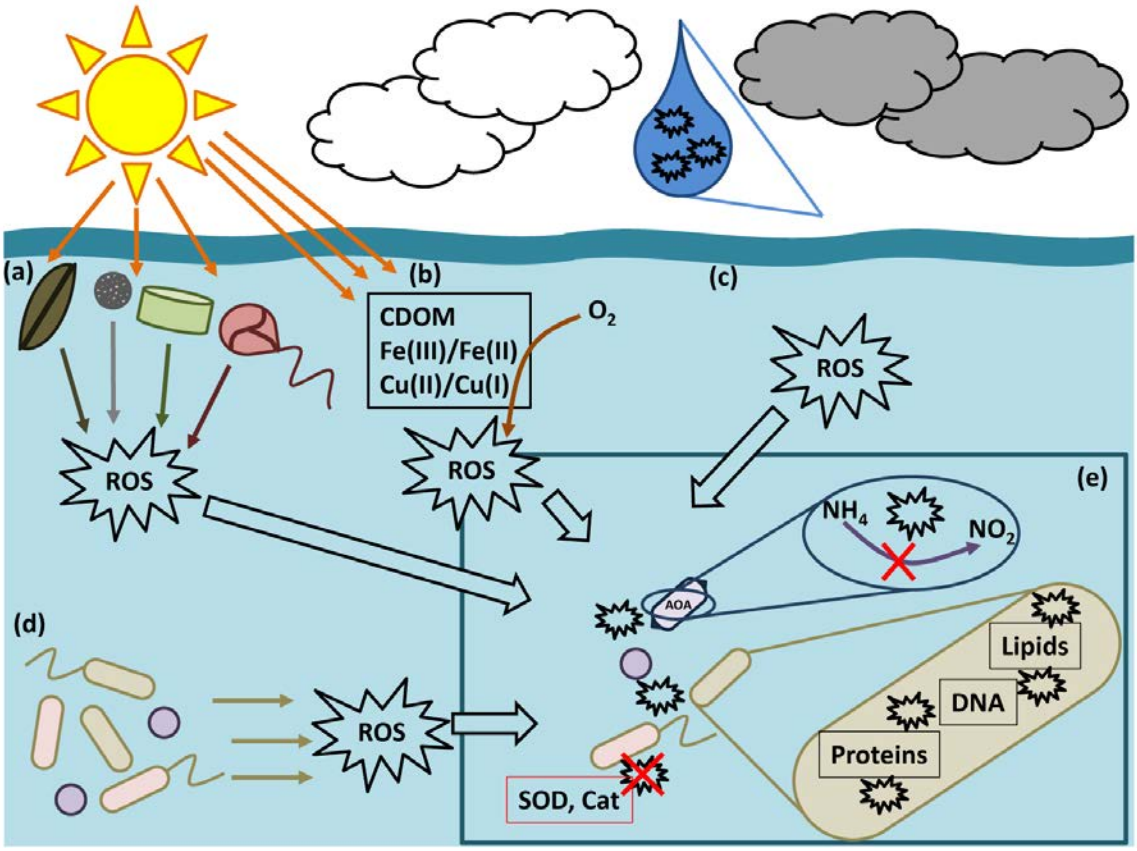
(a)
(b)
(c)
CDOM
Fe(III)/Fe(II)
Cu(II)/Cu(I)
O_2
ROS
ROS
ROS
(d)
ROS
SOD, Cat
(e)
NH_4
NO_2
AOA
Lipids
DNA
Proteins

Figure 6.2: Locations of sample sites where H_2O_2 experiments were performed. (a) Gulf of Mexico; **(b)** Southern Ocean west of the Antarctic Peninsula; **(c)** Gulf of Alaska.

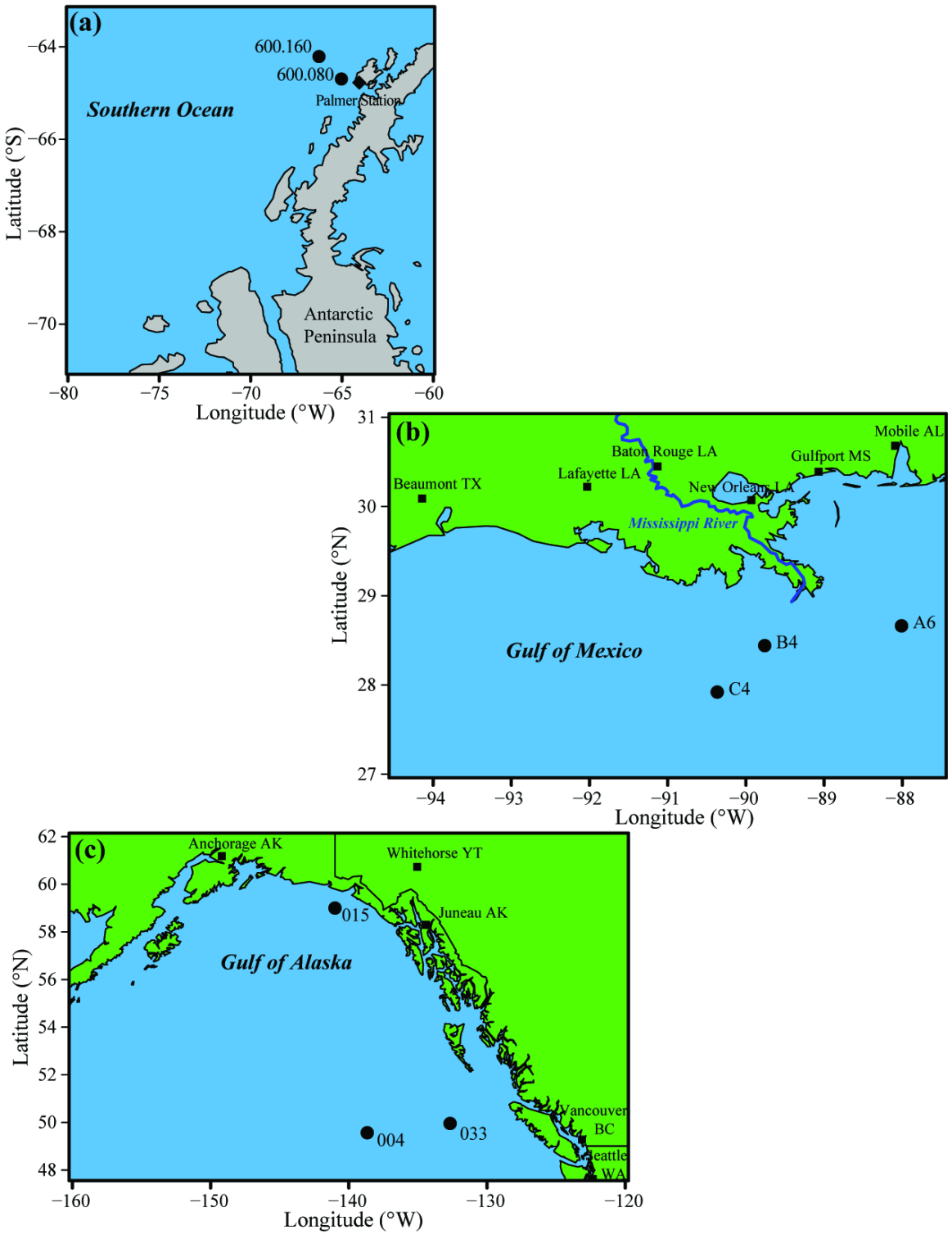
(a)
600.160
600.080
Palmer Station
Southern Ocean
Antarctic
Peninsula
Latitude (°S)
Longitude (°W)
(b)
Mobile AL
Baton Rouge LA
Gulfport MS
Lafayette LA
Beaumont TX
New Orleans LA
Mississippi River
A6
B4
C4
Gulf of Mexico
Latitude (°N)
Longitude (°W)
(c)
Anchorage AK
Whitehorse YT
015
Juneau AK
Gulf of Alaska
Vancouver
BC
Seattle
WA
004
033
Latitude (°N)
Longitude (°W)

Figure 6.3: ^{15}N-Ammonia oxidation rates. Rates of ammonia oxidation as measured with a ^{15}N-ammonium tracer after addition of H_2O_2 in the Southern Ocean (**a, b**; symbols represent sample depth), Gulf of Mexico, and Gulf of Alaska (**c** and **d**, respectively; symbols represent stations sampled).

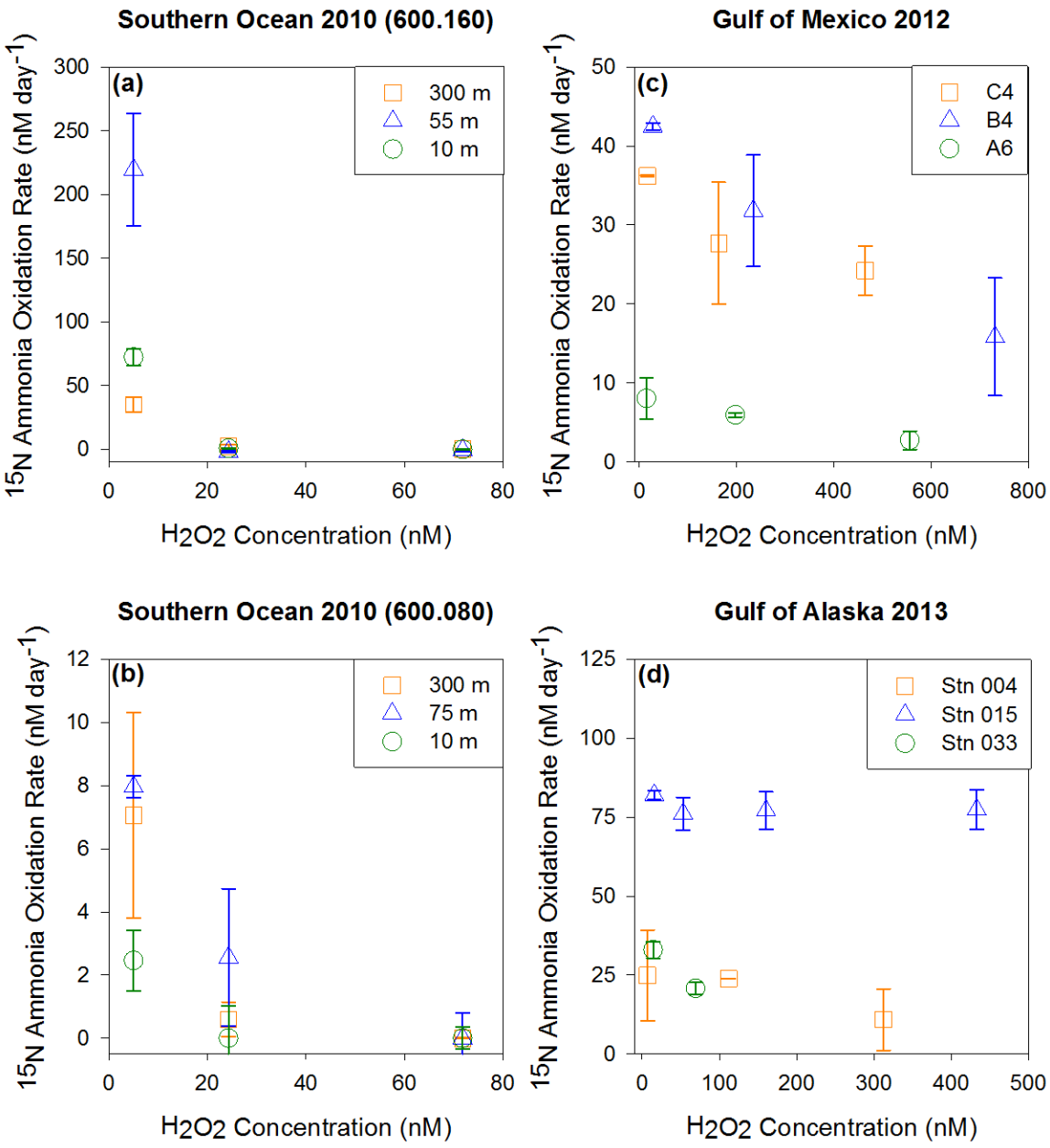
Southern Ocean 2010 (600.160)
(a)
300 m
55 m
10 m
15N Ammonia Oxidation Rate (nM day-1)
H2O2 Concentration (nM)
Gulf of Mexico 2012
(c)
C4
B4
A6
15N Ammonia Oxidation Rate (nM day-1)
H2O2 Concentration (nM)
Southern Ocean 2010 (600.080)
(b)
300 m
75 m
10 m
15N Ammonia Oxidation Rate (nM day-1)
H2O2 Concentration (nM)
Gulf of Alaska 2013
(d)
Stn 004
Stn 015
Stn 033
15N Ammonia Oxidation Rate (nM day-1)
H2O2 Concentration (nM)

Figure 6.4. Archaeal *amoA* transcripts quantified by RT-qPCR using RNA collected from the Southern Ocean (**a, b**; symbols represent sample depth), Gulf of Mexico, and Gulf of Alaska (**c** and **d**, respectively; symbols represent station sampled).

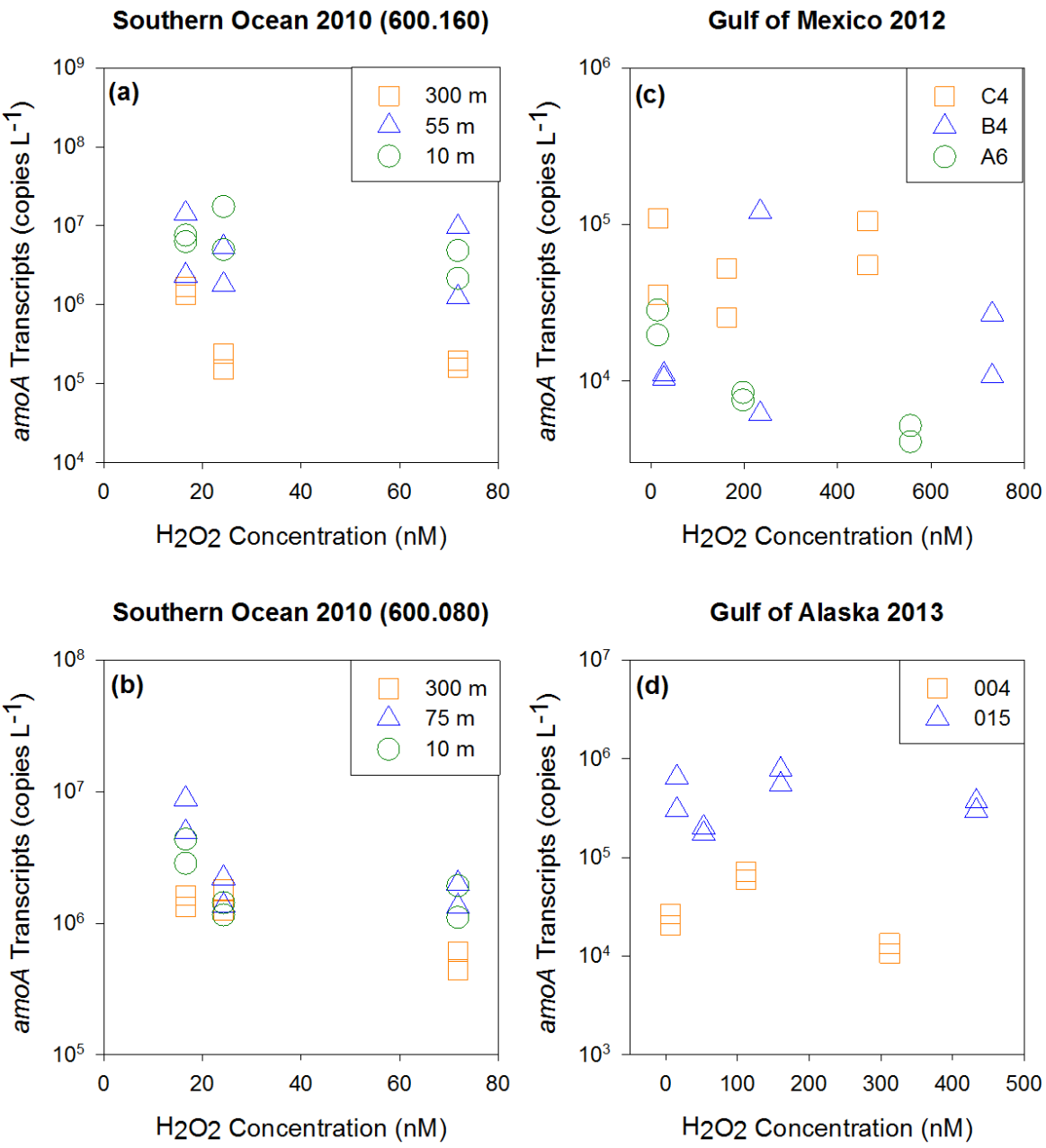
Southern Ocean 2010 (600.160)
(a)
300 m
55 m
10 m
amoA Transcripts (copies L-1)
H2O2 Concentration (nM)
Gulf of Mexico 2012
(c)
C4
B4
A6
amoA Transcripts (copies L-1)
H2O2 Concentration (nM)
Southern Ocean 2010 (600.080)
(b)
300 m
75 m
10 m
amoA Transcripts (copies L-1)
H2O2 Concentration (nM)
Gulf of Alaska 2013
(d)
004
015
amoA Transcripts (copies L-1)
H2O2 Concentration (nM)

Figure 6.5. Bacterial incorporation of L-leucine measured in the Southern Ocean (**a**; symbols represent sample depth), the Gulf of Mexico, and the Gulf of Alaska (**b, c**, respectively; symbols represent station sampled). Incubations were performed using ^{3}H- **(a)** or ^{13}C-labeled **(b, c)** L-leucine.

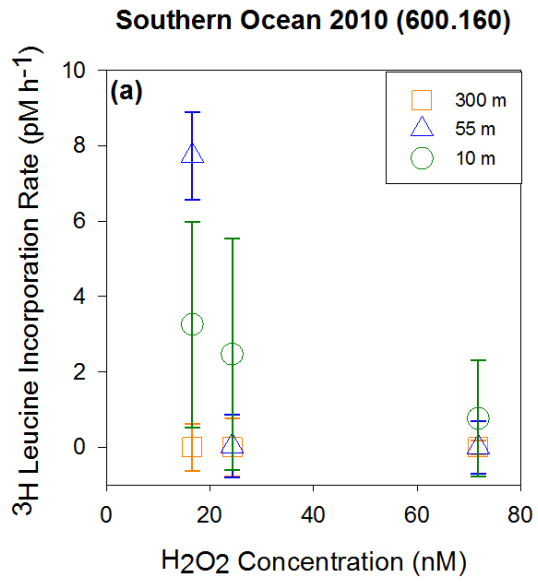
Southern Ocean 2010 (600.160)
(a)
300 m
55 m
10 m
3H Leucine Incorporation Rate (pM h-1)
H2O2 Concentration (nM)

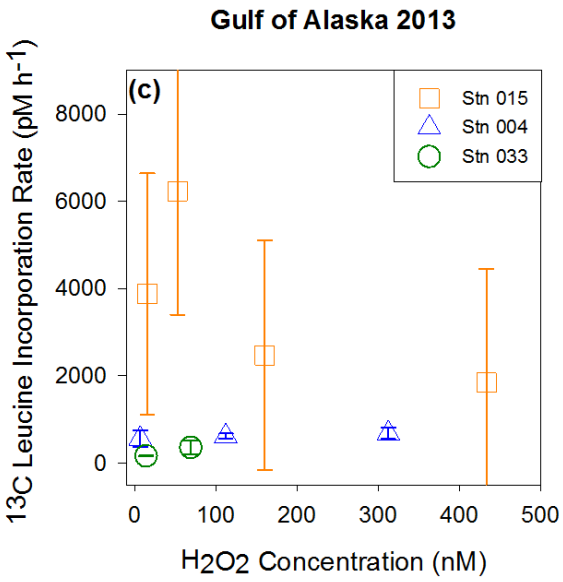
Gulf of Alaska 2013
(c)
Stn 015
Stn 004
Stn 033
13C Leucine Incorporation Rate (pM h-1)
H2O2 Concentration (nM)

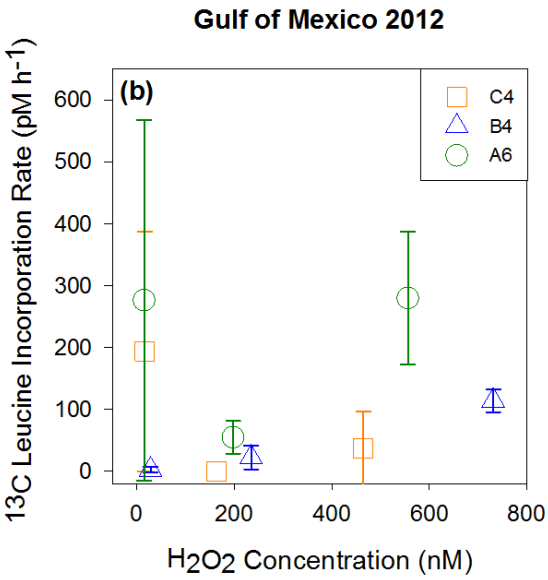
Gulf of Mexico 2012
(b)
C4
B4
A6
13C Leucine Incorporation Rate (pM h-1)
H2O2 Concentration (nM)

Figure 6.6: Decay of hydrogen peroxide in ROS experiments from the Gulf of Mexico **(a-c)** and Gulf of Alaska **(d-f)** in control (black), 30 nM H_2O_2 (purple), 100 nM H_2O_2 (orange), and 300 nM H_2O_2 (blue) incubations. Symbols represent measured H_2O_2 concentrations, while curves represent modeled decay rates.

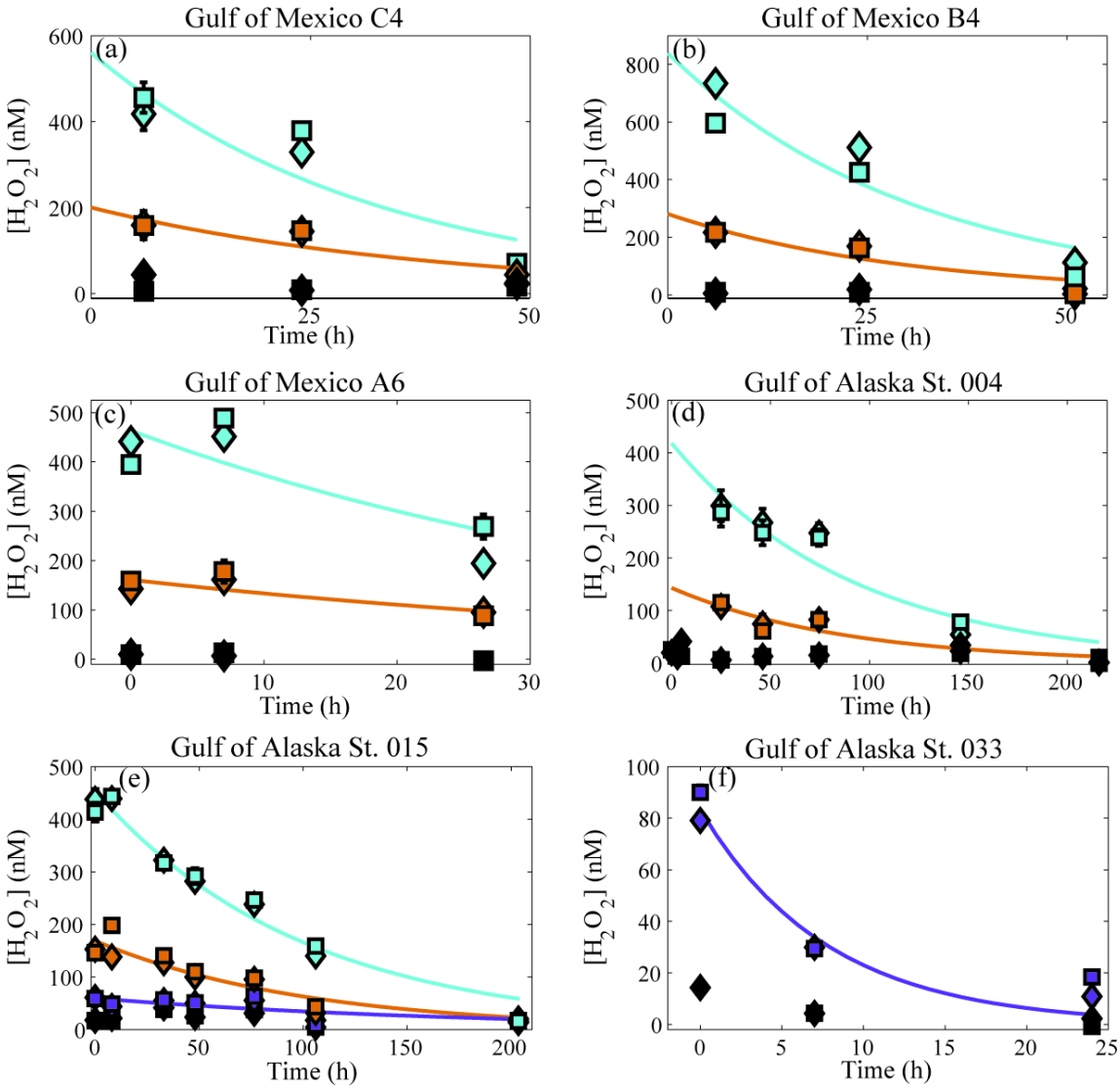
Gulf of Mexico C4
(a)
[H2O2] (nM)
Time (h)
Gulf of Mexico B4
(b)
[H2O2] (nM)
Time (h)
Gulf of Mexico A6
(c)
[H2O2] (nM)
Time (h)
Gulf of Alaska St. 004
(d)
[H2O2] (nM)
Time (h)
Gulf of Alaska St. 015
(e)
[H2O2] (nM)
Time (h)
Gulf of Alaska St. 033
(f)
[H2O2] (nM)
Time (h)

Figure 6.7: Modifications to the FeLume parameters as described in King *et al*. (2007). Operating conditions indicated with bracketed numbers [#] described in the Methods section.

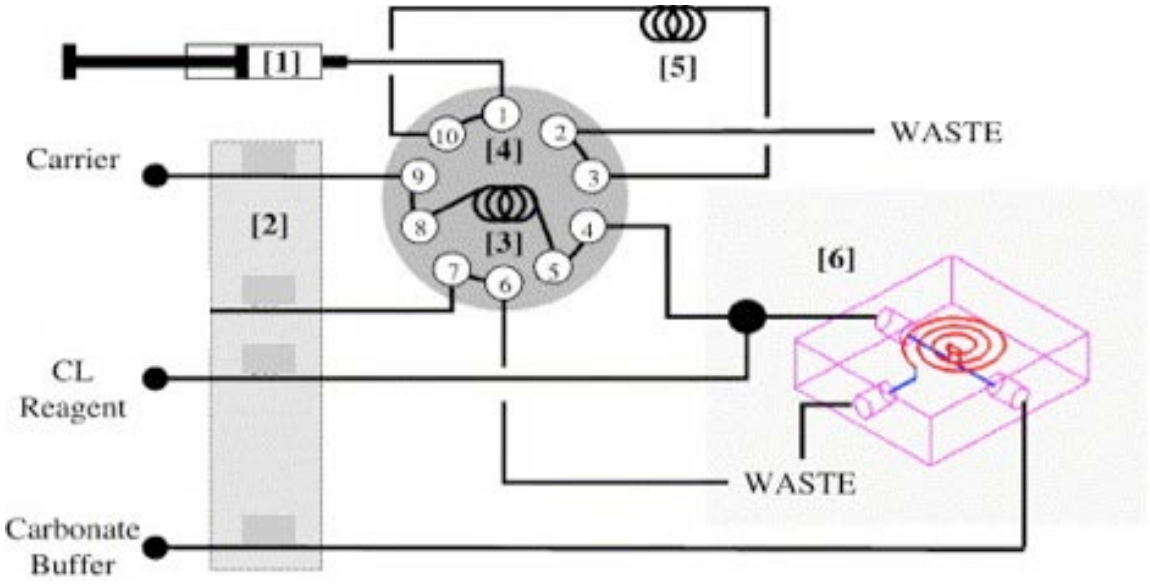
[1]
[5]
WASTE
Carrier
[4]
[2]
[3]
[6]
CL
Reagent
WASTE
Carbonate
Buffer

CHAPTER 7

CONCLUSIONS

This dissertation aimed to determine the factors controlling distribution patterns of Thaumarchaeota abundance and ammonia oxidation in a variety of marine environments. I collected samples from coastal (Sapelo Island, Georgia) and open ocean environments (Gulf of Mexico, Gulf of Alaska), as well as polar (Southern Ocean) and temperate (South Atlantic Bight) waters to gain a broad understanding of global distributions of marine Thaumarchaeota. Quantitative PCR (qPCR) was primarily used to determine this abundance, and I used assays targeting Thaumarchaeota genes (16S rRNA – *rrs*, *amoA*, *accA*, *ureC*) and transcripts (*amoA*, *ureC*) in addition to pSL12 *rrs* (a proposed group of AOA), Bacteria *rrs*, AOB *amoA* genes and transcripts, *Nitrospina rrs* (NOB), and Diatom 18S rRNA. This combination of assays allowed me to compare distributions of Thaumarchaeota against other microorganisms in the same water sample, especially those involved in the nitrogen cycle. I also used ^{15}N-labeled ammonia to determine rates of ammonia oxidation and thus query the apparent activity of Thaumarchaeota (AOA) in a given system. We examined a suite of environmental variables in each study presented here, to determine correlations with Thaumarchaeota abundance, transcriptional activity, and ammonia oxidation through the use of a variety of statistical techniques including Principal Components Analysis (PCA) and Multi-Dimensional Scaling (MDS).

As a preliminary survey of natural populations of Thaumarchaeota to test qPCR primers and to identify factors responsible for their distribution, samples were collected in the northern Gulf of Mexico in March 2010 (Chapter 2). I surveyed the region influenced by the Mississippi River plume and found that Thaumarchaeota abundances correlated with depth, temperature, oxygen concentration, and pH. I found a diverse community of Thaumarchaeota in the Gulf of Mexico, with distinct differences in composition at different sample depths. Finally, estimates of Thaumarchaeota *rrs* relative abundance determined using qPCR and pyrosequencing were strongly correlated ($r^2 = 0.82$), indicating that either method is an acceptable means for determining Thaumarchaeota distributions in marine systems.

A second research cruise was taken to Palmer Station, Antarctica, in September 2010, where samples were collected to measure abundance, activity, and nitrification rates during the austral spring (Chapter 3). These samples were analyzed with others collected in the same region during the summer (January 2011, and 2006). Comparison of the data sets showed that Thaumarchaeota abundances were equivalent at surface and mid-depths in the spring (Antarctic Surface Water, AASW), but were virtually absent from surface waters sampled in summer (Summer Surface Water, SSW) and had decreased in abundance at mid-depths (Winter Water, WW). Thaumarchaeota abundance in deep waters (Circumpolar Deep Water, CDW) was relatively constant, regardless of season. Regardless of water mass, nitrification rates were high in this region (0.52-140 nM d^{-1}) compared to previous measurements made in the Southern Ocean, indicating that this process has been significantly underestimated in Antarctic waters. Interestingly, ammonia oxidation rates did not show a consistent relationship with the abundance of

Thaumarchaeota ammonia monooxygenase (*amoA*) genes or transcripts, or with the ratio of genes to transcripts, which calls into question the use of these molecular measurements as a proxy for ammonia oxidation rates. Overall, properties of Southern Ocean water masses (depth, salinity, temperature) were the most significant in explaining differences in Thaumarchaeota gene abundances, indicating distinct communities between the WW and CDW in particular.

Quarterly sampling at Marsh Landing in the shallow coastal waters around Sapelo Island, Georgia, from 2008-2014 revealed a mid-summer "bloom" of Thaumarchaeota (increase in abundance 100- to 1000-times) that appears to occur each year. This dynamic is in stark contrast to distribution patterns elsewhere, where Thaumarchaeota are only abundant in deeper waters or are only found in surface waters in winter. In Chapter 4, I analyzed samples collected weekly at Marsh Landing to tease out fine-scale temporal variability in Thaumarchaeota abundance. I found that this bloom corresponded with increased temperature and nitrite, and decreased pH and oxygen; any of these factors could potentially "cause" this bloom on Sapelo Island (save for nitrite, which is produced by ammonia oxidation resulting from the bloom), but another perhaps unmeasured factor (possibly copper or another trace metal) could be involved. Additional samples collected in waters surrounding Sapelo Island and in shelf waters of the South Atlantic Bight (Appendix D) indicate that this bloom is restricted to coastal regions in summer (August) and fall (October), and Thaumarchaeota abundances are not above background anywhere during spring (April).

Previous studies suggested the possibility that Thaumarchaeota could be mixotrophic, and anomalous *amoA*:*rrs* ratios detected in the Antarctic WW layer during a

cruise in 2006 suggested that the Southern Ocean could be an ideal location to investigate further. I used a variety of ^{15}N-labeled organic substrates, including urea, to test this hypothesis. Subsequently, it was proposed that Thaumarchaeota in polar regions (and elsewhere) could use urea as an alternate substrate for ammonia oxidation, particularly in situations where ammonia concentrations were limiting. I used both ^{15}N-labeled urea and ammonia as tracers to compare rates of NO_x production in both polar and temperate regions (Chapter 5). The results from this study showed that oxidation of urea-N was variable, with the majority of samples we tested exhibiting rates of ammonia oxidation 1.3 to 130-fold higher than oxidation of urea-N. The exceptions where oxidation of urea-N was faster than oxidation of NH_4 (15 versus 5.4 nM d^{-1}, respectively) were all at high latitudes (Southern Ocean and Gulf of Alaska) and between 70-200 m depth (including Antarctic Winter Water samples). Additional evidence indicates that the N in urea is released into the ammonia pool by hydrolysis prior to oxidation. This implies that direct oxidation of urea-N by marine Thaumarchaeota is not likely to contribute significantly to either nitrification or to the energetics of Thaumarchaeota, except in polar waters. The cases we found for preferential use of urea over ammonia suggest that there may be specific ecotypes of Thaumarchaeota adapted to using urea either directly or more efficiently.

Thaumarchaeota distributions are commonly observed to covary with depth and oxygen in my data sets (and elsewhere). I pursued a hypothesis that reactive oxygen species (ROS) could be important to determining Thaumarchaeota distributions. These studies are described in Chapter 6. Near surface waters are subjected to photochemical perturbation by solar irradiation, which can react with oxygen and dissolved organic

matter to form ROS. ROS are also formed as by-products of photosynthesis and respiration, and could be why Thaumarchaeota are absent in surface waters. Although most organisms produce enzymes to combat ROS, Thaumarchaeota do not have catalase, which detoxifies H_2O_2. This hypothesis was tested in a variety of marine environments using seawater incubations with varying H_2O_2 additions. We measured transcription and nitrification rates and found that in all locations, nitrification is inhibited with increased H_2O_2, with the most sensitive populations coming from Antarctic waters and the least sensitive populations from Sapelo Island, Georgia (Appendix E). We believe this is a result of differences in the surrounding microbial community's ability to remove H_2O_2 via catalase and reduce the toxicity to Thaumarchaeota.

As methods to study uncultured organisms improve – including single-cell genomics and transcriptomics, advanced microscopy techniques, better cultivation strategies, etc. – molecular-based surveys of gene distributions like those showcased in this dissertation will become useful for preliminary ecosystem analysis. Correlations between Thaumarchaeota abundances and environmental measurements are important for targeting more experimental-based approaches and manipulations (much like ROS additions presented in Chapter 6) to tease out factors that directly influence the growth and activity of this group. Environmental factors (including water temperature and pH) that I found to be potentially important drivers of Thaumarchaeota distributions will change as a result of global climate change. Therefore, directed experiments using mesocosms, enrichment cultures, or pure cultures are crucial to understand and predict the effects of a changing world on the global nitrogen cycle.

APPENDIX A

SUPPLEMENTARY MATERIAL: AN ANALYSIS OF THAUMARCHAEOTA POPULATIONS FROM THE NORTHERN GULF OF MEXICO[1]

[1] Tolar, B.B., G.M. King, and J.T. Hollibaugh. 2013. *Frontiers in Microbiology*. 4:72. Reprinted here with permission of the publisher.

SUPPLEMENTARY METHODS

Quantitative PCR (qPCR) standards

Standards for qPCR reactions were constructed as in Kalanetra *et al.* (2009). Briefly, environmental DNA was amplified using gene-specific sequencing primers (Thaumarchaeota *rrs*, Archaeal *amoA*, Bacterial *amoA*) or qPCR primers (*accA*) under standard PCR conditions. For Bacterial *rrs* qPCR, *E. coli* genomic DNA was used. The resulting PCR product was loaded onto an agarose gel, electrophoresed, and a band of expected product size was excised. This band was purified using the QIAquick® Gel Extraction Kit (QIAGEN) and cloned into *E. coli* TOP10 chemically competent cells after insertion into a TOPO 4 vector (Invitrogen) using the manufacturer's instructions. Clones were selected at random and sequenced to check insert specificity. Those with positive insertions were grown overnight in LB broth with ampicillin, and plasmids were extracted using the QIAprep Spin Miniprep Kit® (QIAGEN). Plasmids were linearized using the restriction enzyme *NotI* (New England Biolabs), then purified in the same manner as PCR products above. Concentrations of linearized plasmid DNA were measured with the Quant-iT™ PicoGreen® dsDNA reagent (Invitrogen) using a Picofluor handheld fluorometer (Turner Designs). Gene concentration calculations were based on measured DNA concentrations, plasmid length, and insert sequence length. Standards were then diluted to a range of 10^7 to 10^1 copies μL^{-1} for each reaction.

Thaumarchaeota hcd *gene assay*

In addition to *accA*, another gene in the 3-hydroxypropionate/4-hydroxybutyrate pathway, *hcd*, encoding the enzyme 4-hydroxybutyryl-CoA dehydratase, has been

suggested as a potential marker for carbon fixation in Thaumarchaeota (Offre *et al.*, 2011). Primers for this gene have been developed and tested on soil Thaumarchaeota populations (Offre *et al.*, 2011). We explored using these primers to quantify *hcd* abundance in our samples. We were unable to obtain the desired amplification specificity with these primers and our samples (determined by agarose gel electrophoresis then cloning and sequencing putative amplicons, see below).

Gene abundance and ratio calculations

The number of gene copies detected by qPCR (copies per reaction) was converted to environmental concentrations (copies L^{-1}) using the original sample volume filtered (~1 L), the portion of the lysate purified (800 of 2000 μL), the final volume of the purified extract (50 μL, we also measured DNA concentration in this extract), and the portion of the purified DNA extract used in each qPCR reaction (2 μL). This calculation assumes that all bacterioplankton cells were collected on the filter, that the DNA contribution from eukaryotes was negligible, that all of the DNA from all of the cells collected on each filter was released into the lysate, then extracted and purified from the lysate and detected by qPCR with 100% efficiency by our methods (see discussion and calibration in Kalanetra *et al.*, 2009). The contribution of Thaumarchaeota to the prokaryotic population was estimated from Thaumarchaeota and Bacteria *rrs* abundance by assuming 1.8 *rrs* per Bacteria genome (Biers *et al.*, 2009), 1.0 *rrs* per Thaumarchaeota genome (IMG database) or 2.0 *rrs* per NOB genome (Mincer *et al.*, 2007). Thaumarchaeota abundance was then divided by the total prokaryotic abundance (Bacteria plus Thaumarchaeota; Euryarchaeota were present in some samples but were

never abundant, see below, and were not measured by qPCR) to calculate the contribution of Thaumarchaeota cells to the prokaryotic community. Ratios of gene abundance in a given sample were calculated directly from the qPCR data (copies μL^{-1} of extract).

BEST analysis

BEST analysis was performed for all samples collected in addition to the subset of samples for which nutrient data were available. Nutrient data were collected by researchers interested in modeling phytoplankton growth and thus were only available for near-surface samples. For these samples, gene abundances were log transformed and resemblance distances for each gene between samples were calculated using Bray-Curtis similarity; resemblances for environmental data were calculated using the Euclidean distance. The resultant similarity matrices were combined and analyzed with Biota and/or Environment matching (BioEnv) through the BEST (Clarke, 1993) procedure in PRIMER (Clarke and Gorley, 2006). The significance of BEST results for each gene was tested using 999 permutations, and the null hypothesis of no species-environment relationship was rejected for all results with $p \leq 0.001$.

SUPPLEMENTARY RESULTS

Gene ratios

Ratios of archaeal *amoA*:Thaumarchaeota *rrs* ranged from 0.001 (B5-760 m) to 6.6 (G1-15 m) when using the Wuchter primers to quantify Thaumarchaeota *amoA* (Table 2.2, Figure A.5a). Low ratios of *amoA*:*rrs* seemed to coincide with deep (>100 m)

samples (Table 2.2, Figure A.5a). In contrast, ratios of *amoA*:*rrs* ranged from 0.002 to 1.9 with an average of 0.5 when Thaumarchaeota *amoA* abundance was estimated using the Francis primers. The Francis primer set detected more *amoA* genes below 200 m depth, sometimes up to 1000 times more than the Wuchter primer set (Figure A.6). In contrast, estimates of *amoA* abundance in near-surface (≤100 m) samples using the Wuchter primers were 10 to 100-fold greater than estimates based on the Francis primers (Figure A.6). Ratios of *accA*:Thaumarchaeota *rrs* ranged from 0.0002 to 1.3 (Table 2.2). We detected the fewest copies of *accA* per Thaumarchaeota *rrs* in near-surface (≤100 m) samples (Figure A.5b).

Thaumarchaeota hcd genes

hcd PCR products were also obtained using the primer set from Offre *et al.* (2011). However, the *hcd* primers yielded 3 bands of ~200 bp, ~350 bp and ~400 bp by agarose gel electrophoresis. Analysis of sequences from the ~200 bp band indicated non-specific amplification, so these sequences are not considered further. Sequences from the ~350 and ~400 bp bands were most similar to *hcd* from Thaumarchaeota (BLASTx to the RefSeq database). Since non-specific amplification prevented reliable qPCR quantification of *hcd* in our samples, we did not pursue this marker further. The sequences obtained from ~350 and ~400 bp bands have been submitted to GenBank (NCBI) under accession numbers KC409223 to KC409237.

Community composition

As expected, phylogenetic analysis of *amoA* nucleotide sequences (Figure A.1a) revealed more diversity than was apparent in inferred amino acid sequences, with 47 OTUs (97% similarity cutoff; Table A.4) identified in the 100 m and 200 m samples from Station D5. Seventeen of the 47 *amoA* OTUs only contained sequences from 100 m (1-22 sequences in each OTU), while 23 OTUs only contained sequences from 200 m (1-8 sequences in each). The *amoA* sequence most similar to either "*Candidatus* Nitrosopumilus maritimus" strain SCM1 or to Nitrosopumilus sp. NM25 was obtained from the 100 m library, and it was only 91% similar to either sequence.

The *accA* nucleotide alignment contained 51 OTUs (97% similarity cutoff; Table A.4) that clustered primarily by depth (Figure A.1b). Sequences from deep samples (200 m and 450 m) were assigned to 26 OTUs (1-13 sequences in each); only 4 of these OTUs contained any near-surface (2 m, 50 m, or 100 m) sequences. Twenty-one of the OTUs contained sequences exclusively from near-surface (≤100 m) samples (1-34 sequences in each). Almost half (101) of the sequences we retrieved were at least 77% similar to *accA* from "*Ca.* N. maritimus" strain SCM1; all of these were retrieved from near-surface waters except for 6 sequences from 200 m.

BEST Analysis

Gene abundances determined by qPCR were compared to environmental data using the BEST procedure (Clarke, 1993). Results of this analysis (Table A.7) show that abundances of Bacterial *amoA*, Archaeal *accA*, and pSL12 *rrs* – but not Bacterial *rrs* – were significantly correlated with fluorescence (chlorophyll *a*). Abundances of both

Thaumarchaeota and Bacteria *rrs* were correlated with beam attenuation (turbidity), in combination with salinity and either fluorescence or temperature. Archaeal *amoA* abundance correlated with latitude, fluorescence, and salinity. Interestingly, BEST analysis (Table A.7a) showed that *amoA* abundance estimates obtained using the Wuchter *et al.* (2006) primers correlated with temperature ($\rho = 0.442$; $p < 0.001$), while *amoA* abundance estimated with the Francis *et al.* (2005) primers correlated with oxygen concentration ($\rho = 0.474$; $p < 0.001$).

Nutrient data (including nitrite, nitrate, ammonia, phosphate, and silicate; provided by S. Lohrenz) were only available for near-surface samples. Gene abundances for Bacterial *rrs*, pSL12 *rrs*, and Archaeal *amoA* amplified with Wuchter primers (Table A.7b) correlated with silicate in combination with other variables, although only the Bacterial *rrs* result was significant ($p < 0.001$). Only the results with the highest Spearman's rank correlation coefficient (ρ) are shown in Table A.7b; however, weaker correlations to nutrients were found with the second highest result. Archaeal *amoA* amplified with Francis primers ($\rho = 0.446$; $p \leq 0.010$; data not shown) and Bacterial *rrs* ($\rho = 0.583$; $p < 0.001$; data not shown) were correlated with nitrate, while Thaumarchaeota *rrs* ($\rho = 0.409$; $p \leq 0.018$; data not shown) also correlated with nitrite and silicate together.

SUPPLEMENTARY DISCUSSION

Community composition

Almost all of the near-surface (≤100 m) Thaumarchaeota *rrs* sequences were ≥ 98% similar to the *rrs* from "*Ca.* N. maritimus" strain SCM1, as well as to

Nitrosopumilus sp. NM25, retrieved from sand taken from a *Zostera* seagrass bed (Matsutani *et al.*, 2011). The group containing these sequences included a sequence retrieved from cloned PCR amplicons sequenced from a tidal creek (the Duplin River) adjacent to Sapelo Island, Georgia (Hollibaugh *et al.*, 2011), as well as "*Candidatus* Nitrosoarchaeum limnia" strain SFB1 (Blainey *et al.*, 2011), which was enriched from a sample taken in the oligohaline reach of North San Francisco Bay. This contrasts with clones recovered from 200 m in the northern Gulf of Mexico, where sequences were distributed among 9 OTUs, indicating a richer community of Thaumarchaeota (agreeing with the Shannon index of these samples calculated from pyrosequencing data; Table A.4). We did not recover any clones related to the pSL12-like clade at Station D5, which is consistent with their low *rrs* abundance as estimated by qPCR.

A nucleotide alignment of *accA* genes from this study produced a phylogenetic tree (Figure A.1b) that supported the groupings found in trees generated from inferred amino acid alignments (Figure 2.6b); however, some samples from Station D5 (mostly from 200 m depth) clustered with representatives from Deep Ecotype 1a (Yakimov *et al.*, 2011) at the nucleotide level. Additionally, a novel deep cluster of sequences from the Gulf of Mexico and the South China Sea was identified ('Deep Ecotype 3'; Figure A.1b).

Gene ratios

High ratios of *amoA*:Thaumarchaeota *rrs* genes at certain stations (Figure A.5a) could indicate a population of AOA with multiple *amoA* copies per genome or the presence of a group of Archaea that are not detected by the *rrs* primer set we used (e.g., Beman *et al.*, 2008; Teske and Sorensen, 2008), but that contain a homologue of the

amoA gene (for example the pSL12-like clade). The latter seems less likely for pSL12 in particular, given the low abundance of *rrs* from this group at most stations in the northern Gulf of Mexico. However, in the Mississippi River at station MR1 (salinity of 0), the abundance of pSL12 *rrs* genes was equal to Archaeal *amoA* gene abundance, regardless of the *amoA* primer set used, while Thaumarchaeota *rrs* genes were undetectable. Low ratios of *amoA*:*rrs* have been proposed to indicate a potential for heterotrophy in Thaumarchaeota (Agogué *et al.*, 2008; de Corte *et al.*, 2008; Kalanetra *et al.*, 2009); however, this has yet to be confirmed definitively and may simply reflect depth-dependent shifts in sub-populations that affect our ability to quantify them by qPCR, as shown by Beman *et al.* (2008) and others.

Our data indicate that the ratio of *amoA*:*rrs* gene abundance decreases with depth; however, we also observed increases in the *accA*:*rrs* ratio for deeper waters (Figure A.5b). The *amoA*:*accA*:*rrs* ratios we found are not consistent with the expected 1:1:1 ratio found in the "*Ca.* N. maritimus" strain SCM1 genome (Walker *et al.*, 2010). In samples ≤100 m, this ratio is 1.8:0.1:1 or 0.5:0.1:1, while deeper samples show 0.2:0.6:1 or 0.6:0.6:1 depending on whether the Wuchter or Francis *amoA* primer sets were used. In deeper waters where Thaumarchaeota *rrs* are most abundant, using the Francis primers produces ratios most similar to those found in "*Ca.* N. maritimus" strain SCM1. Direct comparison of *amoA* abundances in our samples as determined by the Wuchter versus Francis primer sets (Figure A.6) demonstrate this clearly.

REFERENCES

Agogué H, Brink M, Dinasquet J, Herndl GJ (2008). Major gradients in putatively nitrifying and non-nitrifying Archaea in the deep North Atlantic. *Nature* **456:** 788-791.

Beman JM, Popp BN, Francis CA (2008). Molecular and biogeochemical evidence for ammonia oxidation by marine Crenarchaeota in the Gulf of California. *ISME J* **2:** 429-441.

Biers EJ, Sun SL, Howard EC (2009). Prokaryotic Genomes and Diversity in Surface Ocean Waters: Interrogating the Global Ocean Sampling Metagenome. *Appl Environ Microbiol* **75:** 2221-2229.

Blainey PC, Mosier AC, Potanina A, Francis CA, Quake SR (2011). Genome of a low-salinity ammonia-oxidizing archaeon determined by single-cell and metagenomic analysis. *PLoS ONE* **6:** e16626.

Clarke KR (1993). Non-parametric multivariate analyses of changes in community structure. *Aust J Ecol* **18:** 117-143.

Clarke KR, Gorley RN (2006). PRIMER v6. *User Manual / Tutorial*. PRIMER-E: Plymouth.

de Corte D, Yokokawa T, Varela MM, Agogué H, Herndl GJ (2008). Spatial distribution of Bacteria and Archaea and *amoA* gene copy numbers throughout the water column of the Eastern Mediterranean Sea. *ISME J* **3:** 147-158.

DeLong EF (1992). Archaea in coastal marine environments. *Proc Natl Acad Sci USA* **89:** 5685-5689.

Francis CA, Roberts KJ, Beman JM, Santoro AE, Oakley BB (2005). Ubiquity and diversity of ammonia-oxidizing archaea in water columns and sediments of the ocean. *Proc Natl Acad Sci USA* **102:** 14683-14688.

Hamady M, Lozupone C, Knight R (2009). Fast UniFrac: facilitating high-throughput phylogenetic analyses of microbial communities including analysis of pyrosequencing and PhyloChip data. *ISME J* **4:** 17-27.

Hollibaugh JT, Gifford S, Sharma S, Bano N, Moran MA (2011). Metatranscriptomic analysis of ammonia-oxidizing organisms in an estuarine bacterioplankton assemblage. *ISME J* **5:** 866-878.

Hornek R, Pommerening-Roser A, Koops HP, Farnleitner AH, Kreuzinger N, Kirschner A, Mach RL (2006). Primers containing universal bases reduce multiple *amoA* gene specific DGGE band patterns when analysing the diversity of beta-ammonia oxidizers in the environment. *J Microbiol Methods* **66:** 147-155.

Kalanetra KM, Bano N, Hollibaugh JT (2009). Ammonia-oxidizing Archaea in the Arctic Ocean and Antarctic coastal waters. *Environ Microbiol* **11:** 2434-2445.

King GM, Smith CB, Tolar B, Hollibaugh JT (2013). Analysis of composition and structure of coastal to mesopelagic bacterioplankton communities in the northern Gulf of Mexico. *Front Microbiol*.

Ludwig W, Strunk O, Westram R, Richter L, Meier H, Yadhukumar, Buchner A, Lai T, Steppi S, Jobb G, Forster W, Brettske I, Gerber S, Ginhart AW, Gross O, Grumann S, Hermann S, Jost R, Konig A, Liss T, Lussmann R, May M, Nonhoff B, Reichel B, Strehlow R, Stamatakis A, Stuckmann N, Vilbig A, Lenke M, Ludwig T, Bode A, Schleifer KH (2004). ARB: a software environment for sequence data. *Nucl Acids Res* **32:** 1363-1371.

Matsutani N, Nakagawa T, Nakamura K, Takahashi R, Yoshihara K, Tokuyama T (2011). Enrichment of a Novel Marine Ammonia-Oxidizing Archaeon Obtained from Sand of an Eelgrass Zone. *Microbes Environ* **26:** 23-29.

Mincer TJ, Church MJ, Taylor LT, Preston C, Karl DM, DeLong EF (2007). Quantitative distribution of presumptive archaeal and bacterial nitrifiers in Monterey Bay and the North Pacific Subtropical Gyre. *Environ Microbiol* **9:** 1162-1175.

Offre P, Nicol GW, Prosser JI (2011). Community profiling and quantification of putative autotrophic thaumarchaeal communities in environmental samples. *Environ Microbiol Rep* **3:** 245-253.

Rotthauwe JH, Witzel KP, Liesack W (1997). The ammonia monooxygenase structural gene *amoA* as a functional marker: Molecular fine-scale analysis of natural ammonia-oxidizing populations. *Appl Environ Microbiol* **63:** 4704-4712.

Schloss PD, Westcott SL, Ryabin T, Hall JR, Hartmann M, Hollister EB, Lesniewski RA, Oakley BB, Parks DH, Robinson CJ, Sahl JW, Stres B, Thallinger GG, Van Horn DJ, Weber CF (2009). Introducing mothur: Open-source, platform-independent, community-supported software for describing and comparing microbial communities. *Appl Environ Microbiol* **75:** 7537-7541.

Suzuki MT, Taylor LT, DeLong EF (2000). Quantitative analysis of small-subunit rRNA genes in mixed microbial populations via 5'-nuclease assays. *Appl Environ Microbiol* **66:** 4605-4614.

Teske A, Sorensen KB (2008). Uncultured archaea in deep marine subsurface sediments: have we caught them all? *ISME J* **2:** 3-18.

Walker CB, de la Torre JR, Klotz MG, Urakawa H, Pinel N, Arp DJ, Brochier-Armanet C, Chain PSG, Chan PP, Gollabgir A, Hemp J, Hügler M, Karr EA, Könneke M, Shin M, Lawton TJ, Lowe T, Martens-Habbena W, Sayavedra-Soto LA, Lang D, Sievert SM, Rosenzweig AC, Manning G, Stahl DA (2010). *Nitrosopumilus maritimus* genome reveals unique mechanisms for nitrification and autotrophy in globally distributed marine crenarchaea. *Proc Nat Acad Sci USA* **107:** 8818-8823.

Wuchter C, Abbas B, Coolen MJL, Herfort L, van Bleijswijk J, Timmers P, Strous M, Teira E, Herndl GJ, Middelburg JJ, Schouten S, Damste JSS (2006). Archaeal nitrification in the ocean. *Proc Natl Acad Sci USA* **103:** 12317-12322.

Yakimov MM, La Cono V, Denaro R (2009). A first insight into the occurrence and expression of functional amoA and accA genes of autotrophic and ammonia-oxidizing bathypelagic Crenarchaeota of Tyrrhenian Sea. *Deep-Sea Res Pt II* **56:** 748-754.

Yakimov MM, La Cono V, Smedile F, DeLuca TH, Juarez S, Ciordia S, Fernandez M, Albar JP, Ferrer M, Golyshin PN, Giuliano L (2011). Contribution of crenarchaeal autotrophic ammonia oxidizers to the dark primary production in Tyrrhenian deep waters (Central Mediterranean Sea). *ISME J* **5:** 945-961.

Table A.1: Primers used in this study

Target Gene*	Primer/Probe**	Sequence (5'→3')	Application	Detection Limit	qPCR Efficiency	Reference
Archaeal *rrs*	21F	TTCCGGTTGATCCYGCCGGA	PCR and Sequencing	N/A	N/A	DeLong (1992)
	958R	YCCGGCGTTGAMTCCAATT				
Thaum-archaeal *rrs*	G1_334F	AGATGGGTACTGAGACACGGAC	qPCR	4.08×10^3 copies L^{-1}	96.5-112.7%	Suzuki *et al.* (2000)
	G1_554R	CTGTAGGCCCAATAATCATCCT				
	TM519AR	TTACCGCGGCGGCTGGCAC				Suzuki *et al.* (2000)
pSL12 *rrs*	pSL12_750F	GGTCCRCCAGAACGCGC	qPCR	1.07×10^4 copies L^{-1}	96.9-103.1%	Mincer *et al.* (2007)
	pSL12_876R	GTACTCCCCAGGCGGCAA				
Bacterial *rrs*	BACT1369F	CGGTGAATACGTTCYCGG	qPCR	1.14×10^4 copies L^{-1}	91.6-113.2%	Suzuki *et al.* (2000)
	PROK1492R	GGWTACCTTGTTACGACTT				
	TM1389F	CTTGTACACACCGCCCGTC				
Universal *rrs*	515F	GCCTTGCCAGCCCGCTCAGGTGTGCCA GCMGCCGCGGTAA	pyro-sequencing	N/A	N/A	King *et al.* (2013)
	806R[#]	GCCTCCCTCGCGCCATCAGNNNNNNNN NNNNGGGGACTACVSGGGTATCTAAT				
Archaeal *amoA* (W^+)	Arch-amoA-for	CTGAYTGGGCYTGGACATC	qPCR	1.44×10^4 copies L^{-1}	95.1-103.6%	Wuchter *et al.* (2006)
	Arch-amoA-rev	TTCTTCTTTGTTGCCCAGTA				
Archaeal *amoA* (F^+)	ArchamoAF	STAATGGTCTGGCTTAGACG	qPCR and Sequencing	1.79×10^4 copies L^{-1}	88.4-96.0%	Francis *et al.* (2005)
	ArchamoAR	GCGGCCATCCATCTGTATGT				
Bacterial *amoA*	amoA-1F	GGGGTTTCTACTGGTGGT	qPCR	1.63×10^4 copies L^{-1}	88.4-95.6%	Rotthauwe *et al.* (1997)
	amoA-r New	CCCCTCBGSAAAVCCTTCTTC				Hornek *et al.* (2006)
Archaeal *accA*	Crena_529F	GCWATGACWGAYTTTGTYRTAATG	qPCR and Sequencing	1.25×10^4 copies L^{-1}	80.5-91.1%	Yakimov *et al.* (2009)
	Crena_981R	TGGWTKRYTTGCAAYTATWCC				
Archaeal *hcd*	hcd-465F (S)	GGHGGTGCWATGACTGAT	PCR, qPCR, Sequencing	N/A	N/A	Offre *et al.* (2011)
	hcd-911F (Q)	AGCTATGTBTGCAARACAGG				
	hcd-1267R (S,Q)	CTCATTCTGTTTTCHACATC				

**rrs* = 16S rRNA gene; *amoA* = ammonia monooxygenase gene, Bacteria *amoA* primers only amplify *amoA* genes from β-Proteobacteria; *accA* = biotin-dependent acetyl-CoA/propionyl-CoA carboxylase gene; *hcd* = 4-hydroxybutyryl-CoA dehydratase. **(S) = Sequencing, (Q) = qPCR, TM = TaqMan Probe. [+]Archaeal *amoA* (W) and (F) refer to Wuchter *et al.* (2006) and Francis *et al.* (2005) primer sets, respectively (as mentioned in text). [#]For primer 806R, N's in sequence = barcode sequence region.

Table A.2: qPCR estimates of the abundance of *rrs*, *amoA*, and *accA* genes in samples from the northern Gulf of Mexico.

Station ID	Depth	Amount Filtered (L)	Wuchter Arch *amoA* copies/L	Francis Arch *amoA* copies/L	Arch *accA* copies/L	Thaum *rrs* copies/L	pSL12 *rrs* copies/L	AOB *amoA* copies/L	Bacteria *rrs* copies/L	Thaum % of Total Prokarya
A2	18 m	1.0	ND	ND	ND	5.85E+05	*1.12E+02*	ND	4.60E+08	0.23%
A4	17m	1.2	ND	ND	ND	2.08E+06	ND	ND	8.70E+08	0.43%
A4	43 m	1.2	ND	ND	ND	2.20E+06	ND	ND	4.32E+08	0.91%
A6	2 m	1.1	2.32E+06	8.82E+05	*6.48E+02*	2.62E+06	*4.50E+01*	*2.79E+02*	5.27E+08	0.89%
A6	20 m	1.1	1.15E+07	3.24E+06	1.33E+05	9.52E+06	*1.72E+03*	*5.23E+03*	1.02E+09	1.66%
A6	80 m	1.1	3.29E+07	7.61E+06	3.30E+05	1.81E+07	*1.52E+03*	*7.07E+03*	3.48E+08	8.54%
A6	160 m	1.1	1.46E+07	5.86E+07	1.80E+07	5.45E+07	1.32E+04	*8.80E+03*	2.42E+08	28.88%
A6	200 m	1.1	4.72E+06	1.25E+07	5.83E+06	2.00E+07	*6.57E+03*	*1.43E+03*	1.77E+08	16.94%
A6	250 m	1.1	1.74E+06	9.41E+06	8.56E+06	2.34E+07	*5.98E+03*	*1.03E+03*	1.28E+08	24.80%
A6	350 m	1.1	5.86E+05	4.64E+06	3.95E+06	8.86E+06	*4.50E+03*	*5.50E+02*	4.46E+07	26.36%
A6	700 m	1.1	2.42E+05	8.36E+06	3.47E+06	9.28E+06	*3.61E+03*	LD	2.49E+07	40.17%
A6	1700 m	1.2	1.53E+05	5.11E+05	1.74E+06	3.23E+06	*1.05E+04*	ND	4.31E+07	11.92%
B4	200 m	1.1	6.20E+06	9.20E+06	1.56E+07	2.28E+07	1.30E+04	*3.52E+03*	3.30E+08	11.06%
B4	530 m	1.2	6.45E+05	6.05E+06	5.46E+06	1.42E+07	*5.78E+03*	*5.24E+03*	1.08E+08	19.11%
B5	2 m	1.1	9.62E+06	8.21E+06	5.54E+05	8.50E+06	*2.71E+03*	*4.71E+03*	6.07E+08	2.46%
B5	200 m	1.1	6.05E+06	3.43E+07	1.21E+07	3.25E+07	3.52E+04	*1.92E+03*	3.68E+08	13.72%
B5	450 m	1.1	9.08E+05	1.60E+07	1.32E+07	3.38E+07	1.54E+04	*2.27E+03*	2.04E+08	23.01%
B5	760 m	1.1	*4.65E+03*	1.36E+06	ND	3.48E+06	*4.17E+03*	*1.34E+02*	4.40E+07	12.49%
C1	12 m	1.1	1.74E+08	1.50E+07	9.53E+05	1.10E+08	LD	2.10E+06	1.08E+10	1.79%
C4	2 m	1.0	ND	ND	ND	1.76E+06	LD	ND	6.03E+08	0.52%
C4	200 m	1.0	7.21E+06	1.66E+07	1.00E+07	4.93E+07	2.39E+04	*3.35E+03*	2.04E+08	30.29%
C4	700 m	1.0	3.84E+05	4.62E+06	7.17E+06	1.26E+07	1.21E+04	*2.35E+03*	4.33E+07	34.30%
D3	25 m	1.1	7.66E+07	1.01E+07	5.10E+05	1.47E+07	*7.17E+03*	2.54E+05	6.60E+08	3.85%
D3	68 m	1.1	8.13E+06	7.53E+05	*1.02E+03*	ND	*5.27E+02*	*1.53E+04*	3.11E+05	0.30%
D5	2 m	1.1	7.31E+06	1.91E+06	1.46E+05	4.71E+06	*6.21E+02*	*4.55E+02*	7.34E+08	1.14%
D5	50 m	1.1	5.42E+06	2.40E+06	3.14E+05	5.37E+06	*1.64E+03*	*1.29E+03*	8.93E+08	1.07%

Station ID	Depth	Amount Filtered (L)	Wuchter Arch *amoA* copies/L	Francis Arch *amoA* copies/L	Arch *accA* copies/L	Thaum *rrs* copies/L	pSL12 *rrs* copies/L	AOB *amoA* copies/L	Bacteria *rrs* copies/L	Thaum % of Total Prokarya
D5	100 m	1.1	2.85E+07	7.08E+06	1.36E+06	2.14E+07	*3.61E+03*	*2.28E+03*	3.89E+08	9.00%
D5	200 m	1.2	1.94E+06	1.08E+07	1.08E+07	1.69E+07	*8.86E+03*	*2.77E+03*	1.23E+08	19.84%
D5	350 m	1.1	9.70E+05	8.69E+06	1.39E+07	2.45E+07	*6.54E+03*	*1.49E+03*	8.53E+07	34.08%
D5	450 m	1.0	4.88E+05	3.76E+06	7.18E+06	1.08E+07	*4.47E+03*	*5.24E+03*	3.56E+07	35.34%
D5	900 m	1.1	4.43E+05	2.72E+06	6.84E+06	7.50E+06	*6.27E+03*	*2.34E+03*	5.50E+07	19.72%
E2	6 m	1.0	ND	LD	ND	ND	ND	ND	4.50E+09	0.00%
E6	200 m	1.1	3.63E+06	1.25E+07	1.55E+07	1.57E+07	1.63E+04	*4.83E+03*	1.80E+08	13.56%
E6	800 m	1.1	5.40E+05	3.49E+06	6.05E+06	4.73E+06	*5.30E+03*	*1.14E+03*	1.49E+08	5.41%
F4	50 m	1.1	1.12E+07	7.60E+05	7.42E+04	5.92E+06	*9.58E+02*	4.23E+04	5.17E+08	2.02%
F6	2 m	1.1	ND	ND	ND	4.79E+04	LD	ND	4.08E+08	0.02%
F6	200 m	1.2	1.03E+07	1.17E+07	1.75E+07	1.56E+07	1.23E+04	*3.18E+03*	2.59E+08	9.80%
F6	950 m	1.1	4.52E+05	1.79E+06	5.42E+06	5.19E+06	*5.43E+03*	*2.78E+03*	3.52E+07	20.99%
G1	15 m	1.1	6.46E+06	2.50E+05	*9.09E+02*	*9.80E+05*	*6.41E+02*	2.37E+04	9.27E+08	0.19%
G5	80 m	1.1	2.39E+07	2.69E+06	5.93E+05	9.77E+06	*2.56E+03*	*6.09E+03*	6.20E+08	2.76%
H1	7 m	1.0	3.79E+05	*9.28E+02*	7.73E+04	5.17E+05	5.93E+04	5.14E+04	5.68E+09	0.02%
H3	20 m	1.2	9.74E+04	6.01E+04	ND	1.37E+05	*1.75E+02*	ND	6.74E+08	0.04%
H6	2 m	1.1	7.64E+04	1.24E+05	*3.16E+02*	4.45E+05	*4.14E+01*	ND	1.04E+09	0.08%
H6	25 m	1.1	3.91E+04	3.95E+05	ND	2.05E+05	*3.41E+02*	*1.67E+02*	1.34E+09	0.03%
H6	45 m	1.1	3.18E+06	1.00E+06	2.67E+04	1.86E+06	*6.21E+02*	*1.02E+03*	9.42E+08	0.35%
H6	80 m	1.1	2.64E+07	1.33E+07	2.79E+06	1.59E+07	*3.98E+03*	*5.64E+03*	4.72E+08	5.74%
H6	110 m	1.1	2.12E+07	1.39E+07	1.48E+06	2.03E+07	*8.10E+03*	*8.18E+03*	3.17E+08	10.33%
H6	200 m	1.2	2.16E+06	ND	ND	1.66E+07	ND	*1.23E+03*	1.13E+08	20.98%
H6	280 m	1.1	2.71E+06	4.57E+06	2.16E+06	4.80E+06	*2.92E+03*	*2.29E+03*	1.83E+09	0.47%
MR1	2 m	0.6	2.02E+05	3.79E+05	2.02E+05	ND	3.30E+05	7.44E+05	1.26E+10	0.00%
MR2	8 m	1.1	6.52E+07	1.02E+07	4.24E+05	2.96E+07	7.68E+04	2.83E+05	7.43E+09	0.71%
MR3	110 m	1.0	5.82E+07	2.97E+07	1.00E+07	4.60E+07	2.93E+04	1.50E+05	1.78E+09	4.46%

ND = Not determined; qPCR abundance undetectable for this specific gene in this sample; LD = Limit of detection; sample ran below limit of detection with high variability in assay. *Note that some values shown below the limit of detection (italicized).

Table A.3: Abundance of Thaumarchaeota, Euryarchaeota, Nitrite-Oxidizing Bacteria (NOB), and Ammonia-Oxidizing Bacteria (AOB) *rrs* sequences in pyrosequenced libraries from DNA samples collected in the northern Gulf of Mexico.

Station ID	Depth	Thaumarchaeota as a % of Prokaryotes by qPCR of *rrs*	Total Number of *rrs* Sequences in Pyrosequenced Library	Bacteria *rrs* Hits in Pyrosequenced Libraries	Thaumarchaeota *rrs* Hits in Pyrosequenced Libraries	Euryarchaeota *rrs* Hits in Pyrosequenced Libraries	NOB *rrs* Hits in Pyrosequenced Libraries	AOB *rrs* Hits in Pyrosequenced Libraries	Thaumarchaeota as a % of Prokaryotes by Pyrosequencing *rrs* amplicons	Euryarchaeota as a % of Prokaryotes by Pyrosequencing *rrs* amplicons	NOB as a % of Prokaryotes by Pyrosequencing *rrs* amplicons	AOB as a % of Prokaryotes by Pyrosequencing *rrs* amplicons
A2	18	0.23%	2297	2283	11	3	0	0	0.86%	0.23%	0.00%	0.00%
A4	17	0.43%	9146	8947	71	128	3	1	1.41%	2.54%	0.03%	0.02%
A4	43	0.91%	6185	5131	727	327	63	0	20.32%	9.14%	0.88%	0.00%
A6	2	0.89%	6288	5888	111	289	2	0	3.28%	8.54%	0.03%	0.00%
A6	20	1.66%	8487	7626	164	697	5	0	3.73%	15.84%	0.06%	0.00%
A6	80	8.53%	8021	7132	583	306	36	1	12.83%	6.73%	0.40%	0.02%
A6	160	28.86%	5787	3578	1779	430	121	0	47.23%	11.42%	1.61%	0.00%
A6	350	26.38%	3552	2415	992	145	24	0	42.51%	6.21%	0.51%	0.00%
A6	700	40.18%	3428	1993	1287	148	20	0	53.75%	6.18%	0.42%	0.00%
A6	1700	11.91%	879	626	232	21	2	0	40.02%	3.62%	0.17%	0.00%
B4	200	11.05%	8564	6925	1383	256	88	0	26.44%	4.89%	0.84%	0.00%
B4	530	19.06%	5539	4243	1154	142	17	0	32.87%	4.04%	0.24%	0.00%
B5	2	2.46%	764	683	12	69	0	0	3.07%	17.63%	0.00%	0.00%
B5	200	13.72%	4053	3191	698	164	51	0	28.25%	6.64%	1.03%	0.00%
B5	450	23.07%	4787	3304	1301	182	30	0	41.48%	5.80%	0.48%	0.00%

Station ID	Depth	Thaumarchaeota as a % of Prokaryotes by qPCR of *rrs*	Total Number of *rrs* Sequences in Pyrosequenced Library	Bacteria *rrs* Hits in Pyrosequenced Libraries	Thaumarchaeota *rrs* Hits in Pyrosequenced Libraries	Euryarchaeota *rrs* Hits in Pyrosequenced Libraries	NOB *rrs* Hits in Pyrosequenced Libraries	AOB *rrs* Hits in Pyrosequenced Libraries	Thaumarchaeota as a % of Prokaryotes by Pyrosequencing *rrs* amplicons	Euryarchaeota as a % of Prokaryotes by Pyrosequencing *rrs* amplicons	NOB as a % of Prokaryotes by Pyrosequencing *rrs* amplicons	AOB as a % of Prokaryotes by Pyrosequencing *rrs* amplicons
B5	760	12.51%	5041	3891	1061	89	15	0	32.92%	2.76%	0.23%	0.00%
C4	2	0.52%	7792	7654	127	11	0	0	2.90%	0.25%	0.00%	0.00%
C4	200	30.33%	5898	4277	1359	262	62	1	36.38%	7.01%	0.83%	0.03%
C4	700	34.40%	3587	2388	1083	116	13	0	44.94%	4.81%	0.27%	0.00%
D3	25	3.84%	7369	6157	751	461	53	1	18.00%	11.05%	0.64%	0.02%
D3	68	0.30%	7208	6231	720	257	2	0	17.22%	6.15%	0.02%	0.00%
D5	2	1.14%	6892	6659	137	96	2	0	3.57%	2.50%	0.03%	0.00%
D5	50	1.07%	7442	7033	134	275	1	1	3.32%	6.80%	0.01%	0.02%
D5	100	9.01%	6019	5161	538	320	24	0	15.80%	9.40%	0.35%	0.00%
D5	350	34.12%	2960	1835	979	146	23	0	48.99%	7.31%	0.58%	0.00%
D5	450	35.39%	1572	945	573	54	10	0	52.19%	4.92%	0.46%	0.00%
D5	900	19.72%	3574	2596	857	121	9	0	37.27%	5.26%	0.20%	0.00%
E2	6	0.00%	8486	7953	444	89	16	0	9.13%	1.83%	0.16%	0.00%
E6	200	13.60%	4454	3334	924	196	67	1	33.28%	7.06%	1.21%	0.04%
E6	800	5.41%	6293	5659	570	64	5	0	15.35%	1.72%	0.07%	0.00%
F6	2	0.02%	6839	6651	56	132	2	0	1.49%	3.52%	0.03%	0.00%
F6	200	9.79%	6863	4953	1445	465	115	0	34.43%	11.08%	1.37%	0.00%
F6	950	21.04%	4945	3800	1036	109	12	0	32.92%	3.46%	0.19%	0.00%

Station ID	Depth	Thaumarchaeota as a % of Prokaryotes by qPCR of *rrs*	Total Number of *rrs* Sequences in Pyrosequenced Library	Bacteria *rrs* Hits in Pyrosequenced Libraries	Thaumarchaeota *rrs* Hits in Pyrosequenced Libraries	Euryarchaeota *rrs* Hits in Pyrosequenced Libraries	NOB *rrs* Hits in Pyrosequenced Libraries	AOB *rrs* Hits in Pyrosequenced Libraries	Thaumarchaeota as a % of Prokaryotes by Pyrosequencing *rrs* amplicons	Euryarchaeota as a % of Prokaryotes by Pyrosequencing *rrs* amplicons	NOB as a % of Prokaryotes by Pyrosequencing *rrs* amplicons	AOB as a % of Prokaryotes by Pyrosequencing *rrs* amplicons
H1	7	0.02%	4997	4942	2	53	0	0	0.07%	1.93%	0.00%	0.00%
H3	20	0.04%	1179	1131	8	40	0	0	1.26%	6.29%	0.00%	0.00%
H6	2	0.08%	7112	7030	6	76	0	0	0.15%	1.94%	0.00%	0.00%
H6	110	10.30%	5364	4195	872	297	115	0	27.23%	9.27%	1.80%	0.00%
H6	280	0.47%	7367	6022	1051	294	75	0	23.91%	6.69%	0.85%	0.00%
MR1	2	0.00%	5265	5259	4	2	4	7	0.14%	0.07%	0.07%	0.24%
MR2	8	0.71%	5759	5607	90	62	4	1	2.81%	1.93%	0.06%	0.03%
MR3	110	4.46%	3356	2849	417	90	36	0	20.85%	4.50%	0.90%	0.00%

Total	221,410	188,177	25,749	7,484	1,127	14	N/A	N/A	N/A	N/A
Average	5,400	4,590	628	183	27	0	21.33%	5.83%	0.41%	0.01%
Max	9,146	8,947	1,779	697	121	7	53.75%	17.63%	1.80%	0.24%
Min	764	626	2	2	0	0	0.07%	0.07%	0.00%	0.00%

Table A.4. Diversity indices for sequenced clones obtained from Station D5 calculated using mothur (v. 1.21.1; Schloss *et al.*, 2009). OTU similarity cutoffs were 2% (*rrs*) or 3% (*amoA*, *accA*). Statistics for *rrs* sequences ("*rrs* 454") obtained from pyrosequencing are included for comparison.

	Observed	Chao	ACE	Shannon	Simpson
accA	51	74.0	109	3.02	0.0862
amoA	47	86.4	107	3.19	0.0615
amoA 100m	22	35.2	55.7	2.39	0.139
amoA 200m	30	39.4	41.8	2.89	0.0801
rrs	10	11.0	12.8	1.30	0.451
rrs 100m	2	2.00	0.000	0.103	0.957
rrs 200m	9	10.0	11.8	1.96	0.141
*rrs*_454	2768	18700	57100	4.15	0.0654

Table A.5: Variables contributing to principal components axes. Coefficients (values) are a measure of contribution of each variable to each of the principal component axes (PC1 and PC2) such that the higher the value, the greater the influence of the variable. A positive or negative sign represents the type of correlation each variable has on each axis. The total amount of variance explained by PC1 was 38.9% and 24.3% for PC2. Depth = water column depth; Rel. Fluorescence = Relative fluorescence, chlorophyll *a* equivalents; beam attenuation = turbidity; euphotic depth = photic zone depth.

Variable	**PC1**	**PC2**
Latitude (°N)	-0.26	+0.30
Longitude (°W)	+0.066	+0.24
Depth (m)	+0.39	+0.21
Temperature (°C)	-0.36	-0.38
Salinity (PSU)	+0.19	-0.49
Dissolved Oxygen (mg/L)	-0.36	-0.12
Rel. Fluorescence (µg/L)	-0.39	+0.15
Beam Attenuation (1/m)	-0.21	+0.44
pH (NBS)	-0.42	-0.32
Euphotic Depth (m)	+0.31	-0.30

Table A.6: Results of CCA analysis of relationship between qPCR-estimated gene abundances and environmental data in the northern Gulf of Mexico. Values for all four canonical axes are shown, but only CCA1 and CCA2 were used to construct a biplot of the data (Figure 2.8).

Axes	**CCA1**	**CCA2**	**CCA3**	**CCA4**
Eigenvalues	0.148	0.135	0.012	0.008
gene-environment correlations	0.655	0.765	0.352	0.230
Cumulative percentage variance				
of gene abundance data	17.0	32.6	34.0	34.9
of gene-environment relation	47.9	91.7	95.7	98.3

Table A.7: Results of BEST analysis comparing gene abundance to **(a)** environmental factors and **(b)** environmental factors and nutrients (only near-surface samples used with nutrients). BEST analysis (Clarke, 1993) performed with PRIMER v6 software (Clarke and Gorley, 2006). Archaeal *amoA* W = amplified with Wuchter *et al.* (2006) *amoA* primer set; Archaeal *amoA* F = amplified with Francis *et al.* (2005) *amoA* primer set; RF = relative fluorescence (chlorophyll *a* equivalents); beam attenuation = turbidity.

(a) BEST analysis with Environmental Variables

Gene	# of Variables	Correlation (ρ*)	Contributing Environmental Variables
Thaumarchaeota *rrs*	3	0.507	salinity, RF, beam attenuation
pSL12 *rrs*	1	0.457	RF
Bacterial *rrs*	3	0.613	temperature, salinity, beam attenuation
Archaeal *amoA* W	4	0.442	latitude, temperature, salinity, RF
Archaeal *amoA* F	4	0.474	latitude, salinity, oxygen, RF
Bacterial *amoA*	1	0.462	RF
Archaeal *accA*	1	0.460	RF

*ρ is the Spearman rank correlation coefficient where $\rho > 0$ rejects the null hypothesis; all results had a significance $p \leq 0.001$, determined from 999 permutations.

(b) BEST analysis with Environmental Variables and Nutrients

Gene	# of Vars	Correlation (ρ*)	*p*-value[+]	Contributing Environmental Variables and Nutrients
Thaumarchaeota *rrs*[#]	1	0.429	0.018	beam attenuation
pSL12 *rrs*	5	0.337	0.102	latitude, salinity, RF, nitrate, silicate
Bacterial *rrs*[#]	2	0.587	0.001	beam attenuation, silicate
Archaeal *amoA* W	3	0.374	0.067	latitude, RF, silicate
Archaeal *amoA* F[#]	2	0.374	0.010	latitude, RF
Bacterial *amoA*	2	0.264	0.269	latitude, RF
Archaeal *accA*	2	0.269	0.246	latitude, RF

*ρ is the Spearman rank correlation coefficient where $\rho > 0$ rejects the null hypothesis.

[+]p is the significance of the result, determined from 999 permutations; [#]$p \leq 0.05$

Figure A.1: P*hylogenetic analysis of (a) amoA* and (b) *accA* genes retrieved from Station D5. Numbers beside groups (in triangles) indicate the number of sequences from each depth sampled according to color – 2, 50, or 100 m (green) and 200 or 450 m (blue). Neighbor-Joining Trees built with ARB (Ludwig *et al.*, 2004) from nucleotide sequences 595 bp (*amoA*) or 411 bp (*accA*) in length. Sequences in bold obtained from isolates or enrichment cultures. Bootstrap values obtained from resampling tree 1,000 times; only values above 75% bootstrap support shown on tree.

(a)

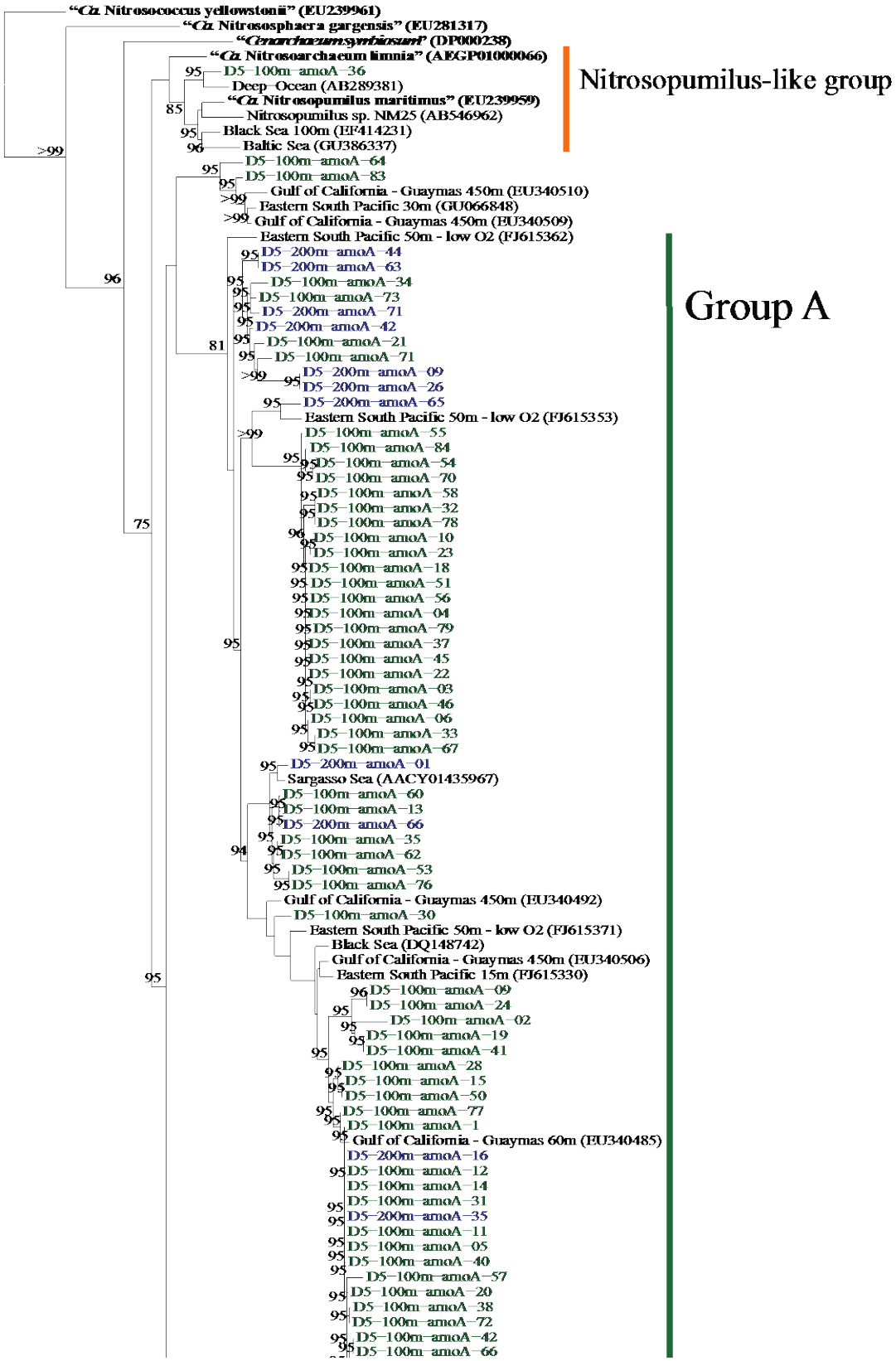
"Ca. Nitrososphaera gargensis" (EU281317)
"Ca. Nitrosocaldus yellowstonii" (EU239961)
"Candidatus Cenarchaeum symbiosum" (DP000238)
"Ca. Nitrosoarchaeum limnia" (AEGP01000066)
D5–100m–amoA–36
Deep–Ocean (AB289381)
"Ca. Nitrosopumilus maritimus" (EU239959)
Nitrosopumilus sp. NM25 (AB546962)
Black Sea 100m (EF414231)
Baltic Sea (GU386337)
Nitrosopumilus-like group
D5–100m–amoA–64
D5–100m–amoA–83
Gulf of California - Guaymas 450m (EU340510)
Eastern South Pacific 30m (GU066848)
Gulf of California - Guaymas 450m (EU340509)
Eastern South Pacific 50m - low O2 (FJ615362)
D5–200m–amoA–44
D5–200m–amoA–63
D5–100m–amoA–34
D5–100m–amoA–73
D5–200m–amoA–71
D5–200m–amoA–42
D5–100m–amoA–21
D5–100m–amoA–71
D5–200m–amoA–09
D5–200m–amoA–26
D5–200m–amoA–65
Eastern South Pacific 50m - low O2 (FJ615353)
D5–100m–amoA–55
D5–100m–amoA–84
D5–100m–amoA–54
D5–100m–amoA–70
D5–100m–amoA–58
D5–100m–amoA–32
D5–100m–amoA–78
D5–100m–amoA–10
D5–100m–amoA–23
D5–100m–amoA–18
D5–100m–amoA–51
D5–100m–amoA–56
D5–100m–amoA–04
D5–100m–amoA–79
D5–100m–amoA–37
D5–100m–amoA–45
D5–100m–amoA–22
D5–100m–amoA–03
D5–100m–amoA–46
D5–100m–amoA–06
D5–100m–amoA–33
D5–100m–amoA–67
D5–200m–amoA–01
Sargasso Sea (AACY01435967)
D5–100m–amoA–60
D5–100m–amoA–13
D5–200m–amoA–66
D5–100m–amoA–35
D5–100m–amoA–62
D5–100m–amoA–53
D5–100m–amoA–76
Gulf of California - Guaymas 450m (EU340492)
D5–100m–amoA–30
Eastern South Pacific 50m - low O2 (FJ615371)
Black Sea (DQ148742)
Gulf of California - Guaymas 450m (EU340506)
Eastern South Pacific 15m (FJ615330)
D5–100m–amoA–09
D5–100m–amoA–24
D5–100m–amoA–02
D5–100m–amoA–19
D5–100m–amoA–41
D5–100m–amoA–28
D5–100m–amoA–15
D5–100m–amoA–50
D5–100m–amoA–77
D5–100m–amoA–1
Gulf of California - Guaymas 60m (EU340485)
D5–200m–amoA–16
D5–100m–amoA–12
D5–100m–amoA–14
D5–100m–amoA–31
D5–200m–amoA–35
D5–100m–amoA–11
D5–100m–amoA–05
D5–100m–amoA–40
D5–100m–amoA–57
D5–100m–amoA–20
D5–100m–amoA–38
D5–100m–amoA–72
D5–100m–amoA–42
D5–100m–amoA–66
Group A

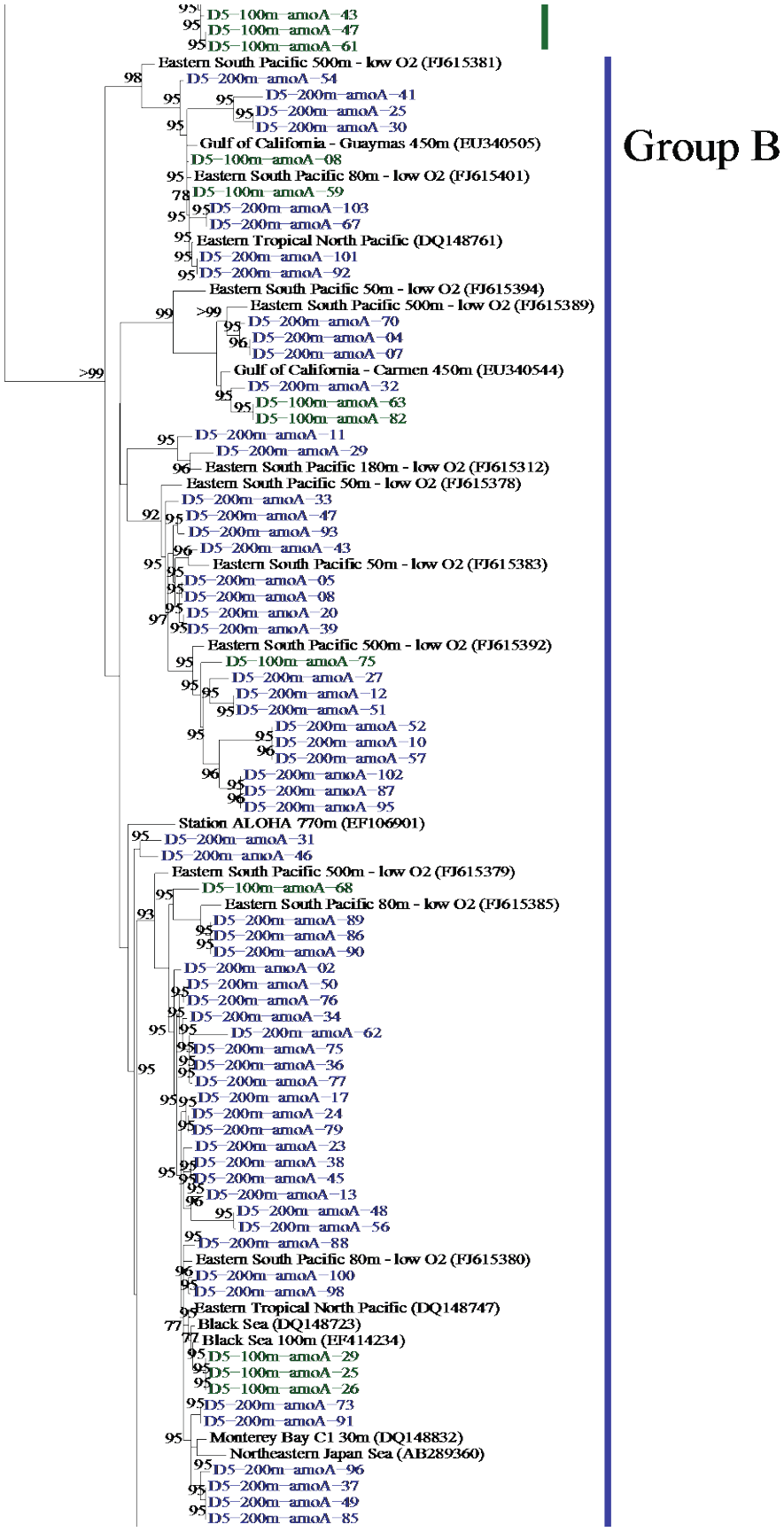
D5_100m_amoA_43
D5_100m_amoA_47
D5_100m_amoA_61
Eastern South Pacific 500m - low O2 (FJ615381)
D5_200m_amoA_54
D5_200m_amoA_41
D5_200m_amoA_25
D5_200m_amoA_30
Gulf of California - Guaymas 450m (EU340505)
D5_100m_amoA_08
Eastern South Pacific 80m - low O2 (FJ615401)
D5_100m_amoA_59
D5_200m_amoA_103
D5_200m_amoA_67
Eastern Tropical North Pacific (DQ148761)
D5_200m_amoA_101
D5_200m_amoA_92
Eastern South Pacific 50m - low O2 (FJ615394)
Eastern South Pacific 500m - low O2 (FJ615389)
D5_200m_amoA_70
D5_200m_amoA_04
D5_200m_amoA_07
Gulf of California - Carmen 450m (EU340544)
D5_200m_amoA_32
D5_100m_amoA_63
D5_100m_amoA_82
D5_200m_amoA_11
D5_200m_amoA_29
Eastern South Pacific 180m - low O2 (FJ615312)
Eastern South Pacific 50m - low O2 (FJ615378)
D5_200m_amoA_33
D5_200m_amoA_47
D5_200m_amoA_93
D5_200m_amoA_43
Eastern South Pacific 50m - low O2 (FJ615383)
D5_200m_amoA_05
D5_200m_amoA_08
D5_200m_amoA_20
D5_200m_amoA_39
Eastern South Pacific 500m - low O2 (FJ615392)
D5_100m_amoA_75
D5_200m_amoA_27
D5_200m_amoA_12
D5_200m_amoA_51
D5_200m_amoA_52
D5_200m_amoA_10
D5_200m_amoA_57
D5_200m_amoA_102
D5_200m_amoA_87
D5_200m_amoA_95
Station ALOHA 770m (EF106901)
D5_200m_amoA_31
D5_200m_amoA_46
Eastern South Pacific 500m - low O2 (FJ615379)
D5_100m_amoA_68
Eastern South Pacific 80m - low O2 (FJ615385)
D5_200m_amoA_89
D5_200m_amoA_86
D5_200m_amoA_90
D5_200m_amoA_02
D5_200m_amoA_50
D5_200m_amoA_76
D5_200m_amoA_34
D5_200m_amoA_62
D5_200m_amoA_75
D5_200m_amoA_36
D5_200m_amoA_77
D5_200m_amoA_17
D5_200m_amoA_24
D5_200m_amoA_79
D5_200m_amoA_23
D5_200m_amoA_38
D5_200m_amoA_45
D5_200m_amoA_13
D5_200m_amoA_48
D5_200m_amoA_56
D5_200m_amoA_88
Eastern South Pacific 80m - low O2 (FJ615380)
D5_200m_amoA_100
D5_200m_amoA_98
Eastern Tropical North Pacific (DQ148747)
Black Sea (DQ148723)
Black Sea 100m (EF414234)
D5_100m_amoA_29
D5_100m_amoA_25
D5_100m_amoA_26
D5_200m_amoA_73
D5_200m_amoA_91
Monterey Bay C1 30m (DQ148832)
Northeastern Japan Sea (AB289360)
D5_200m_amoA_96
D5_200m_amoA_37
D5_200m_amoA_49
D5_200m_amoA_85
Group B

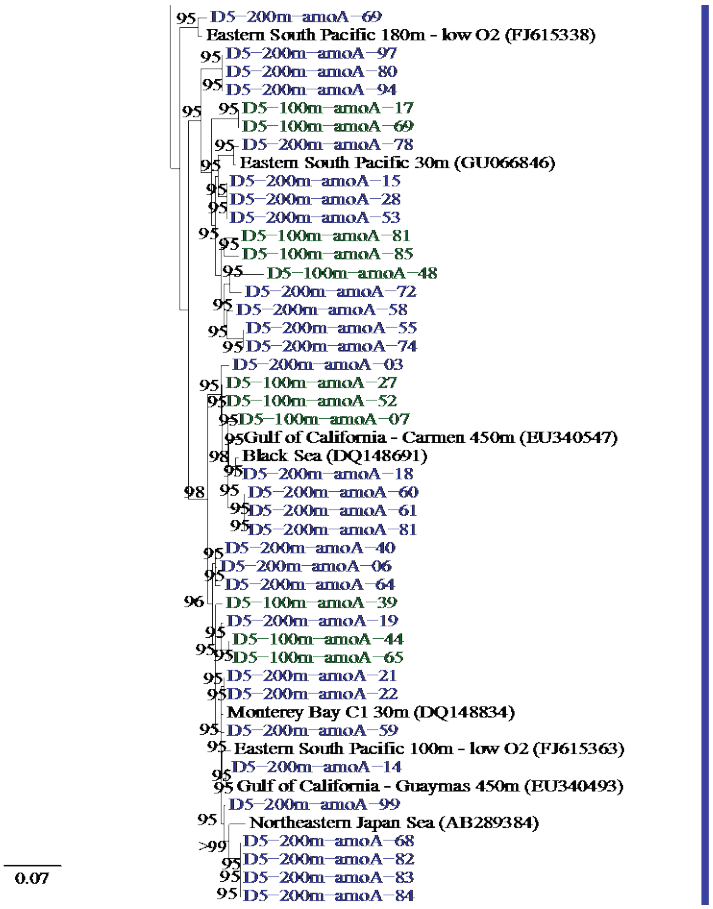
D5–200m–amoA–69
Eastern South Pacific 180m - low O2 (FJ615338)
D5–200m–amoA–97
D5–200m–amoA–80
D5–200m–amoA–94
D5–100m–amoA–17
D5–100m–amoA–69
D5–200m–amoA–78
Eastern South Pacific 30m (GU066846)
D5–200m–amoA–15
D5–200m–amoA–28
D5–200m–amoA–53
D5–100m–amoA–81
D5–100m–amoA–85
D5–100m–amoA–48
D5–200m–amoA–72
D5–200m–amoA–58
D5–200m–amoA–55
D5–200m–amoA–74
D5–200m–amoA–03
D5–100m–amoA–27
D5–100m–amoA–52
D5–100m–amoA–07
Gulf of California - Carmen 450m (EU340547)
Black Sea (DQ148691)
D5–200m–amoA–18
D5–200m–amoA–60
D5–200m–amoA–61
D5–200m–amoA–81
D5–200m–amoA–40
D5–200m–amoA–06
D5–200m–amoA–64
D5–100m–amoA–39
D5–200m–amoA–19
D5–100m–amoA–44
D5–100m–amoA–65
D5–200m–amoA–21
D5–200m–amoA–22
Monterey Bay C1 30m (DQ148834)
D5–200m–amoA–59
Eastern South Pacific 100m - low O2 (FJ615363)
D5–200m–amoA–14
Gulf of California - Guaymas 450m (EU340493)
D5–200m–amoA–99
Northeastern Japan Sea (AB289384)
D5–200m–amoA–68
D5–200m–amoA–82
D5–200m–amoA–83
D5–200m–amoA–84
0.07

(b)

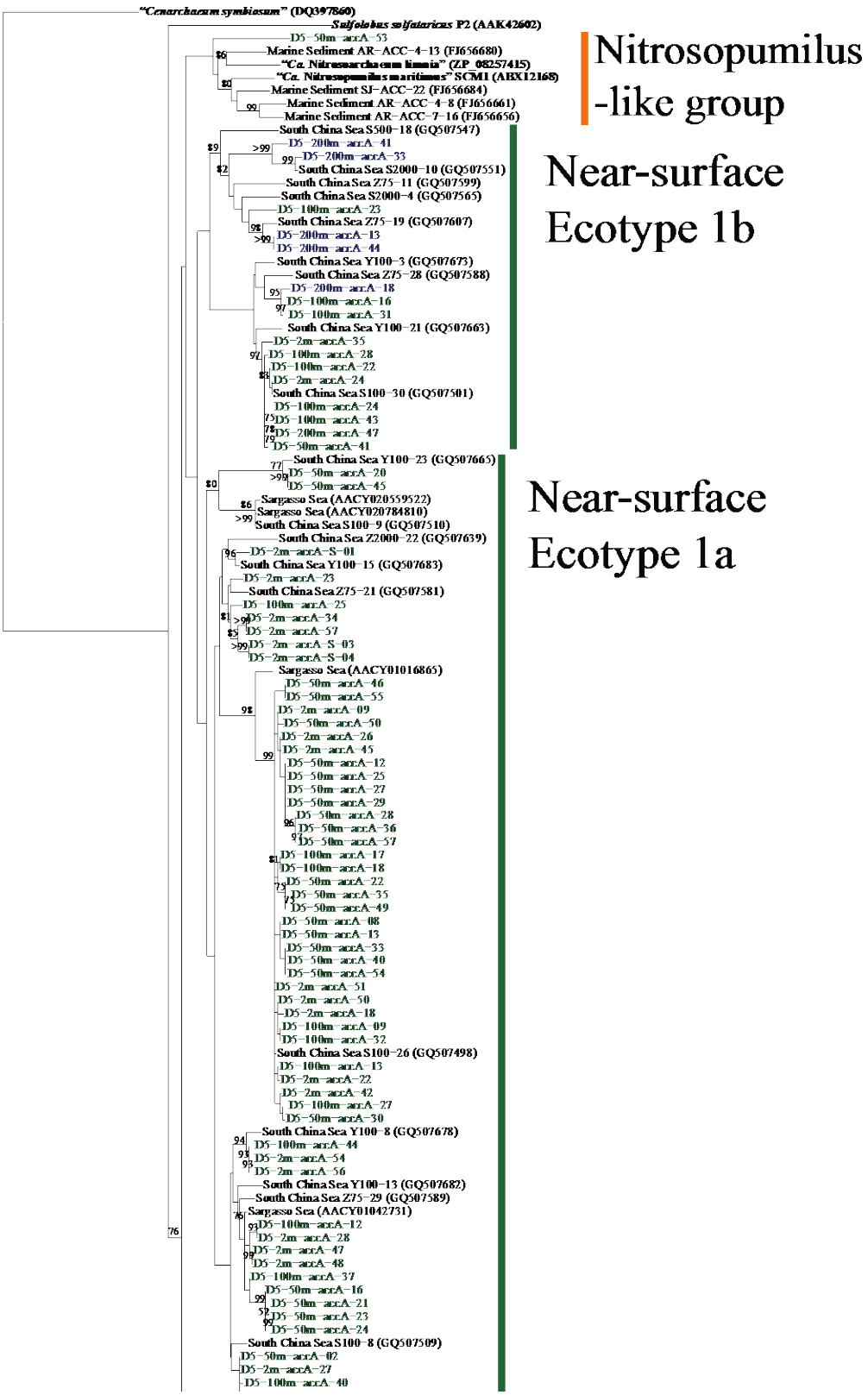
"Cenarchaeum symbiosum" (DQ397860)
Sulfolobus solfataricus P2 (AAK42602)
DS-50m-accA-53
Marine Sediment AR-ACC-4-13 (FJ656680)
"Ca. Nitrosoarchaeum limnia" (ZP_08257415)
"Ca. Nitrosopumilus maritimus" SCM1 (ABX12168)
Marine Sediment SJ-ACC-22 (FJ656684)
Marine Sediment AR-ACC-4-8 (FJ656661)
Marine Sediment AR-ACC-7-16 (FJ656656)
South China Sea S500-18 (GQ507547)
DS-200m-accA-41
DS-200m-accA-33
South China Sea S2000-10 (GQ507551)
South China Sea Z75-11 (GQ507599)
South China Sea S2000-4 (GQ507565)
DS-100m-accA-23
South China Sea Z75-19 (GQ507607)
DS-200m-accA-13
DS-200m-accA-44
South China Sea Y100-3 (GQ507673)
South China Sea Z75-28 (GQ507588)
DS-200m-accA-18
DS-100m-accA-16
DS-100m-accA-31
South China Sea Y100-21 (GQ507663)
DS-2m-accA-35
DS-100m-accA-28
DS-100m-accA-22
DS-2m-accA-24
South China Sea S100-30 (GQ507501)
DS-100m-accA-24
DS-100m-accA-43
DS-200m-accA-47
DS-50m-accA-41
South China Sea Y100-23 (GQ507665)
DS-50m-accA-20
DS-50m-accA-45
Sargasso Sea (AACY020559522)
Sargasso Sea (AACY020784810)
South China Sea S100-9 (GQ507510)
South China Sea Z2000-22 (GQ507639)
DS-2m-accA-S-01
South China Sea Y100-15 (GQ507683)
DS-2m-accA-23
South China Sea Z75-21 (GQ507581)
DS-100m-accA-25
DS-2m-accA-34
DS-2m-accA-57
DS-2m-accA-S-03
DS-2m-accA-S-04
Sargasso Sea (AACY01016865)
DS-50m-accA-46
DS-50m-accA-55
DS-2m-accA-09
DS-50m-accA-50
DS-2m-accA-26
DS-2m-accA-45
DS-50m-accA-12
DS-50m-accA-25
DS-50m-accA-27
DS-50m-accA-29
DS-50m-accA-28
DS-50m-accA-36
DS-50m-accA-57
DS-100m-accA-17
DS-100m-accA-18
DS-50m-accA-22
DS-50m-accA-35
DS-50m-accA-49
DS-50m-accA-08
DS-50m-accA-13
DS-50m-accA-33
DS-50m-accA-40
DS-50m-accA-54
DS-2m-accA-51
DS-2m-accA-50
DS-2m-accA-18
DS-100m-accA-09
DS-100m-accA-32
South China Sea S100-26 (GQ507498)
DS-100m-accA-13
DS-2m-accA-22
DS-2m-accA-42
DS-100m-accA-27
DS-50m-accA-30
South China Sea Y100-8 (GQ507678)
DS-100m-accA-44
DS-2m-accA-54
DS-2m-accA-56
South China Sea Y100-13 (GQ507682)
South China Sea Z75-29 (GQ507589)
Sargasso Sea (AACY01042731)
DS-100m-accA-12
DS-2m-accA-28
DS-2m-accA-47
DS-2m-accA-48
DS-100m-accA-37
DS-50m-accA-16
DS-50m-accA-21
DS-50m-accA-23
DS-50m-accA-24
South China Sea S100-8 (GQ507509)
DS-50m-accA-02
DS-2m-accA-27
DS-100m-accA-40
Nitrosopumilus -like group
Near-surface Ecotype 1b
Near-surface Ecotype 1a

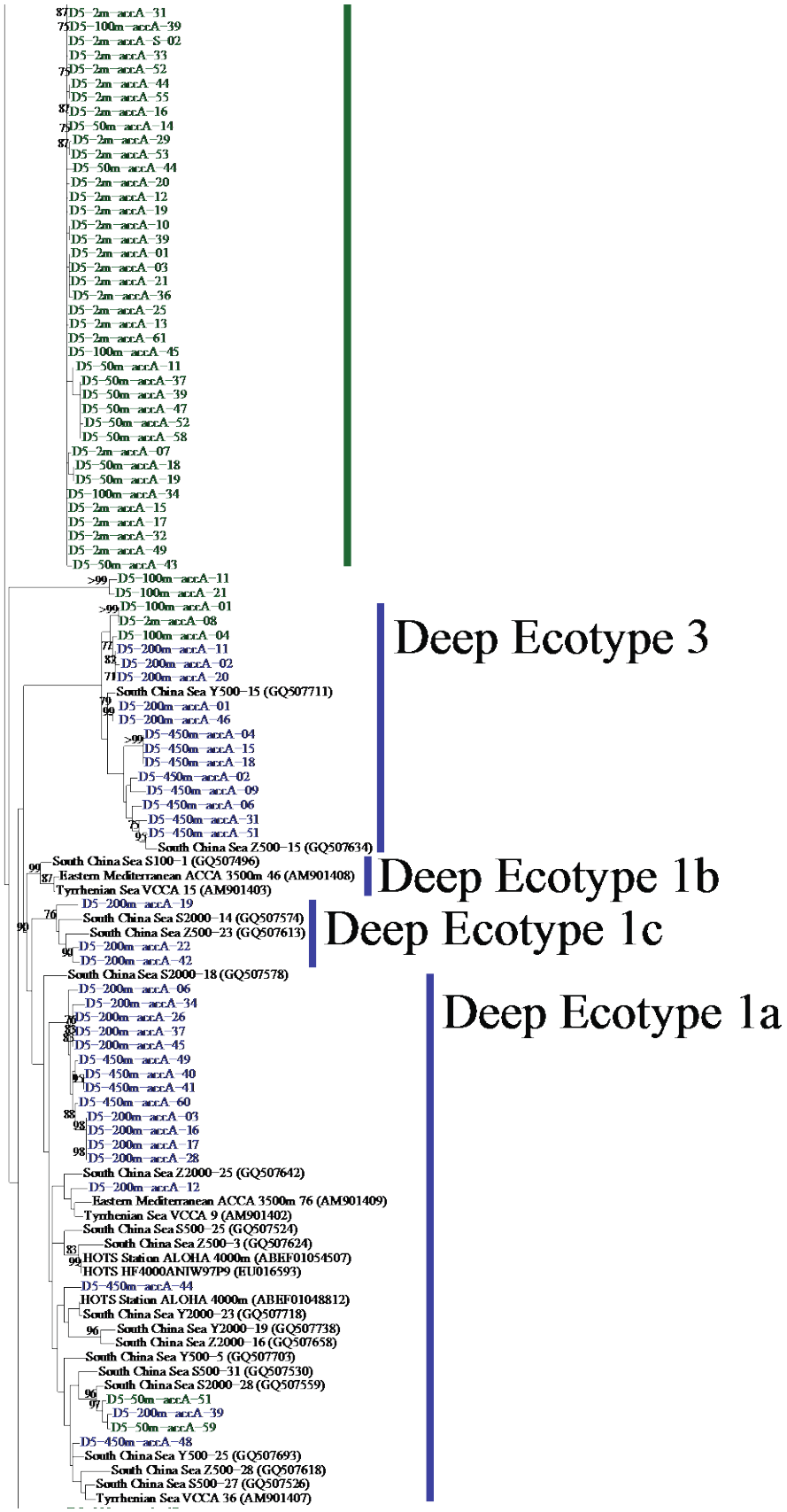
D5_2m_accA_31
D5_100m_accA_39
D5_2m_accA_S_02
D5_2m_accA_33
D5_2m_accA_52
D5_2m_accA_44
D5_2m_accA_55
D5_2m_accA_16
D5_50m_accA_14
D5_2m_accA_29
D5_2m_accA_53
D5_50m_accA_44
D5_2m_accA_20
D5_2m_accA_12
D5_2m_accA_19
D5_2m_accA_10
D5_2m_accA_39
D5_2m_accA_01
D5_2m_accA_03
D5_2m_accA_21
D5_2m_accA_36
D5_2m_accA_25
D5_2m_accA_13
D5_2m_accA_61
D5_100m_accA_45
D5_50m_accA_11
D5_50m_accA_37
D5_50m_accA_39
D5_50m_accA_47
D5_50m_accA_52
D5_50m_accA_58
D5_2m_accA_07
D5_50m_accA_18
D5_50m_accA_19
D5_100m_accA_34
D5_2m_accA_15
D5_2m_accA_17
D5_2m_accA_32
D5_2m_accA_49
D5_50m_accA_43
D5_100m_accA_11
D5_100m_accA_21
D5_100m_accA_01
D5_2m_accA_08
D5_100m_accA_04
D5_200m_accA_11
D5_200m_accA_02
D5_200m_accA_20
South China Sea Y500_15 (GQ507711)
D5_200m_accA_01
D5_200m_accA_46
D5_450m_accA_04
D5_450m_accA_15
D5_450m_accA_18
D5_450m_accA_02
D5_450m_accA_09
D5_450m_accA_06
D5_450m_accA_31
D5_450m_accA_51
South China Sea Z500_15 (GQ507634)
South China Sea S100_1 (GQ507496)
Eastern Mediterranean ACCA 3500m 46 (AM901408)
Tyrrhenian Sea VCCA 15 (AM901403)
D5_200m_accA_19
South China Sea S2000_14 (GQ507574)
South China Sea Z500_23 (GQ507613)
D5_200m_accA_22
D5_200m_accA_42
South China Sea S2000_18 (GQ507578)
D5_200m_accA_06
D5_200m_accA_34
D5_200m_accA_26
D5_200m_accA_37
D5_200m_accA_45
D5_450m_accA_49
D5_450m_accA_40
D5_450m_accA_41
D5_450m_accA_60
D5_200m_accA_03
D5_200m_accA_16
D5_200m_accA_17
D5_200m_accA_28
South China Sea Z2000_25 (GQ507642)
D5_200m_accA_12
Eastern Mediterranean ACCA 3500m 76 (AM901409)
Tyrrhenian Sea VCCA 9 (AM901402)
South China Sea S500_25 (GQ507524)
South China Sea Z500_3 (GQ507624)
HOTS Station ALOHA 4000m (ABKF01054507)
HOTS HF4000ANIW97P9 (EU016593)
D5_450m_accA_44
HOTS Station ALOHA 4000m (ABKF01048812)
South China Sea Y2000_23 (GQ507718)
South China Sea Y2000_19 (GQ507738)
South China Sea Z2000_16 (GQ507658)
South China Sea Y500_5 (GQ507703)
South China Sea S500_31 (GQ507530)
South China Sea S2000_28 (GQ507559)
D5_50m_accA_51
D5_200m_accA_39
D5_50m_accA_59
D5_450m_accA_48
South China Sea Y500_25 (GQ507693)
South China Sea Z500_28 (GQ507618)
South China Sea S500_27 (GQ507526)
Tyrrhenian Sea VCCA 36 (AM901407)
Deep Ecotype 3
Deep Ecotype 1b
Deep Ecotype 1c
Deep Ecotype 1a

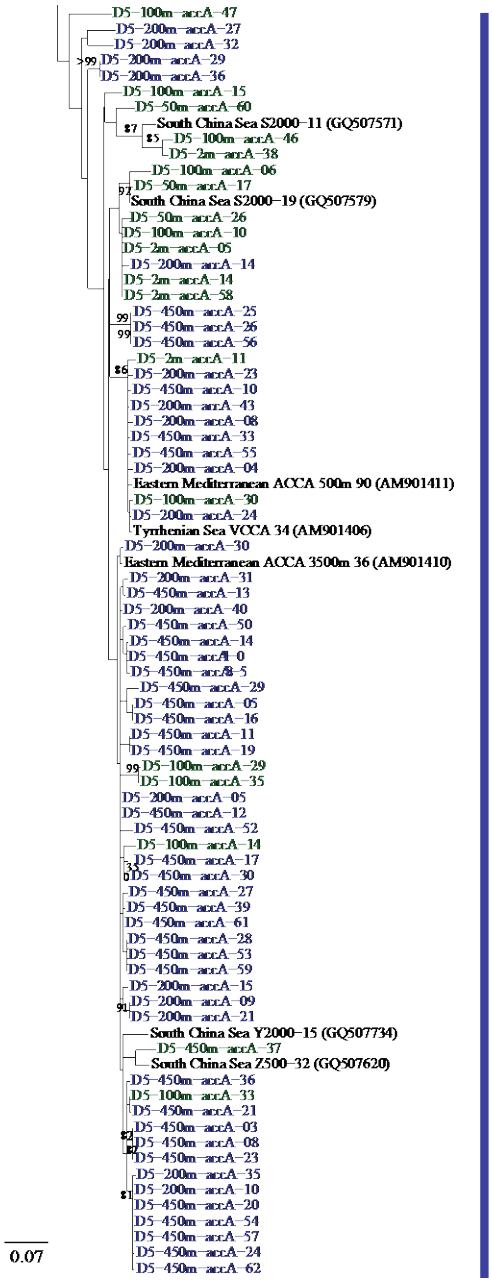

Deep Ecotype 2

Figure A.2: Distribution of various taxa in pyrosequenced libraries of *rrs* in samples from the northern Gulf of Mexico: **(a)** samples taken from depths ≤25 m; **(b)** samples from depths ≥100m.

(a) Sample depth ≤25 m

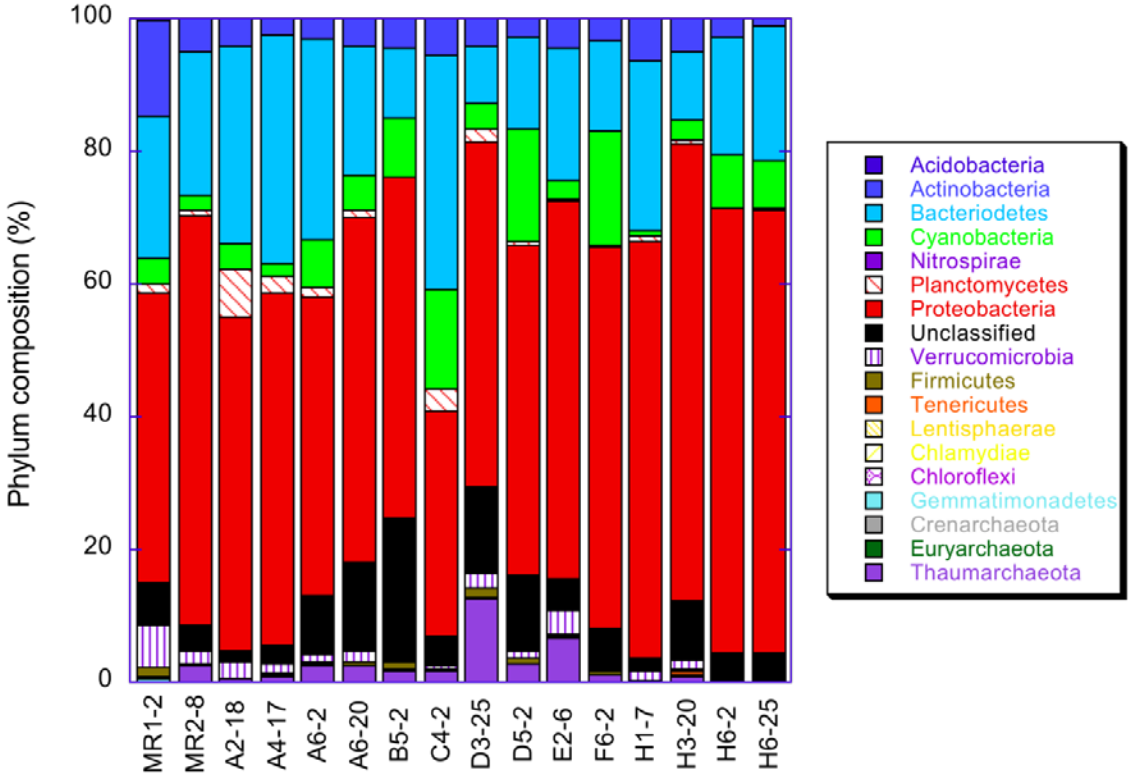

(b) Sample depth ≥100 m

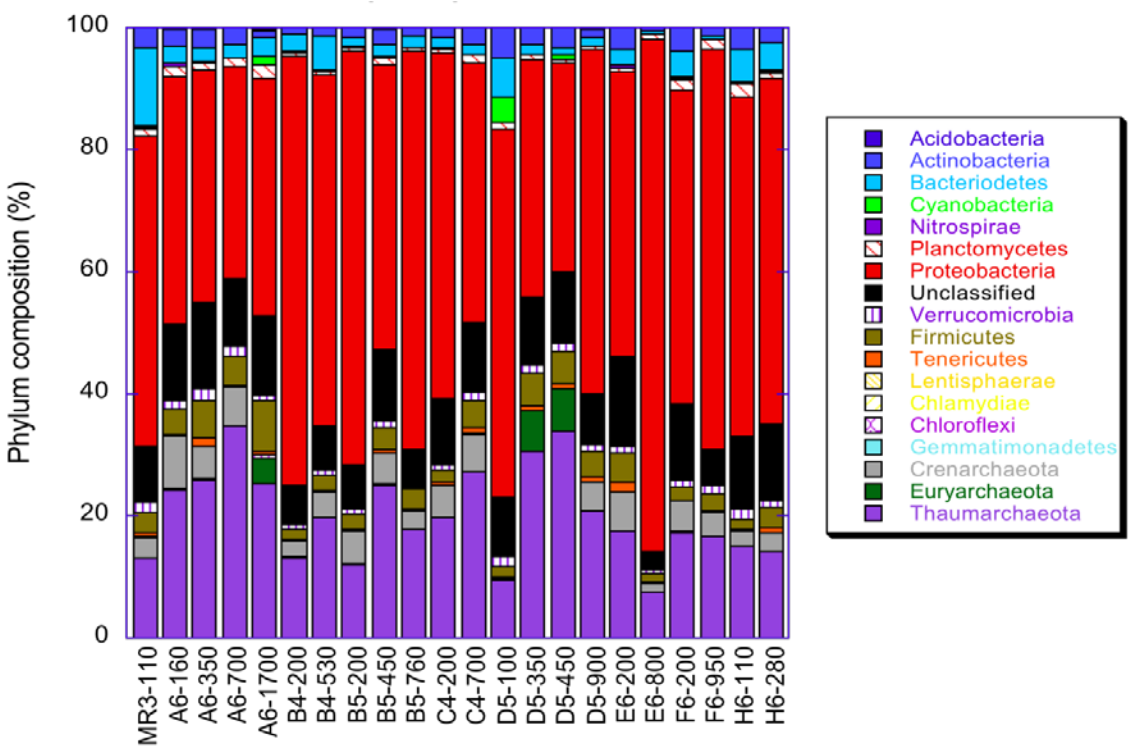

Figure A.3: **Principal components analysis (PCA) of samples using environmental variables**. Fluorescence = relative fluorescence, chlorophyll *a* equivalents; beam attenuation = turbidity. Samples are shown as symbols representing three groupings based on depth and location: orange circles = near-surface inshore (≤100 m depth, over the continental shelf), green diamonds = near-surface offshore (≤100 m depth, shelf break and beyond), and blue squares = deep offshore (>100 m, shelf break and beyond).

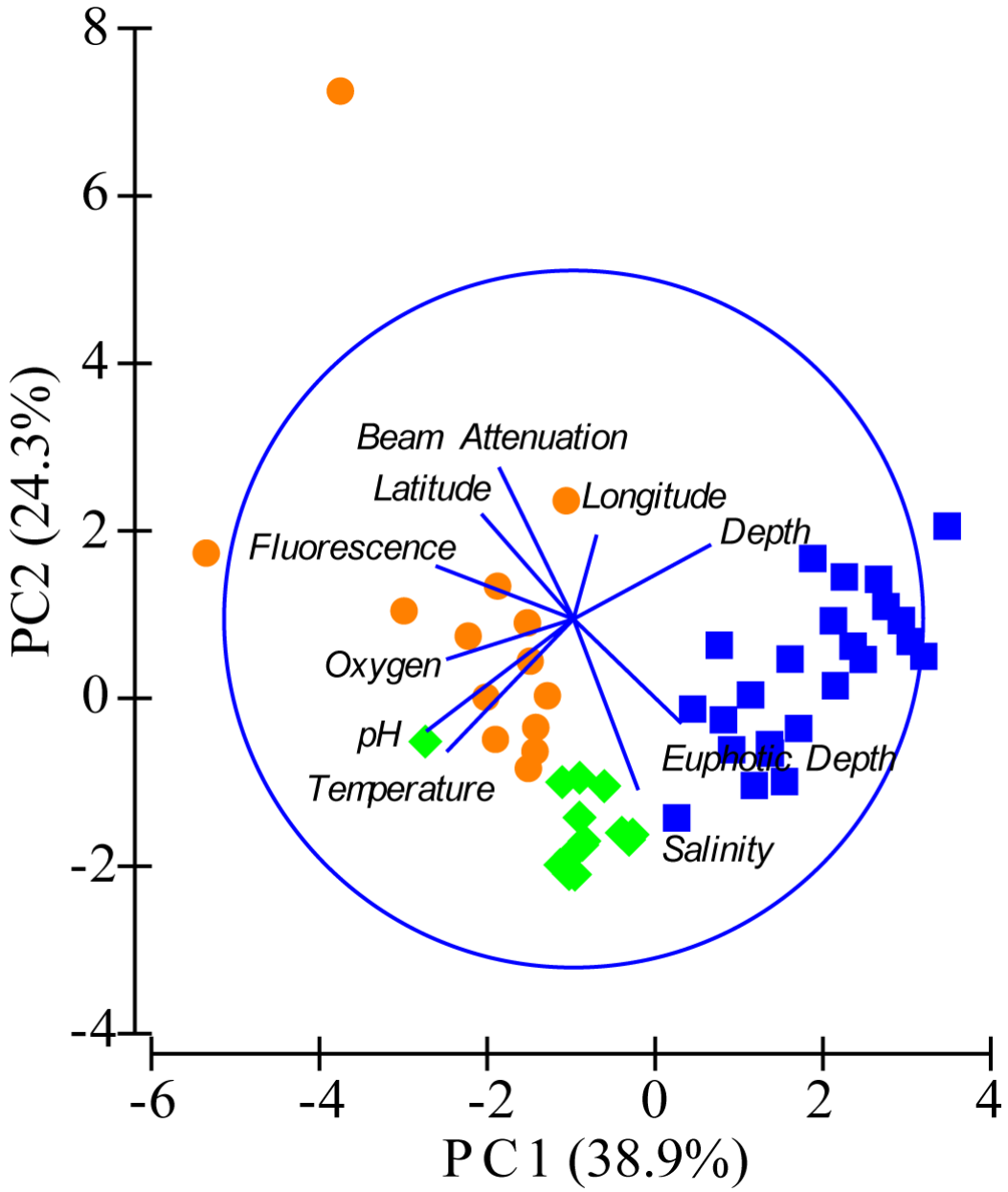
8
6
4
2
0
-2
-4
PC2 (24.3%)
-6
-4
-2
0
2
4
PC1 (38.9%)
Beam Attenuation
Latitude
Longitude
Depth
Fluorescence
Oxygen
pH
Temperature
Euphotic Depth
Salinity

Figure A.4: Jackknife Clustering Analysis of pyrosequenced Thaumarchaeota *rrs* genes using Fast UniFrac (Hamady *et al.*, 2009). Resampling of **(a)** 2 (minimum), **(b)** 100 (1st quartile), or **(c)** 520 (median) sequences were performed for each of 100 iterations of the jackknife analysis. Colors on nodes indicate percentage of iterations where a given cluster was formed – red (>99.9%), yellow (90-99.9%), green (70-90%), blue (50-70%), or grey (<50%). IS# = inshore, near-surface; OS# = offshore, near-surface; OD# = offshore, deep.

(a) Clustering with resampling of minimum (2) sequences for each sample (n=43)

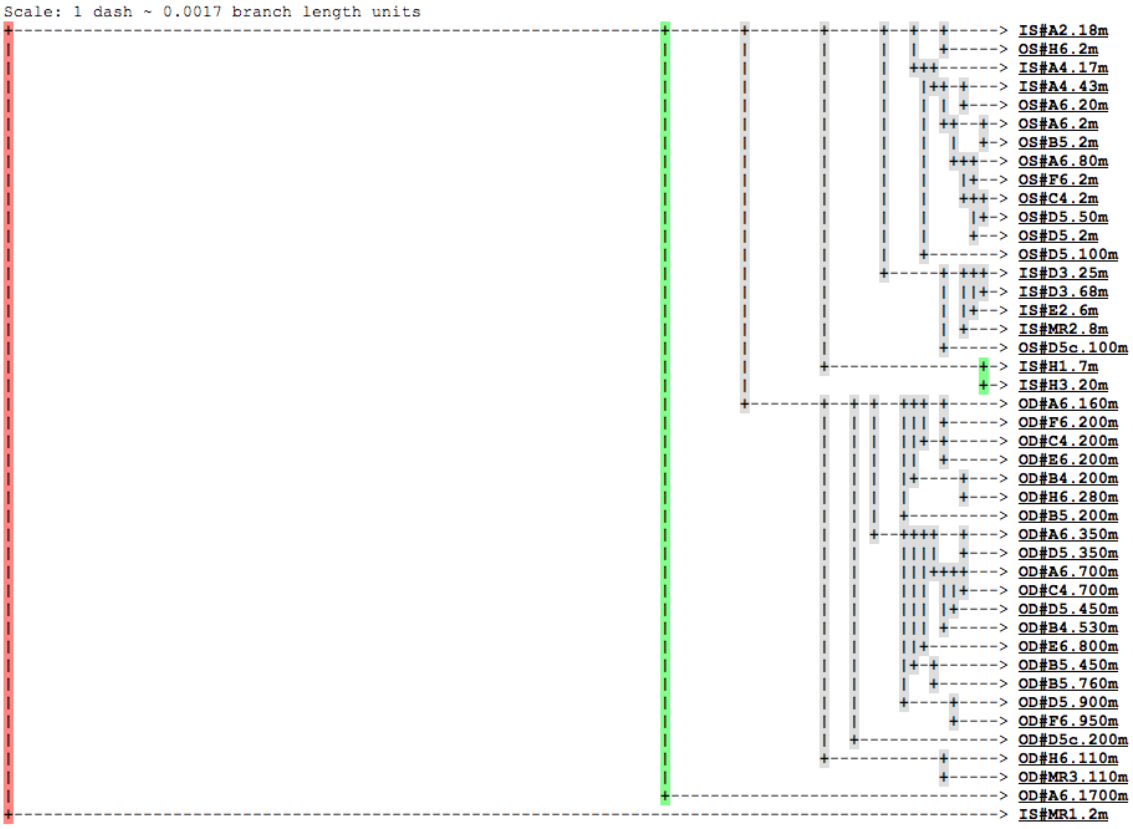

(b) Clustering with resampling of 1st quartile (100) sequences for each sample (n=32)

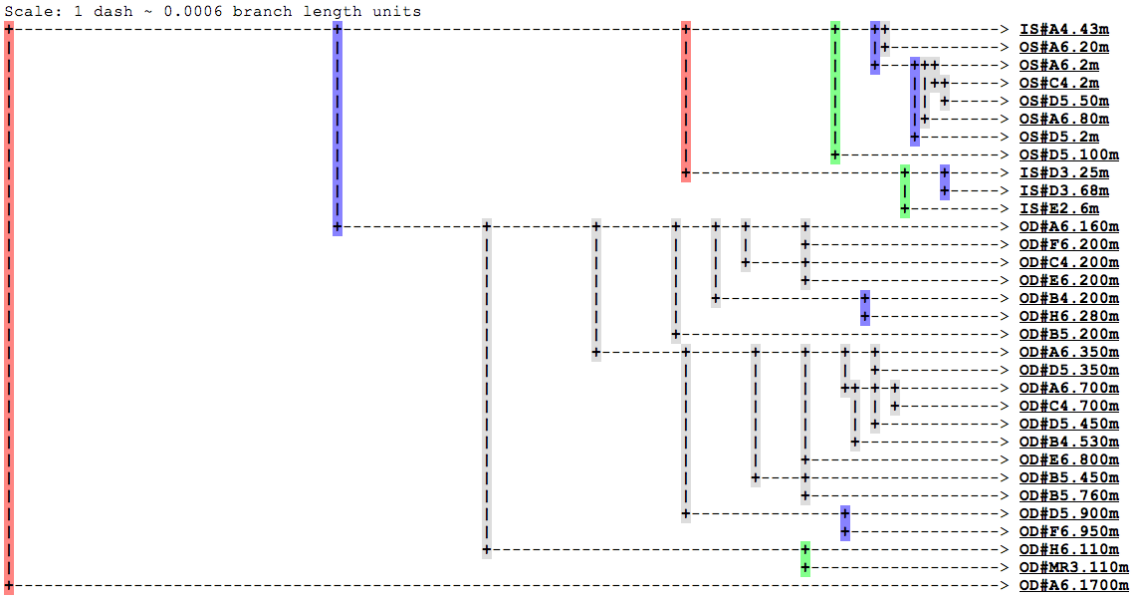

(c) Clustering with resampling of median (520) sequences for each sample (n=22)

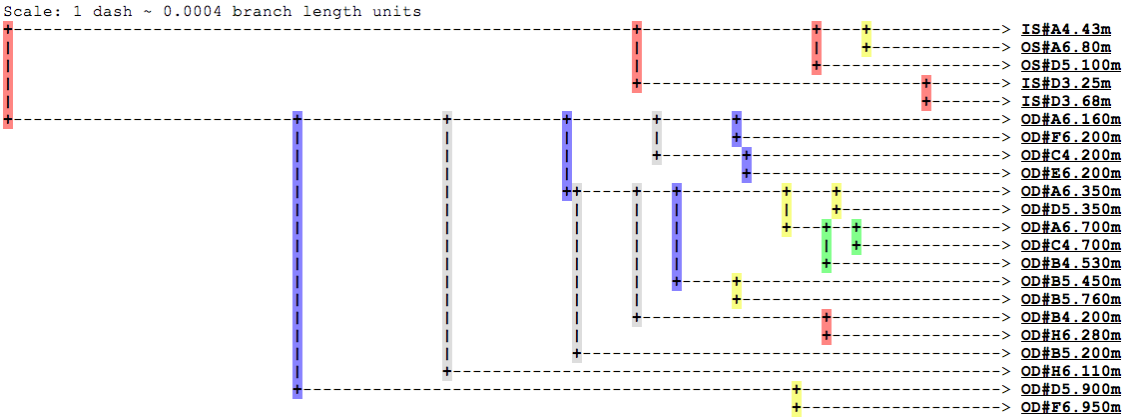

Figure A.5: Scatter plot of Archaeal (a) *amoA* and (b) *accA* versus *rrs* gene abundance in samples from the northern Gulf of Mexico. Solid lines indicate the 1:1 ratios expected from the "*Ca.* N. maritimus" strain SCM1 genome (Walker *et al.*, 2010); dashed lines indicate ratios of 0.1 or 10. 'Inshore' = over the continental shelf; 'offshore' = shelf break and beyond.

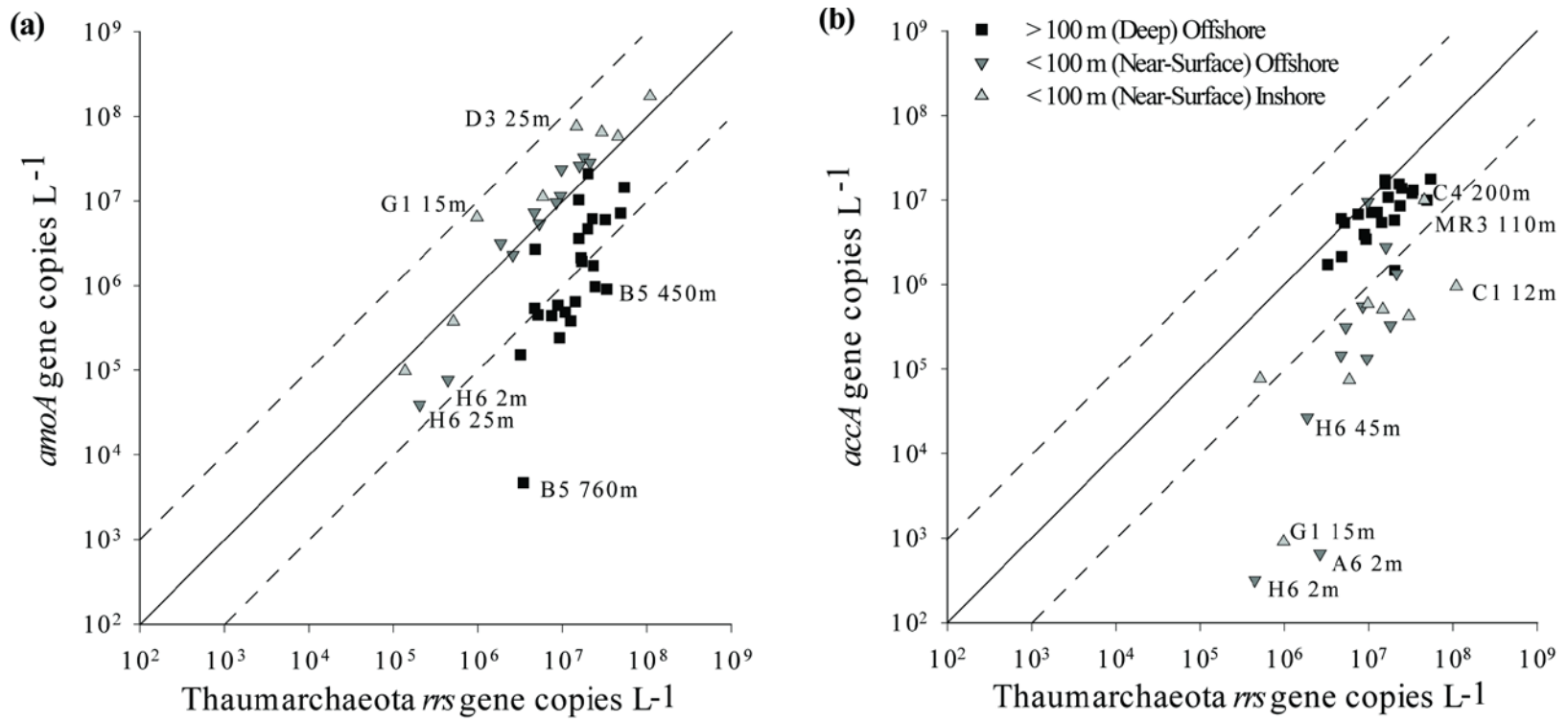
(a)
amoA gene copies L-1
Thaumarchaeota rrs gene copies L-1
D3 25m
G1 15m
B5 450m
H6 2m
H6 25m
B5 760m
(b)
> 100 m (Deep) Offshore
< 100 m (Near-Surface) Offshore
< 100 m (Near-Surface) Inshore
accA gene copies L-1
Thaumarchaeota rrs gene copies L-1
C4 200m
MR3 110m
C1 12m
H6 45m
G1 15m
A6 2m
H6 2m

Figure A.6: Comparison of Archaeal *amoA* gene abundance estimated by qPCR reactions with primers from Wuchter *et al.* (2006) or Francis *et al.* (2005). **(a)** Profiles of *amoA* abundance at Stations A6 and B5 obtained using each primer set. Red diamonds = Wuchter, blue circles = Francis. **(b)** Abundance of *amoA* genes estimated using Francis primers versus abundance estimated using the Wuchter primers. 'Deep' = >100 m sample depth; 'near-surface' = ≤100 m sample depth; 'inshore' = above continental shelf; 'offshore' = shelf break and beyond.

(a) Station profiles of *amoA* quantified with different primer sets

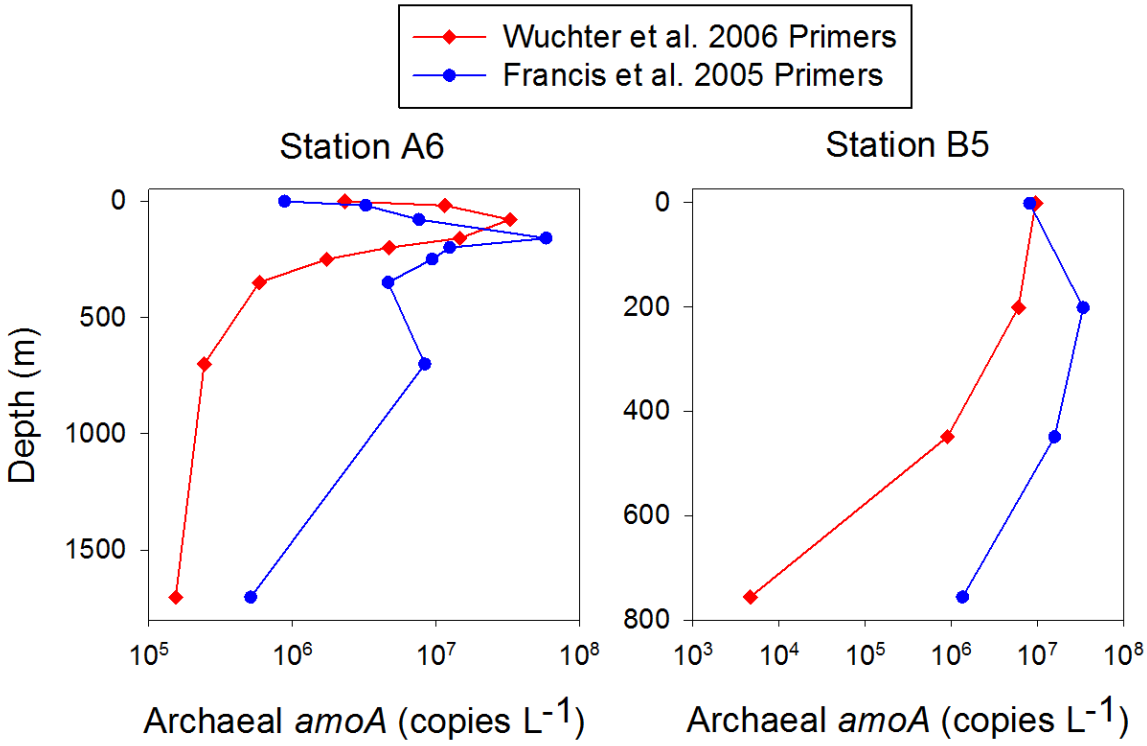

(b) *amoA* quantified by Wuchter *et al.* (2006) primers versus Francis *et al.* (2005) primers

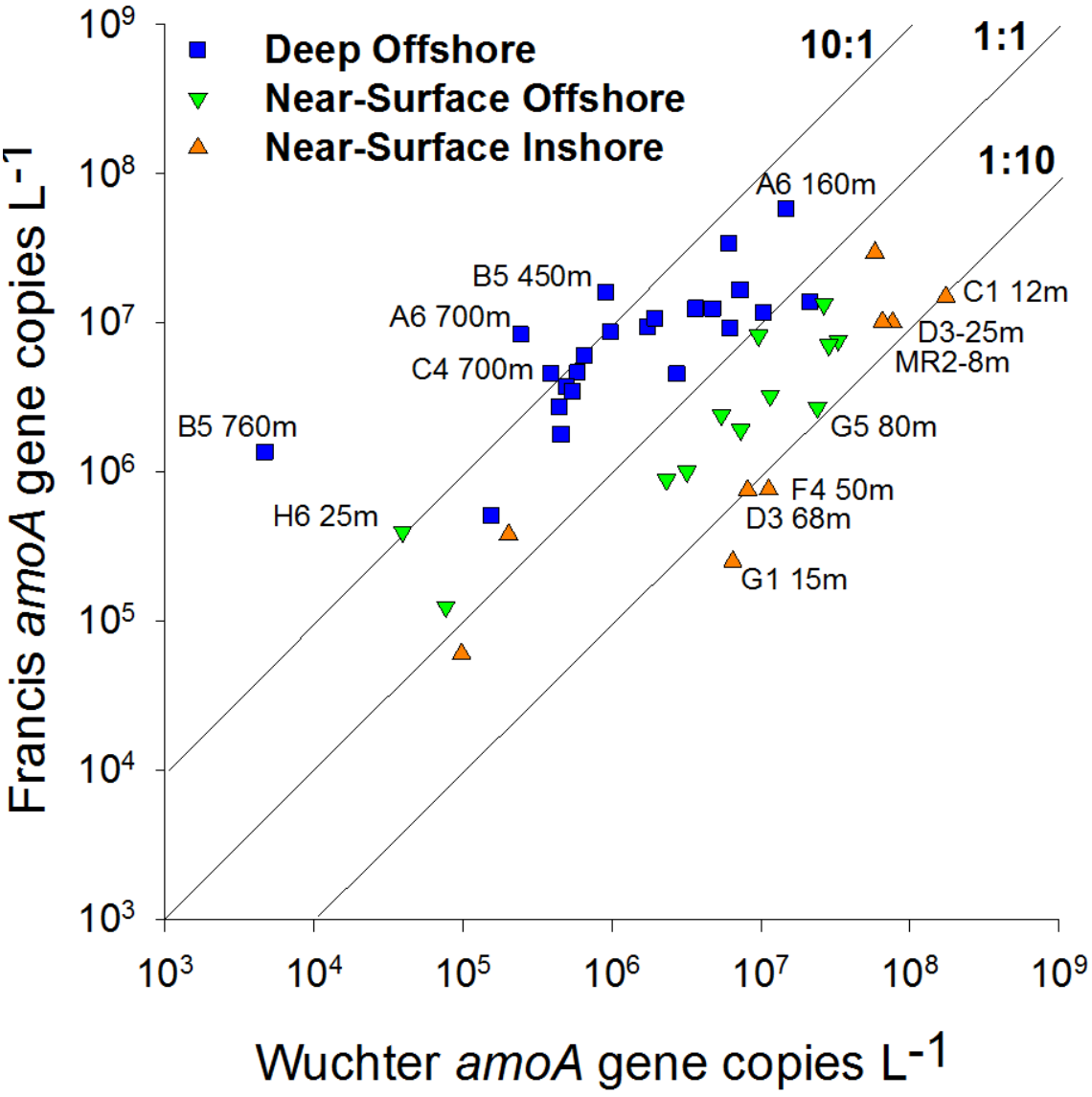

Figure A.7: **Principal Coordinates Analysis (PCoA) of Thaumarchaeota *rrs* sequences obtained through 454 pyrosequencing** of 41 samples and clone libraries generated from two depths at Station D5. Shapes indicate sample groupings: dark grey squares = deep, offshore; open triangles = near-surface, offshore; light grey circles = near-surface, inshore. The percentage of the variance explained by an axis is given in parentheses next to the axis title.

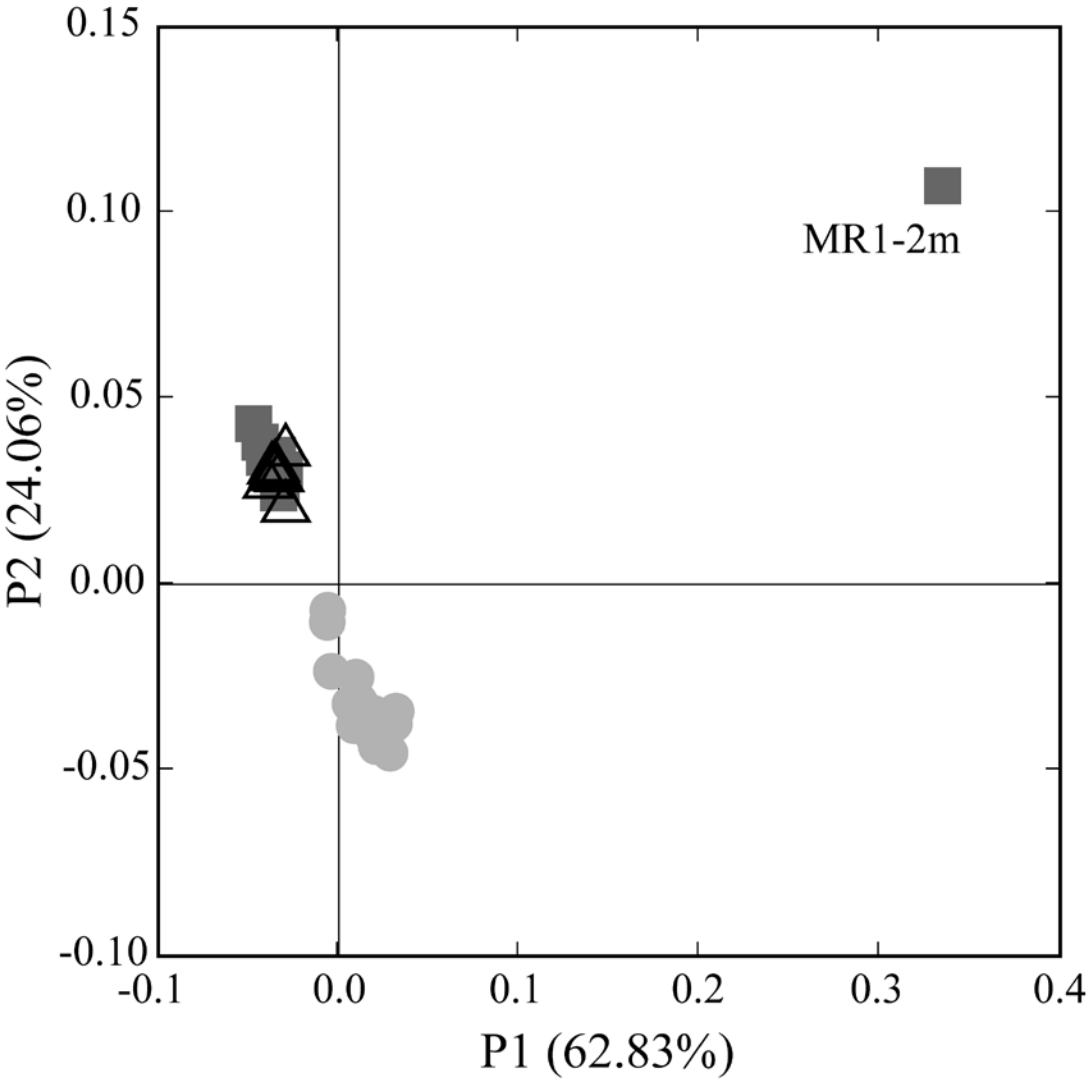
0.15
0.10
0.05
0.00
-0.05
-0.10
P2 (24.06%)
MR1-2m
-0.1
0.0
0.1
0.2
0.3
0.4
P1 (62.83%)

Figure A.8: Mismatches between *amoA* primer sequences and environmental sequences retrieved from samples taken in the northern Gulf of Mexico. Sequences shown were collected from Station D5, 200 m depth, and were trimmed to regions complementary to the Wuchter *et al.* (2006) and Francis *et al.* (2005) primer sets. The top line represents the consensus sequence, while arrows indicate key differences between environmental and primer sequences.

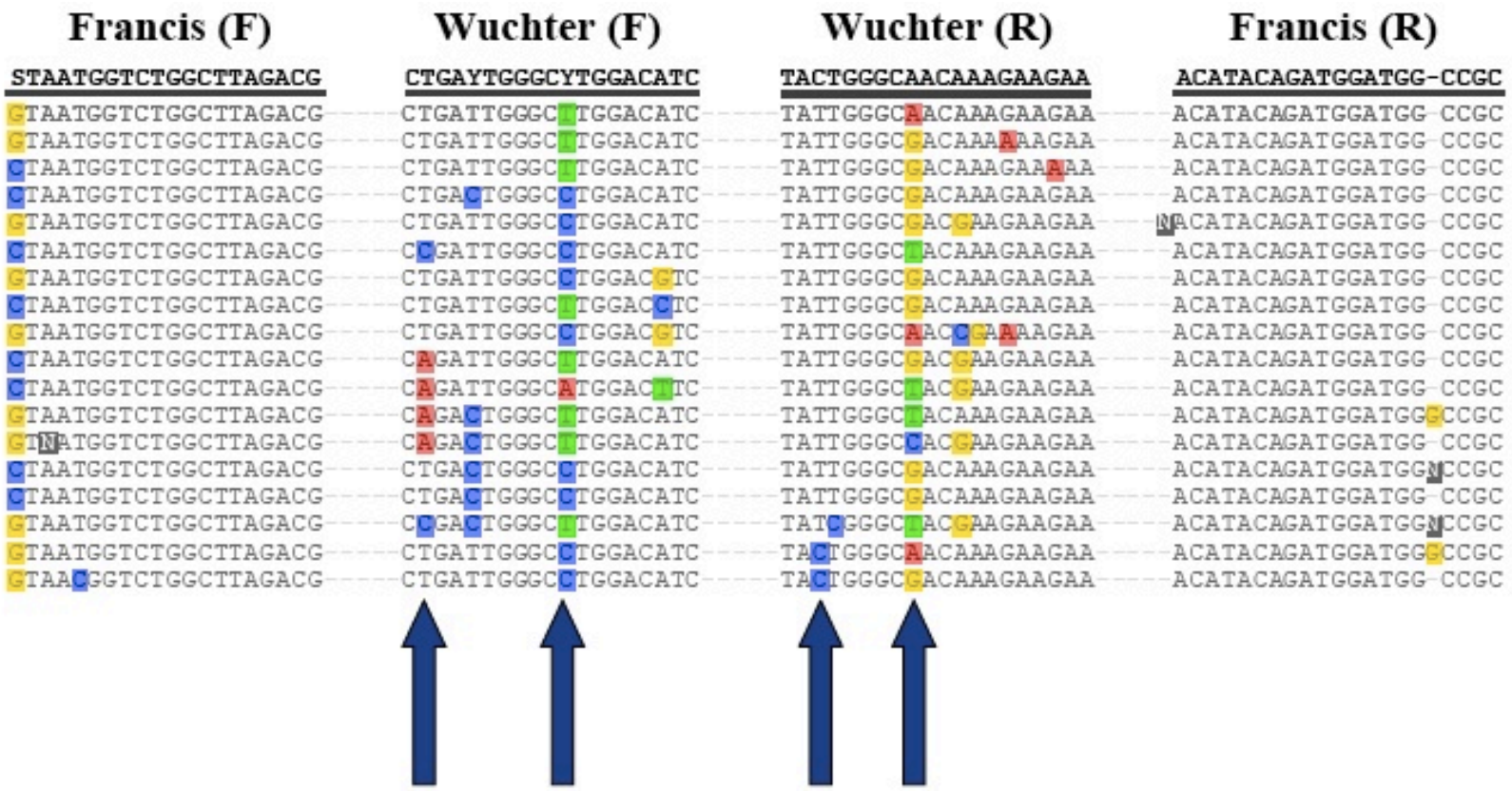
Francis (F)
Wuchter (F)
Wuchter (R)
Francis (R)
STAATGGTCTGGCTTAGACG
CTGAYTGGGCYTGGACATC
TACTGGGCAACAAAGAAGAA
ACATACAGATGGATGG-CCGC

APPENDIX B

SUPPLEMENTARY MATERIAL: SIGNIFICANT AMMONIA OXIDATION RATES IN ANTARCTIC WATERS ATTRIBUTED TO THAUMARCHAEOTA[1]

[1] Tolar, B.B., M.J. Ross, N.J. Wallsgrove, Q. Liu, L.I. Aluwihare, B.N. Popp, and J.T. Hollibaugh. To be submitted to *The ISME Journal*.

REFERENCES

Alonso-Sáez L, Waller AS, Mende DR, Bakker K, Farnelid H, Yager PL, Lovejoy C, Tremblay JE, Potvin M, Heinrich F, Estrada M, Riemann L, Bork P, Pedrós-Alio C, Bertilsson S (2012). Role for urea in nitrification by polar marine Archaea. *Proc Nat Acad Sci USA* **109:** 17989-17994.

Baldi F, Facca C, Marchetto D, Nguyen TNM, Spurio R (2011). Diatom quantification and their distribution with salinity brines in coastal sediments of Terra Nova Bay (Antarctica). *Mar Environ Res* **71:** 304-311.

Biers EJ, Sun SL, Howard EC (2009). Prokaryotic Genomes and Diversity in Surface Ocean Waters: Interrogating the Global Ocean Sampling Metagenome. *Appl Environ Microbiol* **75:** 2221-2229.

Church MJ, DeLong EF, Ducklow HW, Karner MB, Preston CM, Karl DM (2003). Abundance and distribution of planktonic Archaea and Bacteria in the waters west of the Antarctic Peninsula. *Limnol Oceanogr* **48:** 1893-1902.

Francis CA, Roberts KJ, Beman JM, Santoro AE, Oakley BB (2005). Ubiquity and diversity of ammonia-oxidizing archaea in water columns and sediments of the ocean. *Proc Natl Acad Sci USA* **102:** 14683-14688.

Hornek R, Pommerening-Roser A, Koops HP, Farnleitner AH, Kreuzinger N, Kirschner A, Mach RL (2006). Primers containing universal bases reduce multiple *amoA* gene specific DGGE band patterns when analysing the diversity of beta-ammonia oxidizers in the environment. *J Microbiol Methods* **66:** 147-155.

Kalanetra KM, Bano N, Hollibaugh JT (2009). Ammonia-oxidizing Archaea in the Arctic Ocean and Antarctic coastal waters. *Environ Microbiol* **11:** 2434-2445.

Mincer TJ, Church MJ, Taylor LT, Preston C, Karl DM, DeLong EF (2007). Quantitative distribution of presumptive archaeal and bacterial nitrifiers in Monterey Bay and the North Pacific Subtropical Gyre. *Environ Microbiol* **9:** 1162-1175.

Nguyen TNM, Berzano M, Gualerzi CO, Spurio R (2011). Development of molecular tools for the detection of freshwater diatoms. *J Microbiol Methods* **84:** 33-40.

Pester M, Rattei T, Flechl S, Gröngröft A, Richter A, Overmann J, Reinhold-Hurek B, Loy A, Wagner M (2012). *amoA*-based consensus phylogeny of ammonia-oxidizing archaea and deep sequencing of *amoA* genes from soils of four different geographic regions. *Environ Microbiol* **14:** 525-539.

Quast C, Pruesse E, Yilmaz P, Gerken J, Schweer T, Yarza P, Peplies J, Glockner FO (2013). The SILVA ribosomal RNA gene database project: improved data processing and web-based tools. *Nucl Acids Res* **41:** D590-596.

Rotthauwe JH, Witzel KP, Liesack W (1997). The ammonia monooxygenase structural gene *amoA* as a functional marker: Molecular fine-scale analysis of natural ammonia-oxidizing populations. *Appl Environ Microbiol* **63:** 4704-4712.

Schlitzer R (2014). Ocean Data View, 4.6.0 edn.

Schloss PD, Westcott SL, Ryabin T, Hall JR, Hartmann M, Hollister EB, Lesniewski RA, Oakley BB, Parks DH, Robinson CJ, Sahl JW, Stres B, Thallinger GG, Van Horn DJ, Weber CF (2009). Introducing mothur: Open-source, platform-independent, community-supported software for describing and comparing microbial communities. *Appl Environ Microbiol* **75:** 7537-7541.

Suzuki MT, Taylor LT, DeLong EF (2000). Quantitative analysis of small-subunit rRNA genes in mixed microbial populations via 5'-nuclease assays. *Appl Environ Microbiol* **66:** 4605-4614.

Wuchter C, Abbas B, Coolen MJL, Herfort L, van Bleijswijk J, Timmers P, Strous M, Teira E, Herndl GJ, Middelburg JJ, Schouten S, Damste JSS (2006). Archaeal nitrification in the ocean. *Proc Natl Acad Sci USA* **103:** 12317-12322.

Table B.1: Summary of samples from this study.

Cruise	Station*	Depth (m)*	Water Mass[#]	Date	Time (GMT)	Latitude (°S)	Longitude (°W)	Temp-erature (°C)	Salinity (PSU)	Chl *a* Fluor. (mg m^{-3})	Turbidity (m^{-2})	Dissolved Oxygen (mg L^{-1})
LMG 10-06	600.200	10	UAASW	9/17/10	04:47	63.9657	66.8533	-1.79	33.96	ND	ND	ND
		75	LAASW			63.9657	66.8533	-1.76	33.99	ND	ND	ND
		260	CDW			63.9657	66.8533	2.09	34.64	ND	ND	ND
	600.160	10	UAASW	9/17/10	13:34	64.2111	66.2579	-1.76	33.97	0.14	ND	ND
		75	LAASW			64.2111	66.2579	-0.82	34.13	0.09	ND	ND
		300	CDW			64.2111	66.2579	1.57	34.68	0.05	ND	ND
	600.080	10	UAASW	9/22/10	02:03	64.6960	65.0277	-1.83	33.90	0.15	ND	ND
		75	LAASW			64.6960	65.0277	-1.75	33.93	0.14	ND	ND
		300	CDW			64.6960	65.0277	1.39	34.63	0.05	ND	ND
	600.120	10	UAASW	9/22/10	07:25	64.4549	65.6659	-1.84	33.91	0.13	ND	ND
		70	LAASW			64.4549	65.6659	-1.81	33.93	0.12	ND	ND
		330	CDW			64.4549	65.6659	1.32	34.61	0.05	ND	ND
	600.160M	**10**	UAASW	9/23/10	13:29	64.2110	66.2600	-1.77	33.95	0.14	ND	ND
		55	LAASW			64.2110	66.2600	-1.76	33.96	0.13	ND	ND
		300	CDW			64.2110	66.2600	1.57	34.68	0.06	ND	ND
	600.080M	**10**	UAASW	9/24/10	04:27	64.6947	65.0308	-1.84	33.91	0.12	ND	ND
		75	LAASW			64.6947	65.0308	-1.83	33.91	0.12	ND	ND
		300	CDW			64.6947	65.0308	1.38	34.63	0.05	ND	ND
LMG 11-01	**600.100**	**100**	WW	1/7/11	17:32	64.5750	65.3400	0.27	33.96	0.21	-0.04	8.43
		400	CDW			64.5750	65.3400	1.40	34.65	-0.01	-0.07	4.75
	600.200	70	WW	1/8/11	10:15	63.9785	66.8412	-0.11	33.93	0.81	0.01	7.91
		400	CDW			63.9785	66.8412	1.80	34.66	0.00	-0.08	4.05
	500.200	**80**	WW	1/8/11	22:00	64.6033	68.2770	-0.41	34.03	0.38	-0.03	7.56
		400	CDW			64.6033	68.2770	1.90	34.71	0.00	-0.09	4.18

Cruise	Station*	Depth (m)*	Water Mass[#]	Date	Time (GMT)	Latitude (°S)	Longitude (°W)	Temp-erature (°C)	Salinity (PSU)	Chl *a* Fluor. (mg m^{-3})	Turbidity (m^{-2})	Dissolved Oxygen (mg L^{-1})
LMG 11-01	500.120	100	WW	1/9/11	05:45	65.1098	67.0923	-0.06	33.98	0.81	-0.01	7.86
		400	CDW			65.1098	67.0923	1.52	34.69	0.00	-0.08	4.18
	500.060	100	WW		13:30	65.4788	66.1495	-0.53	33.93	0.07	-0.07	7.66
		270	CDW			65.4788	66.1495	1.41	34.65	0.01	-0.05	4.45
	600.040	**80**	WW	1/10/11	00:30	64.9317	64.4027	-0.66	34.00	0.06	-0.06	7.55
		400	CDW			64.9317	64.4027	1.23	34.62	0.02	-0.07	4.34
	400.040	80	WW	1/13/11	04:00	66.2489	67.3354	-0.89	33.97	0.27	-0.01	7.15
		160	CDW			66.2489	67.3354	0.19	34.32	0.07	-0.01	5.66
	400.100	**80**	WW		11:45	65.8825	68.2933	-1.02	34.02	0.20	-0.04	7.75
		350	CDW			65.8825	68.2933	1.59	34.70	0.05	-0.06	3.97
	300.100	**100**	WW	1/14/11	04:37	66.5054	69.3703	-1.13	33.99	0.04	-0.06	7.98
		400	CDW			66.5054	69.3703	1.51	34.71	0.01	-0.07	4.16
	300.040	125	WW		10:05	66.8877	68.9541	-1.02	33.95	0.07	-0.06	7.90
		400	CDW			66.8877	68.9541	1.40	34.68	0.01	-0.05	4.07
	200.100	**100**	WW		21:35	67.1228	71.5432	-1.18	34.00	0.05	-0.06	7.78
		400	CDW			67.1228	71.5432	1.42	34.70	0.02	-0.03	3.87
	200.040	110	WW	1/15/11	03:35	67.5082	70.5797	-1.53	33.93	0.80	0.03	7.79
		440	CDW			67.5082	70.5797	1.38	34.67	0.01	-0.07	4.09
	200.000	100	WW		10:50	67.7717	69.9444	-1.02	33.98	0.04	-0.06	7.98
		400	CDW			67.7717	69.9444	1.43	34.68	0.01	-0.07	4.08
	200.-040	**100**	WW		17:20	68.0320	69.2853	-1.42	33.92	1.53	0.10	7.85
		400	CDW			68.0320	69.2853	1.38	34.67	0.01	-0.07	4.09
	200.160	75	WW	1/17/11	06:45	66.7133	72.4400	-1.61	33.94	0.75	-0.01	7.45
		400	CDW			66.7133	72.4400	2.04	34.69	0.03	-0.08	4.12
	221.-019 P2	80	WW		22:45	67.7740	69.2762	-0.95	33.97	0.25	-0.01	7.73
		80 #2	WW			67.7740	69.2762	-0.89	33.95	1.00	0.09	7.88

Cruise	Station*	Depth (m)*	Water Mass[#]	Date	Time (GMT)	Latitude (°S)	Longitude (°W)	Temp-erature (°C)	Salinity (PSU)	Chl *a* Fluor. (mg m^{-3})	Turbidity (m^{-2})	Dissolved Oxygen (mg L^{-1})
LMG 11-01	203.031 P2-#5	80	WW	1/19/11	18:35	67.5488	70.4117	-1.51	33.90	1.21	0.05	7.32
		400	CDW			67.5488	70.4117	1.35	34.68	0.01	-0.06	4.09
	200.04 #2	**70**	WW	1/23/11	18:15	67.5122	70.5892	-1.38	33.92	0.33	0.02	7.22
		400	CDW			67.5122	70.5892	1.25	34.67	0.01	-0.05	4.08
	100.-040	100	WW	1/24/11	03:24	68.6456	71.0493	-1.20	33.86	0.24	0.02	6.52
		250	CDW			68.6456	71.0493	0.46	34.44	0.07	-0.01	4.82
	100.040	**80**	WW		11:40	68.1191	72.3562	-1.39	33.95	0.25	-0.01	7.16
		325	CDW			68.1191	72.3562	1.45	34.66	0.04	-0.03	3.93
	100.100	80	WW	1/25/11	18:40	67.7060	73.2783	-1.27	33.98	0.08	-0.04	7.81
		400	CDW			67.7060	73.2783	1.51	34.72	0.02	-0.04	4.09
	000.180	70	WW	1/26/11	04:50	67.7110	76.2957	-0.10	33.96	1.44	0.08	8.07
		400	CDW			67.7110	76.2957	1.87	34.71	0.01	-0.06	4.10
	-100.180	70	WW		16:30	68.2487	78.2039	-1.77	33.97	1.20	0.06	7.22
		400	CDW			68.2487	78.2039	2.01	34.67	0.01	-0.06	4.01
	-100.060	**100**	WW	1/27/11	02:40	69.1086	76.4462	-1.41	33.87	0.17	-0.01	7.27
		400	CDW			69.1086	76.4462	1.28	34.65	0.02	-0.06	4.11
	-120.-025	80	WW	1/28/11	03:40	69.8307	75.5068	-1.64	33.83	0.07	-0.02	7.20
		500	CDW			69.8307	75.5068	1.28	34.70	0.03	-0.04	4.08
	-158.-034	100	WW	1/29/11	08:50	70.0881	76.1416	-1.68	33.89	0.13	-0.04	7.38
		285	CDW			70.0881	76.1416	0.52	34.47	0.10	-0.05	4.52
	-100.000	**100**	WW		15:45	69.5291	75.5046	-1.57	33.83	0.60	0.04	7.56
	000.100	**100**	WW	1/30/11	06:40	68.2771	75.1263	-1.38	33.95	0.08	-0.03	7.52
		350	CDW			68.2771	75.1263	1.77	34.70	0.02	-0.06	4.11

*Stations/Depths in **bold** used for pyrosequencing; ND = not determined; data from CTD casts.

#Water Mass Abbreviations: UAASW = Upper Antarctic Surface Water, LAASW = Lower Antarctic Surface Water, WW = Winter Water, CDW = Circumpolar Deep Water

Cruise	Station	Depth (m)	Water Mass	Sigma-T	NO_2 (µM)	NO_3 (µM)	NH_4 (µM)	Biogenic Silicate (µM)	Ammonia Oxidation Rate (nM d^{-1})	Specific Nitrification Rate (λ_{nitrif})	Leucine Incorporation Rate (pM hr^{-1})
LMG 10-06	600.200	10	UAASW	27.3311	0.21	31.98	0.56	ND	15.41	0.028	1.80
		75	LAASW	27.3572	0.19	31.24	0.63	ND	28.13	0.044	2.58
		260	CDW	27.6756	0.21	33.60	1.11	ND	3.11	0.003	1.81
	600.160	10	UAASW	27.3389	0.19	31.81	0.58	ND	61.50	0.105	5.66
		75	LAASW	27.4396	0.18	30.94	0.61	ND	69.32	0.114	9.77
		300	CDW	27.7474	0.03	35.03	0.53	ND	21.55	0.040	2.43
	600.080	10	UAASW	27.2898	0.12	32.88	0.66	ND	43.65	0.066	4.78
		75	LAASW	27.3133	0.13	32.89	0.66	ND	65.05	0.099	4.81
		300	CDW	27.7218	0.08	35.29	0.89	ND	36.41	0.041	5.38
	600.120	10	UAASW	27.2960	0.13	28.18	0.96	ND	73.81	0.077	3.56
		70	LAASW	27.3078	0.12	32.64	0.76	ND	86.39	0.114	3.96
		330	CDW	27.7114	0.08	37.07	0.81	ND	25.89	0.032	0.99
	600.160M	**10**	UAASW	27.3301	0.17	25.71	0.97	ND	77.86	0.080	ND
		55	LAASW	27.3321	0.16	30.05	1.14	ND	143.28	0.126	ND
		300	CDW	27.7464	0.07	29.57	1.11	ND	29.35	0.026	ND
	600.080M	**10**	UAASW	27.2928	0.10	36.94	0.36	ND	2.65	0.007	ND
		75	LAASW	27.2936	0.15	36.55	0.62	ND	7.93	0.013	ND
		300	CDW	27.7188	0.09	38.29	0.69	ND	6.86	0.010	ND
LMG 11-01	**600.100**	**100**	WW	27.2491	0.20	21.04	3.82	LD	3.04	0.001	ND
		400	CDW	27.7372	0.08	26.60	2.10	0.33	85.89	0.041	ND
	600.200	70	WW	27.2448	0.13	30.44	2.05	0.00	LD	ND	ND
		400	CDW	27.7185	0.08	38.30	0.64	0.27	21.46	0.034	ND
	500.200	**80**	WW	27.3419	0.12	28.36	5.60	0.00	18.53	0.003	ND
		400	CDW	27.7449	0.13	31.05	4.04	0.18	9.84	0.002	ND

Cruise	Station*	Depth (m)*	Water Mass[#]	Sigma-T	NO_2 (µM)	NO_3 (µM)	NH_4 (µM)	Biogenic Silicate (µM)	Ammonia Oxidation Rate (nM d^{-1})	Specific Nitrification Rate (λ_{nitrif})	Leucine Incorporation Rate (pM hr^{-1})
LMG 11-01	500.120	100	WW	27.2886	ND	ND	ND	0.00	ND	ND	ND
		400	CDW	27.7595	ND	ND	ND	0.30	ND	ND	ND
	500.060	100	WW	27.2705	ND	ND	ND	0.00	ND	ND	ND
		270	CDW	27.7324	ND	ND	ND	0.00	ND	ND	ND
	600.040	**80**	WW	27.3268	0.19	30.22	0.91	0.30	31.43	0.035	ND
		400	CDW	27.7267	0.08	25.65	2.39	0.28	22.69	0.009	ND
	400.040	80	WW	27.3154	0.15	23.18	1.14	1.42	6.22	0.005	ND
		160	CDW	27.5443	0.14	20.45	1.64	1.34	18.94	0.012	ND
	400.100	**80**	WW	27.3591	0.25	26.66	4.83	LD	13.95	0.003	ND
		350	CDW	27.7630	0.08	34.03	LD	LD	9.78	ND	ND
	300.100	**100**	WW	27.3381	0.26	25.40	5.43	0.00	0.00	ND	ND
		400	CDW	27.7742	0.09	23.41	0.70	0.29	23.17	0.033	ND
	300.040	125	WW	27.3002	0.26	32.08	2.89	LD	37.07	0.013	ND
		400	CDW	27.7612	0.12	37.03	0.05	0.00	16.51	0.307	ND
	200.100	**100**	WW	27.3490	0.14	29.83	1.94	0.34	3.18	0.002	ND
		400	CDW	27.7715	0.13	24.71	1.26	0.48	3.83	0.003	ND
	200.040	110	WW	27.3059	0.21	26.26	1.38	0.00	42.49	0.031	ND
		440	CDW	27.7567	0.07	36.73	0.43	0.00	25.88	0.060	ND
	200.000	100	WW	27.3294	0.14	27.90	2.02	0.16	1.23	0.001	ND
		400	CDW	27.7600	0.05	37.26	0.34	0.17	32.18	0.094	ND
	200.-040	**100**	WW	27.2946	0.21	31.85	0.93	0.00	26.44	0.028	ND
		400	CDW	27.7567	0.14	34.76	2.11	0.00	144.50	0.068	ND
	200.160	75	WW	27.3181	0.13	32.54	1.23	0.00	1.44	0.001	ND
		400	CDW	27.7186	0.05	36.77	0.64	0.00	1.72	0.003	ND
	221.-019 P2	80	WW	27.3200	0.17	27.31	1.49	1.12	1.52	0.001	ND
		80 #2	WW	27.2960	0.17	29.05	1.70	0.00	ND	ND	ND

Cruise	Station*	Depth (m)*	Water Mass[#]	Sigma-T	NO_2 (µM)	NO_3 (µM)	NH_4 (µM)	Biogenic Silicate (µM)	Ammonia Oxidation Rate (nM d^{-1})	Specific Nitrification Rate (λ_{nitrif})	Leucine Incorporation Rate (pM hr^{-1})
LMG 11-01	203.031 P2-#5	80	WW	27.2778	0.13	13.82	1.37	0.00	11.53	0.008	ND
		400	CDW	27.7656	0.08	14.58	0.94	0.14	6.49	0.007	ND
	200.04 #2	**70**	WW	27.2875	0.19	31.16	0.59	1.41	9.81	0.017	ND
		400	CDW	27.7644	0.07	36.35	0.05	0.00	6.30	0.117	ND
	100.-040	100	WW	27.2373	0.17	31.71	1.09	0.00	10.33	0.009	ND
		250	CDW	27.6261	0.09	25.53	1.52	6.09	3.69	0.002	ND
	100.040	**80**	WW	27.3171	0.19	20.29	2.74	0.00	33.20	0.012	ND
		325	CDW	27.7382	0.31	36.23	0.16	0.35	32.61	0.202	ND
	100.100	80	WW	27.3378	0.10	19.14	2.56	LD	0.76	0.000	ND
		400	CDW	27.7813	0.17	35.43	0.30	LD	8.09	0.027	ND
	000.180	70	WW	27.2731	0.19	23.63	1.93	0.00	LD	ND	ND
		400	CDW	27.7491	0.11	33.78	0.15	0.00	1.62	0.011	ND
	-100.180	70	WW	27.3399	0.13	29.86	1.32	0.00	0.52	0.000	ND
		400	CDW	27.7104	0.08	23.69	1.27	0.00	11.59	0.009	ND
	-100.060	**100**	WW	27.2493	0.15	28.74	1.92	0.00	7.69	0.004	ND
		400	CDW	27.7420	0.03	35.41	0.53	LD	39.27	0.074	ND
	-120.-025	80	WW	27.2233	0.25	28.76	1.26	0.00	ND	ND	ND
		500	CDW	27.7829	0.11	12.62	1.11	0.00	ND	ND	ND
	-158.-034	100	WW	27.2765	0.22	28.41	0.94	0.00	19.47	0.021	ND
		285	CDW	27.6528	0.05	34.24	0.18	0.00	16.07	0.090	ND
	-100.000	**100**	WW	27.2212	0.21	29.07	1.27	0.00	5.41	0.004	ND
	000.100	**100**	WW	27.3114	0.09	25.26	1.91	0.29	6.54	0.003	ND
		350	CDW	27.7513	0.02	29.49	0.91	0.00	25.20	0.028	ND

*Stations/Depths in **bold** used for pyrosequencing; ND = not determined; LD = limit of detection; Sigma-T calculated as in text.

#Water Mass Abbreviations: UAASW = Upper Antarctic Surface Water, LAASW = Lower Antarctic Surface Water, WW = Winter Water, CDW = Circumpolar Deep Water

Cruise	Station	Depth (m)	Water Mass	DNA Vol. Filtered (L)	RNA Vol. Filtered (L)	qPCR Data (units are copies L^{-1} sample filtered)					
						Archaeal *amoA*	**Thaum. *rrs***	**Thaum. *ureC***	**Arch. *amoA* Transcripts**	**AOB *amoA***	**AOB *amoA* transcripts**
LMG 10-06	600.200	10	UAASW	14.0	3.1	4.15E+05	5.51E+06	2.58E+05	7.29E+05	1.71E+02	5.66E+03
		75	LAASW	14.5	2.6	1.22E+06	4.97E+06	4.61E+05	1.03E+06	1.12E+05	1.19E+05
		260	CDW	14.0	3.1	4.78E+05	3.39E+06	1.54E+06	3.58E+04	2.61E+03	LD
	600.160	10	UAASW	14.0	3.0	1.68E+06	1.04E+07	8.31E+05	3.11E+06	4.90E+04	9.23E+04
		75	LAASW	14.0	3.5	1.84E+06	1.26E+07	9.32E+05	6.78E+06	9.02E+04	2.89E+05
		300	CDW	14.0	3.5	1.79E+06	6.89E+06	5.26E+06	1.84E+05	7.01E+04	4.60E+03
	600.080	10	UAASW	10.7	3.1	1.53E+06	6.10E+06	6.12E+05	3.40E+06	2.99E+04	1.24E+05
		75	LAASW	4.8	3.0	7.47E+05	1.96E+06	2.49E+05	6.12E+06	3.62E+04	3.77E+05
		300	CDW	11.5	3.4	8.72E+05	9.63E+05	1.35E+06	2.21E+05	1.62E+04	7.27E+03
	600.120	10	UAASW	8.5	3.0	9.07E+05	6.47E+06	5.27E+05	2.87E+06	4.46E+03	8.65E+04
		70	LAASW	10.0	3.1	3.97E+05	3.44E+06	3.73E+05	4.39E+06	8.71E+03	2.73E+05
		330	CDW	13.0	3.1	6.15E+05	3.91E+06	1.69E+06	2.87E+05	3.30E+04	6.44E+03
	600.160M	**10**	UAASW	10.0	29.9	1.13E+06	3.43E+06	3.12E+05	6.68E+04	8.40E+03	6.40E+04
		55	LAASW	9.8	32.8	9.98E+05	4.73E+06	4.05E+05	1.87E+05	7.41E+03	1.15E+05
		300	CDW	9.8	23.5	4.22E+05	1.16E+06	1.21E+06	1.36E+04	4.21E+03	6.00E+03
	600.080M	**10**	UAASW	10.0	31.0	2.40E+06	4.20E+06	6.04E+05	2.28E+05	1.29E+05	2.69E+03
		75	LAASW	9.7	29.8	9.70E+05	3.04E+06	3.41E+05	1.84E+05	5.06E+04	1.60E+04
		300	CDW	10.0	30.0	5.33E+05	1.29E+06	3.00E+06	3.31E+04	7.30E+03	1.45E+02
LMG 11-01	**600.100**	**100**	WW	4.0	1.1	1.75E+04	2.07E+04	2.04E+04	1.88E+04	1.19E+03	6.46E+03
		400	CDW	2.7	1.1	6.41E+06	1.13E+07	2.09E+07	4.58E+05	5.46E+04	8.64E+03
	600.200	70	WW	4.0	1.0	5.36E+04	5.44E+04	1.11E+05	2.41E+04	4.53E+03	1.56E+04
		400	CDW	4.0	1.0	8.60E+06	1.54E+07	2.43E+07	9.53E+05	2.05E+04	1.28E+04
	500.200	**80**	WW	4.3	1.0	5.11E+05	8.15E+05	1.13E+06	4.11E+05	7.21E+04	6.01E+04
		400	CDW	4.3	1.0	3.82E+06	1.38E+07	9.98E+06	4.40E+05	2.69E+03	LD

Cruise	Station*	Depth (m)*	Water Mass[#]	DNA Vol. Filtered (L)	RNA Vol. Filtered (L)	qPCR Data (units are copies L^{-1} sample filtered)					
						Archaeal *amoA*	**Thaum. *rrs***	**Thaum. *ureC***	**Arch. *amoA* Transcripts**	**AOB *amoA***	**AOB *amoA* transcripts**
LMG 11-01	500.120	100	WW	2.0	1.0	1.89E+05	2.33E+05	1.50E+05	2.45E+05	6.15E+04	1.08E+05
		400	CDW	3.5	1.0	7.32E+06	1.31E+07	2.06E+07	5.10E+05	2.15E+04	LD
	500.060	100	WW	3.5	1.0	4.44E+05	6.18E+05	2.77E+05	1.26E+06	9.61E+04	4.34E+05
		270	CDW	4.2	1.1	1.98E+07	3.01E+07	5.32E+07	2.96E+06	4.11E+04	1.89E+04
	600.040	**80**	WW	4.5	1.1	2.15E+06	1.92E+06	2.07E+06	2.01E+06	3.78E+04	5.08E+05
		400	CDW	4.0	1.1	1.15E+07	1.53E+07	2.97E+07	7.11E+05	4.65E+04	9.15E+03
	400.040	80	WW	2.5	0.5	1.42E+06	2.09E+06	9.12E+05	1.64E+06	LD	3.53E+05
		160	CDW	2.3	0.6	7.10E+06	7.22E+06	1.26E+07	2.94E+06	1.24E+05	1.87E+05
	400.100	**80**	WW	3.8	0.8	2.72E+05	3.49E+05	3.38E+05	4.66E+05	2.29E+04	6.20E+04
		350	CDW	3.7	1.0	1.63E+07	2.40E+07	5.07E+07	1.79E+06	2.07E+05	3.66E+03
	300.100	**100**	WW	4.0	1.1	1.14E+06	1.15E+06	2.28E+05	4.83E+05	2.64E+05	1.18E+05
		400	CDW	4.1	1.0	6.48E+07	2.71E+06	3.01E+07	3.05E+06	LD	1.23E+03
	300.040	125	WW	3.3	0.6	2.15E+07	1.78E+07	4.17E+07	6.24E+05	6.97E+04	3.06E+04
		400	CDW	3.5	0.6	8.10E+05	1.28E+06	5.39E+05	1.09E+06	LD	2.48E+03
	200.100	**100**	WW	3.8	1.2	2.16E+06	1.84E+06	8.50E+05	2.29E+06	6.77E+05	2.62E+04
		400	CDW	4.0	1.2	2.97E+07	2.66E+07	1.16E+08	6.61E+06	6.25E+04	1.16E+03
	200.040	110	WW	3.9	1.0	9.51E+06	3.69E+06	1.54E+06	8.18E+06	1.13E+05	4.03E+05
		440	CDW	3.8	1.0	1.62E+07	1.96E+07	3.80E+07	8.80E+05	3.21E+04	2.25E+03
	200.000	100	WW	4.0	1.0	2.89E+05	9.84E+04	1.43E+05	3.09E+05	8.50E+04	8.37E+03
		400	CDW	4.0	1.0	3.12E+07	2.89E+07	1.22E+08	1.09E+06	4.25E+04	9.76E+02
	200.-040	**100**	WW	4.0	1.0	1.15E+07	5.91E+06	4.68E+06	6.19E+06	9.81E+05	6.23E+04
		400	CDW	4.0	1.0	2.76E+07	2.80E+07	5.08E+07	1.01E+06	5.00E+04	LD
	200.160	75	WW	3.0	1.1	2.52E+06	4.42E+05	1.44E+05	5.89E+05	LD	LD
		400	CDW	4.0	1.2	2.67E+06	9.38E+06	1.16E+07	6.48E+04	1.18E+03	8.23E+02
	221.-019 P2	80	WW	3.0	0.9	7.28E+05	8.13E+05	3.74E+05	1.82E+06	1.99E+03	2.12E+03
		80 #2	WW	5.9	1.1	1.26E+04	1.12E+06	2.29E+05	8.26E+05	LD	LD

Cruise	Station*	Depth (m)*	Water Mass[#]	DNA Vol. Filtered (L)	RNA Vol. Filtered (L)	qPCR Data (units are copies L^{-1} sample filtered)					
						Archaeal *amoA*	**Thaum. *rrs***	**Thaum. *ureC***	**Arch. *amoA* Transcripts**	**AOB *amoA***	**AOB *amoA* transcripts**
LMG 11-01	203.031 P2-#5	80	WW	4.0	1.1	3.71E+06	2.63E+06	1.25E+06	7.22E+06	4.81E+04	6.93E+04
		400	CDW	4.0	1.2	5.71E+06	1.58E+07	4.23E+07	7.46E+05	1.28E+04	LD
	200.04 #2	**70**	WW	4.0	0.9	1.44E+06	2.55E+06	4.98E+06	7.43E+06	1.13E+04	1.37E+05
		400	CDW	3.2	1.0	2.43E+06	2.84E+06	7.41E+05	2.58E+06	1.64E+04	1.20E+04
	100.-040	100	WW	4.0	0.9	6.26E+06	1.32E+07	5.46E+06	2.15E+07	1.32E+05	2.40E+05
		250	CDW	0.5	0.6	4.39E+05	ND	ND	3.46E+03	3.68E+04	LD
	100.040	**80**	WW	4.0	0.9	2.15E+06	3.11E+06	2.07E+06	1.01E+07	2.14E+04	1.83E+05
		325	CDW	4.0	1.0	1.23E+07	1.67E+07	1.15E+07	1.60E+07	1.08E+04	2.86E+04
	100.100	80	WW	4.0	0.9	7.33E+05	4.91E+05	2.46E+05	1.74E+06	1.53E+05	6.20E+04
		400	CDW	3.7	1.1	3.69E+06	5.41E+06	1.10E+07	1.10E+07	2.78E+04	9.32E+04
	000.180	70	WW	4.0	1.1	8.46E+04	3.56E+02	1.12E+04	6.67E+03	LD	LD
		400	CDW	4.0	1.1	5.13E+06	1.47E+07	2.66E+07	1.31E+06	1.88E+03	LD
	-100.180	70	WW	4.0	0.9	2.32E+04	2.48E+04	2.36E+04	4.59E+05	LD	12925.93
		400	CDW	4.0	1.1	4.12E+06	9.34E+06	2.11E+07	1.15E+06	1.74E+03	2.77E+03
	-100.060	**100**	WW	4.0	1.1	1.51E+07	1.14E+06	7.63E+05	2.51E+06	LD	2.42E+05
		400	CDW	4.0	1.4	6.77E+06	9.56E+06	3.45E+07	2.39E+06	3.56E+04	6.34E+03
	-120.-025	80	WW	4.0	1.0	8.88E+06	9.06E+06	2.38E+06	2.80E+07	1.16E+06	8.23E+05
		500	CDW	4.0	1.2	1.03E+07	1.49E+07	3.90E+07	3.51E+06	2.03E+04	LD
	-158.-034	100	WW	4.0	1.1	1.45E+07	7.69E+06	2.38E+06	2.47E+07	1.49E+06	3.43E+04
		285	CDW	4.2	1.1	6.48E+06	7.71E+06	2.18E+07	6.87E+06	1.35E+05	3.24E+03
	-100.000	**100**	WW	4.0	1.0	3.64E+06	3.84E+06	8.83E+05	1.18E+06	1.05E+05	1.34E+04
	000.100	**100**	WW	4.0	1.0	3.78E+06	2.49E+06	1.19E+06	2.91E+06	1.30E+05	8.89E+05
		350	CDW	4.0	1.0	2.75E+06	3.13E+06	8.52E+06	1.16E+06	8.44E+03	6.04E+03

*Stations/Depths in **bold** used for pyrosequencing; ND = not determined; LD = limit of detection.

#Water Mass Abbreviations: UAASW = Upper Antarctic Surface Water, LAASW = Lower Antarctic Surface Water, WW = Winter Water, CDW = Circumpolar Deep Water

Cruise	Station	Depth (m)	Water Mass	qPCR Data (units are copies L^{-1})				Pyrosequencing Data (select samples only)**			
				Nitrospina rrs	Bacteria *rrs*	Diatom 18S rRNA	Thaum. % Prok.	Initial # *rrs* Reads	Final # *rrs* Reads	Initial # *amoA* reads	Final # *amoA* Reads
LMG 10-06	600.200	10	UAASW	5.14E+05	1.08E+08	1.60E+07	45.04%	ND	ND	ND	ND
		75	LAASW	9.12E+05	8.09E+07	4.51E+07	48.79%	ND	ND	ND	ND
		260	CDW	3.56E+05	2.97E+07	2.44E+06	64.73%	ND	ND	ND	ND
	600.160	10	UAASW	1.34E+06	1.14E+08	6.60E+07	14.13%	ND	ND	ND	ND
		75	LAASW	1.26E+06	1.19E+08	7.60E+07	16.02%	ND	ND	ND	ND
		300	CDW	5.14E+05	3.62E+07	6.94E+06	25.55%	ND	ND	ND	ND
	600.080	10	UAASW	1.56E+06	2.36E+08	7.31E+07	4.44%	ND	ND	ND	ND
		75	LAASW	3.70E+05	7.27E+07	1.05E+08	4.63%	ND	ND	ND	ND
		300	CDW	1.56E+05	9.17E+06	4.92E+06	15.90%	ND	ND	ND	ND
	600.120	10	UAASW	1.20E+06	2.21E+08	6.97E+07	5.02%	ND	ND	ND	ND
		70	LAASW	5.79E+05	2.20E+08	5.34E+07	2.74%	ND	ND	ND	ND
		330	CDW	4.63E+05	2.75E+07	1.66E+06	20.40%	ND	ND	ND	ND
	600.160M	**10**	UAASW	6.13E+05	1.11E+08	5.02E+07	5.25%	16,475	12,648	7,643	5,683
		55	LAASW	8.65E+05	1.44E+08	7.64E+07	5.60%	18,188	13,757	9,129	6,918
		300	CDW	6.74E+05	1.23E+07	5.69E+06	14.55%	17,481	12,520	6,047	3,793
	600.080M	**10**	UAASW	5.37E+05	9.53E+07	2.06E+07	7.35%	17,625	14,578	9,116	7,048
		75	LAASW	4.85E+05	1.17E+08	5.16E+07	4.47%	60,651	50,498	7,450	5,722
		300	CDW	3.23E+05	1.06E+07	3.86E+06	18.01%	17,650	10,403	7,832	5,073
LMG 11-01	**600.100**	**100**	WW	4.83E+03	6.03E+08	9.99E+07	0.01%	14,932	11,867	4,821	3,598
		400	CDW	1.07E+06	9.81E+07	5.43E+06	17.16%	16,853	10,749	6,071	4,035
	600.200	70	WW	1.09E+04	6.06E+08	1.33E+08	0.02%	ND	ND	ND	ND
		400	CDW	1.27E+06	1.11E+08	9.01E+06	20.08%	ND	ND	ND	ND
	500.200	**80**	WW	1.29E+05	3.24E+08	1.39E+08	0.45%	15,316	11,197	7,310	5,391
		400	CDW	5.99E+05	1.20E+08	9.19E+06	17.11%	15,950	10,608	6,726	4,800

Cruise	Station*	Depth (m)*	Water Mass[#]	qPCR Data (units are copies L^{-1})				Pyrosequencing Data (select samples only)**			
				Nitrospina rrs	Bacteria *rrs*	Diatom 18S rRNA	Thaum. % Prok.	Initial # *rrs* Reads	Final # *rrs* Reads	Initial # *amoA* reads	Final # *amoA* Reads
LMG 11-01	500.120	100	WW	4.15E+04	4.83E+08	1.59E+08	0.09%	ND	ND	ND	ND
		400	CDW	8.86E+05	1.48E+08	9.73E+06	13.76%	ND	ND	ND	ND
	500.060	100	WW	8.68E+04	9.96E+07	6.53E+07	1.10%	ND	ND	ND	ND
		270	CDW	1.37E+06	1.52E+08	7.27E+06	26.24%	ND	ND	ND	ND
	600.040	**80**	WW	2.50E+05	5.22E+08	9.11E+06	0.66%	18,800	14,495	7,525	5,495
		400	CDW	9.20E+05	1.51E+08	9.53E+06	15.42%	10,098	6,605	6,489	3,859
	400.040	80	WW	4.40E+05	8.85E+08	7.37E+07	0.42%	ND	ND	ND	ND
		160	CDW	1.20E+06	2.12E+08	4.15E+07	5.79%	ND	ND	ND	ND
	400.100	**80**	WW	5.86E+04	3.45E+08	1.73E+08	0.18%	20,054	16,745	8,878	7,034
		350	CDW	1.08E+06	2.59E+08	1.07E+07	14.28%	15,608	9,241	7,216	4,349
	300.100	**100**	WW	1.37E+05	7.03E+08	5.19E+07	0.29%	20,488	17,045	8,296	6,587
		400	CDW	9.97E+05	1.19E+08	1.19E+07	3.93%	16,880	9,760	7,116	4,478
	300.040	125	WW	7.08E+05	2.55E+08	4.96E+07	11.19%	ND	ND	ND	ND
		400	CDW	1.01E+05	1.36E+09	7.73E+08	0.17%	ND	ND	ND	ND
	200.100	**100**	WW	4.03E+05	4.47E+08	4.34E+07	0.74%	19,119	15,590	9,324	6,905
		400	CDW	1.66E+06	2.24E+08	1.80E+07	17.60%	19,884	10,152	8,209	5,023
	200.040	110	WW	1.27E+06	4.29E+08	4.43E+08	1.52%	ND	ND	ND	ND
		440	CDW	9.58E+05	8.73E+07	3.70E+07	28.77%	ND	ND	ND	ND
	200.000	100	WW	4.66E+04	1.80E+08	1.55E+07	0.10%	ND	ND	ND	ND
		400	CDW	2.25E+06	2.00E+08	2.40E+07	20.66%	ND	ND	ND	ND
	200.-040	**100**	WW	1.74E+06	5.13E+08	2.54E+08	2.03%	21,278	16,864	7,040	5,231
		400	CDW	1.94E+06	1.49E+08	2.11E+07	25.27%	13,997	8,023	6,746	4,136
	200.160	75	WW	3.94E+04	2.94E+08	3.97E+07	0.27%	ND	ND	ND	ND
		400	CDW	5.79E+05	4.88E+07	1.87E+07	25.71%	ND	ND	ND	ND
	221.-019 P2	80	WW	1.13E+05	7.79E+08	2.16E+08	0.19%	ND	ND	ND	ND
		80 #2	WW	2.12E+05	8.35E+08	7.77E+06	0.24%	ND	ND	ND	ND

Cruise	Station*	Depth (m)*	Water Mass[#]	qPCR Data (units are copies L^{-1})				Pyrosequencing Data (select samples only)**			
				Nitrospina rrs	Bacteria *rrs*	Diatom 18S rRNA	Thaum. % Prok.	Initial # *rrs* Reads	Final # *rrs* Reads	Initial # *amoA* reads	Final # *amoA* Reads
LMG 11-01	203.031 P2-#5	80	WW	5.30E+05	2.99E+08	1.44E+08	1.56%	ND	ND	ND	ND
		400	CDW	7.96E+05	7.66E+07	6.11E+06	27.14%	ND	ND	ND	ND
	200.04 #2	**70**	WW	9.03E+05	7.13E+07	4.39E+06	6.06%	14,387	8,835	7,677	5,225
		400	CDW	5.69E+05	6.13E+08	7.25E+06	0.83%	21,013	17,490	8,684	6,890
	100.-040	100	WW	2.00E+06	4.59E+08	1.04E+08	4.90%	ND	ND	ND	ND
		250	CDW	ND	7.52E+09	ND	ND	ND	ND	ND	ND
	100.040	**80**	WW	8.26E+05	4.53E+08	6.12E+07	1.22%	17,366	14,109	5,471	3,607
		325	CDW	1.56E+06	1.97E+08	1.12E+07	13.24%	15,636	11,877	7,844	5,530
	100.100	80	WW	1.73E+05	5.41E+08	7.14E+07	0.16%	ND	ND	ND	ND
		400	CDW	4.24E+05	1.04E+08	8.02E+06	8.55%	ND	ND	ND	ND
	000.180	70	WW	1.45E+04	7.53E+08	2.30E+08	0.00%	ND	ND	ND	ND
		400	CDW	1.52E+06	1.13E+08	1.73E+07	18.93%	ND	ND	ND	ND
	-100.180	70	WW	3.04E+04	3.75E+08	4.16E+07	0.01%	ND	ND	ND	ND
		400	CDW	8.88E+05	1.34E+08	1.97E+07	11.17%	ND	ND	ND	ND
	-100.060	**100**	WW	3.16E+05	6.06E+08	2.03E+08	0.34%	16,535	14,086	7,732	6,082
		400	CDW	1.94E+06	1.56E+08	2.79E+07	9.94%	15,682	10,284	6,140	4,188
	-120.-025	80	WW	2.98E+06	6.25E+08	2.63E+08	2.54%	ND	ND	ND	ND
		500	CDW	1.82E+06	2.76E+08	2.17E+07	8.86%	ND	ND	ND	ND
	-158.-034	100	WW	7.84E+05	6.69E+08	1.26E+08	2.03%	ND	ND	ND	ND
		285	CDW	1.41E+06	2.86E+08	1.66E+08	4.62%	ND	ND	ND	ND
	-100.000	**100**	WW	4.97E+05	7.28E+08	5.80E+08	0.94%	19,581	16,534	8,726	6,860
	000.100	**100**	WW	8.42E+05	2.61E+08	9.41E+07	1.69%	16,670	13,807	8,159	6,446
		350	CDW	5.92E+05	1.19E+08	3.75E+07	4.51%	13,807	9,022	6,516	4,051
								538,004	399,389	215,933	154,037
								Totals for All Samples			

*ND = not determined; Thaum. % Prok. (Prokaryotes) calculated as described in text.

**Processing of pyrosequencing reads described in Materials and Methods

[#]UAASW = Upper Antarctic Surface Water, LAASW = Lower AASW, WW = Winter Water, CDW = Circumpolar Deep Water

Table B.2: PCR Primers and probes used in this study

Target Gene	Primer/ Probe	Sequence (5'→3')	Application	LD[#]	Reference
Thaumarchaeota 16S rRNA (*rrs*)	G1_751F	GTC TAC CAG AAC AYG TTC	qPCR	2.04 x 10^3 copies L^{-1}	Mincer *et al.* (2007)
	G1_956R	HGG CGT TGA CTC CAA TTG			
	TM519AR	TTA CCG CGG CGG CTG GCA C			Suzuki *et al.* (2000)
	517Fa	GCC TAA AGC ATC CGT AGC	454 Sequencing	N/A	VAMPS project (*vamps.mbl.edu*)
	1058R	CGA CRR CCA TGC ANC ACC T			
Bacterial 16S rRNA (*rrs*)	BACT1369F	CGG TGA ATA CGT TCY CGG	qPCR	5.07 x 10^3 copies L^{-1}	Suzuki *et al.* (2000)
	PROK1492R	GGW TAC CTT GTT ACG ACT T			
	389F	CTT GTA CAC ACC GCC CGT C			
Nitrospina 16S rRNA (*rrs*)	NitSSU_130F	GGG TGA GTA ACA CGT GAA TAA	qPCR	1.60 x 10^3 copies L^{-1}	Mincer *et al.* (2007)
	NitSSU_282R	TCA GGC CGG CTA AMC A			
Diatom 18S rRNA	528F	GCG GTA ATT CCA GCT CCA A	qPCR	1.22 x 10^4 copies L^{-1}	Nguyen *et al.* (2011); Baldi *et al.* (2011)
	650R	AAC ACT CTA ATT TTT TCA CAG			
Archaeal *amoA*	Arch-amoA-for	CTG AYT GGG CYT GGA CAT C	qPCR	7.18 x 10^3 copies L^{-1}	Wuchter *et al.* (2006)
	Arch-amoA-rev	TTC TTC TTT GTT GCC CAG TA			
	ArchamoAF	STA ATG GTC TGG CTT AGA CG	qPCR	8.94 x 10^3 copies L^{-1}	Francis *et al.* (2005)
	ArchamoAR	GCG GCC ATC CAT CTG TAT GT			
	CamoA-19f	ATG GTC TGG YTW AGA CG	454 Sequencing	N/A	Pester *et al.* (2012)
	CamoA-616r	GCC ATC CAB CKR TAN GTC CA			
Thaumarchaeota *ureC*	Thaum-UreC for.	ATG CAA TYT GTA ATG GAA CWA CWA C	qPCR	7.70 x 10^3 copies L^{-1}	Alonso-Sáez *et al.* (2012)
	Thaum-UreC rev.	AGT TGT YCC CCA ATC TTC ATG TAA TTT TA			
Bacterial *amoA**	amoA-1F	GGG GTT TCT ACT GGT GGT	qPCR	8.13 x 10^3 copies L^{-1}	Rotthauwe *et al.* (1997)
	amoA-r New	CCC CTC BGS AAA VCC TTC TTC			Hornek *et al.* (2006)

*Bacterial *amoA* primers amplify genes from β-Proteobacteria only, and not γ-Proteobacteria. [#]LD = limit of detection.

Table B.3: OTUs shared between 2006 and 2010/2011.

rrs	**SSW**	**WW**	**CDW**	**Total**
Cluster #1	6%	3%	11%	7%
Cluster #2	94%	97%	49%	75%
Cluster #3	0%	0%	7%	3%
# Sequences (n)	16	92	91	199

amoA	**SSW**	**WW**	**CDW**	**Total**
Subcluster 13	89%	78%	8%	52%
Subcluster 9.1A	11%	22%	15%	16%
Subcluster 9.1B	0%	0%	77%	32%
# Sequences (n)	9	9	13	31

Figure B.1: Map of the Palmer LTER study region along the Antarctic Peninsula showing the stations sampled. Land is shown in white, while grey-scale shading indicates the bathymetry of the shelf-slope region (medium gray areas bisecting shelf are submarine canyons and troughs). The Palmer LTER sampling grid is set along lines 100 km apart (north to south) with stations 20 km apart (on to offshore, along a line), with standard sampling stations indicated by yellow circles. Green circles show process study stations where extended observations have been made since 2009. Stations colored in blue (LMG10-06) and orange (LMG11-01) were sampled as part of this study. Palmer Station is on Anvers Island, near station 600.040 (top-right, orange circle). Map courtesy of Hugh Ducklow, Lamont-Doherty Earth Observatory.

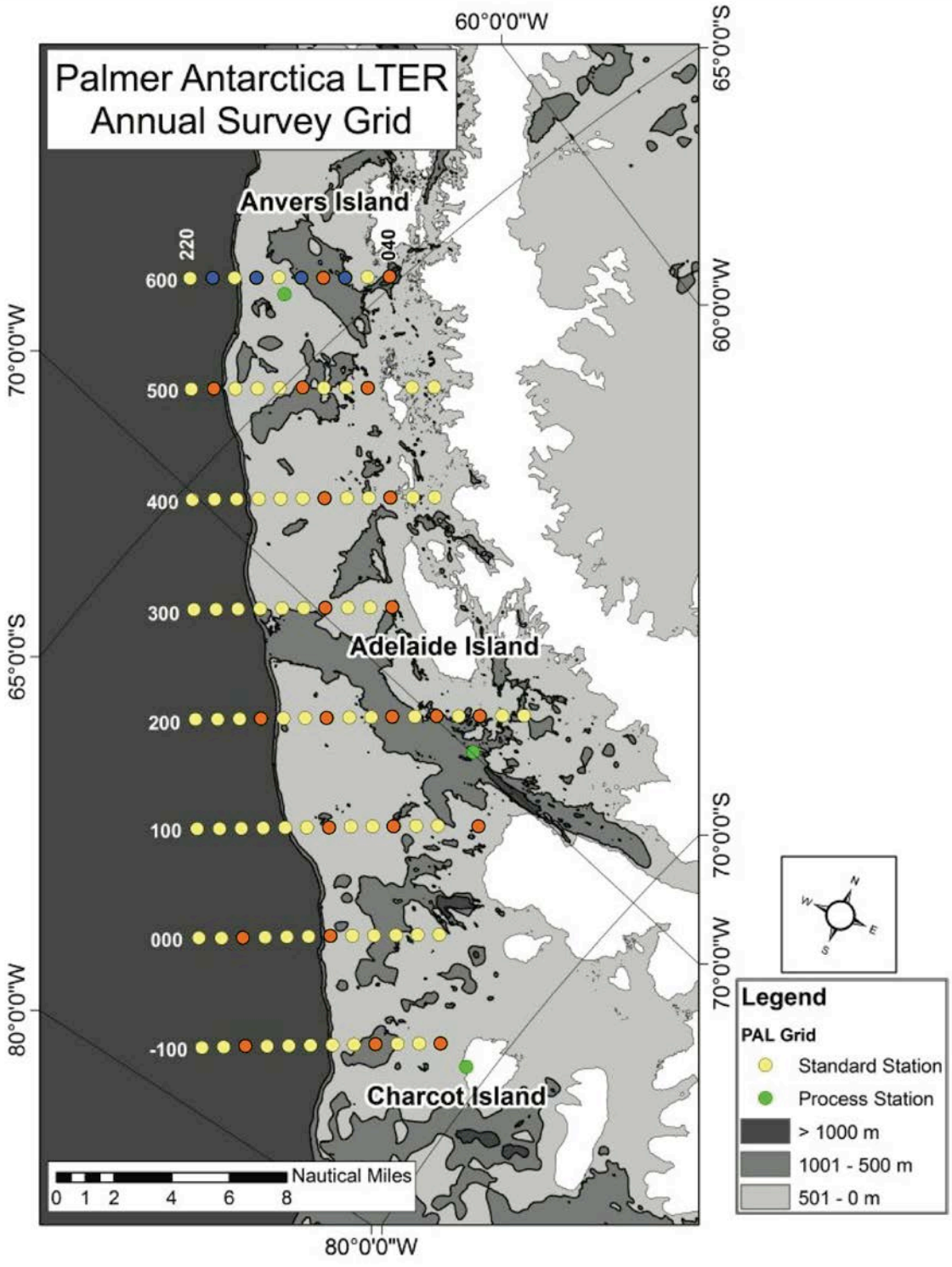
Palmer Antarctica LTER
Annual Survey Grid
Anvers Island
Adelaide Island
Charcot Island
220
040
600
500
400
300
200
100
000
-100
60°0'0"W
65°0'0"S
70°0'0"W
80°0'0"W
Nautical Miles
0 1 2 4 6 8
N
W
E
S
Legend
PAL Grid
Standard Station
Process Station
> 1000 m
1001 - 500 m
501 - 0 m

Figure B.2: Hydrography of the Palmer LTER study region. Water temperature **(top panel)** and salinity **(bottom panel)** from PAL LTER lines 200-500 averaged across summer (Dec 21-Mar 21) samples. Station numbers (using PAL LTER coding) roughly represent the distance from shore in km. Water mass (SSW, WW and CDW) definitions are from Church *et al.* (2003). The section plot was created using Ocean Data View (Schlitzer, 2014) with DIVA gridding. Data for this plot was obtained from the National Oceanographic Data Center's World Ocean Database 2009 (http://www.nodc.noaa.gov/OC5/WOD09/).

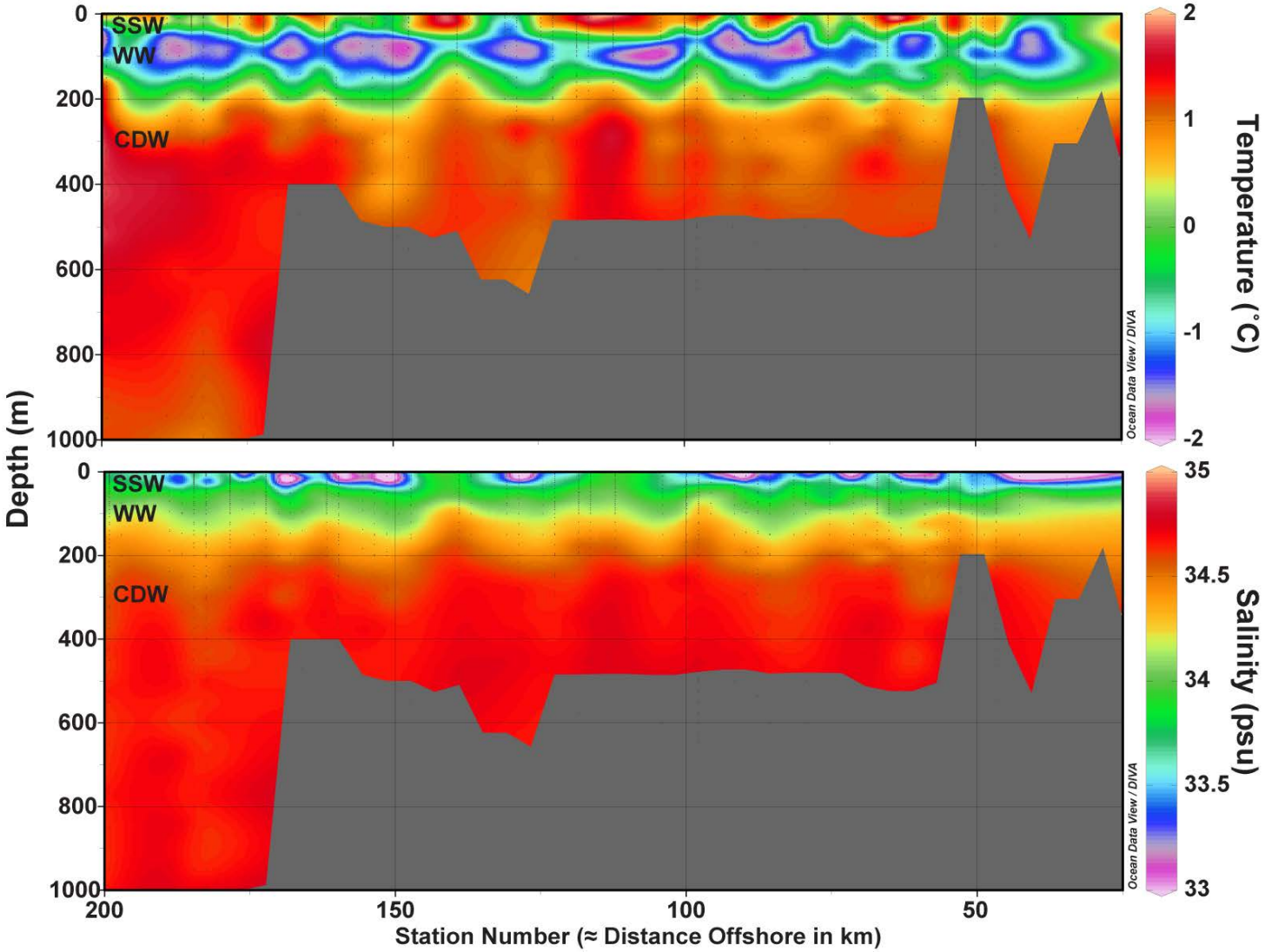
SSW
WW
CDW
Depth (m)
0
200
400
600
800
1000
Ocean Data View / DIVA
Temperature (°C)
2
1
0
-1
-2
35
34.5
34
33.5
33
Salinity (psu)
200
150
100
50
Station Number (≈ Distance Offshore in km)

Figure B.3: Water masses in Antarctic continental shelf waters West of the Antarctic Peninsula (WAP). Temperature versus salinity plot highlighting the differences among three major water masses sampled during Sept 2010 and Jan 2011; the outlier sample of AASW came from the pycnocline. Sigma-t (σ_t, a measure of density at a given temperature) is plotted as contours (dotted lines), with the freezing point of seawater indicated by a dashed line. CDW = Circumpolar Deep water, WW = Winter Water, AASW = Antarctic Surface Water. Figure courtesy Daniela Di Iorio, University of Georgia.

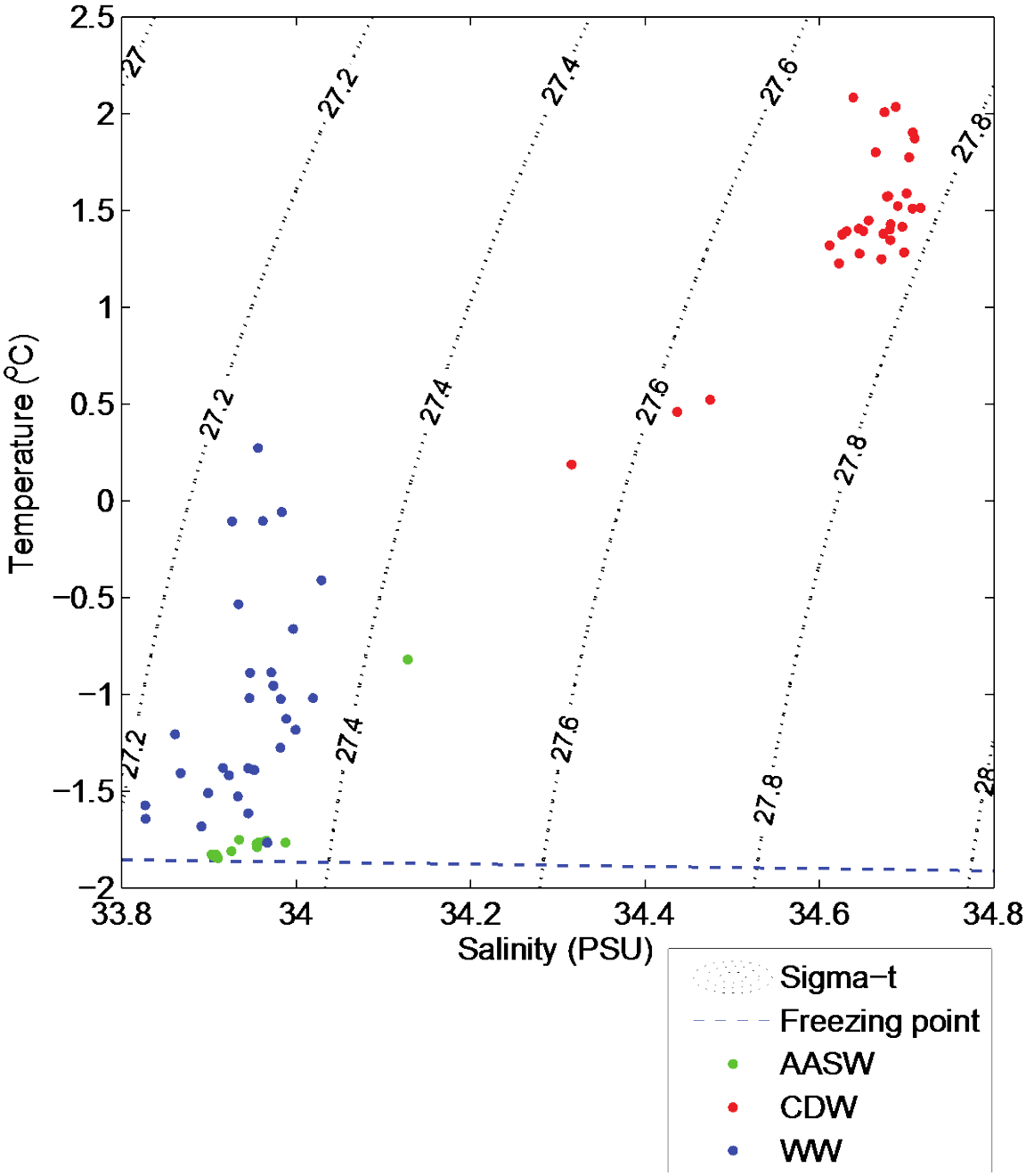
Temperature (°C)
Salinity (PSU)
2.5
2
1.5
1
0.5
0
−0.5
−1
−1.5
−2
33.8
34
34.2
34.4
34.6
34.8
27
27.2
27.4
27.6
27.8
28
Sigma−t
Freezing point
AASW
CDW
WW

Figure B.4: Sample cast data from LMG 10-06 and LMG 11-01. Temperature (blue), salinity (red), chlorophyll (chl) *a* fluorescence (green), and dissolved oxygen (black; LMG 11-01 only) plotted against depth (m). A dashed line represents the depth at which a given sample was collected. Samples collected from stations selected were used in pyrosequencing analysis.

LMG 10-06 Stn 600.160

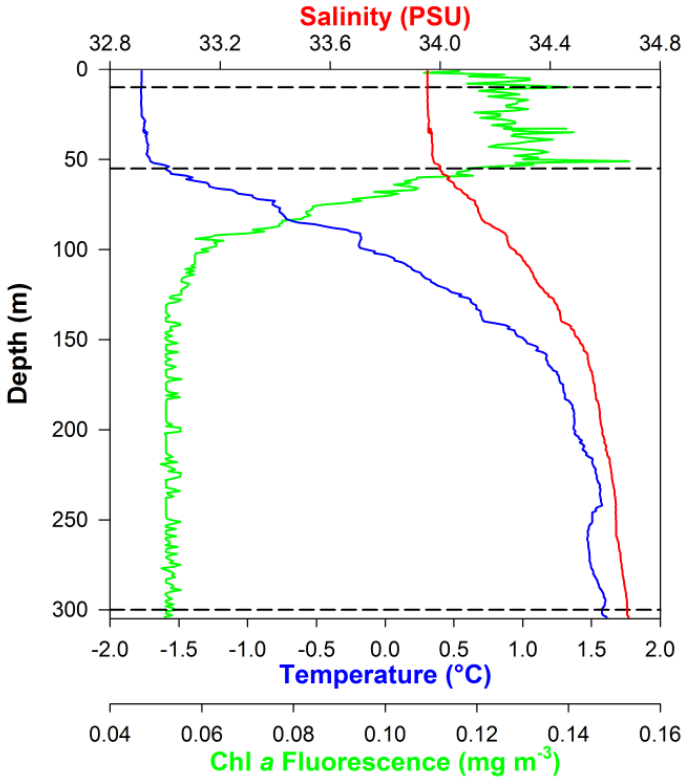

LMG 10-06 Stn 600.080

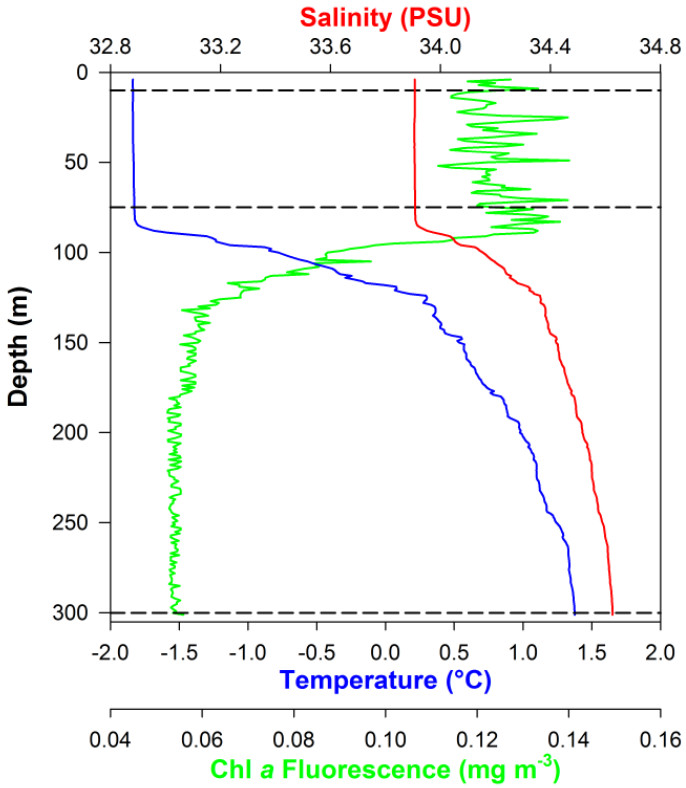

LMG 11-01 Stn 600.100

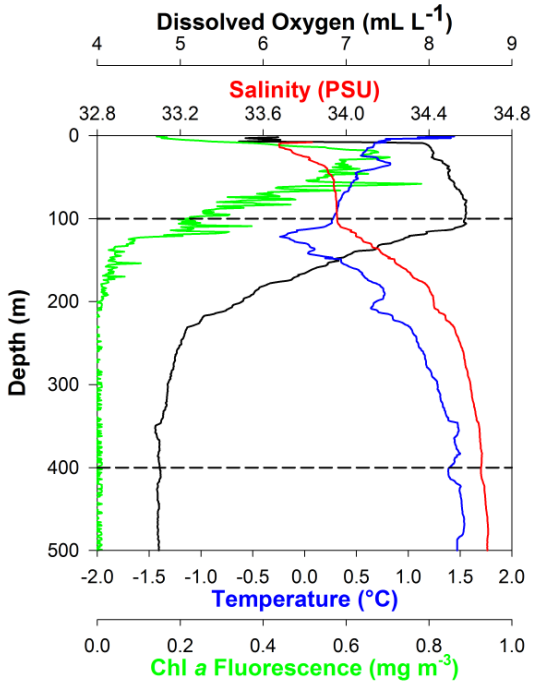

LMG 11-01 Stn 600.040

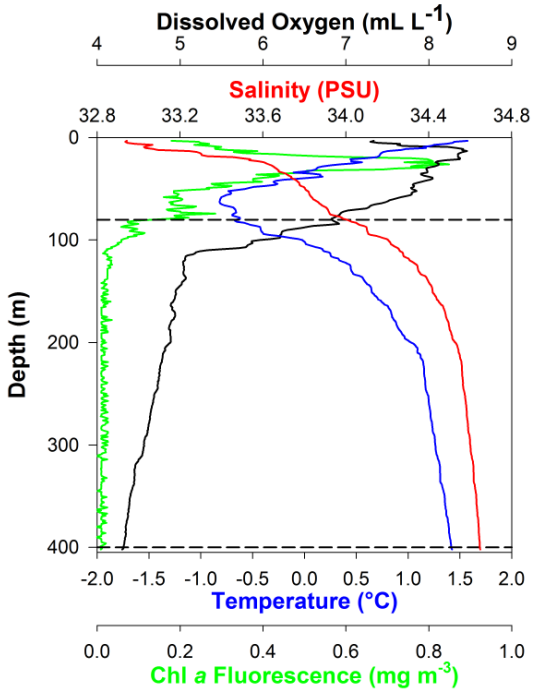

LMG 11-01 Stn 500.200

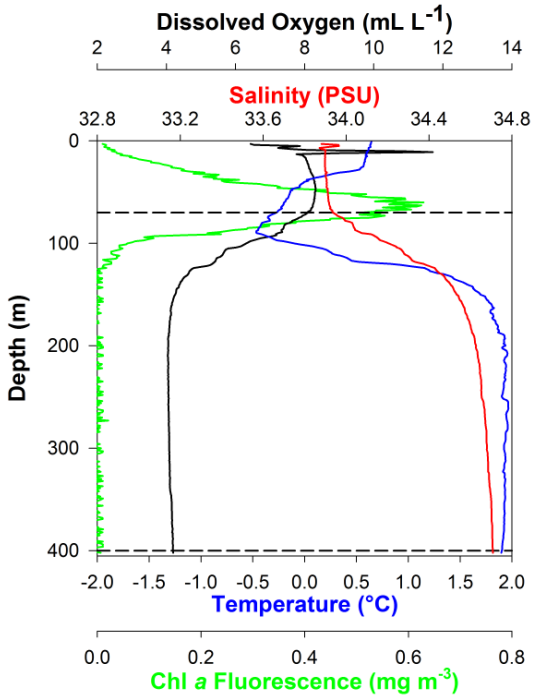

LMG 11-01 Stn 400.100

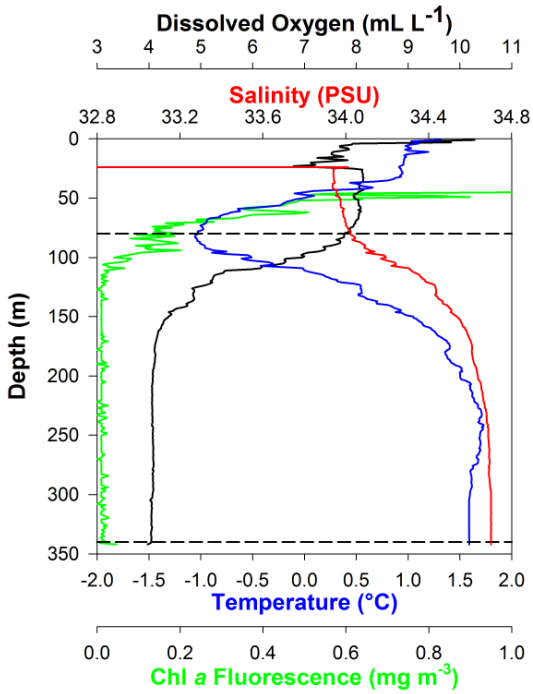

LMG 11-01 Stn 300.100

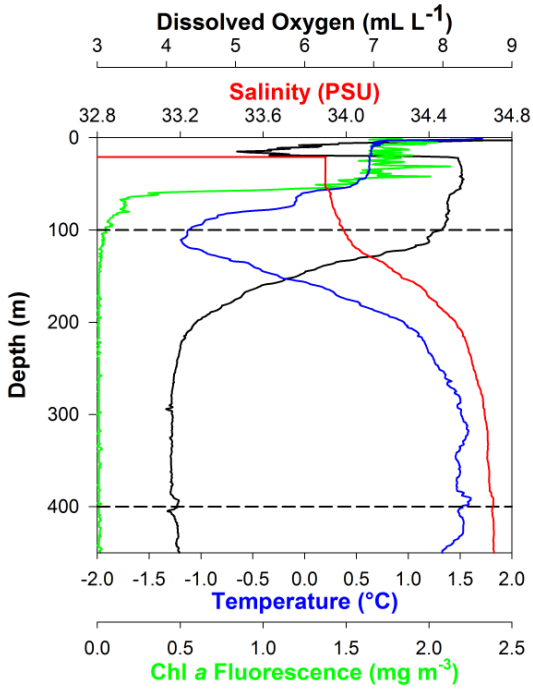

LMG 11-01 Stn 200.100

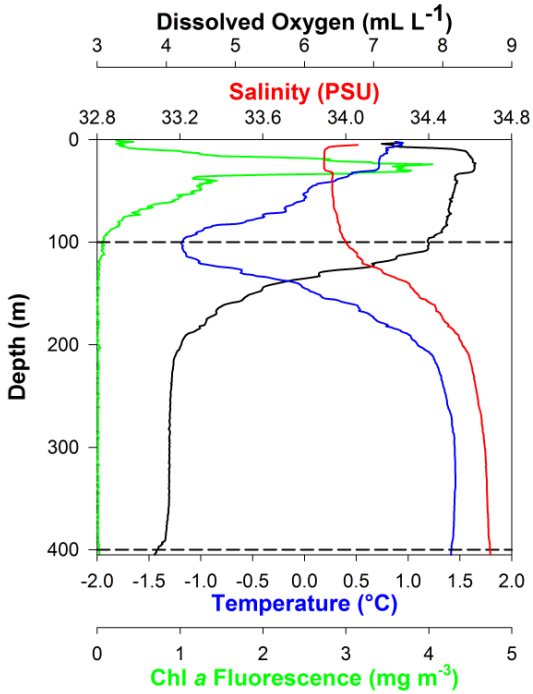

LMG 11-01 Stn 200.040

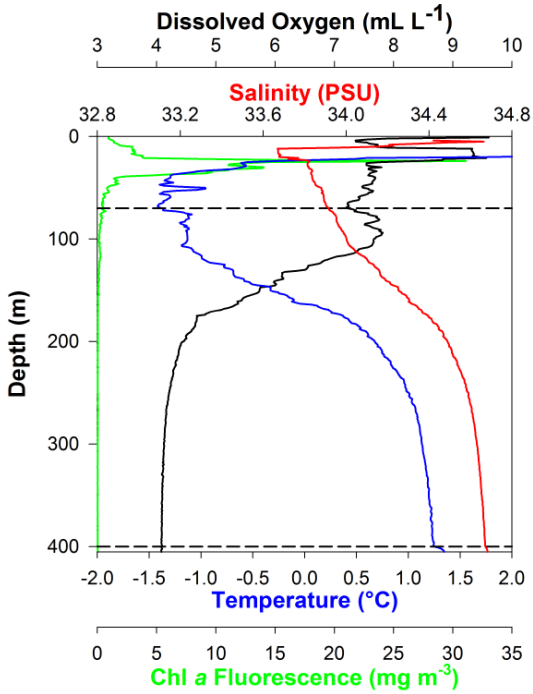

LMG 11-01 Stn 200.-040

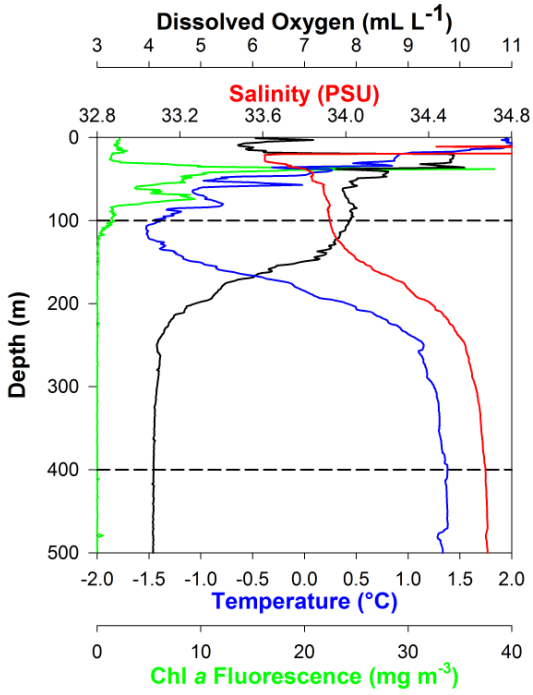

LMG 11-01 Stn 100.040

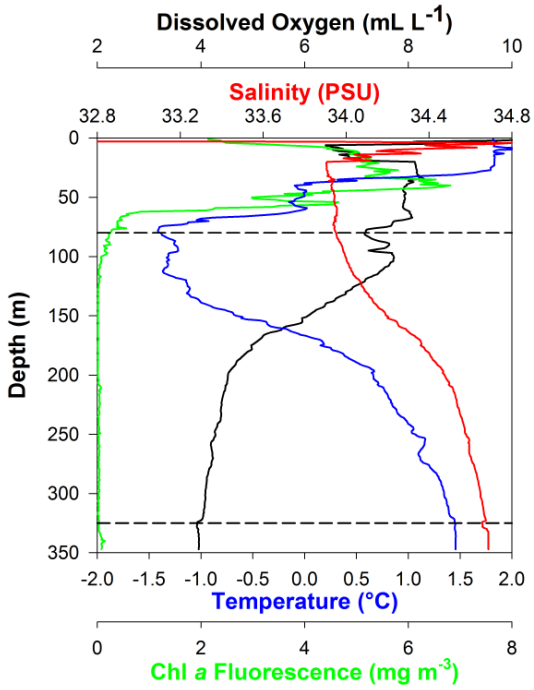

LMG 11-01 Stn 100.000

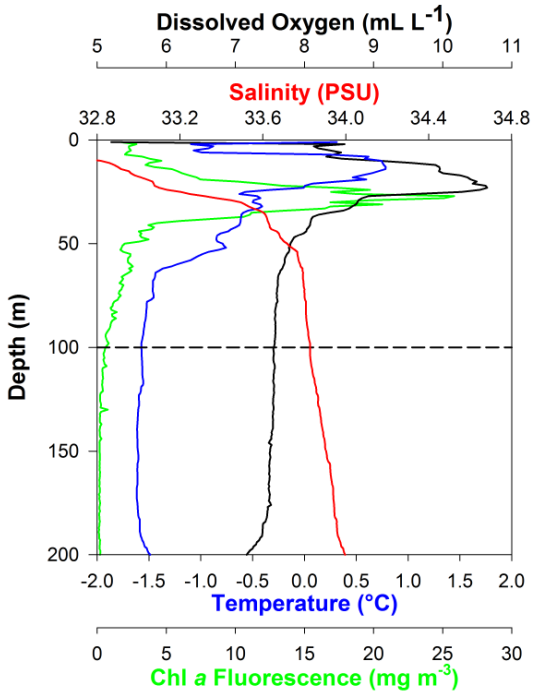

LMG 11-01 Stn 000.100

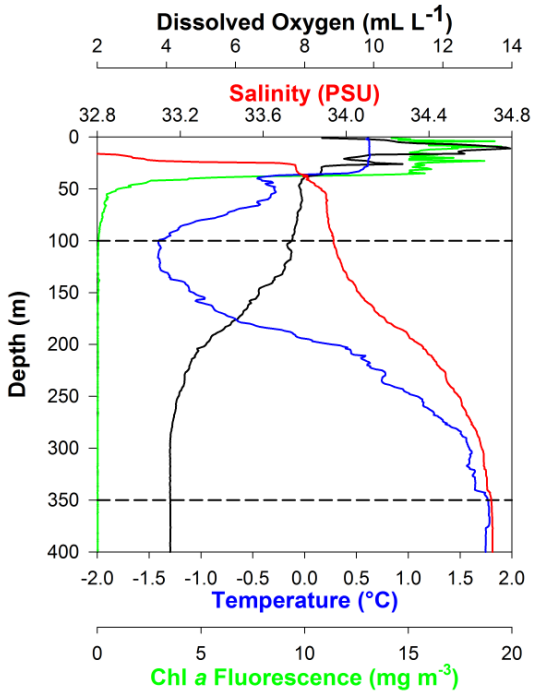

LMG 11-01 Stn -100.060

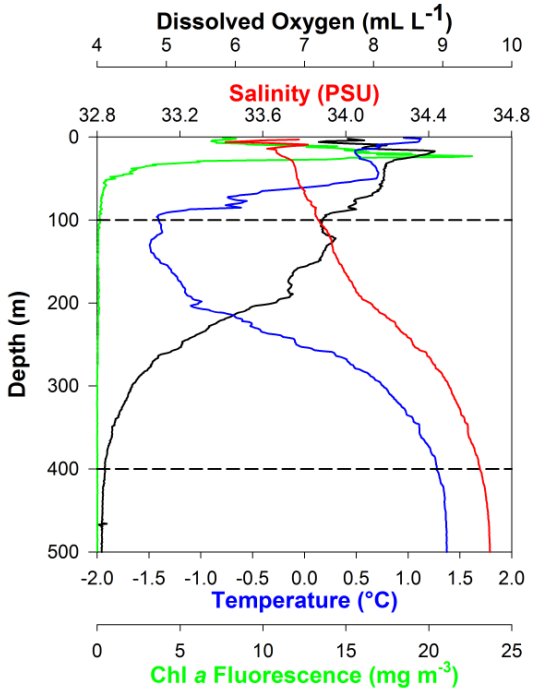

Figure B.5: Thaumarchaeota distribution in summer compared between 2006 and 2011. Gene abundance is plotted as a ratio of Thaumarchaeota *amoA* to *rrs*, against depth. Shapes represent water masses sampled, including Summer Surface Water (SSW; circles), Winter Water (WW; squares), and Circumpolar Deep Water (CDW; triangles). Samples were collected during January-February 2006 (Kalanetra *et al.*, 2009) and January 2011 (this study).

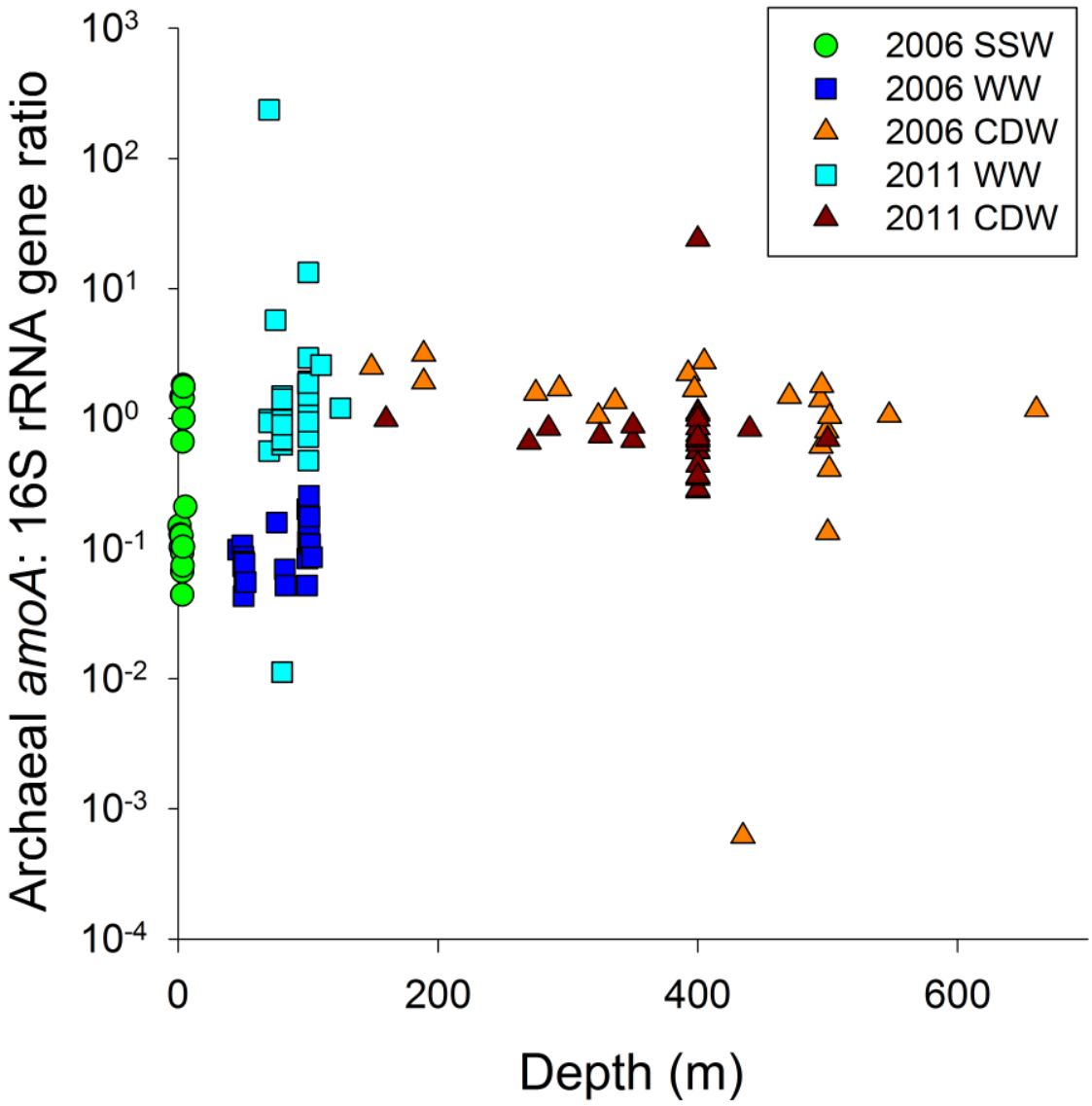
2006 SSW
2006 WW
2006 CDW
2011 WW
2011 CDW
Archaeal amoA: 16S rRNA gene ratio
10^3
10^2
10^1
10^0
10^-1
10^-2
10^-3
10^-4
0
200
400
600
Depth (m)

Figure B.6: Spatial distribution of Thaumarchaeota genes during LMG 11-01.

Distribution of Thaumarchaeota *rrs* **(a-b)** and *ureC* gene **(c-d)** abundance in WW **(a, c)** and CDW **(b, d)** masses of the Palmer LTER study region from summer (January 2011). Spatial plots were created with DIVA gridding using Ocean Data View (Schlitzer, 2014). Note that color scales are identical for panels **(a-c)**.

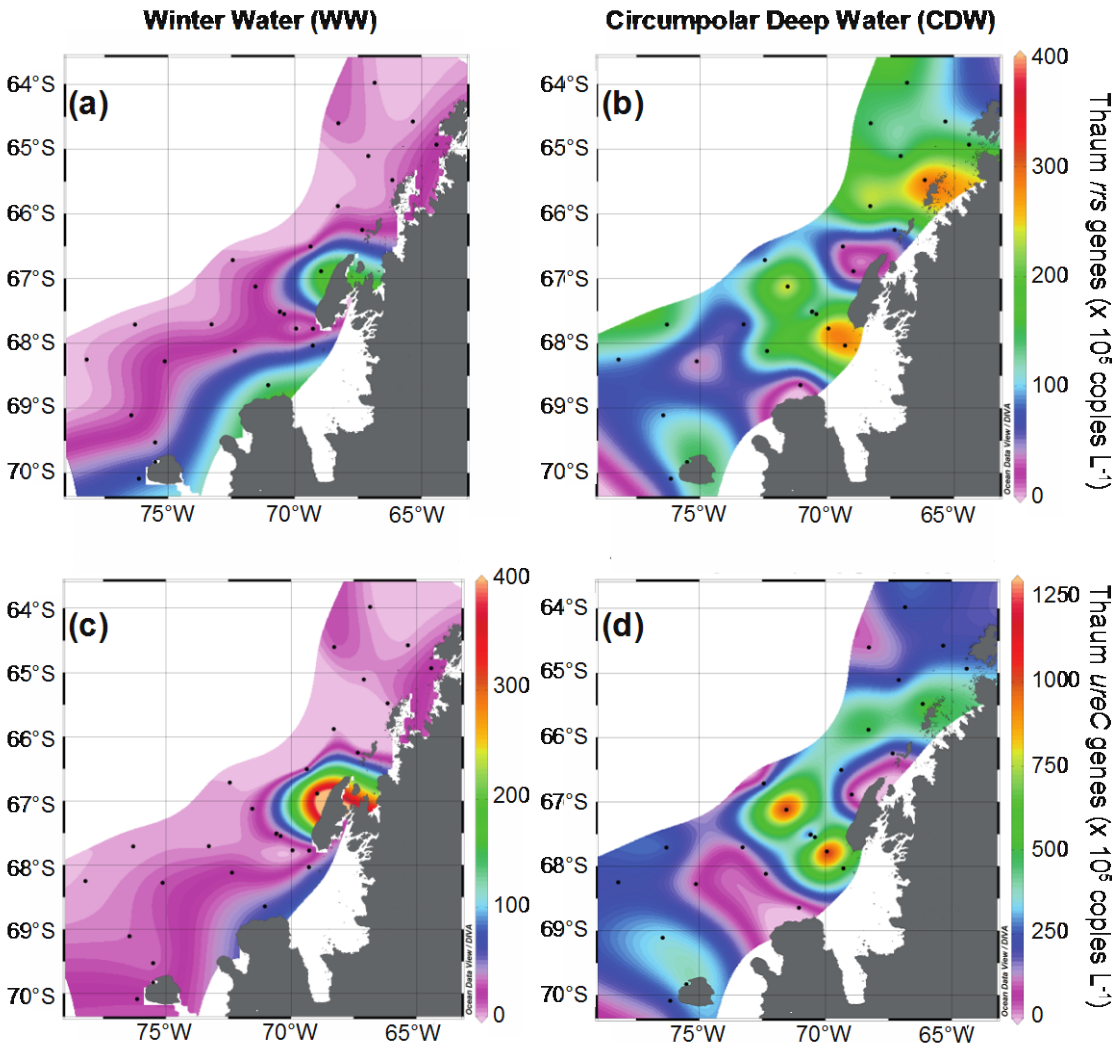
Winter Water (WW)
Circumpolar Deep Water (CDW)
(a)
(b)
(c)
(d)
64°S
65°S
66°S
67°S
68°S
69°S
70°S
75°W
70°W
65°W
400
300
200
100
0
1250
1000
750
500
250
Thaum rrs genes (x 10⁵ copies L⁻¹)
Thaum ureC genes (x 10⁵ copies L⁻¹)
Ocean Data View / DIVA

Figure B.7: Ratios of archaeal *amoA*:Thaumarchaeota *rrs* calculated using different primers. Archaeal *amoA* genes were quantified using either **(a)** Wuchter *et al.* (2006) or **(b)** Francis *et al*. (2005) primer sets. The line represents the expected ratio of 1 *amoA* gene copy per *rrs* gene, based on their copy numbers in sequenced Thaumarchaeota genomes.

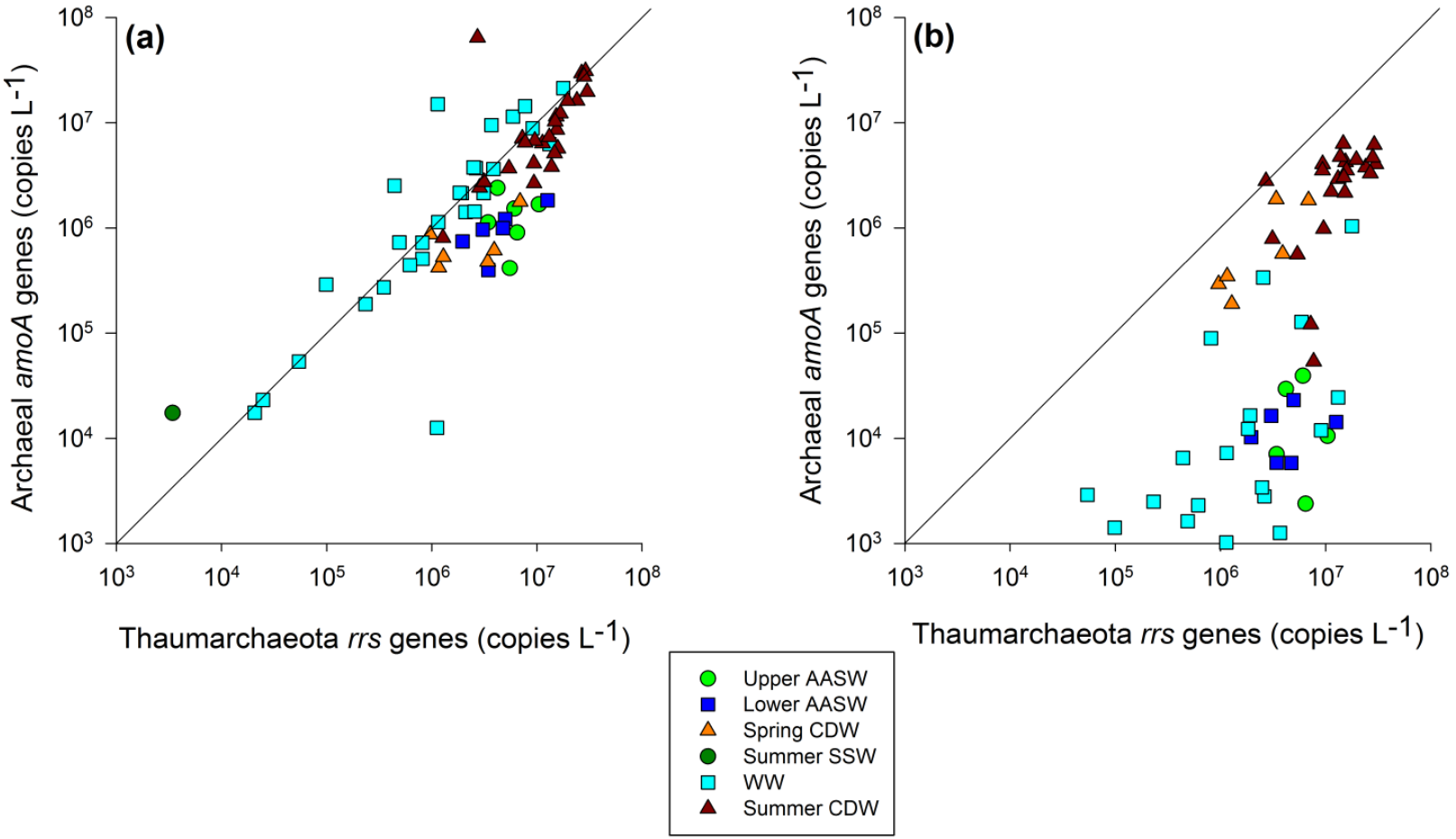
(a)
(b)
Archaeal amoA genes (copies L-1)
Thaumarchaeota rrs genes (copies L-1)
10^3
10^4
10^5
10^6
10^7
10^8
Upper AASW
Lower AASW
Spring CDW
Summer SSW
WW
Summer CDW

Figure B.8: Thaumarchaeota *ureC* gene abundance compared to (a) archaeal *amoA* and (b) Thaumarchaeota *rrs* genes. Line represents the expected ratio of 1 *ureC* gene copy per *rrs* or *amoA* gene based on their copy numbers in sequenced Thaumarchaeota genomes.

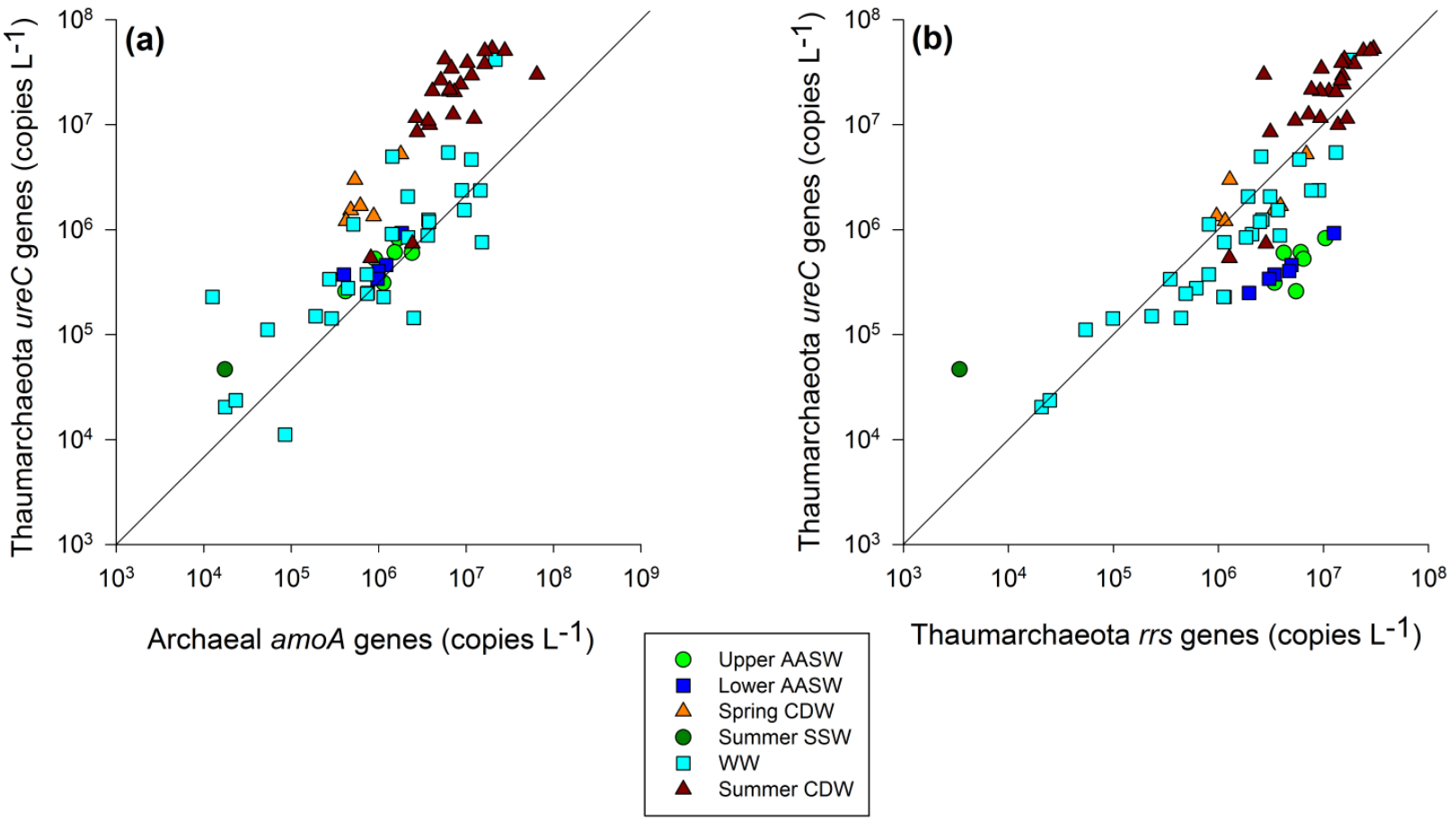
(a)
(b)
Thaumarchaeota ureC genes (copies L-1)
Archaeal amoA genes (copies L-1)
Thaumarchaeota rrs genes (copies L-1)
Upper AASW
Lower AASW
Spring CDW
Summer SSW
WW
Summer CDW

Figure B.9: Ammonia oxidation (AO) rates versus Thaumarchaeota abundance and *amoA* transcription. Measured ^{15}N-AO rates plotted against **(a)** Thaumarchaeota *rrs* genes or **(b)** *amoA* transcripts.

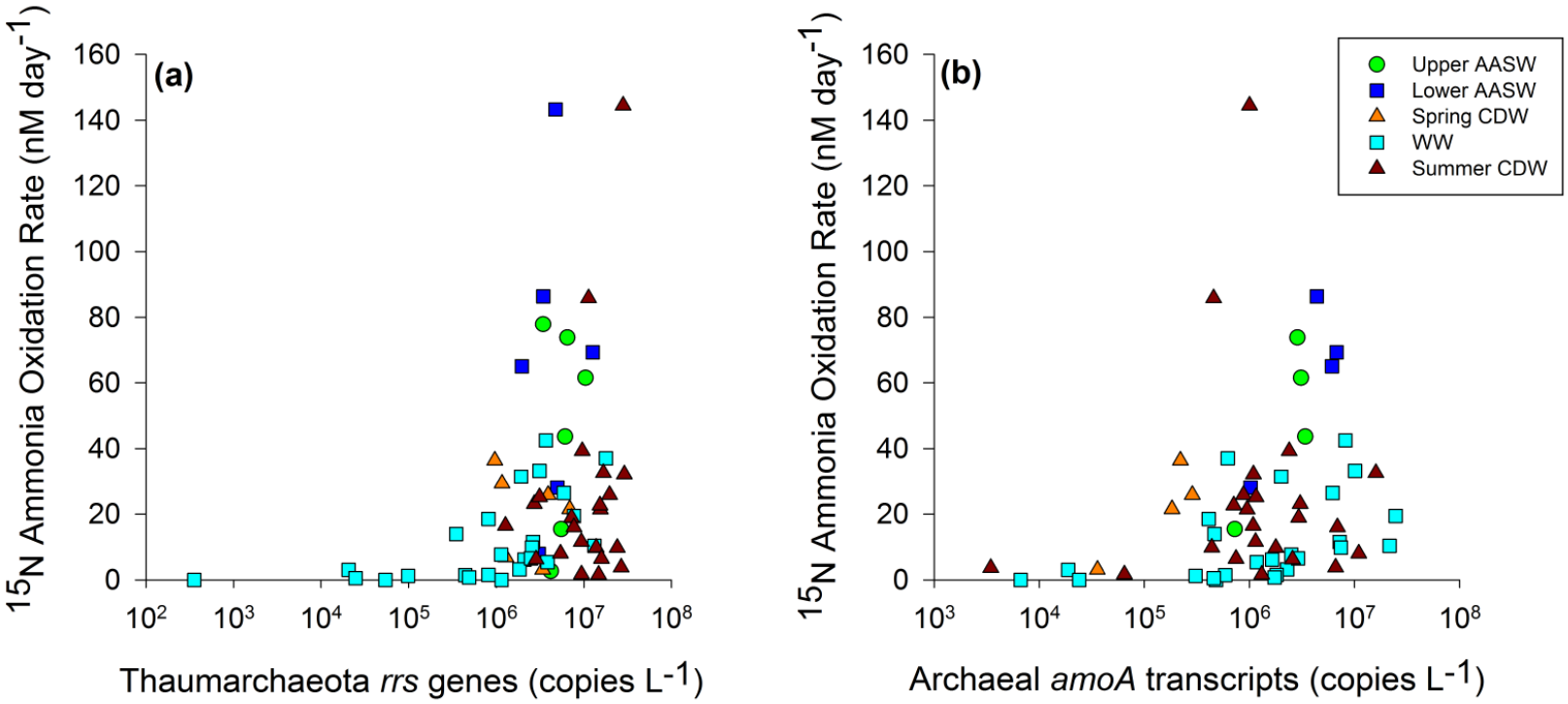
(a)
(b)
^{15}N Ammonia Oxidation Rate (nM day^{-1})
Thaumarchaeota *rrs* genes (copies L^{-1})
Archaeal *amoA* transcripts (copies L^{-1})
Upper AASW
Lower AASW
Spring CDW
WW
Summer CDW

Figure B.10: Distribution of OTUs among water masses. Venn diagrams of OTUs obtained from pyrosequencing samples from **(a-b)** all water masses, **(c-d)** Antarctic Surface Water (AASW) and Winter Water (WW) from the LTER 600 line only, and **(e-f)** Circumpolar Deep Water (CDW) from the LTER 600 line only. Figures show both Thaumarchaeota *rrs* (98% similarity; **a, c, e**) and Archaea *amoA* (97% similarity; **b, d, f**) OTU distributions determined using mothur (Schloss *et al.*, 2009), with singleton OTUs removed. Tables include information on the number of OTUs and sequences from a given water mass, as well as the total number of sequences shared for all water masses shown (the number of shared OTUs is reflected in the figure).

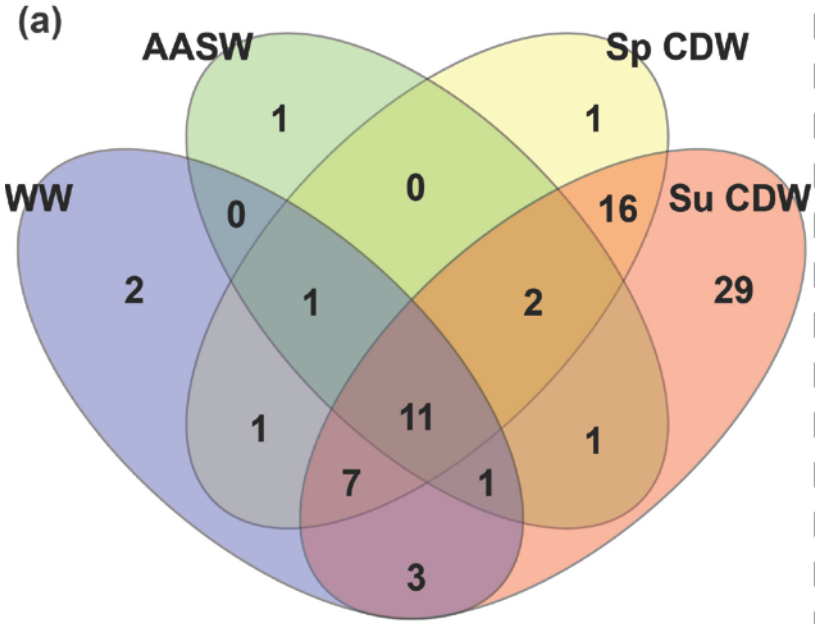

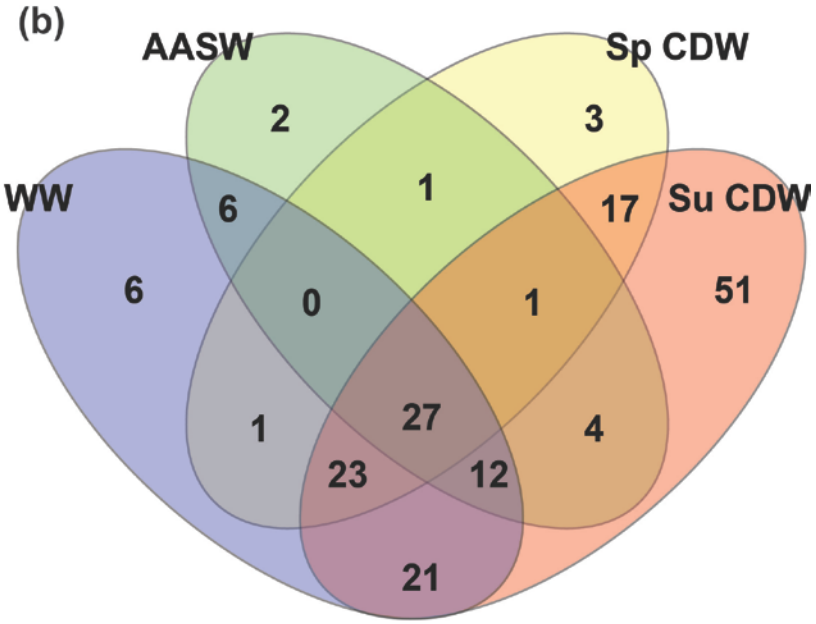

rrs	# OTUs	# Seqs		AASW	Sp CDW	WW	Su CDW
AASW	17	91,480	AASW		114,317	262,601	203,063
Sp CDW	39	22,913	Sp CDW	114,317		194,027	134,741
WW	26	171,169	WW	262,601	194,027		282,856
Su CDW	70	112,037	Su CDW	203,063	134,741	282,856	
Total	76	397,008	Shared # Sequences				

amoA	# OTUs	# Seqs		AASW	Sp CDW	WW	Su CDW
AASW	53	25,358	AASW		33,992	93,644	74,970
Sp CDW	73	8,853	Sp CDW	33,992		76,915	58,563
WW	96	68,427	WW	93,644	76,915		118,243
Su CDW	156	50,076	Su CDW	74,970	58,563	118,243	
Total	175	151,499	Shared # Sequences				

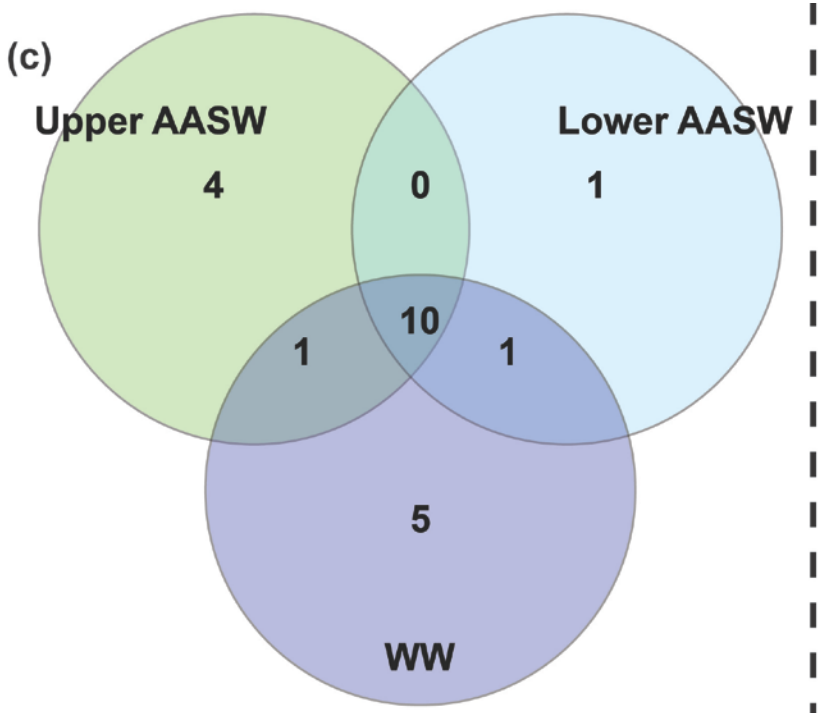

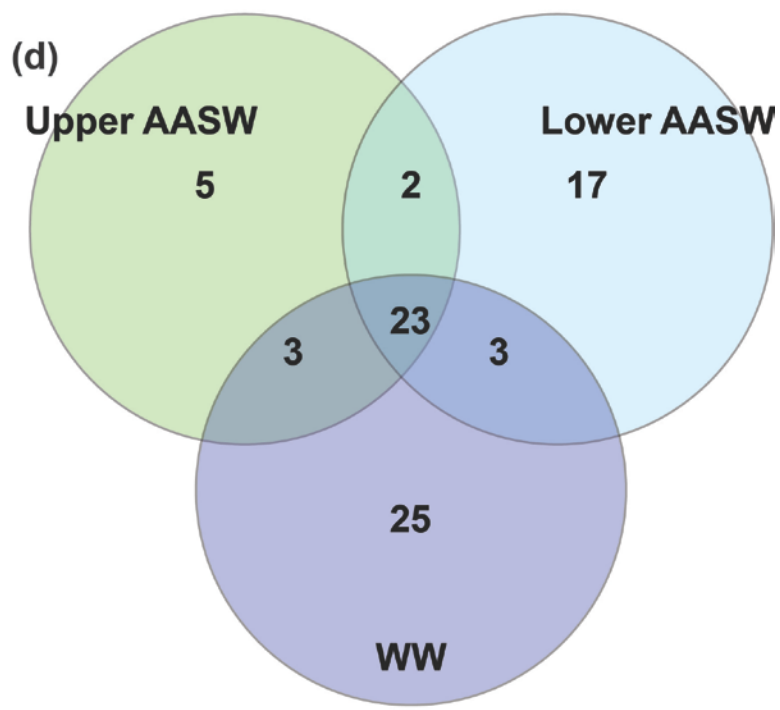

rrs	# OTUs	# Seqs		UAASW	LAASW	WW
UAASW	15	27,226	UAASW		91,457	53,560
LAASW	12	64,254	LAASW	91,457		90,604
WW	17	26,361	WW	53,560	90,604	
Total	10	117,808	Shared # Sequences			

amoA	# OTUs	# Seqs		UAASW	LAASW	WW
UAASW	33	12,722	UAASW		25,320	21,751
LAASW	45	12,636	LAASW	25,320		21,649
WW	54	9,085	WW	21,751	21,649	
Total	104	34,341	Shared # Sequences			

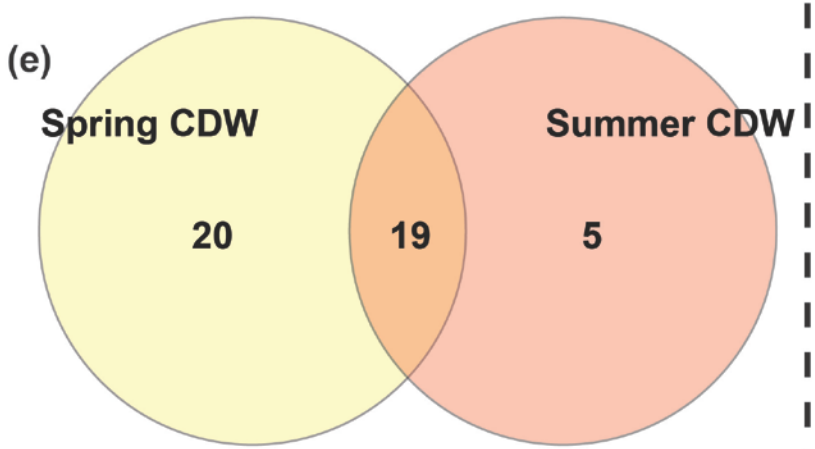

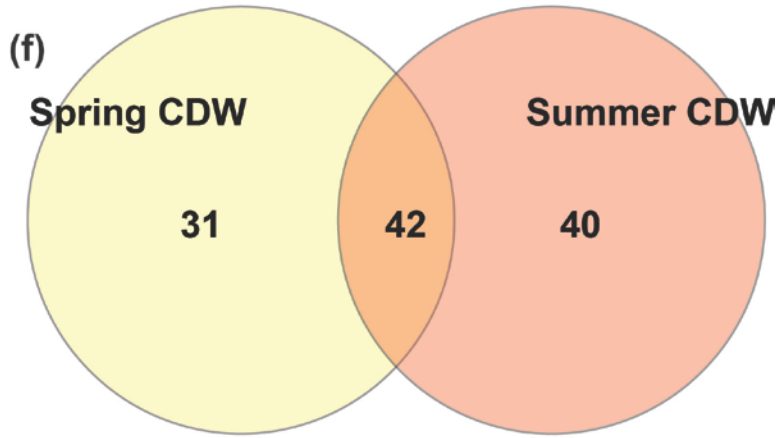

rrs	# OTUs	# Seqs		Spring	Summer
Spring	39	22,913	Spring		40,200
Summer	24	17,351	Summer	40,200	
Total	44	40,200	Shared # Sequences		

amoA	# OTUs	# Seqs		Spring	Summer
Spring	73	8,853	Spring		16,584
Summer	82	7,877	Summer	16,584	
Total	113	16,584	Shared # Sequences		

Figure B.11: Phylogenetic tree of Thaumarchaeota *rrs* genes. Sequences obtained by pyrosequencing (353 bp) were aligned against the SILVA database (Quast *et al.*, 2013), which was also used to construct the tree with OTU representatives set at 98% similarity. Numbers following each OTU represent the number of sequences and the % of total sequences. For the two major clusters (defined by sequences with 95% similarity), additional percentages indicate the distribution of sequences among water masses (AASW, WW, CDW). OTU colors are shaded by the proportion of sequences obtained from each water mass. Sequences labeled "ANT 2006" are from the Kalanetra *et al.* (2009) study. Only bootstrap values ≥50% are shown.

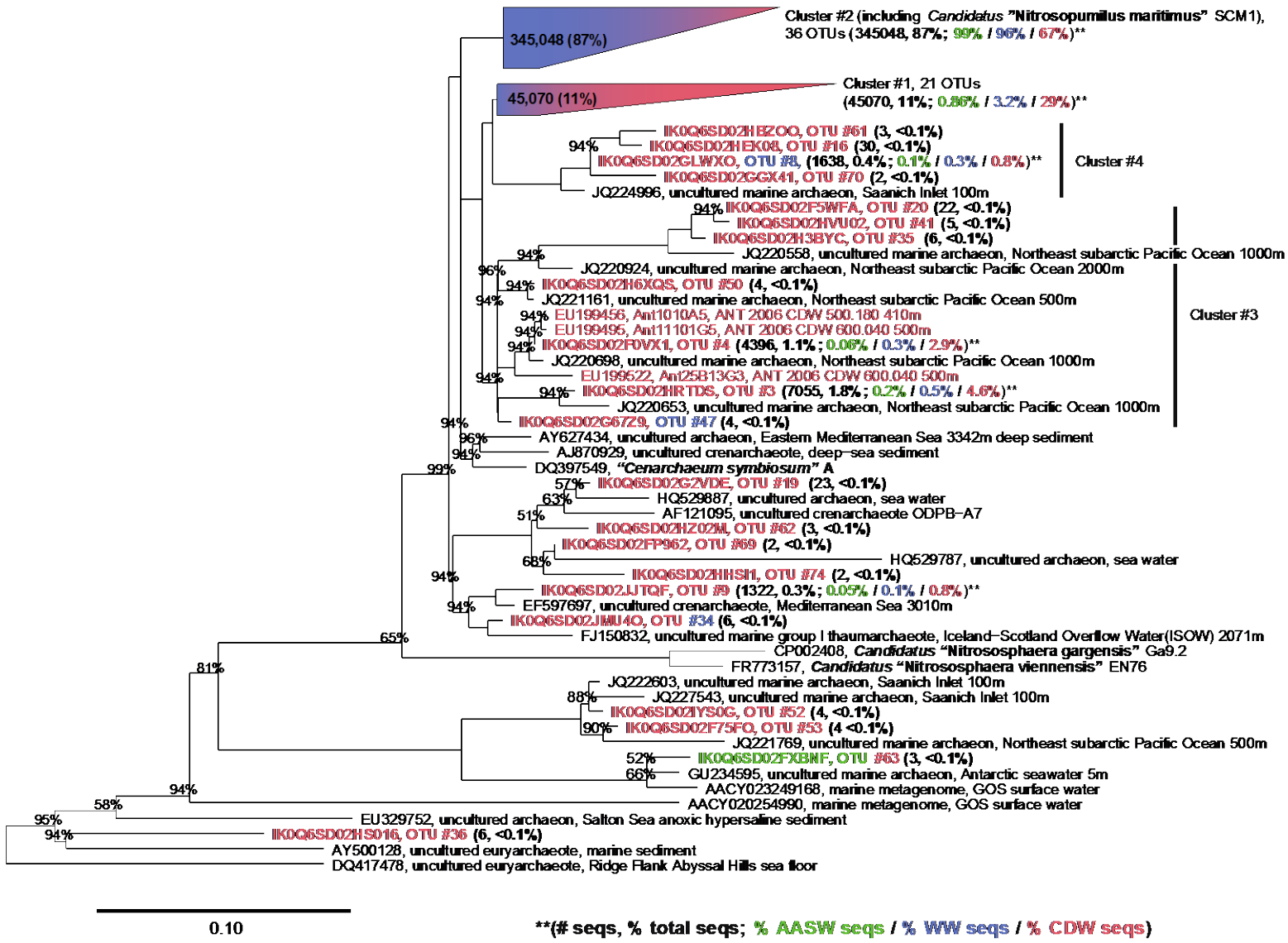
Cluster #2 (including Candidatus "Nitrosopumilus maritimus" SCM1), 36 OTUs (345048, 87%; 99% / 96% / 67%)**
345,048 (87%)
Cluster #1, 21 OTUs (45070, 11%; 0.86% / 3.2% / 29%)**
45,070 (11%)
IK0Q6SD02HBZOO, OTU #61 (3, <0.1%)
IK0Q6SD02HEK08, OTU #16 (30, <0.1%)
IK0Q6SD02GLWXO, OTU #8, (1638, 0.4%; 0.1% / 0.3% / 0.8%)**
IK0Q6SD02GGX41, OTU #70 (2, <0.1%)
JQ224996, uncultured marine archaeon, Saanich Inlet 100m
Cluster #4
IK0Q6SD02F5WFA, OTU #20 (22, <0.1%)
IK0Q6SD02HVU02, OTU #41 (5, <0.1%)
IK0Q6SD02H3BYC, OTU #35 (6, <0.1%)
JQ220558, uncultured marine archaeon, Northeast subarctic Pacific Ocean 1000m
JQ220924, uncultured marine archaeon, Northeast subarctic Pacific Ocean 2000m
IK0Q6SD02H6XQS, OTU #50 (4, <0.1%)
JQ221161, uncultured marine archaeon, Northeast subarctic Pacific Ocean 500m
EU199456, Ant1010A5, ANT 2006 CDW 500.180 410m
EU199496, Ant111101G5, ANT 2006 CDW 600.040 500m
IK0Q6SD02F0VX1, OTU #4 (4396, 1.1%; 0.06% / 0.3% / 2.9%)**
JQ220698, uncultured marine archaeon, Northeast subarctic Pacific Ocean 1000m
EU199522, Ant25B13G3, ANT 2006 CDW 600.040 500m
IK0Q6SD02HRTDS, OTU #3 (7055, 1.8%; 0.2% / 0.5% / 4.6%)**
JQ220653, uncultured marine archaeon, Northeast subarctic Pacific Ocean 1000m
Cluster #3
IK0Q6SD02G67Z9, OTU #47 (4, <0.1%)
AY627434, uncultured archaeon, Eastern Mediterranean Sea 3342m deep sediment
AJ870929, uncultured crenarchaeote, deep-sea sediment
DQ397549, "Cenarchaeum symbiosum" A
IK0Q6SD02G2VDE, OTU #19 (23, <0.1%)
HQ529887, uncultured archaeon, sea water
AF121095, uncultured crenarchaeote ODPB-A7
IK0Q6SD02HZ02M, OTU #62 (3, <0.1%)
IK0Q6SD02FP962, OTU #69 (2, <0.1%)
HQ529787, uncultured archaeon, sea water
IK0Q6SD02HHSI1, OTU #74 (2, <0.1%)
IK0Q6SD02JJTQF, OTU #9 (1322, 0.3%; 0.05% / 0.1% / 0.8%)**
EF597697, uncultured crenarchaeote, Mediterranean Sea 3010m
IK0Q6SD02JMU4O, OTU #34 (6, <0.1%)
FJ150832, uncultured marine group I thaumarchaeote, Iceland-Scotland Overflow Water(ISOW) 2071m
CP002408, Candidatus "Nitrososphaera gargensis" Ga9.2
FR773157, Candidatus "Nitrososphaera viennensis" EN76
JQ222603, uncultured marine archaeon, Saanich Inlet 100m
JQ227543, uncultured marine archaeon, Saanich Inlet 100m
IK0Q6SD02IYS0G, OTU #52 (4, <0.1%)
IK0Q6SD02F75FO, OTU #53 (4 <0.1%)
JQ221769, uncultured marine archaeon, Northeast subarctic Pacific Ocean 500m
IK0Q6SD02FXBNF, OTU #63 (3, <0.1%)
GU234595, uncultured marine archaeon, Antarctic seawater 5m
AACY023249168, marine metagenome, GOS surface water
AACY020254990, marine metagenome, GOS surface water
EU329752, uncultured archaeon, Salton Sea anoxic hypersaline sediment
IK0Q6SD02HSO16, OTU #36 (6, <0.1%)
AY500128, uncultured euryarchaeote, marine sediment
DQ417478, uncultured euryarchaeote, Ridge Flank Abyssal Hills sea floor
0.10
**(# seqs, % total seqs; % AASW seqs / % WW seqs / % CDW seqs)

Figure B.12: Statistical analysis of data from LMG10-06. (a) Principal Components Analysis (PCA) plot of samples arrayed in environmental data space displayed on the first two principal components axes, which represent 69.7% of the variability in the dataset. **(b)** Nonmetric Multidimensional Scaling (NMDS) plot of samples based on qPCR-estimates of gene abundances. Graphs highlight distinct features of Winter Water (WW) and Circumpolar Deep Water (CDW) masses, and show that gene distributions in Antarctic Surface Water (AASW) samples closely match those in the WW layer.

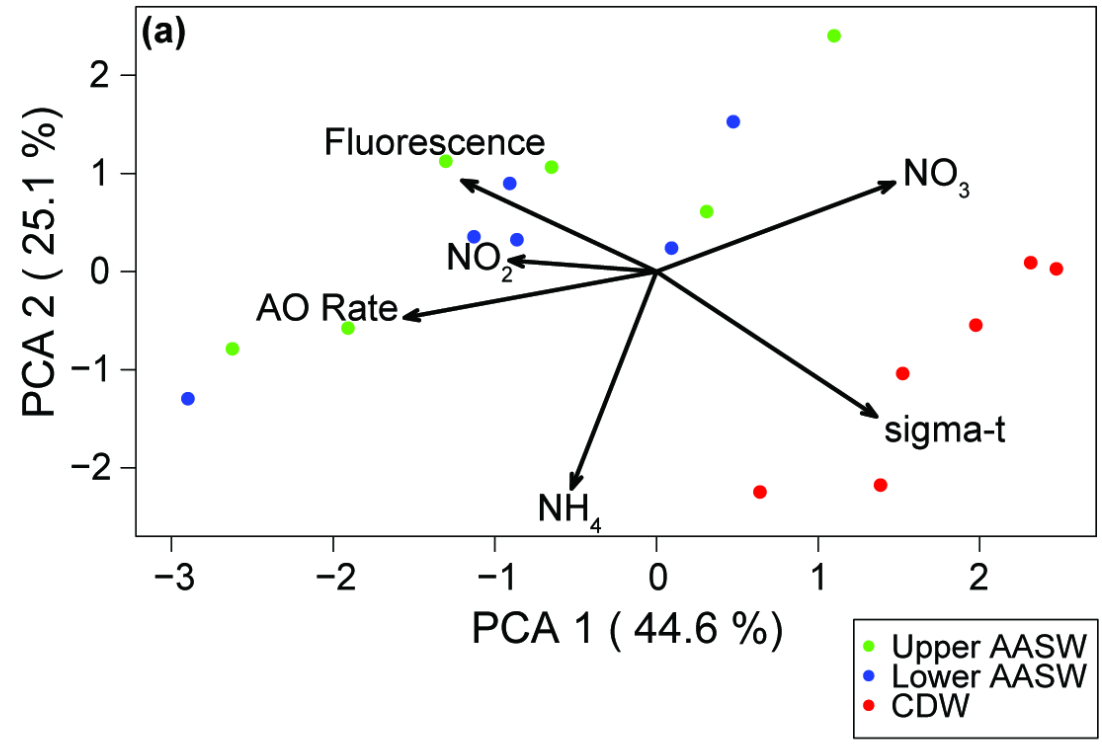
(a)
Fluorescence
NO3
NO2
AO Rate
sigma-t
NH4
PCA 2 (25.1 %)
PCA 1 (44.6 %)
Upper AASW
Lower AASW
CDW

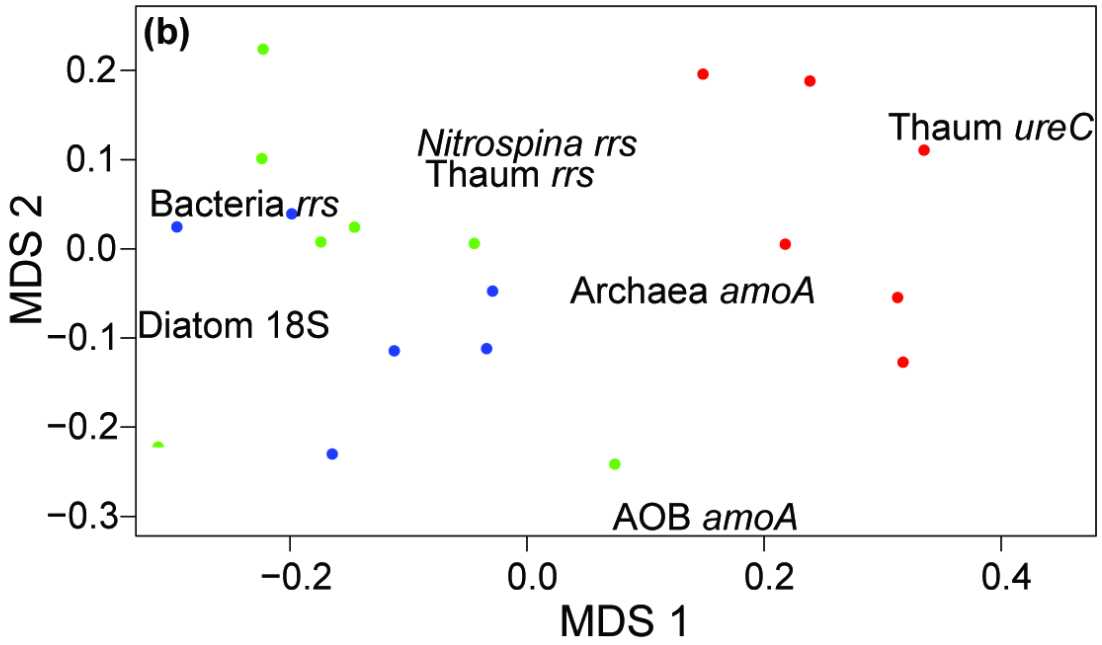
(b)
Nitrospina rrs
Thaum rrs
Thaum ureC
Bacteria rrs
Archaea amoA
Diatom 18S
AOB amoA
MDS 2
MDS 1

Figure B.13: Statistical plots from OTU data obtained by 454 Pyrosequencing. Nonmetric Multidimensional Scaling (NMDS) plots showing Thaumarchaeota *rrs* **(a)** and Archaeal *amoA* **(b)** OTUs. Singleton OTUs were excluded from analysis and OTUs containing two or three sequences were used to construct NMDS plots but were removed for clarity (*rrs* OTUs R55-R77; *amoA* OTUs A98-A176). **(c)** Principal Components Analysis (PCA) plot of samples used for pyrosequencing arrayed in environmental data space; AO = ammonia oxidation. Samples are plotted against the first two axes, which represent 57.1% of the variability in the dataset. The distinction between Winter Water (WW) and Circumpolar Deep Water (CDW) layers is again reflected in this data, with Antarctic Surface Water (AASW) samples grouping with those from the WW layer.

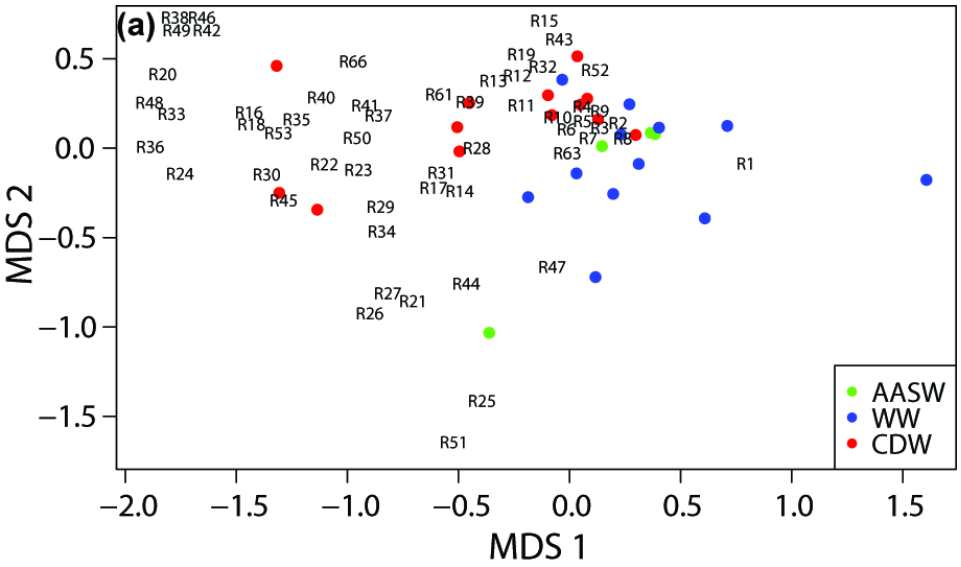
(a)
MDS 2
MDS 1
AASW
WW
CDW

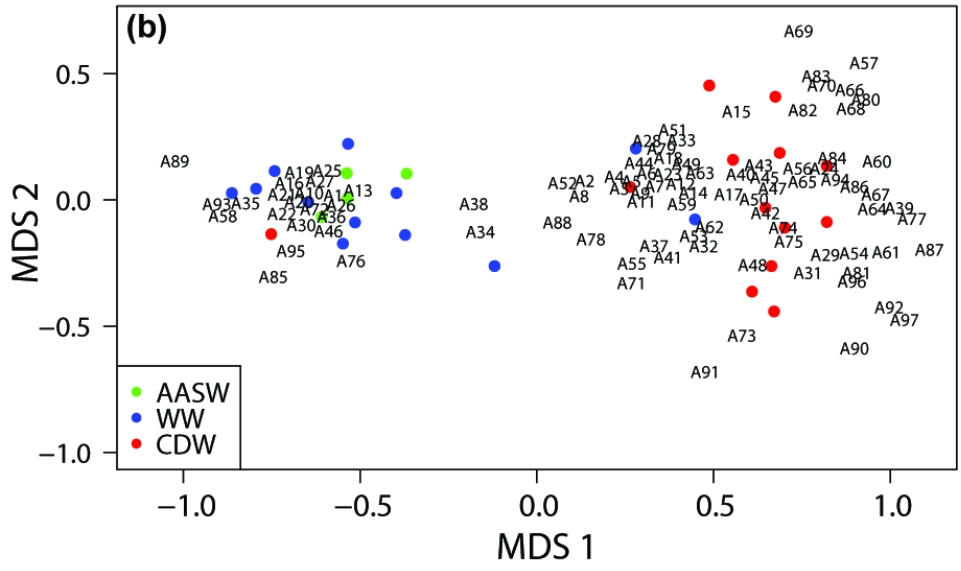
(b)
MDS 2
MDS 1
AASW
WW
CDW

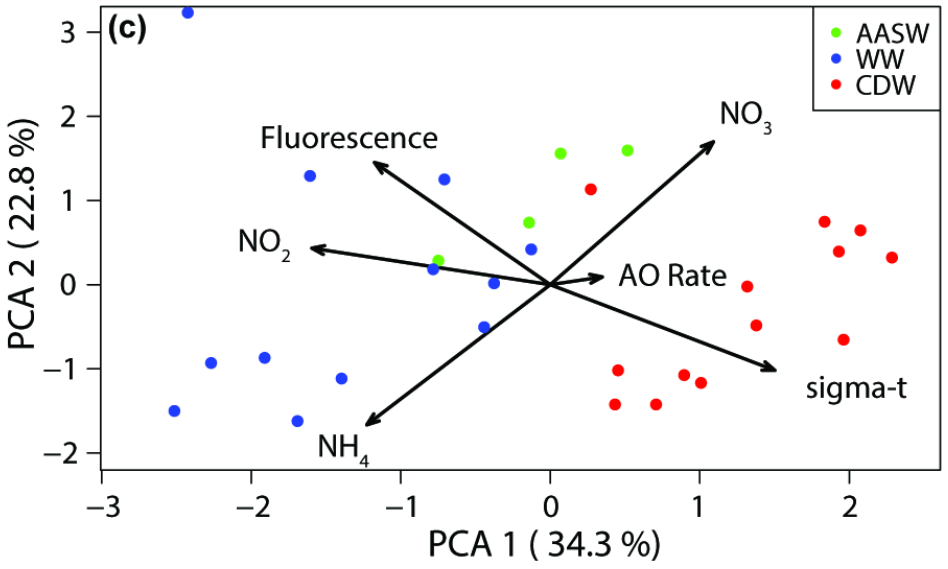
(c)
PCA 2 (22.8 %)
PCA 1 (34.3 %)
Fluorescence
NO3
NO2
AO Rate
sigma-t
NH4
AASW
WW
CDW

Figure B.14: Comparison of prokaryotic abundance measurements. Estimates of prokaryote abundance (Bacteria + Thaumarchaeota) in samples collected during LMG 11-01, were made using *rrs* gene abundance determined by qPCR and corrected using an average of 1.8 Bacteria *rrs* genes per genome (Biers *et al.*, 2009). Flow cytometric cell counts are courtesy of the Palmer LTER (http://pal.lternet.edu/). Samples are coded based on water mass: WW = Winter Water, CDW = Circumpolar Deep Water. Regression includes all data points.

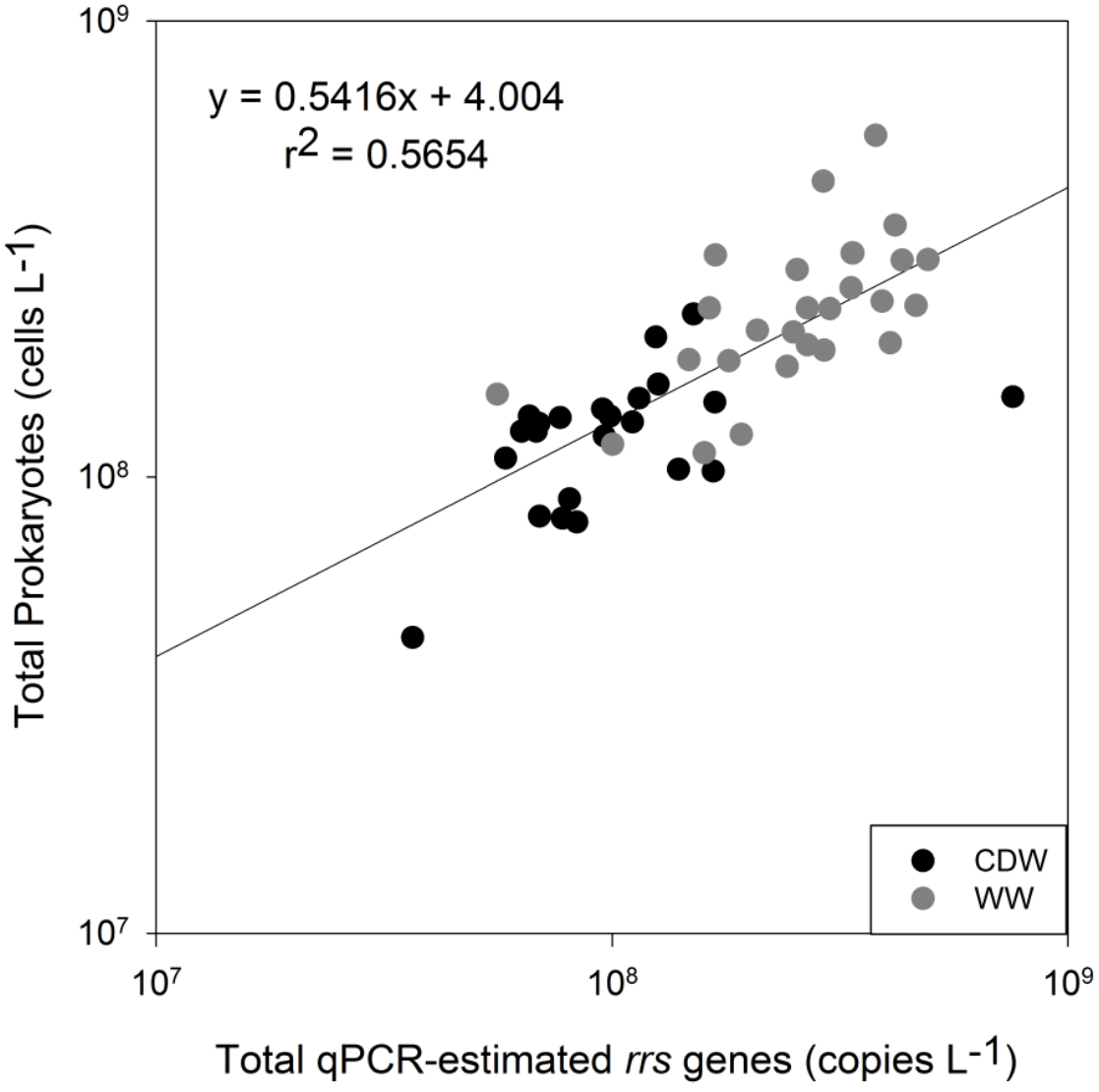
y = 0.5416x + 4.004
r2 = 0.5654
Total Prokaryotes (cells L-1)
Total qPCR-estimated rrs genes (copies L-1)
CDW
WW
10^9
10^8
10^7
10^7
10^8
10^9

APPENDIX C

SUPPLEMENTARY MATERIAL: SHORT-TERM VARIABILITY OF AMMONIA OXIDIZER POPULATIONS IN A SE USA SALT MARSH ENVIRONMENT[1]

[1] Tolar, B.B., P. Hagan, M.J. Ross, and J.T. Hollibaugh. To be submitted to *The ISME Journal*.

MATERIALS AND METHODS

Temperature Experiment

Water from Sapelo Island was collected in August 2008, and has been maintained as an enrichment culture in our laboratory by semi-regular transfers with additions of 50 μM ammonia. It contains both Thaumarchaeota (~5% of Bacteria *rrs*) and *Nitrospina* (nitrite-oxidizing Bacteria, NOB; ~4% of Bacteria *rrs*). Experiments were set up as batch cultures in polycarbonate bottles as 1:9 dilutions of the inoculum with filter-sterilized, low-nutrient offshore water from the South Atlantic Bight (SAB). Care was taken to minimize handling that might inhibit Thaumarchaeota (Könneke *et al.*, 2005), and samples were kept in the dark. Triplicate samples were placed in incubators with temperatures of 10, 15, 20, 25, 30, and 34°C; temperature was monitored in real-time using a HOBO Pendant® temperature data logger (Onset Computer Corporation). Bottles were amended with either ammonia (to monitor ammonia oxidation) or nitrite (to monitor nitrite oxidation) at 50 μM final concentration. Samples were collected regularly over a 10-day period to measure DIN concentrations as above. Thaumarchaeota, NOB, ammonia-oxidizing Bacteria (AOB), and Bacteria abundance was determined by qPCR in the beginning and end of the experiment as described in Chapter 4.

RESULTS

Manipulation of temperature using an enrichment of Thaumarchaeota and NOB from Sapelo Island indicated that this variable has a strong effect on both ammonia and nitrite oxidation (Figure C.6). Nitrite production by Thaumarchaeota was highest at temperatures >25°C, with complete oxidation of ammonia within 5 days at 30 or 35°C

(Figure C.6a); no nitrite production was observed after 10 days at either 10 or 15°C, while the 20°C samples did not have measurable activity until day 6. Measurements of nitrite + nitrate (NO_x; Figure C.6b) in the same samples matched patterns for nitrite alone, with no change in NO_x concentration at 10 or 15°C. Similar trends with temperature were observed for NOB, with the fastest oxidation of nitrite at temperatures >25°C (Figure C.6c); small, inconsistent changes in nitrite were. No change in nitrite concentration was observed for any temperature <20°C (Figure C.6c), and only gradual (but inconsistent) increases in nitrate were measured (Figure C.6d).

REFERENCES

Alonso-Sáez L, Waller AS, Mende DR, Bakker K, Farnelid H, Yager PL, Lovejoy C, Tremblay JE, Potvin M, Heinrich F, Estrada M, Riemann L, Bork P, Pedrós-Alio C, Bertilsson S (2012). Role for urea in nitrification by polar marine Archaea. *Proc Nat Acad Sci USA* **109:** 17989-17994.

Baldi F, Facca C, Marchetto D, Nguyen TNM, Spurio R (2011). Diatom quantification and their distribution with salinity brines in coastal sediments of Terra Nova Bay (Antarctica). *Mar Environ Res* **71:** 304-311.

Hollibaugh JT, Gifford S, Sharma S, Bano N, Moran MA (2011). Metatranscriptomic analysis of ammonia-oxidizing organisms in an estuarine bacterioplankton assemblage. *ISME J* **5:** 866-878.

Hollibaugh JT, Gifford SM, Moran MA, Ross MJ, Sharma S, Tolar BB (2014). Seasonal variation in the metratranscriptomes of a Thaumarchaeota population from SE USA coastal waters. *ISME J* **8:** 685-698.

Hornek R, Pommerening-Roser A, Koops HP, Farnleitner AH, Kreuzinger N, Kirschner A, Mach RL (2006). Primers containing universal bases reduce multiple amoA gene specific DGGE band patterns when analysing the diversity of beta-ammonia oxidizers in the environment. *J Microbiol Methods* **66:** 147-155.

Könneke M, Bernhard AE, de la Torre JR, Walker CB, Waterbury JB, Stahl DA (2005). Isolation of an autotrophic ammonia-oxidizing marine archaeon. *Nature* **437:** 543-546.

Mincer TJ, Church MJ, Taylor LT, Preston C, Karl DM, DeLong EF (2007). Quantitative distribution of presumptive archaeal and bacterial nitrifiers in Monterey Bay and the North Pacific Subtropical Gyre. *Environ Microbiol* **9:** 1162-1175.

Nguyen TNM, Berzano M, Gualerzi CO, Spurio R (2011). Development of molecular tools for the detection of freshwater diatoms. *J Microbiol Methods* **84:** 33-40.

Rotthauwe JH, Witzel KP, Liesack W (1997). The ammonia monooxygenase structural gene *amoA* as a functional marker: Molecular fine-scale analysis of natural ammonia-oxidizing populations. *Appl Environ Microbiol* **63:** 4704-4712.

Suzuki MT, Taylor LT, DeLong EF (2000). Quantitative analysis of small-subunit rRNA genes in mixed microbial populations via 5 '-nuclease assays. *Appl Environ Microbiol* **66:** 4605-4614.

Wuchter C, Abbas B, Coolen MJL, Herfort L, van Bleijswijk J, Timmers P, Strous M, Teira E, Herndl GJ, Middelburg JJ, Schouten S, Damste JSS (2006). Archaeal nitrification in the ocean. *Proc Natl Acad Sci USA* **103:** 12317-12322.

Table C.1: Summary of samples collected weekly at Marsh Landing, Sapelo Island, GA, from March 2011 to September 2014.

Date	Time	qPCR Data (copies L^{-1})						Nutrient Data (μM)				
		Thaum *rrs*	Arch *amoA*	Bacteria *rrs*	AOB *amoA*	*Nitrospina rrs*	Diatom 18S	NO_2	NO_x	NH_4	DIN	Urea
03/28/11		6.54E+04	1.20E+05	6.81E+08	5.28E+04	3.37E+04	3.32E+08	0.21	1.44	6.48	8.13	ND
04/04/11	9:15	1.14E+05	3.62E+04	7.17E+08	1.35E+05	4.99E+04	7.78E+08	0.21	1.85	2.42	4.48	ND
04/11/11	13:30	4.33E+04	2.50E+04	8.39E+08	1.88E+04	1.69E+04	4.29E+08	0.11	0.96	8.97	10.03	ND
04/18/11	10:00	4.48E+04	1.75E+04	2.63E+08	2.53E+04	2.24E+04	3.60E+08	0.23	1.34	19.55	21.12	ND
04/26/11	15:30	1.16E+04	8.06E+03	2.58E+08	1.14E+04	5.39E+03	6.79E+07	0.21	1.60	3.34	5.16	ND
05/04/11	10:30	4.80E+04	1.69E+04	8.93E+08	4.07E+04	1.44E+04	3.90E+08	0.21	1.22	1.92	3.35	ND
05/10/11	12:45	4.35E+04	2.61E+04	7.51E+08	9.68E+03	2.09E+04	5.79E+08	0.11	0.39	3.14	3.63	ND
05/16/11	9:15	1.82E+05	1.02E+05	1.58E+09	8.85E+04	1.58E+05	4.81E+07	0.13	0.22	1.03	1.38	ND
05/24/11	13:15	9.00E+05	4.68E+05	8.97E+09	4.20E+05	4.85E+05	5.52E+09	0.12	0.53	2.82	3.47	ND
06/01/11	9:30	3.11E+05	4.22E+05	1.40E+10	9.55E+05	3.25E+05	8.76E+09	0.11	0.24	0.56	0.91	ND
06/09/11	13:00	1.14E+06	6.63E+05	1.26E+10	8.47E+05	9.84E+05	1.07E+10	0.11	0.84	1.23	2.18	ND
06/16/11	11:30	3.02E+06	1.29E+06	1.87E+10	6.75E+06	3.85E+06	1.40E+10	0.11	0.11	0.42	0.63	ND
06/20/11	13:30	1.99E+06	5.92E+05	2.10E+10	1.03E+06	7.07E+05	1.44E+10	0.18	0.33	0.71	1.22	ND
06/28/11	9:15	1.73E+06	1.69E+06	2.89E+10	3.09E+06	5.36E+05	8.45E+09	0.17	0.37	1.08	1.62	ND
07/14/11	9:20	1.26E+08	7.55E+07	2.79E+10	2.26E+06	1.07E+06	2.53E+10	1.01	1.40	0.68	3.09	ND
07/18/11	11:30	2.18E+08	7.42E+07	9.52E+09	5.43E+05	6.57E+05	1.17E+10	5.08	8.12	2.97	16.17	ND
07/28/11	9:10	2.34E+08	6.94E+07	1.12E+10	8.83E+05	7.34E+05	4.65E+09	4.17	4.86	0.50	9.54	ND
08/02/11	11:20	1.37E+08	1.20E+08	2.91E+10	1.35E+06	7.78E+05	5.25E+09	4.06	5.25	1.49	10.80	ND
08/15/11	11:15	2.12E+08	1.64E+08	1.49E+10	1.54E+05	7.21E+05	4.60E+09	5.82	6.83	0.42	13.07	ND
08/22/11	15:00	1.10E+08	1.11E+08	1.25E+10	1.06E+06	1.90E+05	4.38E+09	0.88	1.17	0.57	2.63	ND
08/31/11	11:15	2.65E+07	1.93E+07	3.12E+09	2.92E+05	2.59E+05	2.60E+09	3.85	5.37	1.54	10.77	ND
09/09/11	9:15	7.82E+07	1.73E+07	2.06E+09	6.74E+07	2.37E+05	2.06E+09	6.78	13.99	1.19	21.96	ND

Date	Time	qPCR Data (copies L^{-1})						Nutrient Data (μM)				
		Thaum *rrs*	Arch *amoA*	Bacteria *rrs*	AOB *amoA*	*Nitrospina rrs*	Diatom 18S	NO_2	NO_x	NH_4	DIN	Urea
09/13/11	11:05	1.51E+08	8.57E+07	5.72E+09	1.31E+06	2.24E+06	3.64E+09	4.72	10.92	1.60	17.24	ND
09/21/11	14:00	5.66E+06	2.97E+06	3.32E+09	3.85E+05	5.37E+04	1.12E+09	1.65	5.03	5.56	12.23	ND
09/29/11	11:00	2.77E+07	1.76E+07	3.37E+09	3.53E+05	8.14E+05	2.56E+09	1.34	8.14	6.12	15.61	ND
10/04/11	14:00	3.97E+07	1.92E+07	4.08E+09	5.39E+05	1.07E+06	4.12E+09	2.05	9.37	2.06	13.47	ND
10/12/11	10:30	4.19E+06	7.86E+06	1.10E+09	1.70E+05	2.82E+05	1.07E+09	0.88	3.73	3.90	8.52	ND
10/18/11	13:30	1.04E+07	1.03E+07	5.79E+08	2.79E+05	5.85E+05	1.11E+09	1.74	6.38	2.74	10.86	ND
10/25/11	9:20	1.09E+07	1.65E+07	1.35E+09	1.70E+05	6.69E+05	6.29E+08	1.11	5.30	2.25	8.67	ND
11/01/11	13:30	5.34E+06	1.57E+07	1.60E+09	8.20E+04	5.22E+05	1.84E+09	0.52	2.69	3.04	6.25	ND
11/09/11	9:30	1.16E+05	2.03E+05	7.03E+07	4.37E+03	4.16E+04	2.44E+07	0.45	1.78	1.82	4.05	ND
11/14/11	10:30	2.04E+06	4.32E+06	1.13E+09	4.75E+04	1.24E+05	1.90E+09	0.50	2.03	2.01	4.53	ND
11/21/11	15:00	1.84E+06	7.44E+06	1.14E+09	9.81E+04	3.28E+05	2.65E+09	0.40	1.33	1.17	2.89	ND
11/28/11	11:00	2.84E+06	9.60E+06	4.57E+09	7.51E+04	2.74E+05	1.56E+09	0.61	2.16	2.06	4.82	ND
12/07/11	9:00	1.90E+06	7.76E+06	4.57E+09	6.51E+04	3.60E+05	7.02E+09	0.48	2.18	1.63	4.29	ND
12/13/11	10:50	1.16E+06	2.36E+06	3.56E+09	3.45E+04	2.87E+05	8.25E+08	0.21	0.43	0.98	1.61	ND
12/20/11	15:15	1.49E+06	2.04E+06	4.19E+08	1.17E+05	2.05E+05	9.34E+08	0.31	1.61	2.20	4.12	ND
12/27/11	10:30	1.32E+06	3.11E+06	3.36E+09	5.69E+04	2.05E+05	1.68E+09	0.23	0.93	1.14	2.30	ND
01/03/12	14:15	5.12E+05	8.15E+05	2.92E+09	5.26E+04	8.41E+04	7.46E+08	0.30	2.29	1.44	4.03	ND
01/12/12	11:30	3.81E+05	1.53E+06	8.36E+08	4.72E+04	1.08E+05	3.18E+09	0.15	0.56	1.08	1.79	ND
01/17/12	16:00	1.93E+06	1.28E+06	1.50E+10	2.96E+05	1.72E+05	3.69E+09	0.03	0.85	0.16	1.00	ND
01/25/12	10:00	2.92E+06	1.72E+06	1.88E+10	1.61E+05	2.54E+05	4.11E+09	-0.06	0.12	0.18	0.30	ND
01/31/12	13:30	5.10E+05	5.90E+05	8.99E+09	1.24E+05	1.15E+05	3.38E+09	-0.03	-0.01	4.53	4.53	ND
02/13/12	13:45	1.46E+06	3.16E+05	5.42E+09	3.31E+04	3.64E+03	1.13E+09	-0.01	0.73	0.28	1.01	ND
02/24/12	9:45	7.64E+05	3.08E+05	1.08E+10	1.84E+05	1.62E+05	3.36E+09	-0.07	0.08	0.08	0.16	ND
02/29/12	14:15	1.06E+06	4.62E+05	1.88E+10	2.31E+05	2.52E+05	4.86E+09	-0.01	0.22	0.26	0.48	ND

Date	Time	qPCR Data (copies L^{-1})						Nutrient Data (μM)				
		Thaum *rrs*	Arch *amoA*	Bacteria *rrs*	AOB *amoA*	*Nitrospina rrs*	Diatom 18S	NO_2	NO_x	NH_4	DIN	Urea
03/07/12	9:10	2.23E+06	6.50E+05	1.56E+10	2.64E+06	7.16E+05	1.83E+09	-0.07	-0.15	0.16	0.01	ND
03/12/12	12:30	2.25E+06	1.93E+05	1.22E+10	1.24E+05	7.07E+04	1.92E+09	-0.06	0.00	0.28	0.28	ND
03/20/12	9:30	6.98E+05	2.96E+05	1.24E+10	3.97E+05	2.85E+05	4.18E+09	-0.07	-0.01	5.36	5.35	ND
03/28/12	12:00	6.33E+05	4.13E+05	1.62E+10	5.36E+05	2.91E+05	6.42E+09	-0.01	-0.04	3.89	3.85	ND
04/05/12	9:30	8.77E+05	3.08E+05	7.86E+09	3.90E+05	1.43E+06	3.40E+09	-0.04	0.15	0.01	0.16	ND
04/11/12	13:20	7.28E+05	3.60E+05	9.76E+09	8.22E+04	3.81E+05	3.51E+09	0.03	0.47	1.05	1.52	ND
04/23/12	10:00	5.45E+05	2.81E+05	1.02E+10	2.11E+05	9.68E+04	5.33E+09	0.04	0.36	3.14	3.50	ND
05/01/12	14:45	4.93E+05	1.37E+05	2.21E+10	1.77E+05	1.05E+05	2.08E+09	-0.02	-0.12	0.06	-0.06	ND
05/07/12	10:00	2.69E+05	2.05E+05	3.72E+10	7.11E+05	6.58E+05	2.06E+09	-0.06	-0.18	1.13	0.95	ND
05/17/12	9:15	2.75E+05	3.23E+05	2.46E+10	8.63E+05	3.56E+05	1.83E+09	-0.02	0.05	0.78	0.83	ND
05/22/12	10:00	3.69E+05	3.34E+05	9.41E+10	9.23E+05	3.61E+05	1.21E+09	0.03	0.14	0.23	0.38	ND
05/30/12	15:15	3.23E+05	1.05E+05	2.49E+10	5.33E+05	2.80E+05	1.25E+09	0.13	0.88	1.15	2.03	ND
05/31/12	15:15	4.77E+05	2.29E+05	2.04E+10	3.98E+05	6.16E+05	7.72E+08	0.06	0.42	0.78	1.20	ND
06/05/12	10:30	2.50E+05	1.75E+05	4.88E+10	9.26E+05	2.89E+05	1.37E+09	0.11	0.28	1.50	1.78	ND
06/11/12	14:45	6.18E+05	2.16E+05	1.34E+10	3.87E+05	2.55E+05	8.38E+08	0.60	1.75	3.44	5.19	ND
06/19/12	10:00	3.39E+06	3.76E+06	2.29E+11	2.14E+06	2.69E+05	8.29E+09	0.10	0.72	0.14	0.86	ND
06/25/12	14:00	1.16E+06	4.84E+05	3.41E+10	5.18E+06	3.01E+05	3.75E+09	0.15	0.37	1.92	2.29	ND
07/05/12	11:30	1.03E+07	5.19E+06	6.59E+10	7.14E+06	4.30E+05	7.37E+09	0.30	1.60	0.14	1.74	ND
07/09/12	12:15	3.27E+07	4.24E+07	2.18E+11	3.87E+05	1.14E+06	1.13E+10	0.43	1.77	-0.05	1.72	ND
07/18/12	9:45	2.64E+07	2.59E+07	1.66E+11	4.60E+04	7.96E+05	8.77E+09	0.35	0.65	8.85	9.51	ND
07/23/12	13:00	3.18E+07	8.24E+06	1.03E+11	1.26E+05	1.47E+06	1.11E+10	0.15	0.25	-0.07	0.17	ND
08/01/12	9:45	5.88E+07	3.70E+07	6.18E+11	1.35E+06	3.31E+06	1.19E+10	0.46	0.78	1.03	1.81	ND
08/06/12	12:00	6.86E+07	7.44E+07	4.03E+11	3.50E+05	1.73E+06	4.09E+09	1.65	2.45	0.12	2.56	ND
08/15/12	9:20	2.26E+08	5.30E+07	5.20E+11	1.05E+06	5.62E+05	4.52E+09	1.11	1.85	-0.21	1.65	ND

Date	Time	qPCR Data (copies L^{-1})						Nutrient Data (μM)				
		Thaum *rrs*	Arch *amoA*	Bacteria *rrs*	AOB *amoA*	*Nitrospina rrs*	Diatom 18S	NO_2	NO_x	NH_4	DIN	Urea
08/22/12	12:30	2.58E+08	1.70E+08	4.07E+11	5.30E+05	8.49E+05	4.40E+09	3.03	3.99	2.43	6.42	ND
08/27/12	16:00	1.55E+08	5.18E+07	4.04E+11	5.57E+05	1.31E+06	3.64E+08	3.06	5.77	0.12	5.89	ND
09/04/12	11:45	5.18E+07	4.24E+07	2.13E+11	8.20E+05	1.08E+06	7.19E+09	1.78	3.51	-0.13	3.39	ND
09/10/12	15:45	2.39E+08	4.75E+07	6.09E+11	8.86E+05	1.58E+05	9.50E+09	1.74	4.39	-0.15	4.24	ND
09/19/12	12:15	2.41E+07	3.16E+06	2.36E+11	5.46E+05	9.12E+04	1.23E+10	0.44	1.17	0.84	2.01	ND
09/24/12	16:00	2.96E+07	2.87E+07	2.95E+11	8.96E+05	9.85E+05	1.23E+10	1.29	3.45	0.71	4.16	ND
10/10/12	15:30	4.27E+07	2.49E+07	2.66E+11	1.06E+06	5.61E+05	6.89E+09	2.23	6.06	3.69	9.75	ND
10/17/12	11:15	3.45E+07	6.78E+06	3.44E+11	1.29E+06	1.37E+06	1.81E+10	0.85	2.63	0.12	2.75	ND
10/22/12	15:00	3.08E+06	1.77E+07	2.08E+11	9.80E+05	1.11E+06	1.60E+10	0.88	3.87	2.45	6.32	ND
11/01/12	12:00	6.92E+06	5.94E+06	2.01E+11	7.73E+05	1.23E+06	2.99E+09	0.40	1.41	0.38	1.80	ND
11/08/12	15:30	1.44E+06	1.16E+06	3.23E+11	3.84E+05	6.61E+05	1.17E+10	0.28	1.16	0.09	1.25	ND
11/15/12	10:00	1.03E+06	5.12E+05	3.44E+10	1.64E+05	3.37E+05	2.07E+09	0.18	0.23	3.23	3.46	ND
11/20/12	1:00	3.37E+06	1.98E+06	9.57E+10	5.46E+05	5.10E+05	6.59E+09	0.06	0.09	0.45	0.54	ND
11/29/12	11:00	9.83E+05	7.70E+05	7.42E+10	7.80E+05	4.41E+05	2.40E+09	0.18	0.80	1.65	2.45	ND
12/05/12	12:00	3.49E+05	8.61E+05	6.16E+10	4.29E+05	1.48E+05	3.45E+09	0.17	0.70	0.94	1.63	ND
12/14/12	4:30	2.23E+06	7.73E+05	6.83E+10	1.03E+06	9.10E+05	4.75E+09	0.17	0.49	8.13	8.62	ND
12/20/12	1:00	7.84E+05	4.26E+05	9.04E+10	4.49E+05	1.13E+05	6.29E+09	0.25	1.25	2.02	3.27	ND
12/26/12	9:30	7.82E+05	5.59E+05	1.25E+11	3.14E+05	2.72E+05	1.39E+10	0.16	0.35	7.28	7.63	ND
01/03/13	12:40	3.93E+05	3.50E+05	2.45E+11	2.44E+05	4.27E+05	1.81E+10	0.06	0.19	0.06	0.25	ND
01/14/13	11:00	2.11E+05	4.07E+05	9.04E+10	7.82E+05	1.38E+05	3.06E+09	0.17	1.38	4.59	5.97	ND
01/25/13	9:45	4.43E+05	2.44E+05	4.92E+10	3.35E+05	3.73E+05	8.33E+09	0.16	1.55	3.50	5.05	ND
01/30/13	11:00	2.77E+05	4.27E+05	1.11E+11	5.32E+05	8.27E+05	8.00E+09	0.06	0.05	0.10	0.15	ND
02/06/13	3:30	8.72E+04	1.47E+05	6.98E+10	3.34E+05	5.00E+05	1.28E+10	0.12	0.22	1.51	1.74	ND
02/19/13	3:00	2.60E+04	3.84E+04	5.09E+10	1.69E+05	7.56E+04	1.19E+10	0.17	2.11	0.13	2.24	ND

Date	Time	qPCR Data (copies L^{-1})						Nutrient Data (μM)				
		Thaum *rrs*	Arch *amoA*	Bacteria *rrs*	AOB *amoA*	*Nitrospina rrs*	Diatom 18S	NO_2	NO_x	NH_4	DIN	Urea
02/28/13	11:00	2.18E+05	2.34E+05	5.78E+10	5.91E+05	4.01E+05	7.45E+09	0.18	2.17	4.34	6.51	ND
03/06/13	2:30	1.61E+05	2.86E+05	7.47E+10	8.06E+05	3.90E+05	3.41E+09	0.06	0.10	0.01	0.11	ND
03/15/13	10:30	1.92E+05	1.16E+05	2.94E+10	4.85E+05	6.15E+05	1.23E+09	0.18	1.22	1.19	2.41	ND
03/21/13	3:00	1.93E+05	7.13E+04	1.37E+11	2.64E+05	1.98E+05	3.41E+09	0.07	0.13	0.54	0.67	ND
03/29/13	10:30	3.19E+05	4.69E+04	1.47E+11	4.35E+05	4.54E+05	1.94E+09	0.15	0.48	0.47	0.95	ND
04/02/13	7:00	1.67E+05	9.33E+05	6.14E+10	2.38E+05	5.13E+05	9.18E+08	0.23	1.01	2.93	3.93	ND
04/16/13	13:00	4.37E+05	4.60E+05	3.44E+10	5.47E+05	2.55E+05	3.63E+09	0.27	0.94	3.62	3.81	0.34
04/29/13	13:00	1.11E+06	2.50E+05	3.73E+10	3.55E+05	4.52E+05	2.46E+09	0.18	1.11	2.10	4.15	0.12
05/10/13	9:30	1.20E+06	7.22E+05	6.23E+10	6.31E+05	3.88E+05	1.15E+10	0.34	2.91	3.17	8.66	0.46
05/15/13	13:00	7.54E+05	5.13E+05	3.74E+10	1.68E+06	2.25E+05	9.32E+09	0.25	1.46	2.98	5.65	1.17
05/24/13	9:45	1.07E+06	2.98E+05	2.80E+10	7.47E+05	4.78E+05	1.17E+10	0.10	-0.04	0.04	-0.15	0.35
05/28/13	12:00	1.75E+06	8.68E+05	5.70E+10	2.55E+06	1.51E+06	1.09E+10	0.14	0.58	1.85	2.87	1.42
06/06/13	9:30	3.25E+06	4.45E+05	4.48E+10	1.23E+06	7.52E+05	1.56E+10	0.13	0.26	2.26	2.65	0.19
06/11/13	10:45	2.86E+06	1.20E+06	1.36E+11	1.81E+06	1.84E+06	5.15E+10	0.24	1.58	0.81	3.73	0.48
06/20/13	9:30	2.06E+06	5.77E+05	6.33E+10	1.40E+06	6.18E+05	1.29E+10	0.25	0.78	3.55	4.86	0.35
06/25/13	10:00	1.64E+06	8.44E+05	3.55E+10	7.72E+05	7.96E+05	1.06E+10	0.51	2.88	8.11	13.35	0.80
07/08/13	10:00	5.25E+07	2.00E+07	1.38E+11	1.25E+06	6.44E+05	3.23E+10	0.38	0.69	1.09	1.23	0.52
07/17/13	15:15	1.01E+07	9.19E+06	2.98E+10	9.57E+04	1.05E+05	8.94E+09	1.09	3.54	2.87	8.85	0.83
07/23/13	11:45	2.08E+07	2.42E+07	9.74E+10	1.05E+06	1.77E+06	1.17E+10	0.83	3.36	3.98	9.87	0.64
08/01/13	15:00	7.27E+06	1.50E+06	5.01E+09	6.97E+05	1.72E+05	3.73E+08	1.09	3.98	3.60	10.47	0.46
08/07/13	10:00	1.62E+07	4.97E+06	6.98E+10	3.69E+06	3.80E+05	1.14E+10	0.46	0.98	0.73	2.23	2.11
08/13/13	13:00	9.61E+07	5.77E+07	8.71E+10	2.97E+05	2.76E+05	5.50E+09	1.23	1.93	1.33	3.94	1.21
08/21/13	12:30	1.88E+08	3.42E+07	4.57E+10	1.55E+05	7.31E+05	5.33E+09	1.26	2.26	0.38	3.64	0.07
08/26/13	10:30	9.84E+07	3.95E+07	6.88E+09	3.06E+05	4.80E+05	3.59E+09	2.49	4.07	0.28	5.93	0.26

Date	Time	qPCR Data (copies L^{-1})						Nutrient Data (μM)				
		Thaum *rrs*	Arch *amoA*	Bacteria *rrs*	AOB *amoA*	*Nitrospina rrs*	Diatom 18S	NO_2	NO_x	NH_4	DIN	Urea
08/30/13	11:30	1.83E+08	4.75E+07	9.48E+10	6.29E+05	3.51E+05	7.72E+09	3.69	4.56	0.03	5.46	0.23
09/10/13	11:00	4.33E+08	1.40E+08	8.20E+10	1.09E+06	7.88E+05	3.35E+10	2.24	2.88	0.49	1.07	0.27
09/19/13	10:00	2.98E+07	4.19E+06	3.97E+10	4.34E+05	1.10E+06	3.00E+09	0.82	1.15	2.70	2.93	0.42
09/25/13	12:30	9.08E+07	1.02E+07	1.75E+10	2.42E+05	7.39E+05	3.18E+09	3.36	7.39	3.74	5.22	0.54
10/03/13	9:30	2.34E+07	8.71E+06	1.80E+10	2.95E+05	5.52E+05	5.01E+09	1.50	3.34	0.07	5.24	0.30
10/08/13	12:00	3.04E+07	6.49E+06	2.76E+10	2.00E+05	8.57E+05	1.91E+09	1.56	4.25	1.42	2.27	0.44
10/17/13	9:45	4.83E+07	8.12E+06	4.28E+10	4.84E+05	2.40E+06	3.77E+09	1.01	3.16	1.45	2.08	0.14
10/22/13	12:00	4.18E+07	3.47E+07	4.14E+10	1.63E+05	2.16E+06	7.01E+09	1.04	2.76	1.38	1.93	0.54
10/31/13	9:45	2.36E+07	9.05E+06	7.71E+09	8.25E+04	6.73E+05	5.98E+09	0.37	0.91	1.00	1.18	0.19
11/08/13	10:00	9.32E+06	9.16E+06	3.63E+09	3.16E+04	1.15E+06	2.64E+09	0.60	1.81	2.62	2.98	0.44
11/12/13	15:00	6.50E+06	1.61E+07	8.40E+10	2.14E+05	9.02E+05	7.71E+09	0.43	1.58	1.36	1.68	0.17
11/21/13	10:30	6.03E+06	6.88E+06	2.60E+10	1.28E+05	3.97E+05	3.70E+09	0.35	1.17	2.63	2.86	0.42
11/25/13	13:30	6.20E+06	1.03E+07	5.81E+10	1.83E+05	6.84E+05	6.15E+09	0.22	0.54	1.64	1.75	0.19
12/03/13	10:00	4.73E+06	7.33E+06	8.16E+10	7.76E+04	3.97E+05	3.84E+09	0.16	0.51	0.99	1.09	0.09
12/11/13	14:30	3.17E+06	5.84E+06	5.10E+10	1.22E+05	5.13E+05	4.12E+09	0.30	1.61	1.90	2.23	0.72
12/18/13	10:30	4.61E+06	1.48E+07	1.37E+10	2.10E+05	1.11E+06	1.83E+09	0.14	0.53	ND	0.53	ND
12/30/13	9:15	4.73E+06	1.52E+07	3.43E+10	9.40E+05	1.78E+06	1.37E+10	0.09	-0.23	ND	-0.23	0.12
01/06/14	12:00	9.74E+06	3.41E+06	9.89E+10	2.88E+06	1.36E+06	3.00E+09	ND	ND	1.16	ND	0.18
01/17/14	9:30	6.45E+05	2.34E+06	3.90E+10	4.10E+05	1.88E+05	7.60E+09	0.08	-0.37	ND	-0.37	0.31
01/21/14	12:00	1.64E+06	2.60E+06	4.95E+10	3.84E+05	2.28E+05	1.67E+10	0.07	-0.28	ND	-0.28	0.03
01/31/14	9:30	1.33E+06	5.56E+06	1.26E+10	4.22E+05	6.97E+05	1.25E+10	0.05	-0.21	ND	-0.21	0.49
02/08/14	11:00	1.31E+06	1.90E+06	8.26E+10	2.00E+05	2.62E+05	6.05E+09	0.1	0.16	1.29	1.45	0.12
02/14/14	9:30	2.30E+06	9.82E+06	3.74E+10	3.19E+05	7.11E+05	9.94E+09	0.04	0.10	0.47	0.57	0.12
02/20/14	11:45	2.20E+06	1.18E+06	1.49E+10	8.74E+04	1.16E+05	4.44E+10	0.04	0.09	0.54	0.63	0.38

Date	Time	qPCR Data (copies L^{-1})						Nutrient Data (μM)				
		Thaum *rrs*	Arch *amoA*	Bacteria *rrs*	AOB *amoA*	*Nitrospina rrs*	Diatom 18S	NO_2	NO_x	NH_4	DIN	Urea
02/27/14	9:15	2.13E+06	5.96E+06	4.04E+10	1.36E+06	1.30E+06	1.00E+10	0.05	0.08	0.39	0.47	0.07
03/03/14	11:00	2.19E+05	8.09E+05	1.68E+10	2.51E+05	6.86E+04	3.29E+09	0.10	0.68	1.01	1.69	0.48
03/13/14	10:00	1.29E+06	8.26E+05	3.04E+10	4.54E+05	1.38E+05	8.37E+09	0.05	-0.02	0.36	0.34	0.06
03/20/14	11:00	3.24E+05	1.52E+06	4.22E+10	5.56E+05	3.01E+05	7.89E+09	0.07	0.13	0.6	0.73	0.58
03/27/14	9:30	4.89E+06	1.49E+07	1.09E+11	5.91E+05	1.62E+06	2.07E+10	0.06	0.06	0.38	0.44	0.1
04/08/14	15:00	1.69E+06	2.06E+06	2.59E+10	3.03E+05	3.74E+05	1.39E+10	0.15	1.50	3.13	4.64	0.24
04/16/14	9:45	1.78E+06	2.71E+06	2.25E+10	4.51E+05	5.79E+05	5.24E+09	0.05	0.40	0.57	0.97	0.16
04/21/14	14:00	1.08E+06	2.72E+06	2.27E+11	3.87E+05	2.16E+05	3.55E+09	0.17	2	3.04	5.04	0.36
04/30/14	13:00	9.72E+05	9.94E+05	8.52E+10	1.88E+05	7.05E+05	2.10E+09	0.21	2.96	1.94	4.89	0.23
05/07/14	15:00	4.29E+05	5.49E+06	5.83E+10	1.27E+04	2.56E+05	4.80E+09	0.16	2.53	2.03	4.55	0.16
05/15/14	11:00	8.51E+05	4.28E+06	3.88E+10	9.49E+04	3.79E+05	2.29E+09	0.12	0.82	1.48	2.3	0.2
05/21/14	15:00	1.93E+06	2.26E+06	3.90E+10	6.78E+05	3.44E+05	1.08E+10	0.06	0.30	0.47	0.77	0.35
05/28/14	10:30	1.26E+06	1.61E+06	4.59E+10	6.33E+04	5.67E+05	2.88E+09	0.08	0.65	1.55	2.20	0.61
06/04/14	14:00	1.04E+06	4.80E+06	2.37E+11	1.16E+06	4.48E+05	2.10E+10	0.05	0.22	0.60	0.82	0.25
06/12/14	9:15	1.05E+06	4.53E+06	2.66E+11	9.22E+05	4.78E+05	1.08E+10	0.05	0.20	0.25	0.44	0.30
06/26/14	9:15	9.21E+05	8.53E+05	1.23E+11	1.06E+06	1.96E+05	1.47E+10	0.08	0.27	0.30	0.56	0.48
07/03/14	12:20	5.85E+05	1.73E+06	1.53E+11	1.89E+06	4.23E+05	1.77E+10	0.08	0.21	0.15	0.36	0.15
07/14/14	10:00	4.07E+06	4.44E+06	1.62E+11	1.61E+06	8.11E+05	1.38E+10	0.10	0.93	4.76	5.69	0.53
07/24/14	9:20	5.66E+07	7.34E+07	1.16E+11	7.24E+05	8.21E+05	1.07E+10	0.66	1.52	1.11	2.63	0.38
07/29/14	11:30	4.73E+07	1.09E+08	1.90E+11	2.32E+06	6.92E+05	5.50E+09	0.27	0.79	0.81	1.60	0.85
08/07/14	9:30	6.24E+07	1.53E+08	5.42E+10	6.08E+06	8.04E+05	5.22E+09	1.95	4.08	0.65	4.73	0.18
08/18/14	14:00	4.92E+08	6.69E+07	6.33E+10	5.10E+05	8.28E+05	1.31E+10	0.43	0.63	ND	ND	ND
08/26/14	10:00	1.29E+07	1.51E+07	1.92E+11	1.67E+06	9.01E+05	1.84E+10	0.11	0.20	ND	ND	ND
09/08/14	9:30	7.72E+06	3.33E+06	1.29E+11	3.73E+05	4.28E+05	9.00E+09	0.23	0.54	ND	ND	ND

Table C.2: Quantitative PCR (qPCR) primers and probes used in this study.

Target Gene	Primer/ Probe	Sequence (5'→3')	Detection Limit	Reference
Thaumarchaeota 16S rRNA (*rrs*)	G1_751F	GTC TAC CAG AAC AYG TTC	2.04 x 10^3 copies L^{-1}	Mincer *et al.* (2007)
	G1_956R	HGG CGT TGA CTC CAA TTG		
	TM519AR	TTA CCG CGG CGG CTG GCA C		Suzuki *et al.* (2000)
Bacterial 16S rRNA (*rrs*)	BACT1369F	CGG TGA ATA CGT TCY CGG	5.07 x 10^3 copies L^{-1}	Suzuki *et al*. (2000)
	PROK1492R	GGW TAC CTT GTT ACG ACT T		
	389F	CTT GTA CAC ACC GCC CGT C		
Nitrospina 16S rRNA (*rrs*)	NitSSU_130F	GGG TGA GTA ACA CGT GAA TAA	1.60 x 10^3 copies L^{-1}	Mincer *et al.* (2007)
	NitSSU_282R	TCA GGC CGG CTA AMC A		
Diatom 18S rRNA	528F	GCG GTA ATT CCA GCT CCA A	1.22 x 10^4 copies L^{-1}	Nguyen *et al*. (2011); Baldi *et al*. (2011)
	650R	AAC ACT CTA ATT TTT TCA CAG		
Archaeal *amoA*	Arch-amoA-for	CTG AYT GGG CYT GGA CAT C	7.18 x 10^3 copies L^{-1}	Wuchter *et al.* (2006)
	Arch-amoA-rev	TTC TTC TTT GTT GCC CAG TA		
Thaumarchaeota *ureC*	Thaum-UreC forward	ATG CAA TYT GTA ATG GAA CWA CWA C	7.70 x 10^3 copies L^{-1}	Alonso-Sáez *et al.* (2012)
	Thaum-UreC reverse	AGT TGT YCC CCA ATC TTC ATG TAA TTT TA		
Bacterial *amoA**	amoA-1F	GGG GTT TCT ACT GGT GGT	8.13 x 10^3 copies L^{-1}	Rotthauwe *et al.* (1997)
	amoA-r New	CCC CTC BGS AAA VCC TTC TTC		Hornek *et al.* (2006)

*Bacterial *amoA* primers amplify genes from β-Proteobacteria only, and not γ-Proteobacteria.

Table C.3: Multi-Dimensional Scaling (MDS) variable score data for each axis based on gene abundance data. Variable scores in **bold** indicate significant contributors to a given MDS axis

(a) All Data

Axis	Archaea *amoA*	Thaumarch. *rrs*	AOB *amoA*	Bacteria *rrs*	*Nitrospina rrs*	Diatom 18S rRNA
MDS1	**0.51**	**0.57**	-0.07	-0.21	-0.05	-0.23
MDS2	0.04	0.11	-0.11	0.31	-0.23	-0.03

(b) SINERR Reduced Dataset

Axis	Archaea *amoA*	Thaumarch. *rrs*	AOB *amoA*	Bacteria *rrs*	*Nitrospina rrs*	Diatom 18S rRNA
MDS1	**0.49**	**0.48**	-0.11	-0.19	0.03	-0.21
MDS2	0.07	0.21	-0.01	0.20	-0.29	0.07

(c) NUT + Urea Reduced Dataset

Axis	Archaea *amoA*	Thaumarch. *rrs*	AOB *amoA*	Bacteria *rrs*	*Nitrospina rrs*	Diatom 18S rRNA
MDS1	0.37	**0.54**	-0.18	-0.15	0.06	-0.18
MDS2	0.28	0.17	-0.06	0.05	-0.26	0.09

Table C.4: Principal Components Analysis (PCA) correlations for each axis of environmental variables measured.

(a) All Data

Axis	% Variance Explained	Temperature	Salinity	Dissolved Oxygen	pH	Turbidity	Air Temperature	Relative Humidity	Barometric Pressure
PC1	27.7%	**0.88**	0.15	**-0.92**	**-0.85**	-0.01	**0.81**	0.16	-0.36
PC2	15.7%	-0.33	0.36	0.13	0.05	-0.09	-0.35	**0.61**	0.32
PC3	11.7%	0.08	-0.07	-0.09	-0.08	0.24	0.10	**0.49**	**-0.54**
PC4	10.4%	-0.13	**-0.47**	0.13	0.11	**0.34**	-0.15	-0.23	-0.27
PC5	9.4%	0.16	**-0.46**	-0.06	0.02	**0.57**	0.25	0.30	**0.36**

Axis	% Variance Explained	Wind Speed	Wind Direction	Total PAR	Cumulative Precipitation	Nitrite	Nitrate	Ammonia	DIN
PC1	27.7%	-0.30	-0.05	0.23	0.23	**0.68**	**0.53**	0.16	**0.56**
PC2	15.7%	-0.27	**-0.64**	**-0.67**	0.24	0.19	**0.42**	**0.44**	**0.48**
PC3	11.7%	**0.44**	0.08	**-0.51**	**0.74**	-0.21	-0.29	-0.11	-0.30
PC4	10.4%	0.31	**0.34**	0.14	0.16	-0.07	0.25	**0.69**	**0.58**
PC5	9.4%	-0.35	**-0.45**	0.25	-0.02	**-0.35**	**-0.31**	0.20	-0.07

(b) WQ Dataset

Axis	% Variance Explained	Temperature	Salinity	Dissolved Oxygen	pH	Turbidity
PC1	53.3%	**0.93**	0.18	**-0.97**	**-0.91**	-0.02
PC2	26.0%	-0.13	**0.79**	0.03	0.01	**-0.81**

(c) NUT Dataset

Axis	% Variance Explained	Nitrite	Nitrate	Ammonia	DIN
PC1	60.3%	0.66	**0.83**	0.60	**0.96**
PC2	29.3%	**-0.63**	-0.32	**0.79**	0.22

(d) MET Dataset

Axis	% Variance Explained	Air Temperature	Relative Humidity	Barometric Pressure	Wind Speed	Wind Direction	Total PAR	Cumulative Precipitation
PC1	30.6%	0.22	**-0.83**	-0.24	0.18	**0.70**	0.78	**-0.46**
PC2	25.5%	-0.24	-0.17	**0.83**	**-0.52**	**-0.46**	0.26	**-0.68**
PC3	21.2%	**0.88**	0.31	-0.20	**-0.60**	-0.19	0.40	0.11

(e) SINERR NUT Dataset

Axis	% Variance Explained	Phosphate	Ammonia	Nitrite	NO_X	Chlorophyll *a*
PC1	45.4%	**0.83**	0.28	**0.77**	**0.91**	-0.29
PC2	26.0%	0.11	**0.75**	**-0.52**	-0.10	**-0.67**

(f) NUT Dataset + Urea

Axis	% Variance Explained	Nitrite	Nitrate	Ammonia	Urea	DIN
PC1	50.8%	0.46	**0.86**	**0.78**	0.30	**0.94**
PC2	23.4%	**-0.75**	-0.28	0.43	**0.58**	0.08

Table C.5: Significant combinations of Multi-Dimensional Scaling (MDS) and Principal Components Analysis (PCA) data using linear models.

PCA Data	PCA Axis	MDS Data	MDS Axis	R^2	*p*-value
All	PC1	All	MDS1	0.37	< 0.00001
WQ	PC1	All	MDS1	0.30	< 0.00001
NUT	PC1	All	MDS1	0.26	< 0.00001
NUT	PC2	All	MDS1	0.30	< 0.00001
SINERR NUT	PC1	SINERR Red.	MDS1	0.55	< 0.00001
NUT + Urea	PC2	NUT+Urea Red.	MDS1	0.39	< 0.00001

*Red. = Reduced dataset

Figure C.1: Time series of quarterly sampling at Marsh Landing, Sapelo Island, GA, from 2008-2011 (Hollibaugh *et al.*, 2011; Hollibaugh *et al.*, 2014). Data are from 4-8 replicate samples of surface water collected over a 48 hr period and thus reflect variability associated with local patchiness. Relative abundances in **(a)** calculated as in Hollibaugh *et al*. (2011). **(a)** qPCR measurements of gene abundance, inset shows AOB *amoA* and NOB *rrs* on a smaller scale; **(b)** DIN concentrations in these samples; **(c)** environmental variables.

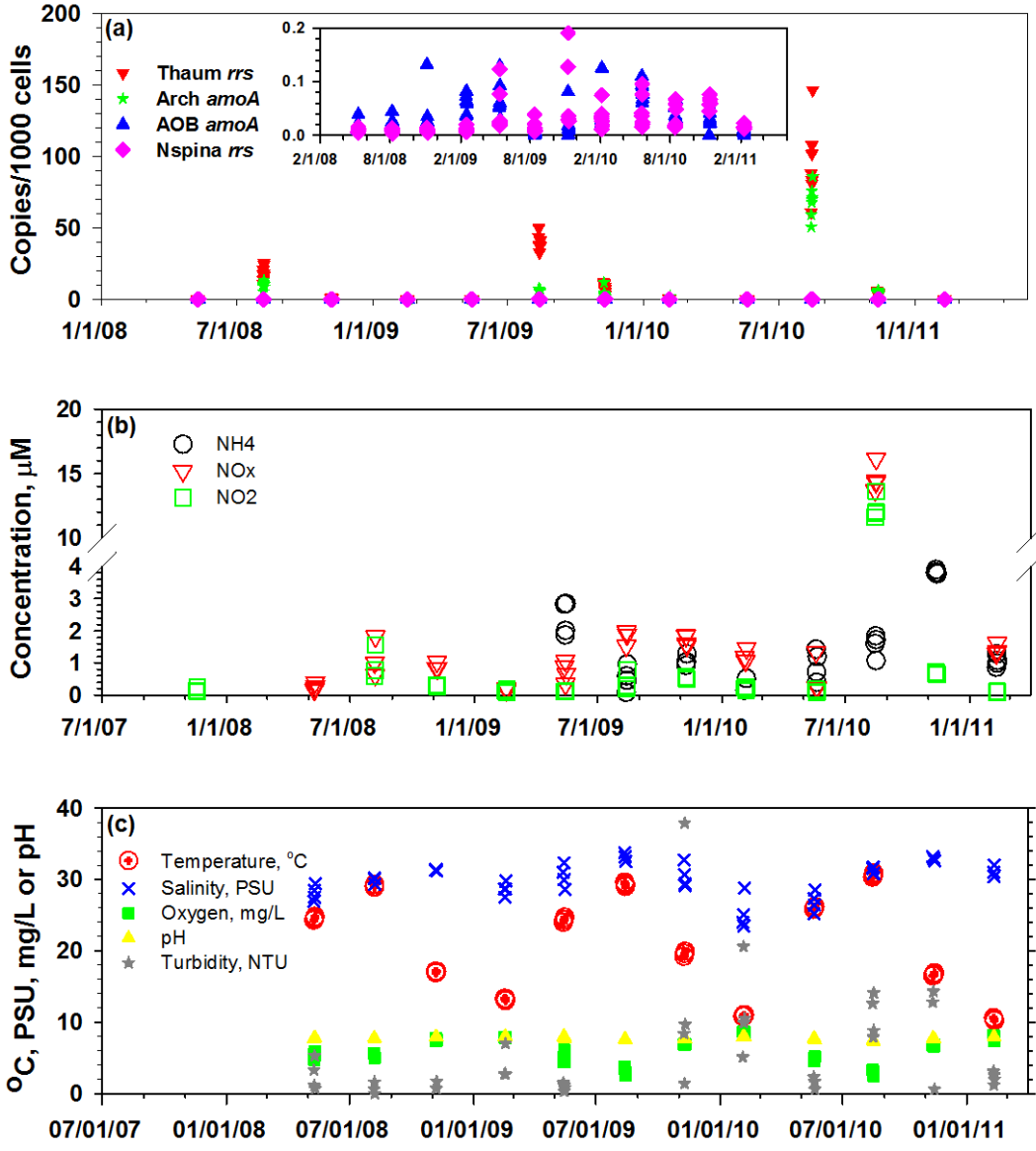
(a)
Thaum rrs
Arch amoA
AOB amoA
Nspina rrs
Copies/1000 cells
200
150
100
50
0
1/1/08
7/1/08
1/1/09
7/1/09
1/1/10
7/1/10
1/1/11
0.2
0.1
0.0
2/1/08
8/1/08
2/1/09
8/1/09
2/1/10
8/1/10
2/1/11
(b)
NH4
NOx
NO2
Concentration, µM
20
15
10
4
3
2
1
0
7/1/07
1/1/08
7/1/08
1/1/09
7/1/09
1/1/10
7/1/10
1/1/11
(c)
Temperature, °C
Salinity, PSU
Oxygen, mg/L
pH
Turbidity, NTU
°C, PSU, mg/L or pH
Turbidity, NTU
40
30
20
10
0
400
300
200
100
0
07/01/07
01/01/08
07/01/08
01/01/09
07/01/09
01/01/10
07/01/10
01/01/11

Figure C.2: Weekly variability in relative abundance of (a) Bacteria *rrs* and (b) Diatom 18S rRNA genes at Marsh Landing, Sapelo Island, GA.

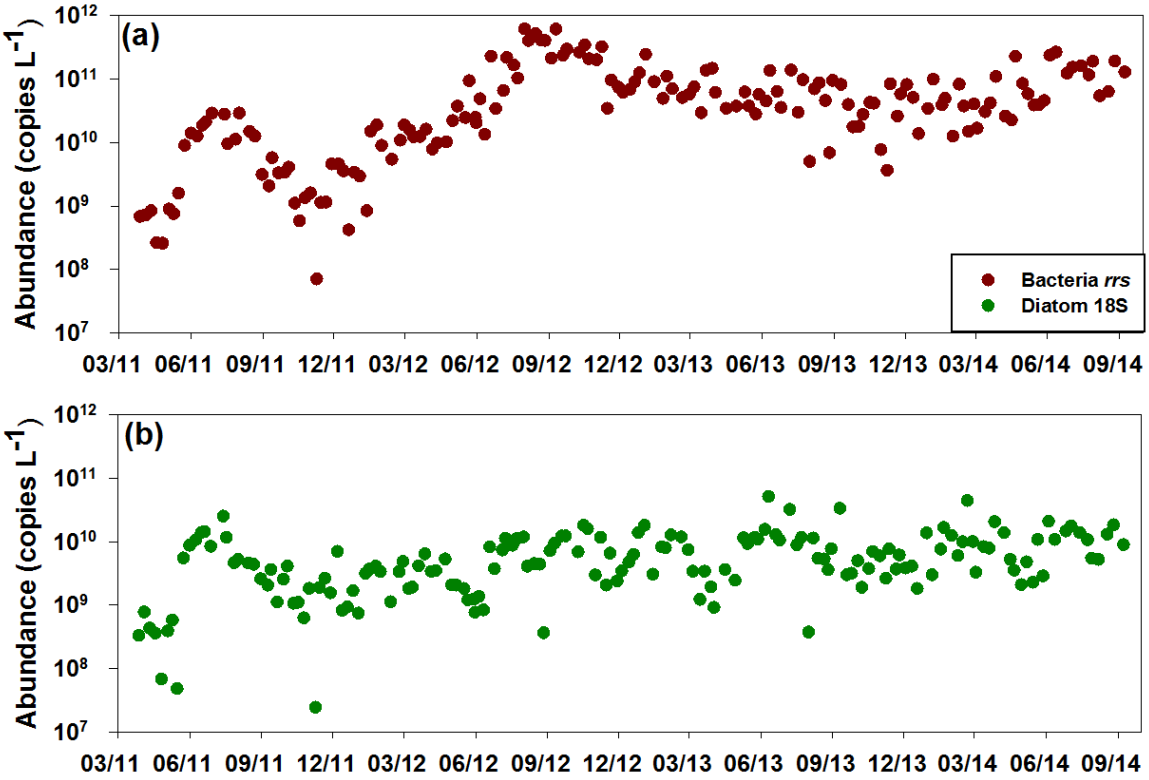
(a)
Abundance (copies L-1)
10^12
10^11
10^10
10^9
10^8
10^7
Bacteria rrs
Diatom 18S
03/11 06/11 09/11 12/11 03/12 06/12 09/12 12/12 03/13 06/13 09/13 12/13 03/14 06/14 09/14
(b)
Abundance (copies L-1)
10^12
10^11
10^10
10^9
10^8
10^7
03/11 06/11 09/11 12/11 03/12 06/12 09/12 12/12 03/13 06/13 09/13 12/13 03/14 06/14 09/14

Figure C.3: **Additional environmental data measured by SINERR at Marsh Landing from March 2011 to September 2014**, including **(a)** dissolved oxygen and **(b)** phosphate concentrations, **(c)** pH, and **(d)** Turbidity.

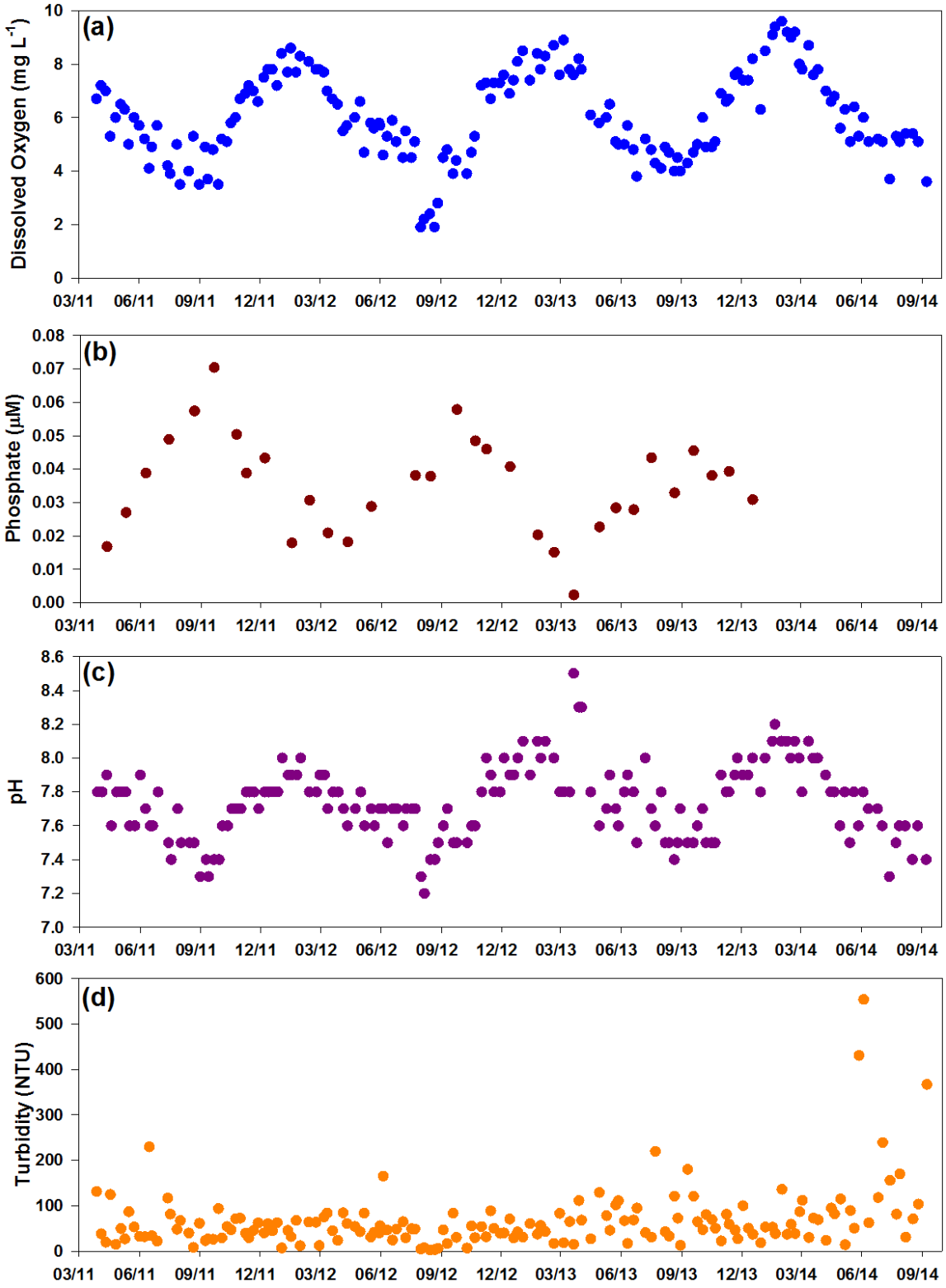
(a)
Dissolved Oxygen (mg L-1)
10
8
6
4
2
0
03/11 06/11 09/11 12/11 03/12 06/12 09/12 12/12 03/13 06/13 09/13 12/13 03/14 06/14 09/14
(b)
Phosphate (µM)
0.08
0.07
0.06
0.05
0.04
0.03
0.02
0.01
0.00
03/11 06/11 09/11 12/11 03/12 06/12 09/12 12/12 03/13 06/13 09/13 12/13 03/14 06/14 09/14
(c)
pH
8.6
8.4
8.2
8.0
7.8
7.6
7.4
7.2
7.0
03/11 06/11 09/11 12/11 03/12 06/12 09/12 12/12 03/13 06/13 09/13 12/13 03/14 06/14 09/14
(d)
Turbidity (NTU)
600
500
400
300
200
100
0
03/11 06/11 09/11 12/11 03/12 06/12 09/12 12/12 03/13 06/13 09/13 12/13 03/14 06/14 09/14

Figure C.4: **Linear models investigating the relationship between biotic and environmental variables** making up the primary axes from Multi-Dimensional Scaling (MDS1; x-axis) and Principal Components Analysis (PC1 or PC2; y-axis), respectively, for various subsets of the data. As Thaumarchaeota abundance corresponded to positive values of MDS1, relationships between Thaumarchaeota and environmental variables can be observed by viewing the regression line in relationship to PC1 or PC2. **(a)** All data, **(b)** SINERR water quality data only, **(c-d)** nutrient data only, **(e)** SINERR nutrient dataset, and **(f)** reduced nutrient dataset to include urea.

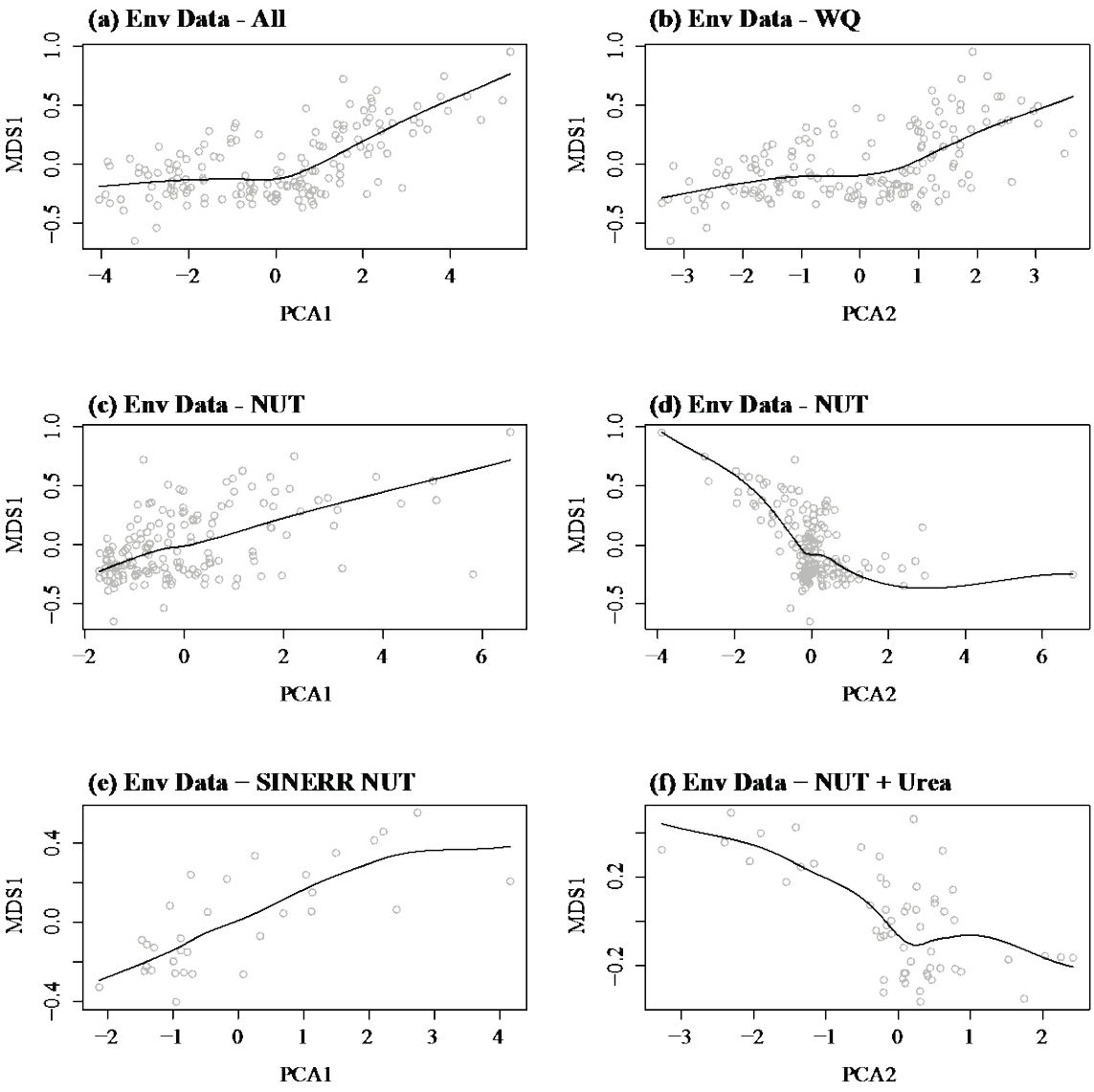
(a) Env Data - All
MDS1
PCA1
(b) Env Data - WQ
MDS1
PCA2
(c) Env Data - NUT
MDS1
PCA1
(d) Env Data - NUT
MDS1
PCA2
(e) Env Data – SINERR NUT
MDS1
PCA1
(f) Env Data – NUT + Urea
MDS1
PCA2

Figure C.5: **Additional statistical analysis plots from subdivided or reduced datasets**: Principal Components Analysis (PCA) plots **(a)** SINERR water quality data only, **(b)** nutrient data only, **(c)** meteorological data only, **(d)** SINERR nutrient dataset, and **(e)** reduced nutrient dataset to include urea; Multi-Dimensional Scaling (MDS) plots **(f**) reduced dataset for SINERR nutrients and **(g)** reduced dataset for nutrients with urea.

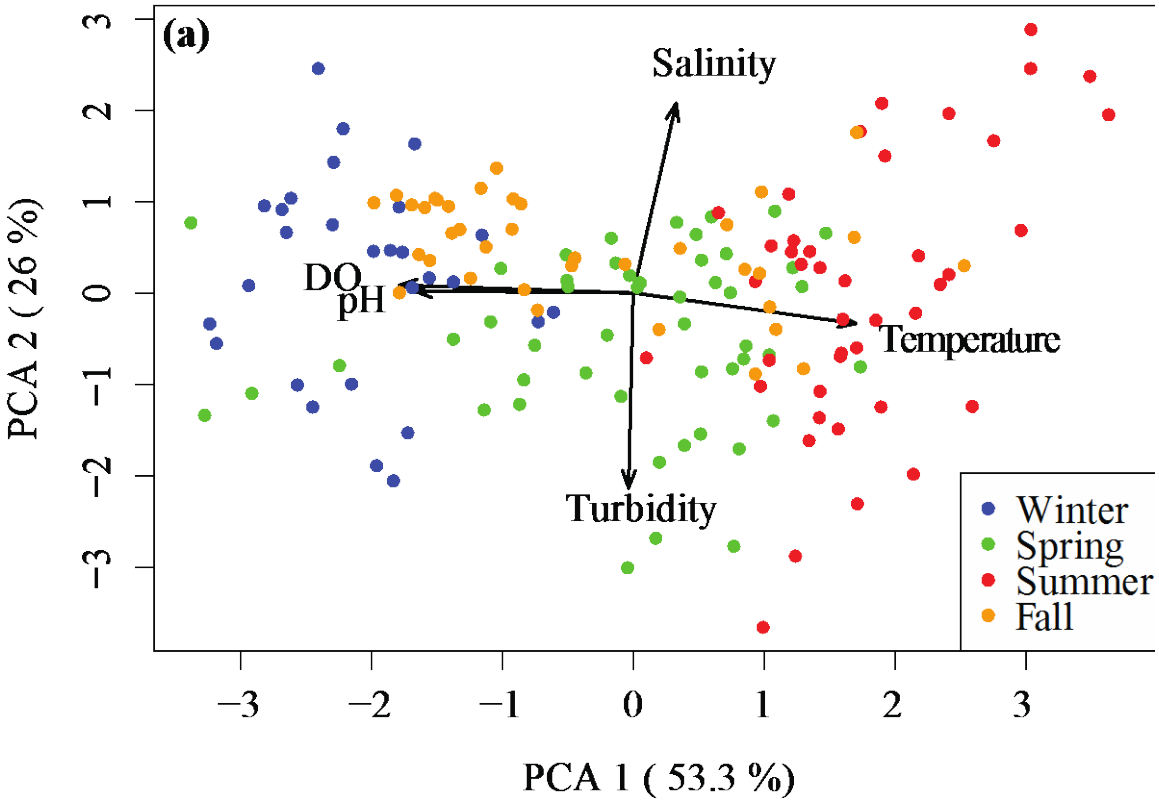
(a)
Salinity
DO
pH
Temperature
Turbidity
Winter
Spring
Summer
Fall
PCA 2 (26 %)
PCA 1 (53.3 %)

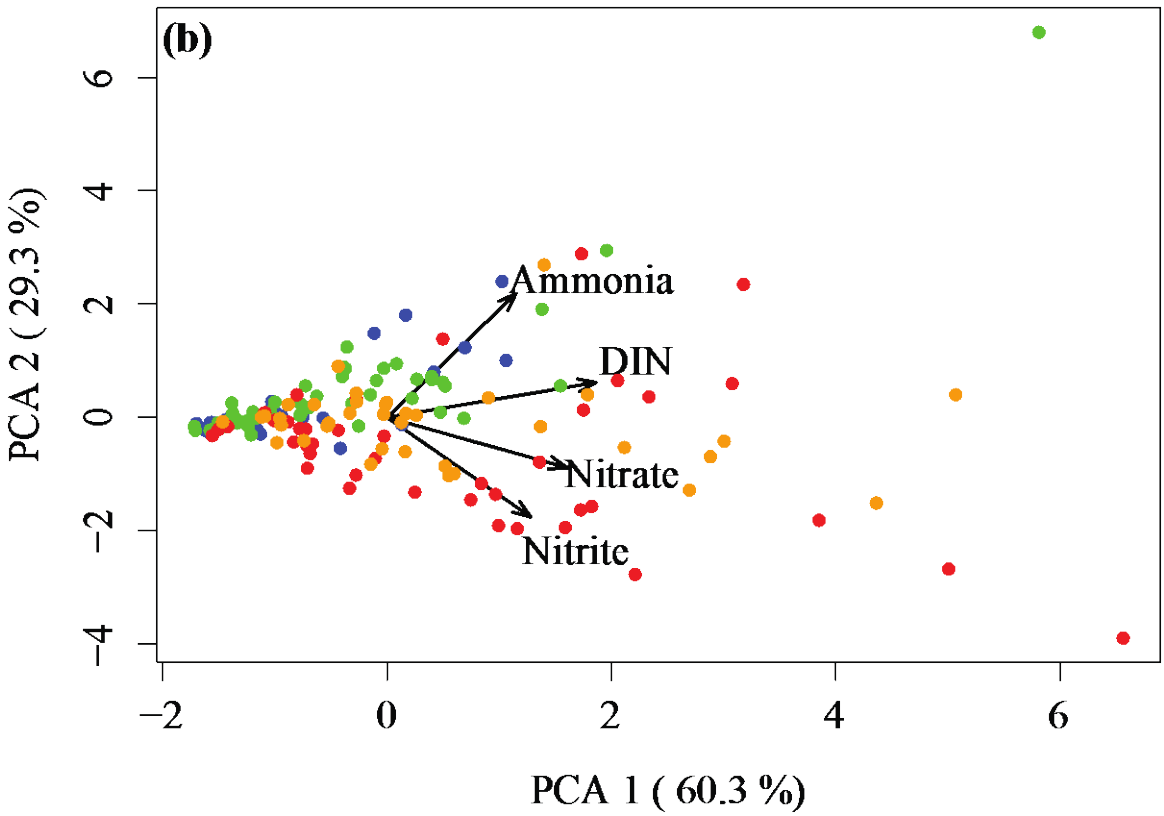
(b)
Ammonia
DIN
Nitrate
Nitrite
PCA 2 (29.3 %)
PCA 1 (60.3 %)

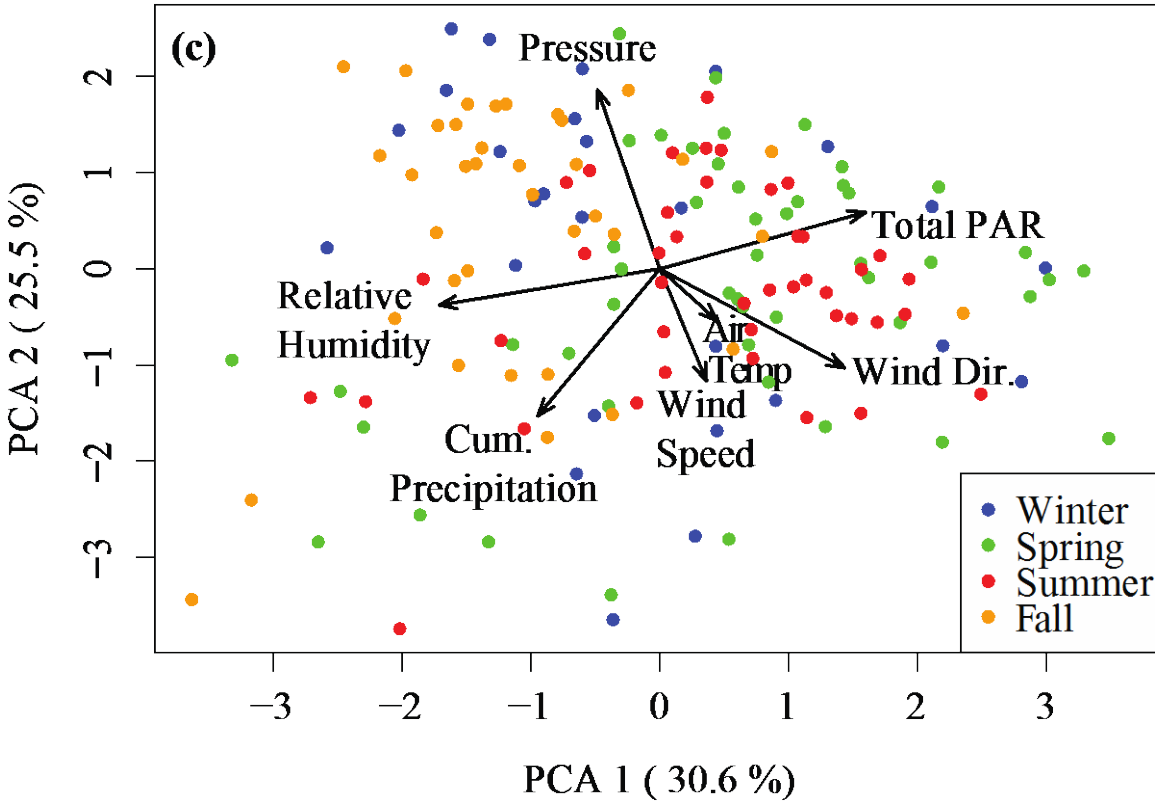
(c)
Pressure
Total PAR
Relative
Humidity
Air
Temp
Wind Dir.
Wind
Speed
Cum.
Precipitation
Winter
Spring
Summer
Fall
PCA 2 (25.5 %)
PCA 1 (30.6 %)

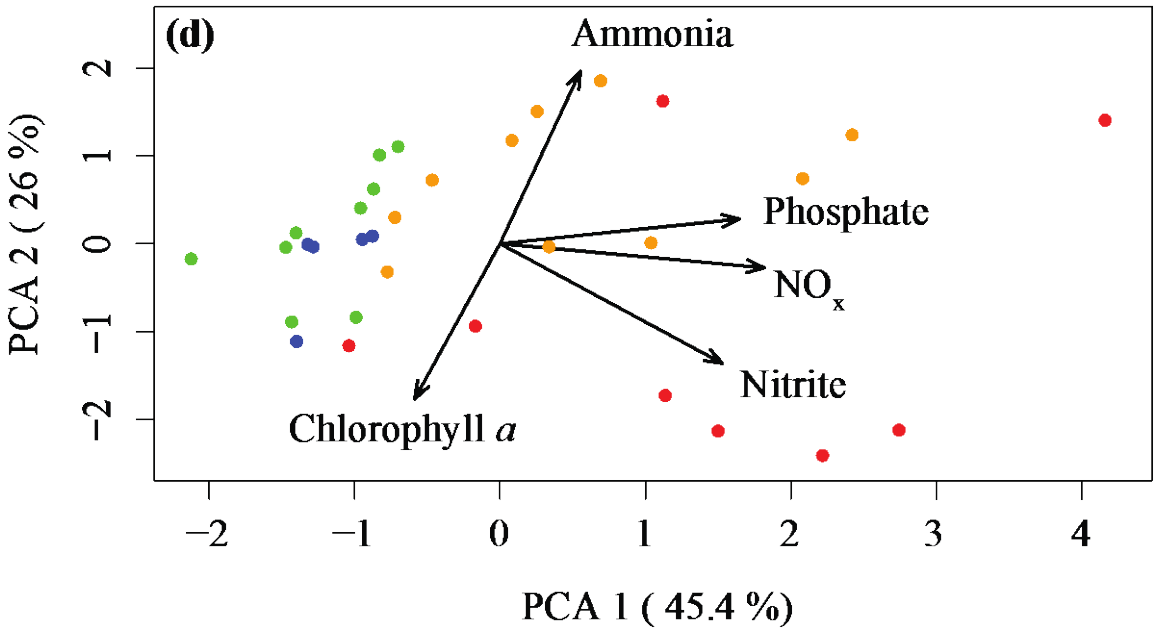
(d)
Ammonia
Phosphate
NO$_x$
Nitrite
Chlorophyll *a*
PCA 2 (26 %)
PCA 1 (45.4 %)

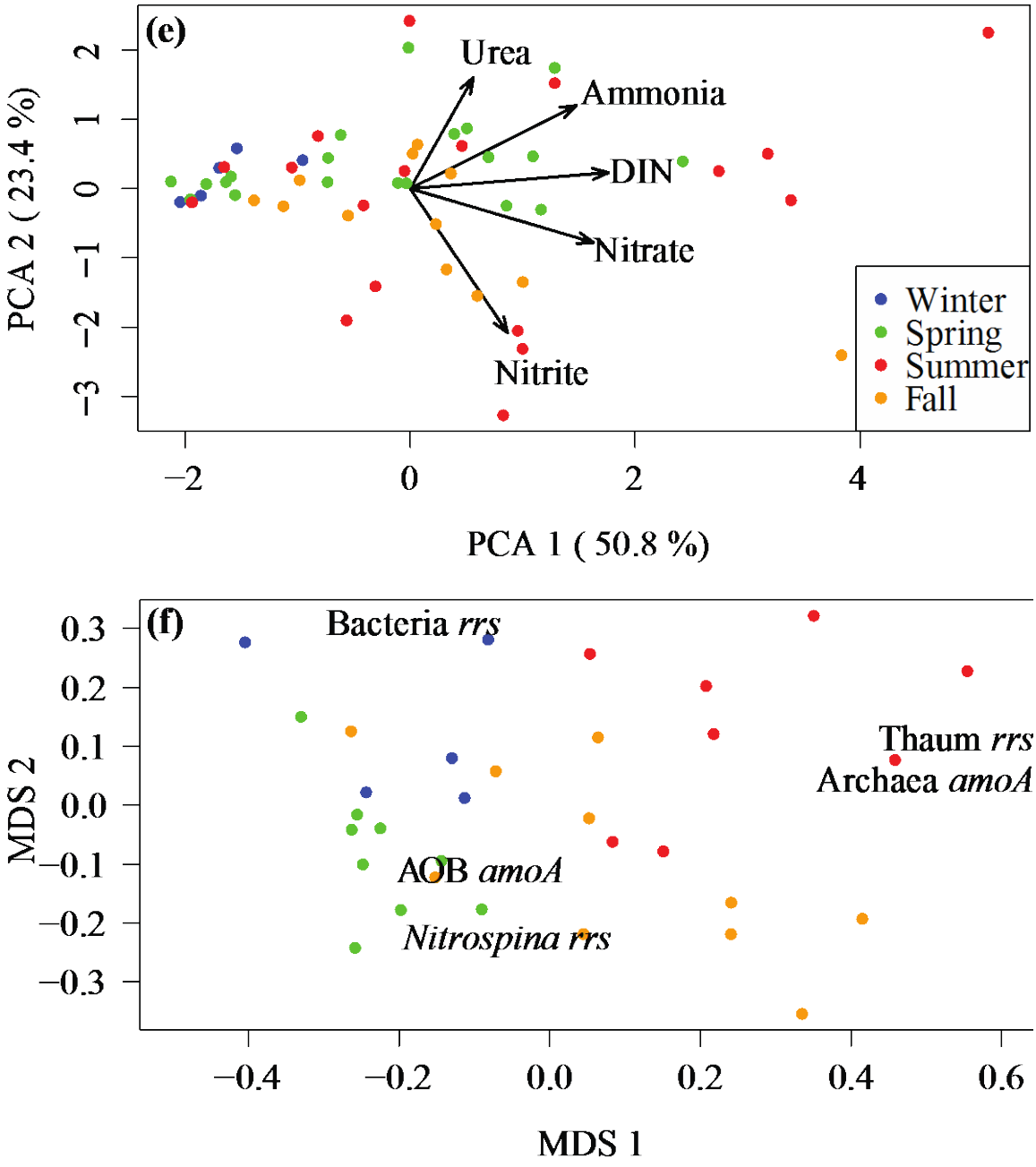
(e)
Urea
Ammonia
DIN
Nitrate
Nitrite
Winter
Spring
Summer
Fall
PCA 2 (23.4 %)
PCA 1 (50.8 %)
(f)
Bacteria rrs
Thaum rrs
Archaea amoA
AOB amoA
Nitrospina rrs
MDS 2
MDS 1

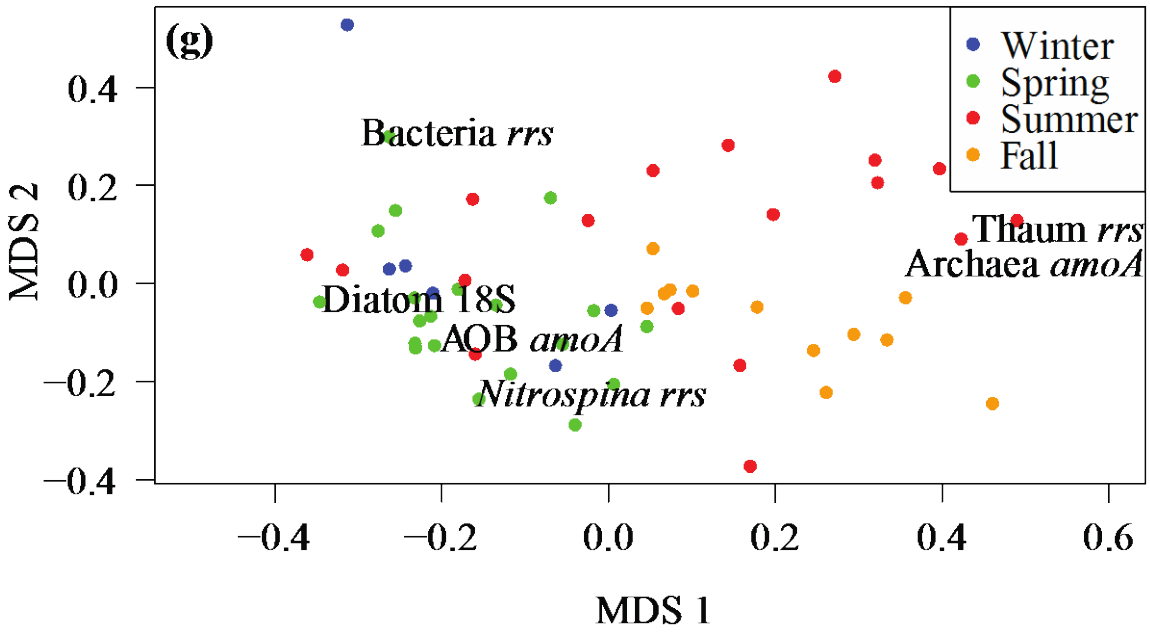
(g)
Winter
Spring
Summer
Fall
Bacteria rrs
Thaum rrs
Archaea amoA
Diatom 18S
AOB amoA
Nitrospina rrs
MDS 2
MDS 1
0.4
0.2
0.0
−0.2
−0.4
−0.4
−0.2
0.0
0.2
0.4
0.6

Figure C.6: Temperature manipulation experiment comparing differences in **(a-b)** ammonia oxidation and **(c-d)** nitrite oxidation using an enrichment from Sapelo Island. Nitrite **(a, c)**, nitrate **(d)**, and nitrite + nitrate **(b)** concentrations are shown for each day and temperature sampled.

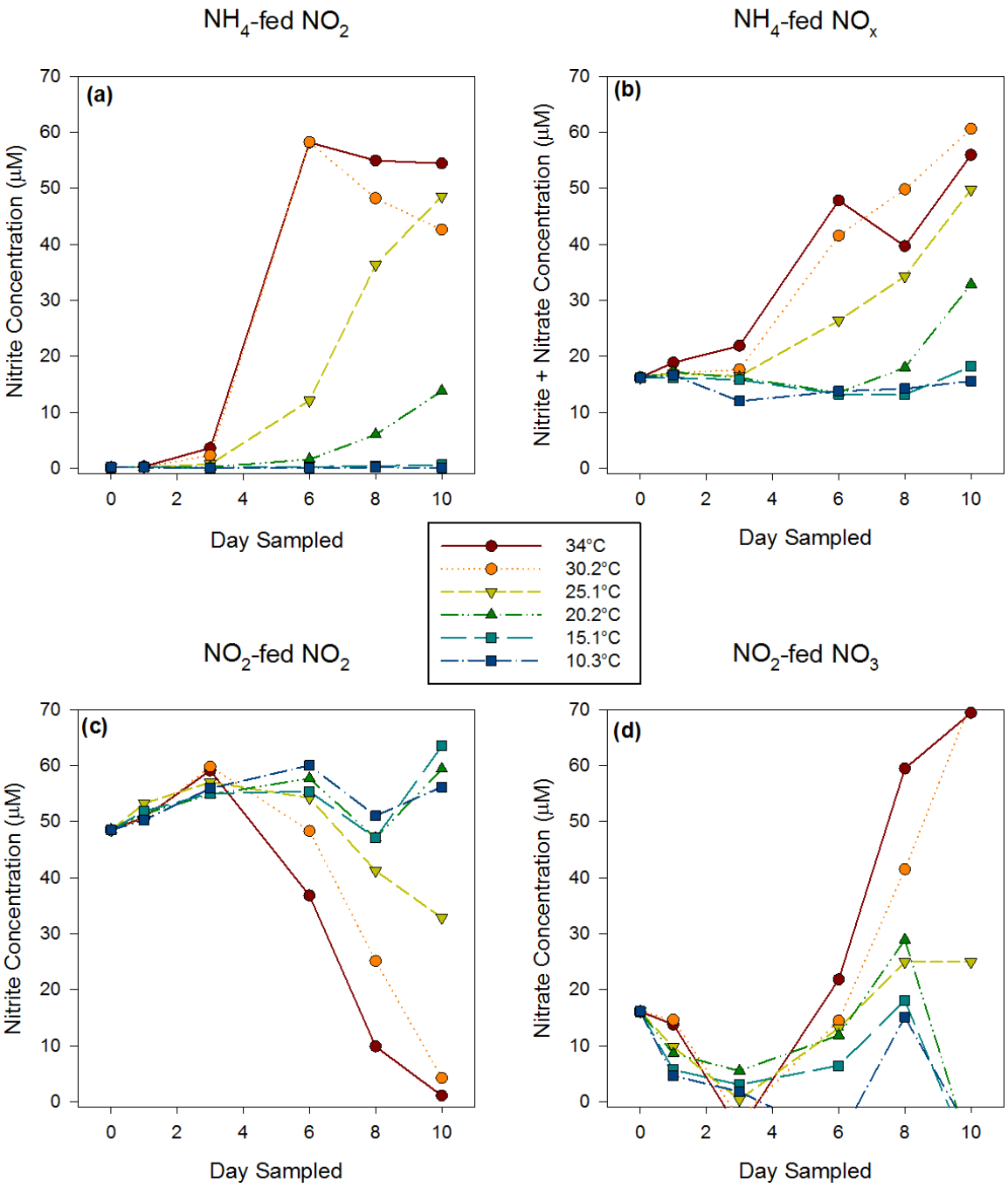
NH4-fed NO2
NH4-fed NOx
(a)
(b)
Nitrite Concentration (µM)
Nitrite + Nitrate Concentration (µM)
Day Sampled
34°C
30.2°C
25.1°C
20.2°C
15.1°C
10.3°C
NO2-fed NO2
NO2-fed NO3
(c)
(d)
Nitrate Concentration (µM)

APPENDIX D

THE SPATIAL EXTENT OF THE SAPELO ISLAND THAUMARCHAEOTA BLOOM INCLUDING THE SOUTH ATLANTIC BIGHT[1]

[1] Tolar, B.B., Q. Liu, and J.T. Hollibaugh. To be submitted to *Applied and Environmental Microbiology.*

PURPOSE

This study aims to determine the spatial constraints of the annual Thaumarchaeota bloom at Sapelo Island (Hollibaugh *et al.*, 2011; Hollibaugh *et al.*, 2014) through samples collected during both bloom and non-bloom periods. We measured Thaumarchaeota abundance and nitrification rates in samples from the estuaries surrounding Sapelo Island, as well as in offshore transects into the South Atlantic Bight (SAB; Atkinson and Menzel, 2013). Additionally, we examined diurnal abundance and activity of Thaumarchaeota at two sites on Sapelo Island to determine if day-night differences observed in ribosomal protein transcripts by Hollibaugh *et al*. (2014) had an effect on nitrification rates.

MATERIALS AND METHODS

Sample collection

Samples were collected from two inshore, estuarine stations at Marsh Landing (ML; 31° 25.068' N, 81° 17.721' W) and Hunt Camp (HC; 31° 25.068' N, 81° 17.721' W) on Sapelo Island, Georgia (Figure D.1, Table D.1), over a 24-hour period on August 13-14, 2011 (ML), April 19-20, 2012 (ML), August 8-9, 2012 (ML, HC), and September 21-22, 2013 (ML, HC). Seawater was obtained directly from the Marsh Landing dock by lowering a sample-rinsed bottle ~10 cm below the surface. Water was transported back to the University of Georgia Marine Institute (UGAMI) laboratory within 15 minutes of collection and immediately filtered (0.4 – 0.7 L) onto duplicate GVWP filters (0.22 μm, 47 mm diameter; Millipore) by vacuum filtration for both DNA and RNA extraction. Filters were stored in WhirlPak bags (Nasco) with 2.0 mL lysis buffer (DNA) or

RNAlater (RNA; Ambion) at -80°C. Fifty milliliters of filtrate was frozen for nutrient analysis at -20°C.

Additional inshore samples were collected from both high and low tides during the Georgia Coastal Ecosystem (GCE) Long-Term Ecological Research (LTER) Network's monthly cruises (Figure D.1; http://gce-lter.marsci.uga.edu/) on the *R/V Salty Dog* from August 13-16, 2011, and April 17-20, 2012. Surface and near-bottom seawater was obtained from bottle casts using a Niskin bottle (Table D.1). DNA was filtered (0.3 – 1.0 L) immediately upon arrival to UGAMI after each tide's sampling as described above, and 50 mL of filtrate was frozen for nutrient analysis at -20°C.

We sampled the South Atlantic Bight (SAB) on three transects from the shore to the Gulf Stream between Savannah, Georgia, and Jacksonville, Florida, on the *R/V Savannah* from April 18-22 (SAV-11-10) and October 2-6 (SAV-11-30), 2011. A total of 14 stations in the SAB were occupied ranging from near-shore, middle shelf, and the shelf-break at the edge of the Gulf Stream (Figure D.2). Seawater was collected using a CTD rosette sampler (Table D.2). Sample water was filtered (0.4 – 1.2 L) immediately upon retrieval as above, 50 mL of filtrate was collected for nutrient analysis, and all samples were stored at -20°C and/or -80°C until analysis.

Nutrient concentrations were determined using previously described methods for ammonia (NH_4; Solórzano, 1969), nitrite (NO_2) and nitrite + nitrate (NO_x; Jones, 1984; Strickland and Parsons, 1972), and urea (Mulvenna and Savidge, 1992; Rahmatullah and Boyde, 1980).

Nucleic acid extraction and quantitative PCR (qPCR)

Sample DNA was extracted from WhirlPak bags using a phenol:chloroform method described in detail previously (Bano and Hollibaugh, 2000; Tolar *et al.*, 2013; Chapters 2-3). DNA was eluted in Tris-EDTA buffer (pH 8.3) and stored at -80°C prior to qPCR. RNA was extracted using previously described methods (Gifford *et al.*, 2011; Poretsky *et al.*, 2009) with slight modifications as described in Chapters 3 and 5. RNA was eluted in nuclease-free water and stored at -80°C. DNA was removed from RNA samples prior to quantitative PCR (qPCR) using the TURBO DNase-Free Kit (Ambion) following manufacturer's instructions with an additional enzyme treatment at 2X concentration.

Methods for quantification of genes and transcripts with qPCR have been described previously (Hollibaugh *et al.*, 2014; Kalanetra *et al.*, 2009; Tolar *et al.*, 2013; Chapters 2-4), and these have been employed for this study using an iCycler iQ^{TM} Real-Time qPCR detection system (BioRad). A list of target genes, including primers and probes used in qPCR, is provided in Table C.2. Bacteria and Marine Group I Archaea (Thaumarchaeota) 16S rRNA (*rrs*) were quantified with TaqMan chemistry using the Platinum Taq qPCR Supermix (Invitrogen); the iQ SYBR Green Supermix (BioRad) was used to quantify all other genes. RT-qPCR targeting *amoA* transcripts (from both Archaea and Bacteria) was performed using the One-Step RT-qPCR SYBR Mix (BioRad). As the coastal, estuarine water samples used in this study contain a number of PCR inhibitors (namely humic acids), both DNA and RNA samples were diluted to a set concentration based on the successful quantification of Bacteria *rrs* as described

previously (Hollibaugh *et al.*, 2014; Chapter 4). All samples were checked for inhibition using this method prior to quantification of any other gene or transcript.

Nitrification Rate Measurements

For a subset of samples (Tables D.1, D.2), seawater was amended with ^{15}N-labeled ammonium chloride ($^{15}NH_4Cl$; Cambridge Isotope Labs) to a final concentration of 50 nM. Incubations were run in duplicate (with a filter-sterilized control) at *in situ* temperature using seawater flow-through tanks at UGAMI or on board the *R/V Savannah* for 24 hours. All samples were frozen at -20°C to terminate incubations, and remained frozen until analysis. Production of $^{15}NO_x$ by ammonium oxidation was measured with the 'denitrifier method' (Sigman *et al.*, 2001) as described in Popp *et al.* (1995) and Dore *et al.* (1998). Briefly, sample seawater was added to *Psuedomonas aureofaciens* cultures to convert NO_2 and NO_3 into N_2O gas; the mass and $\delta^{15}N$ value of N_2O from each sample was measured using a Finnigan MAT-252 isotope ratio mass spectrometer (Thermo Fisher Scientific). Determination of the amount of $^{15}NH_3$ tracer introduced to the NOx pool through ammonia oxidation and calculation of ammonia oxidation rates was performed as described previously (Beman *et al.*, 2008; Beman *et al.*, 2012; Christman *et al.*, 2011).

RESULTS

The annual summer bloom on Sapelo Island (Chapter 4, Appendix C) has only been sampled at one location – Marsh Landing. As is shown here, the bloom is not limited only to this site, but rather extends throughout the GCE-LTER region (Figure

D.3). Abundances of Thaumarchaeota *rrs* were always 10-1000X more abundant in August (2011) than in April (2012), which matches differences observed at Marsh Landing (Figure 4.1a). *amoA* gene abundance reflects *rrs* abundance for this region also (Table D.1).

Diurnal variability in genes did not show a clear trend based on time of day or tide during bloom periods (Figure D.4), while the highest ammonia oxidation (AO) rates were observed during flood tide. Transcripts were lower in abundance than genes (Figure D.4). AO rates for April 2012 (mean = 4.1 nmole L^{-1} d^{-1}; Figure D.4b) were much lower (~110X) than in August (450 nmole L^{-1} d^{-1}; Figure D.4c), indicating that not only are Thaumarchaeota becoming 10-100X more abundant during the bloom (Figure 4.1a) but are also capable of oxidizing ammonia at a much more rapid rate, which would match the disconnect in dissolved inorganic nitrogen (DIN) dynamics discussed in Chapter 4 (Figures 4.1b, 4.2).

In the South Atlantic Bight, the bloom is constrained within the coastal waters (Figure D.5) with increased abundance of Thaumarchaeota genes observed only for inshore stations on two of three transects in October (Figure D.5b, f). The Altamaha River transect (Figure D.5c-d) does not reflect this post-bloom increased abundance inshore (Station #3), but does show an increase at Station #7 surface waters. It does not appear that the Thaumarchaeota are coming from the Gulf Stream, as no increase was observed in mid shelf Stations #6-7, while abundances at offshore Stations #9-12 remained steady between April and October (Figure D.5; $\geq$ 60 m depth). Ammonia oxidation rates measured from SAB samples reflect Thaumarchaeota abundance patterns, with low rates in April (pre-bloom), except in the Gulf Stream (Station #12) at 70 m

depth (Figure D.5e). In October (post-bloom), the only detectable rates were observed at coastal Station #4 and also at 80-200 m depth in the Gulf Stream (Figure D.5f).

ACKNOWLEDGEMENTS

We would like to thank L. Powers, W. Miller, C. Givens, D. Duckett, A. Bratcher, E. Malagón, L. Lim, M. Ross, F. Cao, and X. Liu for assistance with sample collection and processing both in the field and in the laboratory. Additionally, we would like to thank the scientific parties and crew of the R/V *Savannah* and *R/V Salty Dawg*, especially J. Shalack; the GCE-LTER personnel, especially M. Alber and W. Sheldon; and the staff at the UGA Marine Institute on Sapelo Island, especially M. Booth, G. Townsend, and M. Price. Funding for this research was provided by U.S. National Science Foundation grants OCE 09-43278 (EAGER), OCE 13-35838, and OPP 08-38996 to J.T.H; OCE 10-29742 to X. Mou and J.T.H.; and OCE-1129260 to B.N.P.

REFERENCES

Atkinson LP, Menzel DW (2013). Introduction: Oceanography of the Southeast United States Continental Shelf. In: Atkinson LP, Menzel DW, Bush KA (eds). Oceanography of the Southeastern US Continental Shelf. American Geophysical Union: Washington, D. C. pp 1-9.

Bano N, Hollibaugh JT (2000). Diversity and distribution of DNA sequences with affinity to ammonia-oxidizing bacteria of the beta subdivision of the class Proteobacteria in the Arctic Ocean. *Appl Environ Microbiol* **66:** 1960-1969.

Beman JM, Popp BN, Francis CA (2008). Molecular and biogeochemical evidence for ammonia oxidation by marine Crenarchaeota in the Gulf of California. *ISME J* **2:** 429-441.

Beman JM, Popp BN, Alford SE (2012). Quantification of ammonia oxidation rates and ammonia-oxidizing archaea and bacteria at high resolution in the Gulf of California and eastern tropical North Pacific Ocean. *Limnol Oceanogr* **57:** 711-726.

Christman GD, Cottrell MT, Popp BN, Gier E, Kirchman DL (2011). Abundance, Diversity, and Activity of Ammonia-Oxidizing Prokaryotes in the Coastal Arctic Ocean in Summer and Winter. *Appl Environ Microbiol* **77:** 2026-2034.

Dore JE, Popp BN, Karl DM, Sansone FJ (1998). A large source of atmospheric nitrous oxide from subtropical North Pacific surface waters. *Nature* **396:** 63-66.

Gifford SM, Sharma S, Rinta-Kanto JM, Moran MA (2011). Quantitative analysis of a deeply sequenced marine microbial metatranscriptome. *ISME J* **5:** 461-472.

Hollibaugh JT, Gifford S, Sharma S, Bano N, Moran MA (2011). Metatranscriptomic analysis of ammonia-oxidizing organisms in an estuarine bacterioplankton assemblage. *ISME J* **5:** 866-878.

Hollibaugh JT, Gifford SM, Moran MA, Ross MJ, Sharma S, Tolar BB (2014). Seasonal variation in the metratranscriptomes of a Thaumarchaeota population from SE USA coastal waters. *ISME J* **8:** 685-698.

Jones MN (1984). Nitrate Reduction by Shaking with Cadmium - Alternative to Cadmium Columns. *Water Res* **18:** 643-646.

Kalanetra KM, Bano N, Hollibaugh JT (2009). Ammonia-oxidizing Archaea in the Arctic Ocean and Antarctic coastal waters. *Environ Microbiol* **11:** 2434-2445.

Mulvenna PF, Savidge G (1992). A modified manual method for the determination of urea in seawater using diacetylmonoxime reagent. *Estuar Coast Shelf S* **34:** 429-438.

Popp BN, Sansone FJ, Rust TM, Merritt DA (1995). Determination of Concentration and Carbon Isotopic Composition of Dissolved Methane in Sediments and Nearshore Waters. *Anal Chem* **67:** 405-411.

Poretsky RR, Gifford S, Rinta-Kanto J, Vila-Costa M, Moran MA (2009). Analyzing gene expression from marine microbial communities using environmental transcriptomics. *J Vis Exp* **24:** e1086.

Rahmatullah M, Boyde TR (1980). Improvements in the determination of urea using diacetyl monoxime; methods with and without deproteinisation. *Clin Chim Acta* **107:** 3-9.

Sigman DM, Casciotti KL, Andreani M, Barford C, Galanter M, Böhlke JK (2001). A Bacterial Method for the Nitrogen Isotopic Analysis of Nitrate in Seawater and Freshwater. *Anal Chem* **73:** 4145-4153.

Solórzano L (1969). Determination of Ammonia in Natural Waters by the Phenolhypochlorite Method. *Limnol Oceanogr* **14:** 799-801.

Strickland JDH, Parsons TR (1972). Determination of Reactive Silicate. In: Stevenson JC (ed). A Practical Handbook of Seawater Analysis, 2nd edn. Fisheries Research Board of Canada: Ottawa, Canada. pp 65-70.

Tolar BB, King GM, Hollibaugh JT (2013). An analysis of thaumarchaeota populations from the northern Gulf of Mexico. *Front Microbiol* **4:** 72.

Table D.1: Summary of Thaumarchaeota abundance (qPCR) and ammonia oxidation rates for Sapelo Island, Georgia.

Sample ID	Date	Time	Tide	Nutrient Data (μM)					AO Rate (nM d^{-1})	SD	DNA Vol. Filtered (L)	RNA Vol. Filtered (L)
				$[NO_2]$	$[NO_x]$	$[NH_4]$	DIN	Urea				
MLD-1	08/13/11	16:00	Low	5.14	8.57	0.95	14.67	1.31	394.08	56.06	0.50	0.90
MLD-2		21:45	High	2.34	3.85	1.15	7.33	1.20	404.83	69.46	0.70	N/A
MLD-3	08/14/11	4:00	Low	5.42	7.53	0.48	13.43	0.64	314.42	17.83	0.58	N/A
MLD-4		10:15	High	4.42	5.81	0.69	10.91	0.48	326.00	27.79	0.65	N/A
MLD-5		16:04	Low	3.64	5.28	0.98	9.90	0.73	245.03	5.96	0.75	N/A
MLD-6		22:20	High	3.33	4.26	0.52	8.12	3.55	381.94	107.17	0.65	N/A
ML-7	8/15/2011	9:09	High	7.10	10.57	0.13	17.80	0.40	159.50	11.93	0.60	0.65
ML-8		12:10	Low	5.29	7.91	0.84	14.03	ND	ND	ND	0.48	N/A
MLD-1	4/19/2011	13:43	Low	0.05	1.49	1.87	3.37	0.26	3.40	0.09	0.60	0.60
MLD-2		19:39	High	0.06	0.96	0.48	1.44	0.26	0.94	0.15	0.60	0.60
MLD-3	4/20/2011	2:56	Low	0.11	1.78	4.16	5.93	0.61	4.85	1.01	0.60	0.60
MLD-4		7:47	High	0.05	1.27	0.60	1.87	0.34	7.01	0.97	0.60	0.60
MLD-1	08/07/12	3:30	Ebb	2.57	3.81	1.58	5.39	ND	392.80	47.95	0.60	0.60
MLD-2		7:45	Low	2.52	4.04	2.08	6.12	ND	380.74	66.45	0.60	0.60
MLD-3		10:30	Flood	3.29	4.69	2.05	6.75	ND	327.42	8.90	0.60	0.60
MLD-4		13:50	High	1.36	2.56	3.12	5.68	ND	330.38	36.90	0.60	0.60
MLD-5		16:05	Ebb	2.68	4.13	1.38	5.51	ND	456.94	42.70	0.60	0.60
MLD-5R10min		16:15	Rain	2.05	3.09	0.48	3.57	ND	ND	ND	N/A	0.60
MLD-5R30min		16:51	Rain	2.54	3.99	2.56	6.55	ND	ND	ND	N/A	0.60
MLD-5R100min		17:47	Rain	2.84	4.01	1.42	5.43	ND	647.48	65.12	0.60	0.60
MLD-6		20:07	Low	2.61	5.93	1.79	7.72	ND	775.27	33.29	0.65	0.65
MLD-7		23:23	Flood	2.58	7.11	3.15	10.27	ND	270.64	97.85	0.60	0.60
MLD-8	08/08/12	2:39	High	2.17	5.23	1.04	6.26	ND	428.48	35.42	0.60	0.60
MLD-9		16:50	Ebb	2.90	6.94	1.52	8.46	ND	ND	ND	0.60	0.60

Sample ID	Date	Time	Tide	Nutrient Data (µM)					AO Rate (nM d^{-1})	SD	DNA Vol. Filtered (L)	RNA Vol. Filtered (L)
				$[NO_2]$	$[NO_x]$	$[NH_4]$	DIN	Urea				
HCD-1	08/07/12	7:17	Low	0.61	1.66	6.52	8.18	0.39	363.26	26.19	0.60	0.60
HCD-2		13:30	High	1.25	2.17	0.84	3.01	0.42	86.07	26.08	0.60	0.60
HCD-3		19:29	Low	0.22	1.21	1.45	2.66	0.47	2.69	0.57	0.65	0.65
HCD-4	08/08/12	2:01	High	1.97	5.82	2.50	8.32	0.22	385.11	15.61	0.60	0.60
MLD-1	09/21/13	7:18	Flood	2.65	7.42	3.87	11.29	0.05	757.04	32.93	0.60	0.60
MLD-2		10:14	High	2.53	7.42	2.28	9.70	0.04	533.17	17.49	0.65	0.65
MLD-3		13:18	Ebb	2.50	8.36	2.73	11.09	0.05	791.01	22.02	0.40	0.40
MLD-4		16:10	Low	2.30	6.31	2.13	8.44	0.06	373.93	3.30	0.60	0.60
MLD-5		20:04	Flood	2.67	7.02	3.03	10.05	0.04	617.48	41.32	0.60	0.60
MLD-6		23:04	High	2.67	6.01	3.62	9.63	0.05	804.07	13.58	0.60	0.60
MLD-7	09/22/13	3:00	Ebb	1.22	2.13	2.95	5.08	0.02	114.01	16.07	0.50	0.50
MLD-8		5:40	Low	2.33	5.06	2.99	8.05	0.05	482.09	44.45	0.60	0.60
MLD-9		10:45	High	2.73	5.92	2.89	8.81	0.04	531.40	22.22	0.60	0.60

*ND = not determined; N/A = not applicable, no DNA or RNA sample collected.

Sample ID	qPCR Data (all are copies per L sample filtered)									
	Archaea *amoA* gene	**Archaea *amoA* mRNA**	**Thaum. *rrs***	**Thaum. *ureC* gene**	***ureC* mRNA**	**AOB *amoA* gene**	**AOB *amoA* mRNA**	**Bacteria *rrs***	***Nitrospina rrs***	**Diatom 18S rRNA**
MLD-1	6.62E+07	4.63E+05	5.13E+07	2.97E+06	LD	1.16E+05	LD	7.48E+05	1.42E+05	1.48E+09
MLD-2	4.67E+07	ND	1.21E+07	1.20E+06	ND	9.38E+04	ND	1.30E+06	9.13E+04	1.25E+09
MLD-3	7.79E+07	ND	9.15E+07	1.66E+06	ND	2.98E+05	ND	1.10E+06	2.71E+05	3.08E+09
MLD-4	5.15E+07	ND	2.84E+07	2.20E+06	ND	1.72E+05	ND	1.20E+06	8.24E+04	1.51E+09
MLD-5	9.39E+07	ND	5.41E+07	3.02E+06	ND	1.85E+05	ND	1.07E+06	2.33E+05	3.40E+09
MLD-6	2.73E+07	ND	2.16E+07	1.92E+06	ND	9.84E+04	ND	4.79E+05	6.84E+04	1.27E+09
ML-7	5.84E+07	3.44E+05	3.36E+07	2.79E+06	LD	2.40E+05	LD	1.73E+06	3.96E+05	2.02E+09
ML-8	4.14E+07	ND	5.36E+07	2.50E+06	ND	1.10E+05	ND	4.48E+05	7.91E+05	2.34E+09
MLD-1	9.10E+05	5.75E+04	3.84E+05	2.62E+05	LD	2.42E+05	LD	1.79E+10	1.71E+05	1.78E+10
MLD-2	2.94E+05	3.75E+04	1.31E+05	1.45E+05	LD	7.96E+04	LD	8.00E+09	1.75E+05	8.92E+09
MLD-3	3.96E+05	7.46E+04	1.44E+05	8.63E+04	LD	1.14E+05	LD	6.71E+09	1.70E+05	5.14E+10
MLD-4	3.78E+05	2.08E+04	1.07E+06	1.27E+05	LD	1.12E+06	LD	9.30E+09	4.15E+05	1.18E+10
MLD-1	9.43E+07	5.35E+04	6.67E+07	2.09E+07	9.50E+03	1.87E+05	LD	1.01E+11	8.44E+05	1.60E+10
MLD-2	1.74E+08	1.94E+06	1.14E+08	3.44E+07	3.39E+02	6.60E+05	LD	1.93E+11	8.01E+05	2.35E+10
MLD-3	1.27E+08	6.06E+05	1.02E+08	2.24E+07	LD	1.11E+06	LD	7.82E+10	4.48E+05	2.67E+10
MLD-4	1.22E+08	6.27E+04	1.27E+08	4.75E+07	LD	6.58E+05	LD	1.79E+11	6.65E+05	2.53E+10
MLD-5	6.53E+07	3.98E+04	1.73E+07	1.05E+07	LD	7.91E+05	LD	1.33E+10	1.50E+05	1.55E+10
MLD-5R10min	N/A	6.13E+05	N/A	N/A	LD	N/A	LD	N/A	N/A	N/A
MLD-5R30min	N/A	3.23E+04	N/A	N/A	LD	N/A	LD	N/A	N/A	N/A
MLD-5R100min	1.12E+08	1.29E+06	1.02E+08	1.86E+07	LD	5.45E+05	LD	1.37E+11	1.04E+06	1.29E+10
MLD-6	9.52E+07	7.91E+04	8.19E+07	2.98E+07	LD	9.22E+05	LD	1.21E+11	1.02E+06	1.24E+10
MLD-7	8.61E+07	6.04E+04	8.32E+07	2.79E+07	LD	6.27E+05	LD	8.54E+10	7.53E+05	1.99E+10
MLD-8	1.24E+08	6.47E+04	8.13E+07	3.59E+07	LD	7.34E+05	LD	1.18E+11	1.11E+06	1.22E+10
MLD-9	5.13E+07	3.12E+04	1.82E+08	3.30E+07	LD	8.25E+05	LD	2.09E+11	2.35E+06	5.49E+09

Sample ID	qPCR Data (all are copies per L sample filtered)									
	Archaea *amoA* gene	**Archaea *amoA* mRNA**	**Thaum. *rrs***	**Thaum. *ureC* gene**	***ureC* mRNA**	**AOB *amoA* gene**	**AOB *amoA* mRNA**	**Bacteria *rrs***	***Nitrospina rrs***	**Diatom 18S rRNA**
HCD-1	5.62E+07	7.35E+05	3.22E+07	7.76E+06	LD	5.84E+05	LD	3.10E+11	8.56E+05	1.50E+10
HCD-2	8.71E+07	3.99E+06	4.37E+07	1.42E+07	LD	6.43E+05	3.25E+03	2.31E+11	7.97E+05	1.44E+10
HCD-3	6.29E+07	1.83E+05	3.46E+07	1.05E+07	LD	6.17E+05	LD	2.64E+11	8.97E+05	2.09E+10
HCD-4	8.52E+07	2.75E+06	4.70E+07	1.55E+07	LD	1.01E+06	LD	2.14E+11	6.66E+05	2.75E+10
MLD-1	1.89E+06	2.39E+04	8.29E+07	2.83E+07	LD	3.69E+05	LD	2.40E+10	8.16E+05	7.80E+09
MLD-2	1.18E+07	3.22E+05	9.07E+07	2.85E+07	1.11E+04	6.36E+05	LD	4.01E+10	6.74E+05	9.19E+09
MLD-3	2.86E+07	1.69E+05	5.96E+07	1.36E+09	LD	1.66E+06	LD	2.77E+10	3.17E+06	7.29E+09
MLD-4	1.30E+07	1.08E+06	1.41E+08	2.99E+06	1.33E+04	7.78E+05	LD	3.43E+10	9.23E+05	1.01E+10
MLD-5	7.40E+06	3.41E+06	5.79E+07	1.13E+08	6.21E+04	4.79E+05	LD	2.65E+10	7.35E+05	5.58E+09
MLD-6	2.33E+07	3.94E+05	1.28E+08	1.50E+08	9.83E+03	1.01E+06	LD	3.81E+10	9.76E+05	4.66E+09
MLD-7	8.38E+07	1.46E+04	3.28E+08	9.86E+08	LD	1.27E+07	LD	1.02E+11	2.21E+07	1.69E+10
MLD-8	8.55E+06	8.06E+06	7.20E+07	5.12E+07	7.07E+04	9.07E+05	LD	2.87E+10	5.38E+05	4.22E+09
MLD-9	1.04E+07	1.85E+06	6.37E+07	5.28E+07	1.07E+04	5.46E+05	LD	3.07E+10	7.10E+05	3.29E+09

*ND = not determined; LD = below limit of detection; N/A = not applicable, no DNA sample collected

Table D.2: Summary of Thaumarchaeota abundance (qPCR) and ammonia oxidation rates for the South Atlantic Bight.

Stn #	Depth (m)	Station Name	Date	Latitude (N)	Longitude (W)	Nutrient Data (µM)					AO Rate (nM d^{-1})	AO Rate SD
						[NO_2]	[NO_x]	[NH_4]	DIN	Urea		
2	1.6	Wassaw Sound	4/18/2011	31° 55.47'	80° 58.04'	0.04	1.13	1.92	3.06	ND	ND	ND
	11.75					0.02	0.79	0.64	1.43	ND	ND	ND
5	3	Savannah Mid Shelf	4/18/2011	31° 40.15'	80° 08.44'	0.00	0.58	0.92	1.50	ND	ND	ND
	32					0.02	0.54	0.51	1.05	ND	ND	ND
9	10	Savannah Offshore	4/19/2011	31° 23.40'	79° 20.32'	LD	0.50	0.45	0.95	ND	ND	ND
	75					0.08	4.87	0.22	5.09	ND	ND	ND
	433					0.07	30.94	0.25	31.19	ND	ND	ND
6	3	Gray's Reef Mid Shelf	4/19/2011	31° 16.13'	80° 22.65'	0.04	0.40	0.48	0.88	ND	ND	ND
	34					0.02	0.56	0.42	0.99	ND	ND	ND
GR	3	Gray's Reef	4/19/2011	31° 23.50'	80° 51.81'	0.02	0.53	LD	0.25	ND	ND	ND
	18.5					0.05	0.53	LD	0.16	ND	ND	ND
3	2	Altamaha Plume	4/19/2011	31° 18.26'	81° 08.96'	0.05	0.92	0.29	1.22	ND	ND	ND
	6					0.37	0.88	2.15	3.03	ND	ND	ND
4	1.5	St. Mary's	4/20/2011	30° 42.92'	81° 21.36'	0.02	1.49	0.49	1.98	0.12	1.12	1.05
	13					0.02	0.81	0.44	1.25	0.22	0.27	0.00
8	2	St. Mary's Mid Shelf	4/20/2011	30° 31.38'	80° 42.86'	0.04	0.96	0.24	1.20	0.15	**-1.14**	0.03
	30.5					0.00	0.62	LD	0.59	0.13	1.31	0.32
12	10	St. Mary's Offshore	4/20/2011	30° 19.05'	79° 56.12'	LD	0.59	LD	0.50	ND	**-0.05**	0.01
	70					2.03	3.07	2.41	5.48	0.26	82.88	3.46
	500					0.00	32.26	LD	32.13	0.08	0.62	0.41
11	10	Altamaha Offshore	4/20/2011	30° 43.20'	79° 45.93'	0.02	0.39	LD	0.03	ND	ND	ND
	60					0.14	1.96	LD	1.80	ND	ND	ND
	470					0.04	29.07	LD	28.55	ND	ND	ND

Stn #	Depth	Station Name	Date	Latitude (N)	Longitude (W)	Nutrient Data (µM)					AO Rate (nM d^{-1})	AO Rate SD
						$[NO_2]$	$[NO_x]$	$[NH_4]$	DIN	Urea		
7	2	Altamaha Mid Shelf	4/20/2011	31° 02.44'	80° 52.19'	0.04	0.49	LD	0.46	ND	ND	ND
	27.5					0.04	0.50	LD	0.17	ND	ND	ND
GR	4	Gray's Reef	10/3/2011	31° 23.50'	80° 51.81'	0.001	0.58	LD	LD	ND	ND	ND
	17					0.01	0.62	LD	LD	ND	ND	ND
12	20	St. Mary's Offshore	10/4/2011	30° 19.05'	79° 56.12'	0.002	1.21	LD	0.46	0.83	0.17	0.05
	80					0.13	3.10	LD	2.20	0.04	6.04	1.41
	200					0.05	19.29	0.66	19.95	0.20	3.84	0.51
	445					0.001	24.25	LD	23.94	1.00	1.60	7.12
8	4	St. Mary's Mid Shelf	10/4/2011	30° 31.38'	80° 42.86'	0.02	0.42	LD	0.22	1.34	7.90	9.06
	32					0.07	LD	LD	LD	0.08	0.01	0.02
4	4	St. Mary's	10/4/2011	30° 42.92'	81° 21.36'	0.08	0.94	1.10	2.04	0.28	120.29	104.78
	9					0.14	0.76	1.35	2.11	1.18	86.46	48.34
3	4	Altamaha Plume	10/4/2011	31° 18.26'	81° 08.96'	0.05	0.65	0.67	1.33	ND	ND	ND
	11					0.08	0.57	0.87	1.45	ND	ND	ND
7	4	Altamaha Mid Shelf	10/5/2011	31° 02.44'	80° 52.19'	0.06	0.10	0.20	0.31	ND	ND	ND
	27					0.05	0.11	0.99	1.10	ND	ND	ND
11	4	Altamaha Offshore	10/5/2011	30° 43.20'	79° 45.93'	0.01	0.08	LD	LD	ND	ND	ND
	80					0.19	2.61	0.35	2.96	ND	ND	ND
	250					0.02	20.89	0.20	21.09	ND	ND	ND
	400					0.03	17.19	0.28	17.47	ND	ND	ND
10	4	Gray's Reef Offshore	10/5/2011	31° 03.29'	79° 33.19'	0.01	0.03	0.07	0.10	ND	ND	ND
	80					0.07	10.63	0.20	10.83	ND	ND	ND
	260					0.04	9.90	0.56	10.46	ND	ND	ND
	500					0.01	30.18	0.95	31.13	ND	ND	ND

Stn #	Depth	Station Name	Date	Latitude (N)	Longitude (W)	Nutrient Data (µM)					AO Rate (nM d^{-1})	AO Rate SD
						[NO_2]	[NO_x]	[NH_4]	DIN	Urea		
6	4 m	Gray's Reef Mid Shelf	10/5/2011	31° 16.13'	80° 22.65'	0.04	0.16	0.18	0.34	ND	ND	ND
	30 m					0.06	9.62	0.47	10.08	ND	ND	ND
13	4 m	Sapelo Sound	10/6/2011	31° 31.08'	81° 03.12'	0.09	0.20	0.36	0.56	ND	ND	ND
	9 m					0.07	0.25	LD	0.09	ND	ND	ND
1	4 m	Savannah River	10/7/2011	32° 02.37'	80° 55.31'	3.27	10.05	4.73	14.78	ND	ND	ND
	13.5 m					3.11	9.97	2.75	12.73	ND	ND	ND

*ND = not determined; LD = below limit of detection; SD = standard deviation.

AO = ammonia oxidation rate; values in **red are negative, and should be interpreted as below the limit of detection.

Stn #	Depth (m)	DNA Vol. Filt. (L)	RNA Vol. Filt. (L)	qPCR Data (all are copies per L sample filtered)								
				Archaea *amoA* gene	**Archaea *amoA* mRNA**	**Thaum. *rrs***	**Thaum. *ureC* gene**	***ureC* mRNA**	**AOB *amoA* gene**	**AOB *amoA* mRNA**	**Bacteria *rrs***	***Nitro-spina rrs***
2	1.6	0.6	0.6	1.12E+05	ND	9.44E+04	ND	ND	2.78E+04	ND	2.65E+09	2.16E+05
	11.75	0.5	0.5	1.46E+05	ND	3.04E+05	ND	ND	4.07E+04	ND	3.67E+09	9.87E+05
5	3	1.03	1.15	6.16E+03	ND	2.40E+04	ND	ND	6.55E+02	ND	1.00E+09	1.98E+03
	32	1.2	1.1	4.47E+03	ND	3.31E+04	ND	ND	2.25E+03	ND	8.75E+08	2.07E+04
9	10	0.8	0.8	1.21E+03	ND	1.47E+03	ND	ND	5.86E+02	ND	7.47E+08	1.21E+03
	75	0.9	0.9	1.10E+07	ND	2.09E+07	ND	ND	1.51E+03	ND	5.13E+08	9.50E+05
	433	1.0	1.2	4.22E+05	ND	1.45E+07	ND	ND	5.02E+03	ND	9.19E+07	1.27E+06
6	3	1.0	1.0	4.88E+02	ND	1.42E+03	ND	ND	6.63E+02	ND	3.19E+08	4.78E+02
	34	1.1	1.0	1.66E+04	ND	2.31E+04	ND	ND	6.32E+04	ND	1.24E+09	1.81E+03
GR	3	1.0	1.0	1.61E+03	ND	3.05E+03	ND	ND	7.55E+03	ND	1.20E+08	1.18E+03
	18.5	1.0	1.0	5.09E+04	ND	9.25E+04	ND	ND	1.02E+04	ND	1.94E+09	6.18E+03
3	2	0.9	0.9	3.63E+05	ND	1.22E+06	ND	ND	1.23E+06	ND	5.88E+09	6.65E+05
	6	0.9	0.8	3.66E+05	ND	8.07E+05	ND	ND	7.35E+05	ND	1.07E+10	1.35E+06
4	1.5	0.9	0.9	1.18E+05	2.19E+04	2.23E+04	3.04E+05	1.14E+04	5.56E+04	6.41E+04	4.78E+09	1.23E+04
	13	0.9	0.9	1.81E+05	9.09E+03	5.45E+05	4.13E+04	1.19E+04	1.52E+06	LD	6.35E+09	5.96E+05
8	2	1.0	1.0	4.36E+04	1.31E+03	1.07E+04	1.16E+05	LD	5.65E+05	3.82E+03	5.25E+09	2.10E+04
	30.5	1.1	1.1	1.37E+05	6.09E+03	5.68E+04	2.10E+05	1.38E+03	3.13E+04	2.63E+03	2.42E+09	2.31E+04
12	10	1.2	1.2	3.20E+02	1.29E+02	8.04E+02	1.85E+04	LD	9.44E+02	1.21E+03	1.60E+08	8.46E+02
	70	1.0	1.1	6.82E+07	2.27E+06	2.60E+07	2.65E+07	2.19E+03	7.13E+03	3.00E+03	6.45E+08	7.00E+05
	500	1.0	1.0	1.13E+06	2.37E+04	2.56E+07	1.33E+06	3.26E+03	3.94E+03	LD	1.85E+08	1.01E+06
11	10	1.0	1.0	4.73E+02	ND	2.50E+02	ND	ND	6.86E+02	ND	8.62E+08	3.94E+02
	60	1.0	1.0	4.25E+07	ND	3.81E+07	ND	ND	1.24E+04	ND	1.72E+09	6.53E+05
	470	1.0	1.1	9.58E+04	ND	4.24E+05	ND	ND	3.54E+02	ND	3.21E+06	7.94E+03

Stn #	Depth (m)	DNA Vol. Filt. (L)	RNA Vol. Filt. (L)	qPCR Data (all are copies per L sample filtered)								
				Archaea *amoA* gene	Archaea *amoA* mRNA	Thaum. *rrs*	Thaum. *ureC* gene	*ureC* mRNA	AOB *amoA* gene	AOB *amoA* mRNA	Bacteria *rrs*	*Nitro-spina rrs*
7	2	1.0	1.0	2.08E+03	ND	1.39E+03	ND	ND	2.79E+03	ND	2.30E+08	1.24E+02
	27.5	1.0	1.0	1.44E+05	ND	8.30E+04	ND	ND	4.42E+03	ND	1.74E+09	1.38E+03
GR	4	1	1	1.06E+05	ND	3.58E+05	ND	ND	5.83E+04	ND	2.21E+09	1.28E+04
	17	1	1	1.58E+05	ND	3.83E+05	ND	ND	2.60E+05	ND	1.09E+09	5.53E+04
12	20	1	1	1.56E+04	2.04E+03	1.61E+04	2.10E+05	LD	4.53E+03	1.16E+03	5.92E+08	2.93E+03
	80	1	1	2.12E+07	5.97E+06	2.82E+07	3.31E+07	LD	1.27E+04	2.12E+03	1.12E+09	1.05E+06
	200	1	1	2.24E+06	6.26E+04	4.89E+07	4.53E+06	LD	8.19E+03	5.67E+03	1.81E+08	2.39E+06
	445	1	1	7.30E+05	1.99E+05	7.98E+06	2.96E+06	2.68E+03	9.05E+02	1.42E+03	3.38E+07	8.59E+05
8	4	1.01	1	1.26E+05	3.44E+03	2.94E+04	1.36E+06	2.40E+03	4.66E+04	4.66E+03	4.37E+09	1.18E+04
	32	0.8	0.8	5.01E+05	3.15E+03	1.44E+05	4.46E+06	2.08E+03	8.28E+04	5.76E+03	6.66E+09	3.34E+04
4	4	0.95	1	1.96E+07	3.17E+05	2.49E+07	2.35E+06	LD	1.78E+05	1.62E+04	4.18E+09	5.67E+04
	9	0.95	1	5.09E+06	3.34E+05	4.70E+06	3.73E+06	LD	5.76E+05	LD	2.75E+09	4.82E+04
3	4	1	1	2.90E+05	ND	1.21E+05	ND	ND	8.99E+04	ND	7.38E+09	7.88E+04
	11	0.96	1	1.75E+05	ND	2.75E+05	ND	ND	8.64E+04	ND	2.59E+09	1.07E+05
7	4	1.01	1	2.71E+05	ND	5.22E+04	ND	ND	2.88E+04	ND	1.87E+09	4.96E+03
	27	1	1	2.04E+04	ND	7.25E+04	ND	ND	2.79E+04	ND	1.13E+09	7.53E+03
11	4	1	1	2.68E+03	ND	5.31E+03	ND	ND	2.23E+04	ND	1.17E+09	2.31E+03
	80	1	1	1.61E+07	ND	2.38E+07	ND	ND	3.35E+04	ND	6.11E+08	1.43E+06
	250	1	1	2.05E+06	ND	4.00E+07	ND	ND	6.49E+03	ND	1.26E+08	2.36E+06
	400	1	1	1.71E+06	ND	5.23E+07	ND	ND	1.82E+04	ND	1.10E+08	9.28E+05
10	4	1	1	1.76E+04	ND	2.60E+04	ND	ND	4.69E+03	ND	2.03E+08	4.14E+06
	80	1	1	2.54E+07	ND	2.78E+07	ND	ND	4.86E+03	ND	4.50E+08	7.41E+05
	260	1	1	1.38E+06	ND	2.04E+07	ND	ND	4.56E+03	ND	8.83E+07	4.28E+05
	500	1.05	1.05	9.04E+05	ND	2.69E+07	ND	ND	8.91E+03	ND	6.26E+07	1.62E+06

Stn #	Depth (m)	DNA Vol. Filt. (L)	RNA Vol. Filt. (L)	qPCR Data (all are copies per L sample filtered)								
				Archaea *amoA* gene	**Archaea *amoA* mRNA**	**Thaum. *rrs***	**Thaum. *ureC* gene**	***ureC* mRNA**	**AOB *amoA* gene**	**AOB *amoA* mRNA**	**Bacteria *rrs***	***Nitro-spina rrs***
6	4	1	1	5.23E+04	ND	1.64E+04	ND	ND	2.71E+04	ND	8.13E+08	5.36E+03
	30	1	1	8.29E+04	ND	9.98E+04	ND	ND	6.63E+03	ND	1.55E+09	2.44E+03
13	4	1	1	3.08E+06	ND	5.66E+06	ND	ND	1.23E+05	ND	4.39E+10	1.01E+05
	9	1	1	2.61E+06	ND	4.13E+06	ND	ND	9.84E+04	ND	1.67E+10	5.02E+04
1	4	0.7	0.7	2.49E+06	ND	7.01E+06	ND	ND	2.05E+05	ND	3.30E+10	7.43E+06
	13.5	0.7	0.7	2.01E+06	ND	6.27E+06	ND	ND	LD	ND	1.82E+10	3.03E+05

*ND = not determined (RNA not analyzed for given sample); LD = below limit of detection.

Figure D.1: Locations surrounding Sapelo Island, Georgia, where samples were collected for this study. ML (Marsh Landing) is the site where the Sapelo Island Microbial Observatory (SIMO) first identified the Thaumarchaeota bloom (Gifford *et al.*, 2011; Hollibaugh *et al.*, 2011) and a more fine-scale temporal resolution study was done (Chapter 4). Both ML and Hunt Camp (GCE10) were sampled over a 24-hour period for the diurnal study. GCE (Georgia Coastal Ecosystems) sites are part of the Long-Term Ecological Research (LTER) network for Sapelo Island (http://gce-lter.marsci.uga.edu/), which includes the Altamaha River, Altamaha Sound, and both Sapelo and Doboy Sounds.

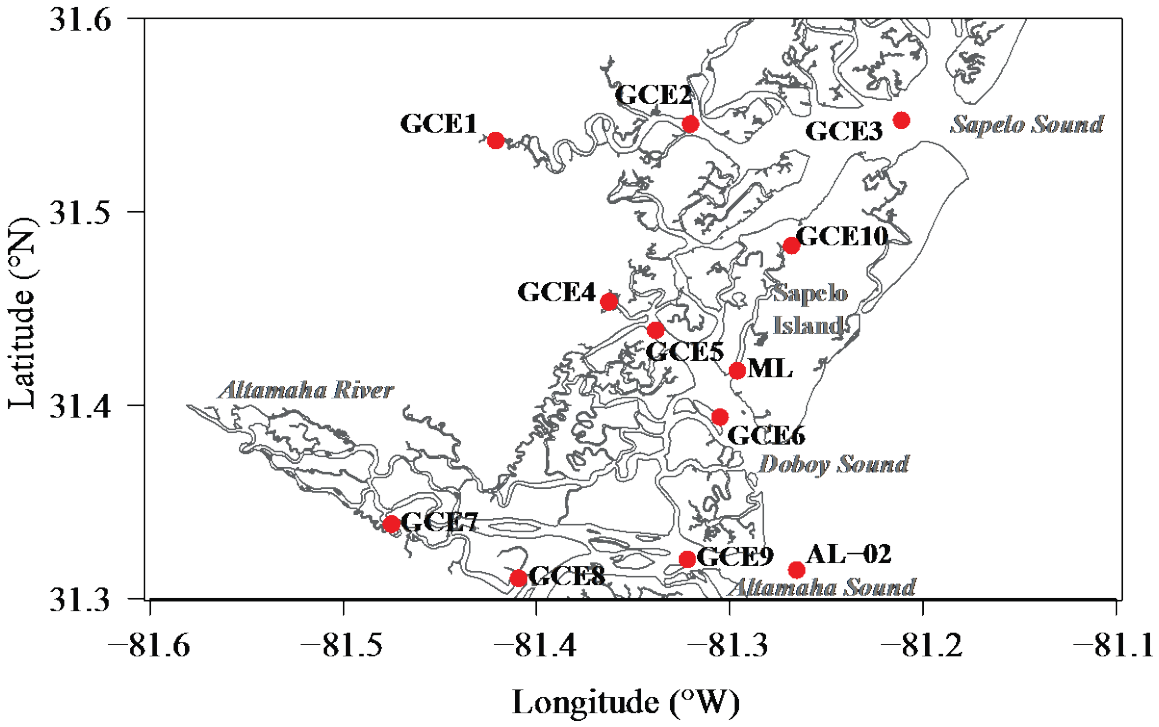
31.6
31.5
31.4
31.3
Latitude (°N)
−81.6
−81.5
−81.4
−81.3
−81.2
−81.1
Longitude (°W)
GCE1
GCE2
GCE3
Sapelo Sound
GCE10
GCE4
Sapelo
Island
GCE5
ML
Altamaha River
GCE6
Doboy Sound
GCE7
GCE9
AL−02
GCE8
Altamaha Sound

Figure D.2: Stations in the South Atlantic Bight (SAB) offshore from Sapelo Island, Georgia, and between Savannah (Georgia) and Jacksonville (Florida) where samples were collected to determine the offshore extent of the Thaumarchaeota bloom in April and October 2011.

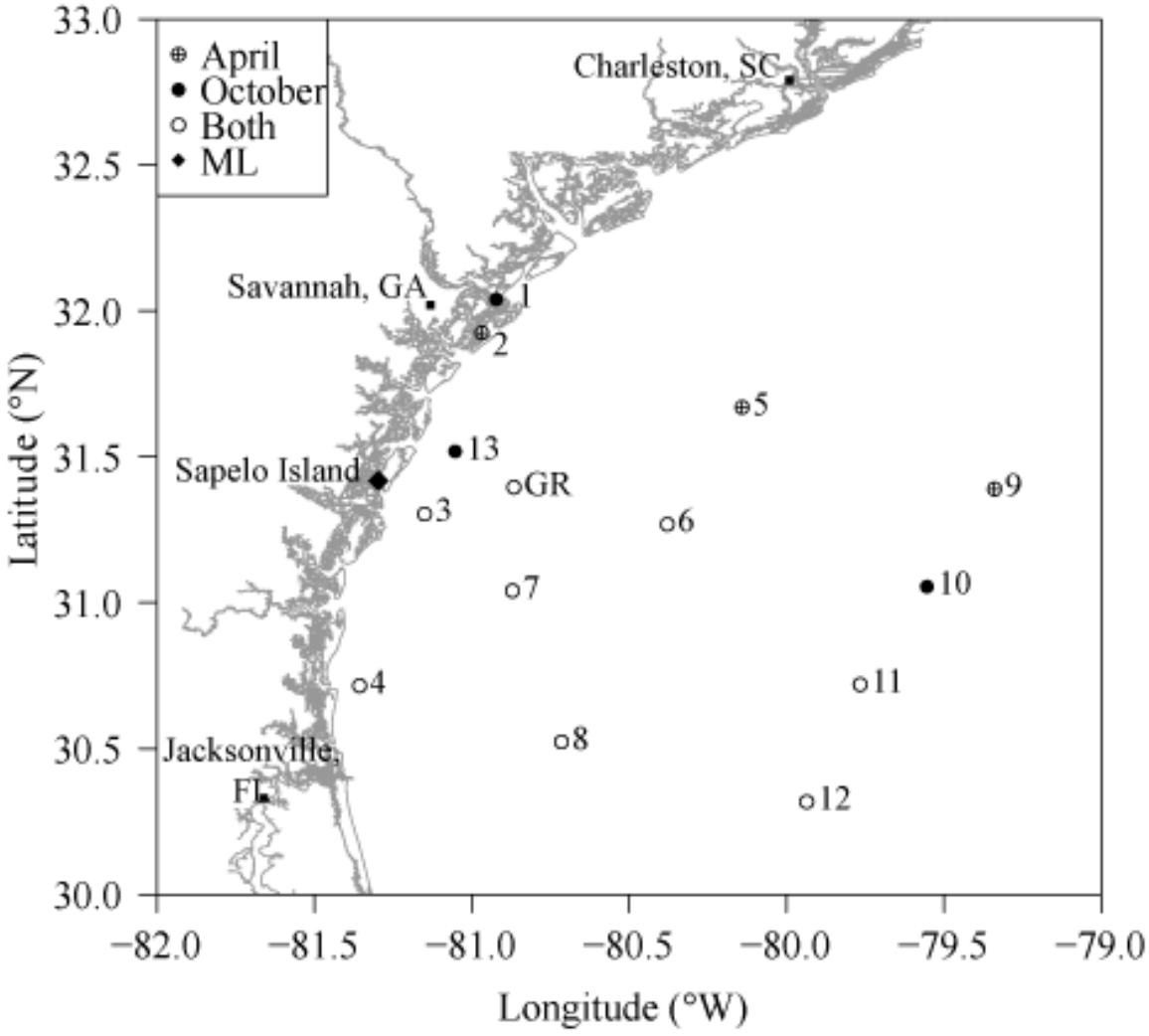
April
October
Both
ML
Charleston, SC
Savannah, GA
Sapelo Island
Jacksonville, FL
1
2
3
4
5
6
7
8
9
10
11
12
13
GR
33.0
32.5
32.0
31.5
31.0
30.5
30.0
Latitude (°N)
−82.0
−81.5
−81.0
−80.5
−80.0
−79.5
−79.0
Longitude (°W)

Figure D.3: Comparison of Thaumarchaeota *rrs* gene abundance around Sapelo Island, Georgia, between bloom (August 2011) and non-bloom (April 2012) periods. Sites are part of the GCE-LTER survey domain (Figure D.1). Sample depth and tide is indicated on the x-axis: HWS = high tide, surface water; HWB = high tide, bottom water; LWS = low tide, surface water; LWB = low tide, bottom water. Samples where no DNA filter was collected are indicated with a *.

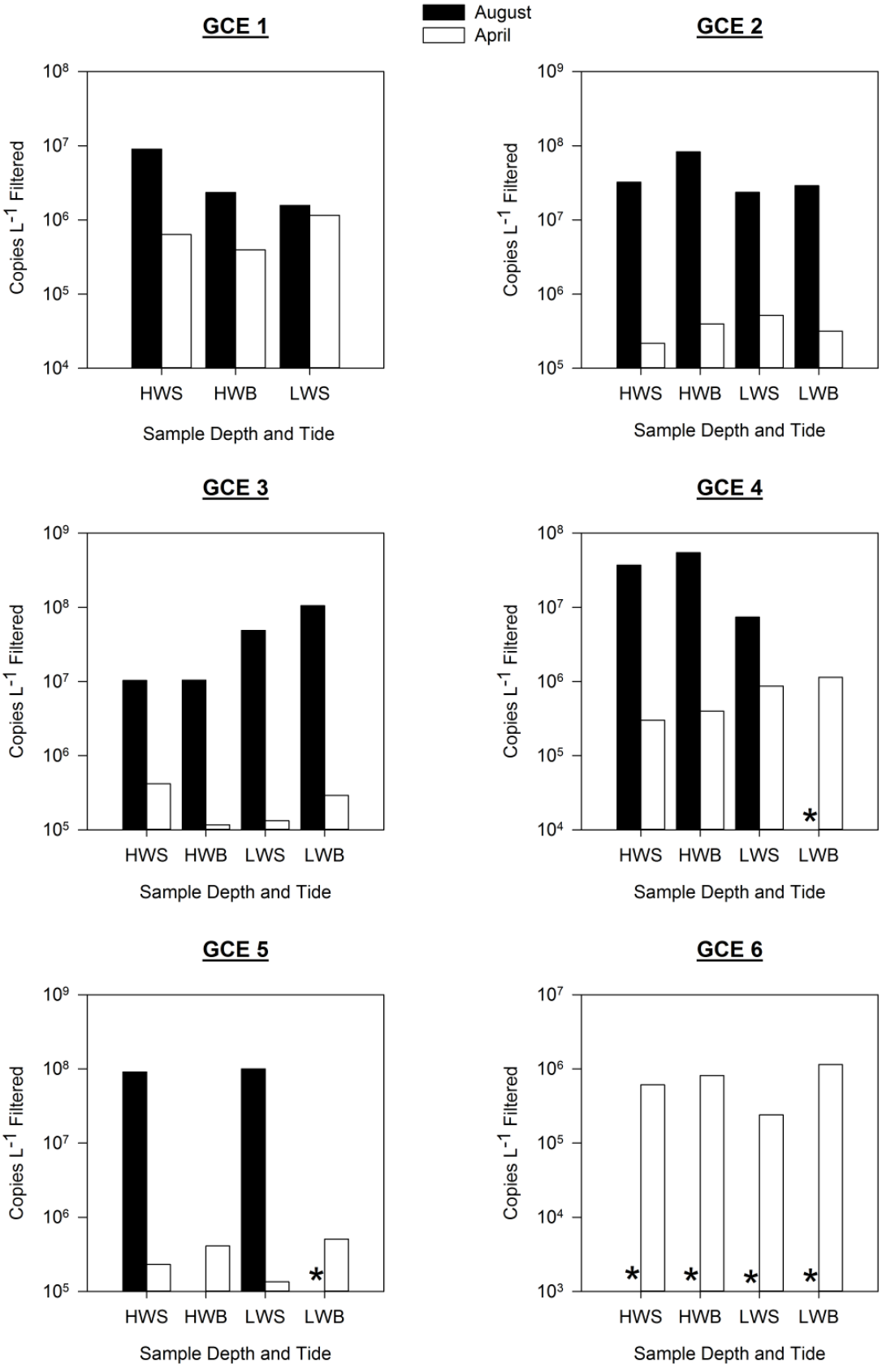
August
April
GCE 1
GCE 2
GCE 3
GCE 4
GCE 5
GCE 6
Copies L-1 Filtered
HWS
HWB
LWS
LWB
Sample Depth and Tide
*

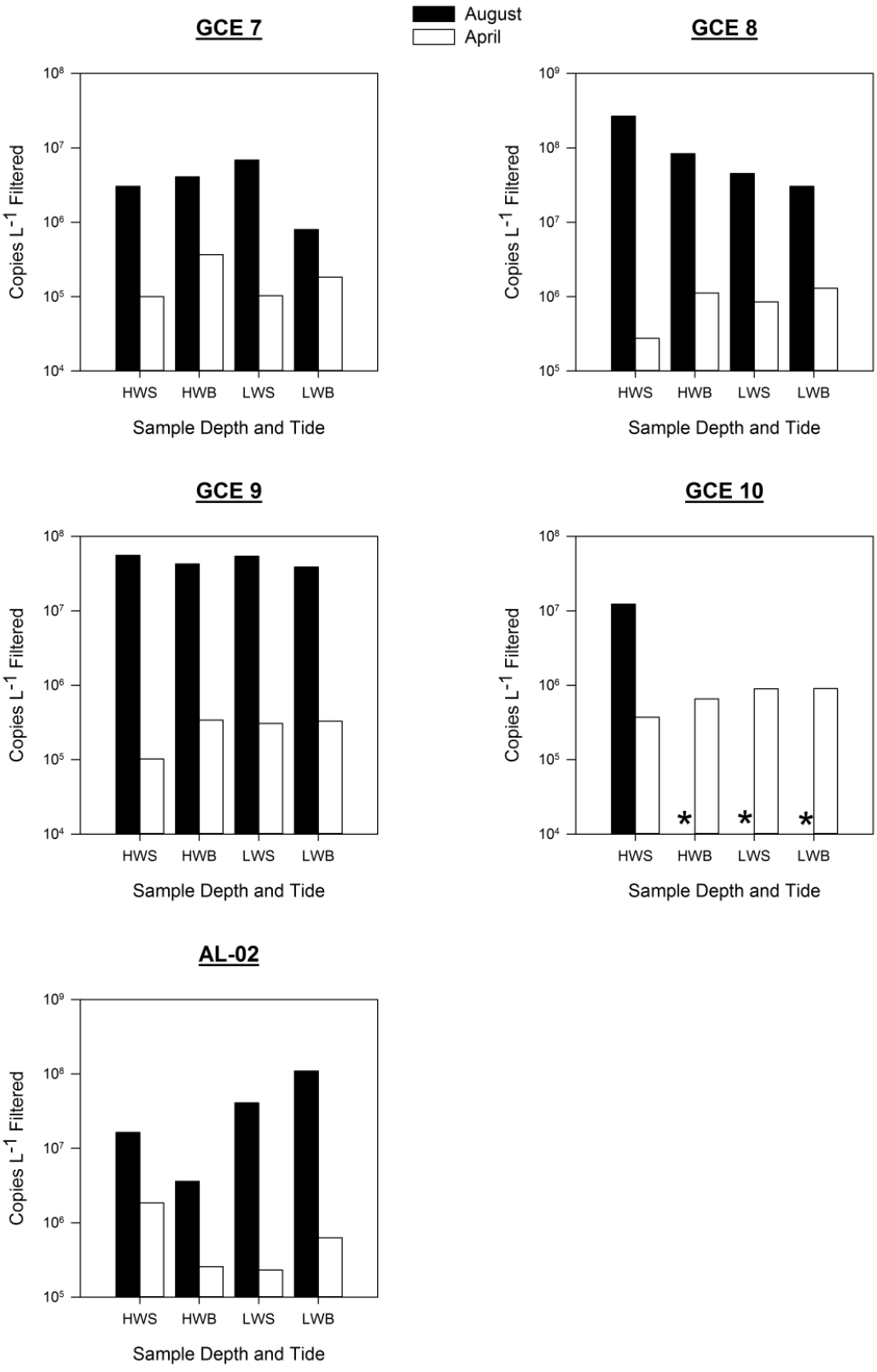
August
April
GCE 7
GCE 8
GCE 9
GCE 10
AL-02
Copies L-1 Filtered
HWS
HWB
LWS
LWB
Sample Depth and Tide
*

Figure D.4: Diurnal measurements of Thaumarchaeota gene and transcript abundance, as well as ammonia oxidation rates in (a) August 2011, (b) April 2012, (c, d) August 2012, and (e) September 2013. Samples collected on Sapelo Island (Figure D.1) at Marsh Landing (ML; **a-c, e**) and Hunt Camp (HC; **d**) over at least two tidal cycles. Thaumarchaeota *amoA* genes (blue circles) and transcripts (red squares) are shown along with ammonia oxidation rates (grey bars). Note the difference in scale between **(b)** April 2012 (y-axis is 100X smaller) and **(d)** HC August 2012 (y-axis for ammonia oxidation is 50% smaller). Photosynthetically active radiation (PAR) is also plotted (orange dashed line) for reference. A thunderstorm occurred during sampling in August 2012, which is noted on panels **c** and **d** and reflected in the rapid decrease in PAR after 2:00 PM.

(a) ML - August 2011

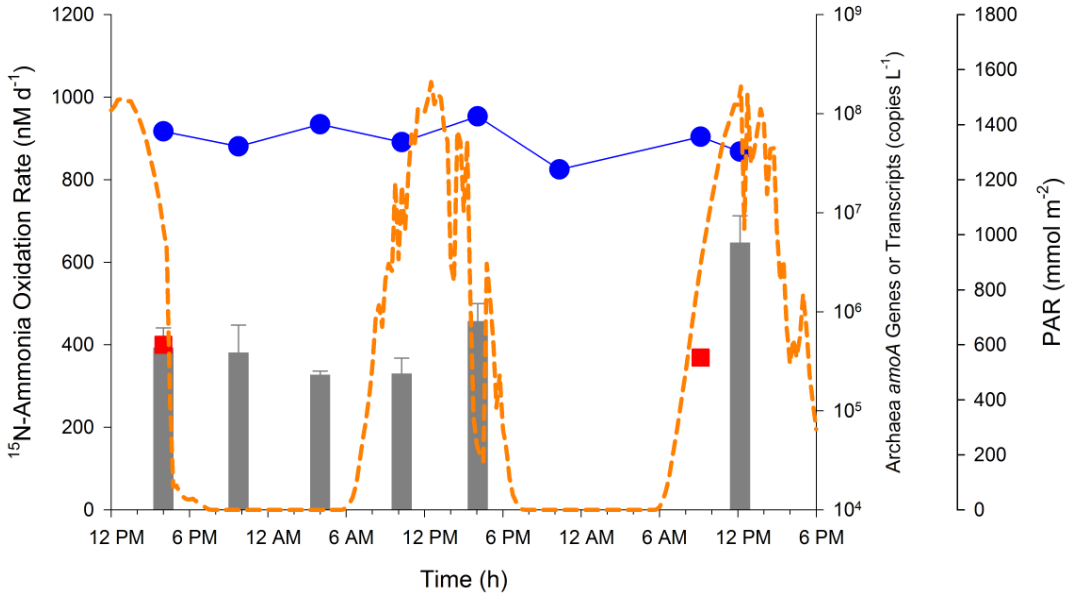

(b) ML - April 2012

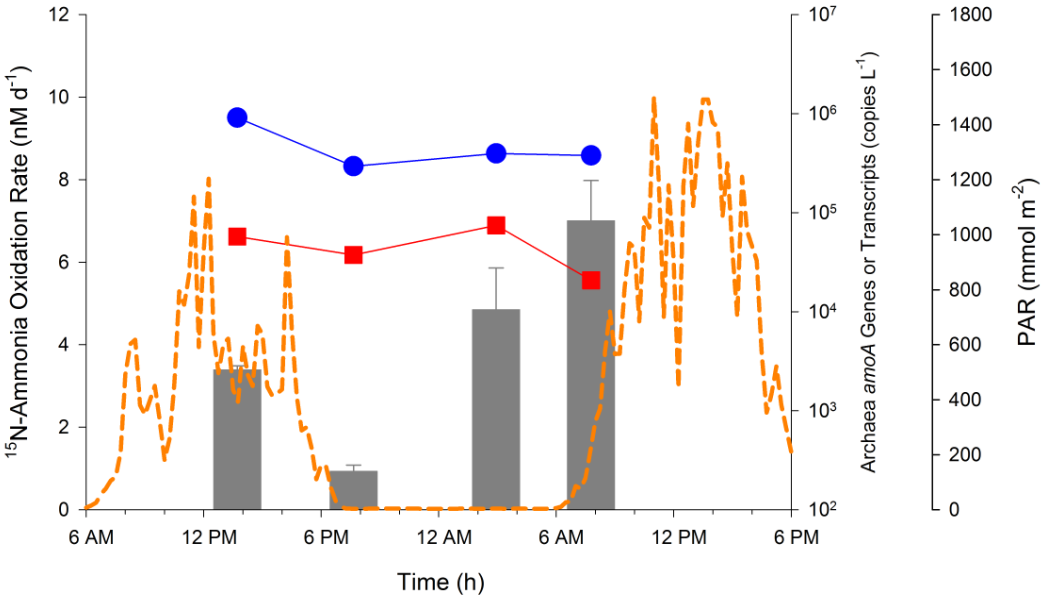

(c) ML - August 2012

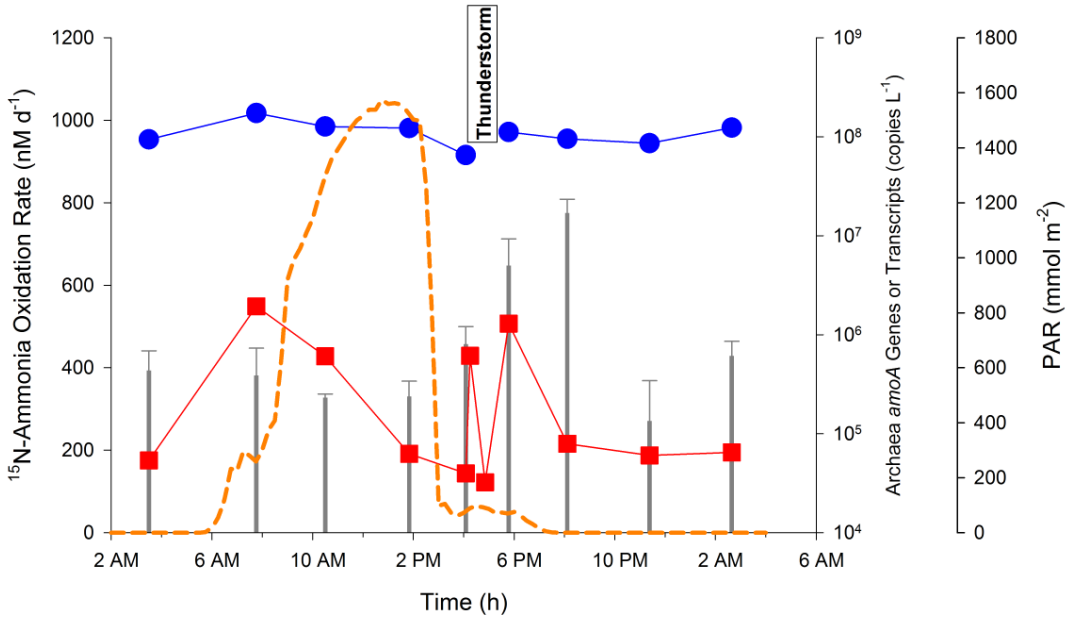

(d) HC - August 2012

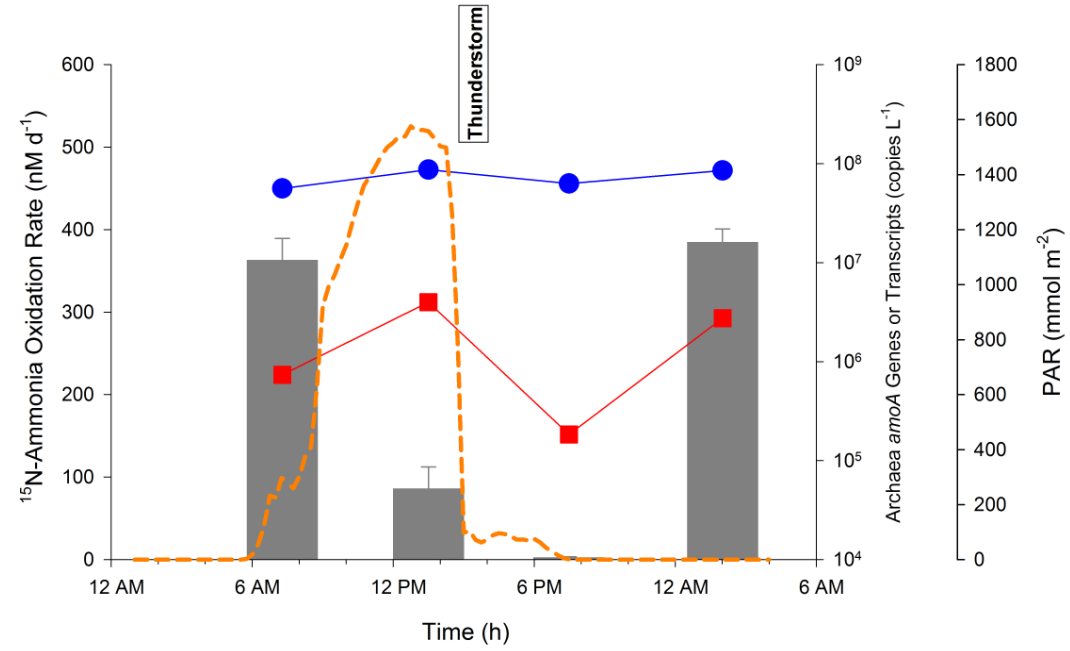

(e) September 2013

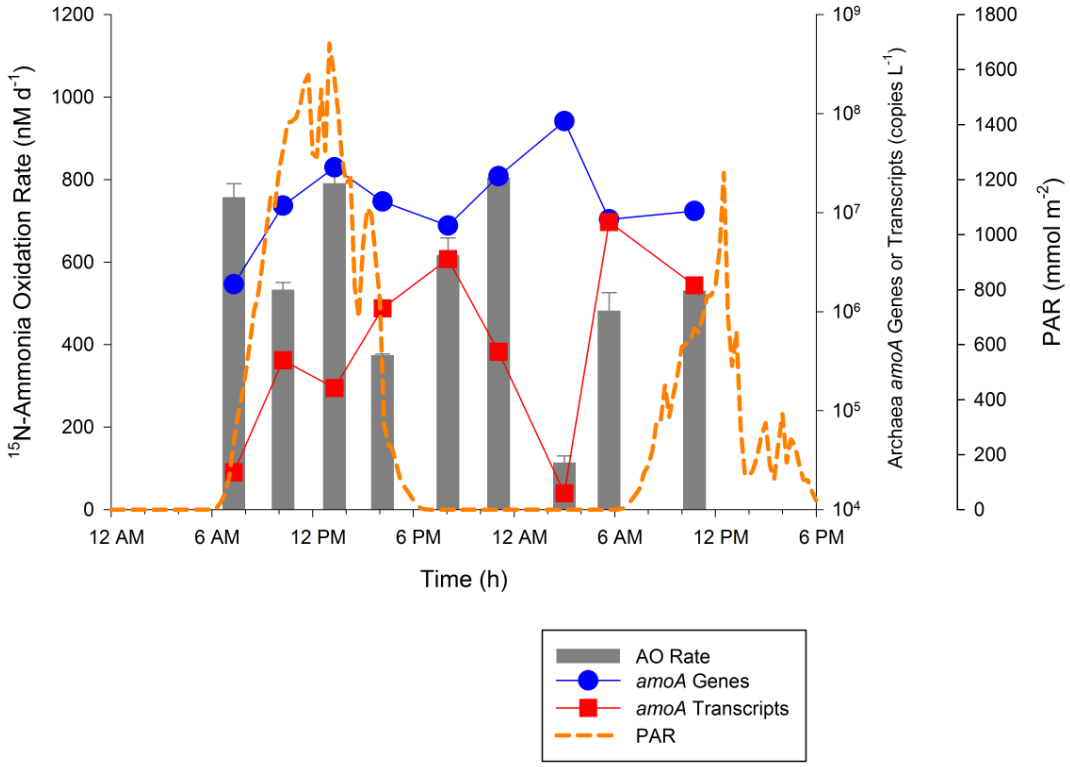

Figure D.5: Thaumarchaeota abundance and ammonia oxidation rates in the South Atlantic Bight (SAB). Samples collected in April **(a, c, e)** and October **(b, d, f)** 2011 on transects offshore from Savannah, GA, and in line with Gray's Reef (**a, b),** out from the Altamaha River plume **(c, d)**, and offshore from St. Mary's, FL **(e, f)**. Thaumarchaeota **(a-f)** gene (*rrs*, *amoA*) and **(e-f)** transcript (*amoA*) abundance based on qPCR. Ammonia oxidation rates were only measured for one representative transect **(e-f)** offshore from St. Mary's, FL (near Jacksonville). Stations are organized from coastal, inshore samples (left; Stations #2-4, 14) to offshore, Gulf Stream samples (right; Stations #9-12) for clarity.

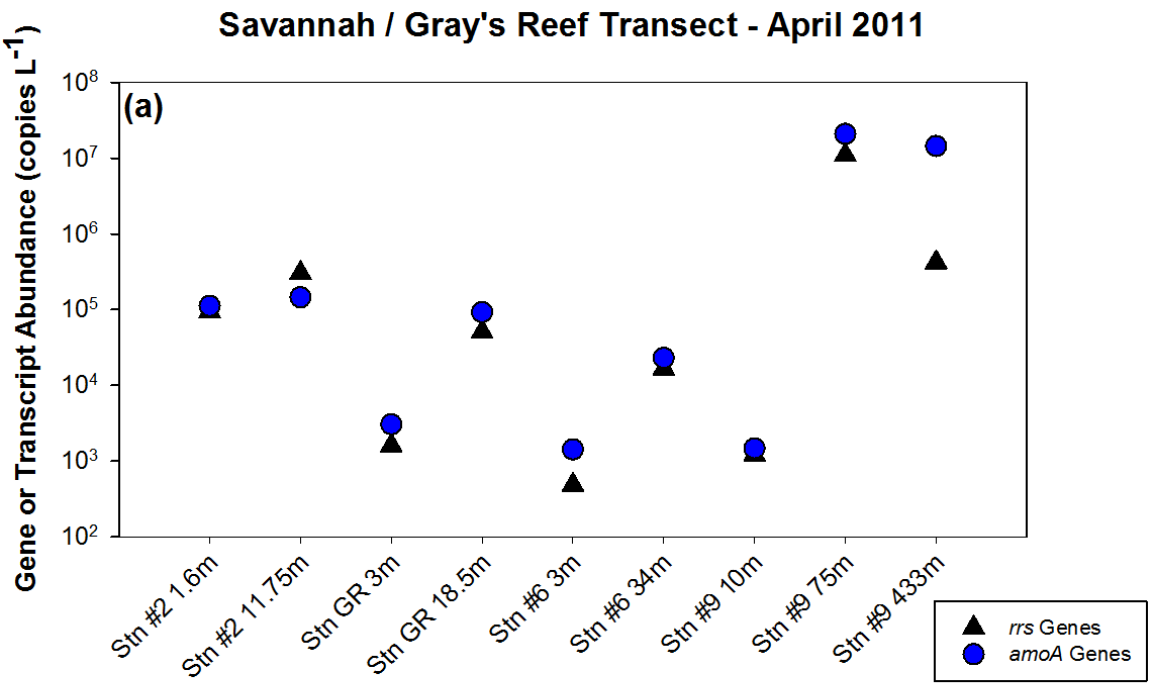
Savannah / Gray's Reef Transect - April 2011
(a)
Gene or Transcript Abundance (copies L-1)
10^8
10^7
10^6
10^5
10^4
10^3
10^2
Stn #2 1.6m
Stn #2 11.75m
Stn GR 3m
Stn GR 18.5m
Stn #6 3m
Stn #6 34m
Stn #9 10m
Stn #9 75m
Stn #9 433m
rrs Genes
amoA Genes

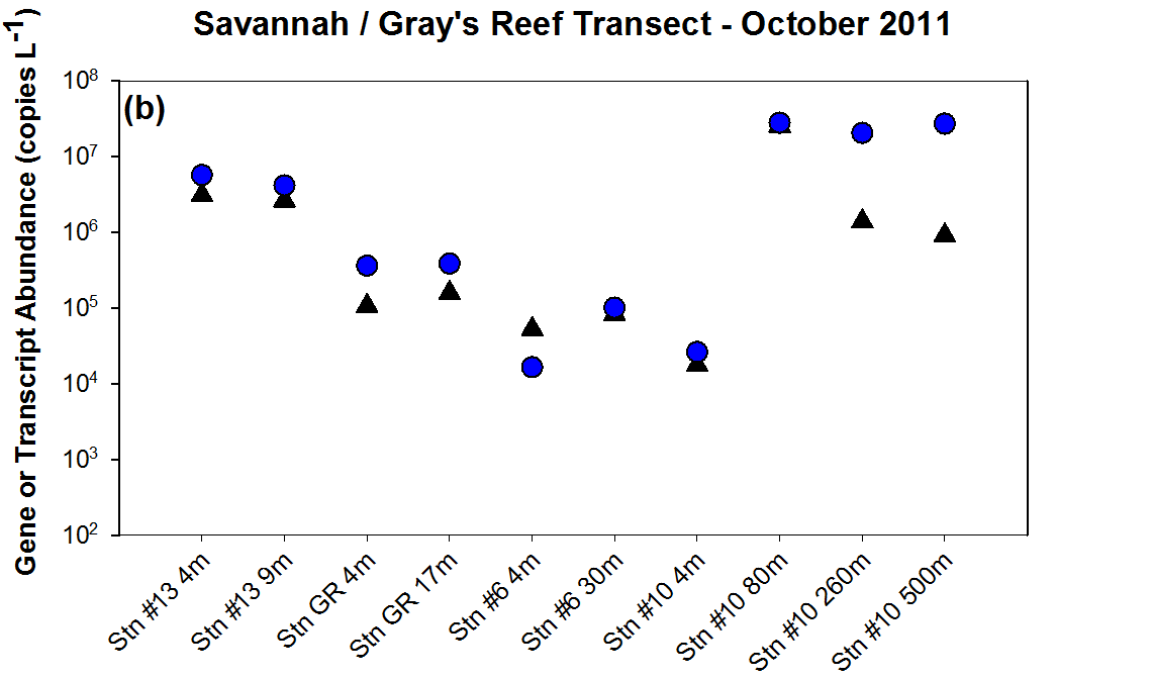
Savannah / Gray's Reef Transect - October 2011
(b)
Gene or Transcript Abundance (copies L-1)
10^8
10^7
10^6
10^5
10^4
10^3
10^2
Stn #13 4m
Stn #13 9m
Stn GR 4m
Stn GR 17m
Stn #6 4m
Stn #6 30m
Stn #10 4m
Stn #10 80m
Stn #10 260m
Stn #10 500m

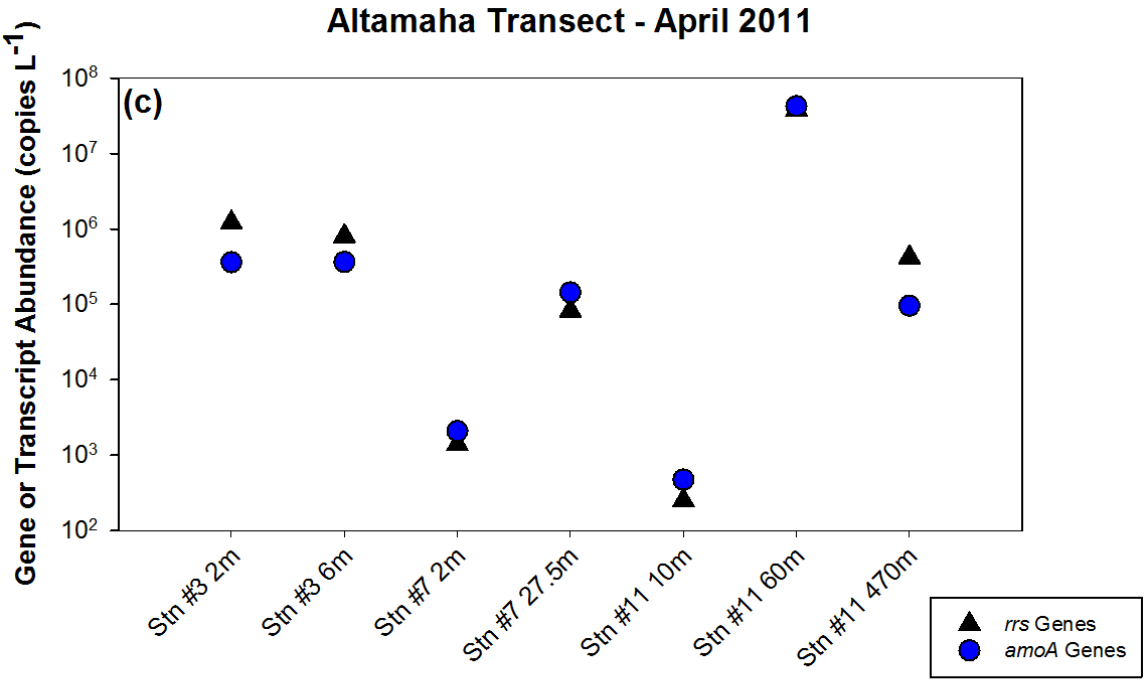
Altamaha Transect - April 2011
(c)
Gene or Transcript Abundance (copies L-1)
10^8
10^7
10^6
10^5
10^4
10^3
10^2
Stn #3 2m
Stn #3 6m
Stn #7 2m
Stn #7 27.5m
Stn #11 10m
Stn #11 60m
Stn #11 470m
rrs Genes
amoA Genes

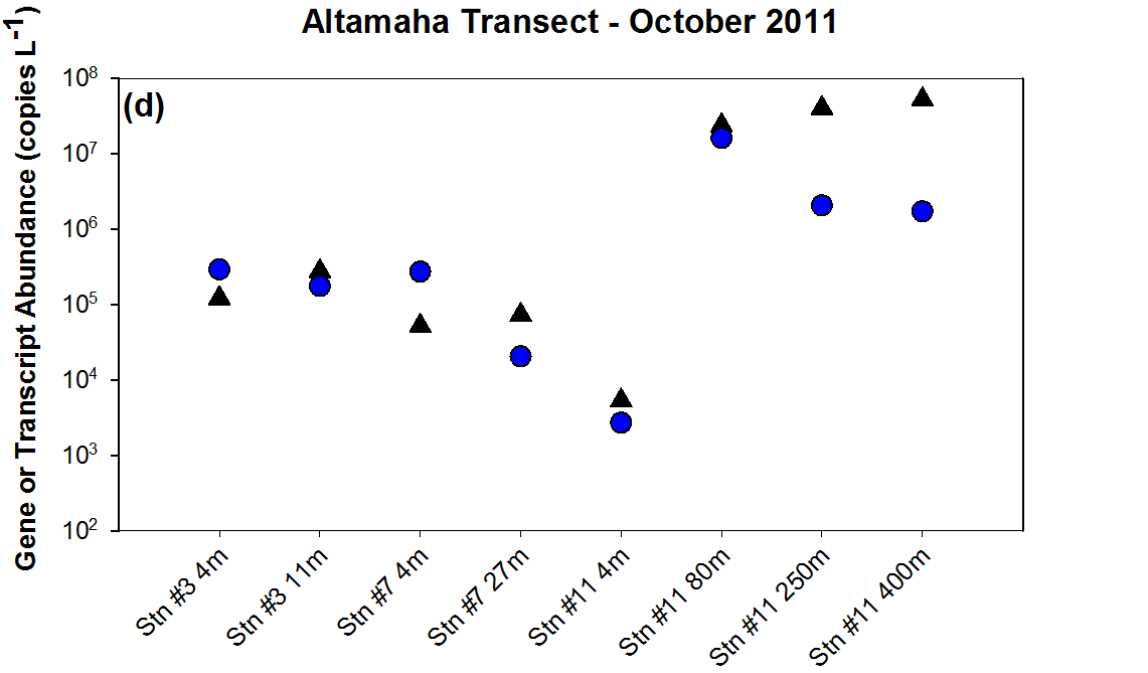
Altamaha Transect - October 2011
(d)
Gene or Transcript Abundance (copies L-1)
10^8
10^7
10^6
10^5
10^4
10^3
10^2
Stn #3 4m
Stn #3 11m
Stn #7 4m
Stn #7 27m
Stn #11 4m
Stn #11 80m
Stn #11 250m
Stn #11 400m

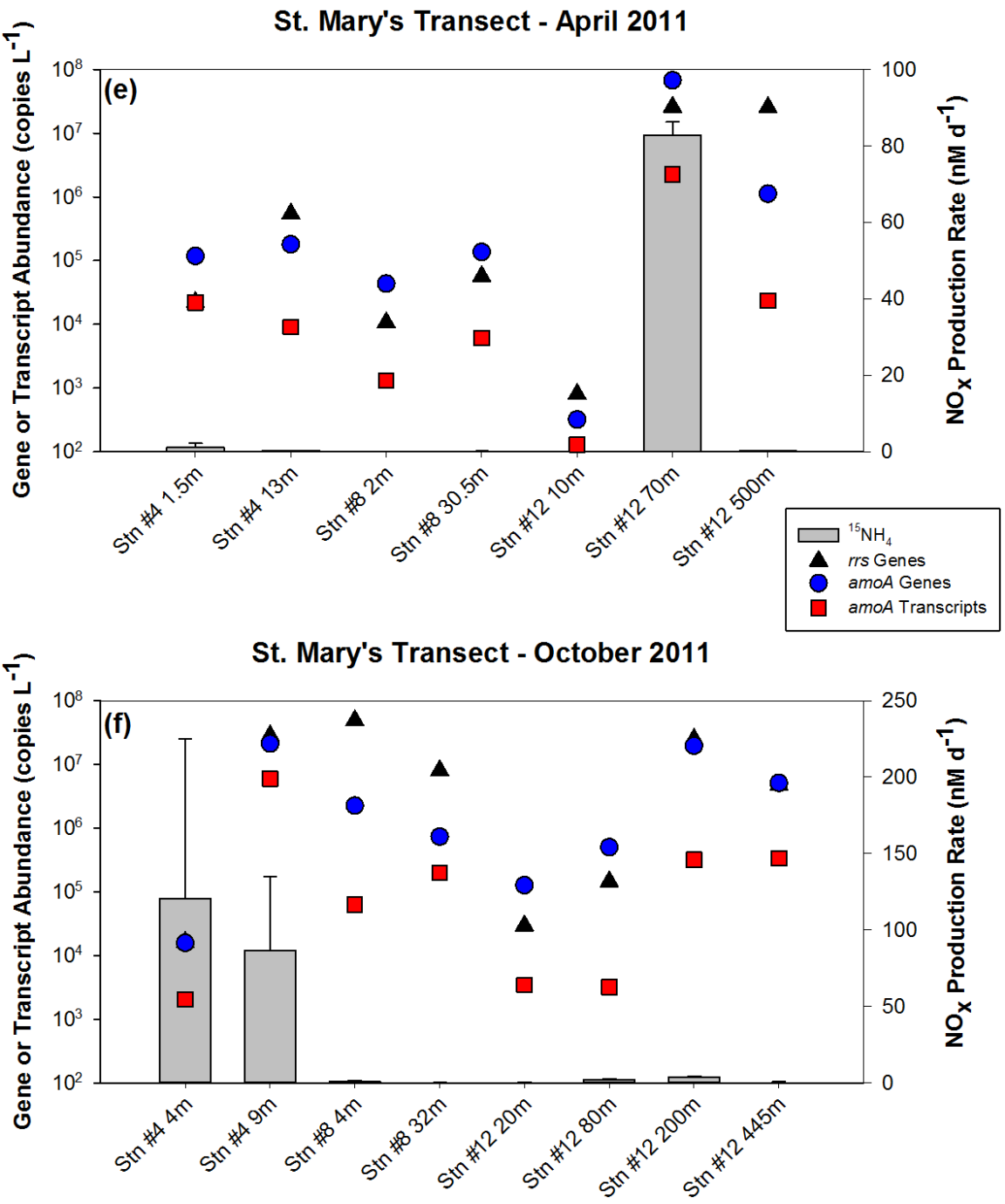
St. Mary's Transect - April 2011
(e)
Gene or Transcript Abundance (copies L-1)
NOX Production Rate (nM d-1)
Stn #4 1.5m
Stn #4 13m
Stn #8 2m
Stn #8 30.5m
Stn #12 10m
Stn #12 70m
Stn #12 500m
15NH4
rrs Genes
amoA Genes
amoA Transcripts
St. Mary's Transect - October 2011
(f)
Gene or Transcript Abundance (copies L-1)
NOX Production Rate (nM d-1)
Stn #4 4m
Stn #4 9m
Stn #8 4m
Stn #8 32m
Stn #12 20m
Stn #12 80m
Stn #12 200m
Stn #12 445m

APPENDIX E

RESPONSE OF SAPELO ISLAND THAUMARCHAEOTA COMMUNITITES TO REACTIVE OXYGEN SPECIES[1]

[1] Tolar, B.B., L.C. Powers, W.L. Miller, N.J. Wallsgrove, B.N. Popp, and J.T. Hollibaugh. To be submitted to *The ISME Journal*.

RESULTS

We examined the sensitivity of AO to the ROS species H_2O_2 in AOO assemblages dominated by Thaumarchaeota (Table E.1) from Sapelo Island, Georgia (Figure 4.1). Whole-seawater incubations were performed at *in situ* temperature with additions of ^{15}N-labeled ammonium (50 nM) to determine rates of AO in the presence of H_2O_2 added at environmentally relevant (10-300 nM) concentrations. We also measured overall microbial activity using leucine incorporation to determine the effects of H_2O_2 on prokaryotic protein synthesis.

Addition of 300 nM H_2O_2 to samples from coastal Georgia, USA, inhibited AO in each of the three years sampled (Figures E.1, E.2). Sapelo Island microbial communities were capable of reducing H_2O_2 concentrations ~6X more quickly (Table E.2, Figure E.3) than communities from open ocean sites (Table 6.2, Figure 6.6). Additional samples collected in 2011 show that AO can be reduced within 6 hours, and no additional reduction (or recovery with 30 nM H_2O_2 additions) was observed after 24 hours (Figure E.2). As with other experiments (Figure 6.4), transcription of *amoA* genes did not reflect any H_2O_2 inhibition (Figure E.4) as observed in AO rates. Overall prokaryotic activity (leucine incorporation) was also reduced by increased [H_2O_2] in Sapelo Island waters (Figure E.5, Table E.1), but it was not significantly different from the reduction in AO rates (average 18% vs 5% reduction; t-test, $p \geq 0.2$). We also found that additions of rainwater inhibited AO rates (Figure E.1). Measured H_2O_2 concentrations in rainwater were 30-50 μM (Table E.2), indicating that storm events could have a significant effect on bacterioplankton and nitification in the ocean's surface layer.

MATERIALS AND METHODS

Samples were collected at Marsh Landing on Sapelo Island, Georgia (Figure 4.1; August 2011 and 2012, September 2013; 31° 25.068' N, 81° 17.721' W). Seawater was added to 10 L carboys and kept at *in situ* temperature (seawater flow-through tank) during the course of the 24-hour incubation. In order to measure ammonia oxidation (AO) rates, ^{15}N-labeled ammonium ($^{15}NH_4Cl$; Cambridge Isotope Laboratories) was added (50 nM final concentration; Beman *et al.*, 2012; Santoro *et al.*, 2010). Hydrogen peroxide (H_2O_2; J.T. Baker) additions ranged from 10 to 300 nM (Table E.2); concentrations were checked using the absorbance of H_2O_2at 240 nm, and its molar absorptivity of 38.1 M^{-1} cm^{-1} (Miller and Kester, 1988). Initial [H_2O_2] was estimated by modeling H_2O_2 decay (Table E.2) as there was variability in measuring stock solutions and with mixing after additions to 10 L carboys.

After a 6-hour incubation with H_2O_2, samples were filtered onto 142 mm, 0.22 µm pore size GVWP filters (Millipore), which were frozen with 5 mL RNA*later* (Ambion) until extraction using previously described methods (Chapters 3 and 6). RT-qPCR was used to quantify *amoA* transcripts as in Chapter 6.

AO samples remained at *in situ* temperature for 24 hours in the dark before termination by freezing at -80°C. Controls were filtered sample water or frozen immediately after addition of tracer. All samples remained frozen until analysis using the previously described 'denitrifier method' (Sigman *et al.*, 2001) with cultures of *Pseudomonas aureofaciens* (Dore *et al.*, 1998; Popp *et al.*, 1995; Chapters 3 and 6). Calculations of AO rates from raw $\delta^{15}N$ values of N_2O produced followed Christman *et al.* (2011) and Beman *et al*. (2012).

Leucine incorporation was used as a proxy for total prokaryotic activity with either ^{13}C-leucine (2012-2013) or ^{3}H-leucine (2011) added to a final concentration of 100 nM. For ^{13}C-leucine incorporation, samples were analyzed as described in Chapter 6. Samples from 2011 amended with ^{3}H-leucine (100 nM) were analyzed as in (Ducklow *et al.*, 2012; Smith and Azam, 1992); briefly, samples were incubated with ^{3}H-leucine at *in* situ temperature for 1 hour in 2.0 mL test tubes, centrifuged to form a pellet, and counted directly using a Beckman LS6500 liquid scintillation counter.

H_2O_2 was measured using a FeLume chemiluminescence (CL) system (Waterville Analytical; Figure 6.8) with modifications to the methods of King *et al*. (2007) as described in Chapter 6. Initial H_2O_2 concentration and decay rates were calculated as in Chapter 6.

ACKNOWLEDGEMENTS

Funding for this research was provided by U.S. National Science Foundation grants OCE 09-43278 (EAGER) and OPP 08-38996 to J.T.H., OCE-1234388 to W.L.M., and OCE-1129260 to B.N.P. We thank Q. Liu, F. Cao, and B. Durham for assistance in field sampling, and the staff at the UGA Marine Institute on Sapelo Island, especially M. Booth and M. Price. We also thank A. Bratcher, D. Duckett, E. Malagón, L. Lim, J.L. Shih, J. Fackrell, and C. Ka'apu-Lyons for assistance in the laboratory.

REFERENCES

Beman JM, Popp BN, Alford SE (2012). Quantification of ammonia oxidation rates and ammonia-oxidizing archaea and bacteria at high resolution in the Gulf of California and eastern tropical North Pacific Ocean. *Limnol Oceanogr* **57:** 711-726.

Christman GD, Cottrell MT, Popp BN, Gier E, Kirchman DL (2011). Abundance, Diversity, and Activity of Ammonia-Oxidizing Prokaryotes in the Coastal Arctic Ocean in Summer and Winter. *Appl Environ Microbiol* **77:** 2026-2034.

Dore JE, Popp BN, Karl DM, Sansone FJ (1998). A large source of atmospheric nitrous oxide from subtropical North Pacific surface waters. *Nature* **396:** 63-66.

Ducklow HW, Schofield O, Vernet M, Stammerjohn S, Erickson M (2012). Multiscale control of bacterial production by phytoplankton dynamics and sea ice along the western Antarctic Peninsula: A regional and decadal investigation. *J Marine Syst* **98-99:** 26-39.

King DW, Cooper WJ, Rusak SA, Peake BM, Kiddle JJ, O'Sullivan DW, Melamed ML, Morgan CR, Theberge SM (2007). Flow injection analysis of H_2O_2 in natural waters using acridinium ester chemiluminescence: Method development and optimization using a kinetic model. *Anal Chem* **79:** 4169-4176.

Miller WL, Kester DR (1988). Hydrogen-Peroxide Measurement in Seawater by (Para-Hydroxyphenyl)Acetic Acid Dimerization. *Anal Chem* **60:** 2711-2715.

Popp BN, Sansone FJ, Rust TM, Merritt DA (1995). Determination of Concentration and Carbon Isotopic Composition of Dissolved Methane in Sediments and Nearshore Waters. *Anal Chem* **67:** 405-411.

Santoro AE, Casciotti KL, Francis CA (2010). Activity, abundance and diversity of nitrifying archaea and bacteria in the central California Current. *Environ Microbiol* **12:** 1989-2006.

Sigman DM, Casciotti KL, Andreani M, Barford C, Galanter M, Böhlke JK (2001). A Bacterial Method for the Nitrogen Isotopic Analysis of Nitrate in Seawater and Freshwater. *Anal Chem* **73:** 4145-4153.

Smith DC, Azam F (1992). A simple, economical method for measuring bacterial protein synthesis rates in seawater using ^{3}H-leucine. *Mar Microb Food Webs* **6:** 107-114.

Zepp RG, Skurlato YI, Pierce JT (1987). Algal-Induced Decay and Formation of Hydrogen Peroxide in Water: Its Possible Role in Oxidation of Anilines by Algae. In: Zika RG, Cooper WJ (eds). Photochemistry of Environmental Systems. American Chemical Society: Washington, D.C.

Table E.1: Summary of ROS incubation experiments, including ammonia oxidation and leucine incorporation rates, and gene and transcript abundance data.

Site	Station	Depth / Time	H_2O_2 Addition (nM)	Avg ^{15}N Oxid. Rate		Avg Leu. Incorp. Rate		Initial [H_2O_2]	
				(nM/d)	SD	(pM/h)	SD	(nM)	SD
Sapelo Island 2011	ML	T = 0	0	66.67	48.05	3295	1701	LD	LD
	ML	6 h	0	23.29	2.48	3558	979.9		
	ML	6 h	100	35.03	0.30	1965	78.98		
	ML	6 h	300	7.62	2.31	2103	112.8		
	ML	12 h	0	ND	ND	2677	324.3		
	ML	12 h	100	ND	ND	2062	70.72		
	ML	12 h	300	ND	ND	2319	123.9		
	ML	24 h	0	41.75	11.41	2262	126.3		
	ML	24 h	100	56.17	5.16	2160	140.6		
	ML	24 h	300	5.47	0.27	2127	157.4		
Sapelo Island 2012	ML	Surface	0	3.46	0.85	4503	398.0	201.50	43.63
	ML	Surface	100	5.12	0.11	3506	427.0		
	ML	Surface	300	1.42	0.26	2974	436.7		
	ML - Rain	Surface	100	4.49	0.54	3413	422.8	*52,890*	*9,690*
Sapelo Island 2013	ML	Surface	0	944.6	36.5	81290	4086	108.20	2.53
	ML	Surface	10	939.2	42.5	69760	19810		
	ML	Surface	30	904.7	64.4	74560	24860		
	ML	Surface	100	904.4	3.9	78060	20710		
	ML	Surface	300	858.9	73.3	78410	21100		
	ML - Rain	Surface	300	814.5	64.1	96700	5966	*33,470*	*470*

Site	Station	Depth / Time	H_2O_2 Addition (nM)	*amoA* mRNA (copies/L)	Gene Abundance (copies/L)			
					Archaeal *amoA*	Thaum. 16S rRNA	AOB *amoA*	Bacteria 16S rRNA
Sapelo Island 2011	ML	T = 0	0	4.14E+07	1.91E+08	5.13E+07	1.16E+05	2.72E+09
	ML	6 h	0	2.78E+07				
	ML	6 h	100	3.46E+07				
	ML	6 h	300	4.27E+07				
	ML	12 h	0	6.33E+06				
	ML	12 h	100	1.27E+06				
	ML	12 h	300	1.11E+07				
	ML	24 h	0	7.20E+07				
	ML	24 h	100	4.97E+07				
	ML	24 h	300	8.94E+06				
Sapelo Island 2012	ML	Surface	0	2.58E+07	3.84E+08	1.82E+08	8.25E+05	2.09E+11
	ML	Surface	100	3.15E+07				
	ML	Surface	300	1.12E+07				
	ML - Rain	Surface	100	2.00E+07				
Sapelo Island 2013	ML	Surface	0	ND	1.04E+07	6.37E+07	5.46E+05	3.07E+10
	ML	Surface	10	ND				
	ML	Surface	30	ND				
	ML	Surface	100	ND				
	ML	Surface	300	ND				
	ML - Rain	Surface	300	ND				

ND = not determined

SD = standard deviation

*[H_2O_2] for rain (*italic*) measured with μM standards or diluted to nM range

Table E.2: Decay rates and initial H_2O_2 concentrations for Sapelo Island ROS Experiments, as well as both nominal and modeled concentrations of added H_2O_2.

Sample	Initial $[H_2O_2]$	$[H_2O_2]$ Addn.	Decay Rate (nM h^{-1})[#] m	SD	R^2	Initial $[H_2O_2]$[$] b	SD	Prokarya Cells / L	$[H_2O_2]_0$ (modeled)[^]	k_{obs} (1/h)	R^2	t 1/2 (h)
SI 2012	201.50	100 nM	-12.97	5.48	0.48	175.5	9.16	2.10E+11	176.4	0.088	0.73	7.88
SI 2012		300 nM	-27.99	5.83	0.79	247.5	11.00	2.10E+11	250.8	0.150	0.86	4.64
SI 2012 Rain		100 nM	-20.09	5.55	0.69	220.9	11.30	2.10E+11	222	0.111	0.92	6.24
SI 2013	108.20	10 nM	-9.63	2.23	0.90	61.1	2.50	3.07E+10	61.01	0.180	0.87	3.85
SI 2013		30 nM	-7.24	1.45	0.93	80.1	1.63	3.07E+10	80.16	0.099	0.93	6.97
SI 2013		100 nM	-22.48	3.88	0.94	137.8	4.34	3.07E+10	138.5	0.200	0.96	3.47
SI 2013		300 nM	-54.07	1.79	0.998	296.6	2.00	3.07E+10	297.4	0.221	0.99	3.14
SI 2013 Rain		100 nM	-28.61	7.64	0.88	167.1	10.80	3.07E+10	167.1	0.210	0.88	3.31

[#]Decay rate determined from slope, a negative slope indicates decay; [$]Initial $[H_2O_2]$ determined from y-intercept;

[^]Calculations for $[H_2O_2]_0$ modeled are described further in the Materials and Methods; Model: $[H_2O_2] = [H_2O_2]_0 * e^{(-k*t)}$

Decomposition of H_2O_2 is overall 2nd order (1st order with respect to $[H_2O_2]$, 1st order with respect to *algal* biomass (Zepp *et al.*, 1987)

*$d[H_2O_2]/dt = -k_{obs}[H_2O_2]$ (modeled using nonlinear curve fit)

*$d[H_2O_2]/dt = -k_d[H_2O_2][biomass]$ (k_d = specific decay rate)

so $k_d = - k_{obs}/[biomass]$

Figure E.1: ^{15}N-Ammonia oxidation rates. Rates of ammonia oxidation as measured with a ^{15}N-ammonium tracer after addition of H_2O_2 in Sapelo Island, Georgia in **(a)** 2012 and **(b)** 2013 (symbols represent H_2O_2 origin, either chemical H_2O_2 or from rainwater).

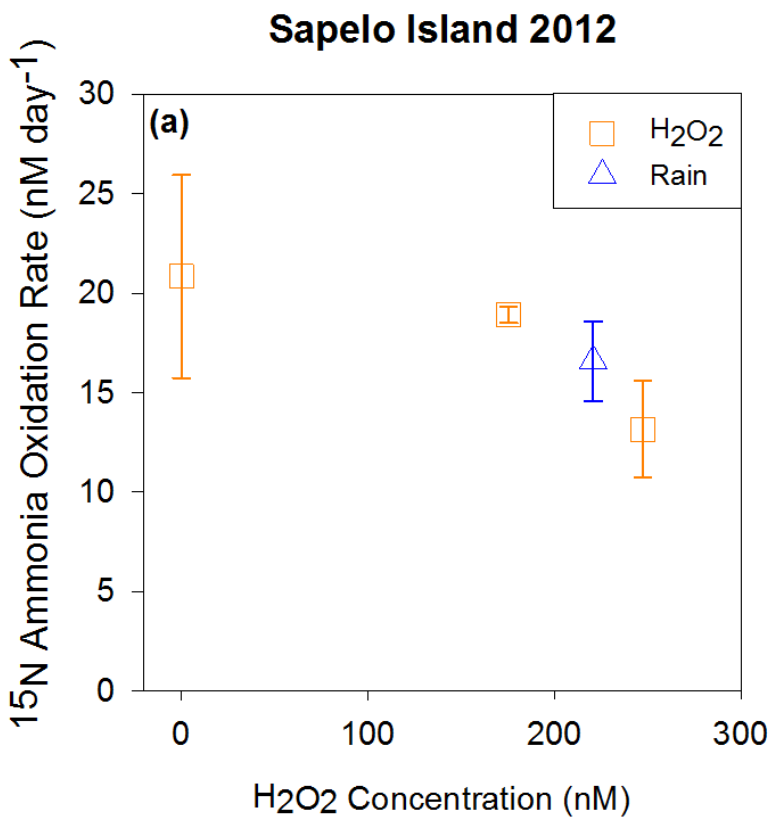
Sapelo Island 2012
(a)
H2O2
Rain
15N Ammonia Oxidation Rate (nM day-1)
30
25
20
15
10
5
0
0
100
200
300
H2O2 Concentration (nM)

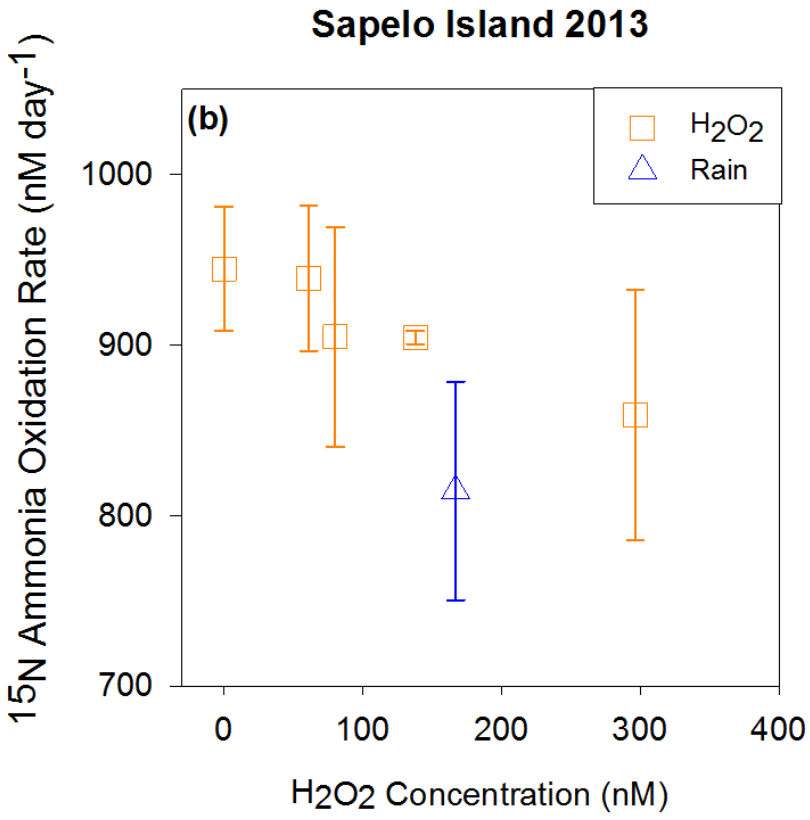
Sapelo Island 2013
(b)
H2O2
Rain
15N Ammonia Oxidation Rate (nM day-1)
1000
900
800
700
0
100
200
300
400
H2O2 Concentration (nM)

Figure E.2: Time course on Sapelo Island, 2011. Ammonia oxidation rates (filled shapes) and Archaeal *amoA* transcripts (open shapes) measured over a 24-hour incubation period after addition of 0 (■), 10 (▲), or 30 nM (●) H_2O_2. Error bars represent the range of duplicate ammonia oxidation rate incubations (note that in some cases the error is too small to be seen outside of the filled shape).

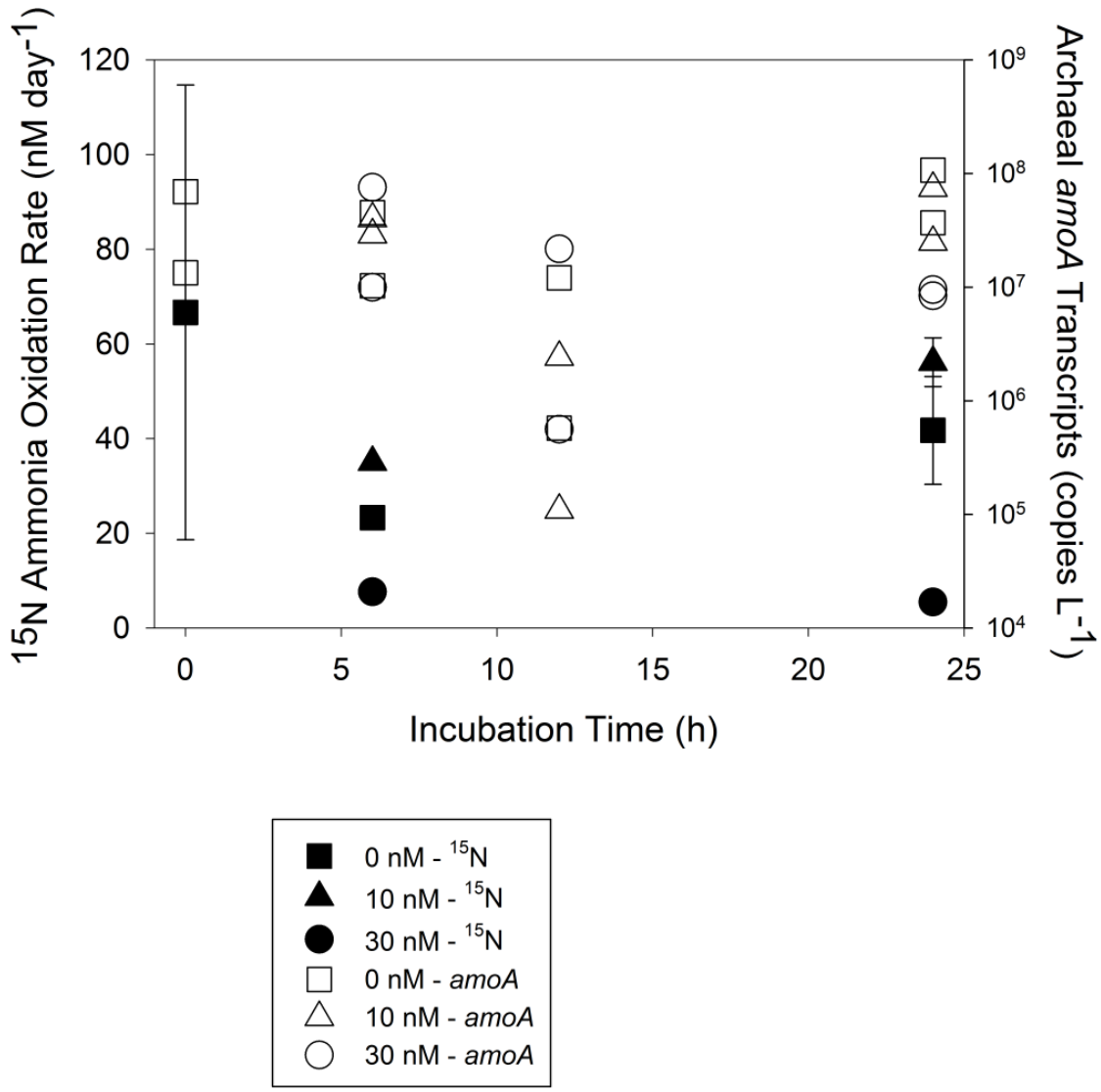
^{15}N Ammonia Oxidation Rate (nM day^{-1})
Archaeal *amoA* Transcripts (copies L^{-1})
Incubation Time (h)
0
20
40
60
80
100
120
0
5
10
15
20
25
10^4
10^5
10^6
10^7
10^8
10^9
0 nM - ^{15}N
10 nM - ^{15}N
30 nM - ^{15}N
0 nM - *amoA*
10 nM - *amoA*
30 nM - *amoA*

Figure E.3: Decay of hydrogen peroxide in ROS experiments from Sapelo Island 2012 **(a)** and 2013 **(b)** in control (black), 10 nM H_2O_2 (green), 30 nM H_2O_2 (yellow), 100 nM H_2O_2 (blue), 300 nM H_2O_2 (purple), and rain (grey) incubations. Symbols represent measured H_2O_2 concentrations, while curves represent modeled decay rates. Variability was greater in Sapelo 2012 **(a)** experiments due to particulate matter in sample water interfering with H_2O_2 measurement.

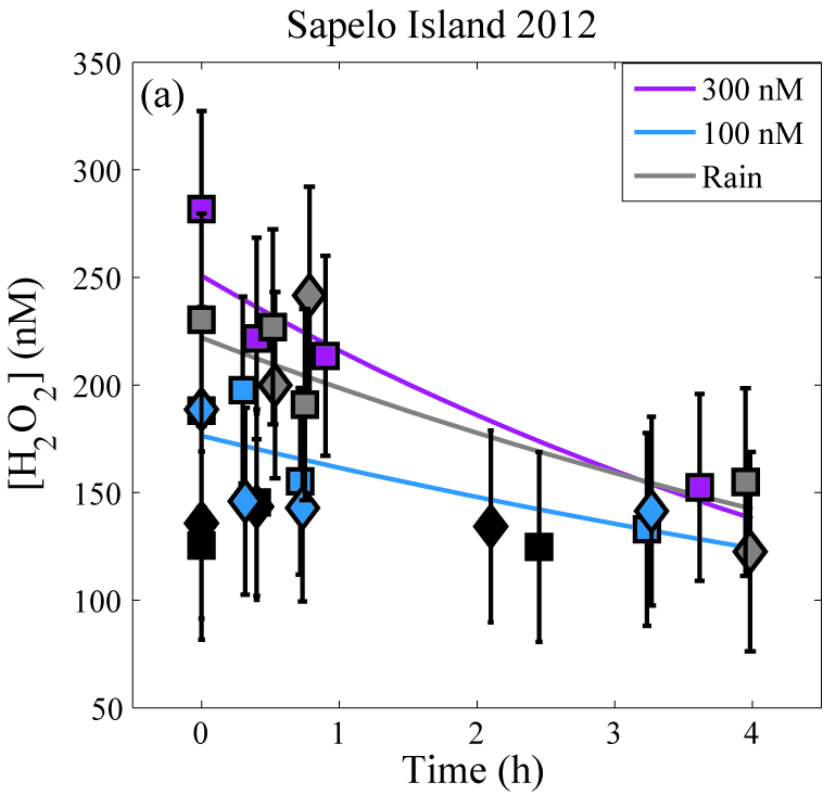
Sapelo Island 2012
(a)
300 nM
100 nM
Rain
[H2O2] (nM)
Time (h)

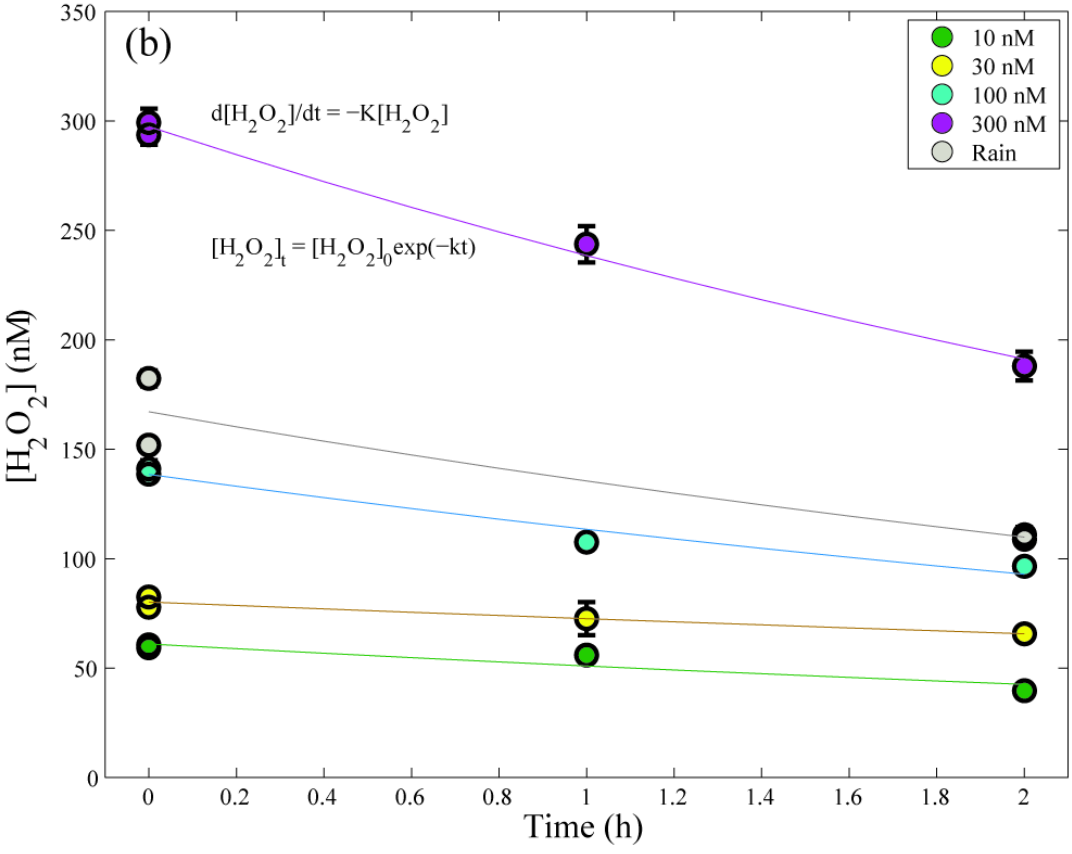
(b)
d[H2O2]/dt = −K[H2O2]
[H2O2]t = [H2O2]0exp(−kt)
10 nM
30 nM
100 nM
300 nM
Rain
[H2O2] (nM)
Time (h)

Figure E.4: Archaeal *amoA* transcripts quantified by RT-qPCR using RNA collected from Sapelo Island, Georgia, in 2011 **(a)** and 2012 **(b)**. Symbols indicate H_2O_2 origin, either chemical H_2O_2 or from rainwater.

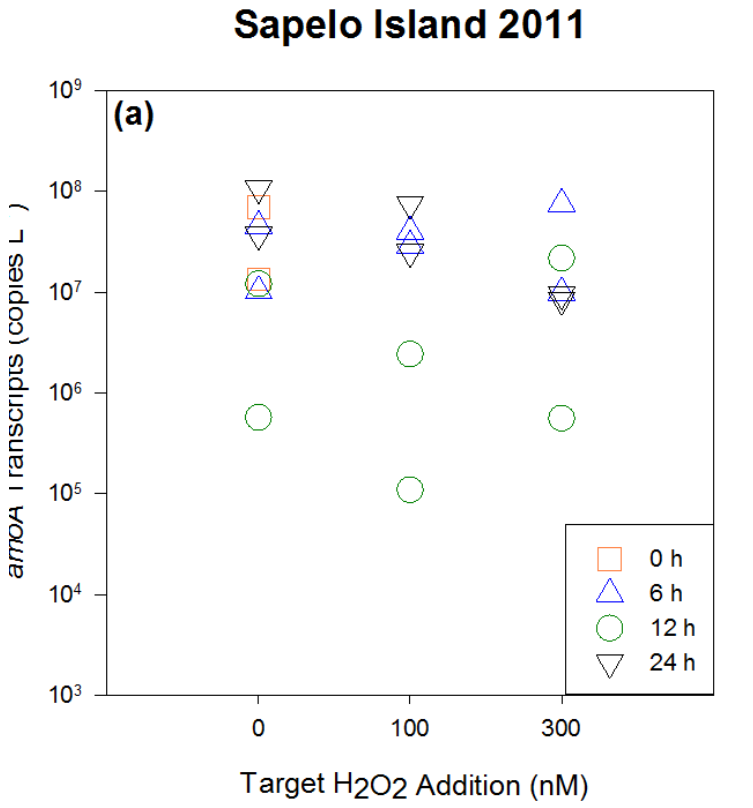
Sapelo Island 2011
(a)
10^9
10^8
10^7
10^6
10^5
10^4
10^3
amoA Transcripts (copies L)
0 h
6 h
12 h
24 h
0
100
300
Target H_2O_2 Addition (nM)

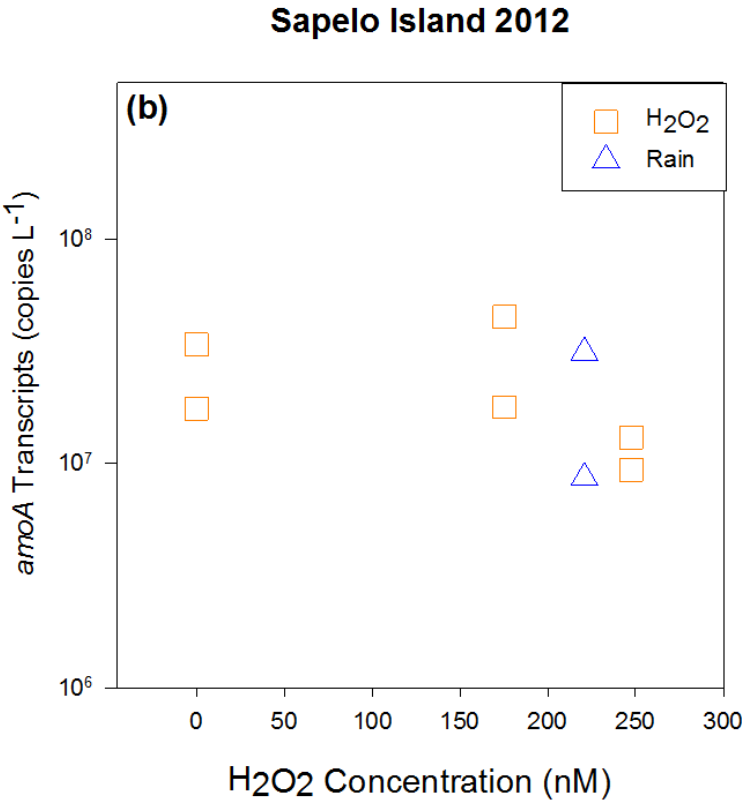
Sapelo Island 2012
(b)
H_2O_2
Rain
10^8
10^7
10^6
amoA Transcripts (copies L^{-1})
0
50
100
150
200
250
300
H_2O_2 Concentration (nM)

Figure E.5. Bacterial incorporation of L-leucine measured Sapelo Island, Georgia in 2011 **(a)**; symbols represent H_2O_2 addition) or 2012 and 2013 (**b** and **c**, respectively; symbols represent H_2O_2 origin, either chemical H_2O_2 or from rainwater). Incubations were performed using ^{3}H- **(a)** or ^{13}C-labeled **(b-c)** L-leucine.

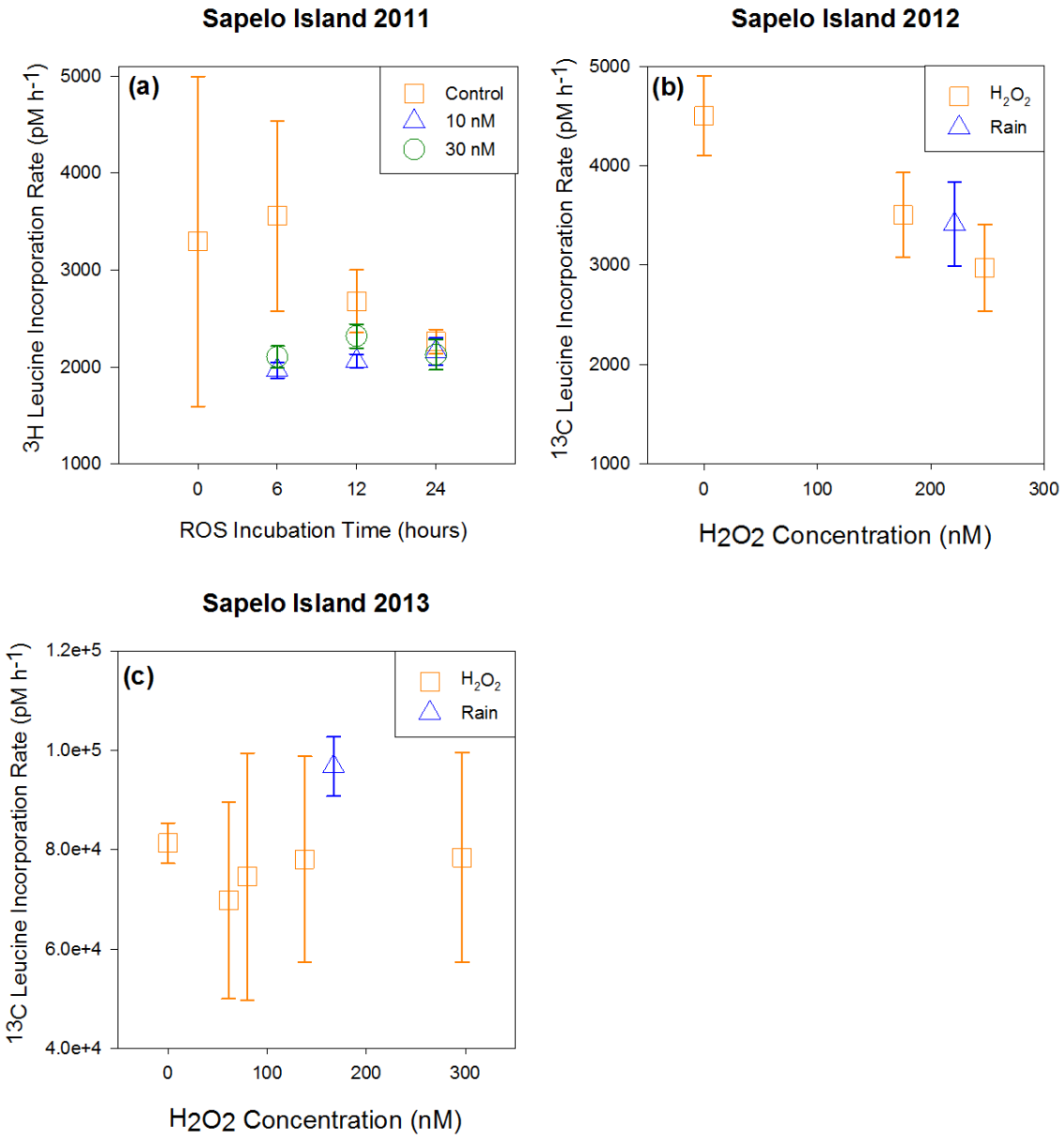
Sapelo Island 2011
(a)
Control
10 nM
30 nM
3H Leucine Incorporation Rate (pM h-1)
5000
4000
3000
2000
1000
0
6
12
24
ROS Incubation Time (hours)
Sapelo Island 2012
(b)
H2O2
Rain
13C Leucine Incorporation Rate (pM h-1)
5000
4000
3000
2000
1000
0
100
200
300
H2O2 Concentration (nM)
Sapelo Island 2013
(c)
H2O2
Rain
13C Leucine Incorporation Rate (pM h-1)
1.2e+5
1.0e+5
8.0e+4
6.0e+4
4.0e+4
0
100
200
300
H2O2 Concentration (nM)